Izaña Atmospheric Research Center

Activity Report 2021-2022

Joint publication of State Meteorological Agency (AEMET) and World Meteorological Organization (WMO)

WMO/GAW Report No. 290

WORLD METEOROLOGICAL ORGANIZATION

GOBIERNO DE ESPAÑA
VICEPRESIDENCIA TERCERA DEL GOBIERNO
MINISTERIO PARA LA TRANSICIÓN ECOLÓGICA Y EL RETO DEMOGRÁFICO

AEMet Agencia Estatal de Meteorología

Cover photograph: Izaña Observatory (Photo: Conchy Bayo-Pérez)

Citation:
Cuevas, E., Milford, C., Barreto, A., Bustos, J. J., García, O. E., García, R. D., Marrero, C., Prats, N., Ramos, R., Redondas, A., Reyes, E., Rivas-Soriano, P. P., Romero-Campos, P. M., Torres, C. J., Schneider, M., Yela, M., Belmonte, J., Almansa, F., López-Solano, C., Basart, S., Werner, E., Rodríguez, S., Alcántara, A., Alvarez, O., Bayo, C., Berjón, A., Borges, A., Carreño, V., Castro, N. J., Chinea, N., Cruz, A. M., Damas, M., González, Y., Hernández, C., Hernández, J., León-Luís, S. F., López-Fernández, R., López-Solano, J., Mármol, I., Martín, T., Parra, F., Rodríguez-Valido, M., Santana, D., Santo-Tomás, F. and Serrano, A.: Izaña Atmospheric Research Center Activity Report 2021-2022. (Eds. Cuevas, E., Milford, C. and Tarasova, O.), State Meteorological Agency (AEMET), Madrid, Spain and World Meteorological Organization, Geneva, Switzerland, NIPO: 666-24-002-7, WMO/GAW Report No. 290, https://doi.org/10.31978/666-24-002-7, 2024.

For more information, please contact:
Izaña Atmospheric Research Center
Headquarters: Calle La Marina, 20
Santa Cruz de Tenerife
Tenerife, 38001, Spain
Tel: +34 922 151 718
Fax: +34 922 574 475
E-mail: ciai@aemet.es
http://izana.aemet.es

State Meteorological Agency (AEMET)
Headquarters: Calle Leonardo Prieto Castro, 8
Ciudad Universitaria
28071, Madrid, Spain
www.aemet.es

World Meteorological Organization (WMO)
7bis, avenue de la Paix
P.O. Box 2300
CH-1211 Geneva 2, Switzerland
www.wmo.int

NIPO: 666-24-002-7
WMO/GAW Report No. 290
https://doi.org/10.31978/666-24-002-7

Izaña Atmospheric Research Center Activity Report 2021-2022

Prepared by:

E. Cuevas[1,*], C. Milford[1], A. Barreto[1], J. J. Bustos[1], O. E. García[1], R. D. García[2,3], C. Marrero[1], N. Prats[1], R. Ramos[1], A. Redondas[1], E. Reyes[1], P. P. Rivas-Soriano[1], P. M. Romero-Campos[1], C. J. Torres[1], M. Schneider[4], M. Yela[5], J. Belmonte[6], F. Almansa[1,7], C. López-Solano[8], S. Basart[9,**], E. Werner[10], S. Rodríguez[11], A. Alcántara[1], O. Alvarez[1], C. Bayo[1], A. Berjón[2], A. Borges[8], V. Carreño[1], N. J. Castro[1], N. Chinea[2,8], A. M. Cruz[1], M. Damas[1], Y. González[7], C. Hernández[1], J. Hernández[12], S. F. León-Luís[2], R. López-Fernández[1], J. López-Solano[2], I. Mármol[1], T. Martín[12], F. Parra[1], M. Rodríguez-Valido[13], D. Santana[14], F. Santo-Tomás[1] and A. Serrano[1]

Editors:

Emilio Cuevas[1], Celia Milford[1] and Oksana Tarasova[15]

[1]Izaña Atmospheric Research Center, State Meteorological Agency (AEMET), Tenerife, Spain
[2]TRAGSATEC, Madrid, Spain
[3]Atmospheric Optics Group, Valladolid University, Valladolid, Spain
[4]Institute for Meteorology and Climate Research, Karlsruhe Institute of Technology (KIT), Karlsruhe, Germany
[5]National Institute for Aerospace Technology (INTA), Torrejón de Ardoz, Madrid, Spain
[6]Universidad Autónoma de Barcelona (UAB), Barcelona, Spain
[7]Cimel Electronique, Paris, France
[8]SIELTEC, La Laguna, Tenerife, Spain
[9]Barcelona Supercomputing Centre, Barcelona, Spain
[10]Sand and Dust Storm Warning Advisory and Assessment Regional Centre, AEMET, Spain
[11]Institute of Natural Products and Agrobiology, IPNA CSIC, Tenerife, Spain
[12]Air Liquide, Tenerife, Spain
[13]University of La Laguna (ULL), Tenerife, Spain
[14]LuftBlick Earth Observation Technologies, Innsbruck, Austria
[15]World Meteorological Organization, Geneva, Switzerland
*now retired
**now at WMO

March 2024

Joint publication of State Meteorological Agency (AEMET) and World Meteorological Organization (WMO)

WMO/GAW Report No. 290

WORLD METEOROLOGICAL ORGANIZATION

Contents

Foreword

The World Meteorological Organization (WMO) coordinates international multidisciplinary research through the Global Atmosphere Watch (GAW) Programme, the World Weather Research Programme (WWRP) and the co-sponsored World Climate Research Programme (WCRP), among others.

The Izaña Atmospheric Research Center (IARC), which is part of the State Meteorological Agency of Spain (AEMET), is a centre of excellence in atmospheric science. It manages four observatories in Tenerife including the high altitude Izaña Observatory. The Izaña Observatory was inaugurated in 1916 and since that date has carried out uninterrupted meteorological and climatological observations, and is now a WMO Centennial Station.

The Izaña Observatory has contributed to the GAW Programme since its inception and is one of 31 GAW Global stations. I would like to highlight the dedication of IARC and collaborating institutions in maintaining the high-quality, long-term (multi-decadal) measurement programmes, which now provide more than 107 years of meteorological data, 40 years of continuous greenhouse gas measurements (CO_2 and CH_4) and more than or close to 30 years of surface and column ozone, ultraviolet and solar radiation, in situ and column aerosols, water vapour and selected reactive gases. These long-term data series are invaluable and require commitment and a rigorous approach.

The urgency of actions related to the state of climate and the environment requires the public and decision-makers to have access to the best available science and high-quality atmospheric composition data, and IARC is highly respected for the quality of the data it provides.

IARC also supports the GAW quality assurance framework by operating the Regional Brewer Calibration Centre for Europe (RBCC-E), which calibrates Brewer spectrometers in Europe and North Africa, maintains the Brewer ozone reference and hosts the European Brewer Network (EUBREWNET). In addition, IARC operates for WMO a Measurement Lead Centre for Aerosols and Water Vapour Remote Sensing Instruments. It also supports the World Radiation Center by maintaining one of the World Optical Depth Research and Calibration Center (WORCC) Precision Filter Radiometer reference instruments at the Izaña Observatory. The Izaña Observatory is also one of three AERONET-EUROPE calibration facilities and ensures the calibration of more than 80 AERONET sites.

IARC also plays an important role in supporting international cooperation. For example, it contributes to activities of the WMO Sand and Dust Storm Warning Advisory and Assessment System (SDS-WAS) and the WMO Barcelona Dust Regional Center (jointly managed by two Spanish institutions, AEMET and the Barcelona Supercomputing Center, BSC) focusing its efforts on the provision of observations, supporting capacity-building activities in the region of Northern Africa, the Middle East and Europe but also, as a reference research centre supporting international atmospheric research projects.

In September-December 2021, the La Palma volcanic eruption took place, and IARC-AEMET responded quickly by deploying a large amount of instrumentation on the island of La Palma, in collaboration with other national and international organisations with the core purpose of helping to save lives and protect the population. The overall response was a clear example of the excellent results that can be achieved through international cooperation and personal and institutional involvement, leading to a significant contribution of science for society.

I would like to express the sincere gratitude of WMO for the exceptional years of service of Dr Emilio Cuevas from the start of the GAW programme in 1989 and later as he became director of IARC. His scientific leadership, dedication, enthusiasm and vision for the Center, as well as his passion for delivering science for society and for innovation in research and development, have been crucial to consolidate IARC as a reference research group on atmospheric science for the international community and to put on the front line the Izaña station as a reference global station.

Dr Cuevas was a key player in the initiation and development of the WMO Barcelona Dust Regional Center and under his stewardship IARC's activities in research and development regarding state-of-the-art measurement techniques, calibration and validation, as well as international cooperation have given it an outstanding reputation in weather, climate and related environmental issues. He will be greatly missed and we wish him all the best for his retirement.

Prof. Jürg Luterbacher

Chief Scientist
Director Science and Innovation
World Meteorological Organization

Dr Emilio Cuevas Agulló

Former Director of Izaña Atmospheric Research Centre (AEMET)

In May 1984, the Izaña Observatory began operating as a World Meteorological Organization Background Atmospheric Pollution MOnitoring Network (BAPMoN) station thanks to an agreement signed at the level of the Ministries of Foreign Affairs of Spain and the Federal Republic of Germany. A basic programme of surface ozone, methane, carbon dioxide, and meteorology continuous measurements was initiated.

I was assigned to the Izaña Observatory in the autumn of 1989. In this year, the WMO Global Atmosphere Watch programme was born as a merger of the BAPMoN program with the Global Ozone Observation System Programme (G030S). In those first five years of operation, the German researchers were the ones who evaluated the data. I learned everything from them, at least in the first years, and they reminded me insistently that "my only valid business card would be the results I obtained." Since then, regular activity reporting became a priority for me.

This is the fifth edition of the biennial report of activities of the Izaña Atmospheric Research Centre co-edited by AEMET and WMO. These reports, prepared in detail, and in which all the IARC staff participate, are intended to show who we are and what we do, both to the citizens who finance us with their taxes, and to the scientific community. They also constitute a written record of the Centre, allowing us to see its evolution over time, as well as a reference in some aspect for other new stations.

These reports are informative and rigorous. The results obtained by Centres like the IARC are immensely valuable to the scientific and wider community because they are subject to numerous external and independent quality controls. The scientific audits of different programmes, the quality controls of the different global databases, and the publication of results in scientific articles with their corresponding peer reviews, are all freely accessible.

Facilities, such as IARC, aside from providing precise information on the characterization and evolution of numerous atmospheric components, are true collaborative hubs of knowledge. In them, global references of atmospheric components are maintained or transferred, new instruments, measurement methodologies, and numerical models of all types are evaluated, and regular intensive measurement campaigns are carried out in order to explain certain atmospheric processes.

The GAW Programme has contributed enormously to creating a multidisciplinary community of atmospheric researchers who can learn from each other and exchange ideas and experience, thereby enhancing scientific progress and expertise.

In the current state of climate emergency, atmospheric processes of characteristics never seen before are beginning to be recorded, and it is a fact that global warming is closely linked to the recovery of the ozone layer and global air quality. In order to adequately monitor the environment, it is necessary to have records of new parameters and products that can only be supplied by R&D institutions. In addition, a continually changing environment requires frequent adjustments and adaptations of monitoring and prediction systems, and this can only be achieved with the active participation of R&D institutions but with operational capacity in products and services delivery. A good example is Copernicus, the EU system aimed to monitor and forecast the state of the environment on land, sea and in the atmosphere, which is basically made up of research institutions. All products and services generated operationally by institutions or research groups are part of what is known as "Science for Society" and constitutes a new paradigm in the development and dissemination of advanced meteorological and atmospheric products and services.

In relation to "Science for Society", in June 2001, the IARC operationally implemented the first prediction model for the ultraviolet index in Spain. A recent example is the atmospheric instrumental deployment carried out in September 2021, in just a few days, on the island of La Palma to monitor and characterize the emissions from the volcanic eruption at Cumbre Vieja with the primary purpose of protecting the health of citizens.

Currently, IARC is implementing the first national network for measuring greenhouse gases in the atmospheric column using the FTIR technique, as well as estimating CO_2 and CH_4 emissions in the cities of Madrid and Barcelona, and which will be part of the COllaborative Carbon Column Observing Network (COCCON). The daily information from this system will be part of a climate service, as well as a greenhouse gas emissions evaluation system for Copernicus.

Climate change can be observed very well in the high-quality meteorological records of Izaña that already cover a period of 107 years. In August of this year, the Izaña Observatory and the Teide astronomical observatory were almost consumed by the flames of a Category 6 wildfire, the first to occur in the Canary Islands, most likely and in part, as a consequence of global warming. The Izaña Observatory turned out to be a unique site to monitor the evolution of the wildfire in a large part of the island and served as a logistics centre to supply water to the firefighting helicopters, knowing, again, to adapt to the circumstances. Until now we had never been able to imagine that something like this could happen.

The importance of Research Centres like the one in Izaña will increase considerably in the coming years in a context of a more intense climate change scenario. However, I hope that these Centres will also be, sooner rather than later, the ones that inform us about the stabilization of the concentrations of greenhouse gases in the atmosphere after the application of drastic measures at a global level to eliminate greenhouse gas emissions.

My professional life has reached this point in time. It has been an immense pride and a privilege to work at IARC with all its staff, both past and present, and collaborating with hundreds of researchers and technicians from many countries within the framework of the GAW programme and those of its associated networks. To those who continue and those who will join in the future, I would like to remind them of the importance of their work for society, and therefore to do it with enthusiasm. I also ask that in a few years the Izaña Observatory could be 100% self-sufficient in energy (with photovoltaic panels) and water (from rain and fog), since it is technically possible, and a facility like this must be environmentally sustainable.

I hope that the moments of tranquillity and silence that the Izaña Observatory will continue to provide will serve its people to think intelligently, and adequately plan the activities without the background noise caused by the successive states of emergency of all kinds that they will have to face from now on.

1 Organization

The Izaña Atmospheric Research Center (IARC) is part of the Department of Planning, Strategy and Business Development of the State Meteorological Agency of Spain (AEMET). AEMET is an Agency of the Spanish Ministry for the Ecological Transition and the Demographic Challenge (MITECO).

2 Mission and Background

The Izaña Atmospheric Research Center conducts observations and research related to atmospheric constituents that have impact on climate (greenhouse gases and aerosols), may cause depletion of the global ozone layer or play key roles in air quality from local to global scales. The IARC is an Associated Unit of the Spanish National Research Council (CSIC) through the Institute of Environmental Assessment and Water Research (IDAEA). The main goal of the Associated Unit "Group for Atmospheric Pollution Studies" is to perform air quality research in both rural and urban environments.

The IARC has contributed to the World Meteorological Organization (WMO) Global Atmosphere Watch (GAW) Programme since its establishment in 1989. GAW integrates a number of WMO research and monitoring activities in the field of atmospheric environment. The main objectives of GAW are to provide data and other information on the chemical composition and related physical characteristics of the atmosphere, its changes and the drivers of these changes. These are required to improve our understanding of the behaviour of the atmosphere and its interactions with the oceans and the biosphere.

The Izaña Atmospheric Research Center also contributes to the Network for the Detection of Atmospheric Composition Change (NDACC). NDACC is an international network for monitoring atmospheric composition using remote measurement techniques. Originally, NDACC was created to monitor the physical and chemical changes in the stratosphere, with special emphasis on the evolution of the ozone layer and the substances responsible for its destruction known as Ozone Depleting Substances. The current objectives of NDACC are to observe and to understand the physicochemical processes of the upper troposphere and stratosphere, and their interactions, and to detect long-term trends of atmospheric composition. IARC also makes an important contribution to the WMO through the Global Climate Observing System and through hosting the WMO Measurement Lead Centre for Aerosols and Water Vapour Remote Sensing Instruments.

Izaña Observatory was inaugurated in its present location on 1 January 1916, initiating uninterrupted meteorological and climatological observations, which constituted a 107-year record in 2022. In 1984, the observatory became a station of the WMO Background Atmospheric Pollution Monitoring Network (BAPMoN). In 1989, BAPMoN and GO3OS (Global Ozone Observing System) merged in the current Global Atmosphere Watch Programme, of which Izaña Observatory is one of 31 GAW Global stations (Figure 2.1). GAW Global stations serve as centres of excellence and perform extensive research on atmospheric composition change. Izaña Observatory is a key example of such a research facility.

Figure 2.1. WMO GAW Global stations.

3 Facilities and Summary of Measurements

The Izaña Atmospheric Research Center (IARC) manages four observatories in Tenerife (Fig. 3.1, Table 3.1): 1) Izaña Observatory (IZO); 2) Santa Cruz Observatory (SCO); 3) Botanic Observatory (BTO); and 4) Teide Peak Observatory (TPO).

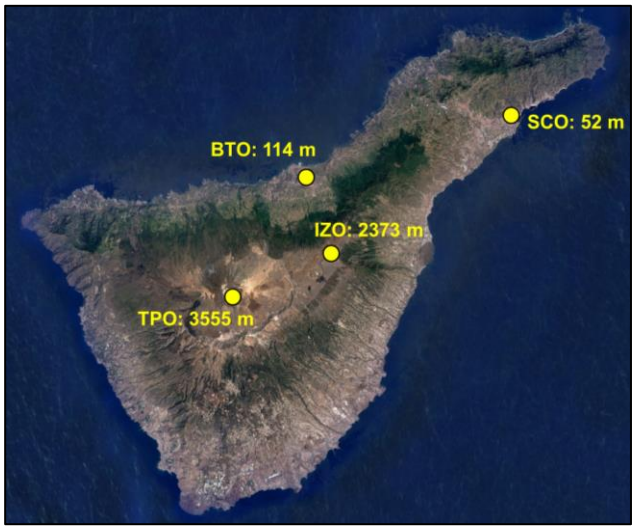

Figure 3.1. Location of IARC observatories on Tenerife.

Table 3.1. IARC observatories.

Observatory	Latitude	Longitude	Altitude (m a.s.l.)
IZO	28.309 ºN	16.499 ºW	2373
SCO	28.473 ºN	16.247 ºW	52
BTO	28.411 ºN	16.535 ºW	114
TPO	28.270 ºN	16.639 ºW	3555

3.1 Izaña Observatory

The Izaña Observatory (IZO) is located on the island of Tenerife, Spain, roughly 300 km west of the African coast. The observatory is situated on a mountain plateau, 15 km north-east of the volcano Teide (3718 m a.s.l.) (Figs 3.2 and 3.3). The local wind regime at the site is dominated by north-westerly winds. Clean air and clear sky conditions generally prevail throughout the year. IZO is normally above a temperature inversion layer, generally well established over the island, and below the descending branch of the Hadley cell.

Figure 3.2. Image of Izaña Observatory.

The station offers excellent conditions for trace gas and aerosol in situ measurements under "free troposphere" conditions, and for atmospheric observations by remote sensing techniques. The environmental conditions and pristine skies are optimal for calibration and validation activities of both ground-based and space-borne sensors. Due to its geographic location, it is particularly valuable for the investigation of dust transport from Africa to the North Atlantic, long-range transport of pollution from the Americas, and large-scale transport from the tropics to higher latitudes.

The Izaña Observatory facilities consist of three separate buildings: the main building, inaugurated in 1916; the aerosols lab, a small nearby building of the same period which was renamed "Joseph M. Prospero Aerosols Laboratory" on 8 April 2016; and the technical tower, completely rebuilt in early 2000, which hosts most of the instruments. Details of the IZO measurement programme are given in Table 3.2.

The main building is a two-storey building with a total area of 1420 m^2, which hosts the following facilities: office space, dining room, kitchen, library, conference hall with audio-visual system, meeting room, engine rooms, a mechanical workshop, and an electronics workshop. In addition, there is residential accommodation available for visiting scientists (seven double en-suite rooms). The technical tower is a seven-storey building with a total area of 900 m^2. It includes 20 laboratories distributed among the different floors (Table 3.3, Fig. 3.8). All the laboratories are temperature-controlled.

Figure 3.3 Izaña Observatory (2373 m) with the volcano Teide (3718 m) to the left of the image.

Table 3.2. Izaña Observatory (IZO) measurement programme.

Parameter	Start date	Present Instrument	Data Frequency
Greenhouse Gases and Carbon Cycle			
CO_2	Jun 1984	CRDS Picarro G2401 (Primary instrument) NDIR Licor 7000 (Secondary instrument)	2″ 30″
CH_4	Jul 1984	CRDS Picarro G2401 GC-FID Varian 3800	2″ 4 samples/hour
N_2O	Jun 2007	GC-ECD Varian 3800 Los Gatos Research 913-0015	4 samples/hour 4″
SF_6	Jun 2007	GC-ECD Varian 3800	4 samples/hour
CO	Jan 2008	CRDS Picarro G2401 GC-RGD Trace Analytical RGA-3 Los Gatos Research 913-0015	30″ 3 samples/hour 4″
In situ Reactive Gases			
O_3	Jan 1987	UV Photometry Teco 49-C (Previous Primary instrument) Teco 49-C (Secondary instrument) Teco 49-i (New Primary instrument)	 1′ 1′ 1′
CO	Nov 2004 - June 2019	Non-dispersive IR absorption Thermo 48C-TL	1′
SO_2	Jun 2006	UV fluorescence Thermo 43C-TL	1′
NO-NO_2-NO_x	Jun 2006	Chemiluminescence Thermo 42C-TL Chemiluminescence EcoPhysics CraNOx II	1′ 1′
Total Ozone Column and UV			
Column O_3	May 1991	Brewer Mark-III #157 (Primary Reference) Brewer Mark-III #183 (for developments) Brewer Mark-III #185 (Travelling Reference)	~100/day ~100/day ~100/day
Spectral UV: 290-365 nm	May 1991	Brewer Mark-III #157 (Primary Reference) Brewer Mark-III # 183 (for developments) Brewer Mark-III #185 (Travelling Reference)	~30′ ~30′ ~30′
Spectral UV: 290-450 nm	May 1998	Bentham DM 150	Campaigns
Column SO_2	May 1991	Brewer Mark-III #157 (Primary Reference) Brewer Mark-III # 183 (for developments) Brewer Mark-III #185 (Travelling Reference)	~100/day ~100/day ~100/day
Column O_3	Oct 2011	Pandora 101 Pandora 121	10′ 10′
Column NO_2	Oct 2011	Pandora 101 Pandora 121	10′ 10′

Parameter	Start date	Present Instrument	Data Frequency
Fourier Transform Infrared Spectroscopy (FTIR)			
Greenhouse gases, reactive gases, and O_3 depleting substances (O_3, HF, HCN, HCl, $ClONO_2$, C_2H_6, HNO_3, CH_4, CO, CO_2, N_2O, NO, NO_2, H_2O, HDO, OCS)	Jan 1999 May 2007 Aug 2022	Fourier Transform Infrared Spectroscopy Bruker IFS 120/5HR (co-managed with KIT) Middle infrared (MIR) solar absorption spectra Near infrared (NIR) solar absorption spectra Bruker IFS 125HR SN149	3 days/week (weather permitting)
Water vapour isotopologues (δD and $\delta^{18}O$)	Mar 2012-Apr 2019	Picarro L2120-I δD and $\delta^{18}O$ Analyser	Continuous (2″)
Greenhouse gases, and reactive gases (CO_2, CH_4, CO, H_2O)	May 2018 Mar 2021	Bruker EM27/SUN SN85 Bruker EM27/SUN SN143	1 day/week (weather permitting)
In situ aerosols			
Chemical composition of particulate matter: PM_T[(1)] PM_1[(2)] $PM_{2.5}$ PM_{10}	 Jul 1987 Aug 2010 Apr 2002 Jan 2005	High-volume sampler custom built/MVC™/MCZ™ Concentrations of soluble species by ion chromatography (Cl^-, NO_3^- and SO_4^{2-}) and FIA colorimetry (NH_4^+), major elements (Al, Ca, K, Na, Mg and Fe) and trace elements by ICP-AES and ICP-MS were determined at CSIC	8h sampling at night
Number of particles with diameter > 3 nm	Nov 2006[(3)]	TSI™, UCPC 3025A	1′
Number of particles > 2.5 nm	Dec 2012	TSI™, UCPC 3776	1′
Number of particles > 10 nm	Dec 2012	TSI™, CPC 3010	1′
Size distribution in the size range 10-400 nm	Nov 2006	TSI™, class 3080 + CPC 3772	5′
Size distribution in the size range 0.7-20 µm	Nov 2006	TSI™, APS 3321	10′
Absorption coeff. (PM_{10}) at 637 nm	Nov 2006	Thermo™, MAAP 5012	1′
Attenuation (PM_{10}) at 370, 470, 520, 590, 660, 880 and 950 nm	Jul 2012	Magee™, Aethalometer AE31-HS	1′
Attenuation (PM_{10}) at 370, 470, 520, 590, 660, 880 and 950 nm	Feb 2022	Magee™, Aethalometer AE33	1′
Scattering coeff. (PM_{10}) at 450, 550 and 700nm	Jun 2008	TSI™, Integration Nephelometer 3563	1′
PM_{10} mass concentration	Jun 2016	Thermo, BETA 5014i	5′
$PM_{2.5}$ and $PM_{2.5-10}$ mass concentrations	Jun 2016	Thermo, TEOM 1405DF	6′

(1) Not operational since 2017

(2) Usually only in summer (August)

(3) Not operational since June 2017

Parameter	Start date	Present Instrument	Data Frequency
Column aerosols			
AOD and Angstrom at 340, 380, 440, 500, 675, 870, 936, 1020 nm	Mar 2003	CIMEL CE318 sun photometer	~ 15′
Fine/Coarse AOD Fine mode fraction	Mar 2003	CIMEL CE318 sun photometer	~ 15′
Optical inversion products	Mar 2003	CIMEL CE318 sun photometer	~ 1h
AOD and Angstrom during night period	July 2012	CIMEL CE318-T sun-sky-lunar photometer	~ 15′ during moon phases
AOD and Angstrom at 368, 412, 500 and 862 nm	July 2001	WRC Precision Filter Radiometer (PFR)	1′
AOD at 769.9 nm	July 1976	MARK-I (at the IAC)	AOD at 769.9 nm
Elastic backscatter and depolarization measurements at 532 nm and 808 nm	Dec 2015	CIMEL CE376 micro-lidar	1’
Vertical Backscatter-extinction at 532 nm, clouds alt. and thickness (with depolarizarion)	Feb 2020	Micro Pulse Lidar MPL-4B	1′
Radiation			
Global Rad. 285-2600 nm	Jan 1977	Pyranometers CM-21 & CM-11 Kipp & Zonen, EKO MS-801 and MS-80S	1′
Global Rad. 300-1100 nm	Feb 1996	YES MFRSR	1′
Estim. Direct Rad.	Feb 1996	YES MFRSR	1′
Direct Rad. 200-4000nm	Aug 2005	Pyrheliometers CH-1 Kipp & Zonen, EKO MS-56 and MS-57	1′
Direct Rad. 200-4000nm	Jun 2014	Absolute Cavity Pyrheliometer PMO6	Calibration campaigns (1′)
Spectral direct Radiation	Dec 2016	Spectroradiometer EKO MS-711	1′
Spectral global and diffuse Radiation	Feb 2020	Spectroradiometer EKO RSB	1′
Spectral global Radiation	Dec 2022	Spectroradiometer EKO MS-713	1′
Diffuse Rad.	Feb 1996	YES MFRSR	1′
Diffuse Rad. 285-2600 nm	Aug 2005	Pyranometers CM-21 Kipp & Zonen, EKO MS-801 and MS-80S	1′
Downward Longwave Rad. 4.5-42 μm	Mar 2009	Pyrgeometers CG-4 Kipp & Zonen and EKO MS-21	1′
UVB Radiation 315-400 nm	Aug 2005	2 Yankee YES UVB-1 Pyranometer (in parallel)	1′
UVA Radiation 280-400 nm	Mar 2009	Radiometers UVS-A-T Kipp & Zonen and EKO MS-10S	1′

Parameter	Start date	Present Instrument	Data Frequency
Radiation (continued)			
Photosynthetically Active Radiation (PAR) 400-700 nm	Aug 2005	Pyranometers Par Lite Kipp & Zonen and Photon Sensor EKO ML-020P	1′
Net Radiation	Nov 2016	Net Radiometer EKO MR-60	1′
Luminance/Radiance	Nov 2020	EKO MS-321LR Sky Scanner	10′
Global and Diffuse Rad.	Jun 2021	SPN1 Sunshine Pyranometer	1′
DOAS (managed by the Spanish National Institute for Aerospace Technology, INTA)			
Column NO_2	May 1993	UV-VIS DOAS EVA and MAXDOAS RASAS II (INTA's homemade; www.inta.es)	Every ~20′ during twilight
Column O_3	Jan 2000	UV-VIS MAXDOAS RASAS II (INTA's homemade)	Every ~20′ during twilight
Column BrO	Jan 2002	UV-VIS MAXDOAS ARTIST-II (INTA's homemade)	Every ~20′ during twilight
Tropospheric O_3	May 2010	UV-VIS MAXDOAS RASAS II (INTA's homemade)	Every ~20′ during twilight
Tropospheric NO_2	May 2010	UV-VIS MAXDOAS RASAS II (INTA's homemade)	Every ~20′ during twilight
Tropospheric IO	May 2010	UV-VIS MAXDOAS RASAS II (INTA's homemade)	Every ~20′ during twilight
Tropospheric HCHO	May 2015	UV-VIS MAXDOAS ARTIST II (INTA's homemade)	Every ~20′ during twilight
Water Vapour			
Precipitable Water Vapour (PWV)	Jul 2008 (ultra-rapid orbits) Jan 2009 (precise orbits)	GPS/GLONASS LEICA GRX1200GGPRO satellite ground-based receiver	15′ (ultra-rapid orbits) and 1h (precise orbits)
PWV Total Column and Profiles for layers from 2.4 km up to 12 km altitude	Dec 1963	Vaisala RS-41	Daily at 00 and 12 UTC
PWV	Mar 2003	CIMEL CE318 sun photometer	~ 15′
PWV	Jan 1999	Fourier Transform Infrared Spectroscopy	3 days/week when cloud-free conditions
Integrated Water Vapour (IWV)	May 2020	Microwave Radiometer LHATPRO G5	1″
Vertical Absolute Humidity Profile (HPC)	May 2020	Microwave Radiometer LHATPRO G5	1′
Vertical Relative Humidity Profile (HRC)	May 2020	Microwave Radiometer LHATPRO G5	1′
Liquid Water Path (LWP)	May 2020	Microwave Radiometer LHATPRO G5	1″
Liquid Water Profile (LPR)	May 2020	Microwave Radiometer LHATPRO G5	1″
Cloud Base Height (CBH)	May 2020	Microwave Radiometer LHATPRO G5	1″

Parameter	Start date	Present Instrument	Data Frequency
Meteorology			
Temperature	Jan 1916	THIES CLIMA 1.1005.54.700 3 VAISALA HMP45C (in parallel) VAISALA PTU300 THIES CLIMA 1.0620.00.000 (thermo-hygrograph) CAMPBELL SCIENTIFIC CS215 (Tower top)	1′ 1′ 1′ Continuous 1′
Relative humidity	Jan 1916	THIES CLIMA 1.1005.54.700 3 VAISALA HMP45C (in parallel) VAISALA PTU300 THIES CLIMA 1.0620.00.000 (thermo-hygrograph) CAMPBELL SCIENTIFIC CS215 (Tower top)	1′ 1′ 1′ Continuous 1′
Wind direction and speed	Jan 1916	Sonic anemometer Thies 2D 4.3820.31.401 Sonic anemometer FT Technologies FT742-D-DM Sonic anemometer FT Technologies FT742-D-DM (Tower Top)	1′ 1′ 1′
Pressure	Jan 1916	SETRA 470 VAISALA PTU 300 BELFORT 5/800AM/1 (Barograph) SETRA 470 (Tower top)	1′ 1′ Continuous 1′
Rainfall	Jan 1916	THIES CLIMA Tipping Bucket THIES CLIMA Tipping Bucket Hellman rain gauge Hellman pluviograph	1′ 1′ Daily Continuous
Sunshine duration	Aug 1916	KIPP & ZONEN CSD3 Campbell Stokes Sunshine recorder	10′ Continuous
Present weather and visibility	Jul 1941	BIRAL 10HVJS	10′
Vertical profiles of T, RH, P, wind direction and speed, from sea level to ~30 km altitude	Dec 1963	RS41+GPS radiosondes launched at Güimar automatic radiosonde station (WMO GRUAN station #60018) (managed by the Meteorological Centre of Santa Cruz de Tenerife)	Daily at 00 and 12 UTC
Soil surface temperature	Jan 1953	2 THIES CLIMA Pt100 (in parallel)	10′
Soil temperature (20 cm)	Jan 2003	2 THIES CLIMA Pt100 (in parallel)	10′
Soil temperature (40 cm)	Jan 2003	2 THIES CLIMA Pt100 (in parallel)	10′
Atmospheric electric field	Apr 2004	Electric Field Mill PREVISTORM-INGESCO	10″
Lightning discharges	Apr 2004	Boltek LD-350 Lightning Detector	1′
Cloud cover	Sep 2008	Sieltec Canarias S.L. SONA total sky camera Sieltec Canarias S.L. SONA total sky camera (Model 201D, daytime) Sieltec Canarias S.L. SONA total sky camera (Model 502N, nighttime)	5′ 5′ 5′

Fog-rainfall	Nov 2009	THIES CLIMA Tipping Bucket with 20 cm^2 mesh Hellman rain gauge with 20 cm^2 mesh	1′ Daily
Sea-cloud cover	Nov 2010	AXIS Camera: West View (Orotava Valley) AXIS Camera: South View (Meteo Garden) AXIS Camera: North View AXIS Camera: East View (Güimar Valley)	5′ 5′ 5′ 5′
Drop size distribution and velocity of falling hydrometeors	May 2011	OTT Messtechnik OTT Parsivel	1′
Aerobiology			
Pollens and spores	Jun 2006	Hirst, 7-day recorder VPPS 2000 spore trap (Lanzoni S.r.l.). Analysis performed with a Light microscope, 600 X at the Laboratori d'Anàlisis Palinològiques, Universitat Autònoma de Barcelona	Continuous (1 h resolution) from April to October

On the ground floor of the technical tower, there are two storage spaces, one of them is for pressured cylinders (tested and certified at the Canary Islands Regional Council for Industry) and the other one is for cylinder filling using oil-free air compressors. This floor also includes the central system for supplying high purity gases (H_2, N_2, Ar/CH_4) and synthetic air to the different laboratories. On the second floor, there is a dark-room with the necessary calibration set-ups for the IZO radiation instruments. On the top of the technical tower there is a 160 m^2 flat horizon-free terrace for the installation of outdoor scientific instruments that need sun or moon radiation. It also has the East and West sample-inlets which supply the ambient air to in situ trace gas analysers set up in different laboratories.

The “Joseph M. Prospero Aerosol Research Laboratory” is a 40 m^2 building used as an on-site aerosol measurement laboratory. It has four sample-inlets connected to aerosol analysers. For more details, see Section 8. Outside Izaña Observatory there are the following facilities: 1) a 160 m^2 flat horizon-free platform with communications and UPS used for measurement field campaigns; 2) the meteorological garden, containing two fully-automatic meteorological stations (one of them is the SYNOP station and the second one is for meteorological research), manual meteorological gauges, a total sky camera, a GPS/GLONAS receiver, a lightning detector, and an electric field mill sensor; and 3) the Sky watch cabin hosting four cameras for cloud observations with corresponding servers. The following sections give further details of some of the facilities located at IZO.

Table 3.3. Izaña Observatory technical tower facilities.

Floor	Facilities	Description
Ground Floor	Mechanical Workshop	33 m^2 room with the necessary tools to carry out first-step mechanical repairs.
	Electronics Workshop	25 m^2 room equipped with oscilloscopes, power supplies, multimeters, soldering systems, etc. to carry out first-step electronic repairs.
	Heating system	Central heating and hot water 90 kW system.
	Air Conditioning System	Central air conditioning system for labs.
	Engine Room: Backup Generators	General electrical panel and two automatic start-up backup generators (400 kVA and 100 kVA, respectively).
	UPS room	Observatory's main UPS (40 kVA redundant) used for assuring the power of the equipment inside the building and an additional UPS (10 kVA) for the outside equipment.
	Compressor room	Room with clean oil-free air compressors used for calibration cylinders filling. It also contains the general pumps for the East and West sample inlets.
	Warehouse / Central Gas Supply System	30 m^2 warehouse authorized for pressurized cylinders. Central system for high purity gas (H_2, N_2, Ar/CH_4) and synthetic air supply.
	Lift	6-floors. No lift access to roof terrace.
First Floor	Archive room	Archive of bands and historical records.
	Technical equipment warehouse	Spare parts for the Observatory's technical equipment.
	Meeting room	8-person meeting room
Second Floor	Optical Calibration Facility	30 m^2 dark room hosting vertical and horizontal absolute irradiance, absolute radiance, angular response, and spectral response calibration set ups.
	T2.1 Laboratory	10 m^2 lab with access to West sample inlet.
	T2.2 Laboratory	9 m^2 lab with access to East sample inlet.
	T2.3 Laboratory	13 m^2 lab hosting Picarro L2120-I δD and $\delta^{18}O$ analyser with access to East sample inlet
Third Floor	Greenhouse Gases Laboratories	70 m^2 shared in two labs hosting CO_2, CH_4, N_2O, SF_6 and CO analysers with access to the East and West sample inlets.
Fourth Floor	All purpose laboratories	Three labs with access to the East and West sample inlets.
Fifth Floor	Reactive Gases Laboratory	10 m^2 lab hosting NO-NO_2 and SO_2 analysers with access to West sample inlet.
	Communications room	Server room and WIFI connection with Santa Cruz de Tenerife headquarters.
	Brewer Laboratory	20 m^2 lab for Brewer campaigns.
Sixth Floor	Surface Ozone Laboratory	10 m^2 laboratory hosting surface O_3 analysers with access to West sample inlet.
	Solar Photometry Laboratory	10 m^2 maintenance workshop for solar photometers.
	Spectroradiometer Laboratory	25 m^2 laboratory hosting two MAXDOAS and two spectroradiometers connected with optical fibre.
Roof	Instrument Terrace	160 m^2 flat horizon-free terrace hosting outdoor instruments, East and West sample-inlets, wind, pressure, temperature and humidity sensors.

3.1.1 Optical Calibration Facility

The optical calibration facility at IZO has been developed within the framework of the Specific Agreement of Collaboration between the University of Valladolid and IARC-AEMET: "To establish methodologies and quality assurance systems for programs of photometry, radiometry, atmospheric ozone and aerosols within the atmospheric monitoring programme of the World Meteorological Organization". The main objective of the optical calibration facility is to perform Quality Assurance & Quality Control (QA/QC) assessment of the solar radiation instruments that support the ozone, aerosols, radiation, and water vapour programs of the IARC. The seven set-ups available are the following:

1) Set-up for the absolute radiance calibration by calibrated integrating sphere (Fig. 3.4A). The system is traceable to the AErosol RObotic NETwork (AERONET) standard at the Goddard Space Flight Center (Washington, USA). This set-up is mainly used by Cimel sun-photometers, but other instruments can also be calibrated. At the end of 2017, in the framework of a competitive scientific infrastructure call of the National Plan for Research, Development and Innovation of Spain, a new integrating sphere was installed at Izaña for AERONET-Europe absolute radiance calibrations as well as optical tests required for QC/QA of reference instruments. The new integrating sphere has a 50.8 cm diameter and 20.3 cm aperture (Fig. 3.4B). This system is also traceable to the AERONET standard at the Goddard Space Flight Center.

2) Set-up for the slit function determination (Fig. 3.4 C). The characterization of the slit function is performed illuminating the entrance slit of a spectrophotometer with the monochromatic light of a VM-TIM He-Cd laser. The nominal wavelength of the laser is 325 nm, its power is 6 mW, and its beam diameter is 1.8 mm.

3) Set-up for the alignment of the Brewer spectrophotometer optics (Fig. 3.4D). It is suitable to perform adjustments of the optics without sending the instrument to the manufacturer.

4) Set-up for the angular response calibration (Fig. 3.4E). It is used to quantify the deviations of the radiometer's angular response from an ideal cosine response. The relative angular response function is measured by rotating the mechanical arm where the seasoned DXW-type 1000 W lamp is located. The rotation over ± 90º is controlled by a stepper motor with a precision of 0.01º while the instrument is illuminated by the uniform and parallel light beam of the lamp.

5) Set-up for the spectral response calibration. It is used to quantify the spectral response of a radiometer (Fig. 3.4F). The light is scattered by an Optronic double monochromator OL 750 within the range from 200 to 1100 nm with a precision of 0.1 nm. An OL 740-20 light source positioned in front of the entrance slit acts as radiation source and two lamps, UV (200-400 nm) and Tungsten (250-2500 nm) are available.

6) Set-up for the absolute irradiance calibration by calibrated standard lamps in a horizontally oriented position (Fig. 3.4G).

7) Set-up for the absolute irradiance calibration by calibrated standard lamps in a vertical oriented position suitable for relatively large spectrophotometers (Fig. 3.4H). The basis of the absolute irradiance scale consists of a set of DXW-type 1000 W lamps traceable to the primary irradiance standard of the Physikalisch-Technische Bundesanstalt (PTB).

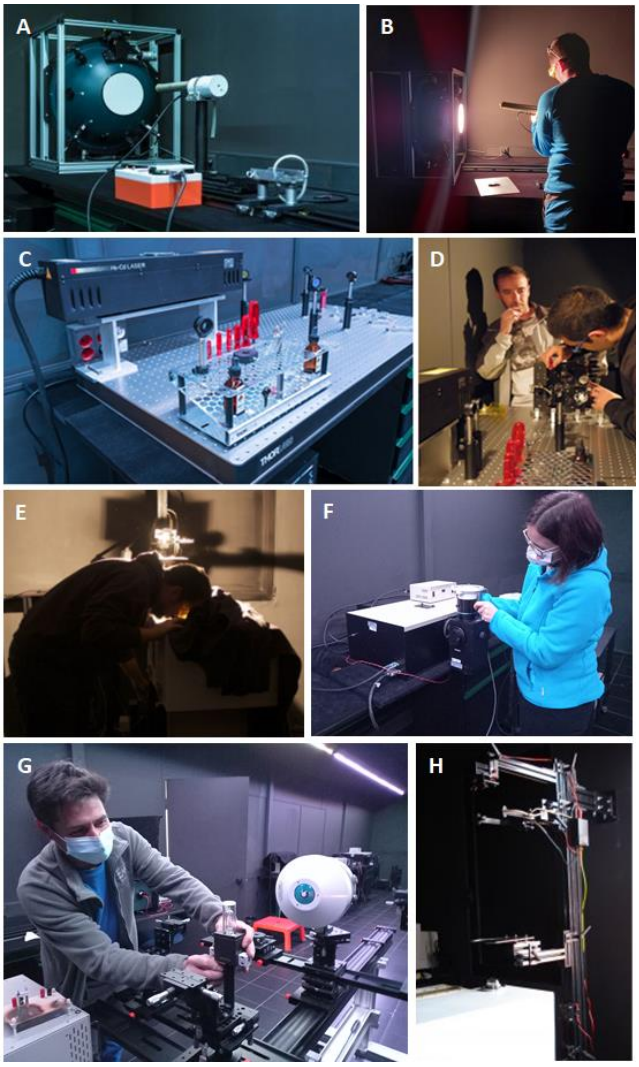

Figure 3.4. Images of the IZO Optical calibration facility. A, B) Absolute radiance calibration of a Cimel CE318 with integrating sphere, C, D) Set up for slit function determination and alignment of a Brewer spectrophotometer optics, E) Angular response function determination of a Brewer, F) Spectral response calibration of a Yankee UVB radiometer, G) Horizontal absolute irradiance calibration of a EKO MS-711 spectroradiometer and (H) Set up for the absolute calibration in a vertical oriented position of a Brewer.

3.1.2 In situ system used to produce working standards containing natural air

GAW requires very high accuracy in the atmospheric greenhouse gas mole fraction measurements, and a direct link to the WMO primary standards maintained by the GAW GHG CCLs (Central Calibration Laboratories), most of which are located at the National Oceanic and Atmospheric Administration-Earth System Research Laboratory-Global Monitoring Laboratory (NOAA-ESRL-GML). To meet these requirements, IARC uses Laboratory Standards prepared (using natural air) and calibrated by NOAA-ESRL-GML. Indeed, the Laboratory Standards used at IARC are WMO tertiary standards. However, due to the fact that the consumption of standard and reference gases by the IARC GHG measurement systems is relatively high, an additional level of standard gases (working standards) prepared with natural air is used.

These working standards are prepared at IZO using an in-situ system (Fig. 3.5) and then calibrated against the Laboratory Standards using the IARC GHG measurement systems. The system used to fill the high-pressure cylinders (up to 120-130 bars) with dried natural air, takes clean ambient air from the East sample-inlet located on top of the IZO tower (30 m above ground), and pumps (using an oil-free compressor) it inside the cylinders after drying it (using magnesium perchlorate), achieving a H_2O mole fraction lower than 3 ppm.

Additionally, it is possible to modify slightly the CO_2 mole fraction of the natural air pumped inside the cylinders. To this end, air from a cylinder containing natural air with zero CO_2 mole fraction (prepared using the same system but adding a CO_2 absorber trap) or a tiny amount of gas from a spiking CO_2 cylinder (5% of CO_2 in $N_2/O_2/Ar$) is added to the cylinder being filled. This system is similar to that used by NOAA-ESRL-GML to prepare WMO secondary and tertiary standards, and it is managed and operated at IZO through a subcontractor (Air Liquide Canarias). The prepared working standards are mainly used in the GHG measurement programme, but some of them are used for other purposes, including for natural air supply for a H_2O isotopologue CRDS analyser located at Teide peak and for a CO NDIR analyser located at SCO.

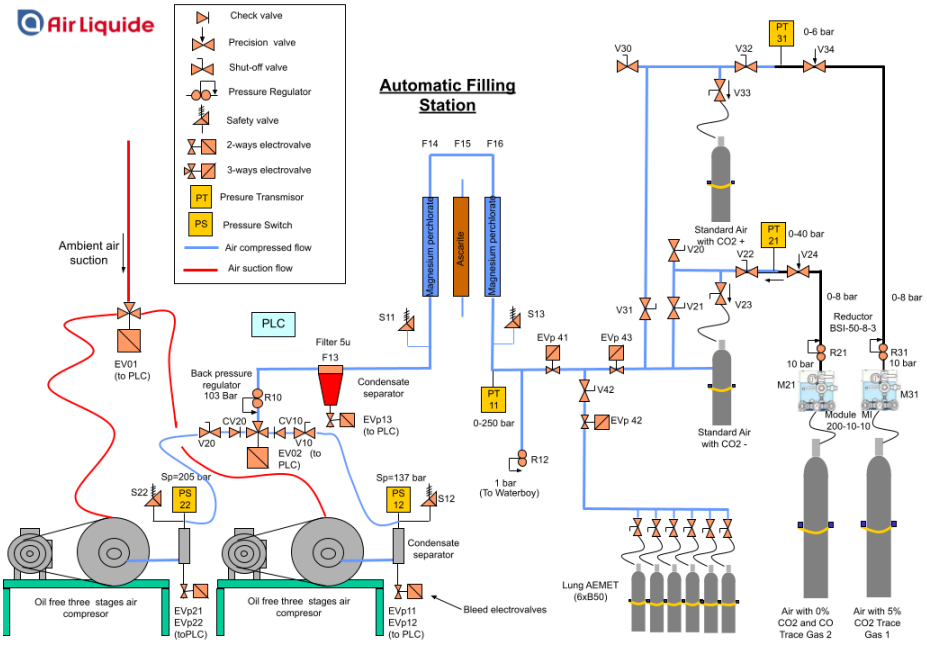

Figure 3.5. In situ system used to produce working standards containing natural air at Izaña Observatory.

3.1.3 Central Gas Supply System

There is a gas central facility located on the IZO tower ground floor for supplying support gases to the different instruments. This central facility supplies high purity: N_2 (used as carrier gas for the GC-FIDs, and for the IZO H_2O isotopologue Cavity Ring-Down Spectroscopy (CRDS) analyser), synthetic air (used as oxidizer in the FIDs, as carrier gas in the GC-RGD, as carrier gas in the IZO H_2O isotopologue CRDS analyser, and as diluting air used in the calibrations of the reactive gas instruments), 99.9995% O_2 (used for O_3 generation in the CraNOx-II analyzer), 95% Ar /5% CH_4 (used as carrier gas for the CD-ECD), and H_2 (used as combustible in the FIDs). The H_2O isotopologue CRDS analyser located at Teide peak has its own dedicated high purity N_2 supply.

Additionally, other gases (provided by Air Liquide) are used at IZO: high purity CO_2 for the calibration of an aerosol nephelometer, high purity N_2O for FTIR instrumental line shape monitoring, liquid N_2 to cryocool the FTIR detectors, and calibrated concentrated gas standards in N_2 (1 ppm NO, 10 ppm NO, 1 ppm SO_2 and 2 ppm CO) for the calibration of the instruments of the reactive gases programme.

3.1.4 Aerosol Filters Laboratory

The Aerosol Filters Laboratory at IZO is equipped with an auto-calibration microbalance (Mettler Toledo XS105DU) with a resolution of 0.01 mg, a set of standard weights, and an oven that reaches 300 ºC. Filters are weighed following the requirements of the UNE-EN-12341-2015 standards. This filter weighing procedure is used for determination of concentrations of PM_{10}, $PM_{2.5}$ and PM_1 by means of standardized methods, within a methacrylate chamber, which also contains the balance used for weighing the filters (Fig. 3.6).

Figure 3.6. IZO Aerosol Filters laboratory: temperature and relative humidity controlled chamber.

3.1.5 Modifications and improvements to the IZO facilities carried out in 2021-2022

In 2022, a new laboratory was completed to house the new FTIR IFS 125HR spectrometer (Fig. 3.7).

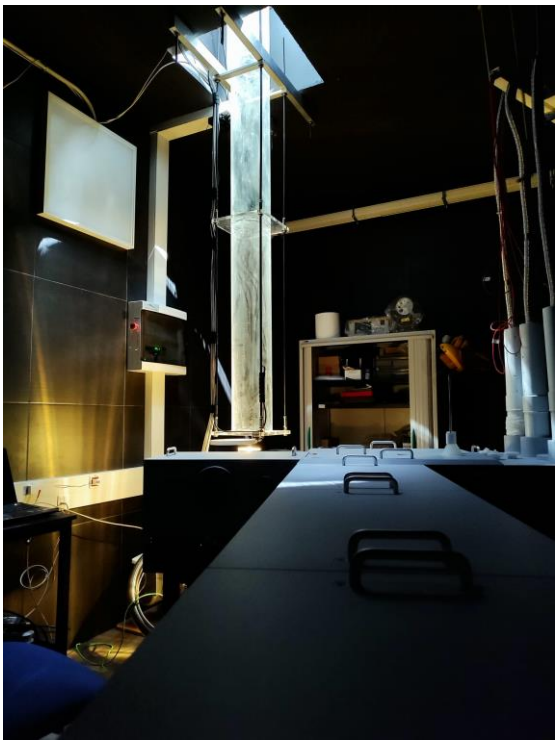

Figure 3.7. New FTIR laboratory at IZO, in August 2022.

The new FTIR IFS 125HR spectrometer was installed in August 2022 at IZO (Fig. 3.8) in order to replace the current instrument (see Section 7 for more details).

Figure 3.8. Installation of the FTIR IFS 125HR at IZO in August 2022.

Figure 3.9. Images of IZO Instrument terrace and technical tower.

3.2 Santa Cruz Observatory

The Santa Cruz de Tenerife Observatory (SCO) is located on the roof of the IARC headquarters at 52 m a.s.l. in the capital of the island (Santa Cruz de Tenerife), close to the city harbour (Figs. 3.10 and 3.11). Details of the SCO measurement programme are given in Table 3.4.

Figure 3.10. Images of Santa Cruz Observatory (SCO).

This observatory has two main objectives: 1) to provide information on background urban pollution to support atmospheric research and to study contribution of the long-range pollution transport driven by trade winds or Saharan dust outbreaks on local air quality and 2) to perform complementary measurements to those at IZO. The IARC headquarters include the following facilities:

- A laboratory for reactive gases measurements (surface O_3, NO-NO_2, CO and SO_2).
- A laboratory hosting Micro Pulse Lidar (MPL) and ceilometer VL-51.
- A laboratory for the preparation of ozonesondes.
- A 25 m^2 flat horizon-free terrace for radiation instruments and air intake.

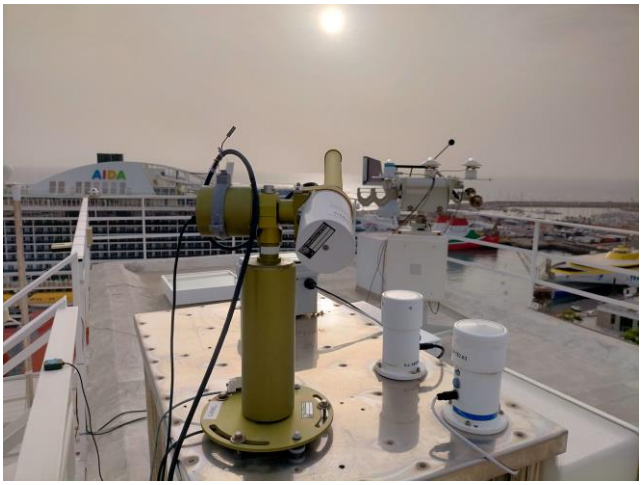

Figure 3.11. Image of SCO instrument terrace.

3.2.1 The Ozonesonde Laboratory

Science Pump Corporation (SPC) Electrochemical Concentration Cell (ECC) ozone sensors (model ECC-6A) are used in the IARC Ozonesonde Programme. Ozonesonde conditioning and pre-flight preparation is performed at the Ozonesonde Laboratory at SCO.

A SPC TSC-1 Ozonizer/Test Unit was used for ozonesonde preparation since 1992. The ozonizer was changed for a new instrument (EN-SCI KTU3) in the beginning of 2022. This unit has been designed for conditioning of ECC ozonesondes with ozone, and for checking the performance of the sondes prior to balloon release. The new KTU3 allows to measure the ECC cell current, down to 0.001 µA, and uses synthetic air (ozone free air) and a UV lamp to produce high concentrations of ozone. The sensing solution used in the ECC sonde is prepared inside a hood in which ambient air is passed through an active charcoal filter to purify the air.

The volumetric flow of the gas sampling pump of each ECC sonde is individually measured at the Ozonesonde Lab before flight. The pump flow rate of the sonde is measured with a bubble flow meter at the gas outlet of the sensing cell and is corrected for temperature and humidity. On the day of release, the ECC-6A ozonesonde is checked for proper operation, filled with the sensing solution and the background current measured. The ECC sonde is transported to the Botanic Observatory ozonesonde launching station (30 km distance) where pre-launch tests are performed.

Table 3.4. Santa Cruz Observatory (SCO) measurement programme.

Parameter	Start date	Present Instrument	Data Frequency
In-situ Reactive Gases			
O_3	Nov 2004	UV Photometry TECO 49-C	1′
CO	Mar 2006	Non-dispersive IR abs. Thermo 48C-TL	1′
SO_2	Mar 2006	UV fluorescence Thermo 43C-TL	1′
NO-NO_2-NO_x	Mar 2006 - Oct 2019	Chemiluminescence Thermo 42C-TL	1′
O_3, NO_2, CO, $PM_{2.5}$, PM_{10}	Mar 2017 - Sept 2021	Vaisala Air Quality Sensor AQT420	1′
Ozone and UV (managed by the AEMET's Special Networks Service at the nearby Met Center)			
Column O_3	Oct 2000	Brewer Mark-II#033	> ~20/day
Spectral UV	Oct 2000	Brewer Mark-II#033	~30′
SO_2	Oct 2000	Brewer Mark-II#033	~30′
Column aerosols			
AOD and Angstrom at 340, 380, 440, 500, 675, 870, 936, 1020 nm	Jul 2004	CIMEL CE318 sun photometer	~ 15′
Fine/Coarse AOD	Jul 2004	CIMEL CE318 sun photometer	~ 15′
Vertical Backscatter-extinction @523 nm, clouds alt. and thickness	Nov 2005- May 2018	Micro Pulse Lidar MPL-3, SES Inc., USA (co-managed with INTA (www.inta.es))	1′
Vertical Backscatter-extinction @532 nm, clouds alt. and thickness (with depolarizarion)	May 2018	Micro Pulse Lidar MPL-4B, provided by NASA Goddard Space Flight Center MPLNET	1′
Vertical backscatter-extinction, AOD profiles @910 nm and clouds altitude	Jan 2011-May 2015 Jun 2015	Vaisala CL-51 Ceilometer Vaisala CL-51 Ceilometer	16" 36"
First Aerosol Layer and Mixing Layer Height	Aug 2016	Vaisala CL-51 Ceilometer	60'
Radiation			
Global Radiation	Feb 2006	Pyranometer CM-11 Kipp & Zonen	1′
Direct Radiation	Feb 2006	Pyrheliometer EPPLEY	1′
Diffuse Radiation	Feb 2006	Pyranometer CM-11 Kipp & Zonen	1′
UV-B Radiation	Aug 2011	Yankee YES UVB-1 Pyranom. (managed by the AEMET's Special Networks Service at the nearby Met Centre)	1′
Global and Diffuse Radiation	Jun 2021	SPN1 Sunshine Pyranometer	1′

Parameter	Start date	Present Instrument	Data Frequency
Water Vapour			
PWV Total Column and Profiles for 13 layers from sea level up to ~12 km of altitude	Dec 1963	Vaisala RS41 launched at Güimar automatic radiosonde station (WMO GRUAN station #60018) (managed by the Meteorological Centre of Santa Cruz de Tenerife)	Daily at 00 and 12 UTC
Precipitable Water Vapour (PWV)	Mar 2003	CIMEL CE318 sun photometer	~ 15′
PWV	July 2008	GPS/GLONASS LEICA GR50 satellite ground-based receiver	15′ (ultra-rapid orbits)
PWV (total column) over SCO when cloudless skies. Cloud base heights when cloudy skies over SCO	Jun 2014	1 SIELTEC Sky Temperature Sensor (infrared thermometer prototype)	Every 30″ during the complete day
Water vapour isotopologues (δD and δ18O)	May 2019	Picarro L2120-I δD and δ18O Analyser	Continuous (2″)
Meteorology*			
Vertical profiles of T, RH, P, wind direction and speed, from sea level to ~30 km altitude	Dec 1963	RS41+GPS radiosondes launched at Güimar automatic radiosonde station (WMO GRUAN station #60018) (managed by the Meteorological Centre of Santa Cruz de Tenerife)	Daily at 00 and 12 UTC
Temperature	Jan 2002	VAISALA HMP45C	1′
Relative humidity	Jan 2002	VAISALA HMP45C	1′
Wind Direction and speed	Jan 2002	RM YOUNG wind sentry 03002	1′
Pressure	Jan 2002	VAISALA PTB100A	1′
Rainfall	Jan 2002	THIES CLIMA Tipping Bucket	1′
Aerobiology			
Pollens and spores	Oct 2004	Hirst, 7-day recorder VPPS 2000 spore trap (Lanzoni S.r.l.).	Continuous (1 h resolution)

* Meteorological data from Santa Cruz de Tenerife Meteorological Center headquarters, 1 km distant, are also available since 1922.

3.3 Botanic Observatory

The Botanic Observatory (BTO) is located 13 km north of IZO at 114 m a.s.l. in the Botanical Garden of Puerto de la Cruz (Fig. 3.12). BTO is hosted by the Canary Institute of Agricultural Research (ICIA). The Botanic Observatory includes the following facilities:

- Ozone Sounding Monitoring Laboratory: equipped with a Digicora MW41 receiver with Vaisala data acquisition and processing software.
- Launch container: equipped with a Helium supply system used for ozonesonde balloons filling.

In addition to the ozonesonde measurements, there is a fully equipped automatic weather station (temperature, relative humidity, pressure, precipitation, wind speed and direction) and a global irradiance pyranometer. For details of the BTO measurement programme, see Table 3.5.

Figure 3.12. Image of Botanic Observatory (BTO).

Table 3.5. Botanic Observatory (BTO) measurement programme.

Parameter	Start date	Present Instrument	Data Frequency
Reactive Gases and ozonesondes			
Vertical profiles of O_3, pressure, temperature, humidity, wind direction and speed, from sea level to ~33 km altitude	Nov 1992	ECC-A6+RS41/GPS radiosondes	1/week (Wednesdays)
Radiation			
Global Radiation	May 2011	Pyranometer CM-11 Kipp & Zonen	1′
Column Water Vapour			
Precipitable Water Vapour	July 2008	GPS/GLONASS TRIMBLE NETR9 satellite ground-based receiver	15′ (ultra-rapid orbits)
Meteorology			
Temperature	Oct 2010	VAISALA F1730001	1′
Relative humidity	Oct 2010	VAISALA F1730001	1′
Wind direction and speed	Oct 2010	VAISALA WMT702	1′
Pressure	Oct 2010	VAISALA PMT16A	1′
Rainfall	Oct 2010	VAISALA F21301	1′

3.4 Teide Peak Observatory

The Teide Peak Observatory (TPO) is located at 3555 m a.s.l. at the Teide Cable Car terminal in the Teide National Park (Fig. 3.13). TPO was established as a satellite station of IZO primarily for radiation and aerosol observations at very high altitude. TPO station, together with Jungfraujoch (3454 m a.s.l.) in Switzerland, are the highest permanent radiation observatories in Europe.

This measurement site provides radiation and aerosol information under extremely pristine conditions and in conjunction with measurements at SCO and IZO allows us to study the variation of global radiation, UV-B and Aerosol Optical Depth (AOD) from sea level to 3555 m a.s.l. In addition to radiation and aerosol measurements, there is a meteorological station and a water vapour isotopologues analyser. Full details of the measurement programme are given in Table 3.6.

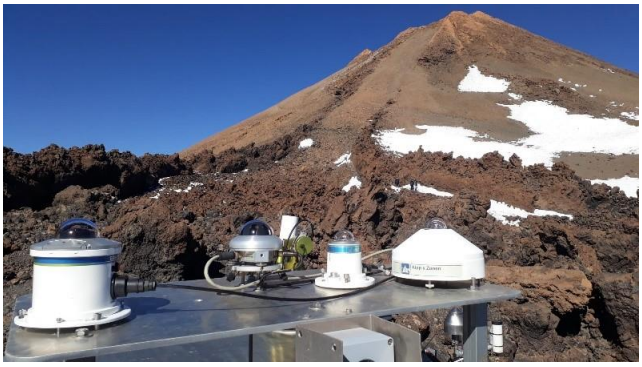

Figure 3.13. Measurements at Teide Peak Observatory.

Table 3.6. Teide Peak Observatory (TPO) measurement programme.

Parameter	Start date	Present Instrument	Data Frequency
Column aerosols			
AOD and Angstrom at 340, 380, 440, 500, 675, 870, 936 and 1020 nm	Jun 1997	CIMEL CE318 sun photometer (Co-managed with the University of Valladolid Atmospheric Optics Group)	~ 15′ (during Apr-Oct)
Fine/Coarse AOD Fine mode fraction	Jun 1997	CIMEL CE318 sun photometer (Co-managed with the University of Valladolid Atmospheric Optics Group)	~ 15′ (during Apr-Oct)
Radiation			
Global Radiation	Jul 2012	Pyranometer CM-11 Kipp & Zonen	1′
UVB Radiation	Jul 2012	Pyranometer Yankee YES UVB-1	1′
Global and diffuse radiation	Sep 2019	SPN1 Sunshine Pyranometer	1′
Water vapour			
Water vapour isotopologues (δD and $\delta^{18}O$)	June 2013	Picarro L2120-I δD and $\delta^{18}O$ analyser	2″
Precipitable Water Vapour	Feb 2020	GPS/GLONASS TRIMBLE NETR9 satellite ground-based receiver	15′ (ultra-rapid orbits)
Meteorology			
Wind direction and speed	Oct 2011	THIES CLIMA Sonic 2D	1′
Temperature	Aug 2012	VAISALA HMP45C	1′
Relative humidity	Aug 2012	VAISALA HMP45C	1′
Pressure	Aug 2012	VAISALA PTB100A	1′

3.5 Computing Facilities and Communications

The computing facilities and communications form an integral component of all measurement programmes and activities in the Izaña Atmospheric Research Center. In the IARC headquarters there is a temperature-controlled room hosting server computers devoted to different automatic and continuous tasks (Network-Attached Storage (NAS), modelling, spectra inversion, etc.) for the research groups. Details of the computing facilities are given in Table 3.7.

Table 3.7. IARC computing facilities.

Computing Hardware				
	Storage	**Virtualization**	**Modelling**	**Total**
H.D.	34 TB	12 TB	10 TB	56 TB
Cores	7	28	68	105
RAM	12 GB	56 GB	46 GB	114 GB

A EUMETCast (European Organisation for the Exploitation of Meteorological Satellites (EUMETSAT) Broadcast System for Environmental Data) reception station is available at SCO. It consists of a multi-service dissemination system based on standard Digital Video Broadcast (DVB) technology. Most of the satellite information is received via this system (see Section 13 for more details).

Data communications were notably improved at the IARC in 2020 by its incorporation into the Advanced Communications Network for Spanish Research (IRIS NOVA network).

RedIRIS-NOVA is the high-capacity optical network of RedIRIS, which connects the regional networks of all the autonomous regions and the main research centers in Spain with the rest of international academic networks, especially the Portuguese academic and research networks and the European research network GÉANT. Fibre optics makes it possible to easily deploy 10Gbps or 40Gbps circuits, and soon 100Gbps, at a much lower cost than the network model based on capacity rental. RedIRIS-NOVA connects more than 50 Points of Presence with each other, making up a mesh network on which the RedIRIS IP Trunk Network and the regional networks are deployed. This network for research allows collaboration between researchers and the deployment of next-generation services.

IARC is the only AEMET unit that has IRIS NOVA Network communications due to its status as a research center.

IARC currently has two data networks, the AEMET network, with access from the central headquarters in Santa Cruz, and linked to the Izaña Observatory by a microwave link (Fig. 3.14), and the IRIS NOVA Network with a double entry. The IARC offices in Santa Cruz are linked to the IRIS NOVA network through a fibre optic connection to the IGN node located in the same building, and to the Izaña Observatory through a fibre optic connection, approximately 1 km long, with the IRIS NOVA node at the Teide Observatory of the Instituto de Astrofísica de Canarias (IAC) (Institute of Astrophysics of the Canary Islands).

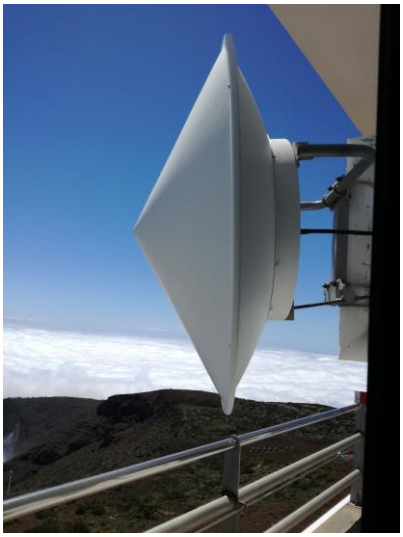

Figure 3.14. Microwave link antenna between Santa Cruz (SCO) and the Izaña Observatory (IZO) of the AEMET data network.

3.6 Staff

Activities universal to all measurement programmes such as operation and maintenance of IARC facilities, equipment, instrumentation, communications and computing facilities are made by the following staff:

Ramón Ramos (AEMET; Head of Scientific instrumentation and infrastructures)

Enrique Reyes (AEMET; IT development specialist)

Néstor Castro (AEMET; IT specialist)

Antonio Cruz (AEMET; IT specialist)

Rocío López (AEMET; IT specialist)

Concepción Bayo (AEMET; Meteorological Observer-GAW Technician)

Virgilio Carreño (AEMET; Meteorological Observer-GAW Technician)

Cándida Hernández (AEMET; Meteorological Observer-GAW Technician)

Antonio Alcántara (AEMET; Meteorological Observer-GAW Technician)

4 Greenhouse Gases and Carbon Cycle

4.1 Main Scientific Goals

The Greenhouse Gases and Carbon Cycle programme conducted by IARC supports two independent in-situ greenhouse gases (GHG) measurement stations, the GAW station and the ICOS station. The new ICOS station has been in development during the years 2021-2022 (see Section 20 for more details). The main goal of the GAW station is to carry out highly accurate continuous in-situ measurements of long-lived GHG in the atmosphere at IZO in order to contribute to the WMO/GAW programme, following the GAW recommendations and guidelines. Additional goals are: 1) to study with precision the long-term evolution of the GHGs in the atmosphere, as well as their daily, seasonal and inter-annual variability; 2) To incorporate continuously technical instrumental improvements and new data evaluation and calibration methodologies in order to reduce uncertainty and improve the accuracy of the GHG measurements; 3) to carry out research to study the processes that control the variability and long-term changes of the GHGs in the atmosphere; and 4) to contribute to international research and its documentation via recommendations and guidelines.

In addition, there has been a growing demand to provide reliable near-real-time GHG data for data assimilation by atmospheric models, to exchange data with the remote sensing community, and to inform policy makers since GHG information is now an object of great social interest and great media impact. Such data exchange requires an enormous effort and represents a technical challenge as it calls for a combination of the classic evaluation of very precise background data (a task that can take at least 6 months) with the delivery of data of an acceptable quality and minimally validated within hours or minutes of being obtained. As an example, IARC agreed with the Canary Islands Government to provide data from Izaña as a new station in the Canary Islands Air Quality Control and Surveillance Network. Among many other data, near-real-time measurements of CO taken with GHG analyzers are provided.

4.2 Measurement Programme

Table 4.1 gives details of the in-situ analysers (owned by AEMET) at IZO used for measuring atmospheric greenhouse gases for the GAW programme, and some details about the measurement schemes. Details of the in-situ measurement systems and data processing can be found in Gomez-Pelaez et al. (2012, 2013, 2014, 2016 and 2019). Additional information can be found in the last IZO GHG GAW scientific audit reports: Scheel (2009), Zellweger et al. (2009, 2015 and 2020).

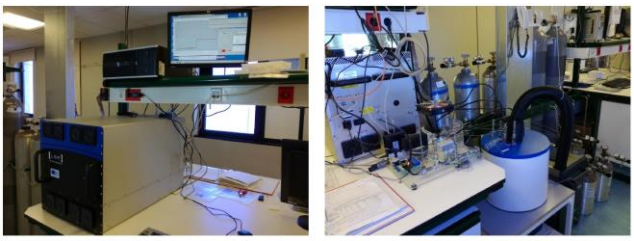

Figure 4.1. Front and rear view of the Los Gatos Research (LGR) CO/N_2O analyser at Izaña Observatory.

Additionally, weekly discrete flask samples have been collected at IZO for the National Oceanic and Atmospheric Administration-Earth System Research Laboratory-Global Monitoring Laboratory Carbon Cycle Greenhouse Gases Group (NOAA-ESRL-GML CCGG) Cooperative Air Sampling Network (since 1991). Weekly discrete flask samples are collected at IZO and subsequently shipped to NOAA-ESRL-GML.

Figure 4.2. IZO Gas Chromatograph measurement system for N_2O and SF_6.

The air inside the flasks has been measured for the following gas species mole fractions: 1) CO_2, CH_4, CO, and H_2 since 1991; N_2O and SF_6 since 1997 (NOAA/ESRL/GML CCGG); 2) Isotopic ratios Carbon-13/Carbon-12 and Oxygen-18/Oxygen-16 in carbon dioxide since 1991 (INSTAAR Stable Isotope Lab); 3) Methyl chloride, benzene, toluene, ethane, ethene, propane, propene, i-butane, n-butane, i-pentane, n-pentane, n-hexane and isoprene were measured from 2006 to 2018 (INSTAAR).

Two-week integrated samples of atmospheric carbon dioxide have also been collected for Heidelberg University (Institute of Environmental Physics, Carbon Cycle Group) since 1984 to measure the radiocarbon (^{14}C) isotopic ratio in carbon dioxide. These data are part of a cooperative CO_2 background air sampling network for high-precision ^{14}C analysis in the Heidelberg Radiocarbon laboratory, and are utilized to study global and hemispheric trends of $\Delta^{14}C$-CO_2 which provide constraints for ^{14}C-free fossil CO_2 emission changes on both global and regional scales (Levin et al., 2022). The data have also been utilized in various carbon cycle modelling activities (e.g. Graven et al., 2017).

Table 4.1. Atmospheric greenhouse gases measured in situ at IZO and measurement methods and analysers used.

Gases	Start Date	Method	Model	Ambient air measurement period	Reference gas/es calibration frequency	Status
CO_2	1984	NDIR	Siemens Ultramat 3	10 s	Biweekly using 4 S	Retired
CO_2	2007	NDIR	Licor 6252	1 s	Biweekly using 4 S	Retired
CO_2	2008	NDIR	Licor 7000	1 s	Biweekly using 4 S	Active
CH_4	1984	GC-FID	Dani 3800	30 min	Biweekly using 2 S	Retired
CH_4	2007	GC-FID	Varian 3800	15 min	Biweekly using 2 S	Retired
N_2O, SF_6	2007	GC-ECD	Varian 3800	15 min	Biweekly using 5 S	Retired
CO	2008	GC-RGD	Trace Analytical RGA-3	20 min	Biweekly using 5 S	Retired
CO_2, CH_4, CO	2015	CRDS	Picarro G2401	2 s	Monthly using 4 S	Active
N_2O, CO	2018	LGR	LGR N2OCM-913	4 s	Monthly using 4 S	Active
N_2O, SF_6	2021	GC-ECD	Agilent 8890	15 min	Monthly using 4 S	Active

Nondispersive Infrared sensor (NDIR), Laboratory Standard (S), Gas Chromatography (GC), Flame Ionization Detector (FID), Electron Capture Detector (ECD), Reduction Gas Analyser (RGD), Cavity Ring-Down Spectroscopy (CRDS), Los Gatos Research (LGR)

4.3 Summary of remarkable activities during the period 2021-2022

This programme has continued performing continuous high-quality greenhouse gas measurements and annually submitting the data to the WMO GAW World Data Centre for Greenhouse Gases (WDCGG), where data are publicly available, as well as included in the data summaries (e.g., WDCGG, 2022). The WMO GAW CO_2 calibration scale (WMO-CO_2-X2007) has been revised and updated to WMO-CO_2-X2019 (Hall et al., 2021). All the IZO CO_2 data since 2007 have been reprocessed to adapt them to the new scale.

The complete CO_2 time series is shown in Fig. 4.3. The average growth rate of CO_2 throughout the period (1985-2022) is approximately 1.9 ppm/yr. However, the increase in CO_2 is accelerating, and in the period 2015-2022 it is about 2.5 ppm/yr, significantly higher than the value of 1.3 ppm/yr which was recorded at the beginning of the CO_2 measurements at IZO in the period 1985-1993 (see Section 4.3.1 for more details).

The Varian 3800 gas chromatograph (GC) was retired in July 2021 and replaced by an Agilent 8890 GC. The new system is based on the GC-ECD three-column method described in Hall et al. (2011), capable of improving the SF_6 measurement precision while maintaining the N_2O measurement performance.

The CH_4, N_2O, SF_6 and CO time series at IZO are shown in Fig. 4.4. All the collected data are used for analysis and investigation of the carbon cycle and understanding of the role of anthropogenic and natural factors that control GHG variability. The curve fitting methods applied to the IZO time series are those used by NOAA/ESRL/GML (Thoning et al., 1989).

IARC has also continued contributing to the data products GLOBALVIEW and OBSPACK led by NOAA-ESRL-GML CCGG (e.g., Schuldt et al., 2022; 2023). ICOS ERIC has developed a similar product, the European atmospheric CO_2 and CH_4 Mole Fraction data product (Apadula et al., 2022). IARC has contributed as well to this data compilation by providing its long-term CO_2 and CH_4 data series.

IARC-AEMET participated in the 7th WMO/IAEA Round Robin Comparison Experiment, whose primary goal is to assess the level to which participating laboratories maintain their link to the WMO mole fraction scales using normal operating procedures. The test consisted of measuring the CO_2, CH_4, CO, N_2O and SF_6 mole fractions of two cylinders with compressed air using the GHG analyzers installed in IZO. The results of the experiment are not yet published.

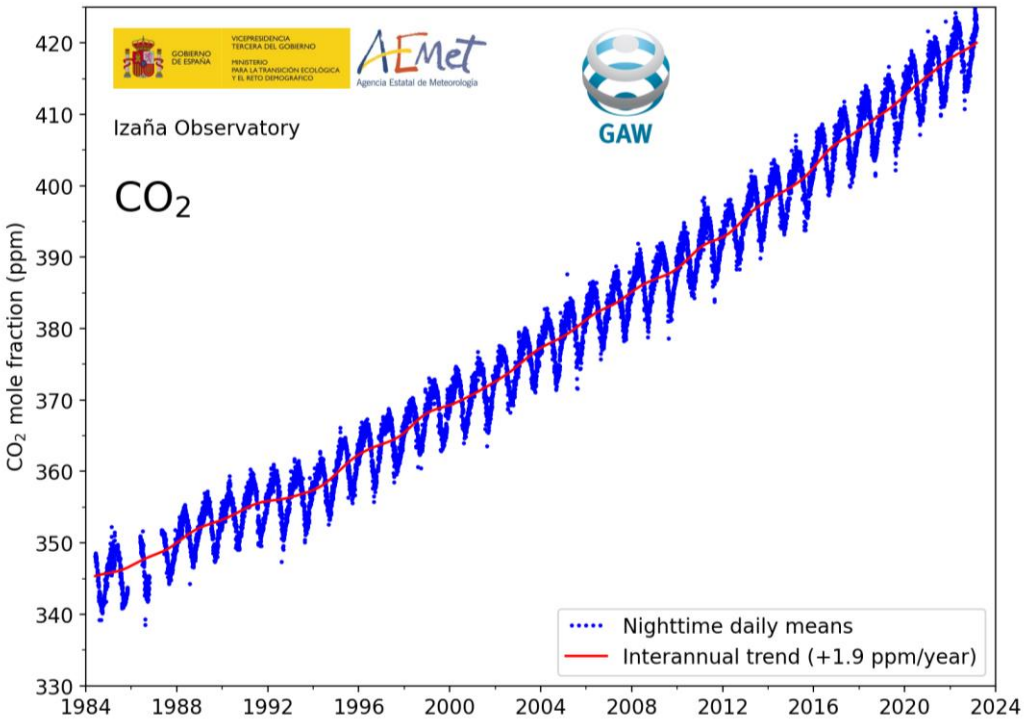

Figure 4.3. Izaña Observatory CO_2 time series (1984-2022).

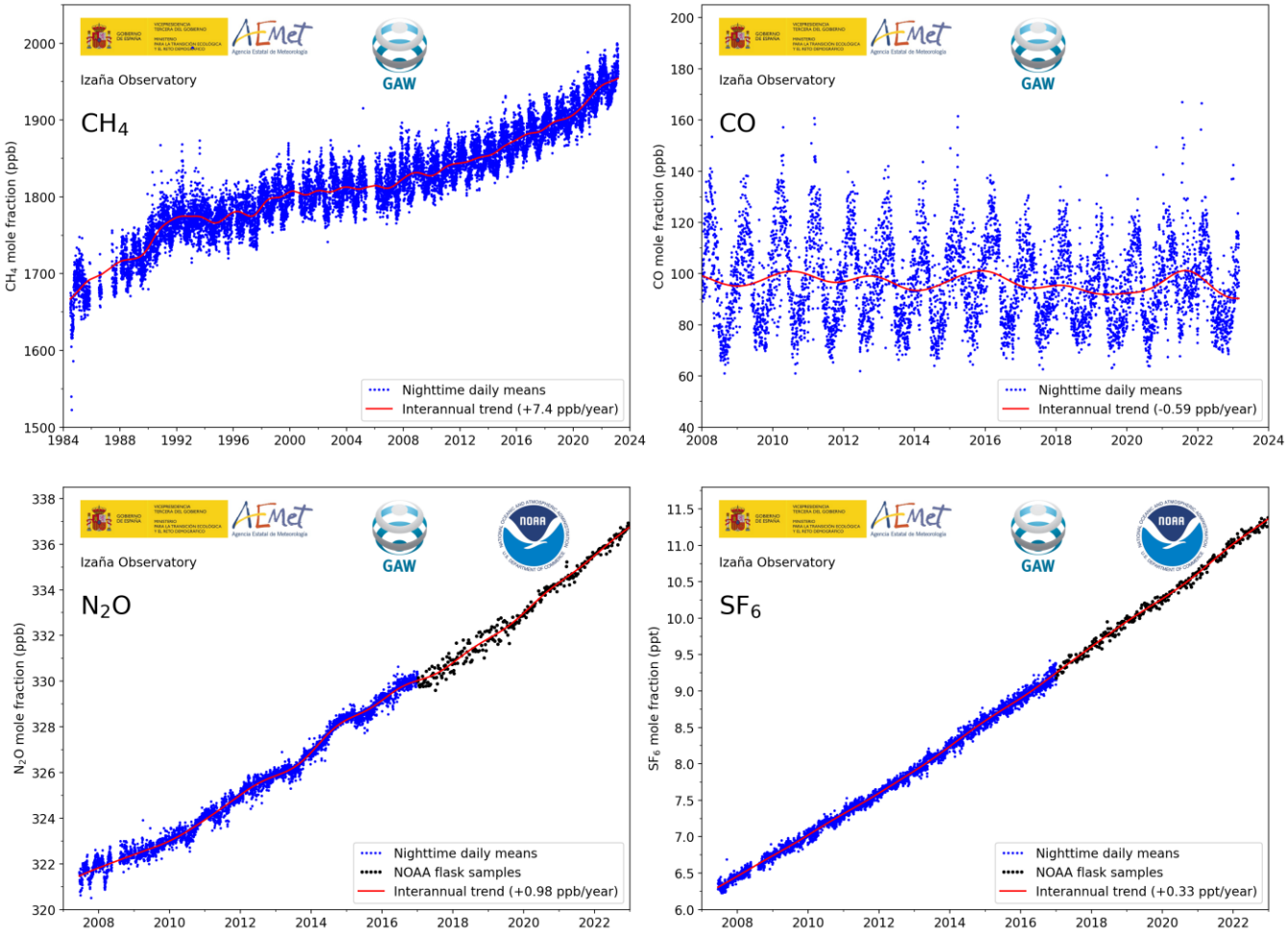

Figure 4.4. CH_4, CO, N_2O and SF_6 IZO time series. N_2O and SF_6 measurements by IZO analysers from the year 2017 onwards are temporarily unavailable due to technical problems and system updates. Data from 2017 to 2022 in these figures come from the NOAA Cooperative Air Sampling Network and are shown as black points.

As part of the implementation of the new ICOS station, two new gas analyzers were purchased and put into operation, a Picarro G2401 and a LGR 907-0015 (see Section 20 for more details).

The Greenhouse Gases group contributed to activities carried out by IARC-AEMET during the 2021 La Palma volcanic eruption. Personnel from the group aided the emergency deployment in La Palma and measurements in Tenerife at Izaña Observatory recorded the direct impact of the volcanic eruption, causing the concentrations of gases such as CO_2 and CO to exceed, by several orders of magnitude, the values of these gases under usual background conditions at IZO (see Section 23.7.2 for more details).

4.3.1 Comparison with Mauna Loa Observatory data series

The CO_2 long-term data series from IZO can be compared with the NOAA Mauna Loa Observatory (MLO) (Hawaii, USA) measurements (Figure 4.5). Both observatories are one of 31 GAW Global stations (see Fig. 2.1), and are part of a small group of high mountain stations that are representative of background free troposphere conditions, and specifically of the subtropical region.

When the average monthly CO_2 mole fractions of both stations, separated from each other by more than 13,000 km, are compared, the datasets largely overlap (Figure 4.5). This is a consequence of both stations measuring very clean air masses, normally coming from the middle layers of the troposphere, and the fact that CO_2 has a very long life-time, which allows it to mix well throughout the atmosphere.

The monthly series of IZO and MLO both demonstrate the CO_2 seasonal variations driven by the respiration cycle of the vegetation in the northern hemisphere; the annual CO_2 maximum occurs in spring, between end of April and beginning of May.

The amplitude of the seasonal CO_2 cycle slightly differs between the observatories, as shown in the zoomed-in detail of Fig. 4.5. The IZO measurements show a slightly greater seasonal amplitude than MLO ones due to its location about 8° latitude further north; it is known that CO_2 concentration has a latitudinal gradient. Despite the seasonal cycle at both stations being slightly different, the deseasonalized data series overlap as shown in Figure 4.5.

Table 4.2 shows the mean annual increases in CO_2 evaluated for different periods at IZO and MLO. Measurements at both stations demonstrate how the mean annual increase of CO_2 in the atmosphere is accelerating. In the 1980s the average annual increase in the background mole fraction of CO_2 was approximately 1.3 ppm/year, in the 2015-2022 period it is about 2.5 ppm/year (Table 4.2).

Table 4.2. Mean annual increase in background CO_2 mole fraction (ppm/year) in IZO and MLO for different time periods.

Period studied	IZO (ppm/yr)	MLO (ppm/yr)
1985-1993	1.28 ± 0.02	1.37 ± 0.02
1994-2003	2.00 ± 0.02	1.90 ± 0.01
2004-2014	2.05 ± 0.02	2.07 ± 0.01
2015-2022	2.47 ± 0.02	2.49 ± 0.02

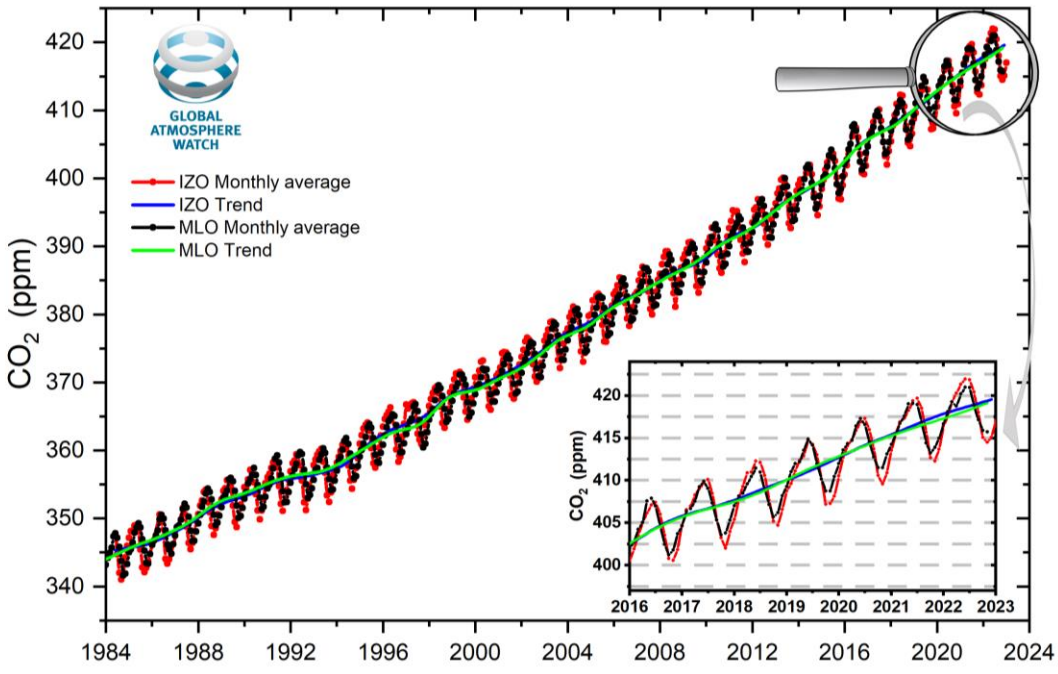

Figure 4.5. Mean monthly CO_2 mole fraction (ppm) measured at Izaña (red) and Mauna Loa (black) Observatories under background conditions and seasonally fitted data (blue and green, respectively) for each station. In the zoomed image it can be seen how the seasonal cycle of IZO has a slightly greater amplitude and a slight lag with respect to that of MLO.

4.4 References

Apadula, F., Arnold, S., Bergamaschi, P., Biermann, T., Blanc, P.-E., Brunner, D., Chen, H., Chmura, L., Colomb, A., Conil, S., Couret, C., Cristofanelli, P., De Mazière, M., Delmotte, M., Emmenegger, L., Forster, G., Frumau, A., Gerbig, C., Gheusi, F., ICOS ERIC. (2022). European atmospheric CO_2 and CH_4 Mole Fraction data product - 2022 (Version 1.0). ICOS ERIC -- Carbon Portal. https://doi.org/10.18160/1RE0-2GKH

Gomez-Pelaez, A.J., R. Ramos, V. Gomez-Trueba, R. Campo-Hernandez, E. Dlugokencky, T. Conway "New improvements in the Izaña (Tenerife, Spain) global GAW station in-situ greenhouse gases measurement program" in GAW report (No. 206) of the "16th WMO/IAEA Meeting on Carbon Dioxide, Other Greenhouse Gases, and Related Measurement Techniques (GGMT-2011) (Wellington, New Zealand, 25-28 October 2011)", edited by Gordon Brailsford, World Meteorological Organization, 76-81, 2012.

Gomez-Pelaez, A. J., Ramos, R., Gomez-Trueba, V., Novelli, P. C., and Campo-Hernandez, R.: A statistical approach to quantify uncertainty in carbon monoxide measurements at the Izaña global GAW station: 2008–2011, Atmos. Meas. Tech., 6, 787-799, doi:10.5194/amt-6-787-2013, 2013.

Gomez-Pelaez, A.J., R. Ramos, V. Gomez-Trueba, R. Campo-Hernandez, E. Reyes-Sanchez: "Izaña Global GAW station greenhouse-gas measurement programme. Novelties and developments during October 2011-May 2013" in GAW report (No. 213) of the "17th WMO/IAEA Meeting on Carbon Dioxide, Other Greenhouse Gases, and Related Measurement Techniques (Beijing, China, June 10-14, 2013)", edited by P. Tans and C. Zellweger, World Meteorological Organization, 77-82, 2014.

Gomez-Pelaez, A.J., R. Ramos, V. Gomez-Trueba, R. Campo-Hernandez, E. Reyes-Sanchez: "GGMT-2015 Izaña station update: instrumental and processing software developments, scale updates, aircraft campaign, and plumbing design for CRDS" in GAW report (No. 229) of the "18th WMO/IAEA Meeting on Carbon Dioxide, Other Greenhouse Gases, and Related Measurement Techniques (GGMT) (La Jolla, CA, USA, 13-17 September, 2015)", edited by P. Tans and C. Zellweger, World Meteorological Organization, 125-131, 2016.

Gomez-Pelaez, A. J., Ramos, R., Cuevas, E., Gomez-Trueba, V., and Reyes, E.: Atmospheric CO_2, CH_4, and CO with the CRDS technique at the Izaña Global GAW station: instrumental tests, developments, and first measurement results, Atmos. Meas. Tech., 12, 2043–2066, https://doi.org/10.5194/amt-12-2043-2019, 2019.

Graven, H., Allison, C. E., Etheridge, D. M., Hammer, S., Keeling, R. F., Levin, I., Meijer, H. A. J., Rubino, M., Tans, P. P., Trudinger, C. M., Vaughn, B. H., and White, J. W. C.: Compiled records of carbon isotopes in atmospheric CO_2 for historical simulations in CMIP6, Geosci. Model Dev., 10, 4405–4417, https://doi.org/10.5194/gmd-10-4405-2017, 2017

Hall, B. D., Crotwell, A. M., Kitzis, D. R., Mefford, T., Miller, B. R., Schibig, M. F., and Tans, P. P.: Revision of the World Meteorological Organization Global Atmosphere Watch (WMO/GAW) CO_2 calibration scale, Atmos. Meas. Tech., 14, 3015–3032, https://doi.org/10.5194/amt-14-3015-2021, 2021.

Hall, B. D., Dutton, G. S., Mondeel, D. J., Nance, J. D., Rigby, M., Butler, J. H., Moore, F. L., Hurst, D. F., & Elkins, J. W. (2011). Improving measurements of SF6 for the study of atmospheric transport and emissions. Atmospheric Measurement Techniques, 4(11), 2441-2451. https://doi.org/10.5194/amt-4-2441-2011

Levin, I., Hammer, S., Kromer, B., Preunkert, S., Weller, R., & Worthy, D. (2022). Radiocarbon in Global Tropospheric Carbon Dioxide. Radiocarbon, 64(4), 781-791. doi:10.1017/RDC.2021.102

Scheel, H.E. (2009), System and Performance Audit for Nitrous Oxide at the Global GAW Station Izaña, Tenerife, Spain, November 2008, WCC-N2O Report 2008/11, http://www.aemet.izana.org/publications/Rep_WCCN2O_2008_IZOAudit.pdf

Schuldt, K. N., John Mund, Ingrid T. Luijkx, Tuula Aalto, James B. Abshire, Ken Aikin, Arlyn Andrews, Shuji Aoki, Francesco Apadula, Bianca Baier, Peter Bakwin, Jakub Bartyzel, Gilles Bentz, Peter Bergamaschi, Andreas Beyersdorf, Tobias Biermann, Sebastien C. Biraud, Harald Boenisch, David Bowling; et al., Multi-laboratory compilation of atmospheric carbon dioxide data for the period 1957-2021; obspack_co2_1_GLOBALVIEWplus_v8.0_2022-08-27; NOAA Earth System Research Laboratory, Global Monitoring Laboratory. http://doi.org/10.25925/20220808, 2022.

Schuldt, K. N., Tuula Aalto, Arlyn Andrews, Shuji Aoki, Francesco Apadula, Jgor Arduini, Bianca Baier, Jakub Bartyzel, Peter Bergamaschi, Tobias Biermann, Sebastien C. Biraud, Harald Boenisch, Gordon Brailsford, Willi A. Brand, Huilin Chen, Aurelie Colomb, Sébastien Conil, Cedric Couret, Paolo Cristofanelli,...Carina van der Veen; Multi-laboratory compilation of atmospheric methane data for the period 1983-2021; obspack_ch4_1_GLOBALVIEWplus_v5.1_2023-03-08; NOAA Earth System Research Laboratory, Global Monitoring Laboratory. http://doi.org/10.25925/20230308, 2023.

Thoning, K.W., P.P. Tans, and W.D. Komhyr; Atmospheric carbon dioxide at Mauna Loa Observatory, 2. Analysis of the NOAA/GMCC data, 1974 1985. J. Geophys. Res. ,94, 8549 8565, 1989.

Zellweger, C., J. Klausen, B. Buchmann, H.-E. Scheel (2009), System and Performance Audit of Surface Ozone, Carbon Monoxide, Methane and Nitrous Oxide at the Global GAW Station Izaña, Spain, March 2009, WCC-Empa Report 09/1, https://www.empa.ch/documents/56101/250799/Izana09.pdf/8dd7d439-c6cb-4122-bcea-bc3fcda5a367

Zellweger, C., M. Steinbacher, B. Buchmann, R. Steinbrecher (2015), System and Performance Audit of Surface Ozone, Methane, Carbon Dioxide, Nitrous Oxide and Carbon Monoxide at the Global GAW Station Izaña, September 2013. WCC-Empa Report 13/2, https://www.empa.ch/documents/56101/250799/Izana13.pdf/da8bbb9f-8623-404e-bdab-6949d6e16282

Zellweger, C., M. Steinbacher, B. Buchmann, R. Steinbrecher (2020), System and Performance Audit of Surface Ozone, Carbon Monoxide, Methane, Carbon Dioxide and Nitrous Oxide at the Global GAW Station Izaña, Spain, May 2019. WCC-Empa Report No. 19/2, https://www.empa.ch/documents/56101/250799/Izana+2019/ac2d85ce-12d1-4c30-a53d-b4d7f70ed913

World Data Centre for Greenhouse Gases (WDCGG), WMO WDCGG Data Summary, GAW Data (Volume IV-Greenhouse and Related Gases), WDCGG No. 46, Japan Meteorological Agency in Co-operation with World Meteorological Organization, 2022.

4.5 Staff

Pedro Pablo Rivas Soriano (AEMET; Head of programme)

Ramón Ramos (AEMET; Head of Infrastructure and instrumentation)

Enrique Reyes (AEMET; Software and data processing)

Antonio Ángel Serrano De La Torre (AEMET; Software and data processing)

Dr Sergio León-Luís (TRAGSATEC; ICOS)

Dr Rosa García (TRAGSATEC/UVA)

Jaime Hernández-Estévez (Air Liquide)

Tomás José Martín Afonso (Air Liquide)

5 Reactive Gases and Ozonesondes

5.1 Main Scientific Goals

The main scientific objectives of this programme are:

- Long-term high-quality observations and analysis of tropospheric O_3 in both the free troposphere (FT) and the Marine Boundary Layer (MBL).
- Long-term high-quality observations of reactive gases (CO, NO_x, SO_2) in the FT and in the MBL to support other measurement programmes at IARC.
- Air quality studies in urban and background conditions.
- Analysis of long-range transport of pollution (e.g. transport of anthropogenic and wildfire pollution from North America).
- Study of the impact of mineral dust and water vapour on tropospheric O_3.
- Characterization of the vertical profile of ozone in subtropical latitudes.
- Analysis and characterization of the Upper Troposphere-Lower Stratosphere (UTLS).
- Analysis of Stratosphere-Troposphere Exchange processes.

5.2 Measurement Programme

The measurement programme of reactive gases (O_3, CO, NO_x and SO_2) includes long-term observations at IZO (Fig. 5.1), SCO and BTO (see Tables 3.2, 3.4 and 3.5) and ozonesonde vertical profiles at Tenerife (now at BTO). In addition, IARC (through AEMET and INTA) has a long-term collaboration with the Argentinian Meteorological Service (SMN) and in the framework of this collaboration, ozone vertical profiles are measured at Ushuaia GAW Global station (Argentina). Surface O_3 measurements started in 1987, CO in 2004, and SO_2 and NO_x measurements were implemented since 2006 at IZO. At SCO, surface O_3 measurements started in 2001, and CO, SO_2 and NO_x programmes were also implemented since 2006.

Figure 5.1. Sample inlet for reactive gas measurements located on top of the Izaña Observatory technical tower in front of the Teide volcano.

Details of the reactive gases and ozonesondes measurement programme are described in González (2012) and Cuevas et al. (2013).

5.2.1 Reactive gases

The surface ozone measurement programme is developed within the framework of the WMO/GAW for the measurement of reactive gases, and its main objectives are high-quality monitoring of surface ozone, as well as other reactive gases, under background conditions in the free atmosphere at IZO, and the analysis of chemical and transport processes that impact O_3 levels. The almost uninterrupted 36-year time series of surface O_3 at IZO is shown in Fig. 5.2.

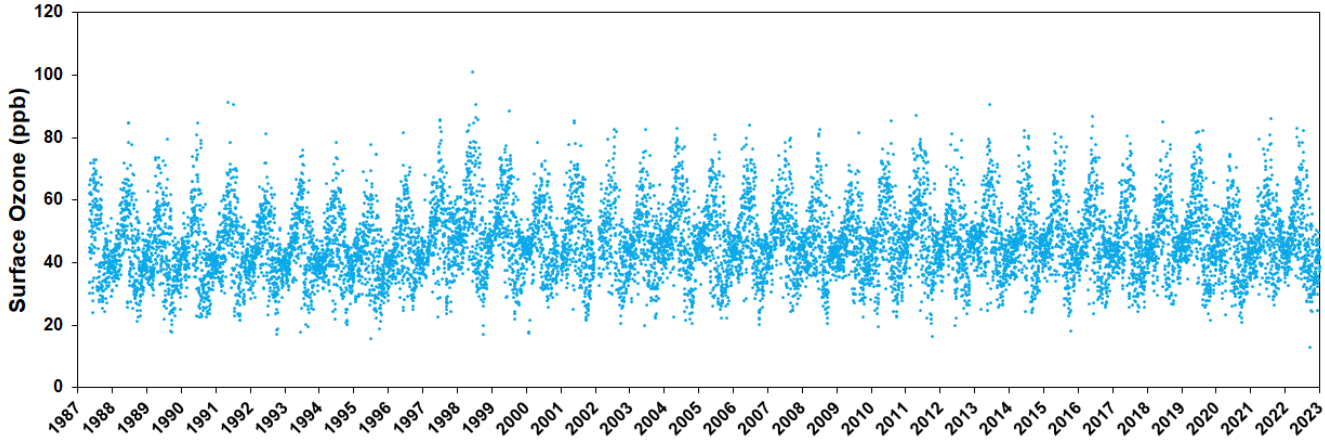

Figure 5.2. Long-term daily (night period) surface O_3 at IZO (1987-2022).

Surface ozone is measured with two ozone analyzers, main and auxiliary, which are measuring simultaneously. A third reserve analyzer is used in case any of the two operational analyzers have a problem. All analyzers determine the ozone mixing ratio by UV absorption; this is the recommended measurement technique for analyzers which are part of the GAW Programme (WMO, 2013). The main analyzer belongs to the new series of Thermo Scientific 49i analyzers, and the other two (auxiliary and reserve) belong to the old series of Thermo Scientific 49C analyzers. All analyzers are compared every three months with the IARC primary ozone standard (Thermo Scientific 49C-PS, since August 2008) (Figure 5.3), which has previously been calibrated against a reference instrument (SRP#15) from the World Calibration Centre for Surface Ozone, Carbon Monoxide, Methane and Carbon Dioxide (WMO/WCC-Empa) to check if there is any drift in the instruments. The error must be less than 1% to ensure that the analyzer has not changed and therefore maintains the WCC-Empa calibration.

Figure 5.3. Ozone analysers (TEI 49i and two TEI 49C in the rack) at Izaña Observatory: comparison of the analysers with primary ozone standard (TEI 49C-PS).

In addition, all analyzers and their installation are audited every 2-3 years by the WCC-Empa to check if the calibration has been maintained over time. This redundancy of equipment, together with the rigorous verification and calibration protocols, are necessary to maintain the quality and continuity of ozone measurements required by the GAW Programme.

The surface O_3 programme at IZO has been audited by the WCC-Empa in 1996, 1998, 2000, 2004, 2009, 2013 and 2019. The most recent audit took place in June 2023. All Empa's audit reports are available in the link: https://www.empa.ch/web/s503/wcc-empa.

During the May 2019 audit the three IZO analysers (TEI 49i #1153030026, TEI 49C #72491-371 and #62900-337) and the primary ozone standard (TEI 49C-PS #56085-306) were compared against the WCC-Empa travelling standard (TS) with traceability to a Standard Reference Photometer (SRP). Good agreement between the WCC-Empa travelling instrument and the IZO calibrator was found, which confirms the validity of the last calibration made at Empa in 2017. The ozone analysers were all in agreement within 1 ppb at the relevant mole fraction range from 0-100 ppb ozone (Fig. 5.4), which confirms that the quality control and maintenances made periodically in IZO are appropriate.

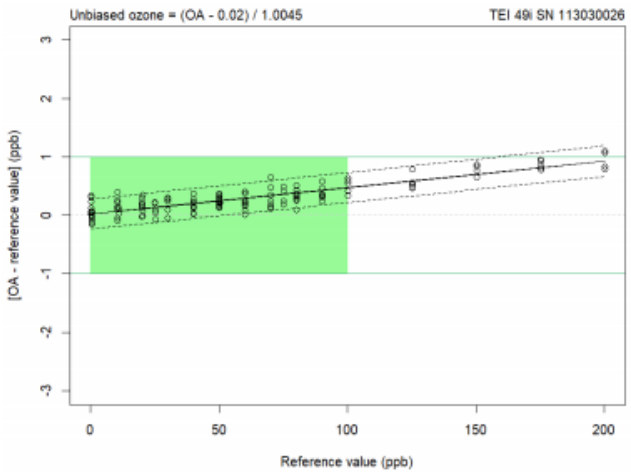

Figure 5.4. Bias of the IZO ozone analyser (TEI 49i #1153030026, principal analyser) with respect to the SRP as a function of mole fraction. Each point represents the average of the last five 1-minute values at a given level. The green area corresponds to the relevant mole fraction range, while the Data Quality Objectives (DQOs) are indicated with green lines. The dashed lines about the regression lines are the Working-Hotelling 95% confidence bands (WMO, 2020).

On the other hand, the WCC-Empa 2019 audit noted that the C-series instruments (TEI 49C) are reaching the end of their lifetime and these instruments should be replaced. During 2022, two TEI 49i analysers and a 49i-PS primary ozone standard have been purchased. Both sets of analysers were operating in parallel to ensure consistent datasets. The new instruments replaced the old 49C-series analysers, once the WCC-Empa audit was completed in June 2023.

NO_x and SO_2 instruments at IZO usually operate below the detection limit (50 ppt) during the night-time period when we can ensure background conditions. However, these measurements are quite useful for studies of local or regional pollution during daytime, when concentrations are modulated by valley-mountain breeze, and help to understand the impact of regional pollution and of long-range transport of pollution on the background atmosphere. For example, high concentrations of SO_2 were measured in IZO at the end of 2021, during episodes of transport of the volcanic plume associated with the eruption on the island of La Palma (see Section 23 for more details).

In order to ensure continuity to the NOx measurement programme at IZO, to improve the quality of measurements and increase precision, the EcoPhysics CraNOx II analyzer was acquired, as part of the project "Equipment for Monitoring and Research from the Global Atmospheric Watch station at Izaña (Tenerife) of Atmospheric Parameters and Components that modulate Climate Change (MICA)" (EQC2018-004376-P). The infrastructure project was approved at the end of 2018, and the new equipment was installed in October 2020 (Fig. 5.5).

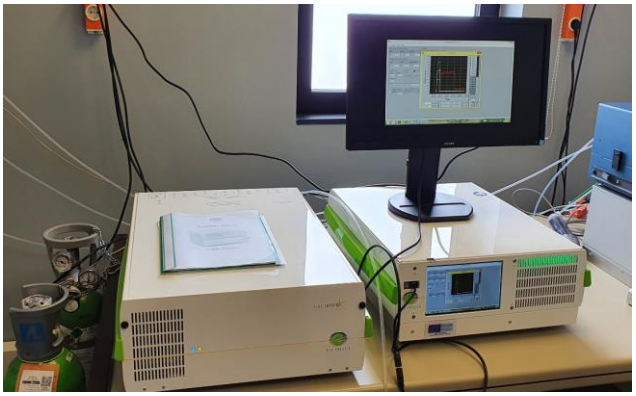

Figure 5.5. EcoPhysics CraNOx II analyser at the Izaña Observatory.

CO is measured with high accuracy at IZO by the Greenhouse Gases and Carbon Cycle Programme, following the GAW recommendations (see Section 4 for more details). CO measurements are also performed at SCO with the non-dispersive IR absorption technique and are utilized for air quality research.

5.2.2 CraNOx II analyzer

The CraNOx analyser is a high-performance device based on a chemiluminescence detection principle (O_3-CLD, Ozone Chemiluminescence Detection), which detects NO directly and NO_2 after converting it into NO with a photolytic converter (PLC, Photolytic Converter). This NO measurement technique is recommended by GAW at its NO_x measurement stations (WMO, 2011 and 2017) given its reliability, linearity and proven reproducibility in a wide range of conditions. The technique consists of enriching the air sample, whose concentration of NO is to be studied, with O_3, which produces a set of reactions resulting in the generation of NO_2 and release of radiation proportional to the initial concentration of NO. This radiation is measured using a photomultiplier tube (PMT) with a signal proportional to NO in the initial sample.

In order to obtain the concentration of NO_2 in the sample, all the NO_2 must first be converted into NO, and then subsequently, the same direct NO measurement process is repeated with the O_3-CLD detector. There are several methods to produce NO_2 from NO, e.g. using a photolytic converter or a heated molybdenum converter. At GAW stations, photolytic conversion is recommended (WMO, 2011) since it is a more selective method, avoiding the overestimation of NO_2, by preventing other nitrogen compounds in the air from being transformed into NO during the process. The air sample is irradiated in a photolytic cell and a fraction of the NO_2 is converted into NO, depending on an efficiency factor related to the intensity and type of lamp, e.g. mercury or xenon arc lamp or UV-LEDs.

The CraNOx II installed in the Izaña Observatory complies with GAW recommendations in terms of measurement technique, precision and detection limit for the measurement of NO and NO_2 under background conditions (WMO, 2011 and 2017). It is a compact instrument consisting of a double O_3-CLD detector for the simultaneous measurement of NO and NO_2, with a pre-chamber, to minimise interference due to the reaction of ozone with other compounds present in the air, and uses a photolytic converter with a metal halide lamp (200W). For the ozone required in the O_3-CLD chemiluminescence detector, the analyser has an internal ozone generator. This ozone is generated by applying an electrical discharge to a constant flow of oxygen (O_2), taken from a bottle, breaking the O_2 molecules down into more unstable atoms, which recombine to form ozone. Thanks to this design, the analyser allows the measurement of NO and NO_2 mole fractions < 25 ppt, with great stability and precision (Fig 5.6).

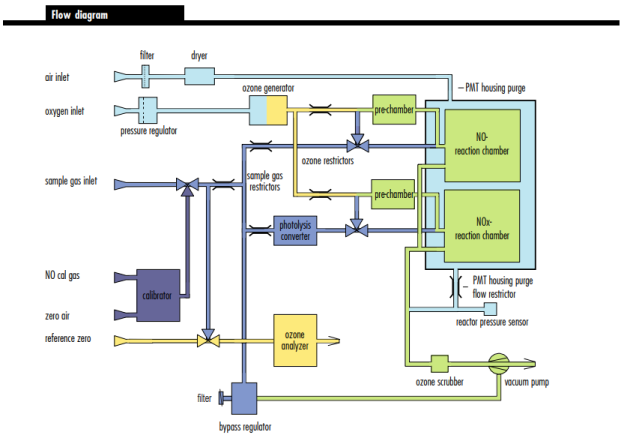

Figure 5.6. Flow diagram of the EcoPhysics CraNOx II (https://www.ecophysics.com/environmental/supreme-line/cranox-ii/).

The CraNOx II also incorporates an internal calibration module that allows the automatic verification/calibration of the analyser: NO-zero (synthetic air with zero NO mole fraction), NO-span (measurement of a known dilute amount of NO) and efficiency of the PLC converter. The high degree of instrument automation always allows control of both the quality of the measurement and of the equipment itself. The CraNOx II is completed with an internal O_3 analyzer, by UV photometric absorption, which measures O_3 mole fraction of the air sample simultaneously with the NO and NO_2 measurements, which will allow the detailed

study of how the chemical reactions that connect these three compounds occur under background conditions. Measurements of NOx (NO + NO_2) from Jan-May 2021 at IZO are shown in Fig. 5.7.

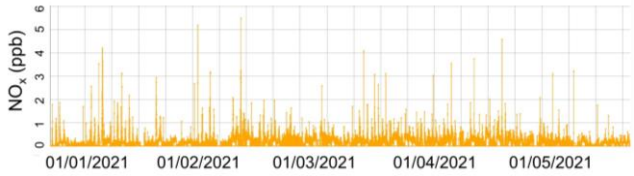

Figure 5.7. 10-minute average of NO_x mole fraction (ppb, preliminary data) from January to May 2021 at IZO.

5.2.3 30 years of Ozone soundings

The geographical location of the island of Tenerife, at the subtropical limit of the North Atlantic, makes the vertical ozone profiles measured in this region exceptionally valuable, not only because the island is frequently located at the northern limit of the Hadley Cell, under the descending branch in which a subsidence regime prevails in the free troposphere, but also due to the scarcity of stations in this region. This makes Tenerife a privileged place for studying the evolution of tropospheric-stratospheric ozone and for analyzing the influence of the subtropical jet stream (STJ) on the stratosphere-troposphere exchange.

With the support of WMO/GAW, the IARC Ozone Sounding Programme began in November 1992. The first ozonesonde was launched on 4 November 1992 from Santa Cruz Station (Fig. 5.9 upper panel). After that first ozone sounding, a weekly launch routine was established, every Wednesday, which has continued uninterrupted to this day. The frequency of ozone soundings is significantly increased during intensive campaigns. In 2011 the launch site was changed to the BTO (Fig. 5.8 and 5.9 lower panel). The launch equipment and stations used during these 30 years are listed in Table 5.1.

Figure 5.8. Inflating the balloon with helium at BTO.

The ozone soundings programme uses ECC sondes along with a helium balloon (TOTEX TA 1200) to obtain the ozone profiles from the ground to the burst level (generally between 30 and 35 km) with a resolution of about 10 metres. A constant mixing ratio above burst level is assumed for the determination of the residual ozone if an altitude equivalent to 17 hPa has been reached (Vaisala Software).

Ozonesondes are checked before launch with a Ground Test with Ozonizer/Test Unit EN-SCI KTU3 (see Section 3.2.1). The ECC-ozone sensor used is an electrochemical cell consisting of two half cells, made of Teflon, which serve as cathode and anode chambers, respectively. Both half cells contain platinum mesh electrodes. They are immersed in a KI-solution, always with the same sensing solution type (SST1.0: 1.0% KI & full pH-buffer). The two chambers are linked together by an ion bridge in order to provide an ion pathway. Each ozone molecule reacts with the KI releasing 2 electrons and the current generated between the two cells is measured to provide the ozone content in the sampled air.

The preparation and conditioning of the ozonesondes follows the protocol established in "Assessment of Standard Operating Procedures for Ozonesondes (ASOPOS)" (Smit, 2013) and ASOPOS 2.0 (WMO, 2021).

Figure 5.9. Preparation and launch of the ozonesonde from Santa Cruz Station (upper panel, first soundings 1990s) and BTO (lower panel, at the present).

Table 5.1. Ozonesonde Programme equipment used during different time periods and launch stations since November 1992.

Instrument manufacturer and model	Frequency	Period/Launching station
OZONESONDES: Nov 1992 – Sep 1997: Science Pump Corp. Model ECC-5A Sep 1997 – present: Science Pump Corp. Model ECC-6A **GROUND EQUIPMENT:** Nov 1992 – Oct 2010: VAISALA DigiCora MW11 Rawinsonde Oct 2010 – Feb 2018: VAISALA DigiCora MW31 Mar 2018 – present: VAISALA DigiCora MW41 **RADIOSONDES:** Nov 1992 – Oct 1997: VAISALA RS80-15NE (Omega wind data) Oct 1997 – Sep 2006: VAISALA RS80-15GE (GPS Wind data) Sep 2006 - Dec 2018: VAISALA RS92-SGP (GPS Wind data) Dec 2018 - present: VAISALA RS41-SGP (GPS Wind data)	1/week (Wed)	Nov 1992 – Oct 2010: From Santa Cruz Station (28.46°N, 16.26°W; 36 m a.s.l.) Oct 2010 – Feb 2011: From Santa Cruz/ BTO (In alternate launches) Feb 2011 – present: From BTO Station (28.41°N, 16.53°W; 114 m a.s.l.)

5.3 Summary of remarkable results during the period 2021-2022

5.3.1 Software for the evaluation of reactive gases data (O_3, NO_x, SO_2, CO)

The software for reactive gases data evaluation was developed during 2015 and 2016, and is improved each year. This software makes it possible to carry out the evaluation and processing of the data of the reactive gases programme (surface O_3, NO_x, SO_2 and CO). The software works in a web environment that facilitates consultations with the database and data processing.

The raw data of the TEI analysers are acquired by a CR1000 Campbell datalogger, which interrogates each instrument every minute. The data are automatically stored in a database; zeros, span and calibration coefficients of the analysers are also recorded. NO, NO_2 and NO_x data from the CraNOx-II are also stored in the same database. The software uses all this information to process data automatically and it allows us to choose the desired component to evaluate and visualize its record along with that of another component and/or together with the meteorological information (temperature, relative humidity, pressure and wind). The software has an option to download the processed data in the EBAS format.

5.3.2 World Data Center for Reactive Gases (WDCRG)

The World Data Center for Reactive Gases (WDCRG) is the data repository and archive for reactive gases of the GAW Programme and is managed by the Norwegian Institute for Air Research (NILU). The WDCRG was established on 1 January 2016 and took over the responsibility for RG data archiving from the Japan Meteorological Agency, which continues to host the World Data Centre for Greenhouse Gases (WDCGG). Some of the reactive gases hosted at WDCRG are SO_2, oxidized nitrogen species, surface O_3 and VOCs. We developed the necessary software to edit surface O_3 data in the EBAS NASA-Ames format required by the WDCRG. Hourly surface O_3 data from 2014 to 2022 have been submitted directly to WDCRG (http://ebas.nilu.no) and O_3 data from 1987 to 2013 have been transferred from the WDCGG to WDCRG in the EBAS format. Monthly average values of surface O_3 data for 1987 to 2022 at IZO are shown in Fig. 5.10.

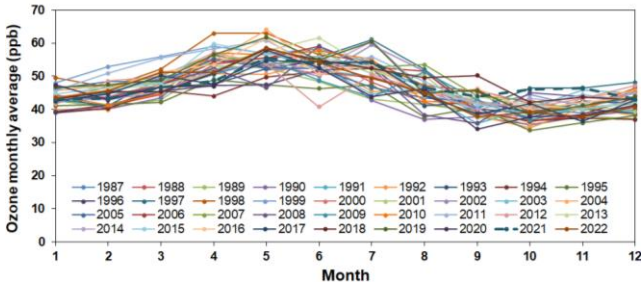

Figure 5.10. Surface ozone mean seasonal cycle from 1987 to 2022 at IZO.

5.3.3 Network for the Detection of Atmospheric Composition Change (NDACC)

In 2004, the Izaña Atmospheric Research Center joined the Network for the Detection of Atmospheric Composition Change and began routinely archiving the ozonesonde data into the NDACC database; in addition, all the ozonesonde records since 1995 were uploaded to the NDACC at this time. Ozonesonde data archived in the NDACC database must meet certain quality criteria. Currently 92% of the ozone soundings performed in the period 1995-2022 are available in the NDACC database (Figure 5.11). Ozonesonde data from the early period (November 1992-1994) need to be reprocessed and reanalysed carefully.

All NDACC data is available at https://www-air.larc.nasa.gov/missions/ndacc/data.html or through search tools available on the NDACC website. At present, NDACC is working on the homogenization of the ozone soundings of all NDACC-stations' data and implementation of a new data format.

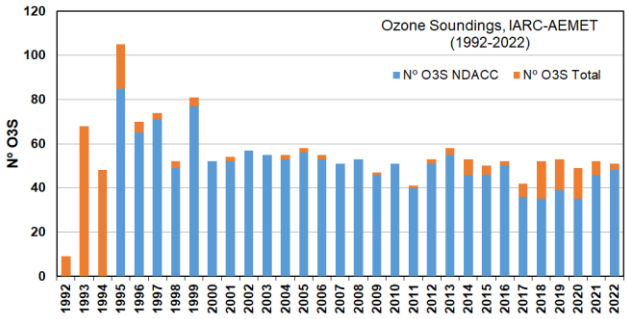

Figure 5.11. Number of ozone soundings (O3S) since the beginning of the programme and the number of ozonesonde datasets recorded in the NDACC database that meet the quality assurance criteria (1992-2022).

5.3.4 Ozonesonde data homogenization activity

An Ozonesonde Data Quality Assessment (O3S-DQA) activity was initiated in 2011 to homogenize temporal and spatial ozonesonde data records under the framework of the SI2N (SPARC [Stratosphere-troposphere Processes And their Role in Climate], IO3C [International Ozone Commission], and NDACC) initiative on "Past Changes in the Vertical Distribution of Ozone". The aim of O3S-DQA activity is to correct for biases related to instrumental (such as sonde type or sensing solution strength) or processing changes to reduce the uncertainty (from 10–20% down to 5–10%), and to provide an uncertainty estimate for every single ozone partial pressure measurement in the profile.

In this context, some O_3-sounding stations (Figure 5.12), one of them being the IZO station, were selected to be involved in the homogenization process, following the "Guidelines for Homogenization of Ozone Sonde Data" (Smit et al., 2012) prepared by the O3S-DQA panel members and the new WMO-GAW report No. 268 (Annex C & D) (WMO, 2021). The reprocessing carried out for IZO station is being supervised by Dr H. Smit (FZJ, Germany), leader of the O3S-DQA panel, and Dr R. Van Malderen (KMI, Belgium).

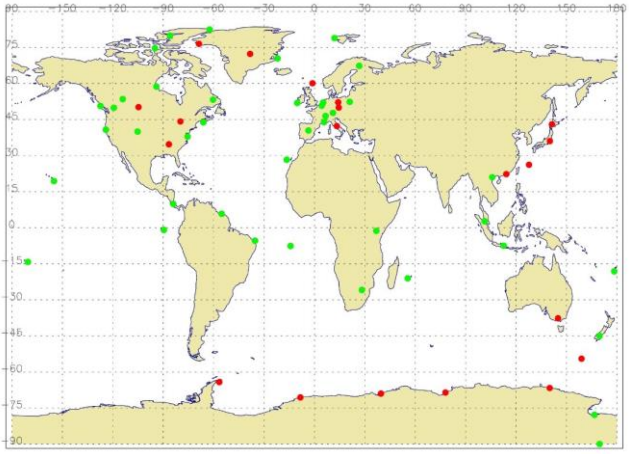

Figure 5.12. Global map of around 60 active ozonesonde sites. Green dots mark the stations with homogenized data available at the HEGIFTOM ftp-server.

At present, the O3S-DQA activity continues to support the TOAR-II Focus Working Group "HEGIFTOM" (Harmonization and Evaluation of Ground-based Instruments for Free Tropospheric Ozone Measurements). (see Section 5.3.6 for more details). The homogenized O3S-data (HO3S) are available at the HEGIFTOM ftp-server (KMI - Datasets).

In our case, although there have not been any changes in ECC ozonesonde manufacturer (Vaisala ECC-SPC) or changes in sensing solution type (STT 1.0% KI & full pH-buffer) since the beginning of the Ozonesonde Programme (Nov 1992), some non-uniformity in ozonesonde and data processing could have occurred during the programme implementation period: changes in the ozonesonde type (ECC5A, Nov. 1992 to Sep. 1997 and ECC6A, Sep. 1997 to present), in the pump temperature measurement, in the background current, in the correction (temperature and humidity) of the pump flow or in the method of determining the ozone residual. All this can lead to some inhomogeneities in the time series and may influence the trends derived from such data dramatically (Figure 5.13).

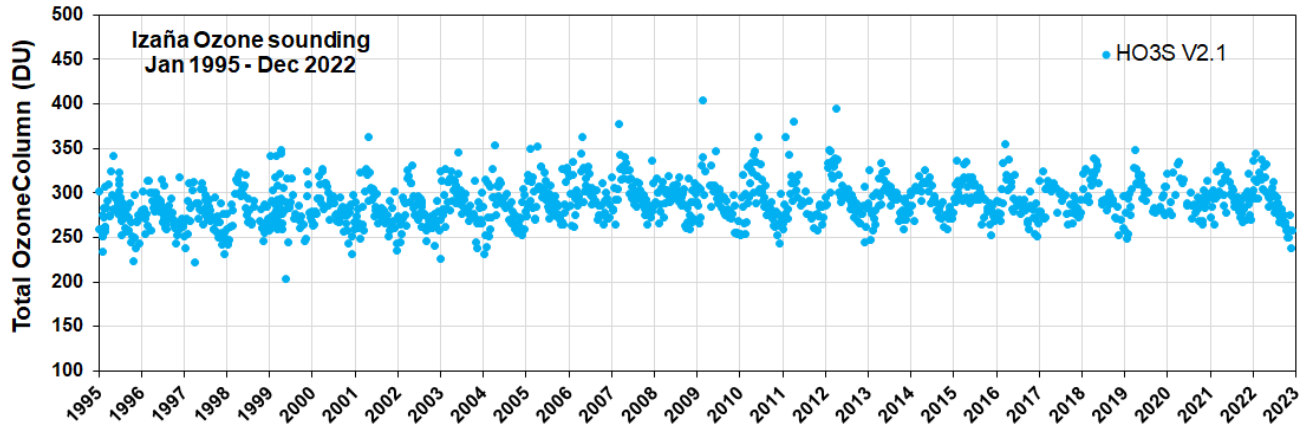

Figure 5.13. Long-term Total Ozone Column with Izaña homogenized ozone sounding data (1995-2022). A satellite ozone climatology is used to determine the residual ozone from 10 hPa.

5.3.5 Tropospheric Ozone Trends: Impact of the COVID-19 Economic Downturn

There are many studies that have been published quantifying the effect that the reduction in industrial, commercial and transport activity has had on the environment, due to the impact of COVID-19, but a complex analysis is required if we want to determine the effect that this crisis has had on the temporal trend of tropospheric ozone on a regional scale. This is the purpose of the paper "*Impact of the COVID-19 economic downturn on tropospheric ozone trends: an uncertainty weighted data synthesis for quantifying regional anomalies above western North America and Europe*" (Chang et al., 2022), where, in addition to quantifying the impact that the reduction of emissions in Europe and North America has had on tropospheric ozone during 2020, a novel method is presented to merge ozone profiles from different stations and measurement techniques, in order to determine the regional anomalies of the trend of the vertical distribution of tropospheric ozone in the period 1994-2020. For this, the ozone soundings of more than 20 stations distributed throughout the world have been analyzed, including Izaña, as well as ozone profiles measured by LIDAR (Light Detection and Ranging) and by the In-Service Aircraft for a Global Observing System (IAGOS) program.

From the individual analysis of the tropospheric ozone time series for each station, we see that before 2020, there are stations with both positive and negative trends, but when including the tropospheric ozone data for 2020, they have been affected by the decrease in the emission of precursors of ozone on a global scale due to COVID-19 (Steinbrecht et al., 2021), a decrease in positive trends is generally observed while negative trends become even more negative. Thus, in the case of Izaña, the trend prior to 2020 for tropospheric ozone (700-300 hPa) is 3 (± 1.00) ppb/decade, and this decreases to 2.65 (± 0.97) ppb/decade if we consider the profiles of ozone in 2020, which corresponds to a reduction of 12% (Figure 5.14).

Ozone Trends in the Free Troposphere (700–300 hPa) Since 1994 (Some Stations Have Different Reference Years, and the TMF Lidar Trends are Limited to 600—300 hPa)

		Through 2019		Through 2020		
Site	Reference	Trend (±2-σ)	p-value	Trend (±2-σ)	p-value	Change (%)
Edmonton	1994	***−3.87 (±2.29)***	<0.01	***−3.79 (±2.13)***	<0.01	2
Kelowna/Port Hardy	2003	1.54 (±2.31)	0.18	1.21 (±2.07)	0.25	−22
Trinidad Head (THD)	1997	−1.38 (±1.91)	0.15	**−1.89 (±1.80)**	0.04	−37
Boulder	1994	***−1.38 (±0.79)***	<0.01	***−1.37 (±0.75)***	<0.01	1
Table Mountain (TMF)	2002	1.07 (±2.21)	0.33	0.58 (±2.00)	0.56	−45
IAGOS (WNA)	1994	***3.97 (±1.80)***	<0.01	–	–	–
Fused (WNA)	1994	***0.35 (±0.21)***	<0.01	0.14 (±0.21)	0.19	−61
Legionowo	1994	***−1.52 (±1.02)***	<0.01	***−1.60 (±0.98)***	<0.01	−5
Lindenberg	1994	−1.73 (±2.01)	0.09	***−2.85 (±1.83)***	<0.01	−65
De Bilt	1994	***2.26 (±1.04)***	<0.01	***1.86 (±1.02)***	<0.01	−18
Uccle	1994	***1.49 (±0.89)***	<0.01	**1.00 (±0.90)**	0.03	−33
Hohenpeissenberg (HPB)	1994	−0.17 (±0.73)	0.63	−0.48 (±0.75)	0.20	−173
Payerne	1994	***−1.56 (±0.85)***	<0.01	***−1.81 (±0.83)***	<0.01	−16
Haute Provence (OHP)	1994	**1.29 (±1.13)**	0.02	1.03 (±1.07)	0.06	−20
Madrid	1994	−0.39 (±1.34)	0.56	−0.88 (±1.29)	0.18	−124
IAGOS (Europe)	1994	***1.16 (±0.77)***	<0.01	**1.02 (±0.75)**	0.01	−12
Fused (Europe)	1994	***0.65 (±0.19)***	<0.01	***0.36 (±0.20)***	<0.01	−44
Broadmeadows	1999	−1.07 (±1.26)	0.09	−0.71 (±1.18)	0.23	34
Lauder	1994	0.34 (±0.77)	0.38	0.27 (±0.73)	0.46	−21
Macquarie Island	1994	***−4.23 (±1.96)***	<0.01	***−3.74 (±1.85)***	<0.01	11
Tateno	2009	−0.58 (±6.32)	0.85	−2.15 (±5.36)	0.42	−269
Izaña	1995	***3.01 (±1.00)***	<0.01	***2.65 (±0.97)***	<0.01	−12
Hong Kong	2000	0.54 (±2.66)	0.69	0.55 (±2.45)	0.66	1
Hilo	1994	0.75 (±1.45)	0.30	0.67 (±1.35)	0.32	−11

Figure 5.14. Tropospheric ozone trend for the period 1994-2019 and 1994-2020 for the analyzed ozone sounding, lidar and IAGOS stations. The value of the trend and the uncertainty are obtained from the monthly averages and applying a linear regression model. Reprinted from Chang et al. (2022).

To carry out the analysis of the impact of COVID-19 on the tropospheric ozone trend at a regional scale, it is necessary to have not only a long time series of data, but also the sampling frequency must be high enough for the data to be representative. In the case of ozone soundings, we find ourselves with the problem that the frequency of launches is usually low together with a high spatial dispersion of the stations, to which the high variability of tropospheric ozone and the reduction of soundings during 2020 due to the decrease in the operation of the stations are added.

In order to solve the problem of dispersion and sampling frequency, Chang et al. (2022) presented a fusion method of vertical ozone profiles obtained by various measurement techniques (ozone soundings, LIDAR profiles and IAGOS profiles) for two regions: Europe and western North America. This method obtained a monthly time series of ozone distribution, with high vertical resolution, which allowed for the analysis of anomalies from surface to mid-stratosphere on a regional scale.

The time series of fused ozone profiles for Europe was generated from 45,000 ozone profiles over 27 years (1994-2020) which corresponds to an average sampling frequency of 140 profiles/month. In the case of western North America, to obtain the time series of fused ozone profiles for that region, it was only possible to use 9,900 profiles covering the same period and obtained from four ozone sounding stations, one LIDAR station and IAGOS profiles from that region. Also, because the stations were representative of different environments (rural, urban, maritime, etc.), only data above 700 hPa were analysed (in the case of western North America) to eliminate this influence. Data from the Tenerife ozone soundings were not used in Chang et al. (2022), as this study only analysed the regions of Europe and western North America.

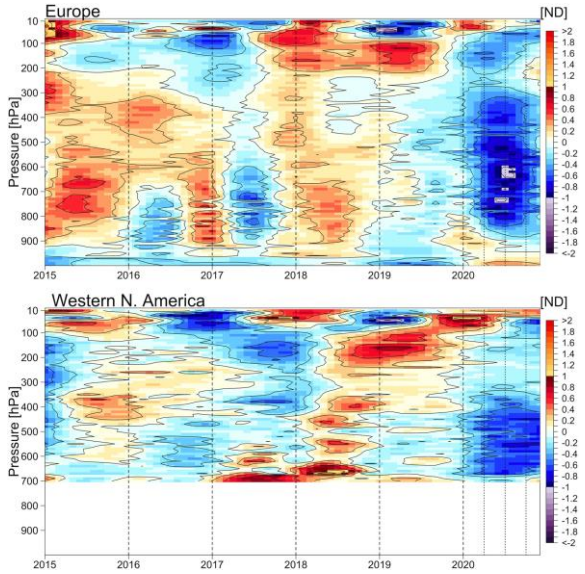

Figure 5.15. Detail of the mean vertical distribution of the ozone normalized deviation (ND) for the merged time series of Europe and western North America, for the period 2015-2020. Data for western North America only analysed above 700 hPa. Reprinted from Chang et al. (2022).

From the analysis of the ozone anomalies of the merged profiles of 2020 compared to the period 1994-2019, an average anomaly of -3.60 (±1.75) ppb over Europe and -2.77 (±1.92) ppb is obtained over western North America, corresponding to a percent deviation of -6.0 (±2.9) % and -4.8 (±3.3) %, respectively. In addition, 2020 is the only year since 1994 where such an intense negative anomaly is observed simultaneously in the two regions.

Figure 5.15 shows a detail of the 2015-2020 period of the mean vertical distribution (10 hPa layers) of the ozone normalized deviation (ND) over Europe and western North America, where the merged ozone time series for each layer has been deseasonalized with the monthly climatological series and normalized with the standard deviation of each layer. The negative anomaly is the strongest around July in Europe, and somewhat weaker for western North America. In mid-latitudes, the tropospheric ozone maximum occurs around June, coinciding with a greater photochemical ozone production, this indicates that in the negative anomaly of 2020, the reduction at the global level of precursors has a greater influence than the atmospheric dynamics itself (Steinbrecht et al., 2021).

5.3.6 TOAR II project

As of February 2020, TOAR (Tropospheric Ozone Assessment Report: Global metrics for climate change, human health and crop/ecosystem research) Activity of the International Global Atmospheric Chemistry Project (IGAC), has entered its second phase (TOAR-II), the first phase was completed in 2019. For further details see Izaña Activity Report 2019-2020 (Cuevas et al., 2022).

In the second phase, the goals of TOAR-II (2020-2024) are:

1. TOAR Ozone Data Portal: Update the ozone observations in the TOAR surface ozone database to include all recent observations (since 2014), and include data from new sites and regions, as well as ozone precursor and meteorological data. Develop methods for including historical data (pre-1975) and create working links to repositories of free tropospheric ozone observations.
2. TOAR publications: Exploit the new observational datasets collected by Goal 1 (with data through 2020) to provide an updated state of the science related to ozone's global distribution and trends relevant to climate, human health and vegetation. Extend the statistical toolbox and metrics of the TOAR trend analyses.
3. Involve scientists from the atmospheric sciences community, as well as statisticians and scientists who focus on broader issues of global change and sustainability, to identify outstanding science questions in relation to tropospheric ozone. The range of topics can be expanded beyond the scope of the original TOAR effort to investigate the impacts of tropospheric ozone on climate, human health and vegetation, and to address urban-scale issues in addition to the regional and global scale.
4. Maximize exploitation of the TOAR Surface Ozone Database by, 1) helping scientists around the world, beyond the TOAR effort, to apply the database to new analyses, and 2) exploring new data science methods to improve the analysis of global ozone trends and their attribution.

The TOAR-II virtual workshop organized in late January and early February 2021, was designed to gather the community and develop the working groups that will produce the papers for the TOAR-II Community Special Issue (the first step of the second Tropospheric Ozone Assessment Report), as well as identify new datasets for the assessment of tropospheric ozone and its impact on climate, health and vegetation. The working groups that were set up are focussing on: Chemical Reanalysis, East Asia,

Harmonization and Evaluation of Ground Based Instruments for Free Tropospheric Ozone Measurements (HEGIFTOM), Ozone over the Oceans, Ozone and Precursors in the Tropics (OPT), Radiative Forcing, Satellite Ozone, Statistics, and Urban Ozone.

IARC participates in TOAR-II within the HEGIFTOM working group with surface ozone measurements, ozonesonde profiles and FTIR ozone profiles (for further details refer to Section 7). The HEGIFTOM working group brings together different networks of ground-based instruments measuring free tropospheric ozone, not only to strengthen, speed up, and expand existing activities of harmonization of instruments, but also to compare Quality Assurance/Quality Control (QA/QC) procedures and reports, and harmonization efforts between the different networks.

5.3.7 Contributions to the 2021 La Palma volcanic eruption emergency response

The Reactive Gases group contributed to activities carried out by IARC-AEMET during the 2021 La Palma volcanic eruption. In particular, the group contributed to the Canary Islands Government implementation of an emergency air quality network with deployment of instrumentation to measure in situ SO_2 and O_3 in Tazacorte (La Palma), measurements started on 24/9/2021 (for more details see García et al., 2022 and Section 23.4).

In addition, measurements on Tenerife at Izaña Observatory recorded episodes of direct impact of the volcanic eruption, causing the SO_2 concentration to increase, by several orders of magnitude, compared to SO_2 values under usual background conditions at IZO. As a consequence of the first episode of very high levels of SO_2 from the volcanic eruption, recorded at IZO, IARC established an internal operating procedure aimed at minimizing the health risks associated with the presence of volcanic pollution. From this emergency IZO procedure, an "Action guide for high levels of volcanic pollution. Izaña Atmospheric Observatory" was published by AEMET (Prats et al., 2022), see Section 23.7 for more details.

Subsequently, IARC-AEMET in collaboration with many participating organisations, conducted a comprehensive evaluation of the impact of the 2021 volcanic eruption on air quality, concentrating on the air quality impacts of SO_2 and PM concentrations (for more details see Section 23.4 and Milford et al., 2023).

5.4 References

Chang, K.-L., Cooper, O. R., Gaudel, A., Allaart, M., Ancellet, G., Clark, H., Godin-Beekmann, S., Leblanc, T., Van Malderen, R., Nédélec, P., Petropavlovskikh, I., Steinbrecht, W., Stübi, R., Tarasick, D.W., Torres, C.: Impact of the COVID-19 economic downturn on tropospheric ozone trends: An uncertainty weighted data synthesis for quantifying regional anomalies above western North America and Europe. AGU Advances, 3, e2021AV000542, https://doi.org/10.1029/2021AV000542, 2022.

Cuevas, E., González, Y., Rodríguez, S., Guerra, J. C., Gómez-Peláez, A. J., Alonso-Pérez, S., Bustos, J., and Milford, C.: Assessment of atmospheric processes driving ozone variations in the subtropical North Atlantic free troposphere, Atmos. Chem. Phys., 13, 1973-1998, doi:10.5194/acp-13-1973-2013, 2013.

Cuevas, E., Milford, C., Barreto, A., Bustos, J. J., García, O. E., García, R. D., Marrero, C., Prats, N., Ramos, R., Redondas, A., Reyes, E., Rivas-Soriano, P. P., Romero-Campos, P. M., Torres, C. J., Schneider, M., Yela, M., Belmonte, J., Almansa, F., López-Solano, C., Basart, S., Werner, E., Rodríguez, S., Afonso, S., Alcántara, A., Alvarez, O., Bayo, C., Berjón, A., Carreño, V., Castro, N. J., Chinea, N., Cruz, A. M., Damas, M., Gómez-Trueba, V., González, Y., GuiradoFuentes, C., Hernández, C., León-Luís, S. F., López-Fernández, R., López-Solano, J., Parra, F., Pérez de la Puerta, J., Rodríguez-Valido, M., Sálamo, C., Santana, D., Santo-Tomás, F., Sepúlveda, E. and Serrano, A.: Izaña Atmospheric Research Center Activity Report 2019-2020. (Eds. Cuevas, E., Milford, C. and Tarasova, O.), State Meteorological Agency (AEMET), Madrid, Spain and World Meteorological Organization, Geneva, Switzerland, NIPO: 666-22-014-0, WMO/GAW Report No. 276, https://doi.org/10.31978/666-22-014-0, 2022.

García, O., Suárez, D., Cuevas, E., Ramos, R., Barreto, África, Hernández, M., Quintero, V., Toledano, C., Sicard, M., Córdoba-Jabonero, C., Riz, V., Roininen, R., López, C., Vilches, J., Weiss, M., Carreño, V., Taquet, N., Boulesteix, T., Fraile, E., Torres, C., Prats, N., Alcántara, A., León, S. ., Rivas, P., Álvarez, Óscar, Parra, F., de Luis, J., González, C., Armas, C., Romero, P., de Bustos, J., Redondas, A., Marrero, C., Milford, C., Román, R., González, R., López-Cayuela, M., Carvajal-Pérez, C., Chinea, N., García, R. ., Almansa, F., González, Y., Bullón, F., Poggio, M., Rivera, C., Bayo, C., & Rey, F. (2022). La erupción volcánica de La Palma y el papel de la Agencia Estatal de Meteorología. Revista Tiempo Y Clima, 5(76). https://pub.ame-web.org/index.php/TyC/article/view/2516

González, Y., Levels and origin of reactive gases and their relationship with aerosols in the proximity of the emission sources and in the free troposphere at Tenerife, PhD Thesis, Technical Note Nº 12, AEMET, NIPO 281-12-016-1, July 2012.

Milford, C.; Torres, C, Vilches, J.; Gossman, A.K; Weis, F.; Suárez-Molina, D.; García, O.E.; Prats, N.; Barreto, A.; García, R.D.; Bustos, J.J.; Marrero, C. L.; Ramos, R.; Chinea, N.; Boulesteix, T.; Taquet, N.; Rodríguez, S.; López-Darias, J.; Sicard, M.; Córdoba-Jabonero, C.; Cuevas, E. Impact of the 2021 La Palma volcanic eruption on air quality: Insights from a multidisciplinary approach, Science of The Total Environment, Volume 869, 2023, 161652, ISSN 0048-9697, https://doi.org/10.1016/j.scitotenv.2023.161652.

Prats, N., Torres, C., Bayo, C., Ramos, R., Cuevas, E. Guía de actuación ante niveles altos de contaminación volcánica. Observatorio Atmosférico de Izaña. AEMET – Publicaciones en línea. Ministerio para la Transición Ecológica y el Reto Demográfico, Agencia Estatal de Meteorología, Madrid, 2022. NIPO: 666-22-012-X. https://doi.org/10.31978/666-22-012-X.

Smit, H. G. J., Oltmans, S., Deshler, T., Tarasick, D., Johnson, B., Schmidlin, F., Stübi, R., and Davies, J.: SI2N/O3S-DQA Activity: Guide Lines for Homogenization of Ozone Sonde Data, version 19 November 2012, available at: http://www-das.uwyo.edu/~deshler/NDACC_O3Sondes/O3s_DQA/O3S-

DQA-Guidelines%20Homogenization-V2-19 November2012.pdf, 2012.

Smit, H.G.J., and the Panel for the Assessment of Standard Operating Procedures for Ozonesondes (ASOPOS), Quality Assurance and Quality Control for Ozonesonde Measurements in GAW, GAW Report No. 201, World Meteorological Organization (WMO), 92 pp, 2013.

Steinbrecht, W., Kubistin, D., Plass-Dülmer, C., Davies, J., Tarasick, D.W., Gathen, P.V., Deckelmann, H., Jepsen, N., Kivi, R., Lyall, N., Palm, M., Notholt, J., Kois, B., Oelsner, P., Allaart, M., Piters, A., Gill, M., Van Malderen, R., Delcloo, A.W., Sussmann, R., Mahieu, E., Servais, C., Romanens, G., Stübi, R., Ancellet, G., Godin-Beekmann, S., Yamanouchi, S., Strong, K., Johnson, B., Cullis, P., Petropavlovskikh, I., Hannigan, J., Hernandez, J.L., Rodriguez, A.D., Nakano, T., Chouza, F., Leblanc, T., Torres, C., Garcia, O., Röhling, A., Schneider, M., Blumenstock, T., Tully, M., Paton-Walsh, C., Jones, N., Querel, R., Strahan, S., Stauffer, R.M., Thompson, A.M., Inness, A., Engelen, R., Chang, K.L., Cooper, O.R., COVID-19 Crisis Reduces Free Tropospheric Ozone across the Northern Hemisphere, Geophysical Research Letters, 48, e2020GL091987, https://doi.org/10.1029/2020GL091987, 2021.

WMO, 2011: WMO/GAW Expert Workshop on Global Long-term Measurements of Nitrogen Oxides and Recommendations for GAW Nitrogen Oxides Network, Hohenpeissenberg, Germany, 8-9 October 2009, GAW Report 195, (WMO/TD-No. 1570), Geneva.

WMO, 2013: Guidelines for Continuous Measurements of Ozone in the Troposphere, WMO TD No. 1110, GAW Report No. 209, World Meteorological Organization, Geneva, Switzerland.

WMO, 2017: Report of the WMO/GAW Expert Meeting on Nitrogen Oxides and International Workshop on the Nitrogen Cycle, 12-14 April 2016, York, UK, GAW Report No. 232.

WMO, 2020: Research Infrastructure Quality Assurance, System and Performance Audit of Surface Ozone, Carbon Monoxide, Methane, Carbon Dioxide and Nitrous Oxide at the Global GAW Station Izaña, Spain, May 2019, WCC-Empa Report No. 19/2, GAW Report No. 251.

WMO, 2021: Ozonesonde Measurement Principles and Best Operational Practices. ASOPOS 2.0 (Assessment of Standard Operating Procedures for Ozonesondes), Edited by Smit, H.G.J., and Thompson, A.M., and the ASOPOS 2.0 Panel, GAW Report No. 268, World Meteorological Organization, Geneva.

5.5 Staff

Carlos Torres (AEMET; Head of programme)

Dr Natalia Prats (AEMET)

Ramón Ramos (AEMET; Head of Infrastructure)

Virgilio Carreño (AEMET; Meteorological Observer-GAW Technician)

Concepción Bayo (AEMET; Meteorological Observer-GAW Technician)

Nayra Chinea (SIELTEC Canarias / TRAGSATEC; Calibrations and ozonesonde technician)

6 Total Ozone Column and Ultraviolet Radiation

6.1 Main Scientific Goals

The main scientific objective of this programme is to obtain the total ozone column (TOC) and ultraviolet (UV) spectral radiation data with the highest precision and long-term stability that the current technology and scientific knowledge allows to achieve. To reach this objective the group uses two interconnected areas: instrumentation and modelling. The basis of the research is the measurements, supported by strict QA/QC protocols, laboratory calibrations and theoretical modelling. Finally, web-oriented databases and scientific publications are utilised for dissemination of the observational data.

6.2 Measurement Programme

Measurements of total ozone and spectral ultraviolet radiation began in May 1991 at IZO with the installation of Brewer spectrometer #033. Ozone profile measurements were added in September 1992 with two daily (sunrise and sunset) vertical ozone profiles obtained with the Umkehr technique. In July 1997, a double Brewer #157 was installed at IZO and it ran in parallel with Brewer #033 for six months. In 2003, a second double Brewer #183 was installed, and it was designated the travelling reference of the Regional Brewer Calibration Center for Europe (RBCC-E).

Figure 6.1. RBCC-E Brewer spectrophotometer triad located at IZO.

In 2005, a third double Brewer #185 was installed, and it completes the reference triad of the RBCC-E (Fig. 6.1). The measurement programme was complemented with the installation of a Pandora spectroradiometer in October 2011. The technical specifications of both Brewer and Pandora instruments are summarized in Table 6.1.

Table 6.1. Spectrometer specifications.

Brewer	
Slit Wavelengths	O_3 (nm): 303.2 (Hg slit), 306.3, 310.1, 313.5, 316.8, 320.1
Mercury-calibration (O_3 mode)	302.15 nm
Resolution	0.6 nm in UV; approx 1nm in visible
Stability	±0.01 nm (over full temperature range)
Precision	0.006 ± 0.002 nm
Measurement range (UVB)	286.5 nm to 363.0 nm (in UV)
Exit-slit mask cycling	0.12 sec/slit, 1.6 sec for full cycle
O_3 measurement accuracy	±1% (for direct-sun total ozone)
Ambient operating temperature range	0°C a +40°C (no heater) -20°C a +40°C (with heater option) -50°C a +40°C (with complete cold weather kit)
Physical dimensions (external weatherproof container)	Size: 71 by 50 by 28 cm Weight: 34 kg
Power requirements Brewer and Tracker	3A @ 80 to 140 VAC (with heater option) 1.5A @ 160 to 264 VAC 47 to 440 Hz
Pandora	
Instrument spectral range	265-500 nm
Spectral window for NO_2 fit	370-500 nm
Spectral resolution	0.4 nm
Total integration time	20 s
Number of scans per cycle	50-2500
Spectral sampling	3 pixels per Full Width at Half Maximum (FWHM)

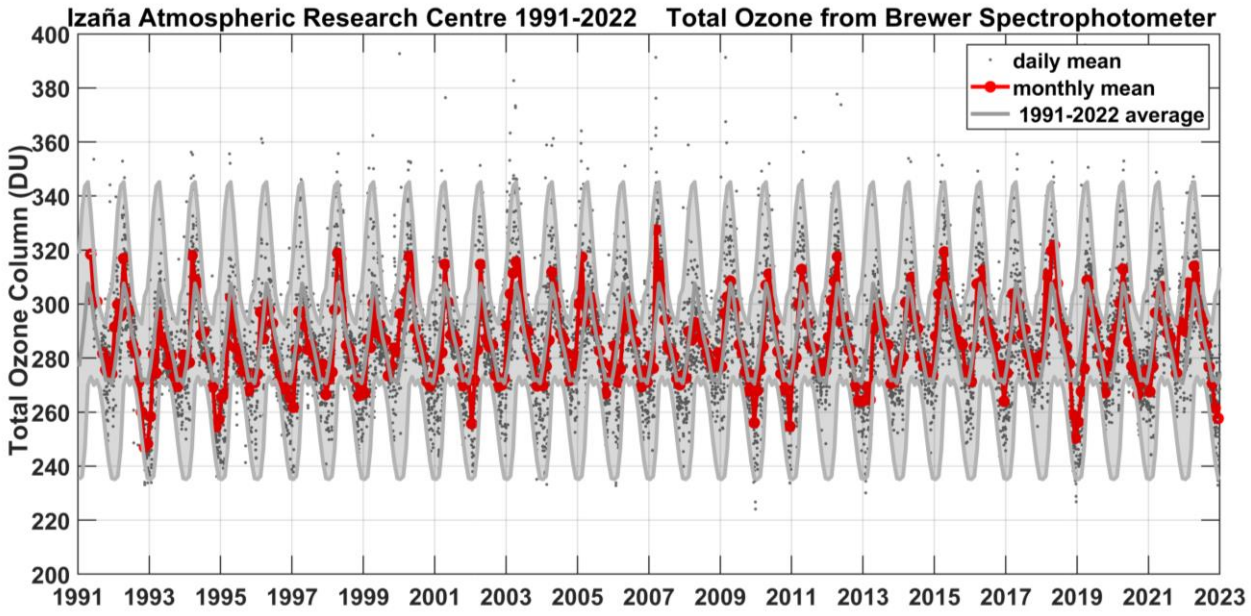

Figure 6.2. Total Ozone time series at Izaña Observatory (1991-2022), daily mean (grey dots) and monthly mean (in red), the long-term daily mean from the period 1991-2022 is also shown (grey line) with the shaded area corresponding to the standard deviation in the long-term mean.

The spectral UV measurements are routinely quality controlled using IZO calibration facilities. The stability and performance of the UV calibration is monitored by 200W lamp tests twice a month. Every six months the Brewers are calibrated in a laboratory darkroom, against 1000W DXW lamps traceable to the Word Radiation Center (WRC) standards. The SHICrivm software tool is used to analyse quality aspects of measured UV-spectra before data transfer to the databases. In addition, LibRadtran model to measurements comparisons are regularly done. Every year the Brewer #185 is compared with the Quality Assurance of Spectral Ultraviolet Measurements (QASUME) International portable reference spectroradiometer from Physikalisch-Meteorologisches Observatorium Davos, World Radiation Center (PMOD/WRC).

Concerning total ozone, the Brewer triad has an exhaustive quality control in order to assure its performance, with routine calibrations performed on a monthly basis. With this procedure, we have achieved a long-term agreement between the instruments of the triad with a precision better than 0.25% in total ozone column.

The Total Ozone programme is a part of the NDACC programme. The total ozone time series for 1991-2022 is shown in Fig. 6.2 and is available at the NDACC website and at the World Ozone and Ultraviolet Data Center (WOUDC). Fig. 6.3 shows the UV index calculated on the basis of UV observations from Brewer spectrophotometer #157, available also at the WOUDC.

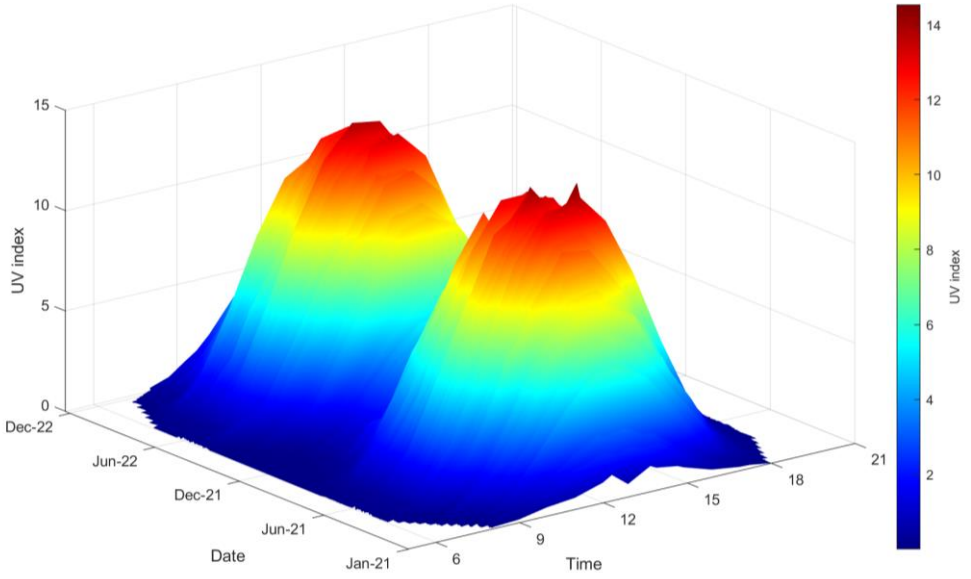

Figure 6.3. UV index during 2021-2022, calculated on the basis of measurements from Brewer #157, at Izaña Observatory.

6.3 Summary of remarkable results during the period 2021-2022

The participation in scientific projects of this measurement programme is intertwined with the activities of the Regional Brewer Calibration Center for Europe (RBCC-E) (see Section 16 for more details).

6.3.1 EUBREWNET

The Vienna Convention for the Protection of the Ozone Layer and the subsequent Montreal Protocol on Substances that Deplete the Ozone Layer have been among the most successful environmental agreements the nations of the world have entered into and have now almost completely eliminated the production of Ozone Depleting Substances. This has led to the halting of the rapid decline of stratospheric ozone observed in the 1980s and 1990s, with some promising early indications of ozone recovery now being apparent. It is therefore important to continue to carefully measure the state of the global ozone layer in the coming decades, noting also that stratospheric conditions are expected to change with the projected increasing concentration of greenhouse gases, and the fact that stratospheric ozone itself has a significant effect on the atmospheric radiation balance and surface climate. For this reason, the Vienna Convention obliges signatory countries to maintain programmes to systematically monitor stratospheric ozone.

The Brewer Ozone Spectrophotometer has, for the last 30 years, been the instrument of choice for ground station measurements of ozone and, in an effort to significantly improve the quality and timeliness of the data. The European Cooperation in Science and Technology (COST) Action (ES1207) was active from April 2013 to July 2017 to form a European Brewer Network – EUBREWNET. The results of this COST Action have been presented in Rimmer, Redondas, and Karppinen (2018).

Since the end of 2018, support to EUBREWNET has been provided by AEMET. Since February 2019, AEMET through TRAGSATEC, provides two staff positions to support the EUBREWNET and the RBCC-E activities. This support has recently been extended until 2026, ensuring and reinforcing the continuation of these two services. Input is provided by the EUBREWNET Management Committee, consisting of A. Redondas (IARC-AEMET, Spain), K. Lakkala (Finnish Meteorological Institute, Finland), A.F. Bais (Aristotle University of Thessaloniki, Greece) and J. Gröbner (PMOD/WRC, Switzerland).

Figure 6.4. Location of Brewer stations currently participating in EUBREWNET. The network started as a European network but now includes 66 spectrometers at 45 stations located world-wide.

EUBREWNET relies on the work of two European calibration Centers, the RBCC-E and the WRC. The RBCC-E plays a key role in EUBREWNET, coordinating the standardization of operation, characterization and calibration of the network instruments as well as providing the Brewer database. Now recognised by the WMO and the International Ozone Commission (IO3C), it represents an extremely valuable network of ground station data points without which the space-borne instruments would not be able to function with any degree of accuracy. In the current times when we are trying to identify ozone recovery rates of 1% per decade, it is highly important that data are both accurate and consistent across all stations.

The purpose of EUBREWNET is to harmonise observations, data processing, calibrations and operating procedures so that a measurement at one station is entirely consistent with measurements at all the others. Additionally, the Brewer spectrophotometers are also used to measure spectral UV irradiance, the sulphur dioxide column and aerosol optical depth. Some Brewer spectrophotometers are also able to measure the nitrogen dioxide column. This harmonised Brewer network (Fig. 6.4) constitutes the largest harmonised ground-based UV network in the world, available for assimilation into satellite retrievals and models to greatly improve accuracy of the satellite data and ozone and UV radiation forecasting. Another important point is the link to climate change where tropospheric ozone and aerosols are still regarded as having the largest effect on uncertainties in climate models. The Brewer instruments are suitable for the measurement of total column ozone which includes both tropospheric and stratospheric ozone whereas satellites struggle with the lower altitudes.

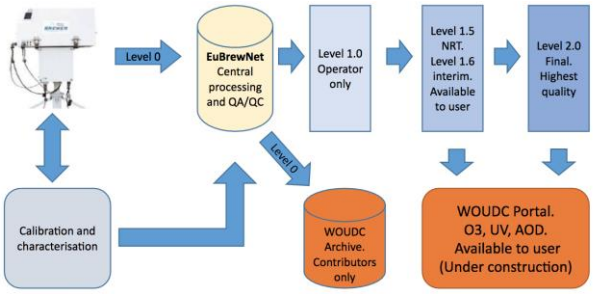

Figure 6.5. EUBREWNET database architecture.

The actual implementation of the network can be summarized as follows:

- Automated data transfers to central database (Fig. 6.5) started in September 2014. Data submission now became automatic with little operator involvement so improving overall submission rates.
- Calibration data are stored in a central database. This allows for central processing of all stations' data so ensuring consistency and use of up-to-date calibration and processing.
- Near Real Time (NRT) data. Central data processing in addition to data processing at the stations: including part of QC by comparison with near instruments and state of the art algorithms. NRT data is essential for NRT validation of satellite data and model assimilations.
- Central re-processing. Historical data or changes in constants recommended by WMO Ozone and UV SAG.
- Central QA/QC systems (QA/QC validated in one place): stations with a problem can be easily identified.

As part of the support provided by AEMET, a new domain has been registered for EUBREWNET. The new address to access the EUBREWNET site is https://eubrewnet.aemet.es. This domain will be used by default and will come to replace the eubrewnet.org domain that will be removed in a few months. In the meantime, all access to eubrewnet.org will be redirected to the new domain.

6.3.2 Ozone developments in EUBREWNET

The determination of the total ozone column uncertainty has been fully implemented in EUBREWNET for both the standard (V1) and the improved (V2) Brewer algorithms. Access functions to download the data are available for product levels 1 and 1.5, as described in the EUBREWNET wiki. Furthermore, monthly data files are being produced in various formats, including the NASA GEOMS.

New tools for the ozone calibration of Brewer spectrophotometers are also now available at EUBREWNET's data server. These include a new function to determine the Extra-terrestrial Constant (ETC) using the Langley-plot method (Fig. 6.6), as well as functions to determine the so-called ETC filter corrections by different methods. For more details, see the Calibration Functions section in the EUBREWNET wiki.

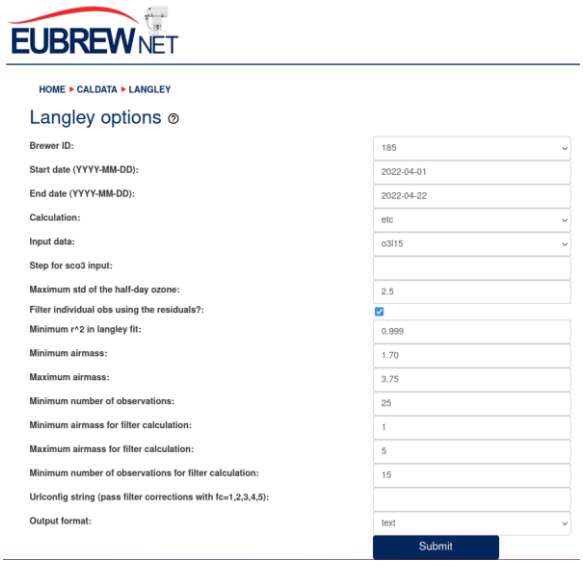

Figure 6.6. EUBREWNET new calibration tool for the determination of the ETC via the Langley-plot method.

Zenith Sky (ZS) measurements are now also fully processed by EUBREWNET's data server, and ozone ZS level 1, 1.5, and 2 products are available here.

Automatic monthly ozone data submission to the WOUDC and ESA Validation Data Center (EVDC) is now available as an option for the stations registered in EUBREWNET.

6.3.3 New UV products in EUBREWNET

Raw UV data is available at EUBREWNET since 2014. Following the ozone and AOD products scheme, we have now implemented four new levels for UV products (Fig.6.7):

- **Level 1** starts from the raw data and implements the dark-count and deadtime corrections to the counts. For Mk II and IV Brewers, the stray-light correction is also added. Finally, the raw counts are converted to irradiances using the UVR files previously uploaded to EUBREWNET.
- **Level 1.5** builds up from level 1 and adds spike and temperature corrections. The spike correction follows the method described in Meinander et al. (2003). The data required for the temperature correction can be obtained following the experimental procedure described in Lakkala et al. (2008). Brewer operators can also define an exclusion list to remove unwanted data.
- **Level 1.6** returns corrected irradiances calculated by the SHICrivm code developed by Harry Slaper at the National Institute of Public Health and the Environment (RIVM). SHICrivm's QA/QC is also available.
- **Level 2.0** adds the cosine correction as implemented in the BUVIC code developed by Basile Maret and Julian Gröbner at PMOD/WRC (Gröbner and Maret, 2020).

These UV product levels, and the access functions available to retrieve the information, are described in more detail in the EUBREWNET wiki.

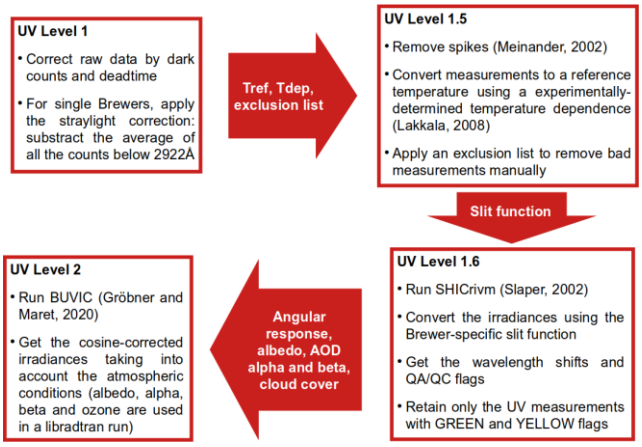

Figure 6.7. Summary of the new levels of UV products implemented in EUBREWNET.

Note that, besides the Brewer UV measurements, the Brewer operator is expected to provide a UV configuration. We have implemented a web interface (Fig. 6.8) similar to that for ozone and AOD, with different sections where the operator can provide the UV response file to convert raw counts to irradiances, plus the required data to perform the temperature and cosine corrections. See the EUBREWNET wiki for a complete description of the configuration interface.

Figure 6.8. UV configuration interface showing the UV response section. Note there are also sections for the temperature and cosine corrections, plus another for the exclusion list.

6.3.4 AOD updates in EUBREWNET

We have continued to process and evaluate AOD in the 306-320 nm wavelength range. This near-real-time product is derived from the same data used in the ozone Direct Sun (DS) measurements, as described in the EUBREWNET wiki. As a field exercise, during the Davos 2021 RBCC-E campaign, we transferred the AOD configuration of Brewer#185 (the RBCC-E travelling reference) to most of the participating Brewers. The AOD calculated using these configurations was then found to be in a reasonable agreement in most cases (Fig. 6.9).

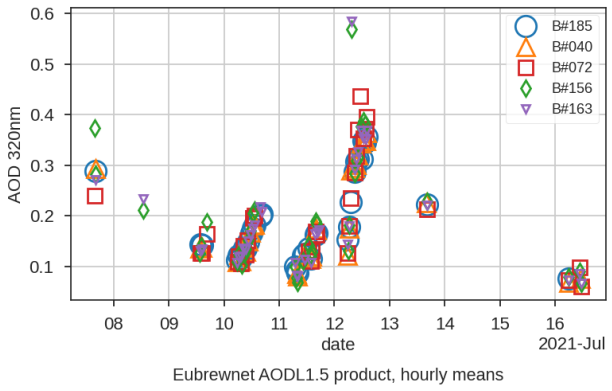

Figure 6.9. Hourly means of the EUBREWNET AOD L1.5 product at 320 nm, for instruments participating in the Davos 2021 RBCC-E campaign. Brewer#185 was calibrated by the Langley-plot method using measurements at the Izaña Observatory. The other instruments were calibrated by transfer from Brewer#185 during the campaign.

Furthermore, the AOD-specific "JG" Brewer measurements are now fully parsed and processed by EUBREWNET's data server. For Brewer spectrophotometers with the required AOD calibration parameters, these measurements allow for the determination of the AOD in an extended wavelength range, reaching up to ~360 nm for Mk III instruments. See the EUBREWNET wiki for further details on accessing and downloading the data. Although work on the determination of the optimal calibration parameters is on-going, a preliminary comparison with data from AERONET shows promising results (Fig. 6.10).

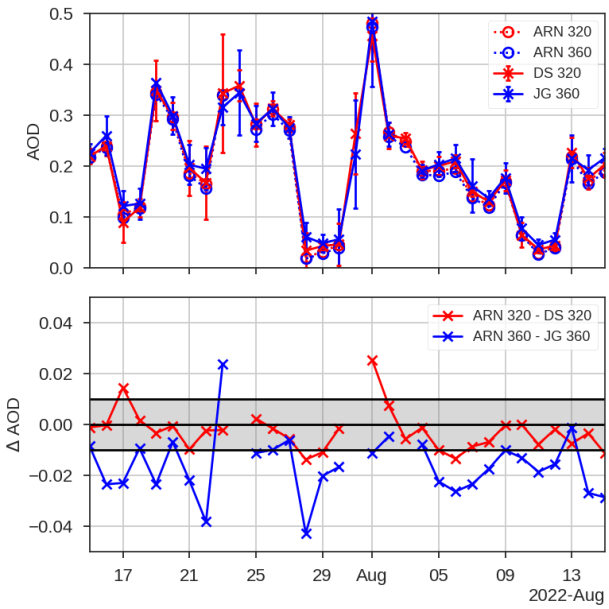

Figure 6.10. Comparison between AERONET (ARN) and EUBREWNET (DS and JG measurements) AOD data. The upper panel shows the daily medians of AOD at 320 (red) and 360 nm (blue). In the case of AERONET, both datasets have been extrapolated from the 340 nm data using the 340-440 nm Ångström exponent. The lower panel shows the AOD differences, the shaded grey area marking the ±0.01 difference which approximately corresponds to the limit of the WMO traceability criteria.

6.3.5 Pandonia Global Network

The Pandora Spectrometer System is a ground-based, sun/sky/lunar passive remote sensing instrument for the retrieval of trace gases in the UV/Vis spectral wavelengths. It was developed in 2005 by NASA and the Sciglob company, and since that time the Pandora spectrometer system has evolved. The Pandonia Network, funded by ESA through the LuftBlick company, has unified the operating and calibration procedures for the Pandora instruments since 2011.

NASA and ESA are currently collaborating to expand the global network of standardized, calibrated Pandora instruments focused on atmospheric composition. Through this collaboration the Pandonia Network became the Pandonia Global Network (PGN), which emphasizes: homogeneous calibration of instrumentation, low instrument manufacturing and operation costs, remote operative assistance, and central data processing and formatting for near-real-time delivery of final data products.

A major joint objective is to support the validation and verification of more than a dozen of Low Earth Orbit (LEO) and Geostationary Orbit (GEO) satellites, most notably Sentinel 5P, TEMPO, GEMS and Sentinel 4. PGN participants are primarily comprised of governmental and academic researchers and technicians. The launch of the PGN in early 2018 represented a programmatic shift by NASA and ESA away from primarily operating and supporting the research and field campaign operations, to establishing long-term fixed locations that are focused on providing long-term quality observations of total column and vertically resolved concentrations of a range of trace gases. The major trace gases observed by the Pandora systems across the range of 280 - 530 nm include: O_3, NO_2, HCHO, SO_2 and BrO.

Figure 6.11. Pandora 101 mounted at IZO.

The Izaña Observatory is one of the most important Pandora instrument testing sites together with the Innsbruck Atmospheric Observatory (University of Innsbruck, Austria). Two Pandora instruments were in operation at Izaña during 2021-2022, the Pandora 101 (1S model, UV, 270-530 nm) owned by the Izaña Observatory (Fig.6.11) and the Pandora 121 (2S model, UV 270-530 nm + VIS 400-900 nm) owned by LuftBlick (Fig. 6.12).

Figure 6.12. Daniel Santana and the Pandora 121 mounted at IZO.

Both instruments received funds from the PGN operational project from ESA to go through an important hardware upgrade at LuftBlick laboratories which includes a new tracker model which improves significantly the pointing accuracy. This upgrade has now been applied to P121 and P121 was back in operation at IZO in December 2022. P101 was sent to LuftBlick in February 2022 to receive the upgrade and is awaiting return.

In addition, funds were received through ESA to purchase and test a third Pandora instrument at Izaña Observatory (P209). This instrument includes a new set of filters and a new technology of high-speed low noise Complementary Metal-oxide-Semiconductor (CMOS) spectrometers (Avantes EVO). P209 was installed in IZO in July 2022 (Fig. 6.13).

Figure 6.13. Pandora 209 installed at IZO in July 2022.

Izaña is an invaluable PGN testing location, not only for testing the performance of the hardware, but also for data intercomparison (e.g. total ozone column) and algorithm development due to its remote location, the large fleet of auxiliary datasets and highly experienced staff. Trace gas column amounts from Pandora data are retrieved utilizing a DOAS like algorithm, where the gas absorption features in a measured spectrum are compared to an absorption-free reference spectrum.

The standard method to process total ozone column in PGN is based on the use of a theoretical reference spectrum, assuming a fixed effective ozone temperature in the atmosphere. This leads to seasonal differences of up to 1% and a 3 % bias between the standard Pandora and Brewer TOC data (Zhao et al., 2016). Currently, updated total ozone column algorithms are being implemented within the PGN. The first algorithm is similar to the current standard but includes the correction of the effective ozone temperature by using the TOMS v8 ozone profile climatology. The second algorithm relies on a novel calibration technique to create an absorption-free synthetic reference spectrum for the retrieval and also derives the effective ozone temperature explicitly.

The current activities at Izaña related to PGN are focused on maintaining the operation of the instruments, testing new hardware improvements on demand, and serving as a testbed for algorithm refinement and development.

We participated as authors or co-authors in Berjon et al. (2021a, b, c; 2022), García et al. (2021a, 2021b), Hedelt et al. (2022), López-Solano (2021a, b, c; 2022), Parra-Rojas et al. (2021a, b, c, d, e: 2022a, b) and Redondas et al. (2021a, b; 2022).

6.4 References

Berjon, A., Redondas, A., López-Solano, J., Carreno, V., Parra-Rojas, F., León-Luis, S.F.: Reprocessing of the RBCC-E triad ozone series. Talk presented at 18th WMO-GAW Brewer Workshop (online), June 14, 2021a.

Berjon, A., Redondas, A., López-Solano, J., Carreno, V., Parra-Rojas, F., León-Luis, S.F.: Reprocessing of the RBCC-E Izaña Observatory triad ozone series. Talk presented at Quadrennial Ozone Symposium (online), October 9, 2021b. Available from: http://qos2021.yonsei.ac.kr/

Berjon, A., Redondas, A., Rimmer, J.S., López-Solano, J., Parra-Rojas, F., Carreno, V., León-Luis, S.F.: EUBREWNET Updates. Talk presented at Nordic Ozone and UV group annual meeting 2021 (online), April 20, 2021c.

Berjon, A., Redondas, A., Rimmer, J.S., López-Solano, J., Parra-Rojas, F., Carreno, V.: Eubrewnet. Sharing data with other databases (WOUDC, NDACC, EVDC). Talk presented at Nordic Ozone and UV group annual meeting 2022 (Kjeller, Norway), April 26, 2022.

García, O.E., E. Sanromá, M. Schneider, F. Hase, S.F. León-Luis, T. Blumenstock, E. Sepúlveda, A. Redondas, V. Carreño, C. Torres, and N. Prats, Ozone monitoring by NDACC FTIR spectrometry: improved retrieval strategy and impact of instrumental line shape characterisation, Quadrennial Ozone Symposium, virtual, 3-9 October, 2021a.

García, O., Sanromá, E., Schneider, M., Hase, F., León-Luis, S.F., Blumenstock, T., Sepúlveda, E., Redondas, A., Carreño, V., Torres, C., and Prats, N., Ozone monitoring by NDACC FTIR spectrometry: improved retrieval strategy and impact of instrumental line shape characterization, TCCON/COCCON/NDACC Meeting 2021 (online), 8-10 June, 2021b.

Gröbner, J. and Maret, B. 2020. BUVIC – Brewer UV Irradiance Calculation, https://github.com/pec0ra/buvic

Hedelt, P., D. Loyola, A. Redondas, A. Barreto, O. Garcia, L. Doppler, J. Reichardt, Analysis of the 2021 Cumbre Vieja eruption and the long-range transport of SO_2 to Europe using TROPOMI and ground-based measurements, Sentinel-5P Mission: 5 years anniversary, Taormina (Italy), 10 – 14 October, 2022.

Lakkala K., Arola, A., Heikkilä, A., Kaurola, J., Koskela, T., Kyrö, E., Lindfors, A., Meinander, O., Tanskanen, A., Gröbner, J., Hülsen, G., Quality assurance of the Brewer spectral UV measurements in Finland, Atmospheric Chemistry and Physics, 8, 3369-3383, 2008.

López-Solano, J., Redondas, A., León-Luis, S.F., Berjón, A., Carreño, V., Parra-Rojas, F.C.: Aerosol Optical Depth in EUBREWNET. Talk presented at Brewer Ozone Spectrophotometer Open Workshop (online), June 14, 2021a.

López-Solano, J., Redondas, A., León-Luis, S.F., Berjón, A., Carreño, V., Parra-Rojas, F.C.: Aerosol Optical Depth in EUBREWNET. Talk presented at Nordic Ozone and UV group (NOG) annual meeting 2021 (online), April 21, 2021b.

López-Solano, J., Redondas, A., Rimmer, J., Berjón, A., Parra-Rojas, F.C., Carreño, V., León-Luis, S.F.: EUBREWNET: An Overview of Recent Advances. Talk presented at Quadrennial Ozone Symposium (online), October 9, 2021c.

López-Solano, J., Redondas, A., Gröbner, J., Maret, B., Lakkala, K., León-Luis, S.F., Carreño, V., Berjón, A., Parra-Rojas, F.C.: New UV products in EUBREWNET. Talk presented at Nordic Ozone and UV group annual meeting 2022 (online), April 27, 2022.

Meinander O., Josefsson, W., Kaurola, J., Koskela, T., Lakkala, K., Spike detection and correction in Brewer spectroradiometer ultraviolet spectra, Optical Engineering, 42(6), 1812-1819, 2003.

Parra-Rojas, F.C., Redondas, A., Berjón, A., López-Solano, J.: Total ozone uncertainty model on Brewer Algorithm. Talk presented at Quadrennial Ozone Symposium (online), October 3, 2021a.

Parra-Rojas, F.C., Redondas, A., Berjón, A., López-Solano, J.: Total ozone uncertainty model on Brewer Algorithm. Talk presented at WMO-GAW Brewer Workshop (online), June 14, 2021b.

Parra-Rojas, F.C., Redondas, A., Berjón, A., López-Solano, J.: A new data set for the Brewer spectrophotometer uncertainty budget in the total ozone column measurements. Talk presented at EGU General Assembly 2021 (online), April 30, 2021c. Available from: https://doi.org/10.5194/egusphere-egu21-15316

Parra-Rojas, F.C., Redondas, A., Berjón, A., López-Solano, J.: Total ozone uncertainty model on Brewer Algorithm and its implementation in EuBrewNet. Talk presented at Metrology for Meteorology and Climate Webminar (online), April 26, 2021d.

Parra-Rojas, F.C., Redondas, A., Berjón, A., López-Solano, J.: Total ozone uncertainty model on Brewer Algorithm. Talk presented at Nordic Ozone and UV group annual meeting (online), April 20, 2021e.

Parra-Rojas, F.C., Redondas, A., Berjón, A., López-Solano, J.: Total ozone uncertainty model implemented on EuBrewNet. Talk presented at Internal Radiation Symposium (Thessaloniki), July 4, 2022a.

Parra-Rojas, F.C., Redondas, A., Berjón, A., López-Solano, J.: Total ozone uncertainty model implemented on EuBrewNet. Talk presented at Nordic Ozone and UV group annual meeting 2022 (online), April 26, 2022b.

Redondas, A., Parra-Rojas, F.C., Berjón, A., López-Solano, J., Bais, A., Gröbner, J., De Bock, V., Karppinen, T., Vilaplana, J.M.: Eubrewnet Brewer updated algorithm, total ozone in seven European stations: Sodankyla, Davos, Uccle, Thessaloniki, Madrid, El Arenosillo and Izaña. Talk presented at Quadrennial Ozone Symposium (online), October 9, 2021a.

Redondas, A., Parra-Rojas, F.C., Berjón, A., López-Solano, J., Bais, A., Gröbner, J., De Bock, V., Karppinen, T., Vilaplana, J.M.: Eubrewnet Brewer updated algorithm, total ozone in seven European stations: Sodankyla, Davos, Uccle, Thessaloniki, Madrid, El Arenosillo and Izaña. Talk presented at Nordic Ozone and UV group annual meeting (online), April 20, 2021b.

Redondas, A., López-Solano, J., Gröbner, J., Maret, B., Lakkala, K., León-Luis, S.F., Carreño, V., Berjón, A., Parra-Rojas, F.C.: UV in EUBREWNET. Poster presented at International Radiation Symposium (Thessaloniki), July 4, 2022.

Rimmer, J. A. Redondas, and T. Karppinen, EuBrewNet – A European Brewer network (COST Action ES1207), an overview, Atmospheric Chemistry and Physics, 18, 10347–10353, 2018.

Zhao, Xiaoyi, Vitali Fioletov, Alexander Cede, Jonathan Davies, and Kimberly Strong. 2016. "Accuracy, Precision, and Temperature Dependence of Pandora Total Ozone Measurements Estimated from a Comparison with the Brewer Triad in Toronto." Atmospheric Measurement Techniques 9 (12): 5747–61. https://doi.org/10.5194/amt-9-5747-2016.

A list of publications involving EUBREWNET is available here.

A list of publications involving the Pandonia Global Network is available here.

6.5 Staff

Alberto Redondas Marrero (AEMET; Head of programme)

Virgilio Carrreño (AEMET; Meteorological Observer-GAW Technician)

Dr Alberto Berjón (TRAGSATEC; Research Scientist)

Dr Javier López Solano (TRAGSATEC; Research Scientist)

Dr Francisco Parra Rojas (Universidad Interamericana de Puerto Rico; Associate Professor)

Daniel Santana Díaz (LuftBlick; Pandonia Global Network Research Scientist)

Dr Sergio León Luis (TRAGSATEC; Research Scientist)

7 Fourier Transform Infrared Spectroscopy (FTIR)

7.1 Main Scientific Goals

Earth observations are fundamental for understanding the drivers of climate change and thus for supporting decisions on adaptation and mitigation strategies. Atmospheric remote sounding from space and ground are essential components of the observational strategy. In this context, the Fourier transform infrared spectroscopy (FTIR) programme at the IARC was established with the main goals of long-term monitoring of atmospheric gas composition (ozone related species and greenhouse gases) and for the validation of satellite remote sensing measurements and climate models. Much effort within the FTIR programme has been put in developing new strategies for observing tropospheric water vapour isotopologues from ground and space-based remote sensors, since these observations play a fundamental role in understanding atmospheric water cycle and its links to the global energy and radiation budgets.

The FTIR programme at the IARC is the result of the close and long-lasting collaboration of more than two decades between the IARC-AEMET and the IMK-ASF-KIT (Institute of Meteorology and Climate Research-Atmospheric Trace Gases and Remote Sensing, Karlsruhe Institute of Technology, Germany). The IMK-ASF has operated high-resolution ground-based FTIR systems for almost three decades and they are leading contributors in developing FTIR inversion algorithms and quality control of FTIR solar measurements. As a result of this collaboration, the FTIR observations at IZO have contributed to the prestigious international networks NDACC and TCCON since 1999 and 2007, respectively.

7.2 Measurement Programme

A ground-based high-resolution FTIR experiment (HR FTIR in the following) for atmospheric composition monitoring has two main components: a precise solar tracker that captures the direct solar light beam and a high-resolution Michelson interferometer (IFS) (Fig. 7.1). IARC's FTIR activities started in 1999 with a Bruker IFS 120M spectrometer, which was replaced by a Bruker IFS 120/5HR spectrometer in 2005 (see technical specifications in Table 7.1).

In the framework of TCCON and NDACC, a new IFS 125HR spectrometer was purchased by AEMET and installed in August 2022 at IZO in order to replace the current instrument (lower panel of Figure 7.1). Both instruments will operate side-by-side for at least one year to ensure the consistency of the FTIR time series at IARC.

Figure 7.1. Upper panel: the ground-based FTIR experiment implemented in 2005 at the IARC. Lower panel: the new ground-based FTIR experiment implemented in 2022. For both experiments, the scientific laboratory is shown on the left panel, and the Michelson interferometer is shown on the right panel.

In order to derive trace gas concentrations from the recorded FTIR solar absorption spectra, synthetic spectra are calculated by the line-by-line radiative transfer model PRFWD (Schneider and Hase, 2009). Then, the synthetic spectra are fitted to the measured ones by the software package PROFFIT (PROFile FIT, Hase et al., 2004)

PROFFIT allows to retrieve volume mixing ratio (VMR) profiles and to scale partial or total VMR profiles of several species simultaneously. There have been a lot of efforts for assuring and even further improving the high quality of the FTIR data products: e.g., monitoring the instrumental line shape (Hase et al., 1999), monitoring and improving the accuracy of the applied solar trackers (Gisi et al., 2011), as well as developing sophisticated retrieval algorithms (Hase et al., 2004). The good quality of these long-term ground-based FTIR data sets has been extensively documented by theoretical and empirical validation studies (e.g., Schneider et al., 2008; Schneider et al., 2010; García et al., 2012; Sepúlveda et al., 2012).

In 2021 a portable and low-resolution FTIR spectrometer (LR FTIR in the following), the Bruker EM27/SUN, was acquired by IARC. This instrument operates within the Collaborative Carbon Column Observing Network (COCCON) (Frey et al., 2019, Alberti et al., 2022) and is mainly dedicated to the participation in field campaigns (see section 7.3.2).

Table 7-1. Technical Specifications for Bruker IFS 120/5HR (in brackets, if different for 120M).

Manufacturer, Model	Bruker, IFS 120/5HR [IFS 120M]
Spectral range (cm^{-1})	700 - 4250 (NDACC) and 3500 - 9000 (TCCON) Optional: 20 - 43000
Apodized spectral resolution (cm^{-1})	0.0025 [120M: 0.0035]
Resolution power ($\lambda/\Delta\lambda$)	$2 \cdot 10^5$ at 1000 cm^{-1}
Typical Scan velocity (cm/s)	2.5 (scan time about 100 s @ 250 cm of Optical Path Difference)
Field of view (°)	0.2
Detectors	MCT and InSb (NDACC); InGaAs (TCCON)
Size (cm)/Weight (kp)/Mobility	320 x 160 x 100 [120M: 200 x 80 x 30] 550 + 70 (Pump) [120M: 100 + 30 (Electronics)] Installed inside container, limited mobility
Quality assurance system	Routine N_2O and HCl cell calibrations to determinate the Instrumental Line Shape

The FTIR programme at the IARC was complemented by two Picarro L2120-I δD (standardized ratio between $H_2{}^{16}O$ and $HD^{16}O$) and $\delta^{18}O$ (standardized ratio between $H_2{}^{16}O$ and $H_2{}^{18}O$) analysers installed at IZO and TPO (González et al., 2016). The instrument, which had been operational at the SCO station since 2019 to monitor the isotopic footprint of the maritime boundary layer, ceased functioning at the end of 2020. The Picarro spectrometers are based on the Wavelength-Scanned Cavity Ring-Down Spectroscopy (WS-CRDS) technology and are calibrated by injecting liquid standards in a Standard Delivery Mode (SDM). The 0.6 Hz-precision of the analyzer on δD is <13.5‰ at 500 ppm H_2O and is <2‰ for 4000 ppm. The absolute uncertainty for δD is <13.7‰ at 500 ppm and <2.3‰ at 4500 ppm. The absolute uncertainty for $\delta^{18}O$ is <0.12‰ at 12,500 ppm at 0.1 Hz. The error estimation accounts for instrument precision as well as errors due to the applied data corrections (Standards Delivery Module (SDM) effects + instrumental drifts <1‰, liquid standard bias <0.7‰, calibration bias <0.5‰) for δD.

7.3 Summary of remarkable results during the period 2021-2022

The FTIR activities from 2019 to 2020 have been focused on ground and space-based remote sensing FTIR spectrometry.

7.3.1 Ground-based high-resolution FTIR spectrometry

The ground-based HR FTIR observations have a large potential to support analysis of the composition of the troposphere, the stratosphere and their exchange processes. This is fundamental to monitor and study, for example, the sources and sinks of greenhouse gases or the evolution of the ozone layer. Routinely, the IARC HR FTIR have contributed to NDACC with C_2H_6, $ClONO_2$, CO, CH_4, COF_2, HCl, HCN, HF, H_2CO, HNO_3, N_2O, NO_2, NO, O_3 and OCS observations (total column amounts and VMR vertical profiles) since 1999. Within TCCON, total column-averaged abundances of CO_2, N_2O, CH_4, HF, CO, H_2O and HDO have been measured since 2007 (Fig. 7.2).

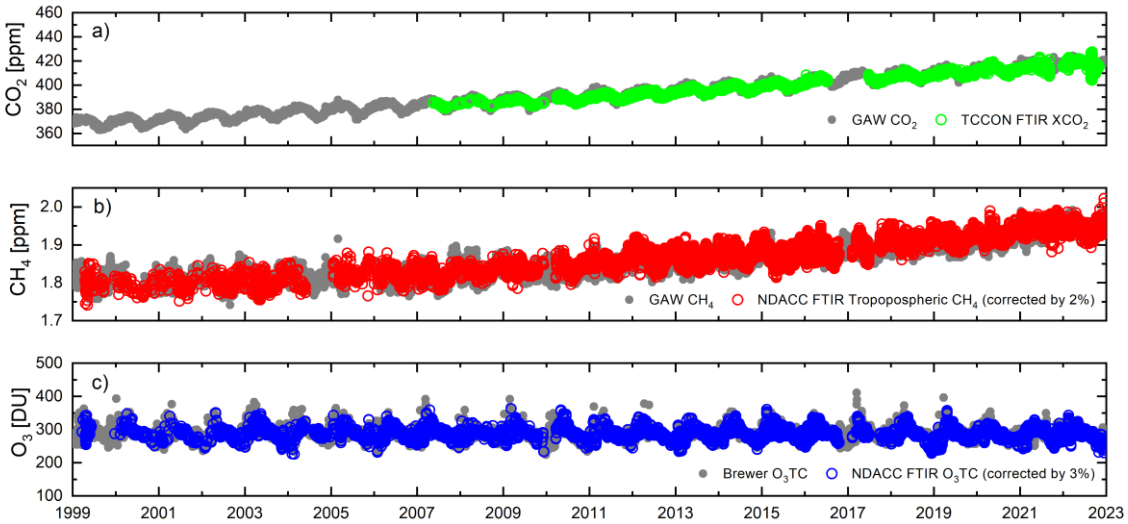

Figure 7.2. Time series of the total column-averaged abundances of a) carbon dioxide (XCO_2) in the framework of TCCON, b) tropospheric methane (CH_4) and c) ozone total column (O_3TC) amounts in the framework of NDACC as observed by the IARC FTIR. For comparison, the time series of these trace gases as observed by other high-quality measurement techniques available at the IARC are also displayed (GAW in-situ records for CO_2 and CH_4, and Brewer O_3TC amounts for O_3)

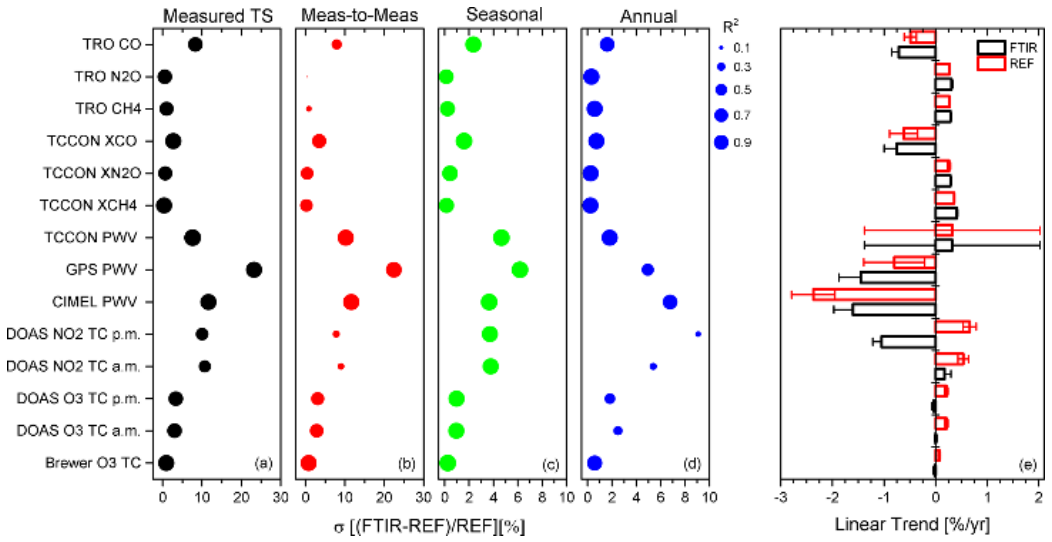

Figure 7.3. Summary of timescale comparison between FTIR and IZO reference data sets: standard deviation of the relative differences (σ, in %) is displayed on the x axis, and the size of dots represents the determination coefficient, R^2. These statistics are shown for the comparison of (a) measured and decomposed time series: (b) measurement-to-measurement, (c) seasonal, and (d) long-term variations (annual means). (e) Linear trends (in % yr^{-1}) for coincident FTIR and reference data sets. Errors represent the 95 % confidence interval. Note that TRO refers to the comparison of the tropospheric quantities (GAW in-situ records and FTIR VMR averages). Reprinted from García et al. (2021).

Coinciding with the 20th anniversary of the implementation of the NDACC program at IARC, reached in 2019, the study by García et al. (2021a) documents the quality and long-term consistency of the IZO NDACC FTIR products by using all reference observations available at IZO within the period 1999–2018. Note that this comparison exercise is performed only for those NDACC trace gases for which other high-quality measurement techniques are available at IZO (CH_4, CO, H_2O, NO_2, N_2O, and O_3) on different timescales (see Fig. 7.3, and García et al., 2021a for more details).

With these refined time series, we have participated in numerous studies at a global scale. For example, the IARC HR FTIR station has been one of the 20 NDACC FTIR stations used to investigate the level of optical resonances ("channeling") of each FTIR spectrometer within NDACC (Blumenstock et al., 2021). Dedicated spectra were recorded using a laboratory mid-infrared source and two operational detectors. In the indium antimonide (InSb) detector domain (1900–5000 cm^{-1}), the amplitude of the most pronounced channeling frequency amounts from 0.1‰ to 2.0‰ of the spectral background level. In the mercury cadmium telluride (HgCdTe) detector domain (700–1300 cm^{-1}), stronger effects were documented with the largest amplitude ranging from 0.3‰ to 21‰ (see Fig. 7.4). The observed channeling frequencies were found to be caused by the optical thickness of the beam splitter substrate, and the air gap in between the beam splitter and compensator plate. A new beam splitter design was proposed to potentially reduce channeling impacts on the NDACC FTIR spectrometers, thereby increasing the quality of recorded spectra across the network (Blumenstock et al., 2021).

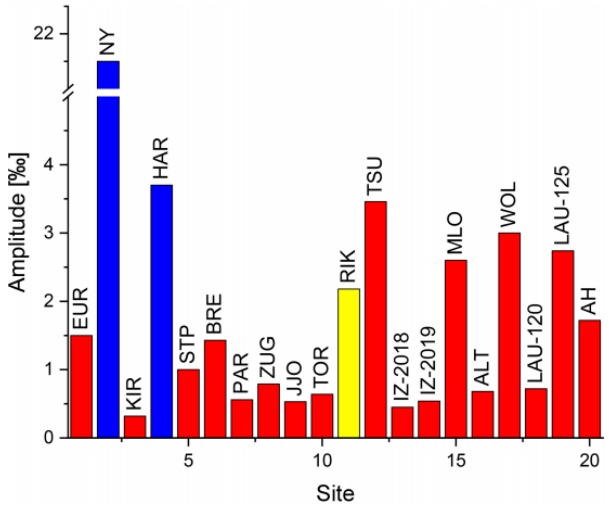

Figure 7.4. Amplitude of channelling in the HgCdTe spectrum. Red, yellow, and blue bars indicate channelling due to the beam splitter air gap, beam splitter substrate, and detector window, respectively. Note that IZO NDACC station is named as "IZ". Reprinted from Blumenstock et al. (2021).

Other studies have investigated changes in key elements in the atmosphere such as CO_2, carbonyl sulphide (OCS) or formic acid (HCOOH). For example, Byrne et al. (2022) presented a pilot dataset of country-specific net carbon exchange (NCE; fossil plus terrestrial ecosystem fluxes) and terrestrial carbon stock changes aimed at informing countries' carbon budgets. These estimates are based on "top-down" NCE outputs from the v10 Orbiting Carbon Observatory (OCO-2) modeling intercomparison project (MIP), wherein an ensemble of inverse modelling groups conducted standardized experiments assimilating OCO-2 column-averaged dry-air mole fraction retrievals (ACOS v10), in situ CO_2 measurements or combinations of these data.

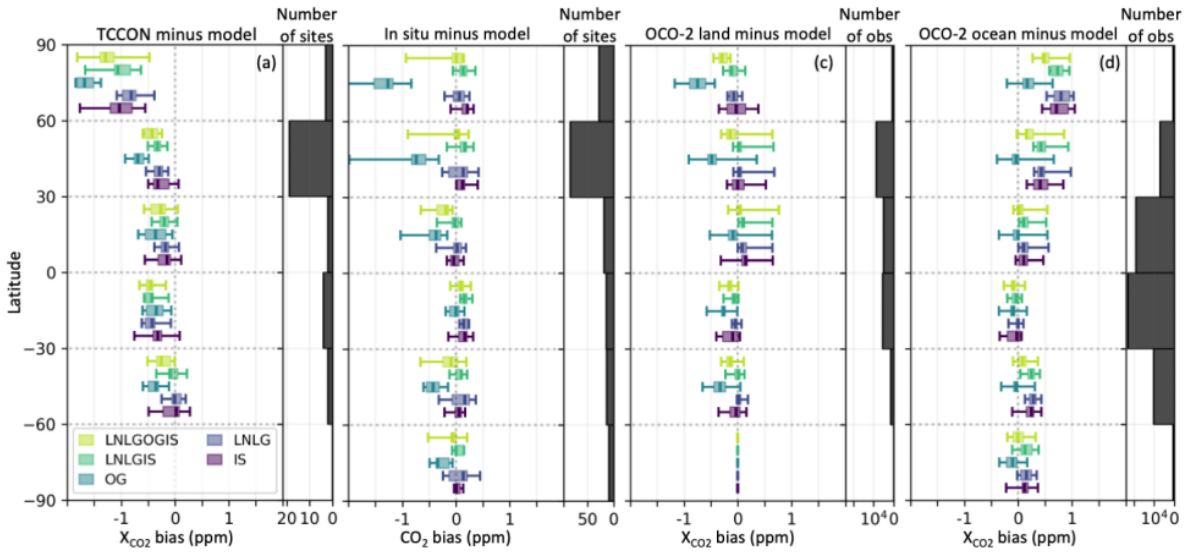

Figure 7.5. Median bias (data minus model) over 30º latitude bins averaged over 2015–2020 for (a) TCCON XCO_2 retrievals, (b) withheld in situ CO_2 measurements, (c) withheld OCO-2 land XCO_2 retrievals and (d) withheld OCO-2 ocean XCO_2 retrievals. The number of TCCON sites per 30º latitude bins are: 3 (60ºN-90ºN), 18 (30ºN-60ºN), 3 (0-30ºN), 3 (0-30ºS) and 2 (30ºS-60ºS). Reprinted from Byrne et al. (2022).

The v10 OCO-2 MIP NCE estimates are combined with "bottom-up" estimates of fossil fuel emissions and lateral carbon fluxes to estimate changes in terrestrial carbon stocks, which are impacted by anthropogenic and natural drivers. All v10 OCO-2 MIP experiments have been compared with co-located TCCON FTIR data at a global scale (Fig. 7.5), showing some biases against TCCON sites. In particular, low biases (high modelled CO_2) are found for 0º– 30ºS and 60º–90ºN. The underlying cause for these differences is unknown.

Regarding OCS, this compound is the most abundant sulphur containing gas in the atmosphere. It is important to quantify and understand OCS as it can be used to understand CO_2 and the carbon cycle, and also since it eventually is transported into the stratosphere, where it maintains the sulphate aerosol layer at about 20 km into the atmosphere. As recently pointed out by Hannigan et al. (2022), analyses of NDACC OCS partial columns at a global scale (including IZO among them, Fig. 7.6) allowed to detect that stratospheric OCS is increasing, north and south of the equator, but decreasing near the equator and increasing in the troposphere to 2016 and decreasing since then until 2020 (data not shown). The main drivers of OCS in the troposphere are the cumulative anthropogenic sources.

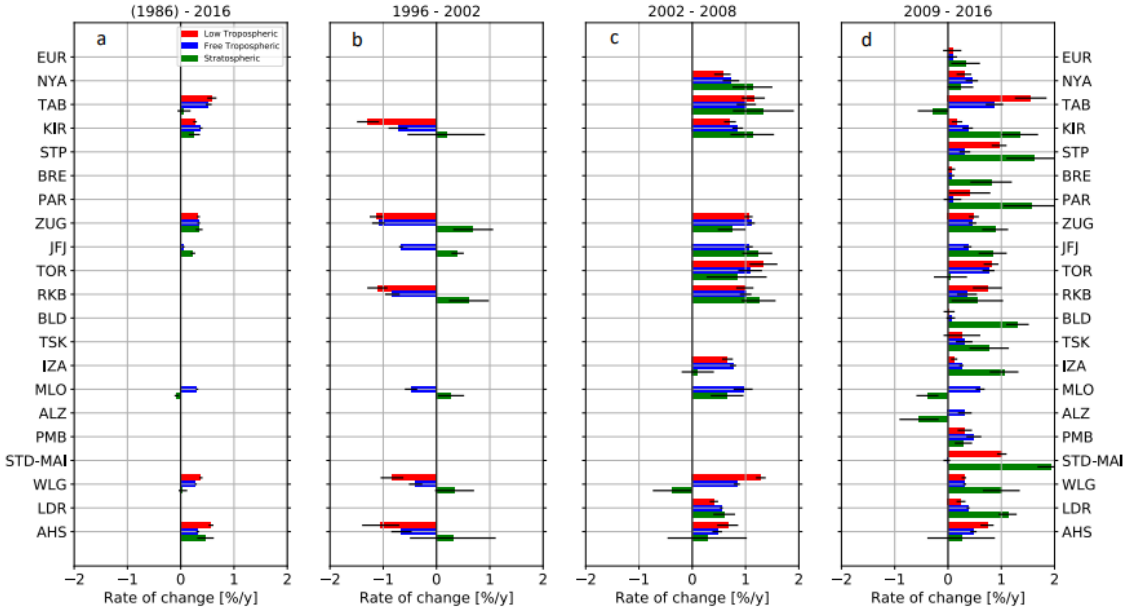

Figure 7.6. OCS trends by time period for all NDACC FTIR stations and for all three altitude ranges, listed by high to low latitude. Red represents the lower troposphere, blue the free troposphere and green the stratosphere. The left panel (a) are trends for only those sites with data from 1996, then increasing time period left to right, (b) 1996-2002, (c) 2002-2008, and (d) 2009-2016. Note that IZO NDACC station is named as "IZA". Reprinted from Hannigan et al. (2022).

In addition, CO_2 along with organic acids increasingly determine atmospheric acidity. Among the organic acids, formic acid facilitates the nucleation of cloud droplets and contributes to the acidity of clouds and rainwater. As recently shown by the Franco et al. (2021) study, published in the prestigious journal Nature, their findings reconcile model predictions and measurements of formic acid abundance. The additional formic acid burden increases atmospheric acidity by reducing the pH of clouds and rainwater by up to 0.3. The diol mechanism presented here probably applies to other aldehydes and may help to explain the high atmospheric levels of other organic acids that affect aerosol growth and cloud evolution.

Among the atmospheric gases with important climate effects, O_3 plays a vital role in atmospheric chemistry. Hence, high-quality and long-term O_3 measurements are essential for further improving our understanding of the O_3 response to natural and anthropogenic forcings, as well as to estimate consistent trends at a global scale. In this context, the IARC FTIR programme has developed several studies to improve O_3 monitoring by ground-based FTIR spectrometry by examining the performance of different O_3 retrieval strategies. As shown by García et al. (2022a), combining a simultaneous temperature retrieval with the optimal selection of single O_3 micro-windows results in superior FTIR O_3 products, with a precision of better than 0.6 % to 0.7 % for O_3 total columns (TCs) as compared to coincident NDACC Brewer observations taken as a reference. However, this improvement can only be achieved provided the FTIR spectrometer is properly characterized and stable over time. For unstable instruments, the temperature fit is found to exhibit a strong negative influence on O_3 retrievals due to the increase in the cross-interference between the temperature retrieval and instrumental performance (given by the instrumental line shape function and measurement noise), which leads to a worsening of the precision of FTIR O_3 TCs of up to 2 %. This cross-interference becomes especially noticeable beyond the upper troposphere/lower stratosphere, as documented theoretically as well as experimentally by comparing FTIR O_3 profiles to those measured using electrochemical concentration cell (ECC) sondes within NDACC (see Fig. 7.7).

In addition, García et al. (2022b) studied in more detail the impact of instrumental line shape (ILS) characterization on O_3 monitoring by FTIR spectrometry. This work concludes that, in order to ensure the independence of the O_3 retrievals and the instrumental response, the optimal approach to deal with the FTIR instrumental characterization is found to be the continuous monitoring of the ILS function by means of independent observations, such as gas cell measurements.

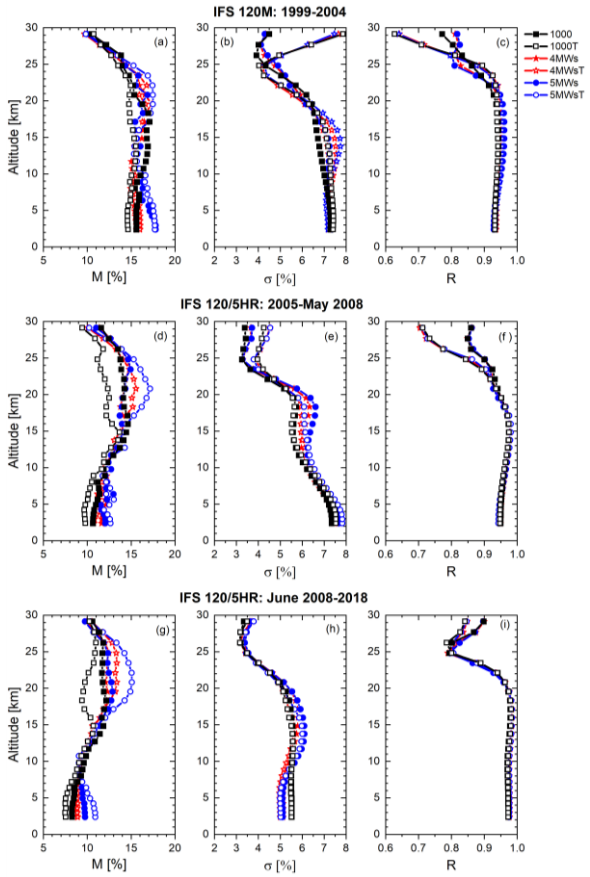

Figure 7.7. Summary of the FTIR–smoothed ECC comparison for the periods 1999–2004, 2005–May 2008, and June 2008–2018. Panels (a), (d), and (g) display the vertical profiles of median (M) RD (FTIR–ECC, in %) for the three periods, respectively. (b, e, h) As for (a), (d), and (g), but for the standard deviation of the RD distribution (σ, in %). (c, f, i) As for (a), (d), and (g), but for the Pearson correlation coefficient. Reprinted from García et al. (2022a).

Regarding O_3 and focused on the troposphere, the IARC HR FTIR O_3 time series also contributes to the Tropospheric Ozone Assessment Report, which has entered its second phase (TOAR-II) in 2020 until 2024 (see details in Section 5.3.6). The first TOAR phase, completed in 2019, offered remarkable results. For example, in Tarasick et al. (2019), various O_3 measurement methods and O_3 data sets are reviewed and selected for inclusion in the historical record of background O_3 levels, based on the relationship of the measurement technique to the modern UV absorption standard, absence of interfering pollutants, representativeness of the well-mixed boundary layer and expert judgement of their credibility. This overview work concludes that the great majority of validation and intercomparison studies of free tropospheric O_3 measurement methods use ECC ozonesondes as reference. Compared to UV-absorption measurements, ECC ozonesondes show a modestly high (~1–5% ± 5%) bias in the troposphere, but no evidence of a change with time. Umkehr, lidar, and FTIR methods all show modestly low biases relative to ECCs, and so, using ECC sondes as a transfer standard, all appear to agree to within one standard deviation with the modern UV-absorption standard. In relation to space-based observations, biases and standard deviations of satellite retrieval are often 2–3 times larger than those of other free tropospheric measurements.

As detailed in Section 5.3.5, Chang et al. (2022) and Steinbrecht et al. (2021) conducted an analysis addressing whether the COVID-19 crisis reduced the Free Tropospheric ozone across the Northern Hemisphere and the FTIR and ECC sonde measurements at Izaña Observatory contributed to these studies (for further details see Section 5.3.5).

In the framework of IZO activities as a WMO Measurement Lead Centre for Aerosols and Water Vapour Remote Sensing Instruments, the water vapour TCCON FTIR data have been used for the validation of new instrumentation for measuring water vapour content (e.g. García et al. 2021c). For further details see Sections 10 and 12.

CARBONSURVEY

In December 2022, the CarbonSurvey project ("Towards the Next Generation of Sensors for Surveying the Atmospheric Carbon Cycle") started, funded by the Spanish Ministry of Science and Innovation (TED2021-131695B-I00). The main expected contribution of this project is to develop a new generation of instruments to enable unprecedented CO_2 monitoring capabilities. These new sensors will provide an accurate measurement of the gas concentration not only at ground level, but also at the different layers of the atmosphere for a full characterization of the CO_2 distribution. Moreover, the sensing systems will be specifically designed for a straightforward in situ deployment in different areas of interest, providing full coverage of the most important blind spots existing today. The IARC CO_2 in situ and total column FTIR observations will serve as the reference for the validation of the new CO_2 sensors developed during this project.

7.3.2 Ground-based low-resolution FTIR spectrometry

The EM27/SUN spectrometer shares the same working principles as HR FTIR and, by covering the near infrared spectral range from 5000 to 11000 cm^{-1} with a spectral resolution of 0.5 cm^{-1}, it is able to measure total column-averaged amounts of O_2, CO_2, CH_4, CO and H_2O.

The IARC EM27/SUNs are operated in accordance with COCCON requirements (Frey et al., 2019; Alberti et al., 2022). This guarantees strict common methods for ensuring the quality of measurements (evaluation of the optical alignment and instrumental line shape), proper calibration of all COCCON spectrometers with respect to the TCCON site Karlsruhe and the COCCON reference EM27/SUN spectrometer operated permanently at KIT (in terms of the standard retrieved species), and adherence to the COCCON data analysis scheme ensures the generation of precise and accurate data products.

MEGEI

COCCON EM27/SUN instruments are a useful complement to the existing TCCON HR network in remote areas as its data can be used for the quantification of local sinks/sources and fluxes of greenhouse gases. With this idea, the IARC is leading the Spanish project, Monitoring greenhousE Gas EmIssions (MEGEI), to monitor greenhouse gas concentrations to evaluated fluxes in different environments by using the COCCON LR spectrometers. MEGEI activities are mainly focused on performing routine measurements at IARC IZO (background conditions) and SCO stations and in addition, on carrying out field campaigns under different atmospheric conditions.

As a result of the MEGEI-MAD experiment (García et al., 2021b), Tu et al. (2022a) developed a methodology to quantify CH_4 emissions from waste disposal sites near the city of Madrid using ground- and space-based observations of COCCON, TROPOMI and IASI. During MEGEI-MAD campaigns, strong CH_4 plumes were detected around the Madrid urban area with increases by about 10% with respect to the regional background. These emissions are likely due to the combined impact of several waste treatment plants located in the surrounding Madrid area, identified from emission inventory data as the only major sources of CH_4 in this area. This methodology was also successfully applied to the estimation of NO_2 emission strengths over Riyadh and Madrid (Tu et al., 2022b).

In December 2022, the first measurements of atmospheric total column-averaged abundances of XCO_2 and XCH_4 were conducted at the Juan Carlos I Antarctic base in the framework of the AEMET Antarctic campaign by using the

IARC COCCON LR instrument (see Fig. 7.8). These measurements mark a milestone in AEMET's observation program in Antarctica and will contribute to a better understanding of the greenhouse gas balance in the Earth climate system.

Figure 7.8. Image of the AEMET technician (Antonio Alcántara) operating the EM27/SUN spectrometer at Juan Carlos I Antarctic base, December 2022.

MAPP

In June 2020, the Metrology for aerosol optical properties (MAPP) project (19ENV04) started, supported by the European Metrology Programme for Innovation and Research (EMPIR). With a consortium of thirteen European organisations (AEMET-IARC among them), the overall goal of MAPP is to enable the SI-traceable measurement of column-integrated aerosol optical properties for assessing the climate radiative forcing. These properties are retrieved from the passive remote sensing of the atmosphere using solar and lunar radiation measurements that are largely lacking traceability to the SI. A secondary objective is to evaluate the retrieval of aerosol optical properties from emerging technologies such as solar and lunar spectroradiometers. The IARC FTIR programme has contributed to this activity by developing the methodology required to retrieved aerosol properties from EM27/SUN instruments (Álvarez et al., 2022a, b, see Fig. 7.9) and participating in the EMPIR field campaign carried out at IZO in September 2022. For further details about the MAPP project and the IARC contributions refer to Section 9 (Column Aerosols).

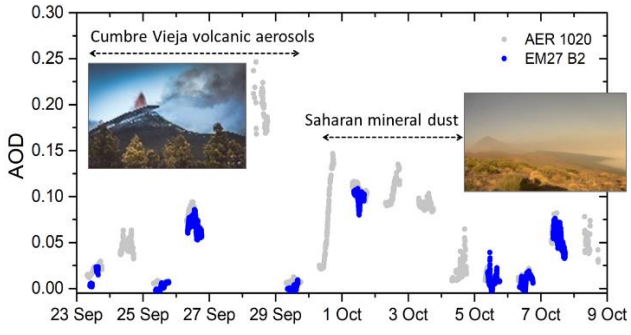

Figure 7.9. AERONET and EM27/SUN aerosol optical depth (AOD) at 1020 nm for a volcanic event followed by a Saharan mineral dust episode affecting IZO in 2021.

7.3.3 Space-based FTIR spectrometry

The IARC's high quality HR FTIR data have been extensively applied for many years for the validation of trace gases measured by different satellite instruments. During the period 2021-2022, particularly, IARC participated in the development and validation of new methodologies for CO, N_2O, O_3, XCH_4 and XCO_2 observations from space-based platforms like TROPOMI, IASI, TANSO-FTS, TANSat, OCO-2 and OCO-3 (Dogniaux et al., 2021; Massie et al., 2021; Noël et al., 2021; Sha et al., 2021; Zhang, et al., 2021a; Zhang, et al., 2021b; Keppens et al., 2022; Lopez et al., 2022; Peiro et al., 2022; Taylor et al., 2022; Vandenbussche et al., 2022; Wang et al., 2022).

Within space-based FTIR spectrometry, the activities of the group are mainly focused on IASI on board MetOp/EUMETSAT satellites and TROPOMI on board Sentinel-5P/ESA satellites through the Spanish project INMENSE (IASI for surveying methane and nitrous oxide in the troposphere) and the German-Swiss project MOTIV (MOisture Transport pathways and Isotopologues in water Vapour). Both projects strongly benefited from the European Research Council project MUSICA (MUlti-platform remote Sensing of Isotopologues for investigating the Cycle of Atmospheric water), which developed the MUSICA IASI processor (Schneider et al., 2022a). The processor performs an optimal estimation of the vertical distributions of H_2O, the δD ratio, N_2O, CH_4, and HNO_3. An example of the MUSICA IASI trace gas products at a global scale is displayed in Figure 7.10.

MOTIV

The MOTIV project aims at using water vapour isotopologues as a diagnostic tool to investigate moisture pathways and evaluate the representation of moist processes in weather and climate models. For this purpose, this project combines high-resolution IASI isotopologue observations, retrieved with the MUSICA processor (Schneider et al., 2022b) with high-resolution modelling from the Consortium for Small-Scale Modelling (COSMOiso). The combination of simulations and MUSICA products provides insight into the diurnal cycle, small-scale variations and effects of large-scale circulation on the moisture in the atmosphere. Within MOTIV, the space-based isotopologue observations are complemented by the in-situ continuous measurements recorded at IZO and PTO since 2012.

Due to its dryness, the subtropical free troposphere plays a critical role in the radiative balance of the Earth's climate system. Stable water isotopes can provide important information about several of the subtropical processes, namely subsidence drying, turbulent mixing, and dry and moist convective moistening.

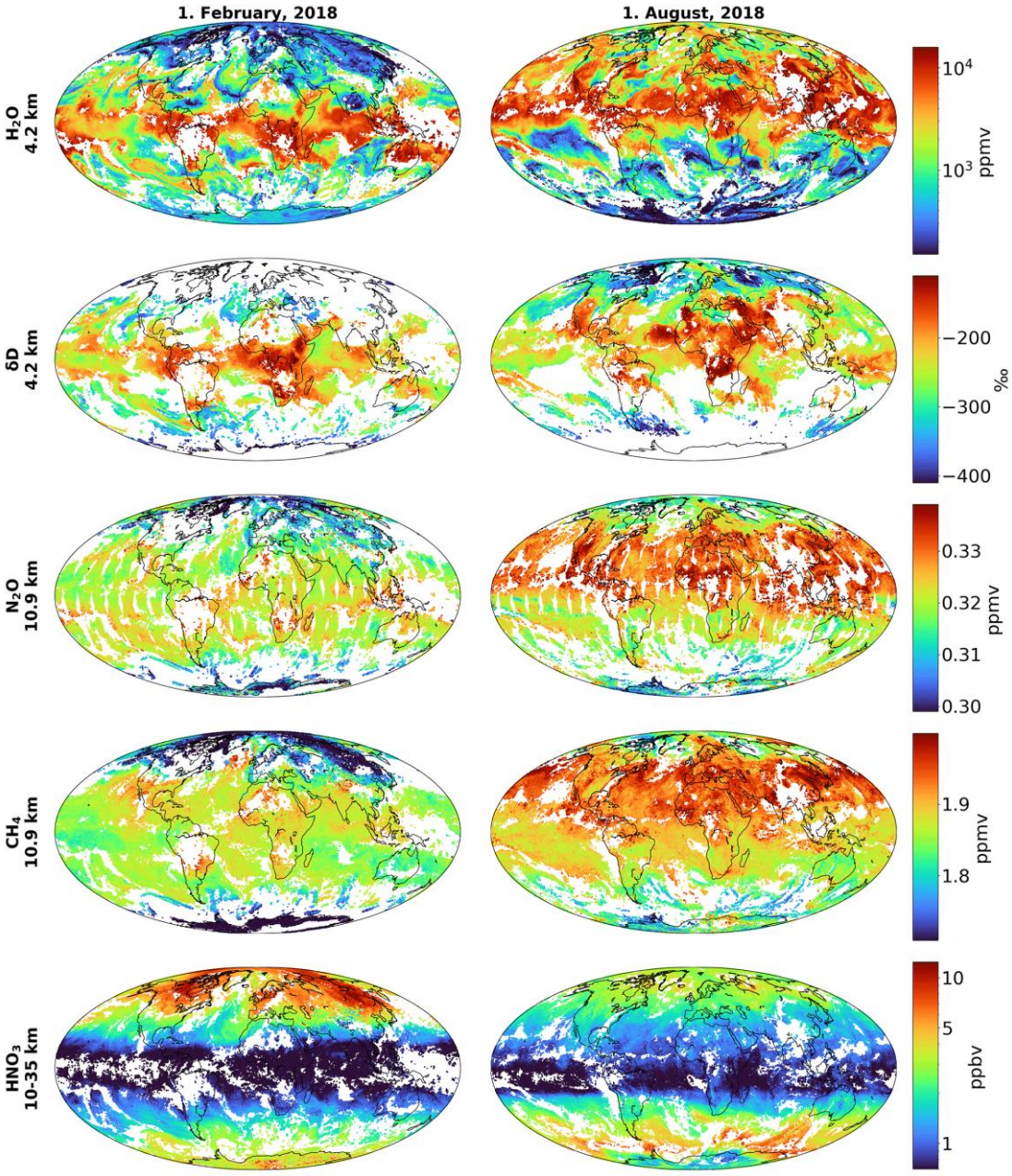

Figure 7.10. Daily maps for 1 February and 1 August 2018 of all MUSICA IASI trace gas products at the altitudes of 4.2 km a.s.l. for H_2O and δD, 10.9 km a.s.l. for N_2O and CH_4, and 10–35 km a.s.l. for HNO_3. Reprinted from Schneider et al. (2022a).

In this context, Dahinden et al. (2021) used high-resolution isotopes simulations from COSMOiso to investigate predominant moisture transport pathways in the Canary Islands region in the eastern subtropical North Atlantic. Comparison of the simulated isotope signals with multi-platform isotope observations (aircraft, ground- and space-based remote sensing) from the MUSICA field campaign in summer 2013 shows that COSMOiso can reproduce the observed variability of stable water vapour isotopes on timescales of hours to days, thus allowing us to study the mechanisms that control the subtropical free-tropospheric humidity. In particular, distinct differences in the location of the North African mid-level anticyclone and of extratropical Rossby wave patterns occur between the four transport pathways identified. Overall, this study demonstrated that the adopted Lagrangian isotope perspective enhances our understanding of air mass transport and mixing and offers a sound interpretation of the free-tropospheric variability of specific humidity and isotope composition on timescales of hours to days in contrasting atmospheric conditions over the eastern subtropical North Atlantic.

INMENSE

The Spanish project INMENSE aims to improve understanding of the atmospheric budgets of two of the most important greenhouse gases, CH_4 and N_2O. Knowledge of the atmospheric CH_4 and N_2O distributions, from local to global scales, as well as their variability in time is essential for a better understanding of their sinks and sources, and for

predicting their evolution in the atmosphere. In order to achieve this core objective, INMENSE has generated a new global observational data set of middle/upper tropospheric mole fractions of CH_4 and N_2O with high and well-documented quality by using the MUSICA IASI processor.

Within MOTIV and in collaboration with the INMENSE team, the potential synergetic use of IASI and TROPOMI space borne sensors for generating a tropospheric CH_4 profile product has been evaluated (Schneider et al., 2022b). The proposed method uses the output of the individual satellite retrievals and combines them a-posteriori in an optimal sense. This approach is largely equivalent to applying thermal (TIR) and short-wave infrared (SWIR) spectra together in a single retrieval procedure, but with the substantial advantage of being applicable to any existing TIR and SWIR retrieval processor, of being very time efficient, and of benefiting from the high quality and most recent improvements of the specific TIR and SWIR retrievals. The combination of IASI and TROPOMI information can detect better the CH_4 tropospheric variations than those by IASI or TROPOMI observations alone. The resulting advantage has been documented theoretically as well as empirically by comparisons to independent free tropospheric in-situ reference data obtained within the frameworks of GAW, NDACC and TCCON FTIR networks.

7.3.4 Contributions to the 2021 La Palma volcanic eruption emergency response

The FTIR group contributed to activities carried out by IARC-AEMET during the 2021 La Palma volcanic eruption by setting up its routine gas observations. At IZO, the IARC HR FTIR instrument was focused on mid-infrared measurements to monitor the main volcanic gas emissions (i.e. H_2O, SO_2, HCl, HF, CO, etc.), while a COCCON LR FTIR spectrometer was dedicated to near-infrared observations tracking secondary species such as CO_2 and aerosols (see Fig. 7.9). As a result, a new strategy to monitor SO_2 from HR FTIR instruments was developed by refining Taquet et al. (2019)'s work. The improved methodology was successfully applied for volcanic emissions at various sites worldwide: Popocatépetl (Mexico), Mont Erebus (Antarctica), Kilauea (Hawaii), Piton de La Fournaise (Reunion Island), and La Palma (Spain) (García et al., 2022c).

In addition, the second IARC COCCON LR FTIR spectrometer was installed in the south of La Palma, in the municipality of Fuencaliente, which allowed for improved monitoring of the volcanic emissions based on their trajectory (Taquet et al., 2022). See Section 23 for further details.

7.4 References

Alberti, C., Hase, F., Frey, M., Dubravica, D., Blumenstock, T., Dehn, A., Castracane, P., Surawicz, G., Harig, R., Baier, B. C., Bès, C., Bi, J., Boesch, H., Butz, A., Cai, Z., Chen, J., Crowell, S. M., Deutscher, N. M., Ene, D., Franklin, J. E., García, O., Griffith, D., Grouiez, B., Grutter, M., Hamdouni, A., Houweling, S., Humpage, N., Jacobs, N., Jeong, S., Joly, L., Jones, N. B., Jouglet, D., Kivi, R., Kleinschek, R., Lopez, M., Medeiros, D. J., Morino, I., Mostafavipak, N., Müller, A., Ohyama, H., Palmer, P. I., Pathakoti, M., Pollard, D. F., Raffalski, U., Ramonet, M., Ramsay, R., Sha, M. K., Shiomi, K., Simpson, W., Stremme, W., Sun, Y., Tanimoto, H., Té, Y., Tsidu, G. M., Velazco, V. A., Vogel, F., Watanabe, M., Wei, C., Wunch, D., Yamasoe, M., Zhang, L., and Orphal, J.: Improved calibration procedures for the EM27/SUN spectrometers of the COllaborative Carbon Column Observing Network (COCCON), Atmos. Meas. Tech., 15, 2433–2463, doi: 10.5194/amt-15-2433-2022, 2022.

Álvarez, O., A. Barreto, O. García, F. Hase, T. Blumenstock, E. Sepúlveda, S. F. León-Luis, V. Carreño, A. Alcántara, F. Almansa, Aerosol properties by ground-based COCCON FTIR spectrometry, International Radiation Symposium (IRS), Thessaloniki (Greece), 4-8 July, 2022a.

Álvarez, O., O. García, A. Barreto, F. Hase, T. Blumenstock, E. Sepúlveda, S. León-Luis, V. Carreño, A. Alcántara, R.D. García, F. Almansa, M. Schneider, Spectral Aerosol Optical Depth Retrievals by ground-based COCCON FTIR spectrometry, TCCON/COCCON/NDACC Meeting 2022 (online), 22-24 June, 2022b.

Blumenstock, T., Hase, F., Keens, A., Czurlok, D., Colebatch, O., Garcia, O., Griffith, D. W. T., Grutter, M., Hannigan, J. W., Heikkinen, P., Jeseck, P., Jones, N., Kivi, R., Lutsch, E., Makarova, M., Imhasin, H. K., Mellqvist, J., Morino, I., Nagahama, T., Notholt, J., Ortega, I., Palm, M., Raffalski, U., Rettinger, M., Robinson, J., Schneider, M., Servais, C., Smale, D., Stremme, W., Strong, K., Sussmann, R., Té, Y., and Velazco, V. A.: Characterization and potential for reducing optical resonances in Fourier transform infrared spectrometers of the Network for the Detection of Atmospheric Composition Change (NDACC), Atmos. Meas. Tech., 14, 1239–1252, doi: 10.5194/amt-14-1239-2021, 2021.

Byrne, B., Baker, D. F., Basu, S., Bertolacci, M., Bowman, K. W., Carroll, D., Chatterjee, A., Chevallier, F., Ciais, P., Cressie, N., Crisp, D., Crowell, S., Deng, F., Deng, Z., Deutscher, N. M., Dubey, M., Feng, S., García, O., Griffith, D. W. T., Herkommer, B., Hu, L., Jacobson, A. R., Janardanan, R., Jeong, S., Johnson, M. S., Jones, D. B. A., Kivi, R., Liu, J., Liu, Z., Maksyutov, S., Miller, J. B., Miller, S. M., Morino, I., Notholt, J., Oda, T., O'Dell, C. W., Oh, Y.-S., Ohyama, H., Patra, P. K., Peiro, H., Petri, C., Philip, S., Pollard, D. F., Poulter, B., Remaud, M., Schuh, A., Sha, M. K., Shiomi, K., Strong, K., Sweeney, C., Té, Y., Tian, H., Velazco, V. A., Vrekoussis, M., Warneke, T., Worden, J. R., Wunch, D., Yao, Y., Yun, J., Zammit-Mangion, A., and Zeng, N.: National CO2 budgets (2015–2020) inferred from atmospheric CO2 observations in support of the Global Stocktake, Earth Syst. Sci. Data Discuss., doi: 10.5194/essd-2022-213, 2022.

Chang, K.-L., Cooper, O. R., Gaudel, A., Allaart, M., Ancellet, G., Clark, H., Godin-Beekmann, S., Leblanc, T., Van Malderen, R., Nédélec, P., Petropavlovskikh, I., Steinbrecht, W., Stübi, R., Tarasick, D.W., Torres, C.: Impact of the COVID-19 economic downturn on tropospheric ozone trends: An uncertainty weighted data synthesis for quantifying regional anomalies above western North America and Europe. AGU Advances, 3, e2021AV000542, doi: 10.1029/2021AV000542, 2022.

Dahinden, F., Aemisegger, F., Wernli, H., Schneider, M., Diekmann, C. J., Ertl, B., Knippertz, P., Werner, M., and Pfahl, S.: Disentangling different moisture transport pathways over the eastern subtropical North Atlantic using multi-platform isotope observations and high-resolution numerical modelling, Atmos. Chem. Phys., 21, 16319–16347, doi:10.5194/acp-21-16319-2021, 2021.

Dogniaux, M., Crevoisier, C., Armante, R., Capelle, V., Delahaye, T., Cassé, V., De Mazière, M., Deutscher, N. M., Feist, D. G., Garcia, O. E., Griffith, D. W. T., Hase, F., Iraci, L. T., Kivi, R., Morino, I., Notholt, J., Pollard, D. F., Roehl, C. M., Shiomi, K., Strong, K., Té, Y., Velazco, V. A., and Warneke, T.: The Adaptable 4A Inversion (5AI): description and first XCO2 retrievals from Orbiting Carbon Observatory-2 (OCO-2) observations, Atmos. Meas. Tech., 14, 4689–4706, doi: 10.5194/amt-14-4689-2021, 2021.

Franco, B., Blumenstock, T., Cho, C., Clarisse, L., Clerbaux, C., Coheur, P.-F., De Mazière, M., De Smedt, I., Dorn, H.-P., Emmerichs, T., Fuchs, H., Gkatzelis, G., Griffith, D. W. T., Gromov, S., Hannigan, J. W., Hase, F., Hohaus, T., Jones, N., Kerkweg, A., Kiendler-Scharr, A., Lutsch, E., Mahieu, E., Novelli, A., Ortega, I., Paton-Walsh, C., Pommier, M., Pozzer, A., Reimer, D., Rosanka, S., Sander, R., Schneider, M., Strong, K., Tillmann, R., Van Roozendael, M., Vereecken, L., Vigouroux, C., Wahner, A., Taraborrelli, D.: Ubiquitous atmospheric production of organic acids mediated by cloud droplets. Nature 593, 233–237, doi: 10.1038/s41586-021-03462-x, 2021.

Frey, M., Sha, M. K., Hase, F., Kiel, M., Blumenstock, T., Harig, R., Surawicz, G., Deutscher, N. M., Shiomi, K., Franklin, J. E., Bösch, H., Chen, J., Grutter, M., Ohyama, H., Sun, Y., Butz, A., Mengistu Tsidu, G., Ene, D., Wunch, D., Cao, Z., Garcia, O., Ramonet, M., Vogel, F., and Orphal, J.: Building the COllaborative Carbon Column Observing Network (COCCON): long-term stability and ensemble performance of the EM27/SUN Fourier transform spectrometer, Atmos. Meas. Tech., 12, 1513-1530, doi: 10.5194/amt-12-1513-2019, 2019.

García, O. E., Schneider, M., Redondas, A., González, Y., Hase, F., Blumenstock, T., and Sepúlveda, E.: Investigating the long-term evolution of subtropical ozone profiles applying ground-based FTIR spectrometry, Atmos. Meas. Tech., 5, 2917-2931, doi:10.5194/amt-5-2917-2012, 2012.

García, O. E., Schneider, M., Ertl, B., Sepúlveda, E., Borger, C., Diekmann, C., Wiegele, A., Hase, F., Barthlott, S., Blumenstock, T., Raffalski, U., Gómez-Peláez, A., Steinbacher, M., Ries, L., and de Frutos, A. M.: The MUSICA IASI CH4 and N2O products and their comparison to HIPPO, GAW and NDACC FTIR references, Atmos. Meas. Tech., 11, 4171-4215, doi: 10.5194/amt-11-4171-2018, 2018.

García, O. E., Schneider, M., Sepúlveda, E., Hase, F., Blumenstock, T., Cuevas, E., Ramos, R., Gross, J., Barthlott, S., Röhling, A. N., Sanromá, E., González, Y., Gómez-Peláez, Á. J., Navarro-Comas, M., Puentedura, O., Yela, M., Redondas, A., Carreño, V., León-Luis, S. F., Reyes, E., García, R. D., Rivas, P. P., Romero-Campos, P. M., Torres, C., Prats, N., Hernández, M., and López, C.: Twenty years of ground-based NDACC FTIR spectrometry at Izaña Observatory – overview and long-term comparison to other techniques, Atmos. Chem. Phys., 21, 15519–15554, doi: 10.5194/acp-21-15519-2021, 2021a.

García, O.E., Eliezer Sepúlveda, Sergio F. León-Luis, Josep-Antón Morgui, Matthias Frey, Carsten Schneider, Ramón Ramos, Carlos Torres, Roger Curcoll, Carme Estruch, África Barreto, Carlos Toledano, Frank Hase, André Butz, Emilio Cuevas, Thomas Blumenstock, Juan J. Bustos, and Carlos Marrero, Monitoring of Greenhouse Gas and Aerosol Emissions in Madrid megacity (MEGEI-MAD), GAW Symposium 2021 (online), 28 June-2 July, 2021b.

García, R.D.; Cuevas, E.; Cachorro, V.E.; García, O.E.; Barreto, Á.; Almansa, A.F.; Romero-Campos, P.M.; Ramos, R.; Pó, M.; Hoogendijk, K.; Gross, J: Water Vapor Retrievals from Spectral Direct Irradiance Measured with an EKO MS-711 Spectroradiometer-Intercomparison with Other Techniques, Remote Sens, 13, 350, doi: 10.3390/rs13030350, 2021c.

García, O. E., Sanromá, E., Schneider, M., Hase, F., León-Luis, S. F., Blumenstock, T., Sepúlveda, E., Redondas, A., Carreño, V., Torres, C., and Prats, N.: Improved ozone monitoring by ground-based FTIR spectrometry, Atmos. Meas. Tech., 15, 2557–2577, doi: 10.5194/amt-15-2557-2022, 2022a.

García, O. E., Sanromá, E., Hase, F., Schneider, M., León-Luis, S. F., Blumenstock, T., Sepúlveda, E., Torres, C., Prats, N., Redondas, A., and Carreño, V.: Impact of instrumental line shape characterization on ozone monitoring by FTIR spectrometry, Atmos. Meas. Tech., 15, 4547–4567, doi: 10.5194/amt-15-4547-2022, 2022b.

García, O. W. Stremme, N. Taquet, F. Hase, I. Ortega, J. Hannigan, D. Smale, C. Vigouroux, M. Grutter, T. Blumenstock, M. Schneider, A. Redondas Sulphur dioxide from ground-based Fourier transform infrared spectroscopy: application to volcanic emissions, IRWG-NDACC Meeting 2022, 28 June-1 July, 2022c.

Gisi, M., F. Hase, S. Dohe, and T. Blumenstock: Camtracker: a new camera controlled high precision solar tracker system for FTIR-spectrometers, Atmos. Meas. Tech., 4, 47-54, 2011.

Hase, F., T. Blumenstock, C. Paton-Walsh: Analysis of the instrumental line shape of high-resolution Fourier transform IR spectrometers with gas cell measurements and new retrieval software, Appl. Opt. 38, 3417-3422, 1999.

Hase, F., J.W. Hannigan, M.T. Coffey, A. Goldman, M. Höpfner, N.B. Jones, C.P. Rinsland, S.W. Wood: Intercomparison of retrieval codes used for the analysis of high-resolution, ground-based FTIR measurements, Journal of Quantitative Spectroscopy & Radiative Transfer 87, 25–52, 2004.

Keppens, A.; Compernolle, S.; Hubert, D.; Verhoelst, T.; Granville, J.; Lambert, J.-C. Removing Prior Information from Remotely Sensed Atmospheric Profiles by Wiener Deconvolution Based on the Complete Data Fusion Framework. Remote Sens., 14, 2197, doi: 10.3390/rs14092197, 2022.

Lopez, F.P.A.; Zhou, G.; Jing, G.; Zhang, K.; Tan, Y. XCO2 and XCH4 Reconstruction Using GOSAT Satellite Data Based on EOF-Algorithm. Remote Sens. 14, 2622, doi: 10.3390/rs14112622, 2022.

Massie, S. T., Cronk, H., Merrelli, A., O'Dell, C., Schmidt, K. S., Chen, H., and Baker, D.: Analysis of 3D cloud effects in OCO-2 XCO2 retrievals, Atmos. Meas. Tech., 14, 1475–1499, https://doi.org/10.5194/amt-14-1475-2021, 2021.

Noël, S., Reuter, M., Buchwitz, M., Borchardt, J., Hilker, M., Bovensmann, H., Burrows, J. P., Di Noia, A., Suto, H., Yoshida, Y., Buschmann, M., Deutscher, N. M., Feist, D. G., Griffith, D. W. T., Hase, F., Kivi, R., Morino, I., Notholt, J., Ohyama, H., Petri, C., Podolske, J. R., Pollard, D. F., Sha, M. K., Shiomi, K., Sussmann, R., Té, Y., Velazco, V. A., and Warneke, T.: XCO2 retrieval for GOSAT and GOSAT-2 based on the FOCAL algorithm, Atmos. Meas. Tech., 14, 3837–3869, doi: 10.5194/amt-14-3837-2021, 2021.

Noël, S., Reuter, M., Buchwitz, M., Borchardt, J., Hilker, M., Schneising, O., Bovensmann, H., Burrows, J. P., Di Noia, A., Parker, R. J., Suto, H., Yoshida, Y., Buschmann, M., Deutscher, N. M., Feist, D. G., Griffith, D. W. T., Hase, F., Kivi, R., Liu, C., Morino, I., Notholt, J., Oh, Y.-S., Ohyama, H., Petri, C., Pollard, D. F., Rettinger, M., Roehl, C., Rousogenous, C., Sha, M. K., Shiomi, K., Strong, K., Sussmann, R., Té, Y., Velazco, V. A., Vrekoussis, M., and Warneke, T.: Retrieval of greenhouse gases from GOSAT and GOSAT-2 using the FOCAL algorithm, Atmos. Meas. Tech., 15, 3401–3437, doi: 10.5194/amt-15-3401-2022, 2022.

Peiro, H., Crowell, S., and Moore III, B.: Optimizing 4 years of CO2 biospheric fluxes from OCO-2 and in situ data in TM5: fire emissions from GFED and inferred from MOPITT CO data, Atmos. Chem. Phys., 22, 15817–15849, doi: 10.5194/acp-22-15817-2022, 2022.

Schneider, M., A. Redondas, F. Hase, C. Guirado, T. Blumenstock, and E. Cuevas: Comparison of ground-based Brewer and FTIR total O3 monitoring techniques, Atmos. Chem. Phys., 8, 5535-5550, 2008.

Schneider, M., P. M. Romero, F. Hase, T. Blumenstock, E. Cuevas, and R. Ramos: Continuous quality assessment of atmospheric water vapour measurement techniques: FTIR, Cimel, MFRSR, GPS, and Vaisala RS92, Atmos. Meas. Tech., 3, 323-338, 2010.

Schneider, M., Ertl, B., Diekmann, C. J., Khosrawi, F., Weber, A., Hase, F., Höpfner, M., García, O. E., Sepúlveda, E., and Kinnison, D.: Design and description of the MUSICA IASI full retrieval product, Earth Syst. Sci. Data, 14, 709–742, doi: 10.5194/essd-14-709-2022, 2022a.

Schneider, M., Ertl, B., Tu, Q., Diekmann, C. J., Khosrawi, F., Röhling, A. N., Hase, F., Dubravica, D., García, O. E., Sepúlveda, E., Borsdorff, T., Landgraf, J., Lorente, A., Butz, A., Chen, H., Kivi, R., Laemmel, T., Ramonet, M., Crevoisier, C., Pernin, J., Steinbacher, M., Meinhardt, F., Strong, K., Wunch, D., Warneke, T., Roehl, C., Wennberg, P. O., Morino, I., Iraci, L. T., Shiomi, K., Deutscher, N. M., Griffith, D. W. T., Velazco, V. A., and Pollard, D. F.: Synergetic use of IASI profile and TROPOMI total-column level 2 methane retrieval products, Atmos. Meas. Tech., 15, 4339–4371, doi: 10.5194/amt-15-4339-2022, 2022b.

Sepúlveda, E., Schneider, M., Hase, F., García, O. E., Gomez-Pelaez, A., Dohe, S., Blumenstock, T., and Guerra, J. C.: Long-term validation of total and tropospheric column-averaged CH4 mole fractions obtained by mid-infrared ground-based FTIR spectrometry, Atmos. Meas. Tech., 5, 1425-1441, doi:10.5194/amt-5-1425-2012, 2012.

Sha, M. K., Langerock, B., Blavier, J.-F. L., Blumenstock, T., Borsdorff, T., Buschmann, M., Dehn, A., De Mazière, M., Deutscher, N. M., Feist, D. G., García, O. E., Griffith, D. W. T., Grutter, M., Hannigan, J. W., Hase, F., Heikkinen, P., Hermans, C., Iraci, L. T., Jeseck, P., Jones, N., Kivi, R., Kumps, N., Landgraf, J., Lorente, A., Mahieu, E., Makarova, M. V., Mellqvist, J., Metzger, J.-M., Morino, I., Nagahama, T., Notholt, J., Ohyama, H., Ortega, I., Palm, M., Petri, C., Pollard, D. F., Rettinger, M., Robinson, J., Roche, S., Roehl, C. M., Röhling, A. N., Rousogenous, C., Schneider, M., Shiomi, K., Smale, D., Stremme, W., Strong, K., Sussmann, R., Té, Y., Uchino, O., Velazco, V. A., Vigouroux, C., Vrekoussis, M., Wang, P., Warneke, T., Wizenberg, T., Wunch, D., Yamanouchi, S., Yang, Y., and Zhou, M.: Validation of methane and carbon monoxide from Sentinel-5 Precursor using TCCON and NDACC-IRWG stations, Atmos. Meas. Tech., 14, 6249–6304, doi: 10.5194/amt-14-6249-2021, 2021.

Steinbrecht, W., Kubistin, D., Plass-Dülmer, C., Davies, J., Tarasick, D.W., Gathen, P.V., Deckelmann, H., Jepsen, N., Kivi, R., Lyall, N., Palm, M., Notholt, J., Kois, B., Oelsner, P., Allaart, M., Piters, A., Gill, M., Van Malderen, R., Delcloo, A.W., Sussmann, R., Mahieu, E., Servais, C., Romanens, G., Stübi, R., Ancellet, G., Godin-Beekmann, S., Yamanouchi, S., Strong, K., Johnson, B., Cullis, P., Petropavlovskikh, I., Hannigan, J., Hernandez, J.L., Rodriguez, A.D., Nakano, T., Chouza, F., Leblanc, T., Torres, C., Garcia, O., Röhling, A., Schneider, M., Blumenstock, T., Tully, M., Paton-Walsh, C., Jones, N., Querel, R., Strahan, S., Stauffer, R.M., Thompson, A.M., Inness, A., Engelen, R., Chang, K.L., Cooper, O.R., COVID-19 Crisis Reduces Free Tropospheric Ozone across the Northern Hemisphere, Geophysical Research Letters, 48, e2020GL091987, doi: 10.1029/2020GL091987, 2021.

Taquet N, Stremme W, Grutter M, Baylón J, Bezanilla A, Schiavo B, Rivera C, Campion R, Boulesteix T, Nieto-Torres A, Espinasa-Pereña R, Blumenstock T and Hase F, Variability in the Gas Composition of the Popocatépetl Volcanic Plume. Front. Earth Sci. 7:114. doi: 10.3389/feart.2019.00114, 2019.

Taquet, N., O. García, R. Campion, T. Boulesteix, W. Stremme,C. Rivera, M. Grutter, A. Barreto, O. Álvarez, S. León-Luis, R. Ramos, V. Carreño, F. Almansa, F. Hase, T. Blumenstock, COCCON activities during the La Palma volcano eruption: gases and aerosols observations, COCCON Meeting (on-line), 23 August, 2022.

Tarasick, D., Galbally, I.E., Cooper, O.R., Schultz, M.G., Ancellet, G., Leblanc, T., Wallington, T.J., Ziemke, J., Liu, X., Steinbacher, M., Staehelin, J., Vigouroux, C., Hannigan, J.W., García, O., Foret, G., Zanis, P., Weatherhead, E., Petropavlovskikh, I., Worden, H., Osman, M., Liu, J., Chang, K.-L., Gaudel, A., Lin, M., Granados-Muñoz, M., Thompson, A.M., Oltmans, S.J., Cuesta, J., Dufour, G., Thouret, V., Hassler, B., Trickl, T. and Neu, J.L., 2019. Tropospheric Ozone Assessment Report: Tropospheric ozone from 1877 to 2016, observed levels, trends and uncertainties. Elem Sci Anth, 7(1), p.39, doi: 10.1525/elementa.376, 2019.

Taylor, T. E., O'Dell, C. W., Crisp, D., Kuze, A., Lindqvist, H., Wennberg, P. O., Chatterjee, A., Gunson, M., Eldering, A., Fisher, B., Kiel, M., Nelson, R. R., Merrelli, A., Osterman, G., Chevallier, F., Palmer, P. I., Feng, L., Deutscher, N. M., Dubey, M. K., Feist, D. G., García, O. E., Griffith, D. W. T., Hase, F., Iraci, L. T., Kivi, R., Liu, C., De Mazière, M., Morino, I., Notholt, J., Oh, Y.-S., Ohyama, H., Pollard, D. F., Rettinger, M., Schneider, M., Roehl, C. M., Sha, M. K., Shiomi, K., Strong, K., Sussmann, R., Té, Y., Velazco, V. A., Vrekoussis, M., Warneke, T., and Wunch, D.: An 11-year record of XCO2 estimates derived from GOSAT measurements using the NASA ACOS version 9 retrieval algorithm, Earth Syst. Sci. Data, 14, 325–360, doi: 10.5194/essd-14-325-2022, 2022.

Tu Q., Hase, F., Schneider, M., García, O., Blumenstock, T., Borsdorff, T., Frey, M., Khosrawi, F., Lorente, A., Alberti, C., Bustos, J. J., Butz, A., Carreño, V., Cuevas, E., Curcoll, R., Diekmann, C. J., Dubravica, D., Ertl, B., Estruch, C., León-Luis, S. F., Marrero, C., Morgui, J.-A., Ramos, R., Scharun, C., Schneider, C., Sepúlveda, E., Toledano, C., and Torres, C.: Quantification of CH4 emissions from waste disposal sites near the city of Madrid using ground- and space-based observations of COCCON, TROPOMI and IASI, Atmos. Chem. Phys., 22, 295–317, doi: 10.5194/acp-22-295-2022, 2022a.

Tu, Q., Hase, F., Chen, Z., Schneider, M., García, O., Khosrawi, F., Blumenstock, T., Liu, F., Qin, K., Lin, S., Jiang, H., and Fang, D.: Estimation of NO2 emission strengths over Riyadh and Madrid from space from a combination of wind-assigned

anomalies and machine learning technique, Atmos. Meas. Tech. Discuss., doi: 10.5194/amt-2022-176, 2022b.

Vandenbussche, S.; Langerock, B.; Vigouroux, C.; Buschmann, M.; Deutscher, N.M.; Feist, D.G.; García, O.; Hannigan, J.W.; Hase, F.; Kivi, R.; Kumps, N.; Makarova, M.; Millet, D.B.; Morino, I.; Nagahama, T.; Notholt, J.; Ohyama, H.; Ortega, I.; Petri, C.; Rettinger, M.; Schneider, M.; Servais, C.P.; Sha, M.K.; Shiomi, K.; Smale, D.; Strong, K.; Sussmann, R.; Té, Y.; Velazco, V.A.; Vrekoussis, M.; Warneke, T.; Wells, K.C.; Wunch, D.; Zhou, M.; De Mazière, M. Nitrous Oxide Profiling from Infrared Radiances (NOPIR): Algorithm Description, Application to 10 Years of IASI Observations and Quality Assessment. Remote Sens., 14, 1810, doi: 10.3390/rs14081810, 2022.

Wang, Hengmao & Jiang, Fei & Liu, Yi & Yang, Dongxu & Wu, Mousong & He, Wei & Wang, Jun & Wang, Jing & Ju, Weimin & Chen, Jing. Global Terrestrial Ecosystem Carbon Flux Inferred from TanSat XCO 2 Retrievals. Journal of Remote Sensing, doi: 10.34133/2022/9816536, 2022.

Zhang, Y., Jacob, D. J., Lu, X., Maasakkers, J. D., Scarpelli, T. R., Sheng, J.-X., Shen, L., Qu, Z., Sulprizio, M. P., Chang, J., Bloom, A. A., Ma, S., Worden, J., Parker, R. J., and Boesch, H.: Attribution of the accelerating increase in atmospheric methane during 2010–2018 by inverse analysis of GOSAT observations, Atmos. Chem. Phys., 21, 3643–3666, doi: 10.5194/acp-21-3643-2021, 2021a.

Zhang S., Bai Yan, He Xianqiang, Huang Haiqing, Zhu Qiangkun, Gong Fang. Comparisons of OCO-2 satellite derived XCO2 with in situ and modeled data over global ocean. Acta Oceanologica Sinica, 40(4): 1–8, doi: 10.1007/s13131-021-1844-9, 2021b.

7.5 Staff and collaborators

The FTIR research group (listed below) is composed of researchers and specialist technicians from IARC-AEMET, from IMK-ASF-KIT, and from TRAGSATEC:

Dr Omaira García (AEMET; Head of programme)

Dr Sergio León-Luis (TRAGSATEC, Research Scientist)

Ramón Ramos (AEMET; Head of Infrastructure)

Antonio Alcántara Ruiz (AEMET; Meteorological Observer-GAW Technician)

Dr Matthias Schneider (IMK-ASF-KIT; Head of the MUSICA group)

Dr Thomas Blumenstock (IMK-ASF-KIT; Head of Ground-based remote-sensing using Fourier-transform interferometers (BOD) group)

Dr Frank Hase (IMK-ASF-KIT; Research Scientist, BOD group)

Benedikt Herkommer (IMK-ASF-KIT; PhD, BOD group)

Jochen Gross ((IMK-ASF-KIT; Research Scientist, BOD group)

8 In situ Aerosols

8.1 Main Scientific Goals

Atmospheric aerosol is composed of a mixture of natural (e.g. sea salt, desert dust or biogenic material) and anthropogenic (e.g. soot, industrial sulphate, nitrate, metals or combustion linked carbonaceous matter) airborne particles whose size range from a few nanometres (nm) to tens of microns (µm). Aerosols contribute to deterioration of air quality with impacts on human health due to cardiovascular, cerebrovascular and respiratory diseases such as asthma and chronic obstructive pulmonary disease; they also influence climate by scattering and absorbing radiation and by influencing cloud formation and rainfall.

The activities of the In situ Aerosols programme (AIS group, *Aerosol In-Situ*) are developed in line with scientific priorities of the Global Atmosphere Watch Programme. One of the main tasks of this group is to maintain the long-term observations of aerosols at IZO. The group focuses its research on: 1) Long-term multi-decadal variability and trends of aerosols; 2) Aerosols and climate interaction and 3) Aerosols and air quality interaction.

8.2 Measurement Programme

The long-term in situ aerosols observation program of Izaña Observatory includes measurements of aerosol mass and number concentration, chemical composition, size distribution and optical properties by in-situ techniques. Instruments are placed in the so-called Aerosols Research Laboratory (ARL) renamed as the Joseph M. Prospero Aerosols Research Laboratory, as a tribute to the pioneer of dust research, in 2016 (Fig. 8.1). The laboratory is equipped with a whole air inlet for aerosol sampling for the on-line analysers (CPCs, SMPS, APS, MAAP, aethalometer, nephelometer), two additional PM_{10} and $PM_{2.5}$ inlets for the aerosol filter samplers and also two additional inlets for TEOM (PM_{10} and $PM_{2.5}$) and BETA (PM_{10}) analysers respectively. The interior of the Aerosols Research Laboratory is maintained at 22 ºC. Driers are not needed during the sampling because of the low relative humidity (RH) of the outdoor ambient air (RH percentiles 25th, 50th and 75th are 15%, 31% and 55%, respectively). Measurements of number concentration, size distribution and optical properties of aerosols are performed with high time resolution (Table 3.2).

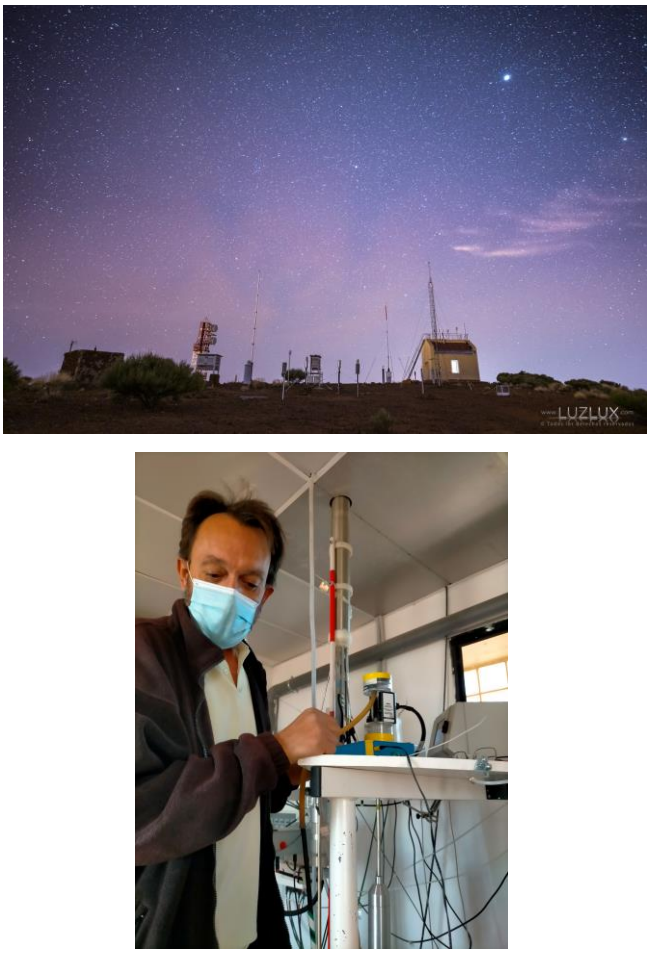

Figure 8.1. Joseph M. Prospero Aerosols Research Laboratory at Izaña Observatory (upper panel: building; lower panel: R. Ramos working in the ARL).

For the automatic instruments in the aerosol laboratory, the QA/QC activities include:

- <daily checks> of the data and status of the instruments
- <weekly checks> of the airflows and leak tests for some instruments (e.g. SMPS)
- <quarterly checks> includes measurements of the instrumental zero (24h filtered air) for all the instruments (CPCs, SMPS, APS, MAAP, aethalometer nephelometer) and calibration checks (e.g. nephelometer)
- <annual intercomparisons> for some instruments
- <regular> calibration of the instruments at the World Calibration Centre for Aerosols Physics (WCCAP).

These activities follow the recommendations of the GAW Programme for aerosols (GAW Report nº227, 2016).

During 2022 the final post-processing of the internal database for all aerosol in-situ parameters measured at ARL was started. This is the final step for making all the QC/QA aerosol information measured at ARL available to the scientific community.

The aerosols chemical composition programme is based on:

- the collection of aerosol samples on filters. Samples are collected at night to avoid the diurnal upslope winds that may bring material from the boundary layer.
- the determination of the aerosol mass concentrations by the gravimetric method. Filters are weighed, before and after sampling, at 20 ºC temperature and 30-35 % relative humidity in the Aerosol Filters Laboratory of the Izaña Atmospheric Research Centre (see Section 3.1.4). The procedure for weighing filters is similar to that described in EN-14907, except that we use a lower relative humidity (30-35 %) due to the relative humidity of the ambient air at IZO being much lower than the 50% stated by EN-14907.
- the determination of chemical composition which currently includes elemental composition (those detected by IPC-AES, i.e. Al, Ca, Fe, Mg, K, Na,…), salts (SO_4^{2-}, NO_3^-, NH_4^+, Cl^-), organic carbon, elemental carbon and trace elements (those detected by IPC-MS, i.e. P, V, Ni, Cd, As, Sb, Sn,...).

The QA/QC procedure for the aerosol chemical composition programme includes:

- airflow checks and calibrations.
- the collection of blank field filters for gravimetry and chemical analysis.
- intercomparison exercises.

The IARC Aerosol In-Situ group has participated in the different ACTRIS in-situ community meetings about data submission, QA/QC, trainings and labelling held online. Other important meetings attended by IARC staff have been related to ACTRIS Week (May 2022 online and October 2022 in person in Prague, Czech Republic), the establishment of the ACTRIS Forum (May 2022) and different ACTRIS IMP meetings.

The AIS group is also responsible for the measurements of different passive samplers, for mercury and persistent organic pollutants. These programmes are led by the Environment and Climate Change Canada and the Spanish National Research Council (CSIC).

8.3 Summary of remarkable results during the period 2021-2022

During the 2021-2022 biennium, the scientific activities of the In situ Aerosols group were focused on measuring the effects of the 2021 La Palma volcanic eruption at our site in addition to new scientific collaborations performed in the framework of the ATMO-ACCESS project (see Sections 21 and 23 for further details).

During this period, international cooperation that began in 2019 continued to provide scientific results. These are the activities related to the projects CREWS (Climate Risk and Early Warning System) West Africa and MAC-CLIMA (Madeira-Azores-Canarias-CLIMA). Further details are given in Section 17 (Sand and Dust Storms Centres).

8.3.1 Focus on volcanic aerosols

In the framework of a collaboration between AEMET/IARC and the University of Azores (Portugal), an aethalometer AE43 was deployed at IARC from November 2021 to April 2022, coincidentally to the volcanic eruption on the island of La Palma, to study the impact of volcanic ash in AE43 signals. An analysis based on Principal Component Analyses (PCA) showed that about one third (33%) of the variance of equivalent BC (eBC) concentration measured in the back trajectories arriving at IZO are explained by the first component (PC1) and that the trajectories passing through Africa represent the largest contribution to PC1 during this period, while the remaining trajectories are explained by PC2 (Henriquez et al., 2023).

Figure 8.2. Visit of researchers from University of Azores to IARC with AIS staff.

8.3.2 Focus on new particle formation processes

IARC hosted the first TransNational Access (TNA) Observation campaign, under the umbrella of the ATMO-ACCESS project during April, May and June 2022 at Izaña Subtropical Access Facility (ISAF) with the Institute for Atmospheric and Earth System Research (INAR) at the University of Helsinki (Fig. 8.3). This campaign was developed with the aim of "Chasing preindustrial aerosols at Izaña" for advancing the understanding of the gas precursors responsible for new particle formation (NPF) processes in pristine conditions such as at Izaña Observatory. For this purpose, the research team installed in our Joseph M. Prospero Aerosols Laboratory a suite of instruments, including APi-TOF for ion clusters measurements, MION-APi-TOF (Rissanen et al., 2019) for H_2SO_4 and oxygenated organic molecules concentrations, Vocus-PTR-TOF for VOCs and oxidation products of DMS (dimethyl sulphide) (Krechmer et al., 2018), and a combo NAIS-PSM for number concentration and size distribution of atmospheric ions and neutral particles with a mobility

diameter of 0.8-42 nm and number concentration of particle with a mobility diameter of 1.25-2.5 nm. Filter samples were also collected and analyzed using a high-resolution time-of-flight chemical ionization mass spectrometer (FIGAERO-HR-TOF-CIMS) for the molecular composition of particulate organics (Lopez-Hilfiker et al., 2014).

Figure 8.3. University of Helsinki and IARC-AIS staff at Joseph M. Prospero Aerosols Laboratory during the field campaign, April - June 2022.

The analysis of the results and the preliminary conclusions suggest the key role of the vertical transport of air masses and the influence of the boundary layer dynamics on the processes associated with NPF. The role of atmospheric precursors and the chemical composition of freshly formed clusters will provide new insights to a better understanding of the preindustrial nucleation mechanisms responsible for NPF. See Wei et al. (2023) and Agro et al. (2023) for further details.

This field campaign was complemented thanks to the collaboration with the University of Granada in a two-month measurement campaign between April and June 2022 at IARC-ARL (Fig. 8.4) using a Cloud Condensation Nuclei (CCN) counter (CCN200, DMT) to measure polydisperse CCN concentrations at different supersaturations (SSs; one column at constant SS of 0.4% and one column varying the SS from 0.1 to 0.8%). $PM_{2.5}$ and PM_{10} were also collected for offline analysis of Ice Nuclei (IN) particles concentrations and for a complete chemical analysis. A Scanning Mobility Particle Sizer and an Aerodynamic Particle Sizer (TSI) were used to measure aerosol size distribution from 12 nm to 20 µm. See Casquero-Vera et al. (2023) for further details.

Figure 8.4. University of Granada and IARC-AIS staff at Joseph M. Prospero Aerosols Research Laboratory during the field campaign, April - June 2022.

8.4 References

Agro, M., Huang, W., Shen, J., Aliaga, D., Okuljar, M., Barreto, A., Rodríguez, S., González, Y., López-Darias, J., Petäjä, T., Lehtipalo, K., Casquero-Vera, J.A., Duplissy, J., Brasseur, Z., Titos, G., Casans, A., Bianchi, F.: Characterization of atmospheric aerosol size distributions at the Izaña station – connections to new particle formation at a high altitude, European Aerosol Science Conference 2023, Málaga, in preparation, 2023.

Casquero-Vera, J.A., Casans, A., Rejano, F., Brasseur, Z., Duplissy, J., Agro, M., Huang, W., Shen, J., Aliaga, D., Okuljar, M., Barreto, A., Rodríguez, S., González, Y., López-Darias, J., Olmo, F.J., Bianchi, F., Petäjä, T., Titos, G. and Alados-Arboledas, L.: Activation properties of aerosol particles as cloud condensation and ice nuclei at Izaña high-altitude station, European Aerosol Science Conference 2023, Málaga, in preparation, 2023.

Henriques, D., Fialho, P., Barreto, A., Gonzalez, Y., Rodriguez, S., Cuevas, E., Pacheco, J.: Aethalometer measurements during Cumbre Vieja volcano eruption, APMG 2023 – 12º Simpósio de Meteorologia e Geofísica da APMG e o XXI Encontro Luso Espanhol de Meteorologia, in preparation

Huang, W., Shen, J., Okuljar, M., Agro, M., Aliaga, D., Barreto, A., Rodríguez, S., Yonzález, Y., López-Darias, J., Casquero-Vera, J.A., Casans, A., Titos, G., Brasseur, Z., Duplissy, J., Petäjä, T., Bianchi, F.: Chemical composition of ambient clusters contributing to clustering events at the pristine high-altitude Izaña Atmospheric Observatory (2367 m a.s.l.), European Aerosol Science Conference 2023, Málaga, in preparation, 2023.

Krechmer, J., Lopez-Hilfiker, F., Koss, A., Hutterli, M., Stoermer, C., Deming, B., Kimmel, J., Warneke, C., Holzinger, R., Jayne, J., Worsnop, D., Fuhrer, K., Gonin, M., and de Gouw, J.: Evaluation of a new reagent-ion source and focusing ion–molecule reactor for use in proton-transfer-reaction mass spectrometry, Anal. Chem., 90, 12011–12018, https://doi.org/10.1021/acs.analchem.8b02641, 2018.

Lopez-Hilfiker, F. D., Mohr, C., Ehn, M., Rubach, F., Kleist, E., Wildt, J., Mentel, Th. F., Lutz, A., Hallquist, M., Worsnop, D., and Thornton, J. A.: A novel method for online analysis of gas and particle composition: description and evaluation of a Filter Inlet for Gases and AEROsols (FIGAERO), Atmos. Meas. Tech., 7, 983–1001, https://doi.org/10.5194/amt-7-983-2014, 2014.

Rissanen, M. P., Mikkilä, J., Iyer, S., and Hakala, J.: Multi-scheme chemical ionization inlet (MION) for fast switching of reagent ion chemistry in atmospheric pressure chemical ionization mass spectrometry (CIMS) applications, Atmos. Meas. Tech., 12, 6635–6646, https://doi.org/10.5194/amt-12-6635-2019, 2019.

WMO/GAW Report nº 227, Aerosol Measurement Procedures, Guidelines and Recommendations, 2016.

8.5 Staff

Dr África Barreto (AEMET; Head of programme)

Dr Sergio Rodríguez (Spanish Scientific Research Council –CSIC, at the Institute of Natural Products and Agrobiology – IPNA; co-Head of the program)

Dr Yenny González (Cimel Electronique; Research Scientist)

Concepción Bayo-Pérez (AEMET; Meteorological Observer-GAW Technician)

Ignacio Mármol (AEMET; ATMO-ACCESS technician)

Ramón Ramos (AEMET; Head of Infrastructure)

Néstor Castro (AEMET; IT Specialist)

Nayra Chinea (SIELTEC Canarias; laboratory technician)

9 Column Aerosols

9.1 Main Scientific Goals

The main scientific goals of this programme are:

- Long-term high-quality measurements of column aerosol properties in the FT and the MBL.
- Aerosol characterization in the Saharan Air Layer and the MBL.
- Development of new methodologies and instrumentation for column aerosols and water vapour observations, as well as new calibration techniques.
- Mineral dust model validation.
- Satellite borne aerosol data validation.
- Provision of accurate sun and lunar photometer calibrations and intercomparisons.

9.2 Measurement Programme

The measurement programme is very extensive, including photometric, lidar and ceilometer observations.

Photometric observations are performed at three of the IARC stations, IZO, SCO and TPO (see Tables 3.2, 3.4 and 3.6). Two of the most important parameters for long-term monitoring of the evolution of atmospheric aerosol are AOD, which accounts for the aerosol loading in the atmospheric column, and the Angström Exponent (AE) which gives information on the size and type of the particles. Both parameters have been measured at IZO since 2004 and SCO since 2005, as AERONET-Cimel stations and at IZO also within the WMO Global Atmosphere Watch - Precision Filter Radiometer (GAW-PFR) network since July 2001.

AOD observations at Izaña can be also dated back to 1982 (Fig. 9.1) when they were performed with the Astronomical Potassium-based Resonance Scattering Spectrometer Mark-I (Barreto et al., 2014).

An IARC collaborative station at Roque de los Muchachos (La Palma) was established in 2019 to extend the monitoring of atmospheric aerosol at key sites.

IARC manages not only the AERONET sites of IZO (Fig. 9.2), SCO (Fig. 9.3), TPO and collaborative stations in Spain, but also collaborates closely and provides technical assistance to AERONET-Africa sites, such as Tamanrasset (Algeria), Cairo (Egypt) and Carthage (Tunis). These observations near dust sources over the Sahara provide key information for the SDS-WAS Regional Center (see Section 17) for dust modelling, verification and validation of satellite-based aerosol products.

IZO is a reference calibration site for radiometric observations and calibrations using the Langley plot technique (since 2011) due to the pristine and relatively stable atmospheric conditions at this site. Together with Mauna Loa (Hawaii), IZO is the site for absolute calibration of the GAW-PFR network of the World Radiation Center (Wehrli, 2000, 2005; Toledano et al., 2018).

Moreover, reference instruments belonging to AERONET, AERONET-Europe and the China Aerosol Remote Sensing NETwork (CARSNET), managed by the China Meteorological Administration (CMA; Key Laboratory of Atmospheric Chemistry, Centre for Atmosphere Watch and Services, Chinese Academy of Meteorological Sciences), are periodically calibrated at Izaña Observatory (Che et al., 2009; Toledano et al., 2018). The absolute calibration of Cimel instruments is complemented by laboratory radiance calibration using the integrating sphere of the Optical calibration facility at IZO (Guirado et al., 2012).

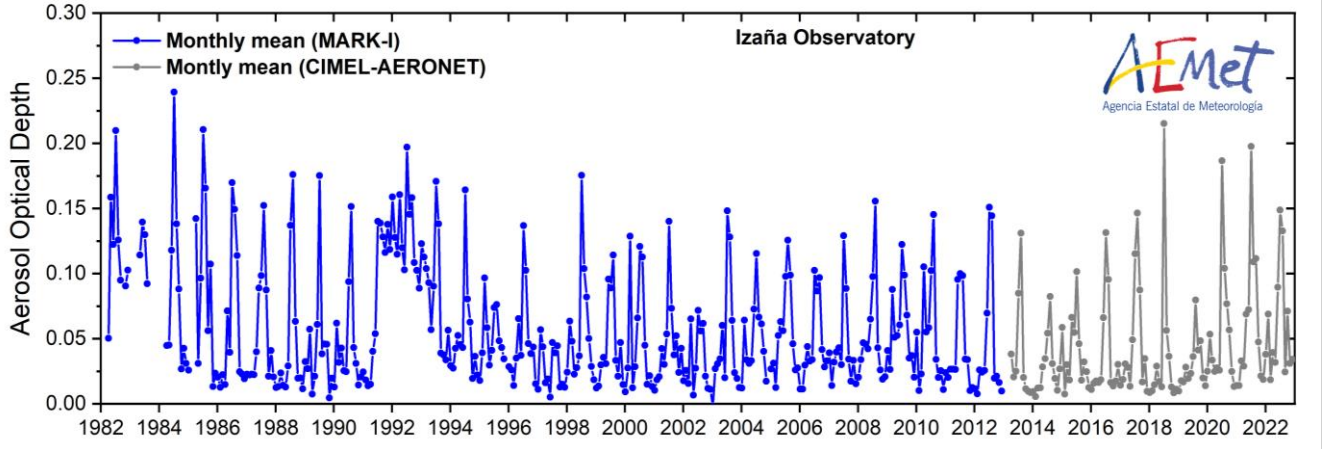

Figure 9.1. Monthly AOD measured at Izaña (in blue) between 1982 and 2012 with the Mark-I spectrometer. AOD measured with Cimel CE318 photometers within AERONET (https://aeronet.gsfc.nasa.gov/) are also included, completing the series between 2012 and 2022 (in grey).

Figure 9.2. Cimel reference instruments of the AERONET-Europe Calibration Facility at Izaña Observatory.

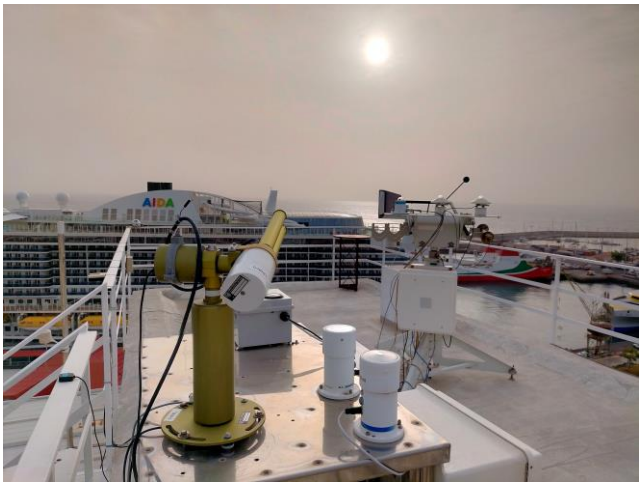

Figure 9.3. Cimel CE318-TS in operation at Santa Cruz Observatory (SCO). On the right, a ZEN, an IR radiometer, radiation instrumentation and a Hirst volumetric spore trap.

9.2.1 Lidar observations

The IARC and the Spanish Institute for Aerospace Technology (PI: Dr Margarita Yela) co-manage a Micropluse lidar (MPL-3) aerosols programme, belonging to the NASA Micro-Pulse Lidar Network (MPLNET), which started a long-term observation programme in 2005. This instrument is part of the NASA MPLNET worldwide aerosol lidar network and operates in full-time continuous mode (24 hours a day / 365 days a year). This instrument operating at SCO can be considered the unique aerosol lidar in Northern Africa that provides regular and long-term information about the vertical structure of the Saharan Air Layer over the North Atlantic.

This lidar was replaced in May 2018 by a new MPL-4B lidar provided by NASA Goddard Space Flight Center MPLNET. The new MPL-4B lidar provides common features of the previous MPL-3 version in addition to dual polarization backscatter measurements allowing researchers to discriminate between aerosol types and clouds phase. A ferroelectric liquid crystal (FLC) is used in these new systems, in addition to a slightly modified measurement strategy to accommodate the difference in polarizer properties. The main technical characteristics of the MPL-4B are detailed in Table 9.1.

Table 9.1. Technical characteristics of the Micro-Pulse Lidar (MPL) at Santa Cruz de Tenerife Observatory.

Micro-Pulse Lidar version 4 (MPL-4B)	
Transmitter	
Laser	Nd:YAG
Wavelength	532 nm
Pulse repetition rate	2500 Hz
Pulse energy	6-8 µJ
Receiver	
Type	Maksutov Cassegrain
Diameter	18 cm
Focal	240 mm
Field of view	Dual field of view configuration: Narrow FOV: 100 µrad Wide FOV: 2 mrad
Polarization	Co-polar and cross-polar components
Detector	
Type	Avalanche photodiode (APD)
Mode	Photocounting

Another MPL-4B was acquired by IARC in February 2020 and installed in the Testbed#2 lidar facility at IZO (Fig. 9.4) in order to provide simultaneous measurements with two MPLs, one located at sea level, and one located in Izaña (2373 m a.s.l.), along with their co-located AERONET sun photometric measurements. These two pieces of information are useful for the characterization of the Saharan Air Layer, its effects in lower (marine boundary layer) and higher (free troposphere) layers and also its impact on mid and high cloud formation.

Figure 9.4 New lidars facility (Testbed#2) at IZO, hosting both the MPL-4B and the CE376 GPN micro-Lidar.

In addition to the two MPL-4B lidars, a Cimel CE376 GPN micro-lidar is also installed at IZO in the same room as the MPL-4B (Fig. 9.4). CE376 performs observations at two wavelengths (532 and 808 nm) with two depolarization channels, complementing the existing MPL data with NIR measurements.

As part of the WMO Measurement Lead Centre for Aerosols and Water Vapour Remote Sensing Instruments, IZO carries out some activities related to column aerosol measurements specifically focusing on methodological and instrument development aspects (see Section 19 for more details).

9.2.2 Ceilometer observations

The Vaisala CL51 ceilometer was installed in SCO in 2011. It has a single channel centered at 910 nm. Every 36 s, it provides atmospheric backscatter profiles up to 15 km altitude as well as cloud base heights at three different altitude levels.

The Vaisala CL51 ceilometer was integrated into the European Meteorological Network (EUMETNET) Automatic Ceilometer and Lidars Network (ALC) within the framework of the EUMETNET Profiling Programme (E-PROFILE) on 24 April 2018.

Figure 9.5. CL51 ceilometer in operation in SCO.

9.3 Summary of remarkable results during the period 2021-2022

The most relevant results obtained during the reporting period are summarized hereinafter.

9.3.1 Aerosol characterisation in the subtropical eastern North Atlantic region using long-term AERONET measurements

A long-term seasonal evolution (2005–2020) of atmospheric aerosols was performed by Barreto et al. (2022b) by using AERONET-NASA observations at four different sites at different altitudes in Tenerife, in the subtropical eastern North Atlantic region. This region is a key location for aerosol monitoring because it is on the pathway of long-range transport such as mineral dust from the Sahel-Sahara regions, dust or sulphates from North America, or sulphates, biomass burning and other pollutants from North America, Europe or Africa. This site is exposed to a strong seasonal dependence of dust transport, representative of the almost pure Saharan dust in summer and winter, a strong vertical stratification in the lower troposphere and contrasting aerosol regimes with very stable and low aerosol turbidity within the free troposphere most of the year.

This comprehensive characterisation was performed at four stations strategically located from the sea level to 3555 m a.s.l. on the island of Tenerife: two stations (Santa Cruz de Tenerife – SCO – at sea level and La Laguna – LLO – at 580 m a.s.l.) within the marine boundary layer, and the other two (Izaña – IZO – at 2373 m a.s.l. and Teide Peak – TPO – at 3555 m a.s.l.) within the free troposphere. Quite consistent measurements across the four sites (Fig. 9.6) confirmed an alternation between predominant background conditions and predominant dust-loaded Saharan air mass conditions caused by seasonal dust transport over the subtropical North Atlantic. Background conditions prevail in the MBL and FT for most of the year, while dust-laden conditions are significant in July and August.

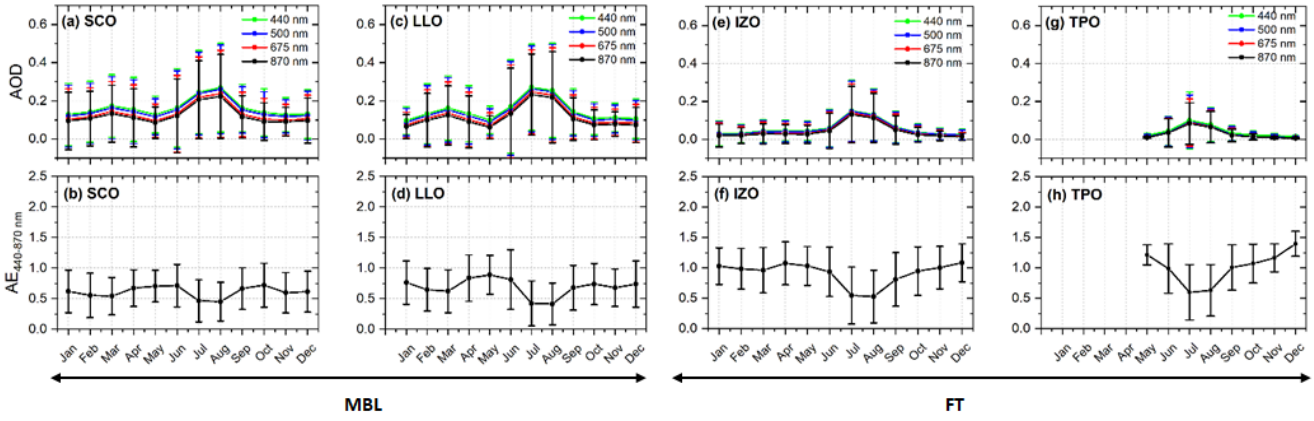

Figure 9.6. Monthly mean aerosol optical depth (AOD) at 440, 500, 675 and 870 nm and Ångström exponent (AE440–870 nm) at the four stations (SCO, LLO, IZO and TPO). Error bars indicate the standard deviation. Reprinted from Barreto et al. (2022b).

9.3.2 Long-term characterisation of the vertical structure of the Saharan Air Layer over the Canary Islands using lidar and radiosondes

The seasonal evolution of atmospheric aerosol extinction and meteorological vertical profiles at Tenerife has been described in Barreto et al. (2022a) over the period 2007-2018 using long-term Micropulse Lidar (MPL-3) and radiosondes observations in Tenerife. These measurements are used to categorise the different patterns of dust transport over the subtropical North Atlantic and, for the first time, to robustly describe the dust vertical distribution in the Saharan Air Layer (SAL) over this region.

Barreto et al. (2022b) found that, under dust presence in summer (Summer-SAL scenario), the SAL appears as a well-stratified layer strongly affecting both the MBL and the free troposphere (Fig. 9.7a). In terms of humidity, the SAL appears relatively dry at lower levels but more humid at higher levels compared with clean FT conditions. Aerosol extinction coefficient (α) peaks at ~ 2.5 km, but dust can be observed up to ~ 6.0 km. This altitude has been defined as the SAL's top or SAL Temperature Inversion (STI), according to the temperature readings from thermodynamic soundings. The winter dust intrusions over the subtropical eastern North Atlantic region (Winter-SAL scenario) appear as a confined dust layer, compressed in the first 2 km (Fig. 9.7b). The most significant features of this layer in winter are the dry anomaly observed at lower levels, the α peak at ~ 1.3 km height, and the STI observed at 2.3 km. Clean FT conditions were found above this level.

The radiative impact of the Summer-SAL has also been studied by these authors. Their findings have revealed that both dust and water vapour play an important role in the radiative balance. A dominant dust-induced shortwave (SW) radiative warming below the dust peak was observed but the combined effect of dust and water vapour appeared as a net SW warming within the SAL, as well as a strong cold anomaly due to longwave adiabatic cooling near the SAL's top. In the case of the Winter-SAL, both dust and atmospheric water vapour have an impact on heating in the atmospheric column. This is the case of the SW heating within the SAL (maximum near the water vapour mixing ratio peak), the dry anomaly at lower levels and the thermal cooling from the temperature inversion upwards.

Finally, a higher occurrence of moderately supercooled mid-level clouds near the SAL top (5-7 km) under the presence of the summer-SAL could point to a possible impact of the SAL on heterogeneous ice nucleation.

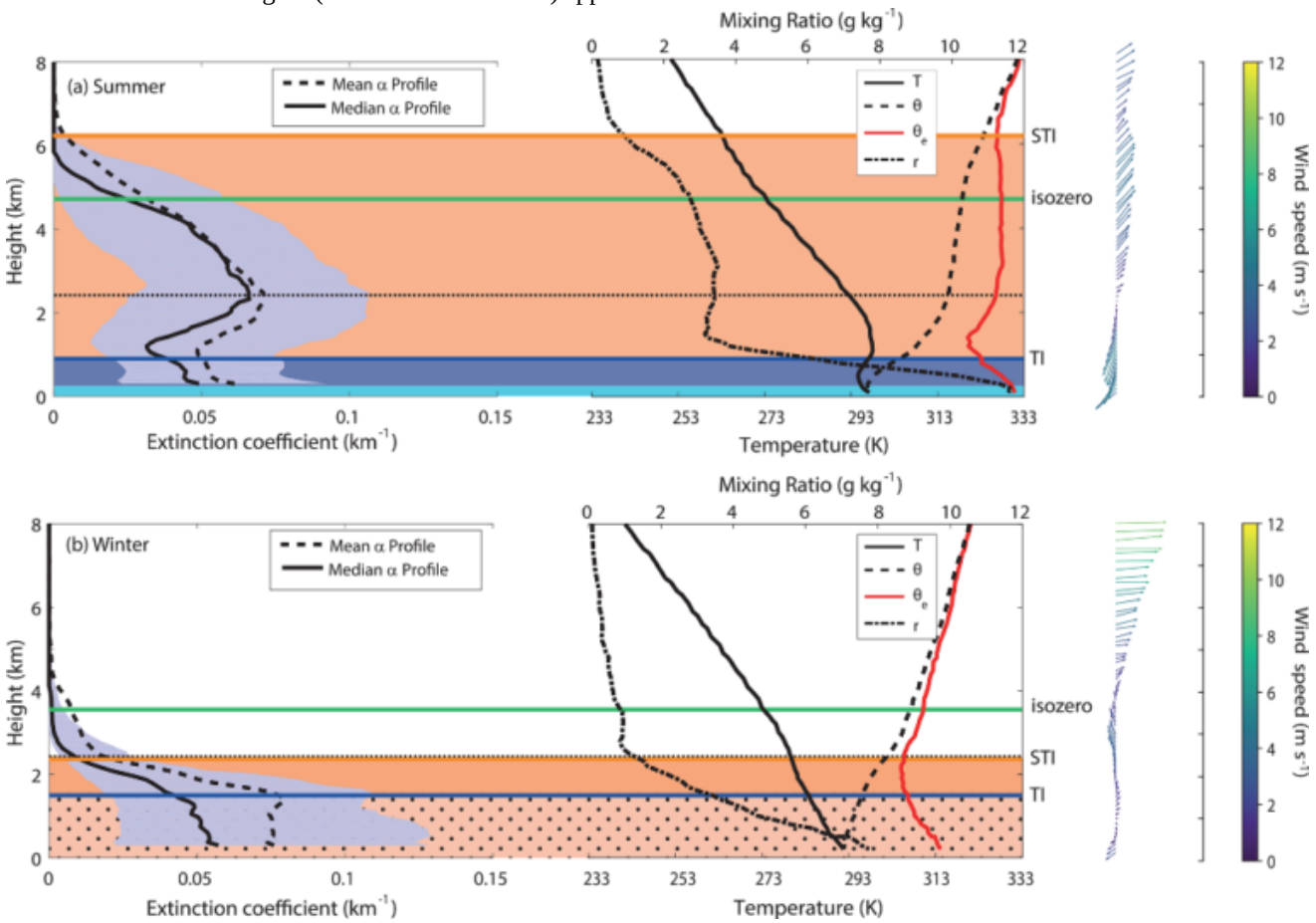

Figure 9.7. Lidar total extinction (at 523 nm) profile (mean and median) and vertical profiles (median) of temperature (T), potential temperature (θ), equivalent potential temperature (θe) and water vapour mixing ratio (r) for Saharan scenarios in (a) summer and (b) winter. 2D-field of wind profiles with arrows (wind direction) and magnitude in m s^{-1} (colour bar) are also presented on the right. Reprinted from Barreto et al. (2022a).

9.3.3 EURAMET/EMPIR project "Metrology for aerosol optical properties" (MAPP)

The European Metrology Programme for Innovation and Research (EMPIR) coordinates research projects including EMPIR-MAPP (Metrology for aerosol optical properties) financed by the European Association of National Metrology Institutes (EURAMET). The EMPIR-MAPP project started in 2020 and is coordinated by PMOD/WRC as a consortium of 14 partners (6 National Metrological Institutes and 8 external partners), in which AEMET is included.

The general objective of EMPIR-MAPP is to improve our understanding of the role that aerosols play in the atmosphere by improving the observation of these components and the intercomparability of the different measurement networks that are currently dedicated to monitoring these components. AEMET was commissioned within this project to organize a measurement campaign to obtain extraterrestrial solar and lunar spectra traceable to the International System of Units (SI) as well as to organize the fourth meeting of EMPIR-MAPP participants.

Figure 9.8. View of the sunset from the Izaña Observatory instrument terrace during the EMPIR-MAPP campaign, September 2022.

The measurement campaign took place at IARC in September 2022 (Fig. 9.8). This campaign involved the most sophisticated instrumentation to date for measuring solar and lunar irradiance using remote sensing techniques from the Earth's surface, including the reference spectral radiometer for the World Radiometric Center (QUASUME), three FTIR spectrometers, belonging to AEMET and the National Physical Laboratory (United Kingdom), as well as reference solar and lunar photometers of the three most important global networks dedicated to the measurement of aerosols (AERONET, WMO GAW and SKYNET). More than 30 instruments for measuring aerosols were involved in this international measurement campaign.

9.3.4 Participation in the fifth Filter Radiometer Campaign (FRC-V) at Davos (Switzerland)

The Fifth Filter Radiometer Comparison (FRC-V) was held in Davos (Switzerland) at the premises of PMOD/WRC in October 2021. Instrumentation belonging to different AOD global networks were invited and participated. In addition, three reference instruments from the Calibration of Aerosol Remote Sensing (CARS) of the pan-European Aerosol, Clouds and Trace Gases Research Infrastructure (ACTRIS) facility participated. In total, 32 filter radiometers and spectroradiometers from 12 countries participated in this campaign (Fig.9.9).

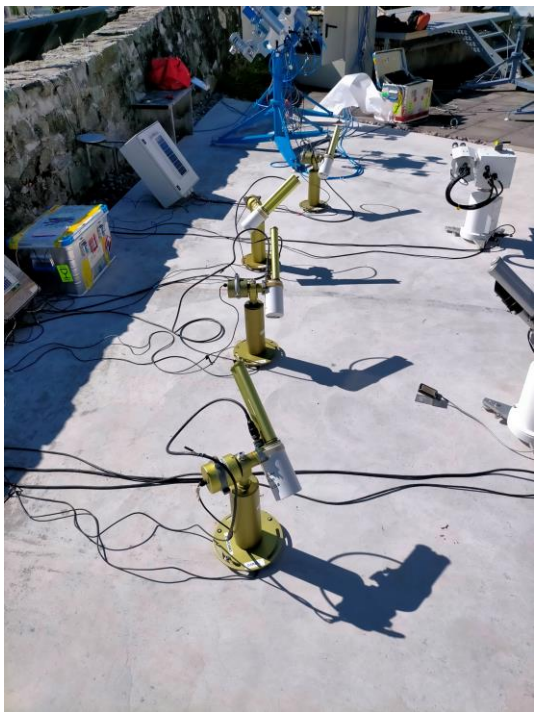

Figure 9.9. Different photometers installed in Davos during the FRC-V field campaign in October 2021.

The objective of this campaign was to compare aerosol optical depth and Ångström exponents (AE) derived from different instruments belonging to different global, regional or national networks in order to quantify the main factors that are responsible for possible deviations. The aim of the whole activity was to initiate action towards homogenization of the AOD measurements on a global scale. The comparison protocol was formulated according to the WMO recommendations. Measurements of each instrument were compared to the WORCC Precision Filter Radiometer (PFR) reference triad. More details of this field campaign can be found in WMO (2023).

9.3.5 SYNERA

The project SYNERA (SYNERgies for assessing short- and long-term variations of Aerosols properties in the subtropical North Atlantic) was approved within the 2020 Call for the National R+D+I Plan "R+D+I Projects" of the Spanish Ministry of Science, Innovation and Universities (MICINN), State Research Agency.

The objective of this project is to improve the current understanding of the transcontinental transport, vertical distribution and physical properties of atmospheric aerosols in the subtropical North Atlantic. To achieve this core objective, a comprehensive and integrated analysis including long-term in situ and remote sensing data will be performed in this project using the GRASP (Generalized Retrieval of Aerosol and Surface Properties) inversion code. This evaluation will be carried out taking advantage of the potential of the IARC as a super-site for aerosol monitoring and a synergistic approach. For this purpose, SYNERA will develop and consolidate new strategies for aerosol monitoring that will produce a multi-platform quality assessment for a coherent analysis of atmospheric change and associated impacts.

9.3.6 New developments for the Cimel CE318 sunphotometer

Satellite downlink communication needs the precise evaluation of the aerosol content in terms of AOD. A new version of the CE318-TS, the CE318-TP9, has been designed in the framework of the ESA project ANAtOLIA (Atmospheric moNitoring to Assess the availability of Optical LInks through the Atmosphere) to assess the aerosol interferences in the satellite communication links. This instrument is able to provide photometric measurements at day and nighttime at two additional spectral bands: 1064 and 1550 nm, the two most common wavelengths used in satellite communication links to the ground. The main objective of ANAtOLIA is to design, manufacture, procure and assemble a self-standing and autonomous ground support equipment for precisely measuring the clouds, aerosols and turbulence conditions for atmospheric transmission characterization.

The new CE318-TP9 has been installed at IARC to calibrate the instrument using solar and lunar measurements in the frame of ATMO-ACCESS and WMO Measurement Lead Centre for Aerosols and Water Vapour Remote Sensing Instruments (see Section 19). For direct sun measurements, the calibration is performed using the common Langley method. However, calibration at nighttime implies the use of a lunar irradiance model to compute the moon's extraterrestrial irradiance and account for the continuous change in the moon's illumination over the moon cycle.

The RIMO (ROLO Implementation for Moon-photometry Observation) is a model (Barreto et al., 2019) based on the USGS Robotic Lunar Observatory, ROLO (Kieffer and Stone, 2005). This model provides exo-atmospheric lunar irradiance for any given location and time, and it is commonly used for AOD retrieval at nighttime (Barreto et al., 2016). As part a of the ATMO-ACCESS EValuation of aerOsol LUnar measuremets at the saTellIte cOmmunication chaNnels (EVOLUTION) TNA at IARC, Cimel will use the measurements taken at Izaña to update the RIMO Corrected Factor model (Barreto et al., 2017; Román et al., 2020) for the two CE318-TP9 new spectral bands. This update is needed to derive accurately AOD during nighttime using this new photometer version.

9.3.7 New developments for the Cimel CE376 GPN Micro-LiDAR

The CE376 GPN micro-Lidar installed at Izaña Observatory in 2015 is one of the initial designs of the CE376 series. Within the framework of the WMO Measurement Lead Centre for Aerosols and Water Vapour Remote Sensing Instruments activities, the optical design of the instrument has undergone upgrades. Furthermore, retrieval methods for determining aerosol properties using this instrument have been developed and incorporated into the data analysis software.

The ATMO-ACCESS TNA project, Characterization Of AerosoLs In The subtropIcal nOrth atlaNtic (COALITION) (see Section 21) took place in November 2022 (Fig. 9.10). During this 5-day on-site mission, the half-wave plates positioned in front of the Polarizer Beam Splitter (PBS) cubes of the two emission channels were updated. Wire-grid polarizers were also installed behind these PBS to mitigate cross-talk in the signals, and the instrument was re-aligned and calibrated. These actions enhance both direct and polarized signals, thereby contributing to an improved characterization of aerosols in the subtropical North Atlantic free troposphere.

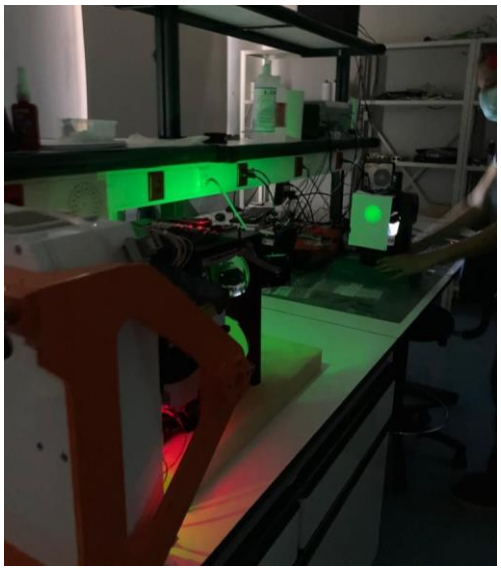

Figure 9.10. CE376 GPN micro-Lidar at IARC during COALITION activities in November 2022.

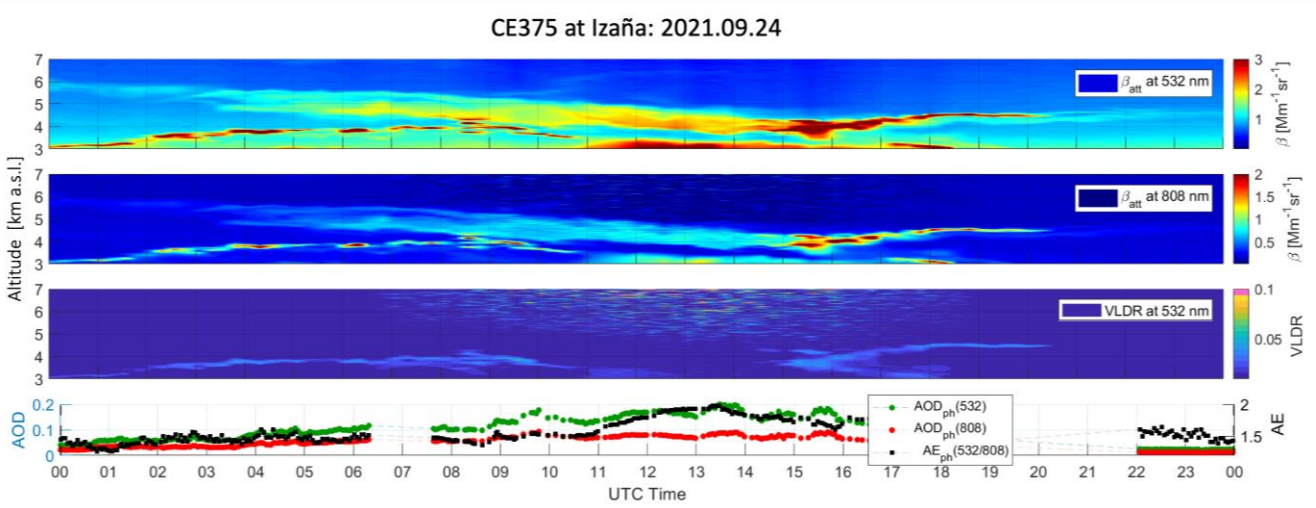

Figure 9.11. CE376 measurements of attenuated backscatter (β_{att}) at 532 and 808 nm and VLDR at 532, as well as photometer measurements of AOD and Angström Exponent (AE) performed at Izaña on 24 September 2021.

Using the two-wavelength modified Klett inversion, effective lidar ratios (LR) at both wavelengths (532 nm and 808 nm) are derived, with concurrent sun photometer measurements available on site. Consequently, AOD obtained from lidar retrievals at both wavelengths and Angström Exponent (AE) (532/808) are determined. Additional metrics providing information of aerosols typing such as Volume Linear Depolarization Ratio (VLDR), Particle Linear Depolarization Ratio (PLDR), lidar extinction coefficients and backscatter profiles at 532 nm and 808 nm can be determined. Quality control of the data was conducted onsite and remotely, following ACTRIS recommendations.

An example of measurements conducted with this instrument is presented in Fig. 9.11. The data correspond to a volcanic plume detected at Izaña Observatory, at the initial stage of the eruptive process of the 2021 La Palma volcanic eruption (approximately 140 km away), on 24 September 2021. On this day, a layer at an altitude of around 4 km a.s.l. was identified, characterized by an effective LR of 47 ± 4 sr at 532 nm and 56 ± 6 sr at 808 nm. The height-temporal variations of attenuated backscatter (β_{att}) signal, low VLDR values (< 0.06) and AE of the photometer exceeding 1.2, suggest the presence of a layer consisting of non-ash particles, specifically fine and spherical aerosols, most likely sulphates.

9.3.8 HARMONIA Cost-Action

In October 2022, the international network for harmonization of atmospheric aerosol retrievals from ground-based photometers (HARMONIA) started.

The objective of this Cost Action is to establish a network involving institutions, instrument developers, scientific and commercial end users, in order to improve and homogenize aerosol retrievals using mainly solar and sky but also lunar and star photometers from different networks. It aims to bridge user needs and the science and technology expertise residing in academia and industry, through:

- Increasing the interactions and knowledge exchanges between several atmospheric aerosol network measurement scientists and users.
- Standardizing and improving existing aerosol products and tools, towards a "harmony" in aerosol photometry.
- Stimulating the communication between operational agencies and academia, with the aim of increasing the applicability of aerosol products.
- Encouraging and organizing the dialogue between researchers and instrument manufacturers, towards innovation actions on current and future photometric-aerosol instrumentation.

The PI of the aerosol group (Dr África Barreto) is a member of the HARMONIA Management Committee.

9.3.9 Contributions to the 2021 La Palma volcanic eruption emergency response

The aerosol group contributed to activities carried out by IARC-AEMET during the 2021 La Palma volcanic eruption both in the emergency deployment in La Palma and in Tenerife at the Izaña Observatory. We participated as co-authors in Bedoya-Velásquez et al. (2022), Córdoba-Jabonero et al. (2023), García et al. (2022), García et al. (2023), Milford et al. (2023), Salgueiro et al. (2023) and Sicard et al. (2022). For more details see ACTRIS (2021) and Section 23.

9.4 References

ACTRIS, ACTRIS-Spain coordinating unprecedented actions for the Cumbre Vieja volcanic emergency, November 2021. Available at: https://www.actris.eu/news-events/news/actris-spain-coordinating-unprecedented-actions-cumbre-vieja-volcanic-emergency

Barreto, A., Cuevas, E., Pallé, P., Romero, P. M., Guirado, C., Wehrli, C. J., and Almansa, F.: Recovering long-term aerosol optical depth series (1976–2012) from an astronomical potassium-based resonance scattering spectrometer, Atmos. Meas. Tech., 7, 4103–4116, https://doi.org/10.5194/amt-7-4103-2014, 2014.

Barreto, Á., Cuevas, E., Granados-Muñoz, M. J., Alados-Arboledas, L., Romero, P. M., Gröbner, J., Kouremeti, N., Almansa, A. F., Stone, T., Toledano, C., Román, R., Sorokin, M., Holben, B., Canini, M., and Yela, M.: The new sun-skylunar Cimel CE318-T multiband photometer – a comprehensive performance evaluation, Atmos. Meas. Tech., 9, 631–654, https://doi.org/10.5194/amt-9-631-2016, 2016.

Barreto, Á., Román, R., Cuevas, E., Berjón, A. J., Almansa, A. F., Toledano, C., González, R., Hernández, Y., Blarel, L., Goloub, P., Guirado, C., and Yela, M.: Assessment of nocturnal aerosol optical depth from lunar photometry at the Izaña high mountain observatory, Atmos. Meas. Tech., 10, 3007–3019, https://doi.org/10.5194/amt-10-3007-2017, 2017.

Barreto, A., R. Román, E. Cuevas, D. Pérez-Ramírez, A.J. Berjón, N. Kouremeti, S. Kazadzis, J. Gröbner, M. Mazzola, C. Toledano, J.A. Benavent-Oltra, L. Doppler, J. Juryšek, A.F. Almansa, S. Victori, F. Maupin, C. Guirado-Fuentes, R. González, V. Vitale, P. Goloub, L. Blarel, L. Alados-Arboledas, E. Woolliams, S. Taylor, J.C. Antuña, M. Yela, Evaluation of night-time aerosols measurements and lunar irradiance models in the frame of the first multi-instrument nocturnal intercomparison campaign, Atmospheric Environment, 202, https://doi.org/10.1016/j.atmosenv.2019.01.006, 2019.

Barreto, Á., García, R. D., Guirado-Fuentes, C., Cuevas, E., Almansa, A. F., Milford, C., Toledano, C., Expósito, F. J., Díaz, J. P., and León-Luis, S. F.: Aerosol characterisation in the subtropical eastern North Atlantic region using long-term AERONET measurements, Atmos. Chem. Phys., 22, 11105–11124, https://doi.org/10.5194/acp-22-11105-2022, 2022a.

Barreto, Á., Cuevas, E., García, R. D., Carrillo, J., Prospero, J. M., Ilić, L., Basart, S., Berjón, A. J., Marrero, C. L., Hernández, Y., Bustos, J. J., Ničković, S., and Yela, M.: Long-term characterisation of the vertical structure of the Saharan Air Layer over the Canary Islands using lidar and radiosonde profiles: implications for radiative and cloud processes over the subtropical Atlantic Ocean, Atmos. Chem. Phys., 22, 739–763, https://doi.org/10.5194/acp-22-739-2022, 2022b.

Bedoya-Velásquez, A.E.; Hoyos-Restrepo, M.; Barreto, A.; García, R.D.; Romero-Campos, P.M.; García, O.; Ramos, R.; Roininen, R.; Toledano, C.; Sicard, M.; Ceolato, R. Estimation of the Mass Concentration of Volcanic Ash Using Ceilometers: Study of Fresh and Transported Plumes from La Palma Volcano. Remote Sens. 14, 5680. https://doi.org/10.3390/rs14225680, 2022

Che, H., Qi, B., Zhao, H., Xia, X., Eck, T. F., Goloub, P., Dubovik, O., Estelles, V., Cuevas-Agulló, E., Blarel, L., Wu, Y., Zhu, J., Du, R., Wang, Y., Wang, H., Gui, K., Yu, J., Zheng, Y., Sun, T., Chen, Q., Shi, G., and Zhang, X.: Aerosol optical properties and direct radiative forcing based on measurements from the China Aerosol Remote Sensing Network (CARSNET) in eastern China, Atmos. Chem. Phys., 18, 405-425, https://doi.org/10.5194/acp-18-405-2018, 2018.

Córdoba-Jabonero, C., M. Sicard, Á. Barreto, C. Toledano, M. Á. López-Cayuela, C. Gil-Díaz, O. García, C. V. Carvajal-Pérez, A. Comerón, R. Ramos, C. Muñoz-Porcar, A. Rodríguez-Gómez, Fresh volcanic aerosols injected in the atmosphere during the volcano eruptive activity at the Cumbre Vieja area (La Palma, Canary Islands): Temporal evolution and vertical impact, Atmospheric Environment, Volume 300, 2023, 119667, ISSN 1352-2310, https://doi.org/10.1016/j.atmosenv.2023.119667.

García, R.D.; García, O.E.; Cuevas-Agulló, E.; Barreto, Á.; Cachorro, V.E.; Marrero, C.; Almansa, F.; Ramos, R.; Pó, M. Spectral Aerosol Radiative Forcing and Efficiency of the La Palma Volcanic Plume over the Izaña Observatory. Remote Sens. 2023, 15, 173. https://doi.org/10.3390/rs15010173

García, O., Suárez, D., Cuevas, E., Ramos, R., Barreto, África, Hernández, M., Quintero, V., Toledano, C., Sicard, M., Córdoba-Jabonero, C., Riz, V., Roininen, R., López, C., Vilches, J., Weiss, M., Carreño, V., Taquet, N., Boulesteix, T., Fraile, E., Torres, C., Prats, N., Alcántara, A., León, S. ., Rivas, P., Álvarez, Óscar, Parra, F., de Luis, J., González, C., Armas, C., Romero, P., de Bustos, J., Redondas, A., Marrero, C., Milford, C., Román, R., González, R., López-Cayuela, M., Carvajal-Pérez, C., Chinea, N., García, R. ., Almansa, F., González, Y., Bullón, F., Poggio, M., Rivera, C., Bayo, C., & Rey, F. (2022). La erupción volcánica de La Palma y el papel de la Agencia Estatal de Meteorología. Revista Tiempo Y Clima, 5(76). Recuperado a partir de https://pub.ame-web.org/index.php/TyC/article/view/2516

Guirado-Fuentes, C., Ramos, R., Frutos, Á., Berjón, A., Redondas, A., López, C., Cachorro, V., Cuevas, E., González-Catón, R., Gonzalez, S., Hernández, M.: Optical calibration facility at the Izaña Atmospheric Research Center. Optica Pura y Aplicada. 45. 57-62. 10.7149/OPA.45.1.57, 2012.

Kieffer, H. and Stone, T.: The Spectral Irradiance of the Moon. The Astronomical Journal. 129. 2887. 10.1086/430185, 2005.

Milford, C.; Torres, C, Vilches, J.; Gossman, A.K; Weis, F.; Suárez-Molina, D.; García, O.E.; Prats, N.; Barreto, A.; García, R.D.; Bustos, J.J.; Marrero, C. L.; Ramos, R.; Chinea, N.; Boulesteix, T.; Taquet, N.; Rodríguez, S.; López-Darias, J.; Sicard, M.; Córdoba-Jabonero, C.; Cuevas, E. Impact of the 2021 La Palma volcanic eruption on air quality: Insights from a multidisciplinary approach, Science of The Total Environment, Volume 869, 2023, 161652, ISSN 0048-9697, https://doi.org/10.1016/j.scitotenv.2023.161652.

Román, R., González, R., Toledano, C., Barreto, Á., Pérez-Ramírez, D., Benavent-Oltra, J. A., Olmo, F. J., Cachorro, V. E., Alados-Arboledas, L., and de Frutos, Á. M.: Correction of a lunar-irradiance model for aerosol optical depth retrieval and comparison with a star photometer, Atmos. Meas. Tech., 13, 6293–6310, https://doi.org/10.5194/amt-13-6293-2020, 2020.

Salgueiro,V., J.L. Guerrero-Rascado, M.J. Costa, R. Román, A. Cazorla, A. Serrano, F. Molero, M. Sicard, C. Córdoba-Jabonero, D. Bortoli, A. Comerón, F.T. Couto, M.Á. López-Cayuela, D. Pérez-Ramírez, M. Potes, J.A. Muñiz-Rosado, M.A. Obregón, R. Barragán, D.C.F.S. Oliveira, J. Abril-Gago, R. González, C. Gíl-Díaz, I. Foyo-Moreno, C. Muñoz-Porcar, M.J. Granados-Muñoz, A. Rodríguez-Gómez, M. Herreras-Giralda, J.A. Bravo-Aranda, C.V. Carvajal-Pérez, A. Barreto, L. Alados-Arboledas, Characterization of Tajogaite volcanic plumes detected over the Iberian Peninsula from a set of satellite and ground-based remote sensing instrumentation,

Remote Sensing of Environment, Volume 295, 2023, 113684, ISSN 0034-4257, https://doi.org/10.1016/j.rse.2023.113684.

Sicard, M.; Córdoba-Jabonero, C.; Barreto, A.; Welton, E.J.; Gil-Díaz, C.; Carvajal-Pérez, C.V.; Comerón, A.; García, O.; García, R.; López-Cayuela, M.-Á.; Muñoz-Porcar, C.; Prats, N.; Ramos, R.; Rodríguez-Gómez, A.; Toledano, C.; Torres, C. Volcanic Eruption of Cumbre Vieja, La Palma, Spain: A First Insight to the Particulate Matter Injected in the Troposphere. Remote Sens. 2022, 14, 2470.

Toledano, C., González, R., Fuertes, D., Cuevas, E., Eck, T. F., Kazadzis, S., Kouremeti, N., Gröbner, J., Goloub, P., Blarel, L., Román, R., Barreto, Á., Berjón, A., Holben, B. N., and Cachorro, V. E.: Assessment of Sun photometer Langley calibration at the high-elevation sites Mauna Loa and Izaña, Atmos. Chem. Phys., 18, 14555-14567, https://doi.org/10.5194/acp-18-14555-2018, 2018.

Wehrli, C.: Calibrations of filter radiometers for determination of atmospheric optical depth, Metrologia, 37, 419, https://doi.org/10.1088/0026-1394/37/5/16, 2000.

Wehrli, C.: GAWPFR: A network of aerosol optical depth observations with precision filter radiometers, GLOBAL ATMOSPHERE WATCH, p. 36, 2005.

WMO-GAW Report, The Fourth WMO Filter Radiometer Comparison (FRC-V), Prepared by Stelios Kazadzis, Natalia Kouremeti, Julian Gröbner Physikalisch-Meteorologisches Observatorium Davos, World Radiation Center, in preparation, 2023.

9.5 Staff

Dr África Barreto (AEMET; Head of programme)

Ramón Ramos (AEMET; Head of Infrastructure)

Dr Fernando Almansa (CIMEL/UVA; Research Scientist)

Dr Yenny González (CIMEL; Research Scientist)

Óscar Alvarez Losada (AEMET; Research Scientist)

Dr Rosa García (TRAGSATEC/UVA; Research Scientist)

Dr Sergio León Luis (TRAGSATEC; Research Scientist)

Pedro Miguel Romero (AEMET; Research Scientist)

Dr Victoria Cachorro (University of Valladolid; Head of Atmospheric Optics Group)

Dr Ángel de Frutos (University of Valladolid Atmospheric Optics Group; Research Scientist)

Dr Margarita Yela (INTA; Co-PI in MPL sub-programme)

10 Radiation

The radiation programme, and specifically the implementation of its core component, the Baseline Surface Radiation Network (BSRN) programme, has been performed in close collaboration with the University of Valladolid Atmospheric Optics Group.

10.1 Main Scientific Goals

The main scientific goals of this programme are:

- To conduct high quality measurement of radiation parameters.
- To investigate the variations of the solar radiation balance and other solar energy parameters at the four radiation measurement stations managed by the IARC.
- To investigate aerosols radiative forcing with a particular focus on the role played by dust taking advantage of the privileged situation of the Canary Islands to analyse dust outbreaks over the North Atlantic and the unique local radiation network with stations at different altitudes (from sea level to 3555 m a.s.l.).
- To recover, digitize and analyse historical radiation data in order to reconstruct long-term radiation series that allow us to make precise studies concerning sky darkening and brightening, and relate radiation and cloud cover and solar flux.
- To conduct the spectral characterization of the solar radiation with respect to impacts of different types of clouds, aerosols, especially mineral dust, and precipitable water vapour.

10.2 Measurement Programme

Direct radiation records from an Abbot silver-disk pyrheliometer are available since 1916, although this information has not yet been analysed. Global solar radiation records from a bimetallic pyranograph are available both in bands and as daily integrated values in printed lists, since 1977. This information has been digitized, recalibrated and processed. The results show an excellent agreement between the bimetallic pyranograph and the BSRN CM21 pyranometer, which allowed the successful reconstruction of a long-term global radiation data series (since 1977), after a careful analysis of historical data (Figure 10.1).

Global and direct radiation measurements started in 1992 as part of a solar radiation project of the Canary Islands Government. In 2005, IZO joined the Spanish radiation network managed by the AEMET National Radiation Center (CNR). Since 2009, IZO has been a BSRN station providing the basic set of radiation parameters (Drieme et al., 2018; García et al., 2019; 2022). In addition, other parameters, including shortwave and long wave upward radiation, UV-A and UV-B radiation are also measured within the BSRN Programme. Later, some basic radiation measurements were implemented at the other three IARC measurement stations (TPO, BTO and SCO, Fig. 10.2).

Radiation measurements are tested against physically possible and globally extremely rare limits, as defined and used in the BSRN recommended data quality control. Shortwave downward radiation (SDR) measurements are compared daily with SDR simulations, which are modelled with the LibRadtran model. This information has been created and shared on the web page http://bsrn.aemet.es/, where real time measurements of global, direct, diffuse and UV-B radiation are shown.

Measurements of spectral direct solar radiation (spectral direct normal irradiance) are performed with an EKO MS-711 spectroradiometer (Fig. 10.3) starting in 2016. This instrument covers a wavelength range from 300 to 1100 nm, exhibiting a Full Width at Half Maximum < 7 nm. It is equipped with its own built-in entrance optics, and the housing is temperature-stabilized at 25° ± 5° (Egli et al., 2016; García et al., 2020; 2021). The main specifications of the EKO MS-711 are given in Table 10.1.

Table 10.1. Main specifications of the EKO MS-711 spectroradiometer

EKO MS-711 spectroradiometer	
Wavelength range	300 to 1100 nm
Wavelength interval	0.3 - 0.5 nm
Optical resolution FWHM	< 7 nm
Wavelength accuracy	+/- 0.2 nm
Cosine Response (Zenith: 0 ~ 80°)	< 5%
Temp. dependency (-10ºC to 50°C)	< 2 %
Temp. Control	25ºC ± 5ºC
Operating temperature	-10ºC to 50ºC
Exposure time	10 msec – 5 sec Automatic adjustment
Dome material	Synthetic Quartz Glass
Communication	RS-422 (Between sensor and power supply)
Power requirement	12VDC, 50VA (from the power supply)

The EKO MS-711 spectroradiometer has been mounted on an Owel INTRA 3 sun-tracker (Fig. 10.3), an intelligent tracker which combines the advantages of automatic-tracking operation (automatic alignment with the system of astronomical coordinates follows after a few days), and actively-controlled tracking (a 4-quadrant sun sensor). It is constructed for use under extreme weather conditions; its operational temperature range is between -10 and +50 °C.

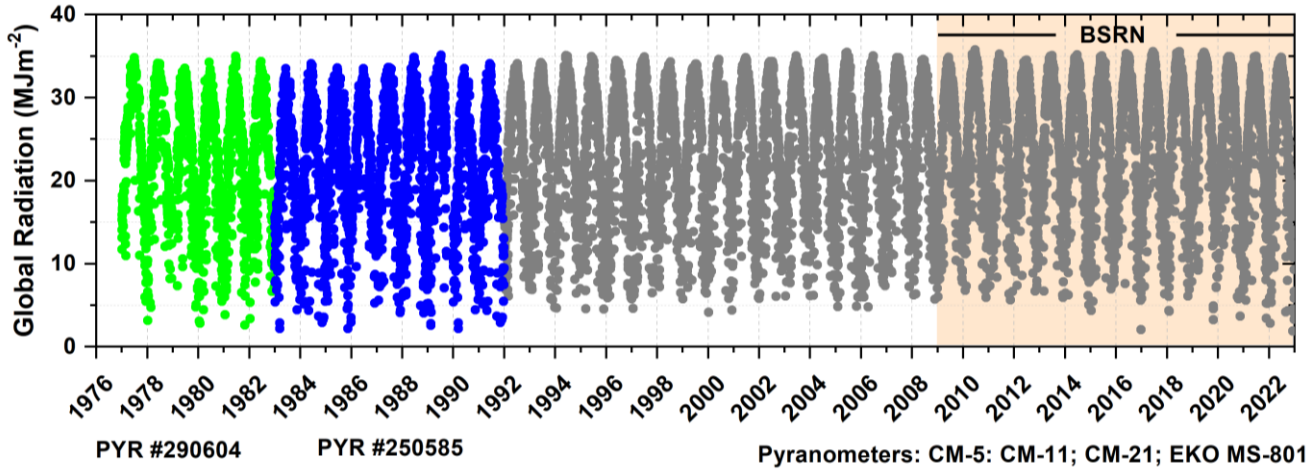

Figure 10.1. Daily GSR_H data time series between 1977 and 2022 at IZO. The green and blue dots correspond to the measurements performed with PYR #290609 and #250585, respectively, between 1977 and 1991, and the grey dots represent the measurements performed with different pyranometers (CM-5, CM-11, CM-21 and EKO MS-801) between 1992 and 2022 (García et al., 2014; 2017; 2019).

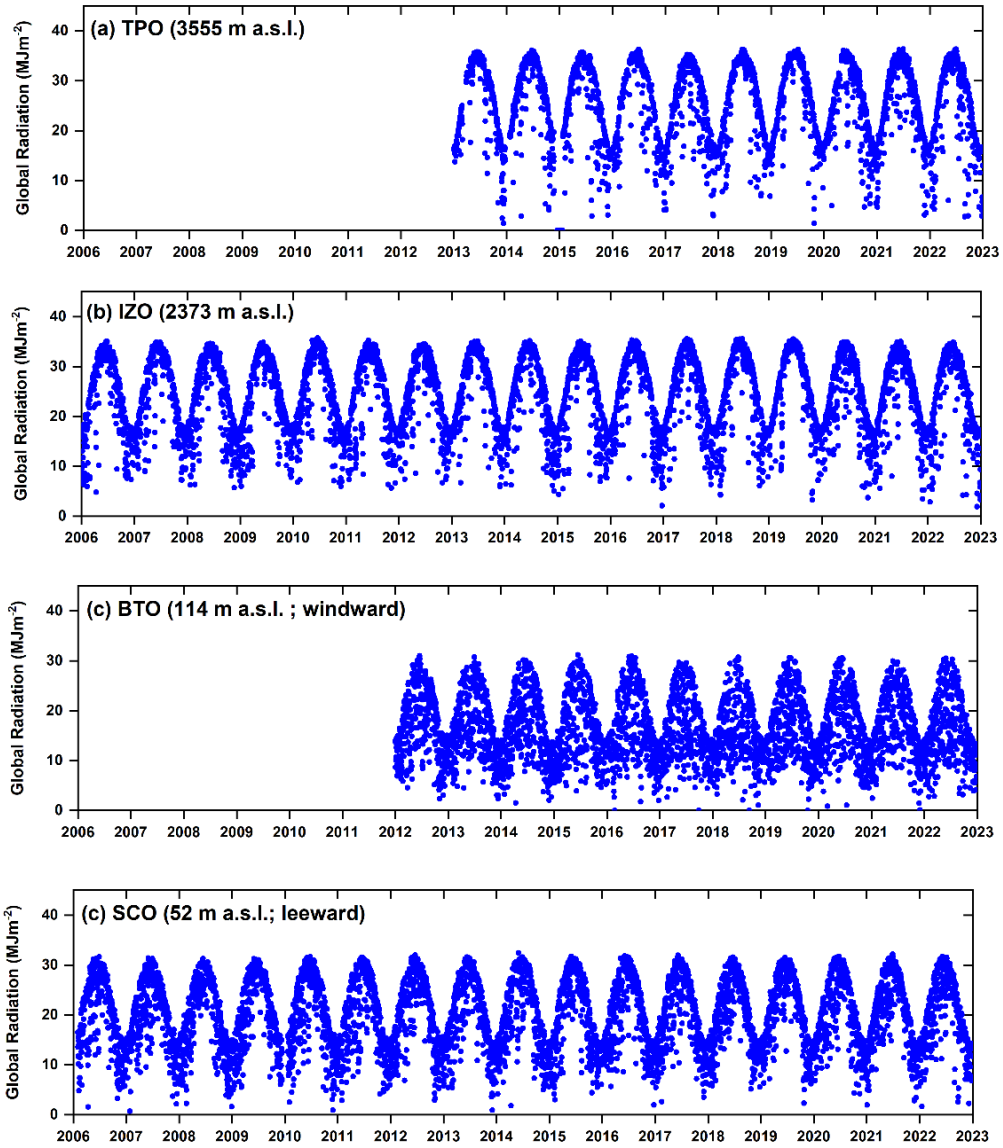

Figure 10.2. Daily global radiation (MJ m^{-2}) data time series at (a) TPO at 3555 m a.s.l., (b) IZO at 2373 m a.s.l., (c) BTO at 114 m a.s.l. and (d) SCO at 52 m a.s.l.

It can sustain about 50 kg of a carefully balanced load. The tracker motors have a special grease for use in low temperatures. The drive unit has an azimuth rotation > 360°. It moves back to the start (morning) position at the corresponding midnight. The drive unit has a zenith rotation > 90°. The unit has an angular resolution ≤ 0.1°, an angular repeatability of ≤ ± 0.05° and an angular velocity ≥ 1.5°/s on the outgoing shafts. The maximum speed is 2.42°/s.

Figure 10.3. The EKO MS-711 spectroradiometer installed at IZO.

The spectral direct solar radiation measurements have been complemented since February 2020 by global and diffuse solar radiation measurements performed with an EKO RSB spectroradiometer (Fig. 10.4). This instrument covers a wavelength range from 300 to 1100 nm. The main specifications of the EKO RSB are given in Table 10.2.

Table 10.2. Main specifications of the EKO RSB spectroradiometer

EKO RSB spectroradiometer	
Wavelength range	300 to 1100 nm
Wavelength accuracy	± 0.2 nm
Directional response	< 5º
Measurement time	10-5000 ms
Precision of Shadow Band Position	± 2º
Measurement Frequency	1 rotation / minute
Operating temperature	-10 to 50 ºC
Temperature control	25º ± 2 ºC
Shielding Angle	5º
Field of view	180º

Figure 10.4. The EKO RSB spectroradiometer installed at IZO.

The atmospheric transmission is a data product that is produced since 2014, it was also processed retrospectively back to 2009, and it has been updated until 31 December 2020. It is available on the IZO BSRN web page. The atmospheric transmission is derived from broadband (0.2 to 4.0 µm) direct solar irradiance BSRN observations. Data are for clear-sky mornings between solar elevations of 11.3° and 30°.

In late 2020, an EKO sky scanner model MS 321-LR was installed at IZO (Fig. 10.5). This instrument is provided with two sensors, one measures the sky luminance (Kcd/m^2) and the other measures the sky radiance (W/m^{2}sr). The sensors are mounted on a tracker. Data from the sky scanner is obtained in 10 min. intervals during daylight (each scan takes up to 4.5 min.). The distribution of both luminance and radiance is obtained by dividing the sky dome in 145 patches with field of view of 11º.

The main specifications of the EKO MS 321-LR are listed in Table 10.4.

Table 10.3. Main specifications of the EKO MS 321-LR sky scanner.

EKO MS 321-LR		
Luminance Sensor	Spectral response	VISIBLE response (CIE)
	Illuminance	0 - 50 Kcd/m^2
	Field of view	11º
	Slope angle	1º
	Linearity	0.3%
Radiance Sensor	Spectral response	0.3 – 3 µm
	Range	0 – 300 W/m^{2}sr
	Field of view	11º
	Slope angle	1º
	Linearity	0.5%

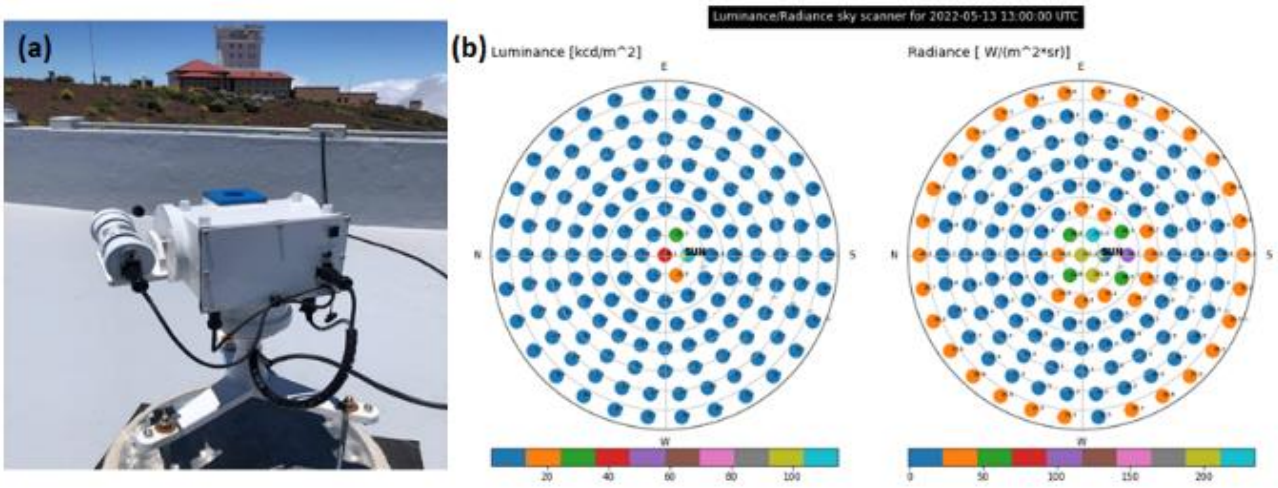

Figure 10.5. (a) The sky scanner EKO MS 321-LR installed at IZO and (b) an example of sky luminance and radiance distribution measurements performed at IZO on 13 May 2022 at 13:00 UTC.

The atmospheric transmission is a data product that has been produced since 2014, it was also processed retrospectively back to 2009, and it has been updated until December 31st, 2020 (Fig. 10.6). It is available on the IZO BSRN web page. The atmospheric transmission is derived from broadband (0.2 to 4.0 µm) direct solar irradiance BSRN observations. Data are for clear-sky mornings between solar elevations of 11.3° and 30°.

Sky images from SONA total-sky cameras at IZO and SCO, meteorological vertical profiles from radiosondes, AOD and AE from Cimel and PFR sunphotometers, column water vapour from Cimel and GPS/GLONASS, column NO_2 from DOAS, and total O_3 from Brewer spectrophotometer are used as ancillary data and/or as input data in LibRadtran SDR simulations.

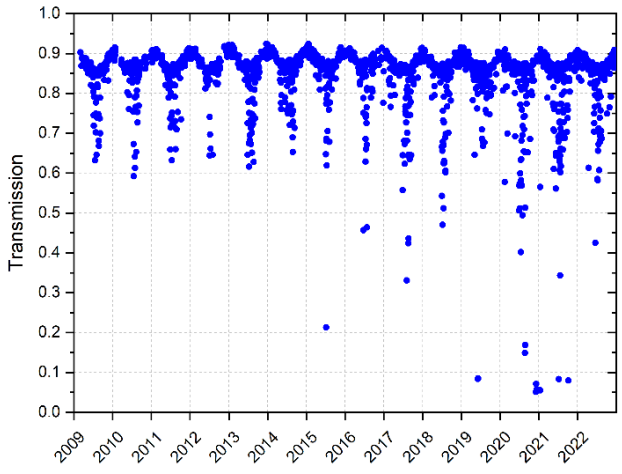

Figure 10.6. Daily atmospheric transmission data (2009-2022) at IZO computed for clear-sky mornings between solar elevations of 11.3° and 30°.

10.3 New instrumentation

10.3.1 BSRN Instrumentation

During 2022, the instrumentation of the BSRN of the Izaña Observatory has been renewed and expanded by solar tracker (EKO STR-32G), two EKO MS-80S pyranometers for global and diffuse radiation measurement, EKO MS-57 pyrheliometer for direct radiation, EKO MS-10S pyranometer for UVA radiation, EKO MS-21 pyrgeometer for longwave downward radiation and ML-020P pyranometer for photosynthetically active radiation (PAR) (Figure 10.7).

Figure 10.7. New instrumentation of the BSRN Izaña installed at IZO during 2022.

10.3.2 EKO MS-713 spectroradiometer

Also in 2022, IZO acquired a grating spectroradiometer EKO MS-713 (Fig. 10.8) to complete the measures of the spectral global radiation in the near infrared wavelength range of 900 to 2500 nm.

Figure 10.8. The EKO MS-713 spectroradiometer installed at IZO.

This instrument has succeeded to control the temperature of the spectrometer at constant to suppress the temperature change in spectrometer, which will greatly affect the measurement uncertainty, allowing maintaining a high performance over a wide operation temperature range. The main specifications of the EKO MS-713 are given in Table 10.4.

Table 10.4 Main specifications of the EKO MS-713 spectroradiometer.

EKO MS-713 spectroradiometer	
Wavelength range	900 to 2500 nm
Wavelength accuracy	± 0.2 nm
Optical resolution FWHM	< 20 nm
Wavelength Interval	1.2 to 2.2 nm
Temp. response (-10ºC to 50°C)	< 2 %
Operating temperature	-30 to 50 ºC
Temperature control	-20 ºC
Exposure time	1 - 30 msec
Cosine Response	< ±5% (within 80°)

10.4 Participation in Scientific Projects and Campaigns/Experiments

10.4.1 Calibration campaign of BSRN instruments with a PMO6 Absolute Cavity Pyrheliometer

As part of the radiation quality assurance system a calibration campaign of BSRN pyranometers and pyrheliometer took place in summers 2021 and 2022 using an Absolute Cavity Pyrheliometer PMO6 as reference (Fig. 10.9). The PMO6 was calibrated by the World Radiation Center, Davos. The BSRN instruments were calibrated following the ISO 9059:1990 (E) and ISO 9846:1993(E), delivering the corresponding official calibration certificates.

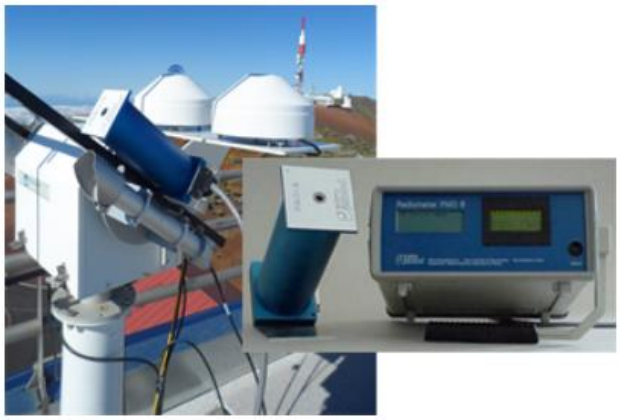

Figure 10.9. Absolute cavity radiometer (PMO6) installed at IZO during summers 2021 and 2022 on the BSRN sun-tracker.

10.4.2 Solar radiation in the Teide National Park

Solar radiation is the fundamental natural factor that governs the climate on Earth, being of vital importance for the development of life. Knowledge of the characteristics of solar radiation is also important in a wide range of applications such as agricultural sciences, the health sector, meteorology, engineering, and numerous fields of natural sciences. In this context, IARC-AEMET and the Teide National Park have created a radiometric network with the aim to monitor the solar radiation in different locations of the Park (Figs. 10.10 and 10.11). For more details of this radiometric network in the Teide National Park see García and Cuevas (2021).

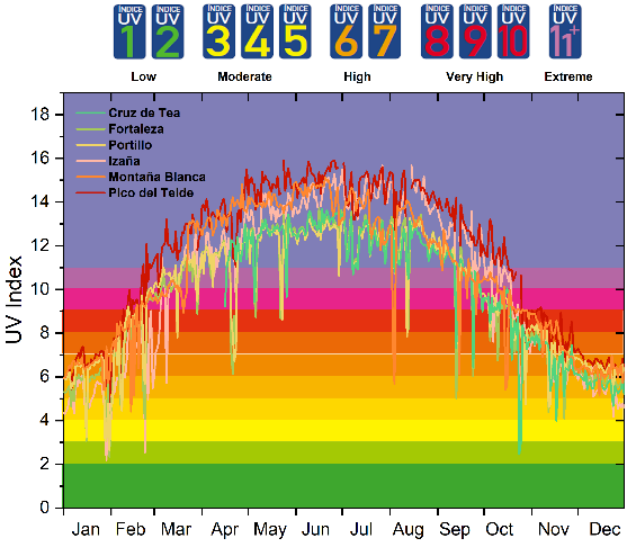

Figure 10.10. UV Index in the different stations of the Teide National Park during 2018. Reprinted from García and Cuevas (2021).

Figure 10.11. Geographical location of the radiometric stations installed in the Teide National Park (TNP). The yellow line represents the limits of the National Park. (Cruz de Tea (TNP), 2053 m a.s.l.; Fortaleza (TNP), 2067 m a.s.l.; Portillo (TNP), 2107 m a.s.l.; Izaña (IARC-AEMET), 2373 m a.s.l.; Montaña Blanca (TNP) 2757 m a.s.l. and Pico del Teide (IARC-AEMET), 3555 m a.s.l.). Reprinted from García and Cuevas (2021).

A summary of the radiation measurement programme managed by the IARC is given in Table 10.5.

Table 10.5. Details of IARC radiation measurement programme.

Instrument	Measurements	Spectral Range
Izaña historical records (2373 m a.s.l.) Start Date: Different dates		
Abbot silver-disk pyrheliometer	Direct Radiation (1916)	~0.3 to ~3.0 μm
Bimetallic pyranograph (analog.)	Global Radiation (Jan 1977)	~0.3 to ~3.0 μm
YES Multi Filter Rotating Shadow-band Radiometer	Global, diffuse and estimated direct radiation (Feb 1996)	300-1200 nm
K&Z CM5 pyranometer	Global radiation (Jan 1992)	310-2800 nm
Izaña BSRN Station (2373 m a.s.l.) Start Date: March 2009		
Pyranometer K&Z CM-21, EKO MS-801, EKO MS-80S	Global and Diffuse Radiation	285-2600 nm
Pyrheliometer K&Z CH-1, EKO MS-56, EKO MS-57	Direct Radiation	200-4000 nm
Pyrgeometer K&Z CG-4, EKO MS-21	Longwave Downward Radiation	4500-42000 nm
Net Radiometer, EKO MR-60	Net Radiation	

Pyranometer K&Z UV-A-S-T, EKO MS-10S	UV-A Radiation	315-400 nm
Pyranometer Yankee YES UVB-1	UV-B Radiation	280-400 nm
Absolute Cavity Pyrheliometer PMO6	Direct Radiation	-
Spectroradiometer EKO MS-711	Spectral Direct Radiation	300-1100 nm
Spectroradiometer EKO RSB	Spectral Global and Diffuse Radiation	300-1100 nm
Spectroradiometer EKO MS-713	Spectral Global Radiation	900-2500 nm
EKO MS-321LR Sky Scanner	Luminance/Radiance	-
EKO Photon Sensor ML-020P	Photosynthetically Active Radiation (PAR)	400-700 nm
SPN1 Sunshine Pyranometer	Global and Diffuse Radiation	400-2700 nm
Izaña National Radiation Center (CNR) Station (2373 m a.s.l.) Start Date: August 2005		
Pyranometer K&Z CM-21	Global and Diffuse Radiation	285-2600 nm
Pyrheliometer K&Z CH-1	Direct Radiation	200-4000 nm
Pyrgeometer K&Z CG-4	Longwave Downward Radiation	4500-42000 nm
Pyranometer Yankee YES UVB-1	UV-B Radiation	280-400 nm
Pyranometer K&Z PQS1	Photosynthetically Active Radiation (PAR)	400-700 nm
SCO (52 m a.s.l.) Start Date: February 2006		
Pyranometer K&Z CM-11	Global and Diffuse Radiation	310-2800 nm
Pyrheliometer EPPLY	Direct Radiation	200-4000 nm
SPN1 Sunshine Pyranometer	Global and Diffuse Radiation	400-2700 nm
BTO (114 m a.s.l.) Start Date: 2009		
Pyranometer K&Z CM-11	Global and Diffuse Radiation	310-2800 nm
TPO (3555 m a.s.l.) Start Date: July 2012		
Pyranometer K&Z CM-11, CM-21	Global and Diffuse Radiation	310-2800 nm
Pyranometer Yankee YES UVB-1	UV-B Radiation	280-400 nm
SPN1 Sunshine Pyranometer	Global and Diffuse Radiation	400-2700 nm

The main on-going and future activities of the radiation programme are focused on:

- Characterization of CIE standard sky types at Izaña station from sky scanner measurements.
- Accurate determination of cloud attenuation impact on global, direct and diffuse spectral radiation performed with EKO RSB spectroradiometer from SCO and IZO.
- Reconstruction and accurate analysis of a new long-term GSR data series (since 1916) in which newly recovered observation data are being incorporated. Long-term records of aerosols (AOD), cloudiness, and solar flux will be compared with GSR data.
- Accurate determination of cloud attenuation impact on global radiation using GSR from SCO and BTO.
- Accurate analysis of UV-B broadband data from the vertical transect formed by SCO (52 m a.s.l.), IZO (2373 m a.s.l) and TPO (3555 m a.s.l.) observatories, with complementary information on cloudiness, AOD and O_3 vertical profiles (ECC O_3 sondes).

10.5 Contributions to the 2021 La Palma volcanic eruption activities

The Radiation group contributed to activities carried out by IARC-AEMET during the 2021 La Palma volcanic eruption, both in La Palma and in Tenerife at the Izaña Observatory, leading a study entitled: "Spectral Aerosol Radiative Forcing and Efficiency of the La Palma Volcanic Plume over the Izaña Observatory" (García et al., 2023). For more details of this study see Section 23.7.5.

10.6 References

Driemel, A., Augustine, J., Behrens, K., Colle, S., Cox, C., Cuevas-Agulló, E., Denn, F. M., Duprat, T., Fukuda, M., Grobe, H., Haeffelin, M., Hodges, G., Hyett, N., Ijima, O., Kallis, A., Knap, W., Kustov, V., Long, C. N., Longenecker, D., Lupi, A., Maturilli, M., Mimouni, M., Ntsangwane, L., Ogihara, H., Olano, X., Olefs, M., Omori, M., Passamani, L., Pereira, E. B., Schmithüsen, H., Schumacher, S., Sieger, R., Tamlyn, J., Vogt, R., Vuilleumier, L., Xia, X., Ohmura, A., and König-Langlo, G.: Baseline Surface Radiation Network (BSRN): structure and data description (1992–2017), Earth Syst. Sci. Data, 10, 1491–1501, https://doi.org/10.5194/essd-10-1491-2018, 2018.

Egli, L., Gröbner, J., Hülsen, G., Bachmann, L., Blumthaler, M., Dubard, J., Khazova, M., Kift, R., Hoogendijk, K., Serrano, A., Smedley, A., and Vilaplana, J.-M.: Quality assessment of solar UV irradiance measured with array spectroradiometers, Atmos. Meas. Tech., 9, 1553-1567, doi:10.5194/amt-9-1553-2016, 2016.

García, R. D., Cuevas, E., García, O. E., Cachorro, V. E., Pallé, P., Bustos, J. J., Romero-Campos, P. M., and de Frutos, A. M.: Reconstruction of global solar radiation time series from 1933 to 2013 at the Izaña Atmospheric Observatory, Atmos. Meas. Tech., 7, 3139-3150, doi:10.5194/amt-7-3139-2014, 2014.

García, R. D., Cuevas, E., García, O. E., Ramón, R., Romero-Campos, P. M., de Ory, F., Cachorro, V. E., and de Frutos, A.: Compatibility of different measurement techniques. Long-term global solar radiation observations at Izaña Observatory, Atmos. Meas. Tech., 10, 731-743, doi:10.5194/amt-10-731-2017, 2017.

García, R. D., Cuevas, E., Ramos, R., Cachorro, V. E., Redondas, A., and Moreno-Ruiz, J. A.: Description of the Baseline Surface Radiation Network (BSRN) station at the Izaña Observatory (2009–2017): measurements and quality control/assurance procedures, Geosci. Instrum. Method. Data Syst., 8, 77–96, https://doi.org/10.5194/gi-8-77-2019, 2019.

García, R. D., Cuevas, E., Barreto, Á., Cachorro, V. E., Pó, M., Ramos, R., and Hoogendijk, K.: Aerosol retrievals from the EKO MS-711 spectral direct irradiance measurements and corrections of the circumsolar radiation, Atmos. Meas. Tech., 13, 2601–2621, https://doi.org/10.5194/amt-13-2601-2020, 2020.

García, R.D.; Cuevas, E.; Cachorro, V.E.; García, O.E.; Barreto, Á.; Almansa, A.F.; Romero-Campos, P.M.; Ramos, R.; Pó, M.; Hoogendijk, K.; Gross, J: Water Vapor Retrievals from Spectral Direct Irradiance Measured with an EKO MS-711 Spectroradiometer-Intercomparison with Other Techniques, Remote Sens, 13, 350. https://doi.org/10.3390/rs13030350, 2021.

García, R. D. and Cuevas, E.: Radiación Solar en el Parque Nacional del Teide. Durban, N & Martín-Esquivel, JL (Eds.). Ciencia en el Parque Nacional del Teide 2009-2019. Cabildo Insular de Tenerife y Ediciones Turquesa. Santa Cruz de Tenerife. Capítulo VIII, ISBN 978-84-16785-84-1, 2021.

García, R.D., Cuevas, E., Ramos, R., Redondas, A. and Cachorro, V.E. "Status of the Izaña BSRN station in 2022", 17th BSRN Scientific Review and Workshop (hybrid, Ispra, VA, Italy) 27-30 June 2022.

García, R.D.; García, O.E.; Cuevas-Agulló, E.; Barreto, Á.; Cachorro, V.E.; Marrero, C.; Almansa, F.; Ramos, R.; Pó, M. Spectral Aerosol Radiative Forcing and Efficiency of the La Palma Volcanic Plume over the Izaña Observatory. Remote Sensing, 15, 173, https://doi.org/10.3390/rs15010173, 2023.

10.7 Staff

Dr Emilio Cuevas (AEMET; Head of programme, until August 2023)

Carlos Torres (AEMET; Head of programme, from September 2023)

Dr Rosa García (TRAGSATEC/UVA; Co-PI)

Ramón Ramos (AEMET; Head of Infrastructure)

Dr Omaira García (AEMET; Research Scientist)

Dr Victoria Cachorro (University of Valladolid; Head of Atmospheric Optics Group)

Dr Ángel de Frutos (University of Valladolid Atmospheric Optics Group; Research Scientist)

11 Differential Optical Absorption Spectroscopy (DOAS)

11.1 Main Scientific Goals

Differential Optical Absorption Spectroscopy (DOAS) and Multi Axis Differential Optical Absorption Spectroscopy (MAXDOAS) techniques allow the determination of atmospheric trace gases present in very low concentrations. The long-term monitoring of atmospheric trace gases is of great interest for trend studies and satellite validation. The detection of gases using DOAS or MAXDOAS technique allows the study of mutual interaction between gases even when detection limits of the gases are low.

The main scientific goals of the DOAS and MAXDOAS programme are:

- To improve the knowledge of the distribution, seasonal behaviour and long-term trends of minor constituents related to ozone equilibrium such as NO_2, BrO and IO and their distribution in the subtropical atmosphere.
- To obtain a climatology of stratospheric NO_2 and BrO in subtropical regions and to study its dependence on environmental and climate variables.
- To study the seasonal variations of NO_2, O_3, formaldehyde (HCHO) and IO in the free troposphere and their interaction with environmental factors such as Saharan dust amongst others.
- To contribute to validation of NO_2 and O_3 satellite products (GOME, GOME2, SCIAMACHY, OMI, TROPOMI) and in the improvement of the methodology to perform such comparisons.

11.2 Measurement Programme

The DOAS technique (Platt and Stutz, 2008) is a method to determine the atmospheric trace gases column density by measuring their absorption structures in the near ultraviolet and visible spectral region.

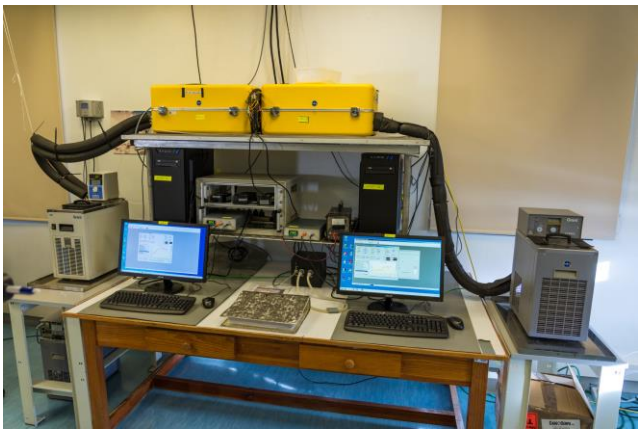

Figure 11.1. RASAS II and ARTIST II MAXDOAS (UV-VIS) spectroradiometers at IARC.

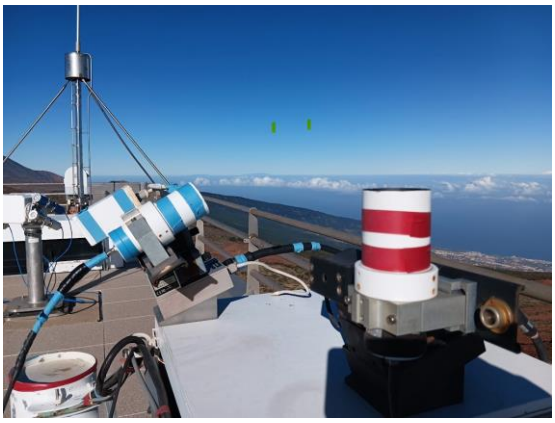

Figure 11.2. DOAS instruments outdoor optics with sky trackers.

The technique is based on measurement of atmospheric absorption of solar radiation at selected wavelength bands where the gas under consideration shows a structured and known absorption cross-section. For stratospheric observations the instrument is pointed at zenith during the twilights.

Although the DOAS technique was developed for stratospheric research, during the last few years it has been largely employed in tropospheric environment and pollution episodes studies. In particular, the so called Multi Axis Differential Optical Absorption Spectroscopy approach allows to infer vertical distribution of minor species from spectrometric measurements of solar scattered light at given angles of elevation (off-axis measurements). The analysis technique makes use of the Optical Estimation Method (Rodgers, 2000) by putting together the off-axis measurements and a radiative transfer algorithm to get the best solution for all used elevation angles.

The instruments (see Figs 11.1 and 11.2) automatically take spectra from an AM SZA = 96º to PM SZA = 96º, every day. As the instrument must work with a stabilized room temperature and also with a stabilized internal temperature and humidity, those parameters are monitored and recorded in data files. Calibration of the instrument grating is performed approximately every year. Calibration of the elevation angle is performed once a month. After the spectral inversion, a quality control of data is carried out. The acquired data are filtered on the basis of the analysis and instrumental error, aerosol optical thickness and the solar zenith angles, to ensure quality.

INTA has performed measurements of stratospheric O_3 and NO_2 at IARC since 1993. Data have been used for the study of stratospheric O_3 and NO_2 distribution in the subtropical region (Gil et al., 2008, Gil et al., 2012 and Yela et al., 2017) and for validation of satellite products (Hendrick et al., 2011, Robles-Gonzalez et al., 2016, Yela et al., 2017). In 2003, the installation of an ultraviolet DOAS spectrometer expanded the measurements of stratospheric gases to the near ultraviolet region, allowing the monitoring of

stratospheric BrO and the estimation of the concentration of BrO in the free troposphere. In 2010, the instruments were adapted to MAXDOAS measurements, allowing the detection of free tropospheric trace gases, such as IO and NO_2 (Puentedura et al, 2012, Gomez et al., 2014, Gil-Ojeda et al., 2015) in the visible region and of BrO and HCHO in the ultraviolet region. Prior to the installation at IZO in 2009, the VIS-MAXDOAS instrument participated in the international blind NO_2 MAXDOAS intercomparison campaign CINDI (Cabauw Intercomparison campaign Nitrogen Dioxide measuring Instrument) (Piters et al., 2012, Pinardi et al., 2013). During the AMISOC campaign in 2013, extensive measurements of IO were performed at three different altitude levels on Tenerife.

11.3 Participation in Scientific Projects and Campaigns/Experiments

11.3.1 Contribution to NDACC data base

The Network for Detection of Atmospheric Composition Change (De Mazière et al., 2018) is one of the most important global networks which primary goal is to establish long-term databases for detecting changes and trends in the chemical and physical state of the atmosphere and to assess the coupling of such changes with climate and air quality. INTA, with DOAS measurements of O_3 and NO_2 at IZO, has contributed to NDACC since 1998. Participation in NDACC requires compliance with strict measurement and data protocols to ensure that the network data is of high and consistent quality. NO_2 and O_3 results are shown in Figs 11.3 and 11.4.

11.3.2 Contribution to CAMS27

The Copernicus Atmosphere Monitoring Service (CAMS) is an integrated service within the Copernicus program that provides information on the atmospheric composition. CAMS27 provides CAMS or high-quality atmospheric data in HDF GEOMS format within a few weeks after measurements acquisition from selected NDACC stations, such as the DOAS measurements at IARC from INTA.

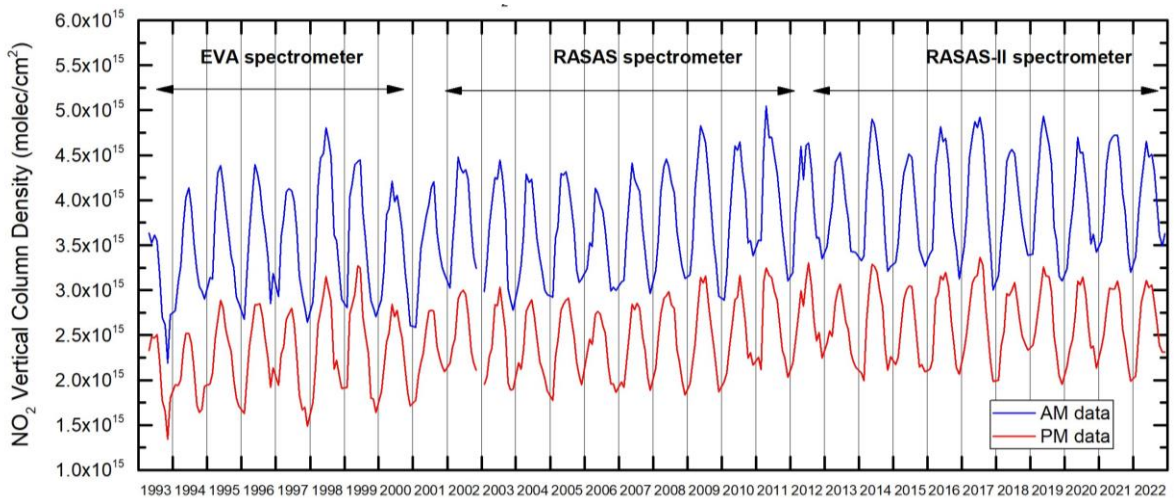

Figure 11.3. Time series of reanalyzed stratospheric NO_2 1993-2022.

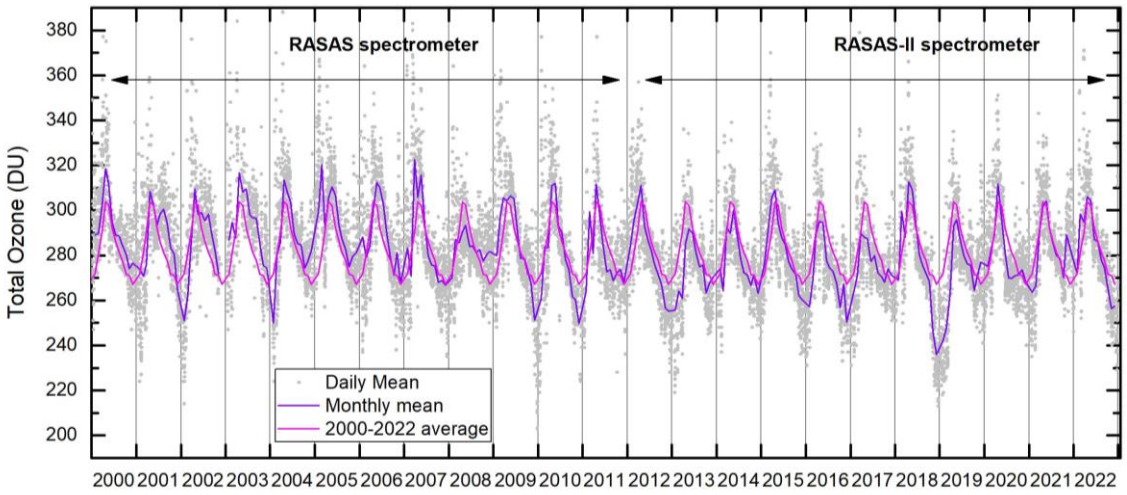

Figure 11.4. Time series of reanalyzed stratospheric O_3 2000-2022.

11.3.3 S5P NItrogen Dioxide and FORmaldehyde Validation (NIDFORVal) using NDACC and complementary FTIR and UV-Vis DOAS ground-based remote sending data

NIDFORVal is an ESA project (ID28607) led by the Royal Belgian Institute for Space Aeronomy (BIRA-IASB) that started in 2016 and extends to 2024. The aim of this project is to establish a network of observations supporting validation for tropospheric products of the Sentinel-5 Precursor (Sentinel-5P). The INTA-MAXDOAS instruments installed at IARC are part of the Sentinel-5P Calibration and Validation Team for NO_2.

11.3.4 Contribution to FRM4DOAS-2.0

Fiducial Reference Measurements (FRM) can be defined as a suite of independent, fully characterized, and traceable ground measurements that follow the guidelines outlined by the project Quality Assured Data for Earth Observation communities (QA4EO). These FRM provide the maximum return on investment for a satellite mission by delivering to users the required confidence in data products, in the form of independent validation of results and satellite measurement uncertainty estimation, over the entire end-to-end duration of a satellite mission. A number of FRM projects have been set up in the past by ESA to build up FRM for different satellites and measurement types.

FRM4DOAS2.0 (FRM for DOAS 2.0), led by BIRA-IASB, started in 2022 and will be completed in 2024, was designed as a continuation of the previous FRM4DOAS project. The main objectives of FRM4DOAS were the specification of best practices for the operation of MAXDOAS instrumentation, the evaluation of the different existing MAXDOAS analysis algorithms, and, finally, the development and implementation of a central and automatic near real-time processing system for the delivery of harmonized and quality-controlled MAXDOAS data products (NDACC MAXDOAS Service). FRM4DOAS-2.0 focuses on the consolidation of existing trace gas algorithms and the development of a new suite of products under the FRM MAX-DOAS activity.

The VIS-MAXDOAS instrument installed at IARC is part of the FRM4DOAS project providing NO_2 and O_3 DOAS/ MAXDOAS data products.

11.4 Summary of remarkable results during the period 2021-2022

11.4.1 Satellite validation

Marais et al. (2021) use Izaña VIS-MAXDOAS tropospheric NO_2 column data to compare and evaluate upper tropospheric NO_2 TROPOMI observations from June 2019 to February 2020. The MAXDOAS instrument at IARC, as a high altitude free tropospheric monitoring site, is a good candidate for this intercomparison. Upper tropospheric NO_2 TROPOMI products are retrieved using cloud-slicing retrieval technique.

Verhoelst et al. (2021) compare tropospheric, stratospheric and total NO_2 column from TROPOMI S5P to globally distributed correlative measurements collected by 19 MAXDOAS, 26 NDACC zenith DOAS, and 25 Pandonia Global Network instruments, in the frame of the NIDFORVal project. Izaña VIS-DOAS zenith NO_2 has participated in this work with the data used for comparison with stratospheric NO_2 column product from TROPOMI S5P.

11.4.2 Comparison to other measurement techniques

Garcia et al. (2021) provides an overview of 20 years of FTIR measurements taken in the framework of NDACC at IARC. In order to examine the quality and long-term consistency of the FTIR observations, a comparison of those NDACC products for which other high quality measurement techniques are available at IZO has been performed in this work. For NO_2 and O_3 total columns, the Izaña VIS-MAXDOAS instrument has been used.

11.5 References

De Mazière, M., Thompson, A. M., Kurylo, M. J., Wild, J. D., Bernhard, G., Blumenstock, T., Braathen, G. O., Hannigan, J. W., Lambert, J.-C., Leblanc, T., McGee, T. J., Nedoluha, G., Petropavlovskikh, I., Seckmeyer, G., Simon, P. C., Steinbrecht, W., and Strahan, S. E.: The Network for the Detection of Atmospheric Composition Change (NDACC): history, status and perspectives, Atmos. Chem. Phys., 18, 4935-4964, https://doi.org/10.5194/acp-18-4935-2018, 2018.

Gil-Ojeda, M., M. Navarro-Comas, A. Redondas, O. Puentedura, F. Hendrick, M. Van Roozendael, J. Iglesias and E. Cuevas. Título: Total ozone measurements from the NDACC Izaña Subtropical Station: Visible spectroscopy versus Brewer and satellite instruments. Quadrennial Ozone Symposium, (QOS 2012). Toronto, Canada. 27-31 August 2012.

Gil-Ojeda, M. Navarro-Comas, L. Gómez-Martín, J. A. Adame, A. Saiz-Lopez, C. A. Cuevas, Y. González, O. Puentedura, E. Cuevas, J.-F. Lamarque, D. Kinninson, S. Tilmes, NO2 seasonal evolution in the north subtropical free troposphere, Atmos. Chem. Phys., 15, pp. 10569-10579, doi:10.5194/acp-15-10567-2015, 2015.

Gil, M., M. Yela, L. N. Gunn, A. Richter, I. Alonso, M. P. Chipperfield, E. Cuevas, J. Iglesias, M. Navarro, O. Puentedura, and S. Rodrıguez, NO2 climatology in the northern subtropical region: diurnal, seasonal and interannual variability Atmos. Chem. Phys. 8, 1635–1648, 2008.

Gomez, L., Navarro-Comas, M., Puentedura, O., Gonzalez, Y., Cuevas, E., and Gil-Ojeda, M.: Long-path averaged mixing ratios of O3 and NO2 in the free troposphere from mountain MAX-DOAS, Atmos. Meas. Tech., 7, 3373-3386, doi:10.5194/amt-7-3373-2014, 2014.

Hendrick, F., J.-P. Pommereau, F. Goutail, R. D. Evans, D. Ionov, A. Pazmino, E. Kyrö, G. Held, P. Eriksen, V. Dorokhov, M. Gil, and M. Van Roozendael, NDACC/SAOZ UV-visible total ozone measurements: improved retrieval and comparison with

correlative ground-based and satellite observations, Atmos. Chem. Phys., 11, 5975-5995, 2011.

Marais, E. A., Roberts, J. F., Ryan, R. G., Eskes, H., Boersma, K. F., Choi, S., Joiner, J., Abuhassan, N., Redondas, A., Grutter, M., Cede, A., Gomez, L., and Navarro-Comas, M.: New observations of NO2 in the upper troposphere from TROPOMI, Atmos. Meas. Tech., 14, 2389–2408, https://doi.org/10.5194/amt-14-2389-2021, 2021.

García, O. E., Schneider, M., Sepúlveda, E., Hase, F., Blumenstock, T., Cuevas, E., Ramos, R., Gross, J., Barthlott, S., Röhling, A. N., Sanromá, E., González, Y., Gómez-Peláez, Á. J., Navarro-Comas, M., Puentedura, O., Yela, M., Redondas, A., Carreño, V., León-Luis, S. F., Reyes, E., García, R. D., Rivas, P. P., Romero-Campos, P. M., Torres, C., Prats, N., Hernández, M., and López, C.: Twenty years of ground-based NDACC FTIR spectrometry at Izaña Observatory-overview and long-term comparison to other techniques, Atmos. Chem. Phys., 21, 15519–15554, https://doi.org/10.5194/acp-21-15519-2021, 2021.

Pinardi, G., Van Roozendael, M., Abuhassan, N., Adams, C., Cede, A., Clémer, K., Fayt, C., Frieß, U., Gil, M., Herman, J., Hermans, C., Hendrick, F., Irie, H., Merlaud, A., Navarro Comas, M., Peters, E., Piters, A. J. M., Puentedura, O., Richter, A., Schönhardt, A., Shaiganfar, R., Spinei, E., Strong, K., Takashima, H., Vrekoussis, M., Wagner, T., Wittrock, F., and Yilmaz, S.: Erratum: MAX-DOAS formaldehyde slant column measurements during CINDI: intercomparison and analysis improvement (Atmospheric Measurement Techniques (2013) 6 (167-185)), Atmos. Meas. Tech., 6 (2), 219, doi: 10.5194/amt-6-219-2013, 2013.

Piters, A. et al..: The Cabauw Intercomparison campaign for Nitrogen Dioxide measuring Instruments (CINDI): design, execution, and early results, Atmos. Meas. Tech., 5, 457-485, doi:10.5194/amt-5-457-2012, 2012.

Platt and Stutz, Differential Optical Absorption Spectroscopy, Principles and Applications, Springler, 2008.

Puentedura, O., Gil, M., Saiz-Lopez, A., Hay, T., Navarro-Comas, M., Gómez-Pelaez, A., Cuevas, E., Iglesias, J., and Gomez, L.: Iodine monoxide in the north subtropical free troposphere, Atmos. Chem. Phys., 12, 4909-4921, doi:10.5194/acp-12-4909-2012, 2012.

Robles-Gonzalez, C., Navarro-Comas, M., Puentedura, O., Schneider, M., Hase, F., Garcia, O., Blumenstock, T., and Gil-Ojeda, M.: Intercomparison of stratospheric nitrogen dioxide columns retrieved from ground-based DOAS and FTIR and satellite DOAS instruments over the subtropical Izana station, Atmos. Meas. Tech., 9, 4471-4485, doi:10.5194/amt-9-4471-2016, 2016.

Rodgers, C.D., Inverse methods for Atmospheric Sounding: Theory and Practice, World Scientific, Series on Atmospheric, Oceanic and Planetary Physics, Vol. 2, 2000.

Verhoelst, T., Compernolle, S., Pinardi, G., Lambert, J.-C., Eskes, H. J., Eichmann, K.-U., Fjæraa, A. M., Granville, J., Niemeijer, S., Cede, A., Tiefengraber, M., Hendrick, F., Pazmiño, A., Bais, A., Bazureau, A., Boersma, K. F., Bognar, K., Dehn, A., Donner, S., Elokhov, A., Gebetsberger, M., Goutail, F., Grutter de la Mora, M., Gruzdev, A., Gratsea, M., Hansen, G. H., Irie, H., Jepsen, N., Kanaya, Y., Karagkiozidis, D., Kivi, R., Kreher, K., Levelt, P. F., Liu, C., Müller, M., Navarro Comas, M., Piters, A. J. M., Pommereau, J.-P., Portafaix, T., Prados-Roman, C., Puentedura, O., Querel, R., Remmers, J., Richter, A., Rimmer, J., Rivera Cárdenas, C., Saavedra de Miguel, L., Sinyakov, V. P., Stremme, W., Strong, K., Van Roozendael, M., Veefkind, J. P., Wagner, T., Wittrock, F., Yela González, M., and Zehner, C.: Ground-based validation of the Copernicus Sentinel-5P TROPOMI NO_2 measurements with the NDACC ZSL-DOAS, MAX-DOAS and Pandonia global networks, Atmos. Meas. Tech., 14, 481–510, https://doi.org/10.5194/amt-14-481-2021, 2021.

Yela, M., Gil-Ojeda, M., Navarro-Comas, M., Gonzalez-Bartolomé, D., Puentedura, O., Funke, B., Iglesias, J., Rodríguez, S., García, O., Ochoa, H., and Deferrari, G.: Hemispheric asymmetry in stratospheric NO2 trends, Atmos. Chem. Phys., 17, 13373-13389, https://doi.org/10.5194/acp-17-13373-2017, 2017.

11.6 Staff

The DOAS research group is composed of researchers and specialist technicians from INTA and IARC-AEMET.

Dr Margarita Yela González (INTA; Head of programme)

Dr Olga Puentedura Rodríguez (INTA; Research Scientist)

Dr Mónica Navarro Comas (INTA; Research Scientist)

Javier Iglesias Méndez, (INTA; Research Scientist)

Dr Laura Gómez Martín (INTA; Research Scientist)

Ramón Ramos (AEMET; Head of Infrastructure)

12 Water Vapour

12.1 Main Scientific Goals

The main scientific goals of this programme are:

- To conduct long-term water vapour monitoring and study its relationship with climate change.
- To study radiative forcing due to water vapour.

To achieve these goals, high-quality measurements are conducted with state-of-the-art instrumentation consisting of a microwave radiometer, Global Navigation Satellite System (GNSS) receiver network, radiosondes, photometers and a Fourier transform infrared spectrometer (see Section 12.2 for more details). From these various measurement datasets, the following products are obtained:

- Precipitable water vapour (PWV) and liquid water (LW) total column content.
- PWV, LW, temperature and humidity vertical profiles.
- Intra-hourly and diurnal PWV variability.
- Diurnal and annual mean cycles of PWV.
- Monthly and annual PWV mean series, analyzing their homogeneity and evaluating their anomalies and evolution over time to detect possible trends.

With these products, IARC-AEMET contributes to the EUMETNET Profiling Programme (E-PROFILE) with measurements from the RPG-LHATPRO-G5 series microwave radiometer, recently acquired and installed at IZO and the EUMETNET GNSS Water Vapour Programme (E-GVAP) through a network of GNSS receivers located at different places and altitudes in Tenerife and La Palma Islands.

12.2 Measurement Programme

Several instruments and measurement techniques are used in this programme as detailed below. Comparisons of column-integrated water vapor (precipitable water) between different techniques and instruments have been carried out during the preceding years (e.g. Romero Campos et al., 2009, Schneider et al., 2010a, García et al., 2020, García et al., 2021). We are currently preparing a technical document to incorporate and validate the column-integrated water vapor measurements obtained from the microwave radiometer with those of the other available techniques.

12.2.1 Global Navigation Satellite System technique

The Global Navigation Satellite System technique consists in determining PWV in the atmospheric column from the observed delay in radio signals at two different frequencies emitted by a network of Global Positioning System (GPS) and Global Navigation Satellite System (GLONASS) satellites received by a GNSS receiver (Fig. 12.1).

Figure 12.1. Global Navigation Satellite System receiver at Izaña Observatory.

Currently, the group works with 11 GNSS receiver stations (Fig. 12.2) at different altitudes, ten of them in Tenerife and one in La Palma. Currently, the San Miguel de Abona (SM), La Orotava (OR), Las Cañadas (CC) and Teide (TE) stations are not operational due to technical problems.

The atmospheric pressure in places where the GNSS antennas are located is a key parameter for obtaining the PWV from the zenith total delay (ZTD) and zenith hydrostatic delay (ZHD). The Spanish National Geographic Institute (IGN) is in charge of managing the GNSS network and data acquisition, as well as the calculation of the ZTD from the GNSS signals, currently using the Bernese 5.4 software version applied for both ultra-fast and precise orbits. The ZHD calculation depends on the temperature and pressure at the GNSS antenna sites. However, atmospheric pressure plays a more important role in determination of PWV than temperature. An uncertainty of 1 hPa in pressure produces, approximately, the same uncertainty in determination of PWV (0.33 mm to 0.36 mm) as an uncertainty of 5K in temperature (Hagemann et al., 2003).

The PWV is calculated from ZTD and pressure values at the different GNSS stations. One of the most important tasks carried out is to estimate the pressure at the GNSS sites where surface pressure measurements are not available due to the absence of barometric sensors. To do this, based on the perfect gas law and the hydrostatic equation, a precise value of pressure as a function of altitude and temperature is calculated for each GNSS station using a grid of ten automatic meteorological stations (EMA) equipped with barometric and temperature sensors, located at different altitudes (Fig. 12.2).

The values of the PWV column are obtained in quasi-real time at each GNSS station from the ZTD from ultra-fast GNSS orbits, which have a temporal resolution of 15 minutes and are available approximately every two hours. Values are plotted as contour maps (Fig. 12.3a). Together with these maps, profiles are obtained that represent the

amount of PWV contained in layers located between GNSS stations. Fig. 12.3b shows one of these profiles.

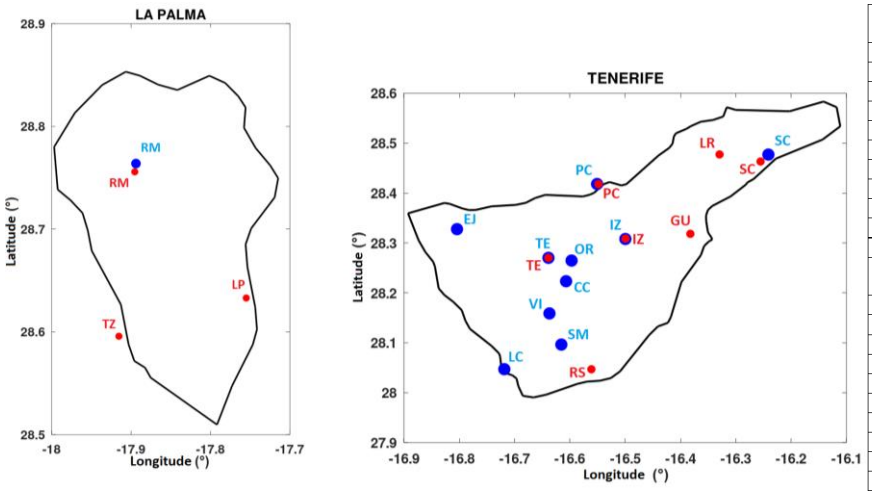

GNSS Stations	Latitude (°)	Longitude (°)	Altitude (m.a.s.l.)
Santa Cruz de Tenerife (SC)	28.477186	-16.241152	7.8
Puerto de La Cruz (PC)	28.418257	-16.550785	8.2
Los Cristianos (LC)	28.047166	-16.718521	14.0
San Miguel de Abona (SM)	28.096470	-16.615437	579.2
Erjos (EJ)	28.327785	-16.804018	1006.9
Vilaflor (VI)	28.158897	-16.636926	1420.7
Roque de Los Muchachos (RM)	28.763874	-17.893826	2155.3
Las Cañadas (CC)	28.223426	-16.606855	2244.0
Izaña (IZ)	28.308069	-16.499678	2369.9
La Orotava (OR)	28.264800	-16.596954	2461.6
Teide (TE)	28.270327	-16.638736	3549.1
Meteorological Stations	**Latitude (°)**	**Longitude (°)**	**Altitude (m.a.s.l.)**
Puerto de La Cruz (PC)	28.418056	-16.548333	25.0
La Palma Airport (LP)	28.633056	-17.755005	33.0
Santa Cruz de Tenerife (SC)	28.463337	-16.255282	35.0
Tazacorte (TZ)	28.595833	-17.915278	62.0
Reina Sofía Airport (RS)	28.046992	-16.561158	64.0
Güímar (GU)	28.318405	-16.382229	115.0
Los Rodeos Airport (LR)	28.477497	-16.329444	632.0
Roque de Los Muchachos (RM)	28.755833	-17.895278	2223.0
Izaña (IZ)	28.308891	-16.499445	2371.0
Teide (TE)	28.270327	-16.638736	3550.0

Figure 12.2. Locations of Global Navigation Satellite System stations and automatic meteorological stations in La Palma and Tenerife.

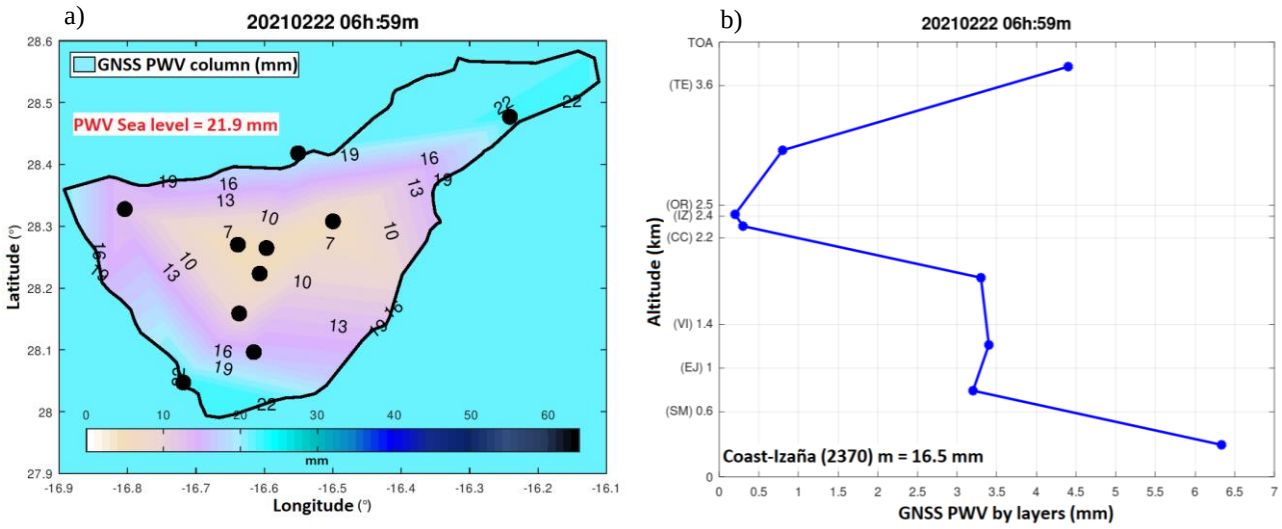

Figure 12.3. PWV at the GNSS stations in Tenerife obtained in quasi-real time at 6:59 UTC on 22 February 2021. a) PWV column values and b) PWV profile between stations.

12.2.2 FTIR

The IARC Fourier transform infrared spectroscopy programme is described in Section 7, where details are given on the atmospheric composition observations conducted within the programme. To obtain column-integrated water vapour, the solar spectra acquired with the standard TCCON settings (Wunch et al., 2011; Schneider et al., 2010b) are used. These measurements are made between 4000 and 9000 cm^{-1} (corresponding to wavelengths between 1111 and 2500 nm) at a spectral resolution of 0.02 cm^{-1}.

12.2.3 Radiosondes

From the vertical profiles of relative humidity obtained with Vaisala RS41 radiosondes, precipitable water content in the atmospheric column is calculated by integrating numerically (using the trapezoidal rule) the density function of atmospheric water vapour for the base and top of each atmospheric layer. The integration is performed from ground level to 12 km altitude. By default, the PWV profile is supplied for the following layers: 1) from ground up to 1.5 km; 2) from 1.5 km to 3 km altitude in layers of 0.5 km thickness; 3) from 3 km altitude up to 12 km in layers of 1 km thickness.

The use of RS41 radiosonde sounding started on Tenerife on 13 December 2017. During the radiosonde's ascent into the atmosphere, a vertical profile of meteorological data is taken and readings within the vertical profile have a temporal resolution of 1 s. Prior to 2017, RS-92 radiosondes were used from 1995-2017, with a temporal resolution of

readings within the vertical profile of 2 s. The high temporal resolution of RS41 radiosondes provides a large number of levels in the vertical profiles of pressure, temperature, humidity and wind.

However, at high altitudes (~14 km in the stratosphere), we have occasionally detected a weak decrease in reported altitude in the RS41 Vaisala Tenerife radiosonde data. It could be due to the combination of an excessively high temporal resolution and longer response times and errors of the different meteorological sensors and GNSS. For these reasons, the erroneous records are filtered from the files before they are evaluated.

12.2.4 Photometric observations

Details of photometric observations conducted at IARC are given in Section 9 (Column Aerosols programme). Since 2012, the CIMEL CE318-T sun-sky-lunar photometer has been utilized (Barreto et al., 2016). Column-integrated water vapour is obtained following the procedure described in Smirnov at al. (2004) with an uncertainty of 10%. According to Schneider et al. (2010a), this uncertainty varies depending on the humidity conditions, with values of 7% for humid conditions and 25% for very dry conditions (IWV < 2 mm).

12.2.5 EKO MS-711 Spectroradiometer

The IARC Radiation programme is described in Section 10, where details are given on water vapor retrievals from spectral direct irradiance measurements with an EKO MS-711 spectroradiometer at Izaña Observatory. These measurements and an intercomparison with other measurement techniques are also described in García et al. (2021).

12.2.6 Microwave Radiometer

In 2019, a high precision microwave radiometer (MWR) was acquired to measure tropospheric temperature and humidity vertical profiles, with high temporal resolution, at the Izaña Observatory (Fig. 12.4). It was installed at IZO on 29 April 2020. The Low Humidity and Temperature Profiling (LHATPRO-G5 series) microwave radiometer (Radiometer Physics GmbH) is specially designed to make humidity measurements under low humidity conditions such as those in the free troposphere above IZO. The radiometer obtains vertical profiles of humidity and tropospheric temperature up to 10 km of height above its emplacement, with a spatial resolution of 200 m to 400 m depending on the height level, with a temporal resolution of 1 second.

The microwave radiometer operates with two receivers. The first one has six channels at different frequencies: around the 183 GHz water vapour line for humidity and water vapour profiling and the second one works with seven channels around the 60 GHz oxygen absorption line for temperature profiling from the brightness temperature measurements.

Figure 12.4. MWR on the Izaña Observatory instrument terrace.

The instrument is also equipped with a double channel coupled infrared radiometer (IRR), a GPS receiver and a conventional weather station with a rain sensor. Fig. 12.5 shows an example of the main types of MWR measurements retrieved with a new software version on 2 March 2023.

Through the radiometer's RPG software, using an artificial neural network (ANN) algorithm, derivative products can be obtained such as Absolute and Relative Humidity (HPC), Full Tropospheric Temperature Profile (TMP), the Liquid Water Path (LWP), Column Integrated Water Vapour (IWV), Hydrostatic and Wet Zenith Delays (DLY) of GPS signals, Infrared Temperatures (IRT), Atmospheric Stability Indices (STA), Cloud Base Height (CBH), Height (BLH) and Temperature Profiles of the Planetary Boundary Layer (TPB) and Atmospheric Attenuation (ATN). The RPG software version (9.41) was updated on 16 June 2022 to a new version (9.49-1).

The MWR is a robust instrument, with a high degree of autonomy, especially designed for outdoor measurements in high mountain conditions that require minimal maintenance. The most important maintenance task is calibration. The equipment requires absolute calibration with liquid nitrogen every six months. The last such calibration took place on 14 November 2022 at IZO. On that same day, the original radome sheet was substituted for a new one since the old one was deteriorated by use and the weather conditions.

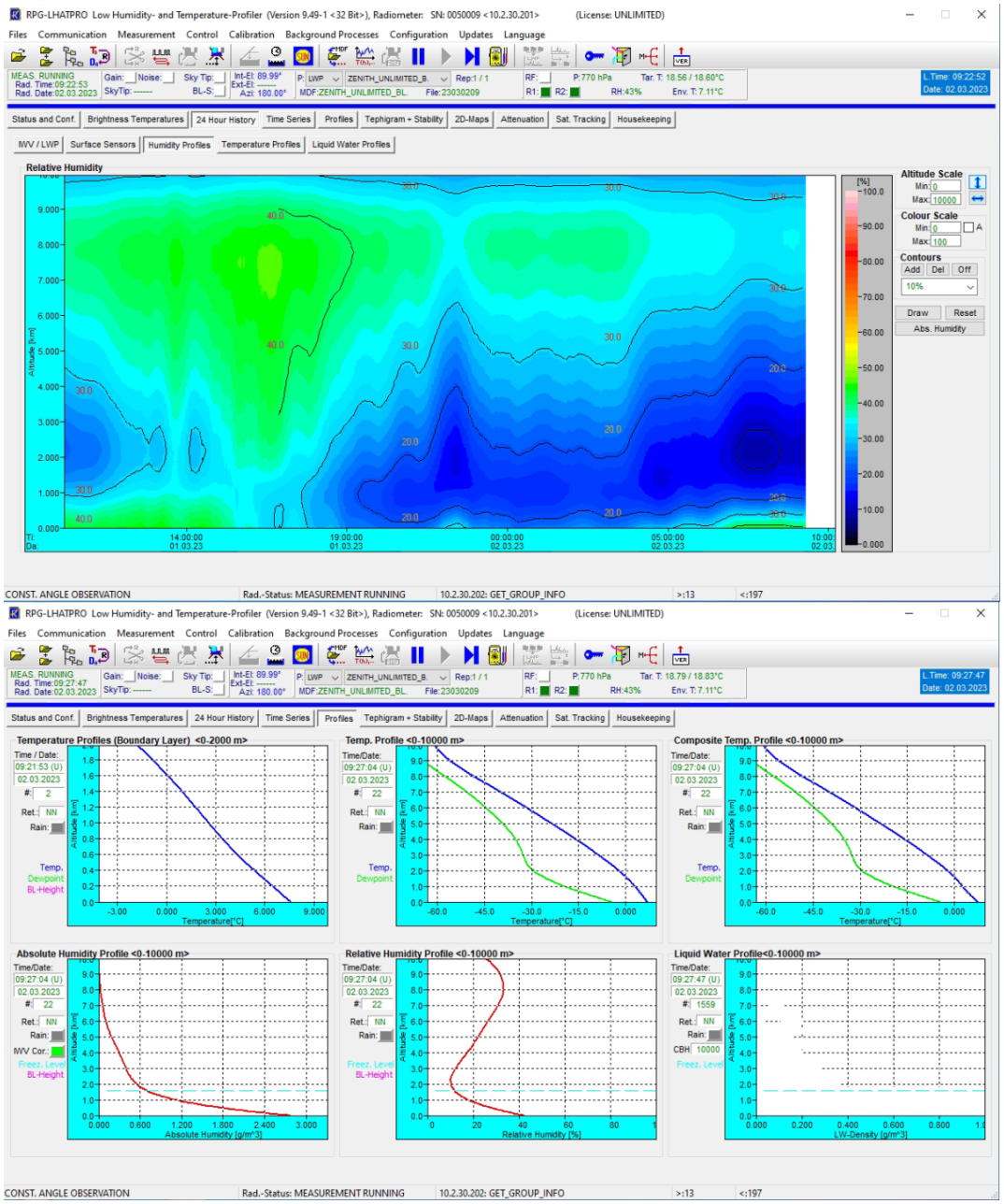

Figure 12.5. Example of the main types of measurements of the MWR on 2 March 2023 UTC at the Izaña Observatory. Upper panel: 24-hour history of the absolute humidity taken at 9:22 UTC and lower panel: different vertical profiles at 9:27 UTC. Graphics produced with the new software version 9.49-1.

Figure 12.6 represents a comparison of the temperature and absolute humidity profiles between the MWR and the radiosondes measurements on 31 December 2022 at 11 UTC at the Izaña Observatory. These results demonstrate that while there is a reasonable agreement between the profiles measured by these two different measurement techniques, the indirect derivation from brightness temperature and the MWR inversion algorithms together with the lower spatial resolution mask certain thermal inversions as well as absolute humidity variations at different levels that the sounding does measure.

On 20 January 2021, we requested the incorporation of the microwave radiometer as a measurement instrument into the E-PROFILE Profiling Programme and on 11 March 2021, IZO was included in a list of potential stations of the new E-PROFILE MWR Network still under development and not operational to date. On 24 March 2023, the MWR was officially registered within E-PROFILE and raw data in hourly files is sent automatically and processed through a centralized hub as part of a pilot program.

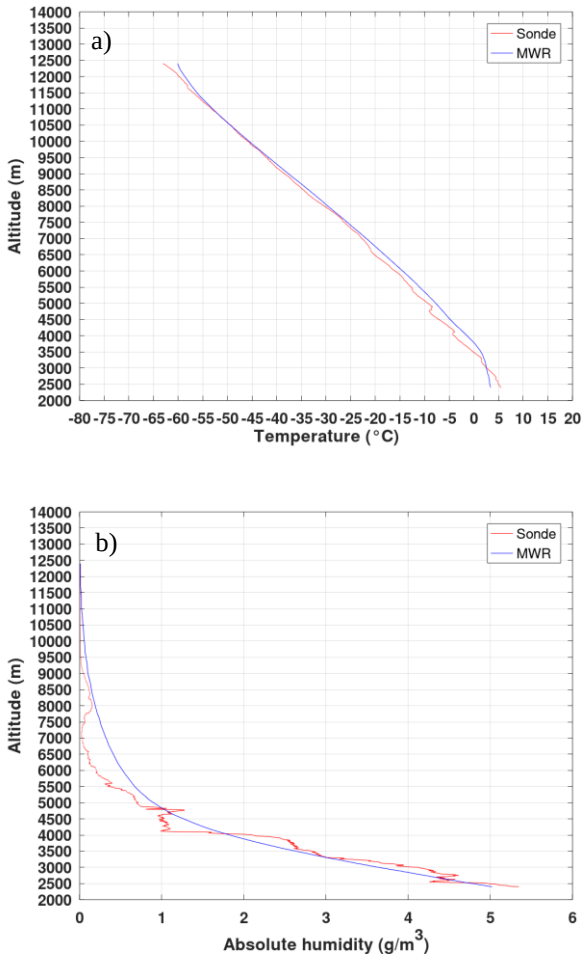

Figure 12.6. a) Temperature and b) absolute humidity profiles from radiosondes (red) and MWR (blue) on 31 December 2022 at 11 UTC at the Izaña Observatory.

12.3 Updating the PWV series: 2021-2022

Following a similar procedure to that of other authors (Botey et al., 2013); diurnal, monthly and annual PWV averages are calculated when the data coverage is ≥ 60%.

12.3.1 Diurnal mean cycle of PWV from GNSS

The averaged diurnal cycles of PWV are shown for GNSS stations at SCO (2008-2022) (Fig. 12.7a) and at IZO (2009-2022) (Fig. 12.7b). Ultrafast orbits (those available) have been used for SCO, and precise orbits were used at IZO. The diurnal cycles have been calculated from average hourly anomalies. For these statistics, we have selected only those hourly average values with at least 60% of high-quality intra-hours values, on days with at least 15 hourly means (60%). The diurnal time anomalies were obtained by subtracting the value of the corresponding diurnal average from the value of the hourly average: hourly mean - diurnal mean.

Then, for each hour, the averages for all the available data anomalies within the period of evaluation are calculated. A total of 4920 diurnal records for IZO and 3709 for SCO have been analyzed for the period 2008-2022.

Diurnal variations are qualitatively similar in SCO and IZO but they are smoother in IZO than in SCO. The minimum of the mean diurnal cycle in SCO is reached around 6UTC-7UTC and in IZO around 8UTC, while the maximum occurs around 14UTC in IZO and around 15UTC in SCO. This suggests that although there is a synoptic cause that modulates the variations, there is also a local influence due to the geography and locations of both stations.

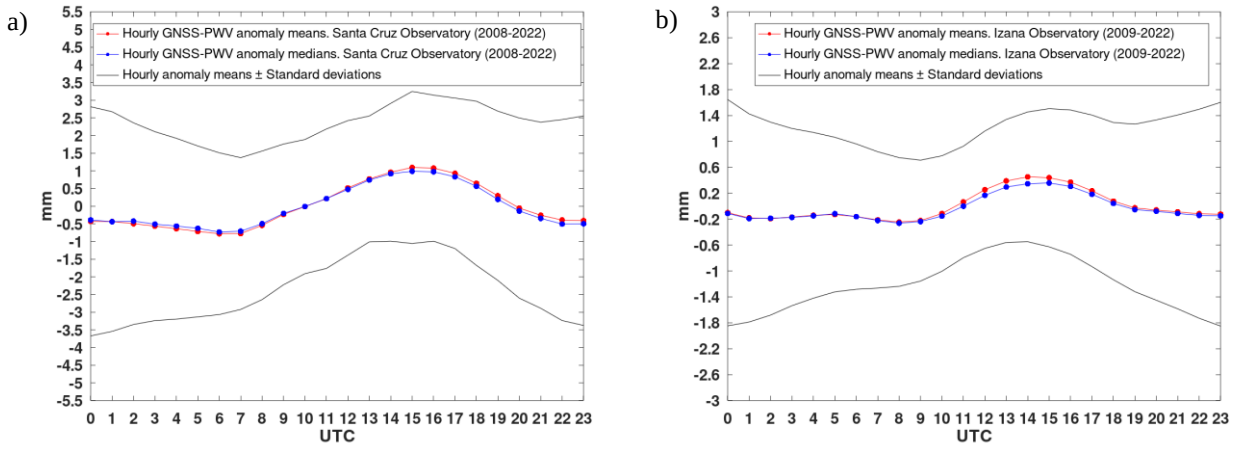

Figure 12.7. PWV mean diurnal cycle at a) SCO and b) IZO, from GNSS during 2008-2022 and 2009-2022 respectively.

12.3.2 Monthly mean PWV data series from radiosondes and GNSS

PWV monthly mean obtained from radiosondes and GNSS at IZO are shown for the period 1995-2022 at 12UTC (Fig. 12.8). These are the values of PWV calculated over the duration of the radiosonde flight (about 2 hours or so) from the time of its release (approximately 12 UTC), and assuming that, during this period of time, the PWV remains constant. An annual cycle with peak in summer-autumn and minimum values in winter is seen in the data. The series was subjected to the corrections for different types of sondes described in (Romero Campos et al., 2011).

Using a 95% confidence level, inhomogeneity was found in the median of the monthly series of the PWV in IZO at 0 UTC in May 2020. The signal-to-noise ratio at the point of change is significant (0.18699 > 0.05). For the rest of the PWV monthly mean series, no lack of homogeneity was detected in the median at a confidence level ≥ 95%. No significant trends have been found in any of the series.

Given that the presence of water vapor above 12,000 m is very small (90% of the water vapor is concentrated in the troposphere below 12,000 m), the values obtained from radiosondes are comparable with those obtained with the GNSS technique. The agreement between the two techniques as depicted in Fig. 12.8 is very good; the small differences observed can be attributed to the fact that the GNSS measurements are zenith, while the radiosondes do not measure vertically, rather its profile moves horizontally, at a greater or lesser distance, depending on weather conditions on launch day.

12.3.3 Annual mean cycle of PWV from GNSS

The PWV seasonal cycles for SCO and IZO for the 2008-2022 and 2009-2022 period respectively are shown in Fig. 12.9 and Fig. 12.10. The seasonal maximum of PWV in Santa Cruz is observed at the end of the summer (September), which represents a one-month delay with respect to Izaña, where seasonal maximum is observed in August.

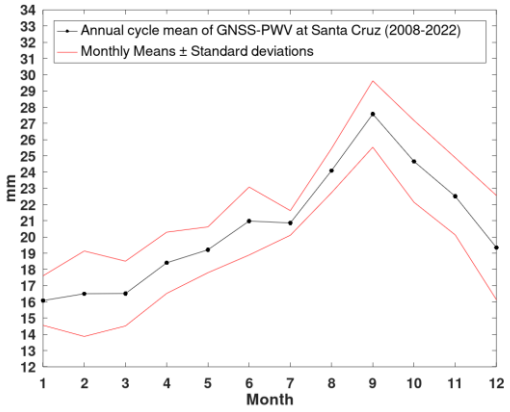

Figure 12.9. GNSS PWV mean seasonal cycle, SCO (2008-2022).

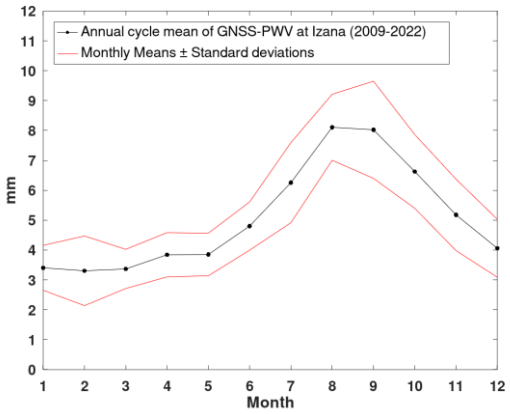

Figure 12.10. GNSS PWV mean seasonal cycle, IZO (2009-2022).

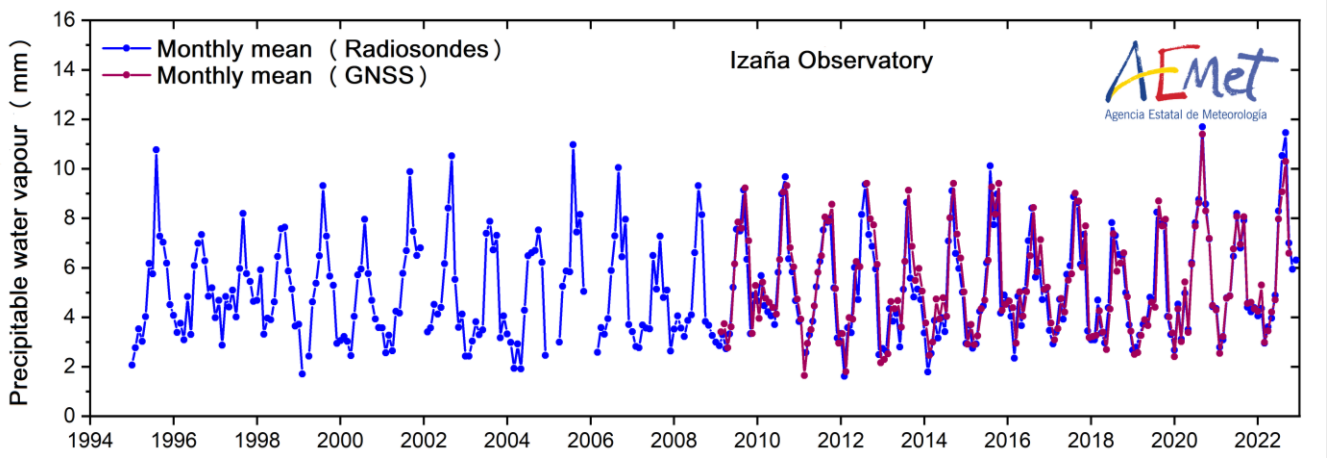

Figure 12.8 PWV monthly data series at IZO at 12UTC from radiosondes and GNSS for 1994–2022.

12.3.4 PWV vertical stratification monthly statistics

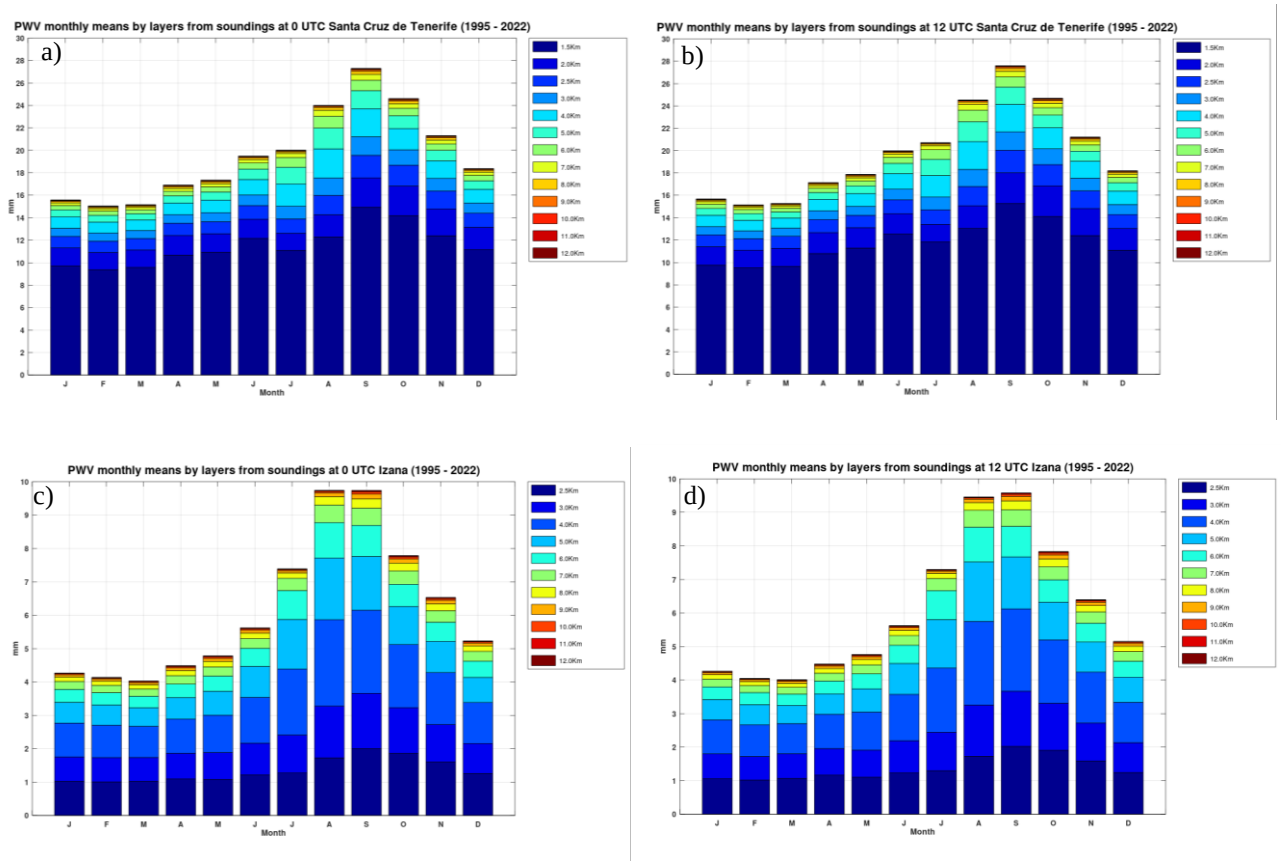

Figure 12.11. Monthly statistics of precipitable water vapour vertical distribution from Tenerife radiosondes for SCO a) 00UTC, b) 12UTC and IZO c) 00UTC and d) 12UTC (1995–2022).

The monthly average of PWV vertical distribution over Tenerife obtained from radiosondes data at 00UTC and 12UTC during the period 1995-2022, are depicted for SCO in Figs. 12.11a-b and for IZO in Figs. 12.11c-d. The total height of each column corresponds to the total monthly averaged PWV at sea level. No significant differences are found between 00UTC and 12UTC.

Most of the PWV is concentrated within the first 1.5 km altitude. There is a “wet” season from August to October, with a maximum in September (~27 mm) in the case of Santa Cruz, and August-September (~ 9.5 mm) in the case of Izaña. Similarly, we observe a "dry" season corresponding to the months of January to March at both sites with minimums in February-March of about (~ 4 mm) at Izaña and (~ 15 mm) at Santa Cruz. The rest are transition months between both seasons.

12.4 Additional activities

12.4.1 Participation in the “Workshop on Ground-based Microwave Radiometry” Jülich (Germany)

Dr África Barreto participated in a training course, jointly organized by the University of Cologne, the Jülich Research Centre, ACTRIS CCRES (Centre for Cloud REmote Sensing) and PROBE COST-Action (PROfiling the atmospheric Boundary layEr), entitled: “Workshop on Ground-based Microwave Radiometry” held at the Jülich Research Centre (Germany), during 31 August - 2 September 2022 (Fig. 12.12).

This workshop was part of the EUMETNET strategy to achieve the goal of establishing a MicroWave Radiometer Network through the E-PROFILE observation program. It took place at the Jülich Research Centre where JOYCE (Jülich ObservatorY for Cloud Evolution) is located. The workshop covered issues related to software, standard operation protocols, data processing, quality control and calibration of the microwave radiometers. The E-PROFILE MWR Network will centrally process the data flow online and distribute the observations in near real time.

Figure 12.12. Participants of the Workshop on Ground-based Microwave Radiometry, held at the Jülich Research Centre (Germany), 31 August-2 September 2022.

12.4.2 Contributions to the 2021 La Palma volcanic eruption emergency response

The Water Vapour group contributed to activities carried out by IARC-AEMET during the 2021 La Palma volcanic eruption, particularly in the emergency deployment in La Palma of the network of vertical profilers (ceilometers and lidar systems), deployed in the context of the Aerosol, Clouds and Trace Gases Research Infrastructure. The vertical profiler network installed at La Palma to monitor the eruption process was aimed at real-time measurement of the height of the volcanic dispersion cloud as well as characterisation of the emitted volcanic aerosols. For more details see ACTRIS (2021) and Section 23. We participated as co-authors in Barreto et al. (2022), Bedoya-Velásquez et al. (2022) and García et al. (2022b).

12.5 References

ACTRIS, ACTRIS-Spain coordinating unprecedented actions for the Cumbre Vieja volcanic emergency, November 2021. Available at: https://www.actris.eu/news-events/news/actris-spain-coordinating-unprecedented-actions-cumbre-vieja-volcanic-emergency

Barreto, Á., Cuevas, E., Granados-Muñoz, M.-J., Alados-Arboledas, L., Romero, P. M., Gröbner, J., Kouremeti, N., Almansa, A. F., Stone, T., Toledano, C., Román, R., Sorokin, M., Holben, B., Canini, M., and Yela, M.: The new sun-sky-lunar Cimel CE318-T multiband photometer – a comprehensive performance evaluation, Atmos. Meas. Tech., 9, 631–654, https://doi.org/10.5194/amt-9-631-2016, 2016.

Barreto, A., M. Sicard, O.E. García, R. Román, V. Rizi, R. Roininen, P.M Romero-Campos, Y. González, S. Rodríguez, R.D. García, C. Torres, M. Iarlori, E. Cuevas, D. Suárez, R. Ramos, C. Córdoba-Jabonero, J. de la Rosa, A. Rodríguez-Gómez, C. Muñoz-Porcar, A. Comerón, A. Bedoya-Velásquez, J.C. Antuña-Sanchez, V. Neustroev, E. Pietropaolo, Y. Lopez-Darias, M.A. López-Cayuela, C. Carvajal-Pérez, J.J. Bustos, O. Álvarez, C. Toledano, C. Aramo, J. Vilches, R. González, F.A. Almansa, R. Ceolato, N. Taquet, Thomas Boulesteix, M. Martínez, N. Prats, A. Redondas, C. Bayo, V. Carreño, C. López, S.L. León, P.P. Rivas, A. Alcántara, F. Parra, P. Martín, La Palma Volcano Eruption: Characterisation of Volcanic Aerosols and Gas Emissions from a Synergetic Perspective, Congreso Nacional de Medio Ambiente (CONAMA), 21-24 November, Madrid, 2022.

Bedoya-Velásquez, A.E.; Hoyos-Restrepo, M.; Barreto, A.; García, R.D.; Romero-Campos, P.M.; García, O.; Ramos, R.; Roininen, R.; Toledano, C.; Sicard, M.; Ceolato, R. Estimation of the Mass Concentration of Volcanic Ash Using Ceilometers: Study of Fresh and Transported Plumes from La Palma Volcano. Remote Sens. 14, 5680. https://doi.org/10.3390/rs14225680, 2022.

Botey, R., J. A. Guijarro y A. Jiménez. "Valores normales de precipitación mensual 1981 – 2010". Agencia Estatal de Meteorología. NIPO: 281-13-007-X. 2013.

García, O. E., Schneider, M., Herkommer, B., Gross, J., Hase, F., Blumenstock, T., & Sepúlveda, E. (2022a). TCCON data from Izana (ES), Release GGG2020.R1 (Versión R1) [Data set]. CaltechDATA. https://doi.org/10.14291/tccon.ggg2020.izana01.R1

García, O., Suárez, D., Cuevas, E., Ramos, R., Barreto, África, Hernández, M., Quintero, V., Toledano, C., Sicard, M., Córdoba-Jabonero, C., Riz, V., Roininen, R., López, C., Vilches, J., Weiss, M., Carreño, V., Taquet, N., Boulesteix, T., Fraile, E., Torres, C., Prats, N., Alcántara, A., León, S. ., Rivas, P., Álvarez, Óscar, Parra, F., de Luis, J., González, C., Armas, C., Romero, P., de Bustos, J., Redondas, A., Marrero, C., Milford, C., Román, R., González, R., López-Cayuela, M., Carvajal-Pérez, C., Chinea, N., García, R. ., Almansa, F., González, Y., Bullón, F., Poggio, M., Rivera, C., Bayo, C., & Rey, F. (2022b). La erupción volcánica de La Palma y el papel de la Agencia Estatal de Meteorología. Revista Tiempo Y Clima, 5(76). https://pub.ame-web.org/index.php/TyC/article/view/2516

García-Cabrera, R. D., Cuevas-Agulló, E., Barreto, Á., Cachorro, V. E., Pó, M., Ramos, R., and Hoogendijk, K.: Aerosol retrievals from the EKO MS-711 spectral direct irradiance measurements and corrections of the circumsolar radiation, Atmos. Meas. Tech., 13, 2601–2621, https://doi.org/10.5194/amt-13-2601-2020, 2020.

García, R.D.; Cuevas, E.; Cachorro, V.E.; García, O.E.; Barreto, Á.; Almansa, A.F.; Romero-Campos, P.M.; Ramos, R.; Pó, M.; Hoogendijk, K.; Gross, J. Water Vapor Retrievals from Spectral Direct Irradiance Measured with an EKO MS-711 Spectroradiometer—Intercomparison with Other Techniques. Remote Sens. 2021, 13, 350. https://doi.org/10.3390/rs13030350.

Hagemann, S., Bengtsson, L., and Gendt, G. (2003), On the determination of atmospheric water vapor from GPS measurements, J. Geophys. Res., 108, 4678, doi:10.1029/2002JD003235, D21.

Romero Campos, P. M., Cuevas Agulló, E., Ramos López, R., Valdés Pérez de Vargas, M., Schneider M., Programa de vapor de agua en columna del Centro de Investigación Atmosférica de Izaña: Análisis e intercomparación de diferentes técnicas de medidas. Ministerio de Medio Ambiente, y Medio Rural y Marino, Agencia Estatal de Meteorología, Madrid, 2009. NIPO: 784-09-009-9. https://doi.org/10.31978/784-09-009-9.

Romero Campos, P.M., Marrero, C., Alonso, S., Cuevas, E., Afonso, S., and Ortiz de Galisteo, J.P.: Una Climatología del Agua Precipitable en la Región Subtropical sobre la Isla de Tenerife basada en Datos de Radiosondeos. NTD nº 6 de AEMET. NIPO: 281-12-007-5. Centro de Investigación Atmosférica de Izaña. Agencia Estatal de Meteorología (España), 2011.

Romero Campos, P.M., Cuevas, E., de Bustos, J.J.: Medida en tiempo cuasi-real y predicción a 24h del contenido atmosférico de agua precipitable a partir de una red de receptores GPS en la isla de Tenerife. NTD nº 20 de AEMET. NIPO: 281-16-002-6. Centro de Investigación Atmosférica de Izaña. Agencia Estatal de Meteorología (España), 2016.

Schneider, M., Romero, P. M., Hase, F., Blumenstock, T., Cuevas, E., and Ramos, R.: Continuous quality assessment of atmospheric water vapour measurement techniques: FTIR, Cimel, MFRSR, GPS, and Vaisala RS92, Atmos. Meas. Tech., 3, 323-338, doi: 10.5194/amt-3-323-2010, 2010a.

Schneider, Matthias & Sepúlveda, E. & García, Omaira & F, Hase & T, Blumenstock. (2010b). Remote sensing of water vapour profiles in the framework of the Total Carbon Column Observing Network (TCCON). Atmospheric Measurement Techniques. 3. 10.5194/amt-3-1785-2010.

Wunch Debra, Toon Geoffrey C., Blavier Jean-François L., Washenfelder Rebecca A., Notholt Justus, Connor Brian J., Griffith David W. T., Sherlock Vanessa and Wennberg Paul O.. 2011 The Total Carbon Column Observing Network. Phil. Trans. R. Soc. A.3692087–2112. http://doi.org/10.1098/rsta.2010.0240.

12.6 Staff

Pedro Miguel Romero Campos (AEMET; Head of programme)

Ramón Ramos (AEMET; Head of Infrastructure)

Dr África Barreto (AEMET; Research Scientist)

Dr Rosa Delia García Cabrera (TRAGSATEC; Research Scientist and AEMET collaborator)

Dr Omaira García (AEMET; Research Scientist)

Dr Antonio Fernando Almansa (CIMEL Electronique; Research Scientist and AEMET collaborator)

13 Meteorology

13.1 Izaña Observatory as a WMO Centennial Observing Station

Today, supercomputers and sophisticated models and satellites are important tools for climate scientists. However, long-term, high quality continuous observations from thermometers, rain gauges and other instruments remain essential. Without them, we could not be certain that the Earth has warmed by one degree centigrade over the past century. These long-term observations are vital to our scientific understanding of climate variability and change and essential for model and satellite validation activities.

To promote the recovery and continuation of these records, governments are nominating Centennial Observing Stations for formal recognition by WMO. Many Centennial Observation Stations are also of outstanding historical and cultural interest, recalling previous eras and the birth of modern meteorology. Taken together as a network, Centennial Observation Stations are uniquely able to tell the story of recent climate history.

Izaña Observatory was recognised as a Centennial Observation Station by the WMO in 2017. More information about the WMO Centennial Observing Stations can be found here.

13.2 Main Scientific Goals

The main goals of the meteorology programme are:

- To provide diagnosis and operational weather forecasting to support routine operation activities at the IARC observatories and issue internal severe weather alerts and special forecasts for planned field campaigns, outdoor calibrations, repairs, etc.
- To configure and operate High Resolution Numerical Weather Prediction Models capable of capturing the complex meteorology of the mountain observatory, as an aid to improve the supporting forecasts.
- To operate back-trajectory models on a monthly basis to keep a database available for other scientific projects up-to-date.
- To investigate the use of machine learning strategies to improve the forecasting of meteorological and air quality parameters.
- To maintain meteorological parameter observations according to WMO specifications, and in the framework of AEMET's Synoptic and Climatological Observation Networks.
- To measure conventional meteorological parameters at different stations on the island of Tenerife, to support other observation programmes.

Figure 13.1. Izaña Observatory weather stations.

- To develop non-conventional meteorological parameters programmes.
- To provide meteorological analysis information and technical advice to interpret and support results from other observation programmes and scientific projects, designing and implementing specific algorithms and databases to reach these goals.

13.3 Measurement Programme

The Izaña Atmospheric Research Center directly manages six weather observation stations, located at IZO (3), SCO, BTO and TPO (see Section 3 for more details).

13.3.1 Izaña Observatory

IZO has three fully automatic weather stations, two of them are located in the weather garden (C430E/60010 and Meteo-STD), which includes a network of five cloud observation webcams, and the third station is on the instrument terrace of the observation tower (Meteo-Tower) at 30 m above ground level. Instrumentation for manual observations (staffed by personnel, Fig. 13.2) with temperature, humidity, pressure and precipitation analog recorders (bands), is also maintained at IZO in order to preserve the historical series that started at Izaña Observatory in 1916.

Figure 13.2. Izaña Observatory, manual meteorological instrumentation.

13.3.2 Santa Cruz Observatory

SCO has a fully automatic weather station located on the instrument terrace.

13.3.3 Botanic Observatory

BTO has a fully automatic weather station installed at the ozonesounding station in the Botanic Garden in Puerto de la Cruz.

13.3.4 Teide Peak Observatory

TPO has an automatic very high-altitude weather station with temperature, humidity and pressure sensors, supplemented by data from a wind sensor installed at the Cable Car tower No.4, managed by the Cable car company.

The meteorology programme also has access to meteorological soundings data of pressure, temperature, humidity and wind from the Tenerife station (ID: WMO 60018) located in the town of Güimar. This station belongs to the AEMET upper-air observation network and is managed by the Meteorological Center of Santa Cruz de Tenerife (AEMET).

13.4 Meteorological Resources

To accomplish the objectives of the meteorology programme we have the following tools.

13.4.1 Man Computer Interactive Data Access System (McIDAS)

LINUX Workstations (Fedora Core) with the Man Computer Interactive Data Access System (McIDAS) provide access, exploitation and visualization of meteorological information from different geo-referenced observations, modelling and remote sensing (satellite, radar) platforms.

The application provides access to all data in real time in the AEMET National Prediction System, including the following data and products:

- Global synoptic surface observation and upper-air networks.
- Outputs of numerical prediction models from ECMWF Integrated Forecasting System (IFS) and AEMET (HIRLAM).
- METEOSAT satellite imagery.
- Images of the AEMET Weather Radar Network.
- Data from the AEMET Electrical Discharge Detection network.
- Products derived from SAF (Satellite Application Facilities) Nowcasting Meteosat Second Generation (MSG) images.

Utilising this application different automated processes for the exploitation of meteorological information have been developed, among which we can highlight:

1) Automatic generation of graphical products from specific model outputs and images from derived MSG products (RGB combinations), for consultation through an intranet website (Fig. 13.3).

2) Calculation of isentropic back trajectories of air masses from analysis outputs (4 cycles per day) and prediction (every 12 hours and range up to 132 hours) for Tenerife at nine different vertical levels (Fig. 13.4).

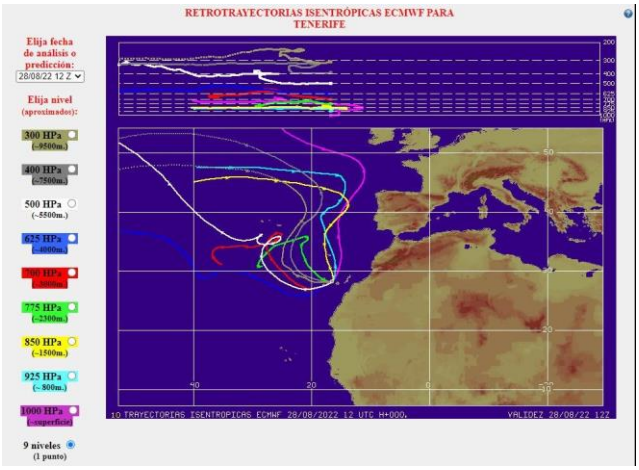

Figure 13.4. Screenshot of isentropic back-trajectories for Tenerife at nine levels on day 28/08/2022 12 UTC.

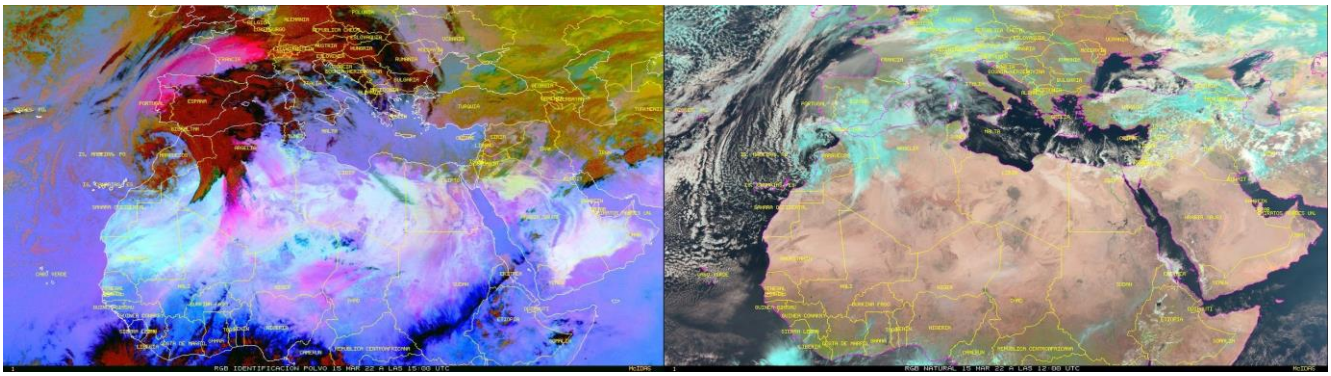

Figure 13.3. Two different RGB composite images from Meteosat-10 satellite for a dust event on 15/03/2022 15:00 UTC. Left panel: dust (channels 7, 9 and 10), right panel: natural (channels 1, 2 and 3).

3) Lightning strikes in situ detection and AEMET lightning detection network warning system, for taking preventive action to avoid damages at the facilities.

4) Automatic seven-day Meteogram generation of temperature, humidity, wind, pressure and clouds for Izaña Observatory using standard isobaric grid points interpolated to 2400 m a.s.l. The statistics have been weighted using the inverse distance to the validity forecast time taking into account the last five available model runs (Fig. 13.5).

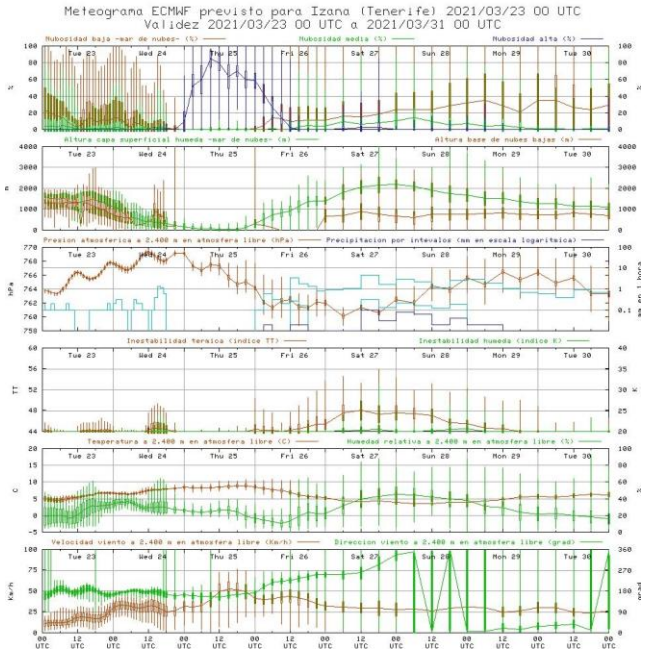

Figure 13.5. Ensemble week length meteogram forecast at IZO on 23/03/2021 at 00 UTC.

13.4.2 EUMETCast receiving system

The EUMETCast real-time receiving system for aerial imagery and meteorological satellite data distributed by EUMETSAT has its own internal web interface for displaying images received, and mass storage system for archiving images of compressed MSG segments in native format.

13.4.3 EUMETSAT Data Center

We have access to the EUMETSAT Data Center for retrieval of images and historical products of Meteosat satellites.

13.4.4 AEMET Server Meteorological Data System

We have access to numerical model databases, observations, bulletins, satellite and radar images available on the AEMET Server Meteorological Data System (SSDM).

13.4.5 ECMWF products and MARS archive

In addition, we have access to the European Centre for Medium-Range Weather Forecasts (ECMWF) computer systems and extractions of the Meteorological Archival and Retrieval System (MARS), which is the archive of all operational products generated in ECMWF. From this system we have developed different exploitation processes such as:

- Routine extraction in two cycles per day of meteorological analysis and prediction fields of the ECMWF IFS model, which are decoded in a compatible format for exploitation from McIDAS and input of initial and boundary conditions for the integration of high-resolution models running locally on our computer systems.
- Monthly extraction of ERA-Interim reanalysis outputs for updating large data series for different projects.
- Extraction of previous analysis fields for computing back trajectories with FLEXTRA.
- Routine extraction in two cycles per day from Copernicus Atmosphere Monitoring Service (CAMS) system (Fig. 13.6).

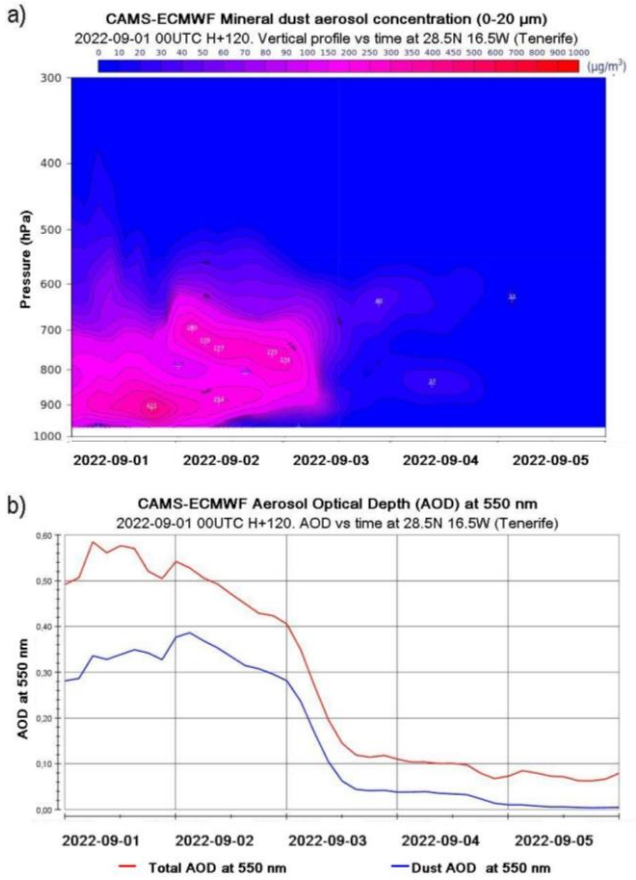

Figure 13.6. Examples of routine output cycles from CAMS. Forecast evolution of a) vertical profile of mineral dust aerosol concentration and b) Aerosol Optical Depth at 550 nm on 01/09/2022 00:00 UTC H+120 for 28.5N 16.5W (Tenerife).

13.4.6 AEMET National Climatological Data Base (BDCN)

We have access to the AEMET National Climatological Data Base (BDCN) for data extraction of observations from the AEMET principal and secondary climatological networks.

13.5 Numerical Models

13.5.1 Statistical forecasting model

A statistical forecasting model based on the analogous method shows the probability of occurrence of pollution events. In addition, meteorological values for a fixed-point NE (29.25 °N 15.75 °W) of the Canary Islands, coloured depending on the quartile position relative to the historical values of the series, show at a glance the adverse meteorological conditions in a forecast range of 108 hours (Fig. 13.7) (for more details see Milford et al., 2008).

DATE	HOUR	DIR	DIR	WS	EPI	BLH	B_ALT	T_ALT	B_TEM	T_TEM	MEDIAN	PER99	>%70	>%80
23-08-2022	00	036	NE	8.6	9.3	488	450	655	19.1	27.3	*****	*****	**	**
23-08-2022	06	026	NNE	9.1	8.0	569	511	734	18.0	25.5	*****	*****	**	**
23-08-2022	12	030	NNE	8.8	7.5	599	579	1021	18.2	26.1	11.0	39.0	23	17
23-08-2022	18	025	NNE	9.1	7.6	604	579	734	18.0	26.4	*****	*****	**	**
24-08-2022	24	032	NNE	9.5	7.5	647	579	821	17.7	25.4	*****	*****	**	**
24-08-2022	30	032	NNE	8.1	6.6	682	650	1126	16.7	24.1	*****	*****	**	**
24-08-2022	36	034	NE	7.8	6.7	663	651	819	17.3	25.1	10.0	316.0	30	13
24-08-2022	42	027	NNE	9.5	6.8	667	579	821	17.6	25.7	*****	*****	**	**
25-08-2022	48	030	NNE	9.3	5.7	713	651	818	16.9	22.6	*****	*****	**	**
25-08-2022	54	030	NNE	9.3	5.3	669	651	912	16.9	21.9	*****	*****	**	**
25-08-2022	60	030	NNE	9.3	5.3	637	579	820	17.3	22.9	11.0	64.0	30	13
25-08-2022	66	027	NNE	9.2	4.7	679	652	818	16.8	22.1	*****	*****	**	**
26-08-2022	72	017	NNE	10.2	5.3	639	579	819	17.2	22.3	*****	*****	**	**
26-08-2022	78	026	NNE	9.0	4.4	761	729	909	15.7	20.5	*****	*****	**	**
26-08-2022	84	024	NNE	8.3	4.2	817	730	1012	16.0	21.2	9.0	64.0	13	10
26-08-2022	90	018	NNE	9.0	4.0	829	815	1010	15.4	20.9	*****	*****	**	**
27-08-2022	96	023	NNE	8.8	3.4	916	906	1116	14.5	19.5	*****	*****	**	**
27-08-2022	102	022	NNE	8.1	2.6	759	1004	1356	13.4	18.1	*****	*****	**	**
27-08-2022	108	015	NNE	6.8	2.2	737	1005	1356	13.2	18.3	8.0	21.0	03	00

Figure 13.7. Meteorological parameters summary table showing wind direction, wind speed, Integrated Stability Parameter (EPI), boundary layer height (BLH), inversion layer height and temperature (base and top), median and 99 percentiles of the analogous selected, and probability of occurrences of exceedances over 80 and 70 percentiles of the historical series of SO_2 concentration.

13.5.2 The PSU/NCAR mesoscale model (MM5)

The meteorology programme has access to a clusters system in LINUX environment of parallel processors for the execution of a non-hydrostatic high resolution weather model (MM5) for the area of the Canary Islands. The initial and boundary conditions are from the ECMWF IFS model, and nested grids of 18, 6 and 2 km resolution are output with a forecasting range up to 144 hours.

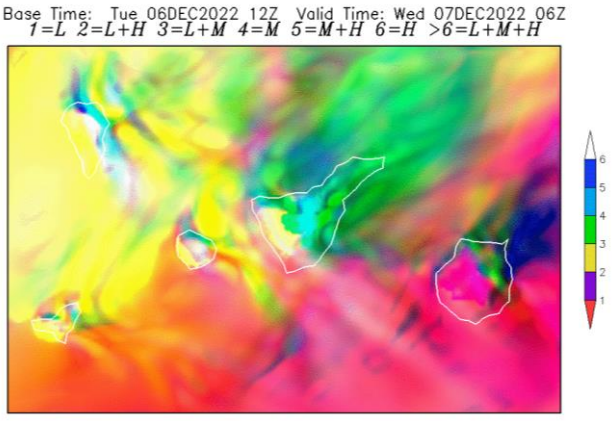

Figure 13.8. Example of graphical representation of total cloud fraction (low+medium+high) shaded in colours on 7 December 2022 at 06 UTC (output of MM5 model).

13.5.3 The Weather Research and Forecasting (WRF) model

A Super Workstation based on the Xeon Phi KNL processor, with 72 cores at 1.5 GHz and RAM 64 GiB, and a CentOs7.3 OS with the Fortran and C++ compiler Intel Parallel Studio XE, is utilised to run the Weather Research and Forecasting - Advanced Research WRF (WRF-ARW) model at very high resolution. The initial and boundary conditions are also from the ECMWF IFS model, and nested grids of 6, 2 and 1 km resolution are output with a forecasting range up to 72 hours. A high-mountain gust parameterization was implemented in WRF which greatly improves the wind gust forecast at both the Izaña Observatory and the Teide Peak Observatory (Fig. 13.9 and 13.10).

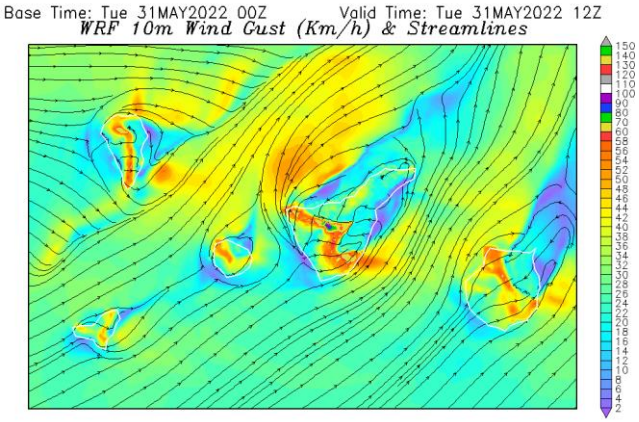

Figure 13.9. Example plot of forecasted wind gust speed, shaded in colours, overlapped with stream lines for a high wind speed episode on 31 May 2022 at 12 UTC.

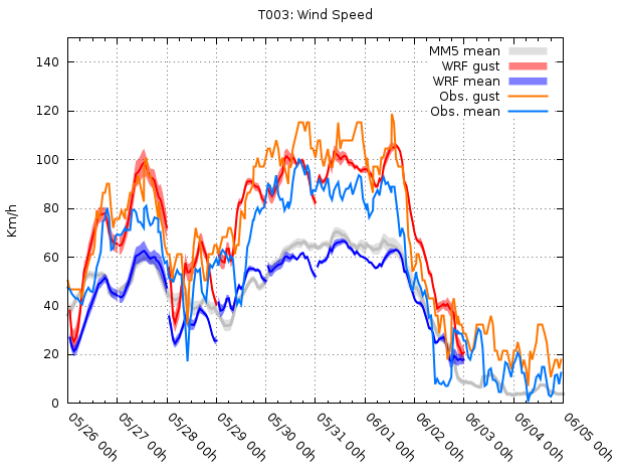

Figure 13.10. Example of validation plot showing observed and forecasted wind and gust speeds from 26 May to 05 June 2022. MM5 wind speed is also plotted.

13.5.4 Post-processed numerical results

The outputs of these models offer the added value of dynamic downscaling of the IFS model predictions for the complex topography of the Canary Islands. Various types of post-processed numerical fields permit a better

understanding of the atmospheric situations. In addition to these outputs an artificial neural network has been implemented that improves the prediction of local temperature and wind at the observatory, granting additional accuracy to the in situ forecast (Fig. 13.11). All these results are presented using a web server installed in the cluster.

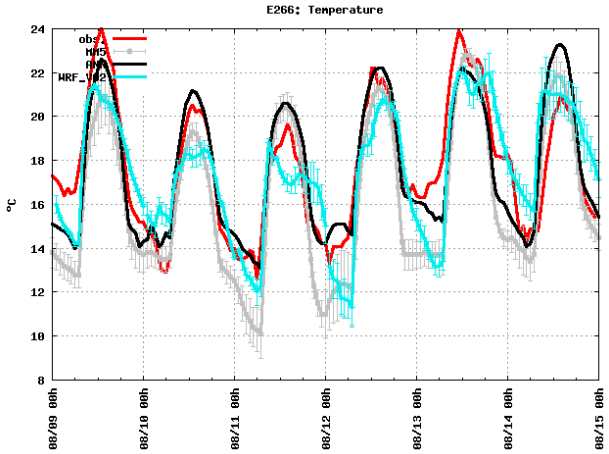

Figure 13.11. Example of the Artificial Neural Network (ANN) 2 m forecast temperature improvement from 9-15 August 2022. Black lines represent the ANN values, while red, grey and blue lines represent observations and direct MM5 and WRF output, respectively.

13.5.5 FLEXible TRAjectory (FLEXTRA) model

The FLEXible TRAjectory (FLEXTRA) model is installed in a dedicated server and simulates 10-day back-trajectories arriving at Izaña Observatory calculated at several levels. The back-trajectories provide relevant information on transport and source regions of air masses affecting the various components and parameters measured at IZO. The back-trajectories have been calculated, and archived, at six hourly intervals for the 1979-2022 period.

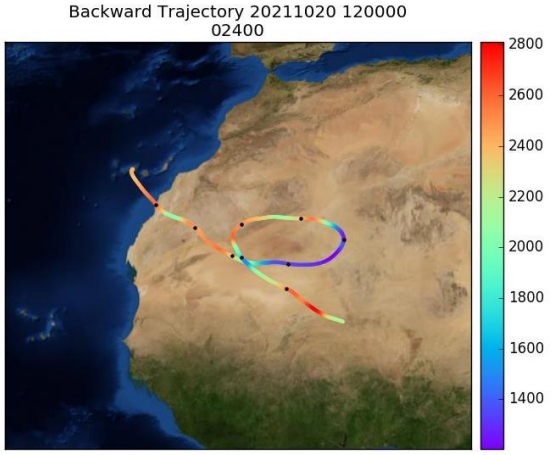

Figure 13.12. Image representing the track and height of a FLEXTRA back-trajectory with track ending on 20/01/2019 at 18 UTC.

Additional graphical information representing the track and its height is shown using a web server as a quick reference in order to select particular episodes (Figure 13.12). A later more exact representation can be requested using a McIdas web-based server (Fig. 13.13).

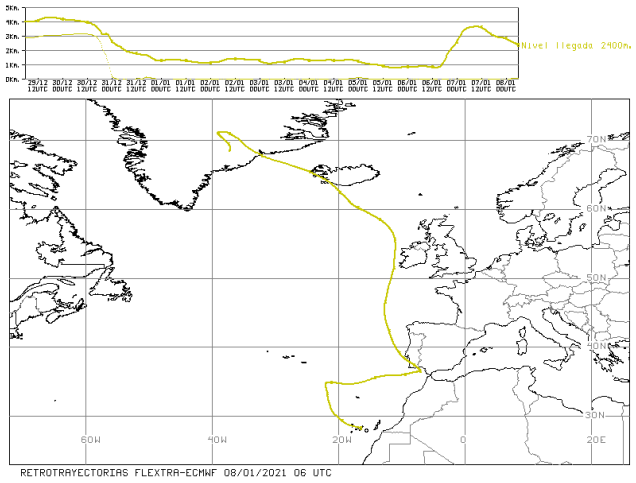

Figure 13.13. Detailed plot of a FLEXTRA back-trajectory with track ending on 08/01/2021 at 06 UTC.

13.5.6 HYbrid Single Particle Lagrangian Integrated Trajectory (HYSPLIT) model

The HYbrid Single Particle Lagrangian Integrated Trajectory (HYSPLIT) model has been installed on the same server as the FLEXTRA model in order to simulate 10-day back-trajectories using the National Centers for Environmental Prediction (NCEP) Global Forecast System (GFS) model as data input. The back-trajectories have been calculated, and archived, at six hourly intervals for the entire 1949-2022 period.

In addition, the HYSPLIT model was also installed in the cluster system using the MM5 output data and was run in dispersion mode using the parallel program settings to determine SO_2 concentrations in areas close to emission sources (Figure 13.14).

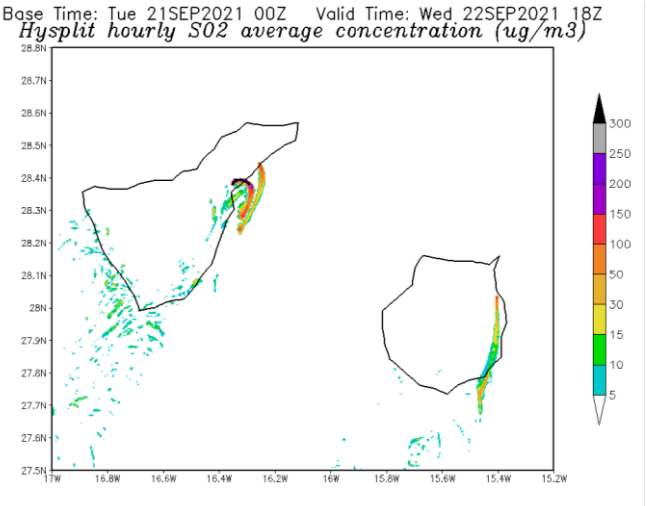

Figure 13.14. Average Hysplit SO_2 concentration forecasted on day 22/09/2021 at 18 UTC.

13.6 Summary of activities during the period 2021-2022

13.6.1 Meteorological long-term records

The series of average temperature, accumulated precipitation, sunshine duration and average atmospheric pressure at Izaña Observatory have been updated for the years 2021 and 2022 (Fig. 13.15). This constitutes over a century of meteorological data and is the oldest uninterrupted climate series in the Canary Islands.

In the series of annual mean temperature at IZO (Fig. 13.15a), the rate of rise in temperature is maintained at 0.15ºC per decade, consistent with the global warming trend. This series is especially relevant since the station is at altitude and is representative of conditions of quasi free troposphere. The annual mean temperature of 2021 and 2022 are situated in the 4th quintile of the 1961-90 reference series, with a classification of very warm, with data of 10.9 and 11.1 ºC, respectively.

Regarding total annual precipitation (Fig. 13.15b), both 2021 and 2022 have precipitation rates less than the 1961-90 median value. 2021 total annual precipitation is 208.1 mm and is classified as very dry (in the 1st quintile), while in 2022 the total annual precipitation is 387.0 mm and is classified as normal (between the 2nd and 3rd quintile).

The total annual sunshine duration series also maintains a significant increasing trend of 40.8 h per decade trend (Fig. 13.15c). In 2021 and 2022, the total annual sunshine duration was 3872.1h and 3774.5 h, respectively.

The evolution of the annual mean atmospheric pressure (13.15d) shows a decrease in the rate of increase of the last decade after the maximum of 2020, with the data for 2021 and 2022 similar at 770.5 and 770.3 hPa, respectively.

An analysis was conducted to compare the meteorology of 2021 and 2022 at IZO to the long-term meteorological records. For example, October 2021 and November 2022 broke the records of highest monthly mean temperature and highest monthly mean of daily maximum temperatures. On the other hand, September 2022 registered two anomalous precipitation events (Table 13.1).

Table 13.1. Meteorology of 2021 and 2022 at IZO in comparison with 1916-2020 meteorological records.

Extreme Event	Data	Date
Highest September daily precipitation 7-7	82.4 mm	24 Sep 2022
Maximum September precipitation intensity	33.6 mm/h	2 Sep 2022
Maximum September precipitation amount in 10′	5.6 mm	2 Sep 2022
Highest October monthly mean temperature	13.9 ºC	Oct 2021
Highest November monthly mean temperature	10.7 ºC	Nov 2021
Highest July monthly mean temperature	25.1 ºC	Jul 2020
Highest October monthly mean of daily maximum temperatures	17.9 ºC	Oct 2021
Highest November monthly mean of daily maximum temperatures	14.1 ºC	Nov 2022

To ensure quality and continuity of observations within national and international meteorological and climatological observation networks in which IARC participates it is required to keep constant maintenance and vigilance of meteorological instrumentation and subsequent quality checking of meteorological data from IZO, SCO, BTO and TPO.

The networks in which IARC participates are the Synoptic Observation Network (WMO Region I, ID: 60010), included in the surface observation network of Global Climate Observing System, the AEMET Climatological Monitoring Network (ID C430E) and the Baseline Surface Radiation Network (BSRN; station # 61).

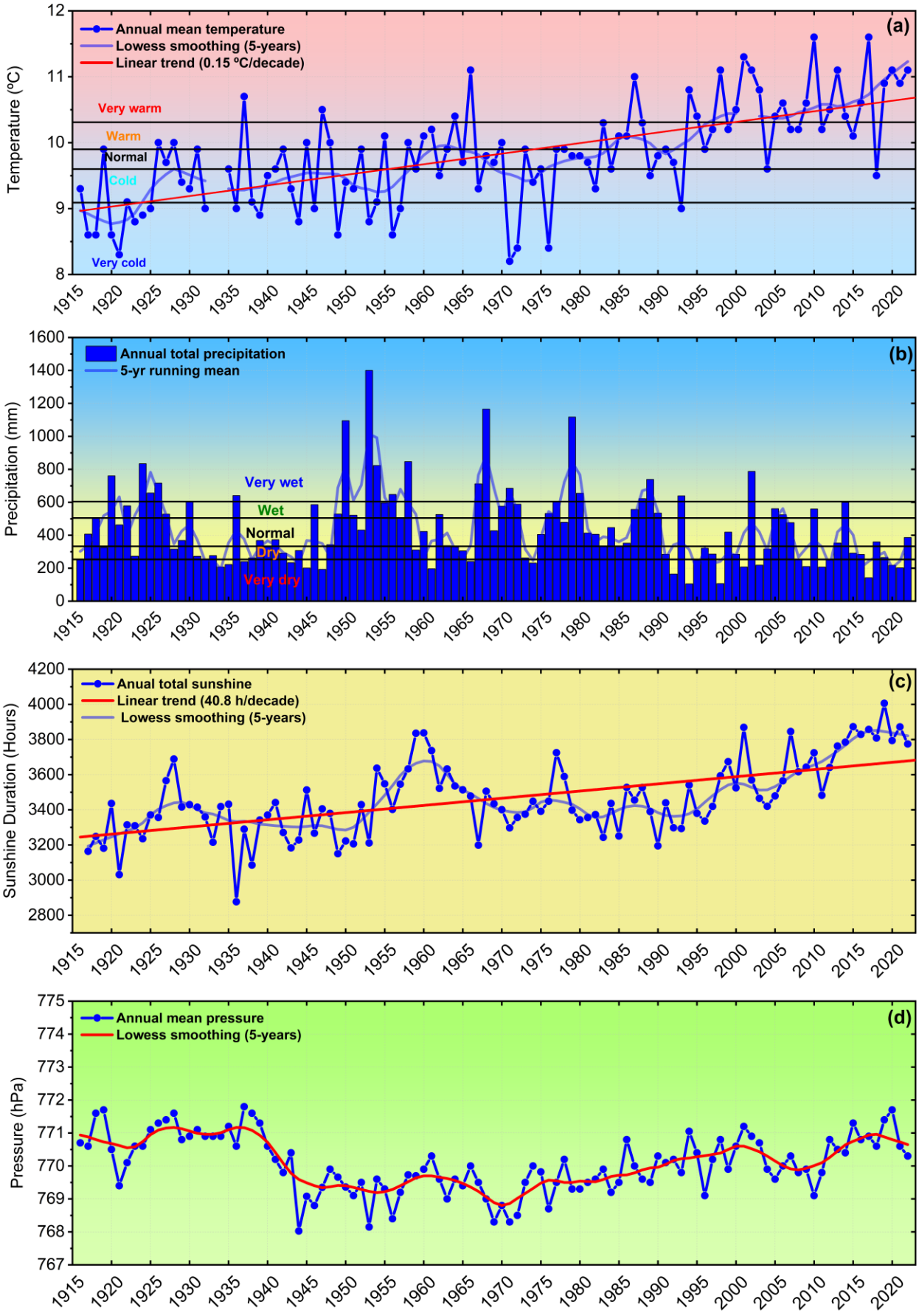

Figure 13.15. Time series (1916-2022) of a) annual mean temperature, b) total annual precipitation, c) annual sunshine duration and d) annual mean pressure at Izaña Observatory.

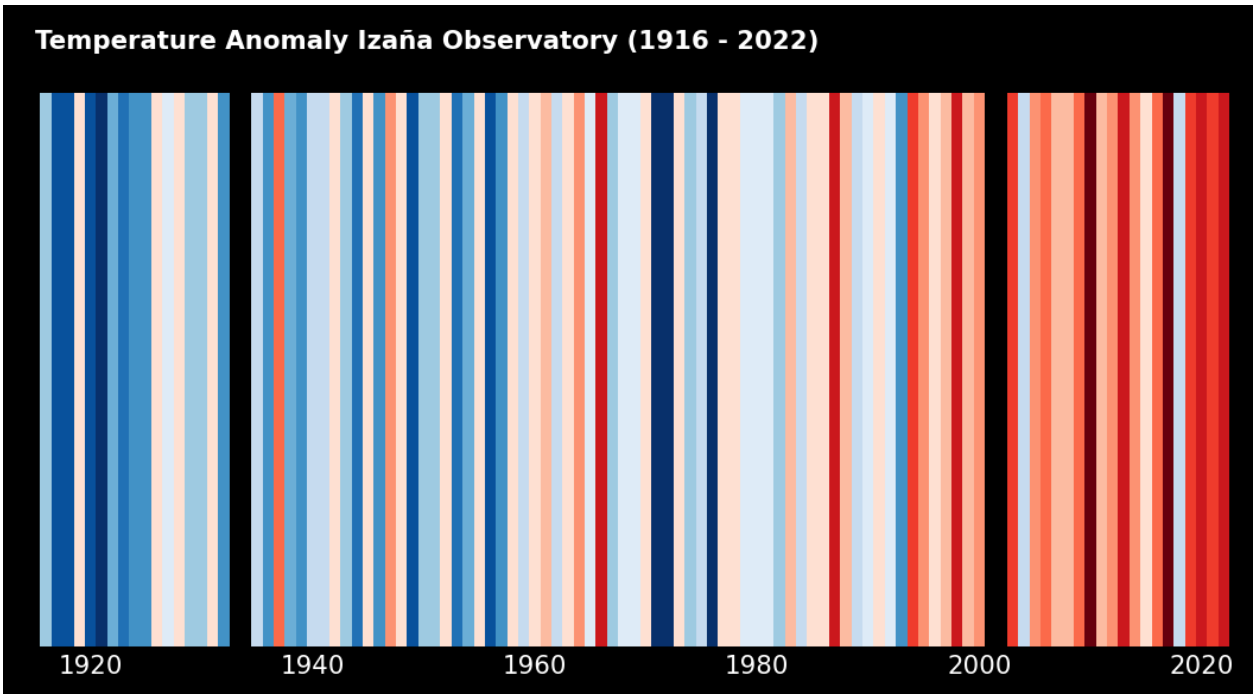

Figure 13.16. Average annual temperature anomaly time series from 1916 to 2022 at Izaña Observatory.

Another representation of the series of average temperature is shown in Fig. 13.16, this shows the average annual temperature anomaly time series at Izaña Observatory for the years 1916 to 2022.

13.6.2 Prediction and analysis of severe weather events

Additional activities of the Meteorology programme include prediction and subsequent analysis of severe weather events that may affect operations of the various observation programmes at the four IARC observatories. We highlight some of the most important episodes during 2021-2022:

On 7-8 January 2021 the named storm Filomena produced strong winds with 124 km/h maximum gust, and a snow event with accumulated 92.6 mm precipitation amount (approximately 69 cm of snow height) (Figs. 13.17 and 13.18).

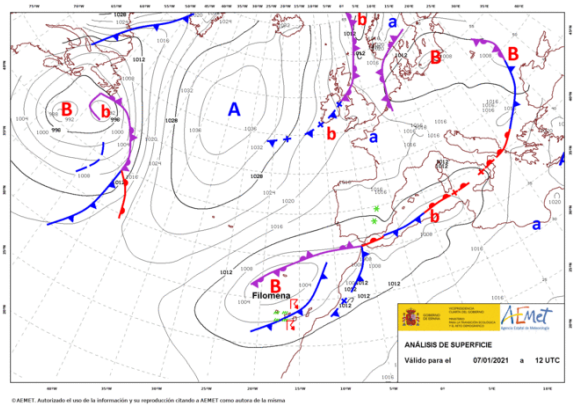

Figure 13.17. Surface pressure analysis and fronts, 07/01/2021 12 UTC.

Figure 13.18. Image taken on 10 January 2021 of the snowfall caused by storm Philomena.

On 14 March 2022 the named storm Celia produced a cold and strong wind event with a 169 km/h maximum wind gust (Figs. 13.19 and 13.20).

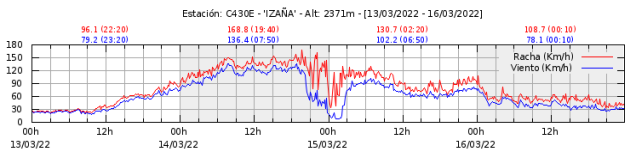

Figure 13.19. Wind speed and gust plot for 13-16 March 2022.

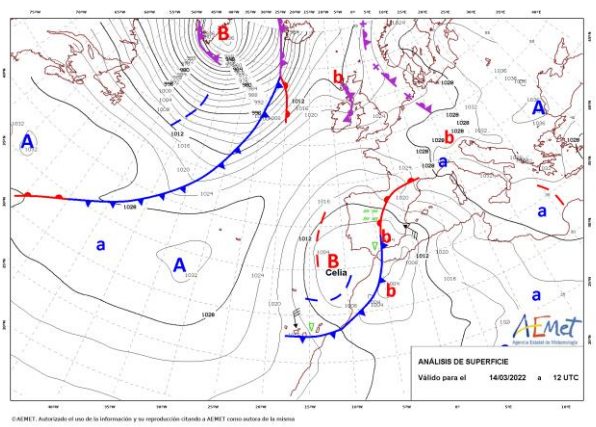

Figure 13.20. Surface pressure analysis and fronts, 14/03/2022 12 UTC.

On 24-26 September 2022 the external moisture circulation of tropical storm Hermine produced an anomalous rain event with accumulated 110.4 mm of precipitation (Figs. 13.21 and 13.22).

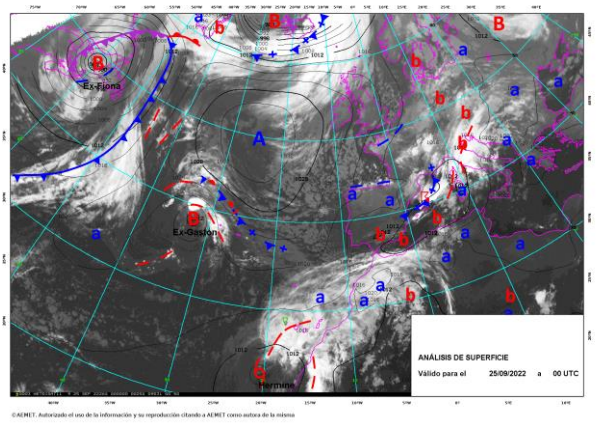

Figure 13.21. Surface pressure analysis and fronts over IR Meteosat images, 25/09/2022 00 UTC.

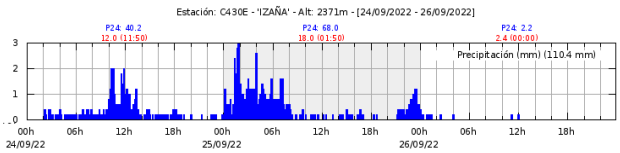

Figure 13.22. Precipitation plot for 24-26 September 2022.

13.6.3 Project to improve the quality of forecasted PM_{10} values during African desert dust outbreaks

The completion of the PM_{10} Prediction Improvement Project for the Canary Islands enables the quantification of more realistic PM_{10} values during African Dust Outbreaks Events. This project has resulted in the publication of a Technical Note (Suárez Molina et al., 2021) that outlines the methodology and findings of the project. Additionally, several new operational products have been implemented to improve air quality management. To better understand the results obtained and make use of the developed products, a specialized training course for forecasters has been offered.

One of the key advancements is the ingestion of real-time PM_{10} data from all stations in the Canary Islands Air Quality Monitoring Network (AQMN). This has allowed for a more comprehensive understanding of air quality patterns and trends, which in turn has improved the accuracy of the predictions.

To make these improved predictions accessible to the forecasters, a new website has been developed that presents the information in a clear and concise manner. This website provides both enhanced predictions as well as real-time observations of PM_{10} concentrations (Fig. 13.23).

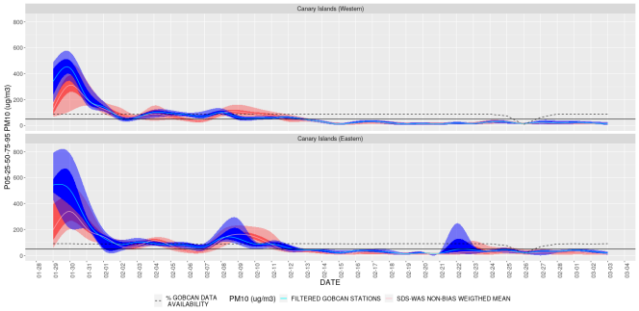

Figure 13.23. PM_{10} values for 05, 25, 50, 75, and 95 percentiles obtained from the SDS-WAS system's component models, statistically corrected and interpolated to the observation station locations. The red colour represents percentiles 25 to 75 with a line marking 50, while lighter shades of red are used for the ranges 05 to 25 and 75 to 95. Observation station data are represented in blue following the same colour scheme. The dotted line indicates the percentage of available data. The upper panel corresponds to the western Canary Islands (El Hierro, La Palma, La Gomera, and Tenerife) while the lower panel includes the eastern Canary Islands (Gran Canaria, Fuerteventura, and Lanzarote). Data for 1 January to 3 March 2022.

13.6.4 Real-time tracking of PM_{10} levels in the Canary Islands

In order to monitor PM_{10} values in the Canary Islands in real-time, a webpage has been developed. The webpage provides daily data, including the daily average value, for each station (represented by a horizontal dotted line that changes as hours are added to the period), and allows users to view detailed information by hovering over data points or the dotted line (Fig. 13.24). This tool offers a valuable means of tracking PM_{10} levels and provides researchers with a new tool for understanding air quality trends in the Canary Islands.

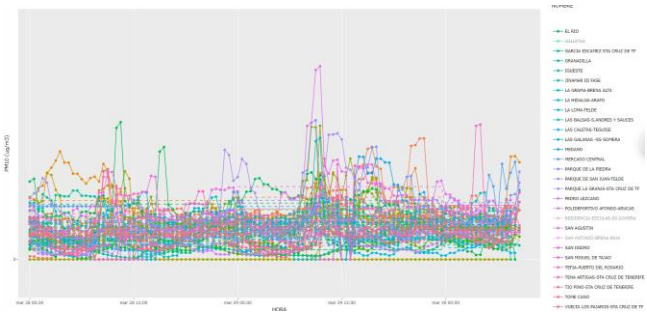

Figure 13.24. Interactive chart of semi-hourly PM_{10} measurements from the Canary Islands Air Quality Monitoring Network. The dashed line represents the daily average, and the dots represent the semi-hourly measurements taken from 28-30 March 2022.

13.6.5 Electric Field Characterization in Izaña

The Previstorm electric field measurements have been characterized through a study conducted in Izaña Observatory. An optimal time interval for statistical characterization of the measured electric field was determined, with information presented as percentiles min, p25, p50, p75, and max for intervals ranging from 1 s to 5 min. The results have been made available on an interactive webpage, allowing for easy access and interpretation (Fig. 13.25). These findings are relevant to the Canary Islands, where understanding and characterizing the electric field can contribute to improved forecasting and management of weather-related events.

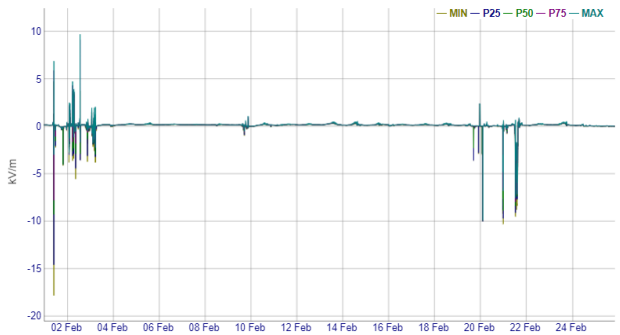

Figure 13.25. Interactive graph of electric field measured with Previstorm every 5 minutes and corresponding percentile statistics (0%, 25%, 50%, 75% and 100%) based on 1 second raw data resolution (February 2022).

13.6.6 Contributions to the CH_4 Emission Quantification from Madrid Waste Sites

This study applies satellite-based measurements from TROPOMI and IASI together with measurements from the ground-based COllaborative Carbon Column Observing Network instruments. The objective is to derive methane (CH_4) emissions of the metropolitan city of Madrid (Spain) from the CH_4 enhancements seen by the space-borne and the ground-based instruments (Tu et al., 2022).

As part of this study, it is necessary to use the wind speed and direction at various locations, which must be simulated due to the lack of observing stations. To do this, data is extracted from the Harmonie-Arome model for wind at various levels and with a spatial resolution of 2.5 km during the period 2017-2020. This extraction is done automatically due to the large amount of data required through query routines to the BigData AMET storage system.

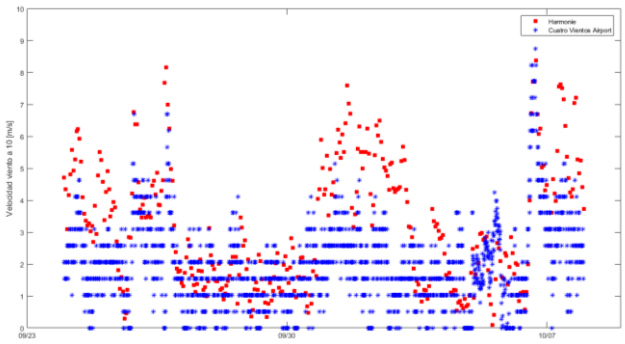

Figure 13.26. Comparison of wind speed between the observation data from Cuatro Vientos airport and the Harmonie model from 23 September - 13 October 2018.

13.6.7 Participation in a study on the relationship between dispensing of asthma medications and PM_{10}

We are currently participating in a study that aims to investigate the relationship between the dispensing of both rescue and long-term maintenance asthma medications in pharmacies and PM_{10} values measured at different stations in the Canary Islands' Air Quality Network. To conduct this study, we extracted the corresponding PM_{10} data from a database and then filtered and purified the data to ensure that the daily average values are of good quality. The study is currently ongoing, and we are working to further analyze the data and investigate any possible correlations between asthma medication dispensing and PM_{10} levels.

13.6.8 New FLEX_EXTRACT Data Extraction System

The FLEX_EXTRACT data extraction system for generating trajectories has been disabled on the new ECMWF (Bologna, Italy) servers due to the disappearance of essential libraries needed to execute the Python and Fortran routines that extract and transform data for the FLEXTRA program. As a result, the only alternative to the FLEX_EXTRACT system is to perform the entire process in local mode. To accomplish this, a virtual machine with an updated Linux (Fedora 37) has been installed to compile all the software, with permissions to access the ECMWF user account through ecmwf-api and cdsapi clients.

The entire system now operates in local mode, eliminating the need to access the ECMWF gateways as a member state user. The processing time depends on the number of users using the services at any given time and is generally similar or slightly longer than the previous method. Back-trajectories can now be processed with any available reanalysis or prediction.

Currently, the back-trajectories have been updated from 1979 to 2022 with ERA5, and trajectories will be calculated from 1959 to 1978 (1959 is currently the earliest date available in ERA5).

13.6.9 Assessing uncertainty in back-trajectories using clustering techniques

The FLEXTRA back-trajectories calculated with ERA5 differ significantly from those calculated with Era Interim. In many of the experiments conducted, a large uncertainty in the trajectories is observed, which changes their destination over small distances and in a few hours. Consequently, we considered it necessary to quantify the uncertainty of the calculated trajectories with ERA5. This uncertainty in the trajectories defined in the FLEXTRA calculations were used to generate 60 elements, which were then grouped using K-means techniques. These elements correspond to the same point at 2400 m used as the main arrival point, the four points surrounding that coordinate, those same coordinates 200 meters above and below, for the periods 00, 06, 12, and 18 of each day, totalling 60 trajectories per day. The trajectories were grouped into four clusters based on their similarity, which optimize the total spatial variance. Using the back-trajectories from 2010 to the present, these four groups were generated for each day with values of percentage of trajectories per group, which provide an idea of the weight that each group has in the impact of their transport. Each group is represented by the mean of the trajectories that compose it. All the information is available on a website that allows for the visualization of the results (Fig. 13.27).

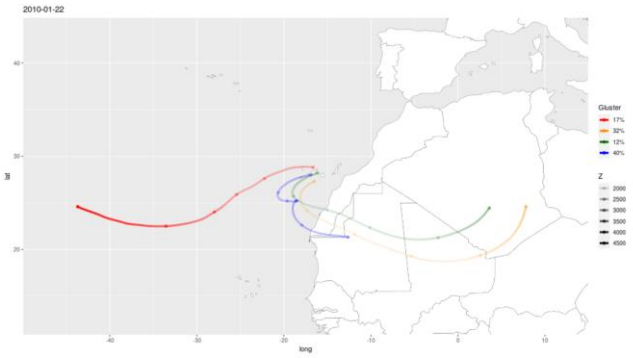

Figure 13.27. Plot representing the mean of the four back-trajectory groups corresponding to 22 January 2010. The legend identifies the percentage of elements in each cluster, and the transparency of the lines indicates the altitude at which they are transported.

13.6.10 Contributions to the 2021 La Palma volcanic eruption emergency response

Air quality data from the Canary Islands Air Quality Monitoring Network was collected from a server every 30 minutes for the following components: SO_2, CO, PM_{10}, PM_{25}, NO, NO_2, NO_X, O_3, HR, DD, TMP and VV. This data was ingested and presented on a website for all stations installed in La Palma (Fig. 13.28). This information allowed for monitoring of the air quality in near real-time.

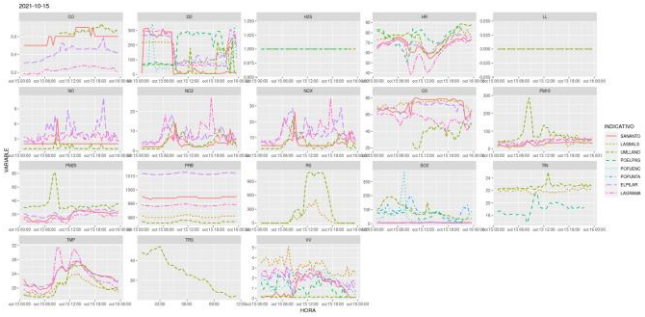

Figure 13.28. Air quality parameters measured on 15 October 2021 at the stations located in La Palma and belonging to the Canary Islands Air Quality Monitoring Network.

Additionally, images from AEMET MOCAGE runs in emergency mode were compiled to create a synthesized and improved presentation on a website, which was automatically updated twice a day (Fig. 13.29).

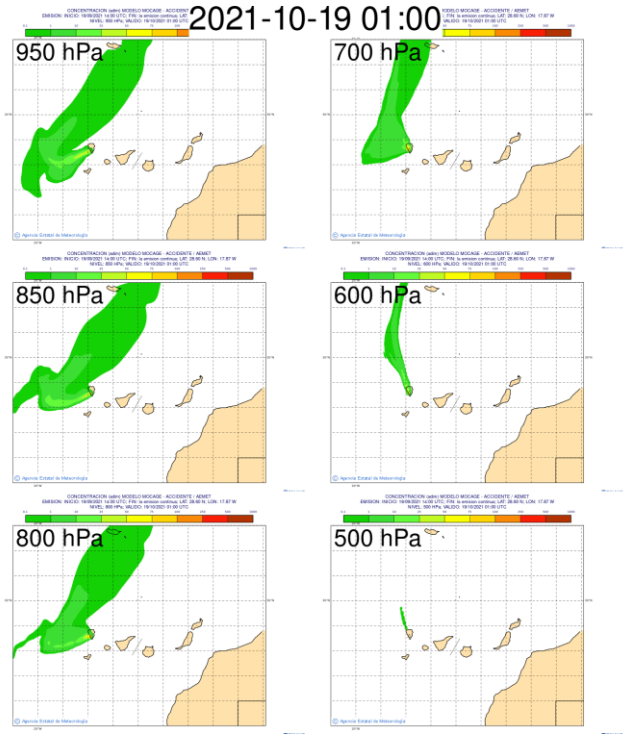

Figure 13.29. Composite images of MOCAGE volcanic ash plume dispersion simulations at different pressure levels on 19 October 2021 at 01:00 UTC.

13.6.11 Contribution to the Calculation of Spectral Aerosol Radiative Forcing and Efficiency of the La Palma Volcanic Plume over IZO

During the 2021 La Palma volcanic eruption, the Izaña Observatory was impacted by various types of aerosols, including volcanic ash, Saharan mineral dust, and a combination of both. Researchers conducted three case studies using data from ground-based and satellite-based instruments, as well as reanalysis data and trajectory analysis (García et al., 2023). These studies were used to examine the optical and micro-physical properties of the aerosols, and ground-based sun-photometry measurements were used to further characterize them.

The study used the FLEXTRA software to compute back-trajectories using ERA5 reanalysis data from ECMWF. The software was configured with input data every 6 hours, covering a large area and resolution in both horizontal and vertical dimensions. The destination coordinate was set to the IZO location, and four pressure levels were used (Fig. 13.30). Back-trajectory coordinates were obtained every 20 minutes using a 3D wind configuration, with horizontal and vertical offset target backward trajectories also computed to estimate uncertainties. This analysis was used to better understand the movement of aerosols during the eruption. For more details on this study see Section 23.

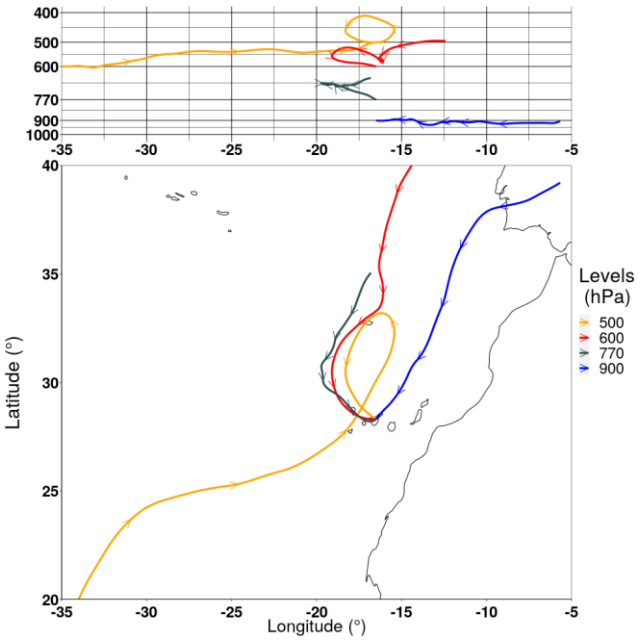

Figure 13.30. FLEXTRA back-trajectories corresponding to 24 September 2021 at 12:00 hours for arrival pressure levels of 900, 770, 600, and 500 hPa at the Izaña Observatory. Reprinted from García et al. (2023).

13.6.12 Contribution to the study on the impact of the 2021 La Palma volcanic eruption on air quality

The determination of the height at which volcanic ash and SO_2 plumes are injected is crucial for determining their transport direction. The strong vertical stratification of the subtropical eastern North Atlantic, which hinders the vertical growth of volcanic plumes and results in a change of wind direction with height, makes FLEXTRA particularly useful in this region. An analysis of the wind direction during the La Palma 2021 eruption showed that lower levels of the troposphere had a dominant E-NE wind direction, leading to transport of plumes to the W-SW, while plumes injected at higher levels were dispersed in various directions (Milford et al., 2023). FLEXTRA forward trajectories helped to confirm these findings and were useful in indicating the transport of the volcanic plume, for more details on this study see Section 23.

13.6.13 Collaboration project with the National Autonomous University of Mexico

We were involved in a collaboration project with the National Autonomous University of Mexico (UNAM), which aimed to estimate SO_2 emission flows from the 2021 La Palma volcanic eruption using data from the TROPOMI/ESA satellite sensor. To achieve this, we used the WRF-ARW model outputs, which routinely run at IARC, and converted them to ARL-compatible outputs with HYSPLIT (Fig. 13.31). This allowed for high-resolution simulations of SO_2 dispersion.

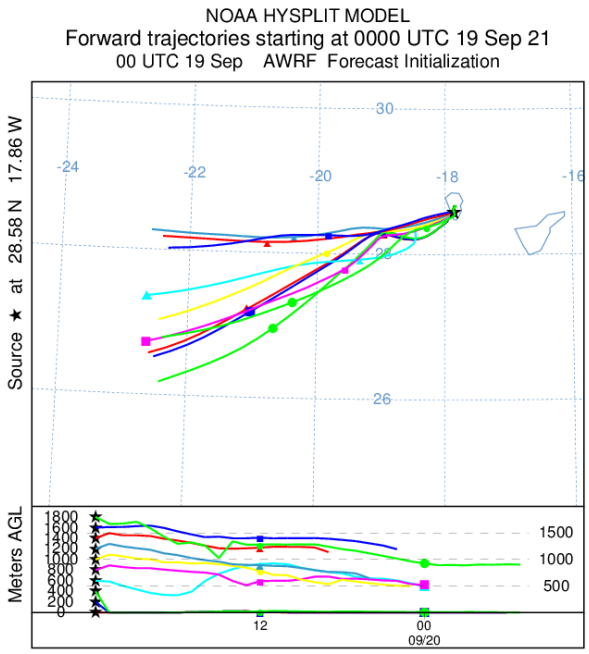

Figure 13.31. Forward trajectories corresponding to a simulation performed with HYSPLIT for the 2021 La Palma volcanic eruption using high-resolution data from WRF-ARW outputs of IARC in the domain of the Canary Islands on 19 September 2021 at 00:00 UTC.

13.6.14 Contribution to characterizing optical properties of aerosols from the 2021 La Palma volcanic eruption, across the Atlantic

After the 2021 La Palma volcanic eruption, gases and aerosols were released that impacted the Canary Islands before crossing the Atlantic and reaching the Caribbean. To determine the days that the volcanic emissions transported from the volcano passed through Izaña and then travelled to San Juan, Puerto Rico, we generated trajectory clusters that allowed us to evaluate the days with a degree of uncertainty. FLEXTRA-ERA5 was run to provide 240 h back-trajectories arriving at San Juan de Puerto Rico at different altitudes and positions (Fig. 13.32).

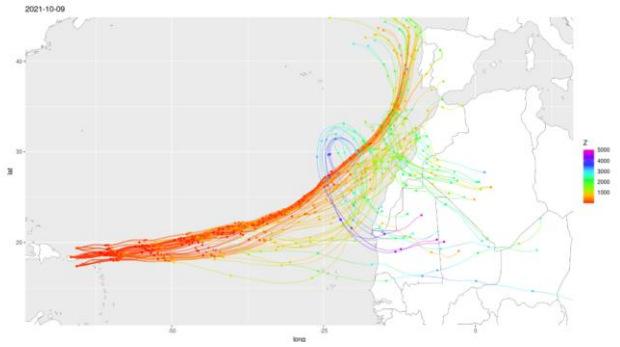

Figure 13.32. Back-trajectories cluster corresponding to arrival altitudes of 0, 64, 100 and 150 m, combined with 4 positions at a distance of 1º with respect to the coordinates of the San Juan de Puerto Rico station on 9 October 2021.

13.6.15 Additional activities

In addition to the activities described in this section, we participated as co-authors in the following studies and publications: Cuevas et al. (2021), Barreto et al. (2022), Fraile-Nuez et al. (2021a, 2021b), García et al. (2021, 2022) and Qiansi et al. (2022).

13.7 References

Barreto, Á., Cuevas, E., García, R. D., Carrillo, J., Prospero, J. M., Ilić, L., Basart, S., Berjón, A. J., Marrero, C. L., Hernández, Y., Bustos, J. J., Ničković, S., and Yela, M.: Long-term characterisation of the vertical structure of the Saharan Air Layer over the Canary Islands using lidar and radiosonde profiles: implications for radiative and cloud processes over the subtropical Atlantic Ocean, Atmos. Chem. Phys., 22, 739–763, https://doi.org/10.5194/acp-22-739-2022, 2022.

Cuevas, E., Milford, C., Barreto, A., Bustos, J. J., García, R. D., Marrero, C. L., Prats, N., Bayo, C., Ramos, R., Terradellas, E., Suárez, D., Rodríguez, S., de la Rosa, J., Vilches, J., Basart, S., Werner, E., López-Villarrubia, E., Rodríguez-Mireles, S., Pita Toledo, M. L., González, O., Belmonte, J., Puigdemunt, R., Lorenzo, J.A., Oromí, P., and del Campo-Hernández, R.: Desert Dust Outbreak in the Canary Islands (February 2020): Assessment and Impacts. (Eds. Cuevas, E., Milford, C. and Basart, S.), State Meteorological Agency (AEMET), Madrid, Spain and World Meteorological Organization, Geneva, Switzerland, WMO Global Atmosphere Watch (GAW) Report No. 259, WWRP 2021-1, 2021.

Fraile-Nuez, E., Cuevas, E., Milford, C., Mosquera, A., Arrieta. J. M., Marrero, C., Vélez-Belchí, P., Bustos, J.J., Barreto, A., García, R. D., Redondas, A., García, O., Romero-Campos, P. M., Presas-Navarro, C., Palomino, D. and González-Vega, A. Climatological Characterisation of Ocean Sites for Ocean Colour System Vicarious Calibration: El Hierro (Canary Islands, Spain), Task 1 Report: Climatological and observational data sets (EUMETSAT study report, EUMETSAT, Darmstadt, Germany), 2021a. https://www.eumetsat.int/media/49924

Fraile-Nuez, E., Cuevas, E., Milford, C., Mosquera, A., Arrieta. J. M., Marrero, C., Vélez-Belchí, P., Bustos, J.J., García, R. D., Barreto, A., García, O., Redondas, A., Romero-Campos, P. M., Berjón, A., Presas-Navarro, C., Palomino, D. and González-Vega, A. Climatological Characterisation of Ocean Sites for Ocean Colour System Vicarious Calibration: El Hierro (Canary Islands, Spain) Task 2 Report: Site Characterisation (EUMETSAT study report, EUMETSAT, Darmstadt, Germany), 2021b. https://www.eumetsat.int/media/49925

García, O.E., Sepúlveda, E., León-Luis, S. F., Josep-Antón Morgui, Matthias Frey, Carsten Schneider, Ramón Ramos, Carlos Torres, Roger Curcoll, Carme Estruch, África Barreto, Carlos Toledano, Frank Hase, André Butz, Emilio Cuevas, Thomas Blumenstock, Juan J. Bustos, and Carlos Marrero, Monitoring of Greenhouse Gas and Aerosol Emissions in Madrid megacity (MEGEI-MAD), GAW Symposium 2021 (online), 28 June-2 July, 2021.

García, O., Suárez, D., Cuevas, E., Ramos, R., Barreto, África, Hernández, M., Quintero, V., Toledano, C., Sicard, M., Córdoba-Jabonero, C., Riz, V., Roininen, R., López, C., Vilches, J., Weiss, M., Carreño, V., Taquet, N., Boulesteix, T., Fraile, E., Torres, C., Prats, N., Alcántara, A., León, S. ., Rivas, P., Álvarez, Óscar, Parra, F., de Luis, J., González, C., Armas, C., Romero, P., de Bustos, J., Redondas, A., Marrero, C., Milford, C., Román, R., González, R., López-Cayuela, M.,

Carvajal-Pérez, C., Chinea, N., García, R. ., Almansa, F., González, Y., Bullón, F., Poggio, M., Rivera, C., Bayo, C., & Rey, F. (2022). La erupción volcánica de La Palma y el papel de la Agencia Estatal de Meteorología. Revista Tiempo Y Clima, 5(76). Recuperado a partir de https://pub.ame-web.org/index.php/TyC/article/view/2516

García, R.D., García, O.E., Cuevas-Agulló, E., Barreto, Á., Cachorro, V.E., Marrero, C., Almansa, F., Ramos, R., Pó, M., 2023. Spectral Aerosol Radiative Forcing and Efficiency of the La Palma Volcanic Plume over the Izaña Observatory. Remote Sensing 15, 173. https://doi.org/10.3390/rs15010173

Milford, C., Torres, C., Vilches, J., Gossman, A.-K., Weis, F., Suárez-Molina, D., García, O.E., Prats, N., Barreto, Á., García, R.D., Bustos, J.J., Marrero, C.L., Ramos, R., Chinea, N., Boulesteix, T., Taquet, N., Rodríguez, S., López-Darias, J., Sicard, M., Córdoba-Jabonero, C., Cuevas, E., 2023. Impact of the 2021 La Palma volcanic eruption on air quality: Insights from a multidisciplinary approach. Science of The Total Environment 869, 161652. https://doi.org/10.1016/j.scitotenv.2023.161652

Milford, C., Marrero, C., Martin, C., Bustos, J. & Querol, X. Forecasting the air pollution episode potential in the Canary Islands. Adv. Sci. Res. 2, 21–26, 2008.

Qiansi T., F. Hase, M. Schneider, O. García, T. Blumenstock, T. Borsdorff, M. Frey, F. Khosrawi, A. Lorente, C. Alberti, J.J. Bustos, A. Butz, V. Carreño, E. Cuevas, R. Curcoll, C. J. Diekmann, D. Dubravica, B. Ertl, C. Estruch, S. F. León-Luis, C. Marrero, J.-A. Morgui, R. Ramos, C. Scharun, C. Schneider, E. Sepúlveda, C. Toledano, C. Torres Quantification of CH_4 emissions from waste disposal sites using ground- and space-based observations of COCCON, TROPOMI and IASI, TCCON/COCCON/NDACC Meeting 2022 (online), 22-24 June, 2022.

Suárez Molina, D., Marrero de la Santa Cruz, C., Cuevas Agulló, E., Werner Hidalgo, E., Prats Porta, N., Basart, S., 2021. Caracterización de las intrusiones de polvo en Canarias. Agencia Estatal de Meteorología. https://doi.org/10.31978/666-20-026-4

Tu, Q., Hase, F., Schneider, M., García, O., Blumenstock, T., Borsdorff, T., Frey, M., Khosrawi, F., Lorente, A., Alberti, C., Bustos, J.J., Butz, A., Carreño, V., Cuevas, E., Curcoll, R., Diekmann, C.J., Dubravica, D., Ertl, B., Estruch, C., León-Luis, S.F., Marrero, C., Morgui, J.-A., Ramos, R., Scharun, C., Schneider, C., Sepúlveda, E., Toledano, C., Torres, C., 2022. Quantification of CH4 emissions from waste disposal sites near the city of Madrid using ground- and space-based observations of COCCON, TROPOMI and IASI. Atmos. Chem. Phys. 22, 295–317. https://doi.org/10.5194/acp-22-295-2022.

13.8 Staff

Carlos Luis Marrero de la Santa Cruz (AEMET; Head of programme)

Juan José Bustos (AEMET; Research Scientist)

Ramón Ramos (AEMET; Head of Infrastructure, Responsible for Meteorological Observation Programme)

Antonio Alcántara (AEMET; Meteorological Observer-GAW Technician)

Concepción Bayo (AEMET; Meteorological Observer-GAW Technician)

Virgilio Carreño (AEMET; Meteorological Observer-GAW Technician)

Cándida Hernández (AEMET; Meteorological Observer-GAW Technician)

Dr Rosa García (TRAGSATEC/UVA; Research Scientist)

Pedro Miguel Romero Campos (AEMET; Research Scientist)

14 Aerobiology

The Aerobiology programme at the IARC is carried out jointly by IARC-AEMET and the Laboratori d'Anàlisis Palinològiques (LAP) of the Universidad Autónoma de Barcelona (UAB) with partial financing from Air Liquide España S.A through the Eolo-PAT project. This programme started in 2004 at SCO with the aim of improving the knowledge of the pollen and spore content in the air of Santa Cruz de Tenerife and its relation to the prevalence of respiratory allergy. A second aerobiological station was implemented at IZO thanks to the financial support of the Research and development (R+D) National Plan CGL-2005-07543 project ("Origin, transport and deposition of African atmospheric aerosol in the Canaries and the Iberian Peninsula based on its Chemical and Aerobiological Characterization"). These two projects also contribute to improvement of knowledge of the biological fraction of aerosols within the GAW Programme.

14.1 Main Scientific Goals

The main scientific goals of this programme are:

- To produce high quality standardized data on the biological component of the atmospheric aerosol.
- To establish the biodiversity and quantity of pollen and fungal spores registered in the air of Santa Cruz de Tenerife and Izaña.
- To establish the distribution pattern over the course of the year of the airborne pollen and fungal spores at Santa Cruz de Tenerife and Izaña, through the daily spectra.
- To put the Canary Islands on the map of the global aerobiological panorama, along with the Spanish (REA; SEAIC) and European networks (EAN).
- To provide information useful for medical specialists and allergic patients.
- To set up the list of the allergenic pollen and spore taxa in the air of Santa Cruz de Tenerife and Izaña that will help doctors to diagnose the allergy aetiology and to rationalize the use of the medication.
- To produce weekly alerts on allergenic pollen and spores for the days ahead to help doctors in the allergy detection and to help people suffering from allergies with a better planning of their activities and to improve the quality of their life.

A detailed description of this programme can be found in Belmonte et al. (2011).

14.2 Measurement Programme

The sampling instrument is a Hirst, 7-day recorder VPPS 2000 spore trap (Lanzoni S.r.l.) (Fig. 14.1) and the analysing instrument is a Light microscope, 600 X (Table 3.2). The pollen and spore analysis are conducted using palynological methods following the recommendations of the Spanish Aerobiology Network management and quality manual and the recommendations of the European Aerobiology Society (Galán et al. 2017). The sampling programme at SCO is continuous through the year, whereas samples are only collected at IZO from April-May to November because of adverse meteorological conditions during the rest of the year.

Figure 14.1. Hirst, 7-day recorder VPPS 2000 spore trap at SCO (left) and at IZO (right).

14.3 Summary of remarkable results during the period 2021-2022

The annual dynamics of the total pollen and total fungal spores taxa in Santa Cruz de Tenerife and Izaña are shown in Figs. 14.2 and 14.3. The plots show mean weekly concentrations of historical data (2004/2006-2021) and data from 2021.

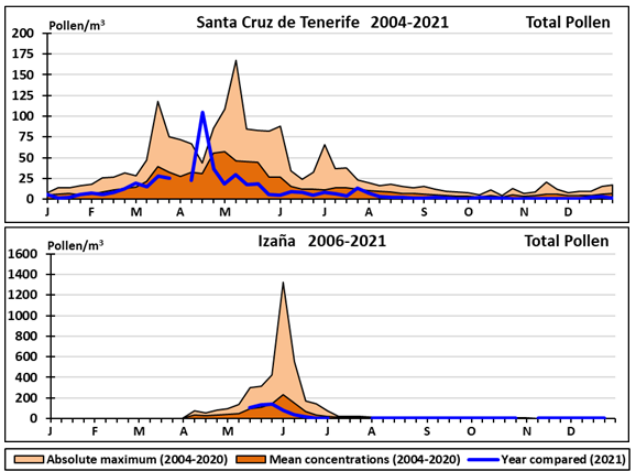

Figure 14.2. Dynamics of the mean weekly Total Pollen concentrations in Santa Cruz de Tenerife (upper panel) and Izaña (lower panel) during 2021 in comparison with 2004-2020 mean and maximum loads.

Table 14.1. Airborne pollen and spore spectrum for SCO, year 2021.

SANTA CRUZ DE TENERIFE
1 January 2021 - 31 December 2021

	YEAR		WEEK		DAY	
	Integral P*day/m³	Percentage %	Maximum P/m³	Week nr. Nr.	Maximum P/m³	Date of the Maximum dd/mm/yyyy
TOTAL POLLEN	**3380**	**100**	**104.7**	**15**	**192.5**	**18/3/2021**
POLLEN FROM TREES	**1326**	**39.2**	**43.2**	**15**	**124.6**	**18/3/2021**
Acacia	0	0.0	0.0		0	
Ailanthus	0.7	0.0	0.1	29	0.7	23/7/2021
Alnus	1	0.0	0.1	1	0.7	6/1/2021
Castanea	11	0.3	1.0	26	7.0	2/7/2021
Casuarina	6	0.2	0.5	51	2.1	8/1/2021
CUPRESSACEAE	69	2.1	1.8	51	7.0	25/12/2021
Eucalyptus	31	0.9	2.0	8	14.0	22/2/2021
Ilex	4	0.1	0.4	11	2.8	17/3/2021
MORACEAE	30	0.9	2.9	11	20.3	17/3/2021
Myrica	561	16.6	35.1	15	121.8	18/4/2021
OLEACEAE	87	2.6	3.1	18	21.7	5/5/2021
PALM TREES	180	5.3	3.9	27	24.5	11/7/2021
Pinus	86	2.5	4.1	15	14.0	13/4/2021
Platanus	1	0.0	0.1	10	0.7	11/3/2021
Populus	6	0.2	0.3	5	1.4	6/2/2021
Quercus total	28	0.8	2.4	8	16.8	22/2/2021
Salix	8	0.2	0.5	3	2.8	22/1/2021
Schinus	213	6.3	5.4	30	30.8	26/7/2021
Tilia	0	0.0	0.0		0.0	
Ulmus	0	0.0	0.0		0.0	
Other pollen from trees	4	0.1	-	-	-	-
POLLEN FROM SHRUBS	**326**	**9.7**	**9.3**	**9**	**37.1**	**4/3/2021**
CISTACEAE	0	0.0	0.0		0.0	
ERICACEAE	305	9.0	9.3	9	37.1	4/3/2021
Ricinus	13	0.4	0.5	34	0.7	21/03/2021; 22/03/2021; 25/03/2021
Pistacia	0	0.0	0.0		0.0	
Other pollen from shrubs	8	0.3	-	-	-	-
POLLEN FROM HERBS	**1657**	**49.0**	**58.4**	**15**	**101.5**	**14/4/2021**
COMPOSITAE total (incl. *Artemisia*)	780	23.1	48.1	15	85.4	14/4/2021
Artemisia	766	22.7	48.1	15	85.4	14/4/2021
BORAGINACEAE	10	0.3	0.5	11	2.1	20/3/2021
CYPERACEAE	8	0.2	0.3	15	0.7	05/01/2021; 20/02/2021; 13/04/2021
CRASSULACEAE	2	0.1	0.2	50	0.7	04/09/2021; 14/12/2021; 16/12/2021
CRUCIFERAE	45	1.3	2.7	12	18.2	23/3/2021
Euphorbia	4	0.1	0.3	19	1.4	15/5/2021
GRAMINEAE (Grasses)	233	6.9	4.5	12	9.1	25/3/2021
Mercurialis	55	1.6	1.1	1	4.2	5/1/2021
Plantago	46	1.4	1.7	11	5.6	5/3/2021
Rumex	156	4.6	3.6	10	7.0	13/03/2021 ; 23/03/2021
AMARANTHACEAE	103	3.0	3.1	5	17.5	3/2/2021
URTICACEAE	151	4.5	3.7	11	7.7	18/3/2021
Other pollen from herbs	66	1.9	-	-	-	-

	YEAR		WEEK		DAY	
	Integral S*day/m³	Percentage %	Maximum S/m³	Week nr. Nr.	Maximum S/m³	Date of the Maximum dd/mm/yyyy
TOTAL SPORES	**62048**	**100.0**	**462.8**	**51**	**966.0**	**24/9/2021**
Alternaria	1064	1.7	15.2	23	28.0	08/06/2021; 09/06/2021
Ascospores	25749	41.5	163.2	51	585.2	1/12/2021
Aspergillus/Penicillium	1025	1.7	30.4	1	165.2	10/1/2021
Clasdosporium	20504	33.0	248.0	38	851.2	24/9/2021
Ustilago	4404	7.1	76.8	28	436.8	15/7/2021
Other fungal spores	9302	15.0	-	-	-	-

Table 14.2. Airborne pollen and spore spectrum for IZO, year 2021.

IZAÑA

10 May 2021 - 26 December 2021

	YEAR		WEEK		DAY	
	Integral	Percentage	Maximum	Week nr.	Maximum	Date of the Maximum
	P*day/m³	%	P/m³	Nr.	P/m³	dd/mm/yyyy
TOTAL POLLEN	**3716**	**100.0**	**138.8**	**21**	**468.3**	**18/5/2021**
POLLEN FROM TREES	**382.2**	**10.3**	**20.8**	**19**	**46.9**	**15/5/2021**
Acacia	0.0	0.0	0.0		0.0	
Ailanthus	0.0	0.0	0.0		0.0	
Alnus	0.0	0.0	0.0		0.0	
Castanea	2.8	0.1	0.2	31	1.4	9/8/2021
Casuarina	0.7	0.0	0.1	46	0.7	21/11/2021
CUPRESSACEAE	14.7	0.4	1.8	51	7.7	22/12/2021
Eucalyptus	0.0	0.0	0.0		0	
Ilex	0.0	0.0	0.0		0	
MORACEAE	0.0	0.0	0.0		0	
Myrica	194.6	5.2	7.8	23	39.9	8/6/2021
OLEACEAE	21.0	0.6	2.2	20	7	19/5/2021
PALM TREES	2.1	0.1	0.1	21	0.7	29/05/2021 ; 31/05/2021 ; 01/09/2021
Pinus	137.2	3.7	12.5	19	30.1	13/5/2021
Platanus	0.0	0.0	0.0		0	
Populus	0.0	0.0	0.0		0	
Quercus total	9.1	0.2	0.9	19	3.5	15/5/2021
Salix	0.0	0.0	0.0		0	
Schinus	0.0	0.0	0.0		0	
Tilia	0.0	0.0	0.0		0	
Ulmus	0.0	0.0	0.0		0	
Other pollen from trees	0.0	0.0	-	-	-	-
POLLEN FROM SHRUBS	**38.5**	**1.0**	**3.4**	**19.0**	**9.1**	**12/5/2021**
CISTACEAE	0.0	0.0	0.0		0.0	
ERICACEAE	33.6	0.9	3.3	19	9.1	12/5/2021
Ricinus	2.8	0.1	0.4	21	2.1	19/5/2021
Pistacia	0.0	0.0	0.0		0	
Other pollen from shrubs	2.1	0.0	-	-	-	-
POLLEN FROM HERBS	**3204.6**	**86.2**	**129.7**	**21.0**	**448.7**	**18/5/2021**
COMPOSITAE total (incl. *Artemisia*)	7.0	0.2	0.3	21	1.4	24/5/2021
Artemisia	4.9	0.1	0.2	19	1.4	21/5/2021
BORAGINACEAE	2.1	0.1	0.3	19	2.1	14/5/2021
CYPERACEAE	1.4	0.0	0.1	32	0.7	14/08/2021 ; 22/10/2021
CRASSULACEAE	0.0	0.0	0.0		0	
CRUCIFERAE	3056.9	82.3	127.0	21	448.7	18/5/2021
Euphorbia	0.0	0.0	0.0		0	
GRAMINEAE (Grasses)	96.6	2.6	5.3	22	15.4	1/6/2021
Mercurialis	0.7	0.0	0.1	24	0.7	17/6/2021
Plantago	2.8	0.1	0.1	19	0.7	14/05/2021 ; 19/05/2021 ; 09/06/2021
Rumex	4.2	0.1	0.4	24	0.7	01/06/2021 ; 14/06/2021 ; 15/06/2021
AMARANTHACEAE	14.0	0.4	0.4	42	2.1	20/10/2021
URTICACEAE	17.5	0.5	0.7	19	1.4	14/05/2021 ; 15/05/2021 ; 21/05/2021
Other pollen from herbs	1.4	0.0	-	-	-	-

	YEAR		WEEK		DAY	
	Integral	Percentage	Maximum	Week nr.	Maximum	Date of the Maximum
	S*day/m³	%	S/m³	Nr.	S/m³	dd/mm/yyyy
TOTAL SPORES	**9929**	**100.0**	**149.6**	**20**	**520.8**	**23/9/2021**
Alternaria	498	5.0	9	20	28	17/9/2021
Ascospores	2856	28.8	24	23	140	24/6/2021
Aspergillus/Penicillium	104	1.0	6	50	44.8	14/12/2021
Clasdosporium	4326	43.6	83	38	481.6	23/9/2021
Ustilago	826	8.3	23	24	50.4	18/6/2021
Other fungal spores	1319	13.3	-	-	-	-

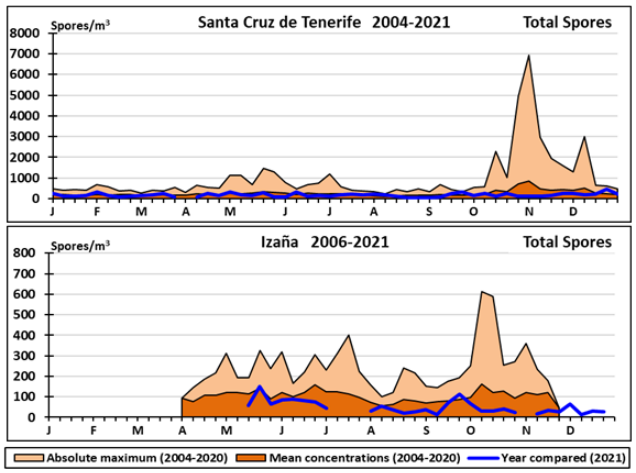

Figure 14.3. Dynamics of the mean weekly Total Fungal Spore concentrations in Santa Cruz de Tenerife (upper panel) and Izaña (lower panel) during 2021 in comparison with 2004-2020 mean and maximum loads.

The plots show that the seasonal cycle of total concentration of pollen and fungal spores at SCO is very different from that observed at IZO. It is also a subject of great interannual variability that depends on weather conditions such as temperature and precipitation. In SCO, concentration of pollen shows a broad maximum covering an extensive spring season (March to early June), that in 2021 occurred mainly in April. While in IZO, higher pollen concentrations during the measurement period happen in two months (usually from May to late June) but centered in May in 2021. Usually, pollen concentration values are somewhat higher for IZO than for SCO (Fig. 14.2). Main pollen taxa in SCO are *Artemisia*, *Myrica*, *Erica*, grasses (*Poaceae*), *Schinus*, Palm trees, *Urticaceae* and *Amaranthaceae*. In IZO, *Brassicaceae* (*Cruciferae*) pollen is predominant, followed by *Myrica*, *Pinus*, grasses (*Poaceae*), *Erica*, *Olea*, *Urticaceae*, *Cupressaceae* and *Amaranthaceae* (Tables 14.1 and 14.2).

The total concentration of fungal spores shows a contrasting seasonal variation to that of total pollen. In 2021, in SCO the concentrations showed small peaks in September and in December that reached values slightly higher than the mean values, but from mid-October and during November concentrations were less than the mean values of the period 2004-2020. At IZO, in 2021, fungal spore concentrations were lower than the mean values for the period 2006-2020. Fungal spore concentrations are higher in SCO than in IZO (Fig. 14.3). Main fungal spore taxa are *Ascospores*, *Cladosporium* and *Ustilago*, followed by *Alternaria* and *Aspergillus/Penicillium* (Tables 14.1 and 14.2).

The results presented here are a summary of the detailed information generated. However individual taxa might have quite a different seasonal behaviour at each station (see Tables 14.1 and 14.2 and graphs that can be generated on the webpage).

A number of products, such as current levels and forecasts of the main allergenic pollens and fungal spores, historical and current data and pollen calendar for SCO can be found at the Tenerife Aerobiology information (Proyecto EOLO-PAT) web page.

14.4 Future Activities

- Continuation of pollens and fungal spores sampling, and aerobiological data analysis.
- Update of the airborne pollen and spores databases.
- Improvement of the information provided through the webpage and services to its users.
- Trend analysis.
- Internannual variability versus meteorology.

14.5 References

Belmonte, J., Cuevas, E., Poza, P., González, R., Roure, J.M., Puigdemunt, R., Alonso-Pérez, S., Grau, F. Aerobiología y alergias respiratorias de Tenerife. Editor: Agencia Estatal de Meteorología/Ministerio de Medio Ambiente y Medio Rural y Marino, 2010. NIPO (versión electrónica): 784-10-006-2.

Belmonte, J., E. Cuevas: Proyecto EOLO-PAT. Estudio de alergenos en Canarias. Resumen anual de datos 2012. Bellaterra: Proyecto EOLO-PAT, 2013.

De Linares, C., Delgado, R., Aira, MJ., Alcázar, P., Alonso-Pérez, S., Boi, M., Cariñanos, P., Cuevas, E., Díaz de la Guardia, C., Elvira-Rendueles, B., Fernández-González, D., Galán, C., Gutiérrez-Bustillo, AM., Pérez-Badia, R., Rodríguez-Rajo, FJ., Ruiz-Valenzuela, L., Tormo-Molina, R., Trigo, MM., Valencia-Barrera, RM., Valle, A., Belmonte, J. Changes in the Mediterranean pine forest: pollination patterns and anual trends of airborne pollen. Aerobiologia, 33: 375-391, 2017.

Galán, C., Ariatti, A., Bonini, M., Clot, B., Crouzy, B., Dahl, A., Fernandez-González, D., Frenguelli, G., Gehrig, R., Isard, S., Levetin, E., Li, D.W., Mandrioli, P., Rogers, C.A., Thibaudon, M., Sauliene, I., Skjoth, C., Smith, M., Sofiev, M. Recommended terminology for aerobiological studies. Aerobiologia, 33: 293-295, 2017.

14.6 Staff

Dr Jordina Belmonte (UAB; Head of programme)

Dr Emilio Cuevas (AEMET; Co-PI)

Ramón Ramos (AEMET; Hirst sampler maintenance)

Virgilio Carreño (AEMET; Sampling)

Rut Puigdemunt (UAB; Technical Analyst)

David Navarro (UAB; Technical Analyst)

Dr Concepción De Linares (UAB; Research Scientist)

Cándida Hernández (AEMET; Meteorological Observer-GAW Technician)

Concepción Bayo (AEMET; Meteorological Observer-GAW Technician)

International Cooperation Programmes

15 ACTRIS

The Aerosol, Clouds and Trace Gases Research Infrastructure (ACTRIS) is the pan-European research infrastructure (RI) producing high-quality data and information on short-lived atmospheric constituents and on the processes leading to the variability of these constituents in natural and controlled atmospheres (simulation chambers).

ACTRIS enables access to high-quality long-term atmospheric data through a single-entry point. It offers access to world-class facilities providing researchers, from academia as well as from the private sector, with the best research environments and expertise promoting cutting-edge science and international collaboration.

ACTRIS is composed of nine connected elements: distributed National Facilities (Observational platforms and Exploratory platforms) both in Europe and globally, and eight Central Facilities (Head Office, Data Centre and six Topical Centres) (Fig. 15.1).

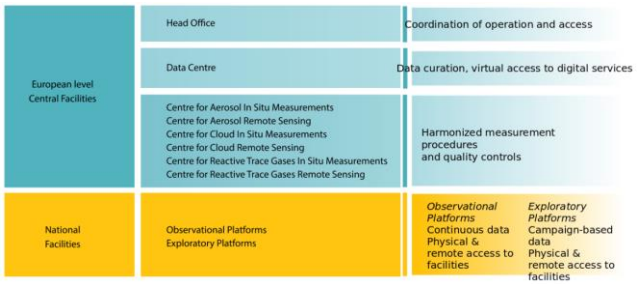

Figure 15.1. ACTRIS research infrastructure core components.

ACTRIS research infrastructure works towards:

- reducing uncertainties in quantification of emission sources, improved understanding of deposition processes that remove short-lived constituents from the atmosphere and quantification of their potential impacts on ecosystems.
- bringing essential information for understanding global biogeochemical interactions between the atmosphere and ecosystems, and how climate-ecosystem feedback loops may change atmospheric composition in the future.
- supporting the development of the required level of understanding of sources of the air pollutants that negatively affect human health.
- complementing Earth Observations from space with the necessary observations, providing unique ground-truthing of remote sensing information collected by current and future satellite missions.

15.1 ACTRIS-Implementation Phase Project

ACTRIS was included in the European Strategy Forum on Research Infrastructures (ESFRI) roadmap in 2016. In April 2023, ACTRIS was legally recognized as a European Research Infrastructure Consortium (ERIC) with the official establishment of the ACTRIS ERIC by the European Commission. After many years of community building, design phase, and three years of ACTRIS Preparatory Phase Project (ACTRIS PPP), ACTRIS is now immersed in a five-year implementation phase (2020-2024) dedicated to constructing and upgrading the National Facilities and Central Facilities, setting-up the user access and service provision, working on the governance and management tasks, increasing the connection with new users and member countries, further developing strategies within ACTRIS and for international collaboration and partnerships, and integrating ACTRIS at different strategic levels (national, European and internationally) (Fig. 15.2).

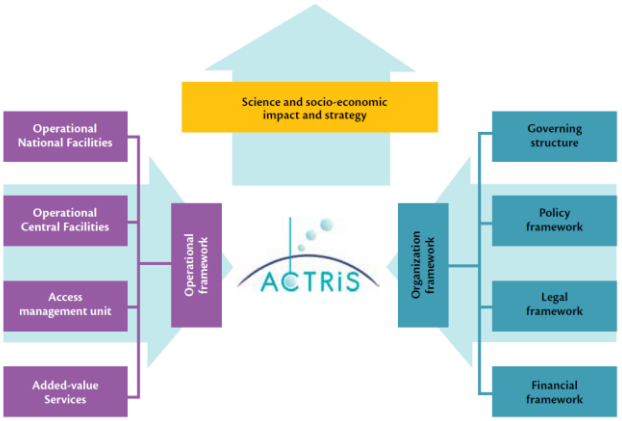

Figure 15.2. ACTRIS Work Breakdown Structure. Each box describes a key action/product. Reprinted from ACTRIS (2018).

The process is funded as ACTRIS Implementation Project (ACTRIS IMP), through the EU Horizon 2020 Coordination and Support Section (grant agreement No 871115) project. ACTRIS IMP started on 1 January 2020 for a period of five years.

The ACTRIS implementation project builds on the achievements of the successful ACTRIS PPP and on the scientific and technical deliveries of the ACTRIS-2 and EUROCHAMP-2020 projects. The ACTRIS IMP project objectives are based on the overall ACTRIS implementation phase objectives which are to coordinate and accomplish the actions required for implementing a globally recognised long-term sustainable research infrastructure with operational services by 2025 (see Fig. 15.3).

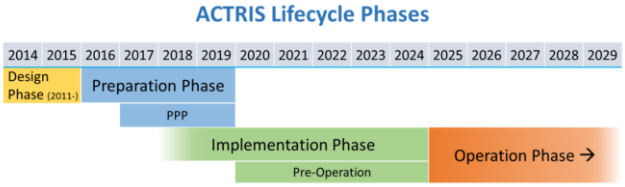

Figure 15.3. ACTRIS lifecycle phases from design to preparation, implementation and operation.

15.2 Centre for Aerosol Remote Sensing

The Centre for Aerosol Remote Sensing (CARS) is one of the six ACTRIS Topical Centres. The mission of CARS is to offer operation support to ACTRIS National Facilities operating aerosol remote sensing instrumentation: aerosol high-power lidars, automatic low power lidars and ceilometers, and automatic sun/sky/polarised/lunar photometers. Additionally, CARS offers specialised services for the above instruments and related ACTRIS variables, to ACTRIS users of various types: academia, business, industry, and public services. CARS is composed of the following units, which are grouped in three clusters, one cluster for each measurement technique (see Fig. 15.4):

1) National Institute of Research and Development for Optoelectronics (INOE), Romania.

2) Meteorological Institute of the Ludwig-Maximilians-University (LMU-MIM), Germany.

3) Consiglio Nazionale delle Richerche (CNR), Italy.

4) Hohenpeissenberg Meteorological Observatory, Deutscher Wetterdienst (DWD), Germany.

5) CNRS-Laboratoire d'Optique Atmospherique, Lille University, France.

6) Atmospheric Optic Group, University of Valladolid (UVA), Spain.

7) Izãna Atmospheric Research Center (AEMET), Spain.

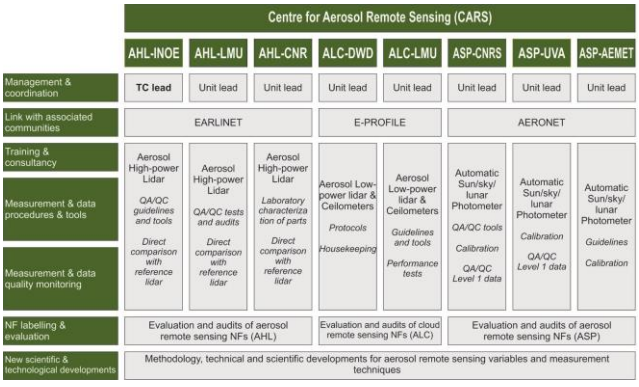

Figure 15.4. CARS organigram.

CARS offers operational support to ACTRIS National Facilities, as well as specialized services to ACTRIS users:

- Training and consultancy for setting up and running an aerosol remote sensing station.
- Measurement and data processing and tools for QA/QC of the lidar and photometer measurements.
- Measurement and data quality monitoring, including calibration of photometers, characterization of lidar optical blocks, direct comparison with reference systems, support for debugging, upgrading, and optimizing the instruments.

The CARS activities related to the measurement technique Automatic Sun/sky/polarised/lunar Photometers (CARS-ASP) are provided by CNSR-LOA (Lille, France), UVA-GOA (Valladolid, Spain) and AEMET-IARC (Izaña, Spain) (see Figs.15.4 and 15.5). Izaña Observatory provides a unique facility for absolute calibration of Master Cimel instruments (Fig. 15.6). For more details about the early AERONET-EUROPE Calibration Service, which is now incorporated into CARS-ASP, see previous IARC Activity Reports (e.g Cuevas et al., 2019).

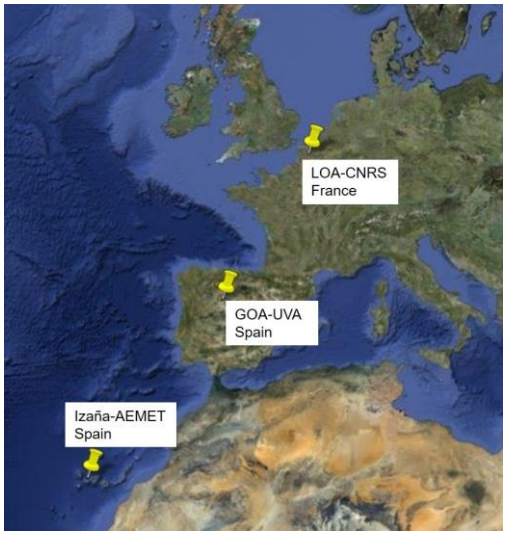

Figure 15.5. Location of the three calibration facilities of CARS-ASP.

IZO continue to host a set of six reference instruments continuously in operation and available for the needs of the LOA and GOA facilities. AERONET-EUROPE master instruments from LOA and GOA are recalibrated every three months at IZO in order to assure measurement accuracy. Master instruments from other networks such as the China Aerosol Remote Sensing NETwork (CARSNET) are also recalibrated at IZO on a regular basis.

All users who operate either a standard or a polarized CIMEL sun/sky or triple (sun/sky/lunar) photometer located in Europe or outside Europe but run in the framework of international cooperation agreements can submit a proposal to ACTRIS CARS-ASP Calibration Service at any time. The instrument calibration and maintenance are performed

free of charge, and proposals are granted on the basis of a TransNational Access (TNA) selection panel review process. Instrument shipping expenses from and to the user site are not included and must be covered by the user institution.

Most of the accesses provided under ACTRIS CARS-ASP allow to assure quality of data on sites operating not only a sun or triple photometer but also multiple complementary in situ, remote sensing, and radiation instruments.

Quality-assured data from AERONET-EUROPE are widely used by modelling and satellite communities through several European programmes and initiatives (ESA, GMES, AEROCOM, etc). By the end of 2023, around 86 AERONET sun-photometers were used for near-real-time validation of dust forecast models by the SDS-WAS Regional Center for North Africa, Middle East and Europe, most of them were calibrated by AERONET-EUROPE (https://aerospain.aemet.es/).

15.3 References

ACTRIS Stakeholder Handbook 2018.

Cuevas, E., Milford, C., Bustos, J. J., R., García, O. E., García, R. D., Gómez-Peláez, A. J., Guirado-Fuentes, C., Marrero, C., Prats, N., Ramos, R., Redondas, A., Reyes, E., Rivas-Soriano, P. P., Rodríguez, S., Romero-Campos, P. M., Torres, C. J., Schneider, M., Yela, M., Belmonte, J., del Campo-Hernández, R., Almansa, F., Barreto, A., López-Solano, C., Basart, S., Terradellas, E., Werner, E., Afonso, S., Bayo, C., Berjón, A., Carreño, V., Castro, N. J., Chinea, N., Cruz, A. M., Damas, M., De Ory-Ajamil, F., García, M.I., Gómez-Trueba, V., Hernández, C., Hernández, Y., Hernández-Cruz, B., León-Luís, S. F., López-Fernández, R., López-Solano, J., Parra, F., Rodríguez, E., Rodríguez-Valido, M., Sálamo, C., Sanromá, E., Santana, D., Santo Tomás, F., Sepúlveda, E., and Sosa, E.: Izaña Atmospheric Research Center Activity Report 2017-2018. (Eds. Cuevas, E., Milford, C. and Tarasova, O.), State Meteorological Agency (AEMET), Madrid, Spain and World Meteorological Organization, Geneva, Switzerland, WMO/GAW Report No. 247, 2019.

15.4 Staff

Dr África Barreto (PI of Izaña-AEMET facility since June 2020)

Dr Philippe Goloub (PI of LOA-CNRS/University of Lille facility)

Dr Carlos Toledano (PI of GOA-University of Valladolid facility)

Dr Natalia Prats (Project Manager)

Figure 15.6. Cimel Masters at the Izaña Observatory Calibration facility.

16 Regional Brewer Calibration Center for Europe (RBCC-E)

16.1 Background

In November 2003 the WMO/GAW Regional Brewer Calibration Center for Europe (RA-VI region) (RBCC-E) was established at IZO. The RBCC-E reference is based on three double Mark-III Brewer spectrophotometers (the IZO triad): a Regional Primary Reference (Brewer 157), a Regional Secondary Reference (Brewer 183) and a Regional Travelling Reference (Brewer 185). As described in Section 3.1, IZO is located in a subtropical region (28ºN) on a mountain plateau (2373 m a.s.l.) with pristine skies and low ozone variability. This location allows routine absolute calibrations of the reference instruments under conditions similar to the Mauna Loa Observatory (MLO), Hawaii, USA. The establishment of the RBCC-E Triad allows the implementation of a self-sufficient European Brewer calibration system that respects the world scale but works as an independent GAW infrastructure.

There are two European Calibration Centers for the two types of ozone spectrophotometers in use: Dobson and Brewer. The Regional Dobson Calibration Center for Europe (RDCC-E) is located at the Meteorological Observatory Hohenpeissenberg (Germany). Since 2009, the RBCC-E activities have largely been funded by the ESA project, "CEOS Intercalibration of Ground-Based Spectrometers and Lidars" which includes the participation of the two European Calibration Centers (RBCC-E and RDCC-E).

16.2 Objectives

The main objectives of this Cooperation programme are:

- To implement a system for routine absolute calibrations of the European Brewer regional reference instruments at IZO, fully compatible with absolute calibrations of the world reference triad at MLO.
- To perform periodical intercomparison campaigns using the Regional Primary Reference B157 (during intercomparisons held at IZO) and the Regional Travelling Reference B185 spectrophotometer (traceable to B157) in continental campaigns (Figs. 16.1 and 16.2).
- To perform regular comparisons of the Regional Brewer Primary Reference B157 with the Regional Dobson Reference D074 to monitor the relationship between both calibration scales in the WMO RA-VI region.
- To study the sources of errors of the absolute calibrations and to determine the accuracy of total ozone measurement achievable by the Brewer spectrophotometer under different atmospheric conditions or instrumental characteristics.

Figure 16.1. Participants at the 17th RBCC-E Intercomparison campaign held at Davos in 2022 (Photo: P. Babal).

16.3 Tasks

The main tasks of this Cooperation programme are:

- To develop quality control protocols and Standard Operating Procedures (SOPs) for establishment of traceability of measurements to the reference standards.
- To maintain laboratory and transfer standards that are traceable to the reference standards.
- To perform regular calibrations and audits at GAW sites.
- To provide, in cooperation with Quality Assurance/Science Activity Centres, training and technical assistance to stations.

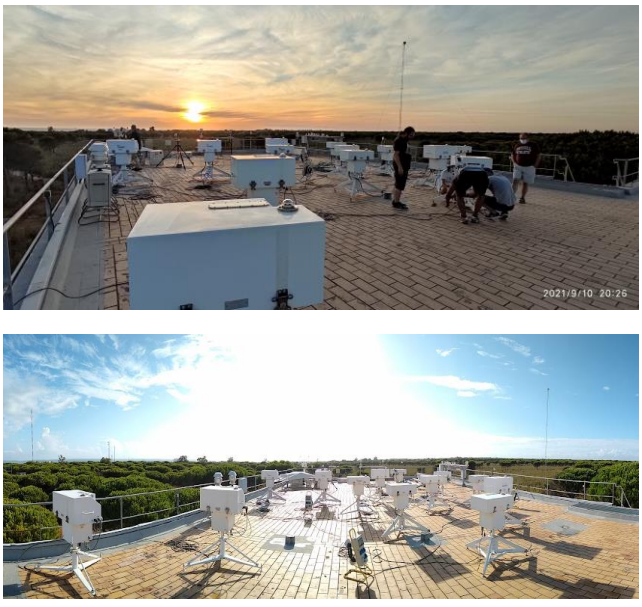

Figure 16.2. Images of the instrument terrace during the El Arenosillo 2021 campaign.

16.3.1 Main activities of the RBCC-E during the period 2021-2022

16.3.2 Absolute calibration transfer

The WMO GAW Scientific Advisory Group on ozone and UV Radiation in 2011 authorized RBCC-E to conduct the transference of its own absolute calibration, based on Langley analysis at IZO. The link to the world reference in this case can be assured either by direct intercomparison with the world triad in Toronto or by common Langley campaigns at MLO or at IZO (Redondas 2014).

During 2021 and 2022 the RBCC-E has worked together with the Environment and Climate Change Canada, Meteorological Service of Canada (ECCC-MSC) to analyse calibration procedures and the feasibility of forming a single Central Calibration Laboratory (CCL) between the two groups. This work has been divided into four parts as follows:

1) Brewer Primary Calibration condition paper: led by ECCC (Xiaoyi Zhao). This work focuses on evaluating the environmental conditions for different Brewer calibration sites globally. This work addresses a key scientific question: What is needed to make sure that the primary calibration performed at different sites (e.g., Mauna Loa Observatory in Hawaii and Izana Observatory in Spain) can be of the same quality? This work has now been completed and published (Zhao et al., 2023).

2) Brewer Total Ozone Uncertainty Budget paper: led by AEMET (Francisco Parra-Rojas and Alberto Redondas). This work will also introduce a new Brewer uncertainty budget model to provide detailed evaluation of uncertainties of Brewer observations (i.e., precision and accuracy).

3) 1st Brewer Central Calibration Laboratory (CCL) paper: led by AEMET (Alberto Redondas). This work describes the primary calibration theory and technical details (e.g., the difference between the Canadian and Spanish primary calibrations of their Brewer instruments).

4) 2nd Brewer CCL paper: led by ECCC (Xiaoyi Zhao). This work focuses on how the primary calibration is transferred to field Brewer instruments worldwide. In the context of having two CCLs instead of the current one CCL, this work will evaluate the transfer results from the Canadian (ECCC) and Spanish (AEMET) primary calibrations to see if the calibration qualities are equivalent. This work will use real campaign data (2022 Davos campaign) to examine the equivalence of the two CCLs.

At present, the RBCC-E maintains a triad of reference instruments (see section 16.1). Each spectrophotometer is calibrated independently with the standard Langley method at IZO and since 2011 transfers their own total ozone calibration at regular calibration campaigns. These instruments are also regularly compared with the Toronto Triad.

During the 2021 Intercomparison campaigns, a change in the ozone absorption coefficient was observed. Initially, it was assumed that this change was due to the uncertainty in the determination of these coefficients, but its effect was also observed during the Davos 2022 campaign. This has led to a revision of the calibration of the Triad configuration for the year 2021 (Redondas et al. 2023a). After this revision, changes in the triad are minor, with ozone changes below 1 DU. An important point of this revision is that the MatSHIC algorithm (Slaper et al., 1995, Egli et al., 2022) has been incorporated into the Triad analysis, which allows us to monitor the wavelength shift in the Brewers.

Redondas et al. (2016) and León-Luis et al. (2018) studied the stability of the RBCC-E Triad during the period 2005-2015, using a mathematical method where the ozone values are fitted to a 2nd grade polynomial (Fioletov et al., 2005) or an extended 3rd grade polynomial (Stübi et al., 2017). Redondas et al. (2016) and León-Luis et al. (2018) took into account two conditions: a) only days with at least 15 measurements distributed around the solar noon and with standard deviation < 0.5 were selected and b) measurement data obtained from Travelling Reference Brewer #185 during campaigns were removed. In addition to this study, the stability of the RBCC-E Triad during the period 2005-2022 is presented in this report. The distribution of the difference between the ozone daily mean obtained by each Brewer with respect to the Triad mean O_3 value (O_{3_mean}) was calculated as follows:

$$O_{3\_mean} = (O_{3\_157} + O_{3\_183} + O_{3\_185})/3. \quad (1)$$

A good Gaussian profile can be observed in the distribution of the differences (Fig. 16.3) which confirms the stability of the IZO Brewer Triad during the period 2005-2022.

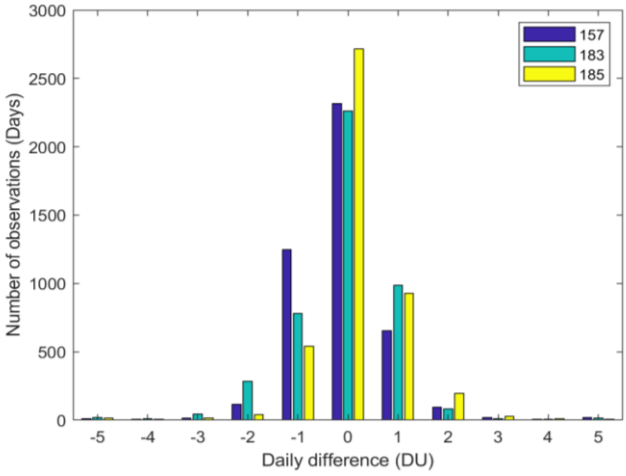

Figure 16.3. Distribution of the differences between the ozone daily mean obtained by each Brewer in the Triad with respect to the mean O_3 value of the RBCC-E Brewer Triad located at IZO for the period 2005-2022.

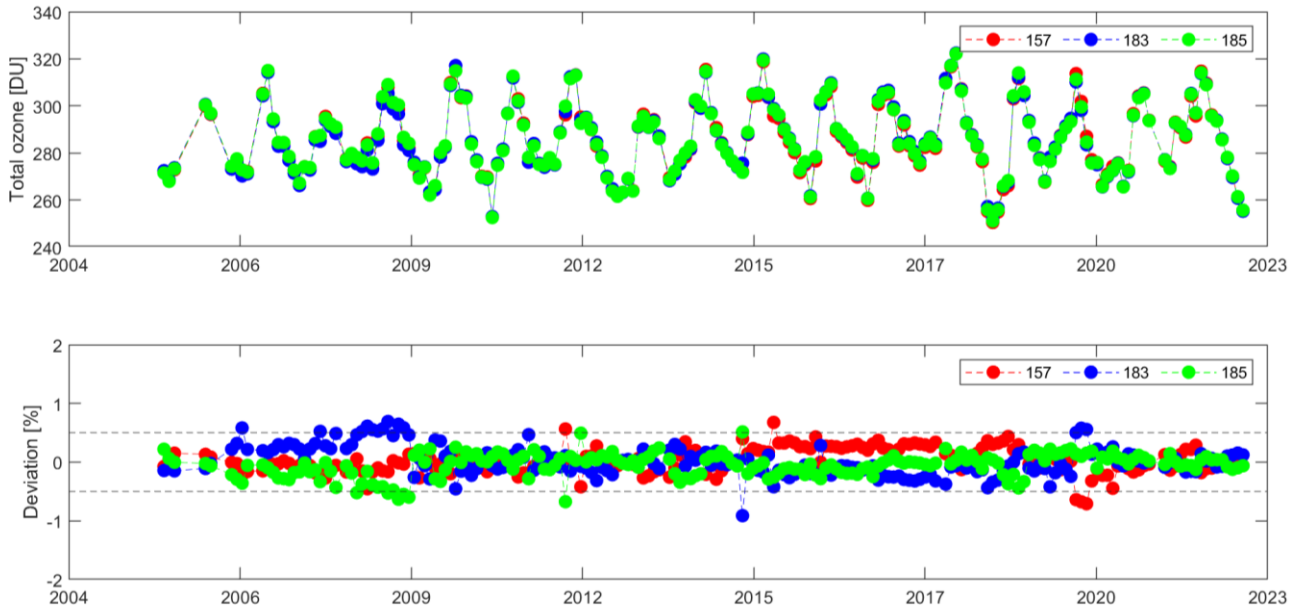

Figure 16.4. a) Monthly mean Total Ozone Column values measured at Izaña Observatory by the RBCC-E Triad and b) Relative deviation of each Brewer from the monthly mean of the RBCC-E Triad during the 2005-2022 period.

Figure 16.4 shows the relative deviations from the RBCC-E Triad monthly mean TOC for each individual Brewer. This plot is used as a benchmark to identify if an instrument of the RBCC-E Triad needs to be recalibrated or for checking that a current calibration applied to a Brewer is good enough. The standard deviation of the relative deviations from the RBCC-E Triad monthly mean have values of 0.21%, 0.25% and 0.19% (Brewer#157, Brewer#183 and Brewer#185) for the period 2005-2022, 52% and 47% less than those reported for the MkII Canada Triad in Fioletov et al. (2005) and in Zhao et al. (2020), and 31% less than the MkIII Canada Triad (Zhao et al., 2020).

16.3.3 RBCC-E Intercomparison campaigns

Figure 16.5. The RBCC-E travelling reference Brewer #185 at the Davos 2021 campaign during a dispersion test. (Photo: F. Zeilinger).

Brewer intercomparisons are held annually, alternating between Davos in Switzerland and the El Arenosillo Sounding Station of INTA (Huelva, Spain). The aim is to collect simultaneous ozone data from a number of Brewers from invited organizations so that their calibration constants can be transferred from the reference instruments. Due to the COVID-19 pandemic, no intercomparison campaign took place in 2020, so the campaign that should have taken place in Davos was moved to 2021. Therefore, two campaigns took place in 2021, the 15th RBBC-E intercomparison campaign held in Davos on 6-16 July 2021 (Fig. 16.5) and the 16th RBBC-E intercomparison campaign held in El Arenosillo on 6-16 September 2021.

In 2022, the 17th RBBC-E intercomparison campaign was held in Davos on 22-31 August (Fig.16.8). The geographical origin of the Brewers calibrated by the RBCC-E is shown in Figure 16.6 and the number of calibrations performed by the RBCC-E every year is shown in Figure 16.7. In 2021, 20 calibrations were performed (6 in Davos, 13 in El Arenosillo and 1 in Izaña), while in 2022, 12 calibrations were performed (9 in Davos and 3 in Izaña). These routine intercomparison campaigns provide the Brewer community with the opportunity to assess the status of the European network instruments.

Figure 16.6. Geographical origin of the Brewers calibrated by the RBCC-E.

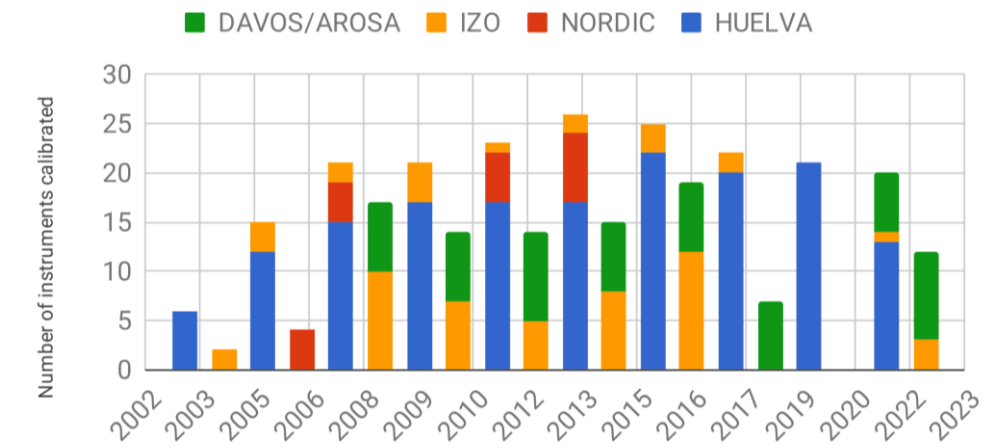

Figure 16.7. Calibrations performed by the RBCC-E per year.

Table 16.1. Participants at the 15th RBCC-E Intercomparison campaign held at Davos in 2021.

Institution	Participants	Instrument	Country
Davos 2021 (Switzerland, 6-16 July) RBCC-E			
Izaña Atmospheric Research Centre-AEMET	Alberto Redondas Francisco Parra Rojas Alberto Berjón	Brewer #185-MKIII	Spain
World Radiation Center (WRC) & MeteoSwiss	Julian Gröbner Luca Eggli Franz Zeilinger Herbert Schill Rene Stubi	Brewer #040-MKIII Brewer #072-MKIII Brewer #156-MKIII Brewer #163-MKIII QASUME Koherento3	Switzerland
Kipp & Zonen (K&Z)	Pavel Babal Erik Noort	Brewer #158-MKIII Brewer #245-MKIII	The Netherlands

Table 16.2. Participants at the 16th RBCC-E Intercomparison campaign held at El Arenosillo in 2021.

Institution	Participants	Instrument	Country
Arenosillo 2021 (Spain, 6–16 September) RBCC-E			
Izaña Atmospheric Research Centre-AEMET	Alberto Redondas Virgilio Carreño Francisco Parra Rojas Javier López Solano	Brewer #185-MKIII	Spain
University of Thessaloniki	Alkis Bais	Brewer #005-MKII	Greece
AEMET	J.M San Atanasio Ana María Díaz Arcadio Blasco	Brewer #033-MKIV Brewer #070-MKIV Brewer #117-MKIV Brewer #151-MKIV Brewer #166-MKIII Brewer #186-MKIV	Spain
UK Meteorological Office (UKMO)	John Rimmer Richard Kift	Brewer #075-MKIV Brewer #126-MKII Brewer #172-MKIII	UK
Instituto Nacional de Técnica Aeroespacial (INTA)	Jose Manuel Vilaplana	Brewer #150-MKIII	Spain
Danmarks Meteorologiske Institut (DMI)	Niss Jepsen Sotirios Skarpalezos	Brewer #202-MKIII Brewer #228-MKIII	Denmark
World Radiation Center (WRC)	Franz Zellinger Gregor Hülsen Julian Gröbner	QUASUME	Switzerland
Universidad de Extremadura	Antonio Serrano Pérez Joaquín Fernando Monserrat Jesús Zarza Belmonte Julio Alberto Hernández Alba Flores María Luisa Cancillo	NILU #119 NILU #145	Spain

Figure 16.8. Brewers participating in the 17th RBCC-E intercomparison campaign held at Davos, 22 – 31 August 2022.

Table 16.3. Participants at the 17th RBCC-E Intercomparison campaign held at Davos in 2022.

Institution	Participants	Instrument	Country
Davos 2022 (Switzerland, 22–31 August) RBCC-E			
Izaña Atmospheric Research Centre-AEMET	Alberto Redondas Virgilio Carreño Alberto Berjón Javier López Solano	Brewer #185-MKIII	Spain
World Radiation Center (WRC) & MeteoSwiss	Julian Gröbner Eliane Maillard Barras Luca Eggli Franz Zeilinger Gregor Hülsen	Brewer #040-MKIII Brewer #072-MKIII Brewer #156-MKIII Brewer #163-MKIII QASUME Koherento3	Switzerland
Environment Canada	Michael Brohart Xiaoyi Zhao	Brewer #190-MKIII	Canada
Kipp & Zonen (K&Z)	Pavel Babal Erik Noort	Brewer #158-MKIII Brewer #245-MKIII	The Netherlands
Royal Netherlands Meteorological Institute (KNMI)	Igor Nedeljkovic Izzy Hendriks	Brewer #189-MKIII	The Netherlands
BOKU-Met	Daniel Rauter	Brewer #093-MKIV	Austria

16.3.4 15th RBCC-E Intercomparison Results

Due to the inconsistencies ob served during the blind days of the 17th RBCC-E Intercomparison Campaign in 2022 (see section 16.3.6), it was decided to revise the RBCC-E Triad for 2021 (Redondas et al. 2023a), and therefore, the configurations for the 15th RBCC-E Intercomparison Campaign (Redondas et al., 2023b). The initial comparison (blind period), using the instruments' original calibration constants, showed that all the operational Brewer instruments were in the ± 1.0% range, while 83% of them (5 instruments out of 6) showed a perfect agreement within ± 0.5% after two years calibration period (Fig. 16.9).

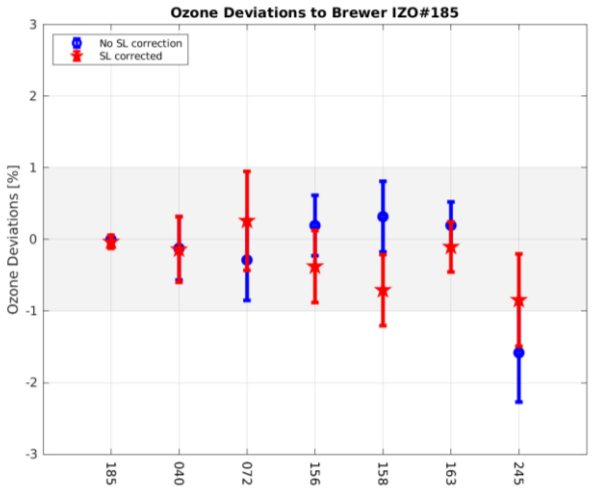

Figure 16.9. Initial period, percentage mean difference with the reference for the simultaneous direct sun measurements for all the participating instruments, with and without the standard lamp correction, in the stray-light free OSC region (OSC < 900).

It is worth noting that these results correspond to the stray-light free region, OSC < 900, but large errors (up to 4%) can be expected for single-monochromator Brewer instruments operating at OSC > 1000 DU. With the final calibration and including a correction for the stray light, all participating Brewer spectrophotometers were within the ± 0.5% agreement range (Fig. 16.10).

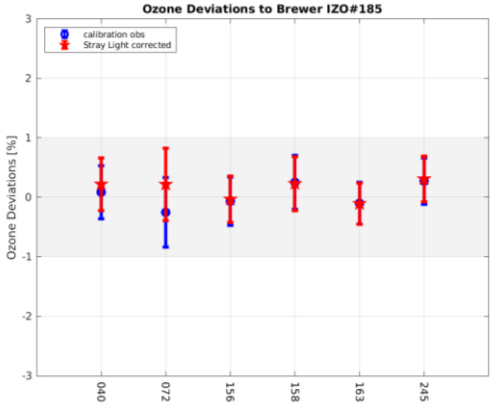

Figure 16.10. Final period, percentage mean difference with the reference for the simultaneous direct sun measurements for all the participating instruments.

16.3.5 16th RBCC-E Intercomparison Results

As with the 15th RBCC-E Intercomparison Campaign, also held in 2021, the 16th RBCC-E Intercomparison Campaign has been revised following the revision of the RBCC-E Triad for 2021. The initial comparison (blind period), using the instruments' original calibration constants, showed that 85% of the operational Brewer instruments were in the ± 1.0% range, while 69% of them (9 instruments out of 13) showed a perfect agreement within ± 0.5% after two years calibration period (Fig. 16.11).

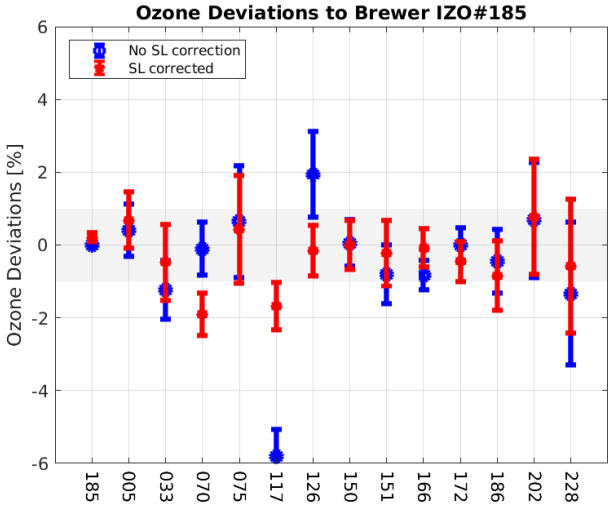

Figure 16.11. Initial period, percentage mean difference with the reference for the simultaneous direct sun measurements for all the participating instruments, with and without the standard lamp correction, in the stray-light free OSC region (OSC < 900).

As mentioned in 16.3.4, these results correspond to the stray-light free region, OSC < 900, but large errors (up to 4%) can be expected for single-monochromator Brewer instruments operating at OSC > 1000 DU. With the final calibration and including a correction for the stray light, the average TOC of all Brewer spectrophotometers was within the ± 0.5% agreement range (Fig. 16.12).

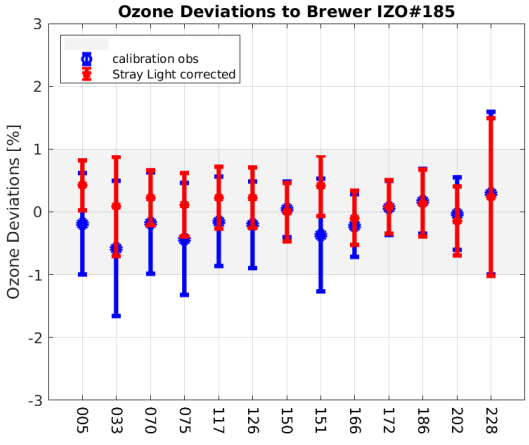

Figure 16.12. Final period, percentage mean difference with the reference for the simultaneous direct sun measurements for all the participating instruments.

16.3.6 17th RBCC-E Intercomparison Results

During the blind comparison of the 17th RBCC-E Intercomparison Campaign, the ozone measured by the Reference Brewer #185 was around 1% higher than the values obtained by the other participants (Fig. 16.13). This includes all six instruments participating in the Davos 2021 campaign, four of which have remained at the Davos station and have shown good stability over the last year. It was found that using the pre-Davos 2021 configurations for the Brewers which participated in that campaign, improved the blind comparison (Fig. 16.13).

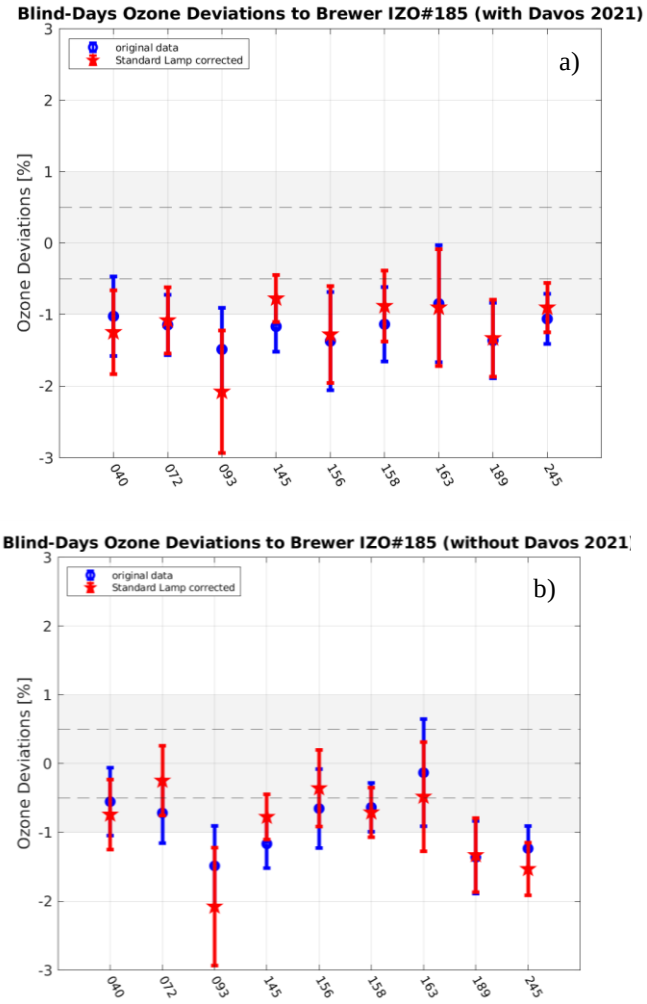

Figure 16.13. Initial period, percentage mean difference with the reference for the simultaneous direct sun measurements for all the participating instruments, with and without the standard lamp correction, in the stray-light free OSC region (OSC < 900). a) Summary of the blind comparison considering the calibration obtained during the 2021 campaign. b) The same results when taking the configurations prior to the 2021 campaign for Brewers #040, #072, #156, #158, #163 and #254.

Preliminary analysis of the 2021 campaign suggests that the ozone measurement position of the monochromator could be shifted one step during the journey to the campaign, and back to the original position on the return journey to Izaña. This situation is very unusual. Changes that occur during the outward or return journey are usually identified in the pre-post campaign analysis and in the SL analysis. However, this time the change was only observed in an anomalous behaviour in the dispersion tests. Due to this issue, it was decided not to use the configurations from the 2021 campaign and use the previous configurations for the blind comparison.

The initial comparison with this configuration showed that 6 of the Brewer instruments were in the ± 1% range, while 22% of them (2 instruments out of 9) showed a perfect agreement within ± 0.5% after two years calibration period. Note three instruments show a difference larger than 1% (Fig. 16.13). With the final calibration and including a correction for the stray light, the average TOC of all participating Brewer spectrophotometers were within the ± 0.5% agreement range (Fig. 16.14). See Redondas et al. (2023c) for more details.

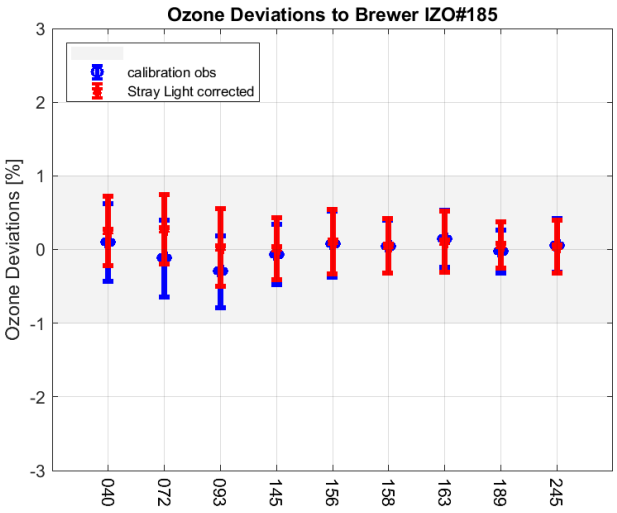

Figure 16.14. Final period, percentage mean difference with the reference for the simultaneous direct sun measurements for all the participating instruments. Blue symbols show results without the stray light correction and red symbols show results with the correction applied to single Brewer spectrophotometers.

16.4 References

Egli, L., Gröbner, J., Hülsen, G., Schill, H., and Stübi, R.: Traceable total ozone column retrievals from direct solar spectral irradiance measurements in the ultraviolet, Atmos. Meas. Tech., 15, 1917–1930, doi: 10.5194/amt-15-1917-2022, 2022.

Fioletev, V.E., Kerr J.B., McElroy C.T., Wardle D.I., Savastiouk V., Granjkar T.S., The brewer reference triad, Geophys. Res. Lett., 32 L208805. 2005.

León-Luis, S. F., Redondas, A., Carreño, V., López-Solano, J., Berjón, A., Hernández-Cruz, B., and Santana-Díaz, D., Internal consistency of the Regional Brewer Calibration Centre for Europe triad during the period 2005--2016. Atmos. Meas. Tech., 11, 4059-4072, 2018.

Redondas, A., Rodríguez-Franco J.J., Carreño, V., and Sierra, M., "Ten years of the Regional Brewer Calibration Center- Europe" COST ACTION ES1207 EUBREWNET OPEN CONGRESS /14th WMO-GAW BREWER USERS GROUP MEETING EUBREWNET & WMO GAW, Tenerife, 24-28 March 2014, 2014.

Redondas, A., S.F. León-Luis, V. Carreño, B. Hernández, J. López-Solano, A. Berjón, D. Santana-Díaz, and M. Rodriguez, Stability of the RBCCE triad during the period 2005-2015, Quadrennial Ozone Symposium 2016, Edinburgh, 4-10 September 2016.

Redondas, A., Carreño, V., León-Luis, S. F., Hernández-Cruz, B., López-Solano, J., Rodriguez-Franco, J. J., Vilaplana, J. M., Gröbner, J., Rimmer, J., Bais, A. F., Savastiouk, V., Moreta, J. R., Boulkelia, L., Jepsen, N., Wilson, K. M., Shirotov, V. and Karppinen, T.: EUBREWNET RBCC-E Huelva 2015 Ozone Brewer Intercomparison, Atmospheric Chemistry and Physics, 18(13), 9441–9455, doi:https://doi.org/10.5194/acp-18-9441-2018, 2018.

Redondas, A., Berjon, A., Lopez-Solano, J., Carreno, V., Parra-Rojas, F., León-Luis, S.F., Santana-Díaz, D., RBCC-E triad Calibration Report. Izaña 2021, RBCC-E triad Calibration Report. Izaña Atmospheric Research Center, AEMET, Santa Cruz de Tenerife, Spain. 2023a. Available from: http://rbcce.aemet.es/svn/iberonesia/RBCC_E/2021/Triad/latex/triada2021.pdf

Redondas, A., Berjon, A., Lopez-Solano, J., Carreno, V., Parra-Rojas, F., RBCC-E Davos 2021 Intercomparison Campaign report, RBCC-E Calibration Campaign Report. Izaña Atmospheric Research Center, AEMET, Santa Cruz de Tenerife, Spain. 2023b. Available from: http://rbcce.aemet.es/svn/campaigns/dav2021/latex/analisys/report_dav2021.pdf

Redondas, A., Berjon, A., Lopez-Solano, J., Carreno, V., Parra-Rojas, F., RBCC-E Davos 2022 Intercomparison Campaign report, RBCC-E Calibration Campaign Report. Izaña Atmospheric Research Center, AEMET, Santa Cruz de Tenerife, Spain. 2023c. Available from: http://rbcce.aemet.es/svn/campaigns/dav2022/latex/analisys/report_dav2022.pdf

Slaper, H., Reinen, H. A. J. M., Blumthaler, M., Huber, M. and Kuik, F.: Comparing ground-level spectrally resolved solar UV measurements using various instruments: A technique resolving effects of wavelength shift and slit width, Geophys. Res. Lett., 22, 2721–24, doi: 10.1029/95GL02824, 1995.

Stübi, R., Schill, H., Klausen, J., Vuilleumier, L. and Ruffieux, D.: Reproducibility of total ozone column monitoring by the Arosa Brewer spectrophotometer triad, Journal of Geophysical Research: Atmospheres, 122(8), 4735–4745, doi:10.1002/2016JD025735, 2017.

Zhao, X., Fioletov, V., Redondas, A., Gröbner, J., Egli, L., Zeilinger, F., López-Solano, J., Arroyo, A. B., Kerr, J., Maillard Barras, E., Smit, H., Brohart, M., Sit, R., Ogyu, A., Abboud, I., and Lee, S. C.: The site-specific primary calibration conditions for the Brewer spectrophotometer, Atmos. Meas. Tech., 16, 2273–2295, https://doi.org/10.5194/amt-16-2273-2023, 2023

16.5 Staff

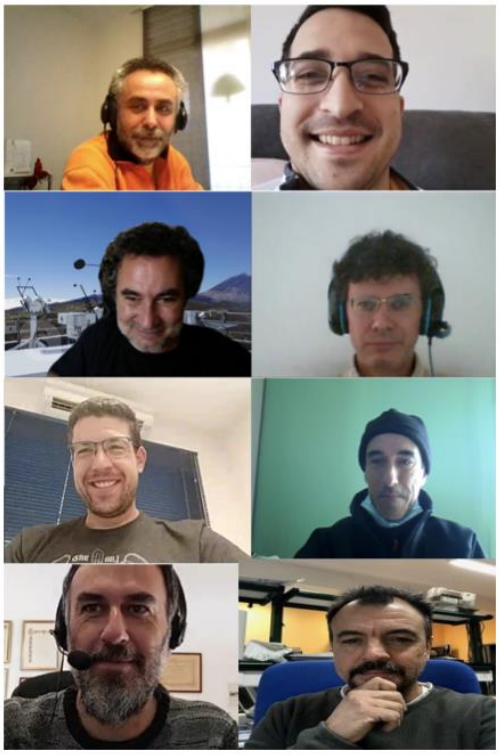

Figure 16.15. Members of the RBCC-E team. Left to right, top to bottom: A. Berjón, D. Santana, A. Redondas, J. López-Solano, S. León Luis, V. Carreño, F. Parra-Rojas and M. Rodriguez Valido.

Alberto Redondas Marrero (AEMET; PI in charge of RBCC-E)

Virgilio Carrreño (AEMET; Meteorological Observer-GAW Technician)

Dr Alberto Berjón (TRAGSATEC; Research Scientist)

Dr Javier López Solano (TRAGSATEC; Research Scientist)

Dr Sergio Fabián León Luis (TRAGSATEC; Research Scientist)

Daniel Santana (LuftBlick; Research Scientist)

Dr Francisco Parra Rojas (Universidad Interamericana de Puerto Rico; Associate Professor)

Dr Manuel Rodriguez Valido (ULL, Research Scientist)

17 Sand and Dust Storm Centres

Following the need for international coordination of a diverse community dealing with the societal impacts of sand and dust storms, WMO took the lead with international partners to develop and implement the Sand and Dust Storm Warning Advisory and Assessment System (SDS-WAS). The WMO Sand and Dust Storm Project was initiated in 2004 and SDS-WAS was launched by the Fifteenth World Meteorological Congress in 2007.

The SDS-WAS mission is to enhance the ability of countries to deliver timely and quality sand and dust storm forecasts, observations, information, and knowledge to users through an international partnership of research and operational communities. SDS-WAS is run jointly under the WMO World Weather Research Programme (WWRP) and GAW Programme and is coordinated by the global SDS-WAS Steering Committee supported by the WMO Secretariat (for more details see WMO, 2020).

SDS-WAS currently operates through three regional nodes:

1) WMO SDS-WAS Regional Node for Northern Africa, Middle East and Europe (NA-ME-E), coordinated by a Regional Centre in Barcelona, Spain, hosted by AEMET and the Barcelona Supercomputing Centre (BSC).

2) WMO SDS-WAS Regional Node for Asia, coordinated by a Regional Centre in Beijing, China, that is hosted by the China Meteorological Administration (CMA).

3) WMO SDS-WAS Pan-American Regional Node, coordinated by a Regional Center in Bridgetown, Barbados, hosted by the Caribbean Institute for Meteorology and Hydrology (CIMH).

17.1 WMO SDS-WAS Regional Centre for Northern Africa, Middle East and Europe

The WMO SDS-WAS Regional Centre for Northern Africa, Middle East and Europe was established in 2007 to coordinate SDS-WAS activities within this region. The Centre, as a consortium of AEMET and the Barcelona Supercomputing Centre, soon evolved into a structure that hosted international and interdisciplinary research cooperation between numerous organizations in the region and beyond, including national meteorological services, environmental agencies, research groups and international organizations.

The WMO SDS-WAS NA-ME-E Regional Centre website (Fig. 17.1) is a place where visitors can find the latest dust-related observations and the most up-to-date experimental dust forecasts. The activities carried out by the SDS-WAS NA-ME-E Regional Centre have been broadly disseminated at international workshops and conferences (Basart et al., 2018a; Cuevas et al., 2017). A detailed description of the main activities of the SDS-WAS NA-ME-E Regional Centre can be found in Basart et al. (2019).

A global observational network is crucial to any forecast and early warning system for real-time monitoring, validation, and evaluation of forecast products, as well as for data assimilation. The main data sources are in-situ aerosol measurements performed at air quality monitoring stations, indirect observations (visibility and present weather) from meteorological stations, sun photometric measurements (e.g. AERONET network), lidar, ceilometers and satellite products.

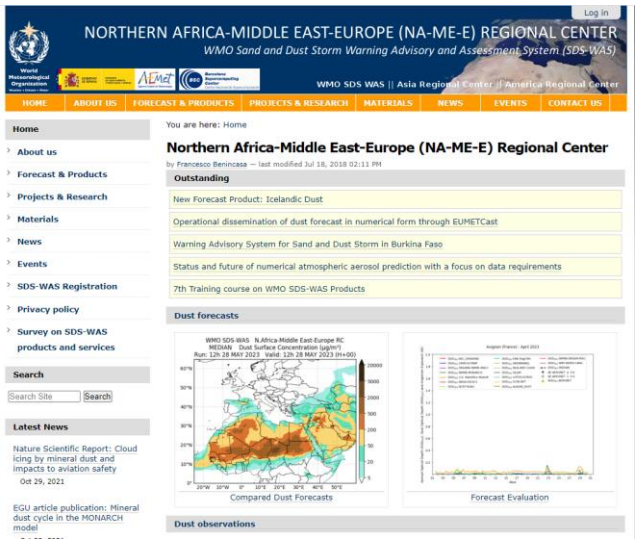

Figure 17.1. SDS-WAS Northern Africa, Middle East and Europe Regional Centre Web portal.

The exchange of forecast products is a core part of the WMO SDS-WAS programme and the basis for the joint visualization and evaluation initiative. The web portal offers dust forecasts (dust surface concentration and Dust Optical Depth (DOD) at 550 nm) generated by various global and regional modelling systems as well as the multi-model median. The models that are currently providing daily dust forecasts to the NA-ME-E are listed here and in alphabetical order are: ALADIN, CAMS-IFS, DREAM8-CAMS, EMA RegCM4, ICON-ART, LOTOS-EUROS, MetOffice-UM, MOCAGE, MONARCH, NASA-GEOS, NCEP-GEFS, NOA-WRF-CHEM, SILAM, WRF-NEMO and ZAMG-WRF-CHEM.

An important element of any forecasting system is the evaluation of the products. The main goal of this process is to assess whether the modelling systems successfully simulate the evolution of dust-related parameters. In addition, the evaluation improves the understanding of the model capabilities, limitations, and appropriateness for the purpose for which they were designed. The evaluation is performed by comparing the model forecasts with

observational data. The individual models and multi-model median forecasts of DOD at 550 nm are compared with AERONET observations of AOD for 40 selected dust-prone stations. In addition to this near-real-time evaluation, a system to assess quantitatively the performance of the different models has been implemented. It yields evaluation scores computed from the comparison of the simulated DOD with the AERONET retrievals of AOD.

The SDS-WAS Regional Centre works toward strengthening the capacity of countries to use the observational and forecast products distributed in the framework of the WMO SDS-WAS programme in partnership with National Meteorological and Hydrological Services (NMHSs) in the region and other relevant organizations.

17.2 The Barcelona Dust Regional Center

In May 2013, in view of the demand of many national meteorological services and the good results obtained by the SDS-WAS related to operationalization, the 65th Session of the WMO Executive Council designated the consortium formed by AEMET and the BSC-CNS as the first Regional Specialized Meteorological Centre with activity specialization on Atmospheric Sand and Dust Forecast (RSMC-ASDF). The Centre operationally generates and distributes predictions for Northern Africa (north of equator), Middle East and Europe.

The Barcelona Dust Regional Centre (BDRC) prepares regional forecast fields using the Multiscale Online Nonhydrostatic AtmospheRe Chemistry model (MONARCH) continuously throughout the year on a daily basis. MONARCH is a chemical weather prediction system that can be used for regional and global modeling at a range of resolutions (for more details see Klose et al., 2021).

In 2022, the BDRC, which coordinates the research activities and operations of the SDS-WAS NA-ME-E Regional Centre launched a new website (Fig. 17.2).

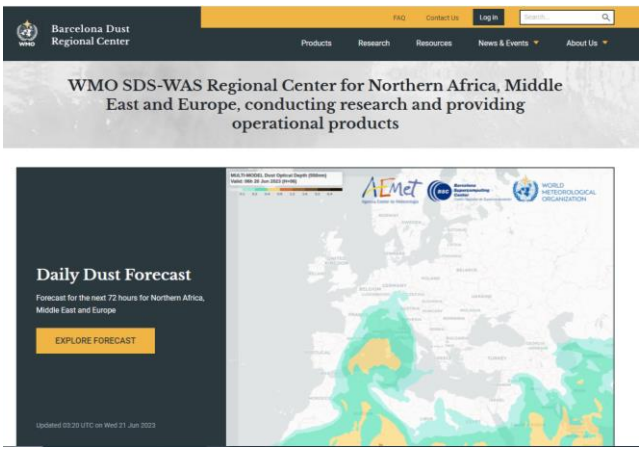

Figure 17.2 SDS-WAS Regional Center for Northern Africa, Middle East and Europe, web portal.

The Barcelona Dust Regional Center provides access to available dust products and coordinates a network of collaborators (researchers, data providers and users' communities) in Northern Africa, the Middle East and Europe. The activities of the center focus on facilitating access to the available dust information. The network around the Center promotes scientific collaborations that aim to deepen our understanding of the dust cycle and its variability, along with its impacts on key socio-economic sectors. Additionally, one of the core activities of the Center is to build capacity of end-users with the aim of promoting the use of dust products to address the risks associated with airborne dust (Basart et al., 2021a).

17.3 AEMET Commission to BSC-CNS for the development and improvement of products and services supplied by the WMO Regional Centers for Atmospheric Sand and Dust Forecast

The director of IARC is the manager, on behalf of AEMET, of the AEMET Commission to BSC-CNS for the development and improvement of products and services supplied by the WMO Regional Centers for Atmospheric Sand and Dust Forecast. The present Commission began in 2020 and it will continue its work for four years.

The AEMET Commission to the BSC-CNS addresses new developments and improvements of products and services of the two regional centers during the 2021-2024 period:

1) Unification and redesign of the information portals of the two Regional Centers.

2) Development of new parameters in the operational dust forecasting system aimed at users of specific socio-economic sectors (such as energy and transportation) that will be available on the website of the Regional Centers:

2.1 Aviation:

• Development and implementation of reduced horizontal visibility forecast associated with the presence of mineral dust.

• Visualization of dust concentration at different heights.

2.2 Solar energy:

• Development and implementation of solar irradiance forecasts including the impact of mineral dust.

• Development and implementation of ice condensation nuclei forecast due to the presence of mineral dust. This new forecast will improve the cloud cover forecast, and consequently, solar irradiance.

3) Maintenance and improvements to the daily mineral dust forecast system:

3.1 Optimization of the daily forecast system.

• External data download such as global weather forecasts that are used as initial conditions for forecasts and observations for evaluation,

• Forecast model and associated post processes execution,

• Products publication on the new unified website of the Regional Centers.

3.2 Optimization of the dust forecast model execution on different BSC-CNS and AEMET HPC platforms.

3. 3 Improvement of the access system to the numerical data of the predictions to prevent security failures and the stability of the download server.

4) Provide a "robust" dust climatology based on reanalysis:

4.1 Design and testing of a new reanalysis (the MONARCH high resolution reanalysis version 2.0; Di Tomaso et al, 2022a, 2022b) over Northern Africa, the Middle East and Europe, with improvements in the model configuration, which includes spatial resolution, emission and deposition schemes, new observations considered in the assimilation (review of new satellite dust products), as well as new initial conditions (i.e. ERA5).

4.2 Extension of the available reanalysis period (i.e. 2007-2016) from 2003 to the present.

17.4 Contribution of SDS Regional Centres to international aerosol dust-related infrastructures and networks

17.4.1 WMO SDS-WAS

WMO released the fifth and sixth issues of "Airborne Dust Bulletin" on July 2021 and September 2022, respectively (Fig. 17.3).

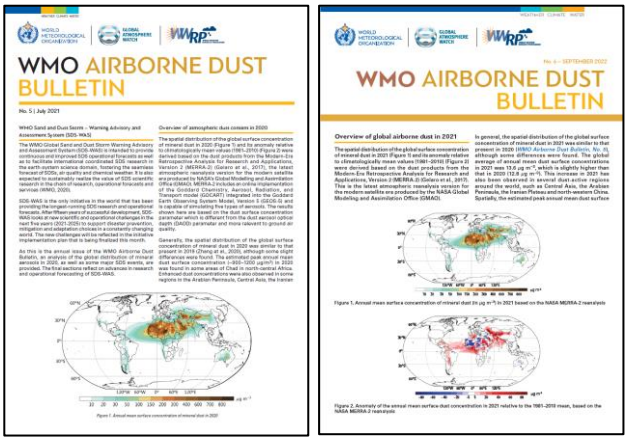

Figure 17.3. WMO Airborne Dust Bulletins, No. 5 (2021) and No. 6 (2022) Available at https://library.wmo.int.

17.4.2 InDust

Managing and mitigating SDS risks and effects requires fundamental and cross-disciplinary knowledge. Due to the significant impacts of sand and dust storms, the design of dust services is one of the major research issues identified by the United Nations Coalition to Combat Sand and Dust Storms, in which WMO is leading the forecasting and early warning strategy. This was the main objective of the European Union Cooperation in Science and Technology (COST) Action entitled "inDust": the International Network to Encourage the Use of Monitoring and Forecasting Dust Products, the COST action officially ended on 30 October 2021.

All activities developed as part of inDust sought to enhance awareness and visibility related to the impacts of sand and dust on various socioeconomic sectors (see, for example, Figure 17.4). It is a fundamental step for building capacity by promoting collaborations and by using the available products (through the organisation of training activities) in a regional context. All inDust outcomes are being considered as the basis for future development of the provision of dust services within the WMO SDS-WAS.

One of the final outcomes for inDust was the creation of a pop-up book: "The Impacts of Sand and Dust Storms" (printed and interactive) and a related animated video presenting the impacts of sand and dust storms on transport and infrastructure, agriculture and energy, health and air quality, and the Earth system.

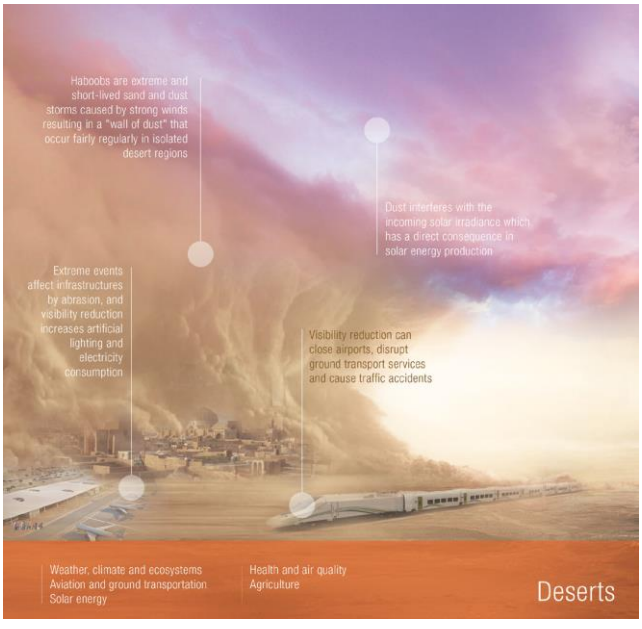

Figure 17.4. Extract from an inDust leaflet that outlines the dust impacts on different sectors. Available at https://cost-indust.eu/media-room/resources.

17.4.3 DustClim

DustClim (Dust Storm Assessment for the development of user-oriented Climate services in Northern Africa, the Middle East and Europe) is a project of several European groups that contribute to the SDS-WAS NAMEE Regional Center node financed by the European Research Area for Climate Services. Several European institutions participate in the project and contribute to the following areas: observations (CNR-DTA/IMAA of Italy, and CNRS- LISA of France), modelling (BSC, and CNR-DTA/ISAC of Italy) and products and services (AEMET, IMF of Finland, and CNR-DTA/ISAC of Italy).

DustClim has five work packages with the following objectives:

• WP1 Review, compilation and treatment of dust observations,

• WP2 Generation of high-resolution dust reanalysis,

• WP3 Development of products and services from the reanalysis model: aviation, solar energy and air quality, together with a visualization tool for the products,

• WP4 Dissemination of products and services,

• WP5 Project Management.

AEMET is responsible for work package 4.

DustClim had a duration of three years, ending in June 2021. The reanalysis, available from 14 Dec 2020, is being used and verified by the groups participating in DustClim.

17.4.4 Development of a dust storm warning system for West Africa: MAC-CLIMA and CREWS

In 2018, a warning advisory system for sand and dust storm was launched for the 13 administrative regions into which the territory of Burkina Faso is divided (Terradellas et al., 2018) (Fig. 17.5). This system has been designed and is operated by the AEMET and BSC in collaboration with the Burkina Faso National Meteorological Agency. Daily dust warnings are released through the WMO SDS-WAS Regional Centre. This was a pilot project funded by the CREWS initiative.

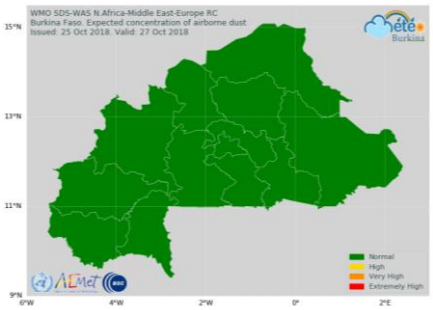

Figure 17.5. Example plot of SDS-WAS Burkina Faso forecasted alert level for 27 October 2018.

Inspired by the Burkina Faso pilot project, the SDS-WAS Regional Center has participated in two projects, MAC-CLIMA and CREWS with complementary strategies, and with a common goal: to implement dust prediction in Western African countries and evaluate them by means of a network of low-cost sensors that measure in-situ (PM_{10}) and column (AOD) aerosols, to be deployed in the region by IARC-AEMET.

The region to be covered in the future by synergies of MAC-CLIMA and CREWS (West Africa) is very large, and includes the following countries: Benin, Burkina Faso, Cape Verde, Gambia, Ghana, Guinea, Guinea-Bissau, Ivory Coast, Liberia, Mali, Mauritania, Niger, Nigeria, Senegal, Sierra Leone and Togo, and in the future, also Chad, Cameroon and Central African Republic (Fig. 17.6).

Figure 17.6. Map of West Africa.

The MAC-CLIMA project aims to generate a meteorological and ocean observation system and using these observations to promote resilience and adaptation to climate change. The objectives of MAC-CLIMA are to promote the progressive creation of an institutional, scientific, and social network among the countries of the cooperation area to work, in a coordinated manner, for the adaptation to and mitigation of climate change. The cooperation area is made up of the outermost regions of Madeira, Azores and the Canary Islands and the three geographically close countries that have accepted to participate in the programme: Cape Verde, Senegal and Mauritania.

The CREWS (Climate Risk and Early Warning Systems) West Africa project, financed by the CREWS Trust Fund managed by WMO, has a main goal to improve short- to medium-range forecast capabilities focusing on severe weather, based on a seamless operational forecast systems and offering technical assistance for capacity building in West Africa.

The collaboration in these two projects, currently covers the following countries: Senegal, Mauritania, Cabo Verde, Mali, Niger and Chad.

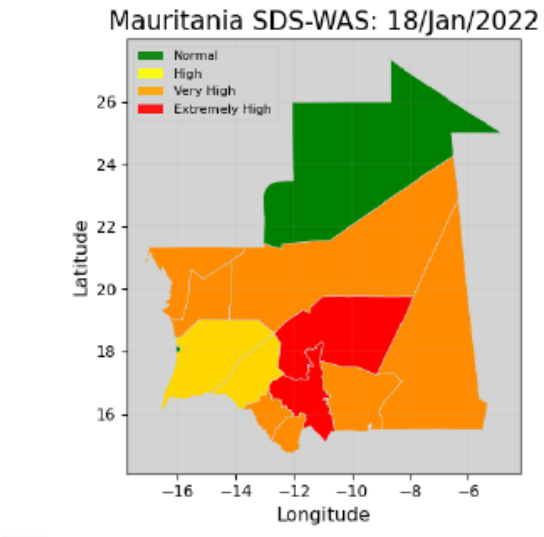

Figure 17.7. Example plot of SDS-WAS Mauritania forecasted alert level for 18 January 2022.

As an example, the forecast of dust storms is shown for the different provinces of Mauritania with a 4-color code map, for 18 January 2022 (Fig. 17.7). A qualitative comparison with mineral dust visibility reduction maps obtained from visibility data from airports in West Africa including Senegal, for the same day, is also presented in Fig. 17.8.

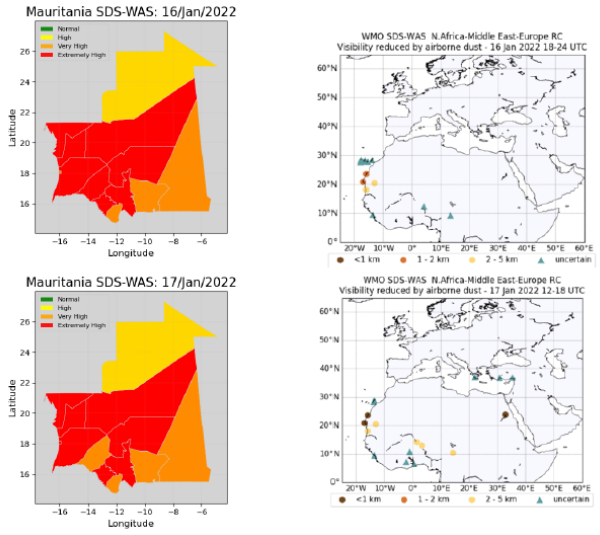

Figure 17.8. Comparison between warning map for Mauritania (16 January 2022) on the left and visibility reduction reported in the country on the right.

In the framework of the MAC-CLIMA project, two tested Particulate Matter – Low-Cost Sensors (PM-LCS) and two hand-held Calitoo sun photometers were installed at Nouakchott Oumtounsy International Airport (Mauritania) in November 2021 (Fig. 17.9a) and at Isla de Sal (Cape Verde) in the offices of the Instituto Nacional de Meteorología e Geofísica (INMG) in June 2022 (Fig. 17.9b). Online workshops on installation, management, and operation of instrumentation, as well as on interpretation of the Warning Advisory System (WAS) and its implementation in the daily work routine have been organized.

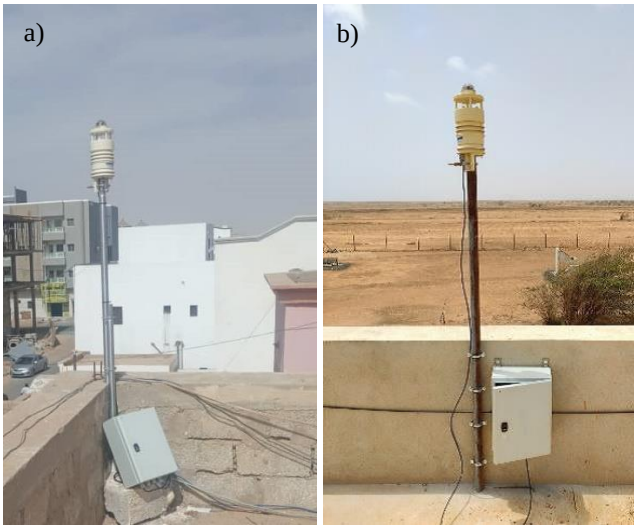

Figure 17.9. PM_{10} data/PM-LCS installation at a) Mauritania and b) Isla de Sal (Cape Verde).

New and improved PM-LCS sensors were specifically designed by the company SIELTEC Canarias S.L. in the frame of CREWS project to improve the PM measurements in remote sites. Four prototypes of the new PM-LCS sensors were installed at Izaña in August 2022 (Fig. 17.10).

Figure 17.10. Installation of new PM-LCS (four sensors) at IARC for the CREWS project.

17.4.5 Development of a surface dust concentration warning system for the Canary Islands

In 2021, the pilot project to implement a surface dust concentration alert system for the Canary Islands based on the outputs of a dust multi-model ensemble of the SDS-WAS Regional Center, was completed. It includes a filtering of the models adjusted for the archipelago using surface PM data from the Canary Islands Air Quality network (Fig.17.11), and the design of surface dust

concentration exceedance probability maps and ENSgrams, see Section 13.6.3 for more details.

Figure 17.11. Stations of the Canary Islands Government Air Quality Network used for dust forecasts evaluation.

17.4.6 SDS-WAS and Copernicus CAMS-84/82 Service

The Copernicus programme consists of a complex set of systems, which collect data from multiple sources: earth observation satellites and in situ sensors such as ground stations, airborne and sea-borne sensors. It processes these data and provides users with reliable and up-to-date information through a set of services related to environmental and security issues.

The Copernicus Atmosphere Monitoring Service (CAMS) has been developed to address environmental concerns, providing data and processed information, aiming at supporting policymakers, business, and citizens with enhanced atmospheric environmental information.

CAMS-84 is a global and regional a posteriori validation activity, with focus on the Arctic and Mediterranean areas. The SDS-WAS Regional Centre, through BSC-CNS as the main partner and AEMET as a third-party, participated in CAMS-84 providing validation and evaluation of dust and aerosols products. Mineral dust validation activities were carried out as CAMS-84 services and published as Quarterly Reports. Since 2021, the Barcelona Dust Regional Center contributes to the new CAMS2-82 (Evaluation and Quality Control (EQC) of global products) activity.

The SDS-WAS Regional Centre participated in the preparation of seven CAMS reports during the period 2021-22 (Arola et al., 2022a, 2022b; Errera et al., 2021; Langerock et al., 2022; Ramonet et al., 2021; Schulz et al., 2021 and Sudarchikova et al., 2021).

17.5 References

Arola, A., S. Basart, A. Benedictow, Y. Bennouna, A.-M. Blechschmidt, E. Cuevas, Q. Errera, H.J. Eskes, J. Kapsomenakis, B. Langerock, A. Mortier, M. Pitkänen, M. Ramonet, A. Richter, M. Schulz, N. Sudarchikova, V. Thouret, T. Warneke, C. Zerefos, Validation report of the CAMS near-real-time global atmospheric composition service: Period September – November 2021, Copernicus Atmosphere Monitoring Service (CAMS) report, CAMS2_82_2022SC1_D82.1.1.1-SON2021.pdf, April 2022, doi:10.24380/e3r1-ga84, 2022a

Arola, A., S. Basart, A. Benedictow, Y. Bennouna, A.-M. Blechschmidt, I. Bouarar, E. Cuevas, Q. Errera, H.J. Eskes, J. Griesfeller, J. Kapsomenakis, B. Langerock, A. Mortier, I. Pison, M. Pitkänen, M. Ramonet, A. Richter, M. Schulz, J. Tarniewicz, V. Thouret, A. Tsikerdekis, T. Warneke, C. Zerefos, Validation report of the CAMS near-real-time global atmospheric composition service: December 2021 – February 2022, Copernicus Atmosphere Monitoring Service (CAMS) report, CAMS2_82_2022SC1_D82.1.1.2-DJF2022.pdf, June 2022, doi: 10.24380/9z4h-5ni, 2022b.

Basart, S., García-Castrillo, G., Cuevas, E., Goloub, P., Cazorla, A., Alastuey, A., Mortier, A., Benedetti, A. and Terradellas, E. Towards continuous evaluation of dust profiles in the WMO SDS-WAS. 9th Internatıonal Workshop on Sand/Dust storms and Associated Dustfall, La Laguna, Tenerife, Spain, 22-24 May 2018.

Basart, S., García-Pando, C.P., Werner, E., Nickovic, S. and Cuevas-Agullo, E.: Understanding the user's needs in risky sand and dust storm environments in Northern Africa, the Middle East and Europe. In NSF Convergence Workshop on Bringing Land, Ocean, Atmosphere and Ionosphere Data to the Community for Hazards Alerts. AGU, 2021a.

Basart, S., Werner, E., Cuevas, E., García-Pando, C.P. (2022). The WMO Barcelona Dust Regional Center: Linking Research with the Development of Dust User-Oriented Services. In: Mensink, C., Jorba, O. (eds) Air Pollution Modeling and its Application XXVIII. ITM 2021. Springer Proceedings in Complexity. Springer, Cham. https://doi.org/10.1007/978-3-031-12786-1_31, 2021.b

Basart, S., Nickovic, S., Terradellas, E., Cuevas, E., Pérez García-Pando, C., García-Castrillo, G., Werner, E. and Benincasa F. The WMO SDS-WAS Regional Center for Northern Africa, Middle East and Europe. E3S Web Conf. 99 04008. DOI: 10.1051/e3sconf/20199904008, 2019.

Cuevas, E., E. Terradellas, and S. Nickovic, Sand and Dust Storm Advisory, 10th Session WWRP Scientific Steering Committee (WWRP SSC10), Geneva, WMO Headquarters, 25-26 October 2017.

Cuevas, E., Milford, C., Barreto, A., Bustos, J. J., García, R. D., Marrero, C. L., Prats, N., Bayo, C., Ramos, R., Terradellas, E., Suárez, D., Rodríguez, S., de la Rosa, J., Vilches, J., Basart, S., Werner, E., López-Villarrubia, E., Rodríguez-Mireles, S., Pita Toledo, M. L., González, O., Belmonte, J., Puigdemunt, R., Lorenzo, J.A., Oromí, P., and del Campo-Hernández, R.: Desert Dust Outbreak in the Canary Islands (February 2020): Assessment and Impacts. (Eds. Cuevas, E., Milford, C. and Basart, S.), State Meteorological Agency (AEMET), Madrid, Spain and World Meteorological Organization, Geneva, Switzerland, WMO Global Atmosphere Watch (GAW) Report No. 259, WWRP 2021-1, 2021.

Di Tomaso, E. et al. (2022). MONARCH Regional Reanalysis of Desert Dust Aerosols: An Initial Assessment. In: Mensink, C., Jorba, O. (eds) Air Pollution Modeling and its Application XXVIII. ITM 2021. Springer Proceedings in Complexity. Springer, Cham. https://doi.org/10.1007/978-3-031-12786-1_33, 2022a.

Di Tomaso, E., Escribano, J., Basart, S., Ginoux, P., Macchia, F., Barnaba, F., Benincasa, F., Bretonnière, P.-A., Buñuel, A., Castrillo, M., Cuevas, E., Formenti, P., Gonçalves, M., Jorba, O., Klose, M., Mona, L., Montané Pinto, G., Mytilinaios, M., Obiso, V., Olid, M., Schutgens, N., Votsis, A., Werner, E., and Pérez García-Pando, C.: The MONARCH high-resolution reanalysis of desert dust aerosol over Northern Africa, the Middle East and Europe (2007–2016), Earth Syst. Sci. Data, 14, 2785–2816, https://doi.org/10.5194/essd-14-2785-2022, 2022b.

Errera, Q., M. Ramonet, N. Sudarchikova, M. Schulz. H. J. Eskes, S. Basart, A. Benedictow, Y. Bennouna, A.-M. Blechschmidt, S. Chabrillat, Christophe, Y., E. Cuevas, A. El-Yazidi, H. Flentje, P. Fritzsche, K.M. Hansen, U. Im, J. Kapsomenakis, B. Langerock, A. Richter, V. Thouret, A. Wagner, T. Warneke, C. Zerefos, Validation report of the CAMS near-real-time global atmospheric composition service: Period March – May 2021, Copernicus Atmosphere Monitoring Service (CAMS) report, CAMS84_2018SC3_D1.1.1_MAM2021.pdf, September 2021, doi:10.24380/qq5mdg18.

Klose, M., Jorba, O., Gonçalves Ageitos, M., Escribano, J., Dawson, M. L., Obiso, V., Di Tomaso, E., Basart, S., Montané Pinto, G., Macchia, F., Ginoux, P., Guerschman, J., Prigent, C., Huang, Y., Kok, J. F., Miller, R. L., and Pérez García-Pando, C.: Mineral dust cycle in the Multiscale Online Nonhydrostatic AtmospheRe CHemistry model (MONARCH) Version 2.0, Geosci. Model Dev., 14, 6403–6444, https://doi.org/10.5194/gmd-14-6403-2021, 2021.

Langerock, B., B., A. Arola, S. Basart, A. Benedictow, Y. Bennouna, A.-M. Blechschmidt, I. Bouarar, E. Cuevas, Q. Errera, H.J. Eskes, J. Griesfeller, J. Kapsomenakis, A. Mortier, I. Pison, M. Pitkänen, M. Ramonet, A. Richter, M. Schulz, J. Tarniewicz, V. Thouret, A. Tsikerdekis, T. Warneke, C. Zerefos, Validation report of the CAMS near-real-time global atmospheric composition service: March – May 2022, Copernicus Atmosphere Monitoring Service (CAMS) report, CAMS2_82_2022SC1_D82.1.1.3-MAM2022.pdf, August 2022, doi:10.24380/akid-u2rr, 2022, 2022.

Ramonet, M., N. Sudarchikova, M. Schulz. Q. Errera, H. J. Eskes, S. Basart, A. Benedictow, Y. Bennouna, A.-M. Blechschmidt, S. Chabrillat, Christophe, Y., E. Cuevas, A. El-Yazidi, H. Flentje, P. Fritzsche, K.M. Hansen, U. Im, J. Kapsomenakis, B. Langerock, A. Richter, V. Thouret, A. Wagner, T. Warneke, C. Zerefos, Validation report of the CAMS near-real-time global atmospheric composition service: Period June – August 2021, Copernicus Atmosphere Monitoring Service (CAMS) report, CAMS84_2018SC3_D1.1.1_JJA2021.pdf, November 2021, doi:10.24380/6x8f-9630, 2021.

Schulz, M., Q. Errera, M. Ramonet, Sudarchikova, N., H. J. Eskes, S. Basart, A. Benedictow, Y. Bennouna, A.-M. Blechschmidt, S. Chabrillat, Christophe, Y., E. Cuevas, A. El-Yazidi, H. Flentje, P. Fritzsche, K.M. Hansen, U. Im, J. Kapsomenakis, B. Langerock, A. Richter, V. Thouret, A. Wagner, T. Warneke, C. Zerefos, Validation report of the CAMS near-real-time global atmospheric composition service: Period December 2020 – February 2021, Copernicus Atmosphere Monitoring Service (CAMS) report, CAMS84_2018SC3_D1.1.1_DJF2021.pdf, June 2021, doi:10.24380/f540-kb09, 2021.

Sudarchikova, N., M. Schulz, Q. Errera, M. Ramonet, H. J. Eskes, S. Basart, A. Benedictow, Y. Bennouna, A.-M. Blechschmidt, S. Chabrillat, Christophe, Y., E. Cuevas, A. El-Yazidi, H. Flentje, P. Fritzsche, K.M. Hansen, U. Im, J. Kapsomenakis, B. Langerock, A. Richter, V. Thouret, A. Wagner, T. Warneke, C. Zerefos, Validation report of the CAMS near-real-time global atmospheric composition service: Period September - November 2020, Copernicus Atmosphere Monitoring Service (CAMS) report, CAMS84_2018SC3_D1.1.1_SON2020.pdf, March 2021, doi: 10.24380/ rysv-7371, 2021.

Terradellas, E., Werner, E., Basart, S. and F. Benincasa 2018: Warning Advisory System for Sand and Dust Storm in Burkina Faso, WMO SDS-WAS, Barcelona, 9 pp. SDS-WAS-2018-001, 2018.

WMO, Sand and Dust Storm Warning Advisory and Assessment System: Science Progress Report. World Meteorological Organization (WMO), GAW Report- No. 254, WWRP 2020-4, 2020. https://library.wmo.int/doc_num.php?explnum_id=10346

WMO, WMO Airborne Dust Bulletin: Sand and Dust Storm Warning Advisory and Assessment System, No. 5 - July 2021, 2021.

WMO, WMO Airborne Dust Bulletin: Sand and Dust Storm Warning Advisory and Assessment System, No. 6 - September 2022, 2022.

17.6 Staff

Dr Emilio Cuevas (AEMET; SDS-WAS Regional Centre NA-ME-E Scientific Advisor (until August 2023))

Dr África Barreto (AEMET; SDS-WAS Regional Centre NA-ME-E Scientific Advisor)

Ernest Werner (AEMET, Technical Director of the SDS WAS Regional Centre NA-ME-E, and the BDRC)

Gerardo García Castrillo (Scientific Support of the SDS WAS Regional Centre NA-ME-E)

Dr Sara Basart (WMO; Research Scientist)

Dr Sergio Rodríguez (CSIC-IPNA, Scientific advisor)

Dr Natalia Prats (AEMET; Research Scientist)

Francesco Benincasa (BSC-AEMET; Technical support)

Kim Serradell (BSC; Technical support)

18 GAW Tamanrasset twinning programme

In 2006, the "GAW-Twinning" between IZO and Tamanrasset GAW stations was initiated with the Saharan Air Layer Air Mass characterization (SALAM) project. This was part of a cooperation programme between the l'Office Nationale de la Météorologie (ONM, Algeria) and AEMET. In September 2006, the AERONET Tamanrasset-AEMET Cimel station was installed (Fig. 18.1). The instruments of the GAW Tamanrasset twining programme are located on the roof of the Regional Meteorological Center (southern regional meteorological department, ONM, Algeria) in Tamanrasset (92,635 inhabitants). This area, free of industrial activities, is in the highlands of the Algerian Sahara. Tamanrasset-Assekrem is a WMO Global GAW station.

Figure 18.1. The AERONET Cimel (upper image) at Tamanrasset on the terrace of the Regional Meteorological Centre (lower image).

This station now has a relatively long time series of AERONET data, covering the period 2006-2022 (Fig. 18.2), despite the enormous environmental and logistical difficulties to keep it in operation, in large part thanks to the effort and great collaboration of the human team in charge of the GAW Tamanrasset-Assekrem facilities.

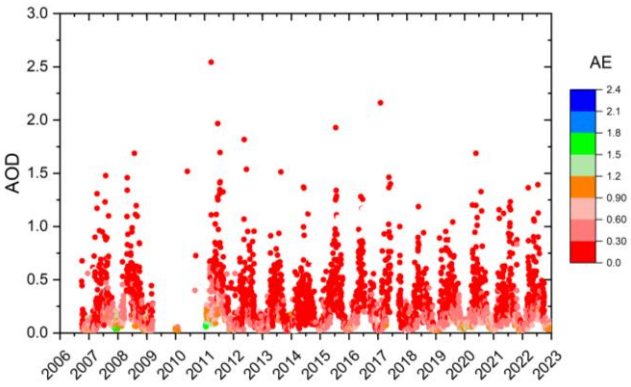

Figure 18.2. The Tamanrasset AERONET AOD data series (2006-2022).

The GAW station Tamanrasset is in the south of Algeria, in the heart of the Sahara, and it provides unique and precious data in an extensive region near important dust sources. Tamanarasset station is the only permanent AERONET observation site in the heart of the Sahara region (Fig. 18.3a). This station is strategic not only for the characterization of atmospheric composition over the Sahara Desert in the frame of the GAW Programme, but also to evaluate atmospheric models and validate satellite data. The Tamanrasset station has been regularly used to evaluate satellite-derived products, such as the IASI aerosols product including desert mineral dust (e.g. Callewaert et al., 2019). In fact, it is a key station to assess the performance of mineral dust prediction models in a challenging region where there are numerous nearby dust sources.

Tamanrasset is a singular station of special attention for the Sand and Dust Storm Warning Advisory and Assessment System Regional Center (e.g. Terradellas et al., 2016) (see Section 17 for more details). This AERONET photometer is calibrated by the IARC on an approximately annual basis. Further details of this programme are provided in Guirado et al. (2014).

An automatic comparison of 12 model forecasts of Dust Optical Depth (DOD) at 550 nm versus AERONET AOD data for the month of March 2021 at Tamanrasset is shown in Fig. 18.3b. This comparison is available at the SDS-WAS website.

b)

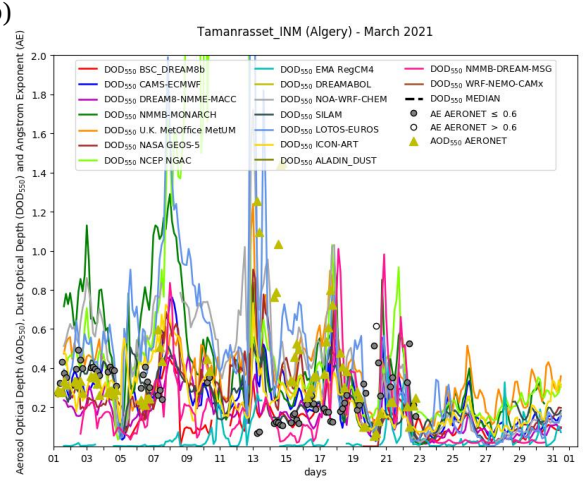

Figure 18.3. a) Map of the AERONET stations in Northern Africa used by the SDS-WAS Regional Centre and b) AERONET dust AOD product comparison with 12 dust models, dust optical depth (DOD) and median of the models at Tamanrasset in March 2021.

Tamanrasset is also a key station for evaluating global operational forecast services, such as CAMS-Copernicus, under conditions of almost pure dust. An automatic comparison of CAMS-Copernicus outputs for several aerosol types with the Tamanrasset AERONET level 1.5 AOD data during the period September-November 2021 (from Arola et al., 2022) is shown in Fig. 18.4 and can be found here, where it is possible to select other intercomparison time periods.

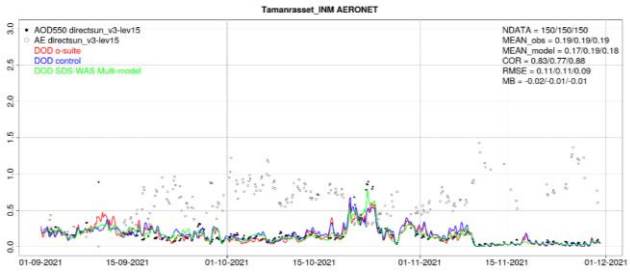

Figure 18.4. Comparison of Copernicus CAMS operational aerosols product and AERONET level 1.5 AOD at Tamanrasset site during the period September-November 2021 (from Arola et al., 2022).

The twinning was completed with the installation at Tamanrasset of a double Brewer Spectrophotometer #201 (MARK-III) in October 2011 (Fig. 18.5), thanks to the project entitled "Global Atmosphere Watch in the Maghreb-Sahara Region" (GAW-Sahara) financed by the Spanish Agency for International Development Cooperation (AECID).

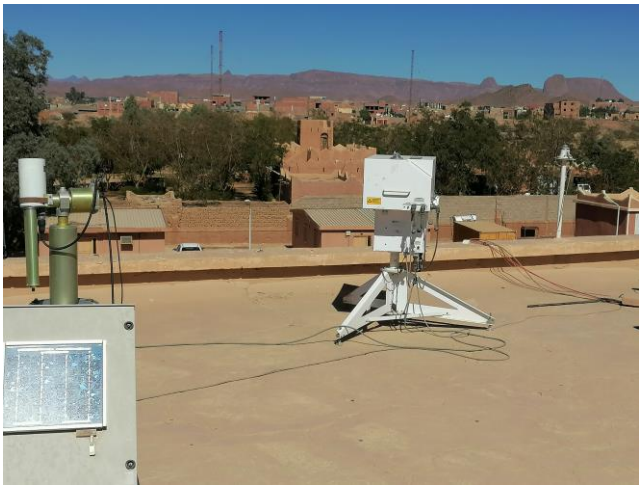

Figure 18.5. Brewer#201 at Tamanrasset on the terrace of the Regional Meteorological Centre. On the left, the AERONET Cimel photometer.

An operational Dobson (#11; WMO station code 002) spectrophotometer has been operated at Tamanrasset since April 1994. This station is now one of the few sites in the world where permanent and long-term intercomparison between the Dobson, the Brewer and the present and future satellite-based sensors could be performed on a routine basis. This initiative has been strongly recommended by the WMO Ozone and UV Radiation Scientific Advisory Group and represents a unique contribution to the total ozone global network Quality Assurance. In addition, the Brewer instrument provides spectral ultraviolet radiation data.

Tamanrasset, with the Brewer Spectrophotometer #201, plays an important role in the context of other global observation networks, e.g. in the EUBREWNET network (Fig. 18.6) (see Section 6.3.1 for more details) providing near-real-time data of column ozone, spectral radiation and AOD in the UV range (see López-Solano et al., 2018).

As an example, Figure 18.6 shows two of the many products that EUBREWNET provides. The total ozone data on 7 March 2022 is shown in Fig. 18.6b. During this day there were clear conditions that allowed more than 100 direct sun measurements, with a very low ozone content of 251 DU and quite stable values, making it a day that can be used for Langley calibration. In Fig. 18.6c, the diurnal cycle of the UV-index at Tamanrasset on 7 March 2022 is shown.

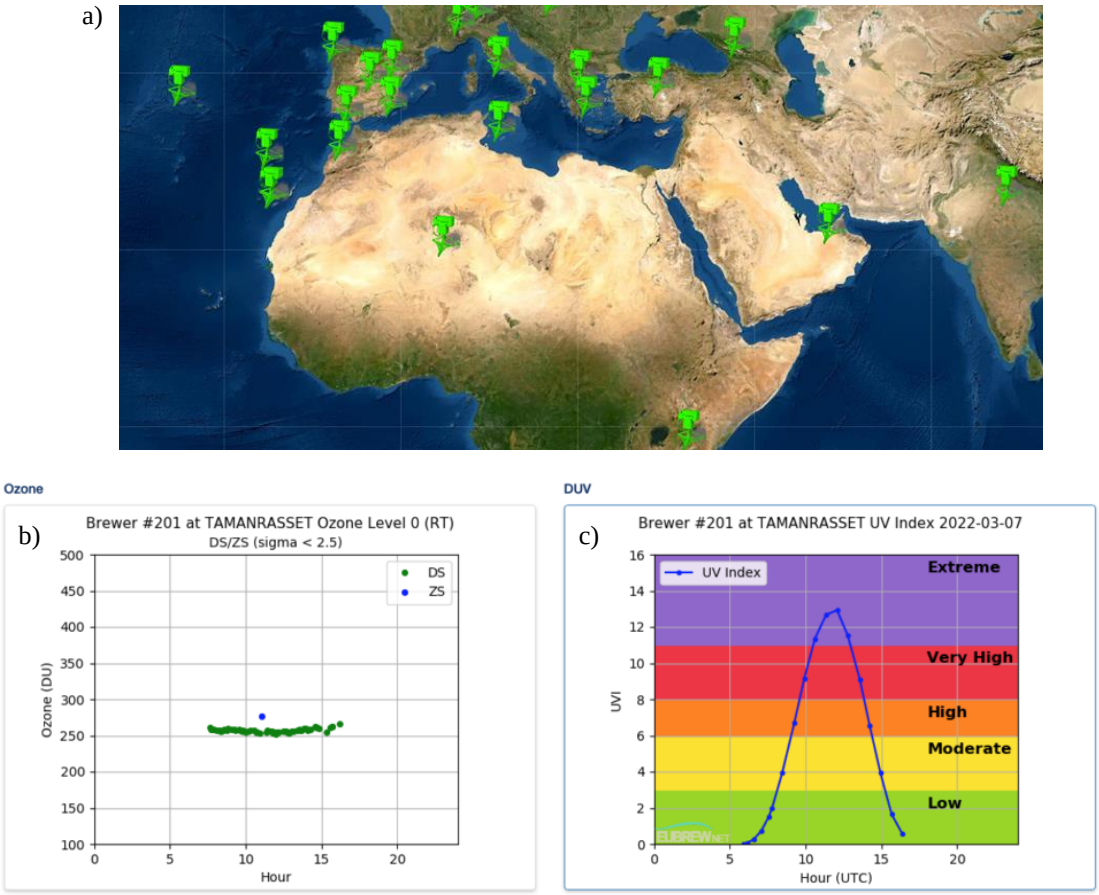

Figure 18.6. a) The Brewer spectrophotometer of Tamanrasset as part of the EUBREWNET network. Data from Brewer #201 at Tamanrasset on 7 March 2022: b) example of total ozone data display and c) example of UV index diurnal cycle. Clear conditions allow for more than 100 direct sun measurements. Total column ozone is low (251 DU) and quite stable, and the UV index reaches 13 UVI.

The Brewer #201 is periodically calibrated by the Regional Brewer Calibration Center for Europe hosted by the IARC taking advantage of the biannual intercomparisons that are held at the INTA station at El Arenosillo-Huelva (Southern Spain). In fact, this instrument was repaired and participated in the 14th RBCC-E intercomparison campaign, which was held at El Arenosillo on 17-28 June 2019, see Redondas et al. (2020). During the 2019 campaign, the instrument had to be repaired by IOS (International Ozone Services) technicians due to deterioration in the spectral response of the instrument. Although it was finally repaired and calibrated, it was not put into operation on its return to Tamanrasset station in 2019.

For the equipment to return to operational status and, given the circumstances due to the Covid-19 pandemic, the WMO set up a team trip to the IARC (Redondas, 2021), where the RBCC-E staff repaired the instrument and subsequently organized training for the instrument operator, Sida Lamine Baika, who has recently been able to reinstall the equipment that provides its valuable observations to the EUBREWNET network (Fig. 18.7).

Figure 18.7. Sida Lamine Baika, Brewer operator at Tamanrasset with the Brewer #201.

Since March 2017, a Calitoo hand-held sun photometer has been operating at Tamanrasset. During this time, the performance of the Calitoo under the challenging conditions in a desert area have been tested with very good results (see Fig. 18.8).

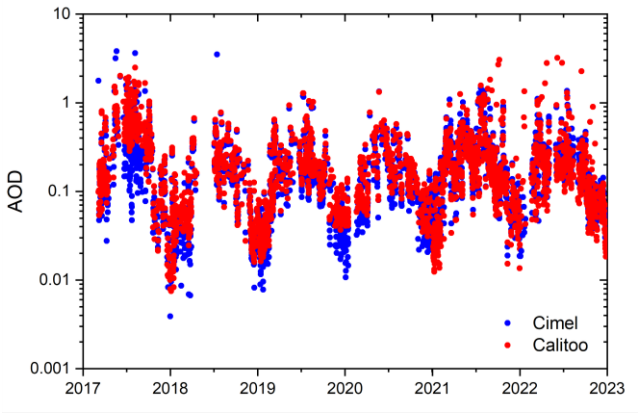

Figure 18.8. AERONET AOD computed at 500 nm from Cimel sun-photometer versus AOD computed at 540 nm from Calitoo hand-held sun-photometer at Tamanrasset (2017-2022). The gap in data in 2018 is due to the replacement of the Calitoo for a newly calibrated one.

18.1 References

Arola, A., Basart, S., Benedictow, A., Bennouna, Y., Blechschmidt, A.E., Cuevas, E.,. Errera, Q., Eskes, H.J., Kapsomenakis, J., Langerock, B., Mortier, A., Pitkänen, M. Ramonet, M., Richter, A., Schulz, M., Sudarchikova, N., Thouret, V., Warneke, T., Zerefos, C,: Validation report of the CAMS near-real-time global atmospheric composition service: Period September – November 2021, Copernicus Atmosphere Monitoring Service (CAMS) report, CAMS2_82_2022SC1_D82.1.1.1-SON2021.pdf, April 2022, doi:10.24380/e3r1-ga84.

Callewaert, S., Vandenbussche, S., Kumps, N., Kylling, A., Shang, X., Komppula, M., Goloub, P., and De Mazière, M.: The Mineral Aerosol Profiling from Infrared Radiances (MAPIR) algorithm: version 4.1 description and evaluation, Atmos. Meas. Tech., 12, 3673–3698, https://doi.org/10.5194/amt-12-3673-2019, 2019.

Guirado, C., Cuevas, E., Cachorro, V. E., Toledano, C., Alonso-Pérez, S., Bustos, J. J., Basart, S., Romero, P. M., Camino, C., Mimouni, M., Zeudmi, L., Goloub, P., Baldasano, J. M., and de Frutos, A. M.: Aerosol characterization at the Saharan AERONET site Tamanrasset, Atmos. Chem. Phys., 14, 11753-11773, doi:10.5194/acp-14-11753-2014, 2014.

López-Solano, J., Redondas, A., Carlund, T., Rodriguez-Franco, J. J., Diémoz, H., León-Luis, S. F., Hernández-Cruz, B., Guirado-Fuentes, C., Kouremeti, N., Gröbner, J., Kazadzis, S., Carreño, V., Berjón, A., Santana-Díaz, D., Rodríguez-Valido, M., De Bock, V., Moreta, J. R., Rimmer, J., Smedley, A.R.D., Boulkelia, L., Jepsen, N., Eriksen, P., Bais, A. F., Shirotov, V., Vilaplana, J. M., Wilson, K. M., and Karppinen, T. Aerosol optical depth in the European Brewer Network, Atmos. Chem. Phys., https://doi.org/10.5194/acp-18-3885-2018, 18, 3885-3902, 2018.

Redondas, A., Berjón, A., López-Solano, J., Carreño, V., León-Luis, S.F., Santana, D.: Fourteenth Intercomparison Campaign of the Regional Brewer Calibration Centre Europe. El Arenosillo Atmospheric Sounding Station, Huelva, Spain, 17–28 June 2019. Vol. WMO/GAW Report No. 257. Joint publication of State Meteorological Agency (AEMET), Madrid, Spain and World Meteorological Organization (WMO), 550 p., 2021. Available from: https://library.wmo.int/doc_num.php?explnum_id=10640

Terradellas, E., S. Basart, and E. Cuevas: 2013-2015 Activity Report of the SDS-WAS Regional Center for Northern Africa, Middle East and Europe, Joint publication of AEMET and WMO; NIPO: 281-16-007-3; WMO / GAW Report No. 230; WMO / WWRP No. 2016-2, 2016.

18.2 Staff

Dr Emilio Cuevas (AEMET, PI of the Tamanrasset-Izaña twinning)

Alberto Redondas (AEMET, PI of the Ozone and UV Programme)

Ramón Ramos (AEMET, logistics and instrumentation)

Dr África Barreto (AEMET, PI of Aerosol Programme)

Virgilio Carreño (AEMET; Meteorological Observer-GAW Technician)

Local contributors:

Mr Sidi Lamine Baika (Tamanrasset-Assekrem GAW station, Head)

Mr Abdessadek Saanoune and Mr Abdelhadi Belmiloud (Technical staff).

19 WMO Measurement Lead Centre for Aerosols and Water Vapour Remote Sensing Instruments

The mission of the Commission for Instruments and Methods of Observations (CIMO) was to promote and facilitate international standardisation and compatibility of instruments and methods of observations used by Members, in particular within the WMO Global Observing System, to improve quality of products and services delivered to/by Members and to meet their requirements (see e.g. Report from the President to Cg-XVII (2015). CIMO XVI nominated Izaña Observatory as WMO Testbed for Aerosols and Water Vapour Remote Sensing Instruments.

Following approval of the WMO Reform package by the Eighteenth World Meteorological Congress in June 2019, a Joint Session of the new Technical Commissions and Research Board agreed on working structures in May 2020. As a result of the WMO reform of the constituent bodies, CIMO was dissolved and its activities were included in the activities of the Commission for Observation, Infrastructure and Information Systems (INFCOM). In 2021, INFCOM decided to replace the existing concepts of WMO Testbeds and Lead Centres with the single concept of WMO Measurement Lead Centres (for more information see here).

The main ongoing activities of the WMO Measurement Lead Centre for Aerosols and Water Vapour Remote Sensing Instruments at Izaña Observatory are related to instrument validation, development of new methodologies and devices for aerosol and water vapour observations (e.g. García et al., 2020, 2021).

19.1 Remote sensing of aerosols at night with the CoSQM sky brightness data

Four novel multispectral Color Sky Quality Meter (CoSQM) photometers were installed in April 2019 in four different locations in Tenerife differently affected by their proximity to the lighting sources and elevation: SCO, IZO, IAC Observatory and TPO. This deployment is considered a first step toward a worldwide CoSQM network. Marseille et al. (2021) presented an innovative method for estimating the aerosol optical depth using an empirical relationship between Zenith Night Sky Brightness (ZNSB) measured at night with the CoSQM and AOD retrieved at daytime from the AErosol Robotic NETwork (Holben et al., 1998; Giles et al., 2019). The empirical relationship is especially suited to light-polluted regions with light pollution sources located within a few kilometres of the observation site. This is the case of Santa Cruz de Tenerife. A coherent day-to-night aerosol optical depth and Ångström Exponent evolution in a set of 354 days and nights from August 2019 to February 2021 was used to verify the suitability of this new methodology (Fig. 19.1), including an estimation of the method uncertainty, set at 0.02 for AOD and 0.75 for AE.

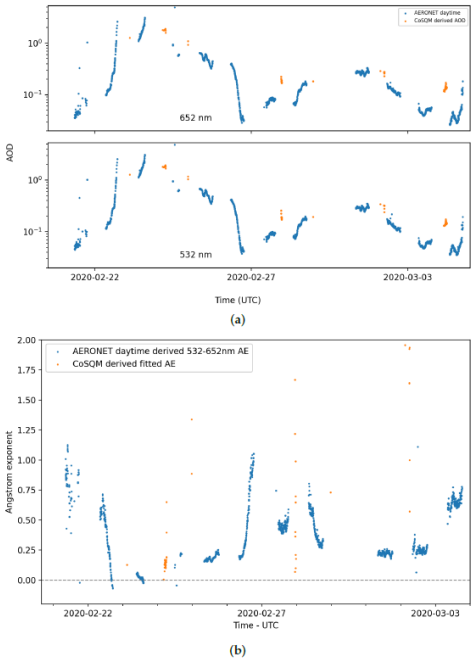

Figure 19.1. Continuity of (a) AOD and (b) Angstrom Exponent (AE) derived by means of CoSQM ZNSB compared to AERONET daytime sun photometer measurements during and after a calima event. AERONET AE values were retrieved with 440–675 nm daytime sun photometer measurements. Reprinted from Marseille et al. (2021).

19.2 Installation of the new CoSQM 2 version

In November 2021, Pr. Martin Aubé from the University of Sherbrooke (Canada) installed the new version of the multispectral Color Sky Quality Meter (CoSQM version 2) in Izaña Observatory (Fig. 19.2). The CoSQM is a portable device which samples the multispectral properties of artificial light scattered by the atmosphere. It is a convenient tool to estimate light pollution and its impact on the environment. CoSQM is an instrument composed of a filter wheel with four different spectral transmittances in the visible range (clear, red, blue, green), placed on a step motor in front of a Sky Quality Meter.

The device comprises a Raspberry pi open source linux computer so that it can be reproduced by anyone. CoSQM also comprises a camera module. The instrument can be operated remotely via the SSH protocol, and the data may be accessed via an integrated web server. This device provides data to demonstrate how humankind can affect their own nocturnal environments. Colour detection capability is an important improvement over existing non-imaging detectors in the context of the drastic change in the colour of light pollution provided by the transition to LED technology.

Figure 19.2. Dr Martin Aubé at Izaña during the installation of the new CoSQM version 2 instrument in November 2021.

This new and updated version of the CoSQM adds improvements on the camera, enclosure, motor, WIFI and filter wheel. It also includes a high-quality raspberry pi. In particular, this new system reacts better to high temperature conditions.

19.3 Spectral lunar spectral irradiance measurement campaign at IARC

A field campaign was conducted at Izaña Observatory between April and September 2022 in the framework of the ESA project "Improving the lunar irradiance model of ESA". This project, launched in 2021, was assigned to a consortium of three members: University of Valladolid/Izaña Atmospheric Reseach Center, National Physical Laboratory (NPL, London) and Flemish Institute for Technological Research (Vlaamse Instelling voor Technologisch Onderzoek, Belgium). The main goal of the project is to use a wider set of ground-based lunar measurements performed with a CE318-TP9 photometer at Izaña and Teide Peak to improve the current Lunar Irradiance Model of ESA (LIME), providing improved spectral interpolation algorithm and uncertainty analysis. This will also provide users in the lunar calibration community a Git hosted python module and GUI to perform lunar calibration using LIME.

In this project, modifications to the ASD FieldSpec spectroradiometer are proposed, including new fore optics, designed to define the field of view over the full spectral range and a scrambler to ensure all the ASD fibers view the full lunar disk. Additionally, a field reference source with dual apertures is proposed for calibration and performance verification. To do that, the ASD was mounted on a lunar tracker ensuring the ASD fore optics to be centred on the lunar disk. The University of Valladolid team was in charge of performing ASD hyperspectral measurements of the lunar disk at Izaña Observatory for a sufficient number of lunar phase angles (at least three lunar cycles) to capture the possible spectral variability of the lunar disk reflectance with phase angles and libration angles (Figure 19.3).

Figure 19.3. Deployment of the ASD spectrometer in Izaña Observatory during the ESA campaign by University of Valladolid and IARC members in April 2022.

19.4 References

Barreto, Á., Cuevas, E., García, R. D., Carrillo, J., Prospero, J. M., Ilić, L., Basart, S., Berjón, A. J., Marrero, C. L., Hernández, Y., Bustos, J. J., Ničković, S., and Yela, M.: Long-term characterisation of the vertical structure of the Saharan Air Layer over the Canary Islands using lidar and radiosonde profiles: implications for radiative and cloud processes over the subtropical Atlantic Ocean, Atmos. Chem. Phys., 22, 739–763, https://doi.org/10.5194/acp-22-739-2022, 2022.

García-Cabrera, R. D., Cuevas-Agulló, E., Barreto, Á., Cachorro, V. E., Pó, M., Ramos, R., and Hoogendijk, K.: Aerosol retrievals from the EKO MS-711 spectral direct irradiance measurements and corrections of the circumsolar radiation, Atmos. Meas. Tech., 13, 2601–2621, https://doi.org/10.5194/amt-13-2601-2020, 2020.

García, R.D.; Cuevas, E.; Cachorro, V.E.; García, O.E.; Barreto, Á.; Almansa, A.F.; Romero-Campos, P.M.; Ramos, R.; Pó, M.; Hoogendijk, K.; Gross, J. Water Vapor Retrievals from Spectral Direct Irradiance Measured with an EKO MS-711 Spectroradiometer—Intercomparison with Other Techniques. Remote Sens. 2021, 13, 350. https://doi.org/10.3390/rs13030350.

Giles, D.M.; Sinyuk, A.; Sorokin, M.G.; Schafer, J.S.; Smirnov, A.; Slutsker, I.; Eck, T.F.; Holben, B.N.; Lewis, J.R.; Campbell, J.R.; et al. Advancements in the Aerosol Robotic Network (AERONET) Version 3 database—Automated near-real-time quality control algorithm with improved cloud screening for Sun photometer aerosol optical depth (AOD) measurements. Atmos. Meas. Tech., 12, 169–209, 2019.

Holben, B.N.; Eck, T.; Slutsker, I.; Tanre, D.; Buis, J.; Setzer, A.; Vermote, E.; Reagan, J.; Kaufman, Y.; Nakajima, T.; et al. AERONET—A federated instrument network and data archive for aerosol characterization. Remote Sens. Environ., 66, 1–16, 1998.

Marseille, C.; Aubé, M.; Barreto, A.; Simoneau, A. Remote Sensing of Aerosols at Night with the CoSQM Sky Brightness Data. Remote Sens., 13, 4623. https://doi.org/10.3390/rs13224623, 2021.

19.5 Staff

Dr Africa Barreto (AEMET; PI of WMO Measurement Lead Centre for Aerosols and Water Vapor Remote Sensing Instruments)

Ramón Ramos (AEMET; Head of Infrastructure)

Pedro Miguel Romero Campos (AEMET; Research Scientist)

Dr Rosa García (TRAGSATEC/UVA; Research Scientist)

Dr Antonio Fernando Almansa (CIMEL/AEMET; Research Scientist)

Dr Yenny González (CIMEL; Research Scientist)

César López Solano (SIELTEC)

Dr Omaira García (AEMET; Research Scientist)

Dr Victoria Cachorro (University of Valladolid; Head of Atmospheric Optics Group)

20 Integrated Carbon Observation System (ICOS)

The Integrated Carbon Observation System (ICOS) is a European Research Infrastructure Consortium (ERIC) producing high-precision and long-term observations to help us to understand the carbon cycle and the response of the Earth system to climate change generated by greenhouse gases. It provides standardized and open data from close to 150 measurement stations across 14 European countries.

The stations observe greenhouse gas concentrations in the atmosphere as well as carbon fluxes between the atmosphere, land surface and oceans. Thus, ICOS is rooted in three domains: Atmosphere, Ecosystem and Ocean. A Thematic Centre, within each domain, coordinates the observations and supports the stations. In addition to the Thematic Centres, there are Central Analytical Laboratories (CAL) that provide gas analyses and calibration gases (see Fig. 20.1). In 2022, more than 500 scientists and 110 renowned universities or institutes are a part of the ICOS community.

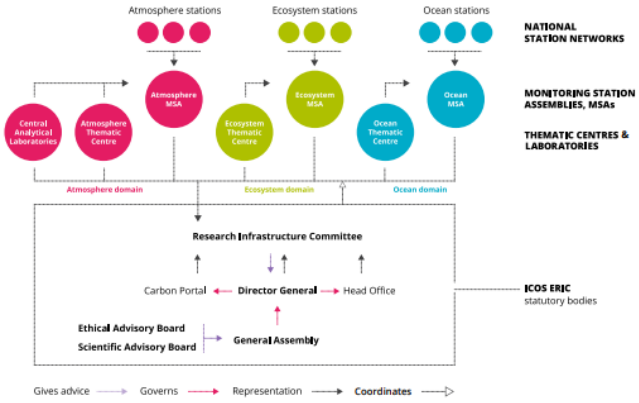

Figure 20.1. ICOS research infrastructure core components. (Reprinted from ICOS Handbook 2022)

ICOS collaborates in international initiatives such as the development of the Integrated Global Greenhouse Gas Information System (IG^{3}IS) of the WMO and since 2019, it is an observer organisation to the United Nations Framework Convention on Climate Change (UNFCCC). Thus, ICOS contributes to the work of the Convention and its Subsidiary Body on Scientific and Technical Advice (SBSTA) and can organise its own side-events in connection with the annual global climate negotiations (COP meetings). Finally, due to its role as observer in the Intergovernmental Panel on Climate Change (IPCC), ICOS can propose the participation of its research community in the writing process of IPCC reports.

20.1 IARC-AEMET: Spanish node technical coordinator task

The membership application of Spain was approved by the ICOS General Assembly on 17 November 2020. The national network, ICOS-Spain, is formed by the group of the Institute of Oceanography and Climate Change (QUIMA) belonging to the University of Las Palmas de Gran Canaria (ULPGC), the National Institute of Aerospace Technology (INTA) and AEMET in charge of the technical coordination tasks of this network at the national level. IARC Director, Dr Emilio Cuevas, was appointed as the focal point for Spain. Each partner is responsible for its station, selecting a Principal Investigator (PI) to participate in the Measurement Station Assembly organized by the thematic centres of each domain.

The incorporation of Spain into the ICOS consortium contributes to the expansion of the geographical coverage of ICOS, allowing the observations to reach the subtropical zone of the Atlantic Ocean. At the end of 2022, ICOS-Spain was formed by three stations covering the two domains: atmospheric (Izaña Observatory and El Arenosillo) and oceanic (CanOA), implemented on a Volunteer Observing Ship (VOS). However, in 2022, the process to incorporate the ESTOC (Estación de Series Temporales en el Océano de las Islas Canarias) oceanic station and the Majadas de Tiétar ecosystem associated station was also initiated. Both stations have been accepted by ICOS headquarters and have officially joined the network as of 1 January 2023 (see Fig. 20.2). The ESTOC will be managed by the Oceanic Platform of the Canary Island (PLOCAN), IEO and ULPGC. The Mediterranean Centre for Environment Studies (CEAM) will manage the associated station of Majadas de Tiétar.

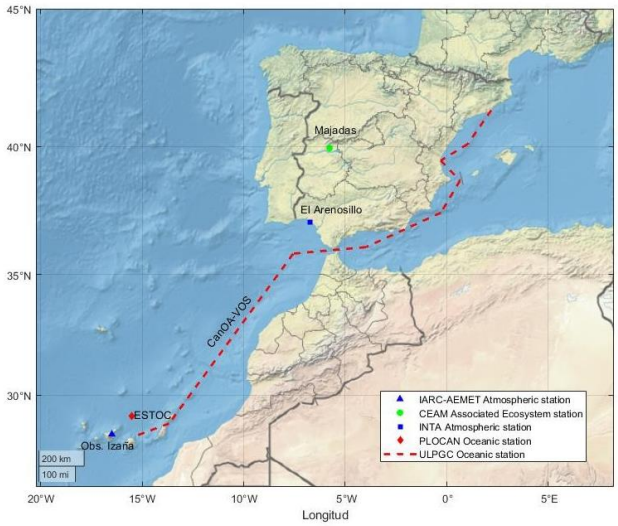

Figure 20.2. The ICOS-Spain station network.

Table 20.1. ICOS-Spain stations and current status in the ICOS certification process.

Station (Institution)	PI	Station domain	Date officially admitted	ICOS certification process stage
Izaña Observatory (IARC-AEMET)	Pedro Pablo Rivas Soriano	Atmosphere (Class 2)	2021	Station validation: 19/4/2021 Instrumentation and facilities certification: completed March 2022 Certification process completed: 23/5/2023
CanOA-VOS (ULPGC)	Melchor Dávila	Oceanic (Class 1)	2021	Station validation: 25/2/2021 Currently certifying instrumentation and facilities
El Arenosillo (INTA)	Jose Antonio Adame	Atmosphere (Class 2)	2022	Station validation: 9/5/2022 Currently certifying instrumentation and facilities
Majadas de Tiétar (CEAM)	Arnaud Carrara	Ecosystem (associated)	2023	Station admitted by ICOS headquarters
ESTOC (PLOCAN, IEO and ULPGC)	Melchor Dávila Eric Delory	Oceanic (Class 1)	2023	Station admitted by ICOS headquarters

For a definition of the acronyms used in the above table, see Section 29

The process of inclusion of a new station is initiated by a formal request from the Focal Point of the national network to ICOS headquarters (see Fig. 20.1). Then, the corresponding thematic Centre initiates the certification process, which has two stages:

1) To validate that the station is located in an area of scientific interest.

2) To certify that the instrumentation implemented in the station meets the ICOS accuracy requirements.

ICOS, depending on the domain, has defined a series of mandatory variables to be measured by each station. In atmosphere and ecosystem, according to the number of monitored variables with respect to the total established, the stations are classified as Class 1 or Class 2. In addition, the ecosystem network is complemented by a set of associated stations, with lower requirements with respect to the number of variables to be monitored. The ocean stations are all Class 1 stations.

In 2021 and 2022, IARC-AEMET organized different coordination meetings with its partners with the main objective to aid them in the certification of their stations. Currently, all stations are in the process of certification, therefore, their observations are not currently publicly available. Table 20.1 summarizes the status of the ICOS-Spain stations within the ICOS certification process.

The most recent ICOS General Assembly was held in Madrid on 22-23 November 2022. IARC-AEMET and the Spanish Ministry of Science and Innovation (person responsible, Maria Vallejo) coordinated the organization of this important event. In this assembly, the Spanish focal point and several PIs presented the current status of the national node as well as the new stations to be incorporated in 2023 and other national research projects on greenhouse gases. IARC-AEMET as coordinator of the activities of the national network has collected the necessary information from its partners to collaborate in the edition of different documents such as the ICOS financial report, ICOS annual report and ICOS handbook. In addition, the ICOS-Spain webpage has been developed to disseminate the activities of the national node.

20.2 Izaña-ICOS atmospheric station

The Izaña Observatory was selected to implement the first atmospheric station of the ICOS network in Spain. Izaña will become a Class 2 ICOS mountain atmosphere station and, therefore, it is required to provide continuous in-situ CO_2 and CH_4 measurements. However, CO measurements are also recommended. In addition to these gases, IARC-AEMET is committed to providing N_2O measurements. Following the ICOS requirements for analysers, we acquired between the end of 2020 and the beginning of 2021 a new Picarro G2401 and a new LGR 907-0015 in order to measure the aforementioned gases.

Both instruments were sent to the ICOS Atmospheric Thematic Center (ATC) Metrology Lab to be guaranteed to fulfill the ICOS high-quality data requirements. Unfortunately, both instruments failed the tests and were returned to the factory for overhaul. Subsequently, the Picarro and LGR passed the ICOS test on 25 November 2021 and 30 March 2022, respectively. In parallel, the documentation to meet the first stage of the certification process (validation of the site) was sent to ATC. Site validation for the Izaña Observatory ICOS station was accepted on 19 April 2021.

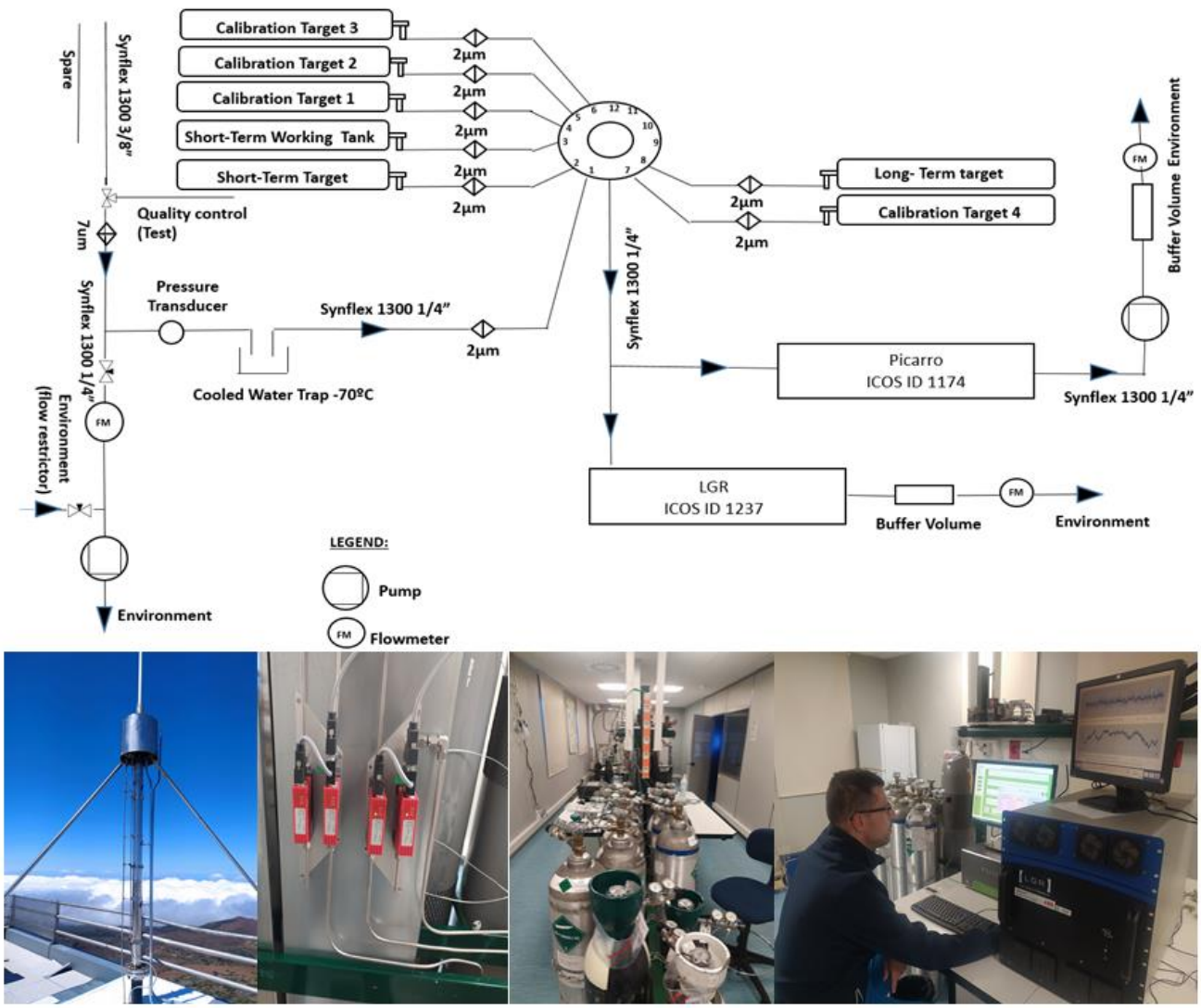

Figure 20.3. Ambient air/gas standard plumbing diagram of the Izaña-ICOS station. At the bottom, from left to right, photographs showing parts of the installation: sampling, flow meters, gas tanks and work station next to the instruments.

A new ambient air/gas standard plumbing system has been designed and implemented for the instrumentation, following ATC recommendations (see Fig. 20.3). In early November 2022, periodic 2-weekly calibrations of both instruments were initiated after receiving the ICOS standard targets from the ICOS-Central Analytical Laboratories. In addition, the daily submission of the measurements together with other ancillary variables to the ATC has been automated for the monitoring of this station as part of the certification process. The data sent follows an automatic QC/QA process but must be finally checked by the station PI through a visualization data program developed by ATC (see Fig. 20.4). Pedro Pablo and Sergio León participated in a training course about this visualization and validation data program organized by ATC.

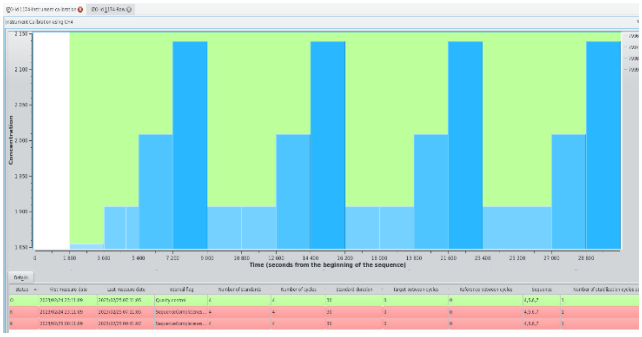

Figure 20.4. Screenshot of data visualization and validation program, developed by ATC, showing a calibration.

During the preparation of this report (on 23/5/2023) the Izaña Observatory has completed the ICOS certification process and has been fully admitted as an atmospheric station and its observations are therefore available on the ICOS-ERIC data portal.

We participated in the ICOS Science Conference 2022 (12-14 September 2022) with the following presentation: "Inter-comparison of CO_2, CO and CH_4 mixing ratios obtained by in-situ and remote measurements techniques in the Izaña Atmospheric Observatory" (García et al., 2022).

In addition, several informative notes have been published to make this new national network more visible. These notes have been published on the ICOS-Spain webpage and in ICOS-ERIC newsletters. These notes have focused on the monthly maximum CO_2 concentration, as well as the high in situ concentrations recorded during the volcanic eruption on La Palma (see Section 23 for more details).

20.3 New project to develop science-based climate services in Africa: KADI

ICOS has over 170 measurement stations in the European continent and on the adjacent oceans. On the African continent, however, there is currently no stable infrastructure to standardise the operation of the existing stations, and to harmonise the data into one portal. Moreover, the current global models and observational instructions have been developed mainly in non-tropical regions, meaning that they need to be fitted to the African environment.

To start addressing these issues, ICOS is now leading a new EU HORIZON-INFRA project called Knowledge and Climate Services from an African Observation and Data Research Infrastructure (KADI). KADI aims at improving the knowledge about climate change in Africa and at developing tools to combat its negative consequences. The project will investigate what kind of climate services are needed in the African continent to tackle the climate crisis. The ultimate aim is to design a pan-African climate observation research infrastructure. IARC-AEMET scientists participate as a team member in this project.

20.4 References

Integrated Carbon Observation System Research Infrastructure. ICOS Handbook 2022.

García Rodríguez, O. E.; Cuevas Agulló, E.; Rivas Soriano, P. P.; León Luis, S. F. Inter-comparison of CO_2, CO and CH_4 mixing ratios obtained by in-situ and remote measurements techniques in the Izaña Atmospheric Observatory. ICOS Science Conference 2022.

20.5 Staff

Dr Emilio Cuevas (Spanish Focal Point (until August 2023) – Former Director of IARC-AEMET)

Carlos Torres (Spanish Focal Point (from September 2023) – Director of IARC-AEMET)

Pedro Pablo Rivas Soriano (AEMET; Head of programme)

Dr Sergio Fabián León Luis (TRAGSATEC; Research Scientist)

Ramón Ramos (AEMET; Head of Infrastructure and instrumentation)

Enrique Reyes (AEMET; Software and data processing)

Dr Omaira García (AEMET; Research Scientist)

Dr África Barreto (AEMET; Research Scientist)

21 ATMO-ACCESS

The aim of the ATMO-ACCESS project (Sustainable Access to Atmospheric Research Facilities), from the European Union Horizon 2020 research and innovation programme, is to address the needs for developing sustainable solutions based on the principles of open access and to develop guidelines and recommendations for governance, management and funding for efficient and effective access provision suited to distributed atmospheric RIs. This project investigates the most suitable mechanisms that could lead to the sustainable provision of access to atmospheric research infrastructures.

The main objectives of ATMO-ACCESS are:

1) To provide coordinated physical, remote and virtual open access to state-of-the-art facilities and services in atmospheric RIs and further enhance their range of products, capabilities and accessibility for a wide range of users, including the private sector. Remote trans-national access is access to resources and services offered by the facility without users physically visiting the facility. Similar to Physical access, it requires competitive selection of the users to be served, as usually it applies to resources that are not unlimited (e.g. computing hours on a supercomputer, digital tools or measurements/experiments performed by the facility staff for the user). In contrast, virtual access is wide, free access provided through communication networks to resources that can be simultaneously used by an unlimited number of users (e.g. a dataset available on the Data Centre).

2) To engage facilities and their national stakeholders and direct them towards improved harmonisation of access procedures across the different member states, while also exploring modalities by which the use of atmospheric RIs can be further enhanced.

3) To explore and test new modalities of access that build on the complementarity and synergies among atmospheric RIs and respond to the evolving needs of users in relation to training, research and technology development, innovation and data services

4) To identify the most suitable conditions for establishing sustainable access procedures across the EU for distributed atmospheric RIs, involving national and international stakeholders.

ATMO-ACCESS currently provides opportunities to access 43 of the most advanced operational European atmospheric research facilities in Europe. The ATMO-ACCESS project began in April 2021, and will be ongoing until March 2025. IARC-AEMET is involved in the following Work Packages:

WP8: Sustainable and strategic framework for access to distributed atmospheric Research Infrastructures: integrates findings from all other WPs to identify the most suitable conditions for making trans-national access sustainable beyond the current EU funding model (through its third-party University of Valladolid – Atmospheric Optics Group)

WP9: Implementing access through TNA activities: deals with central management of TNA in the project, enabling both physical and remote access to a large collection of atmospheric research facilities in a coordinated manner.

Specifically, in WP9 we offer as the Izaña Subtropical Access Facility for Observations (ISAF-Obs), synergistic observation of aerosol and trace gases with in-situ and remote sensing techniques, meteorology and radiation, intercomparisons with operational instruments (reporting data to worldwide networks and programmes such as WMO-GAW, NDACC, etc), study of atmospheric composition in pristine conditions and with desert dust influences, support in specific campaigns to study atmosphere in remote high mountain conditions, for example to study NPF, desert dust aerosols, transatlantic transport, etc.

In addition, as the Izaña Subtropical Access Facility for Calibration (ISAF-Cal), our facility is available as a calibration site for photometric techniques in terms of Langley procedures in pristine conditions (a certificate will be provided) and comparison of photometers with reference instrument enabling improvements and optimization of them. For more information see the Izaña ATMO-ACCESS webpage and the ATMO-ACCESS project webpage.

The following access activities were performed at our facilities during 2022:

- **Chasing preindustrial aerosols at Izaña**
  Understanding the gas precursors responsible for new particle formation process in pristine-like Izaña. TNA Project Leader: Wei Huang, University of Helsinki. Date of access: March-June 2022 (for more details see section 8.3.2).
- **COALITION: Characterization Of AerosoLs In The subtropIcal nOrth atlaNtic**
  The purpose of the access activities was to improve the direct and polarized signals of the CE376 micro Lidar in order to contribute to the aerosol characterization of the subtropical North Atlantic free troposphere. TNA Project Leader: Stephane Victori, CIMEL. Date of access: November 2022 (for more details see Section 9.3.7).

22 Activities in collaboration with IAC

IARC-AEMET, within the framework of the Specific Collaboration Agreement between AEMET and the Instituto de Astrofísica de Canarias (IAC) (Institute of Astrophysics of the Canary Islands), provide information and data to IAC. In particular, IARC provides data that allows IAC to characterize and monitor parameters that determine the astronomical quality of their observatories on the Canary Islands: 1) Teide Observatory (TO), in Tenerife, approximately 1km away from the Izaña Observatory (IZO) of IARC-AEMET and 2) Roque de los Muchachos Observatory (RMO) on the island of La Palma.

IARC provides measurements of aerosol optical depth in different channels, aerosol optical properties and water vapour in the atmospheric column, to IAC, both for TO and RMO, from measurements obtained by sunphotometers enrolled in AERONET installed at IZO and RMO, respectively (Fig. 22.1).

Figure 22.1. The AERONET sunphotometer at Roque de los Muchachos Observatory (RMO), La Palma.

Near-real-time information on column water vapour (precipitable water) is provided from a high-precision GNSS receiver installed at IZO. Real-time PM_{10} particulate matter data is provided from the PM TEOM analyzer installed at IZO, for operational purposes (Fig. 22.2). This information allows decisions to be made about the operability of the telescopes based on aerosols surface concentration; as above at relatively low threshold, aerosols, and specifically mineral dust, can cause damage to the optics and other mechanical elements of the telescopes.

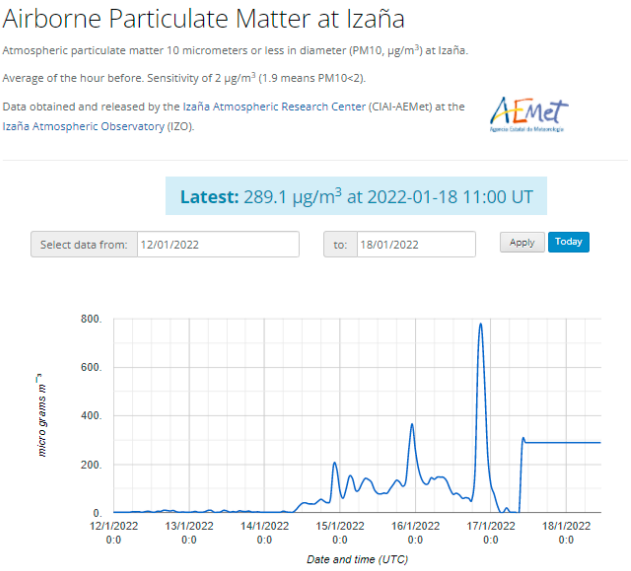

Figure 22.2. IAC Internal web page with PM_{10} real-time information from the TEOM analyzer at IZO (IARC-AEMET).

In addition, data from the radiosondes launched daily at 00 and 12 UTC from the AEMET Güímar (Tenerife) automatic radiosonde station (WMO GRUAN station, #60018) (Fig. 22.3) are provided to the IAC for both operational and scientific purposes.

Figure 22.3. Image of the AEMET GRUAN automatic radiosonde station in Güímar (Tenerife).

IAC also has real-time access to the images obtained with the all-sky and regular cameras installed at IZO, which show the state of the sky every five minutes. Meteorological information from the automatic meteorological stations installed at IZO and RMO is also provided.

In addition to meteorological and atmospheric observations, AEMET provides specific meteorological forecasts at the two sites (TO and RMO), of geopotential height, temperature, relative humidity, wind, precipitation, cloud cover and mineral dust from the Sahara, which allows IAC to carry out a flexible scheduling of telescope operation. Much of this information is very useful for short- and medium-term planning of observations.

23 La Palma 2021 Volcanic Eruption

The most recent eruption in the Canary Islands archipelago occurred on the island of La Palma between 19 September and 13 December 2021 (85 days, 8 h, Figs. 23.1 and 23.2) (PEVOLCA, 2021; González, 2022). This was the first subaerial eruption in a 50-year period in the Canary Islands. The La Palma 2021 volcanic eruption, located in a zone known as Hoya de Tajogaite, was characterised by extensive lava emissions, (12.4 km^2 lava field) which caused considerable destruction and damage to homes, buildings, crops and other infrastructures.

Figure 23.1. Image captured by LuzLux of the La Palma 2021 volcanic eruption.

During the La Palma 2021 volcanic eruption, AEMET as the Spanish National Meteorological Agency, provided different support services to the Scientific Committee and the Advisory Committee of the Canary Islands Volcanic Emergency Plan (PEVOLCA- Plan Especial de Protección Civil y Atención de Emergencias por Riesgo Volcánico en la Comunidad Autónoma de Canarias) as well as to the wider scientific community (García et al., 2022b).

AEMET provided support to the La Palma volcanic emergency crisis in two fundamental aspects. Firstly, from an operational point of view, AEMET, as the meteorological authority, provided specific forecasts and conducted volcanic ash monitoring and surveillance in coordination with the Volcanic Ash Advisory Centre (VAAC) in Toulouse, which is responsible for the Canary Islands region. Secondly, AEMET and IARC, at the research level, devoted special attention to key aspects such as the transport of the volcanic dispersion cloud, its physical properties and chemical composition, and its different impacts in the subtropical region of the North Atlantic, from an air quality and climate point of view.

Some aspects of this work are presented in the following sections, references are provided for further details.

Figure 23.2. Image captured by Fernando Bullón (AEMET) of the La Palma 2021 volcanic eruption.

23.1 Modelling of volcanic plume transport

AEMET operationally employs the chemical transport model MOCAGE (Modélisation de la Chimie Atmosphérique Grande Echelle) (Josse et al., 2004) to provide predictions of the chemical composition of the atmosphere with a focus on air quality. However, for the La Palma volcanic emergency crisis, AEMET provided specialised simulations of volcanic ash cloud dispersion at different pressure levels (from 950 to 300 hPa), executed twice daily (at 00:00 and 12:00 UTC) with hourly outputs of ash dispersion as well as 12-hour accumulated wet and dry deposition and total column values, forecast up to 72 hours ahead. For this purpose, MOCAGE was run on the AEMET Cirrus supercomputer in emergency mode, disabling the chemistry module of the model and running as a dispersion model. Figure 23.3 shows an example of these simulations and the corresponding satellite image.

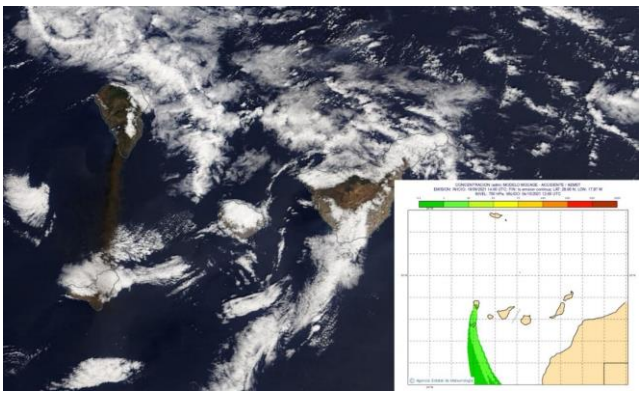

Figure 23.3. Image captured by the MODIS sensor aboard NASA's Terra satellite in the visible channel on 4/10/2021 at 11:55 UTC. The ash plume is seen as a brown band dispersing in a southerly direction (Image: NASA Worldview). In the lower right inset, the ash dispersion map predicted for the same day at 12:00 UTC by the MOCAGE model. Reprinted from AEMET, 2022.

23.2 Instrumentation deployment in La Palma

To complement the observation and monitoring of the evolution of the volcanic ash cloud, AEMET, through the Izaña Atmospheric Research Centre and the Territorial Delegation of AEMET in the Canary Islands (DTCAN) and in collaboration with numerous national and international institutions, deployed scientific instrumentation on La Palma with a double objective:

1) To characterise the vertical structure of the eruptive plume, and to monitor in real time the changes that occur in this structure, as well as to perimeterise the outflow of the dispersion cloud (see Section 23.3).

2) To contribute to the implementation of an emergency air quality network. This network was supported by the Military Emergency Unit (UME), the Government of the Canary Islands and the Island Council of La Palma (see Section 23.4).

Scientific instrumentation was installed at seven measurement stations in La Palma to follow the volcanic eruption by different organisations in collaboration with AEMET (Fig. 23.5). Details of the sites and instrumentation that were installed are as follows:

1) Roque de los Muchachos (2400 m): ARCADE Raman Lidar at Cerenkov Telescope Array and sun-photometer (AERONET);

2) El Paso (650 m): Prototype Vaisala CL61 ceilometer;

3) Tazacorte (110 m): In situ SO_2, O_3, aerosols, micro-pulse lidar (MPL-4B), all-sky cameras, ZEN radiometer, ash deposition collector, meteorological instrumentation;

4) Airport (60 m): Vaisala CL51 ceilometer, meteorological instrumentation;

5) Fuencaliente (680 m, Figs. 23.4, 23.6): sun-lunar photometer (AERONET), CM15k ceilometer (Lufft), EM27 FTS, all-sky camera, DOAS (direct-sun);

6) Los Llanos (295 m): meteorological sondes;

7) Angeles-Alvariño (IEO Ship): AQT420 (in situ SO_2, CO and O_3).

Figure 23.4 Instrumentation in Fuencaliente

Figure 23.5. Location of the seven stations (stars) deployed on La Palma to follow the volcanic eruption by different organisations in collaboration with AEMET. The blue dot represents the location of the eruptive centre, the red area is the area affected by the lava flow, and the circles represent the approximate location of the different earthquakes associated with the eruptive process (Credits (map): Instituto Geográfico Nacional, www.ign.es).

In addition, mobile records were conducted: ash collection and multigas measurements (in collaboration with UNAM).

A video showing the physical deployment, both of resources of personnel and of meteorological and scientific instrumentation, carried out by AEMET on the island of La Palma with the collaboration of other national and international institutions can be found here.

Figure 23.6 Attending to instrumentation in Fuencaliente.

23.3 Network of vertical profilers in La Palma

The vertical profiler network installed at La Palma to monitor the eruption process was aimed at real-time measurement of the height of the volcanic dispersion cloud as well as at characterisation of the emitted volcanic aerosols, and was deployed in the context of the European Aerosol, Clouds and Trace Gases Research Infrastructure (ACTRIS, 2021). This network consisted of five instruments (three ceilometers and two lidar systems), which were installed around the perimeter of the volcanic eruptive centre at five measurement stations (see details in Figs. 23.5 and 23.7).

This rapid scientific collaboration was carried out among some of the research groups that make up ACTRIS-Spain: IARC-AEMET, University of Valladolid (UVa), Atmospheric Optics Group, Optical Remote Sensing CommSensLab group from the Universitat Politècnica de Catalunya (UPC), the University of Granada (UGR), INTA and CSIC. ACTRIS-Italy's University of L'Aquila and other institutions and private companies also strongly supported the volcanic emergency, such as Vaisala (Finland). Data from this new emergency network were provided in real time to PEVOLCA and were incorporated into the EUMETNET E-Profile network, which supported the Toulouse VAAC and the Copernicus observing programme.

Figure 23.7. Images of the different profilers (three ceilometers and two lidar systems), deployed in La Palma. Reprinted from ACTRIS, 2021.

A detailed example of the vertical evolution of the volcanic plume on 3 October 2021 is presented in Fig. 23.8. In this case, volcanic aerosols reached 5 km in height, affecting the surface level with a downward movement of the ash layer.

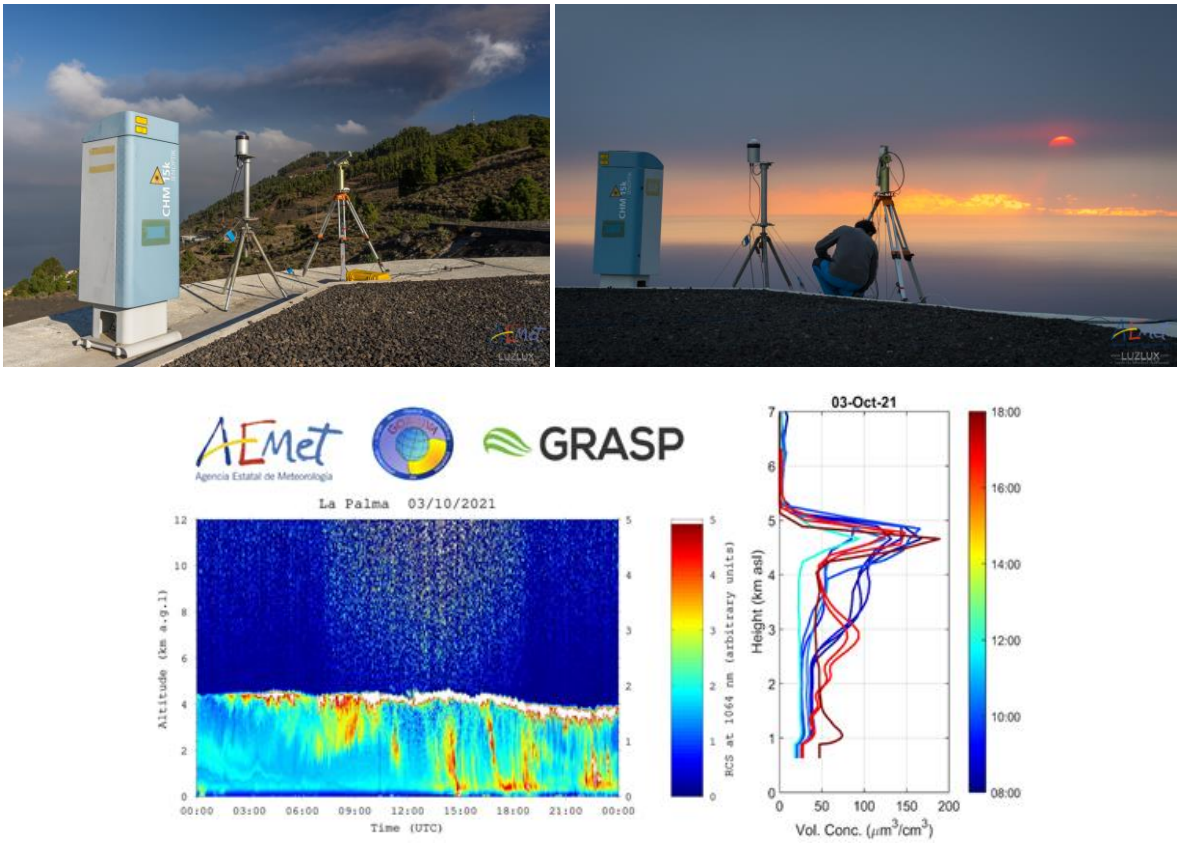

Figure 23.8. Upper panel: Images of instrumentation installed at Fuencaliente station, from left to right: 1) Lufft CHM15k ceilometer, 2) all-sky camera and 3) sun/moon photometer belonging to AERONET. (Image credit: LuzLux). Lower panel: Range Corrected Lidar signal profile extracted from the ceilometer Lufft CHM15k and the corresponding aerosol volume concentration (µm3/cm3) profiles calculated with the GRASP inversion code on 3 October 2021. Reprinted from ACTRIS, 2021.

These measurements advanced our knowledge of the impact of the volcanic eruption on the atmosphere in addition to their contribution to the emergency response during the volcanic eruption.

For example, Córdoba-Jabonero, et al. (2023) conducted a study on "Fresh volcanic aerosols injected in the atmosphere during the volcano eruptive activity at the Cumbre Vieja area (La Palma, Canary Islands): Temporal evolution and vertical impact". The relative mass contribution and vertical impact of the volcanic components (ash and non-ash) particles was examined.

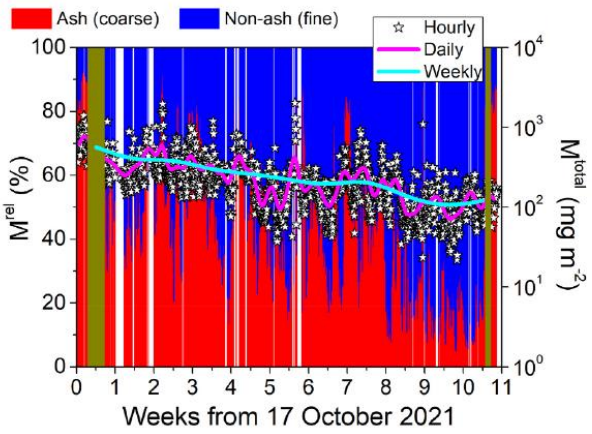

Figure 23.9 Evolution of the ash (a) and non-ash (na) particles along the P-MPL observational period in terms of: (Left axis) Relative mass contribution (Mrel i =Mi/Mtotal, %) with i = a (red) and na (blue); and (Right axis) the total mass loading (Mtotal, g m^{-2}), as represented by its hourly- (stars symbols), daily- (magenta line) and weekly-averaged (cyan line) values. Reprinted from Córdoba-Jabonero et al. (2023).

A representative mass conversion factor was obtained for both ash and non-ash particles: 1.89 ± 0.53 and 0.31 ± 0.06 g m^{-2}, respectively. These factors were used to calculate the ash and non-ash mass concentrations from the polarized Micro-Pulse Lidar (P-MPL) observations, the P-MPL was deployed at Tazacorte, La Palma, on 17 October 2021. The relative ash mass contribution was 73 ± 18% with a total mass loading of 566 ± 281 mg m^{-2} at week 1 (week 5 from the start of the volcanic eruption), reducing gradually down to 38 ± 32% and 120 ± 49 mg m^{-2}, respectively, at week 11 (week 15 from the start of the volcanic eruption) (Fig 23.9).

Bedoya-Velásquez, et al. (2022) conducted a study entitled: "Estimation of the Mass Concentration of Volcanic Ash Using Ceilometers: Study of Fresh and Transported Plumes from La Palma Volcano". The attenuated backscattering ranged from 0.8 to 9.1 x 10^{-6} (msr)$^{-1}$ and the volume depolarization ratio measured nearby the volcano was up to 0.3. The ash plume showed intense episodes that reached mean AOD values of up to 0.4 (Fig 23.10). The ash mass concentration reached moderate levels with maximum values of up to 313.7 µg m^{-3} in the 0-1 km layer, 272.3 µg m^{-3} in the 1-2 km layer and 137.9 µg m^{-3} in the 2-3 km layer.

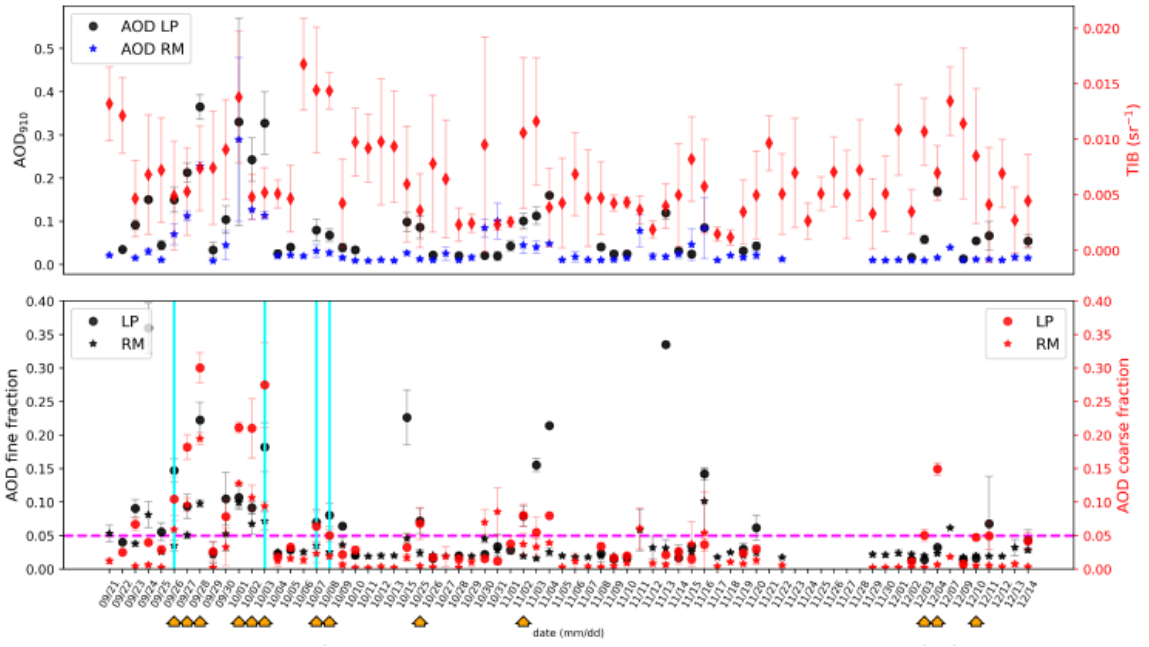

Figure 23.10 Mean AOD at 910 nm in the upper panel (black circles and blue stars for La Palma (LP) and Roque de los Muchachos (RM), respectively) and mean integrated β (red diamonds, all data availability considering all stations). Mean AOD fine/coarse fractions are displayed in the lower panel (black and red circles for LP and black and red stars for RM). Orange arrows highlight the days with dominant coarse mode fractions. Reprinted from Bedoya-Velásquez et al. (2022).

23.4 Impact on Air Quality

The continuous and real-time monitoring of air quality throughout the island of La Palma was one of the priorities of PEVOLCA, the Canary Islands Government and the Cabildo Insular de La Palma. For this reason, an emergency network of air quality stations was deployed from the beginning of the eruption process, monitoring the surface concentrations of the main pollutants expected during the eruption (particulate matter and sulphur compounds, SO_2 and H_2S) (García et al., 2022b). IARC-AEMET contributed to this implementation of an emergency air quality network with deployment of instrumentation to measure in situ SO_2, O_3 and particulate matter in Tazacorte, measurements started on 24/9/2021.

Subsequently, IARC-AEMET in collaboration with many participating organisations, conducted a comprehensive evaluation of the impact of the 2021 volcanic eruption on air quality, concentrating on the air quality impacts of SO_2 and PM concentrations (PM_{10} and $PM_{2.5}$) and utilising a multidisciplinary approach (Milford et al., 2023). High concentrations of SO_2, PM_{10} and $PM_{2.5}$ were observed in La Palma (hourly mean SO_2 up to ~2600 μg m^{-3}) and also sporadically at ~140 km distance, at the Izaña Observatory in Tenerife (hourly mean SO_2 > 7700 μg m^{-3}) in the free troposphere (Fig. 23.11). Exceedances of EU Air Quality limit values (EC, 2008) and WHO Air Quality Guidelines (WHO, 2021) occurred for SO_2, PM_{10} and $PM_{2.5}$.

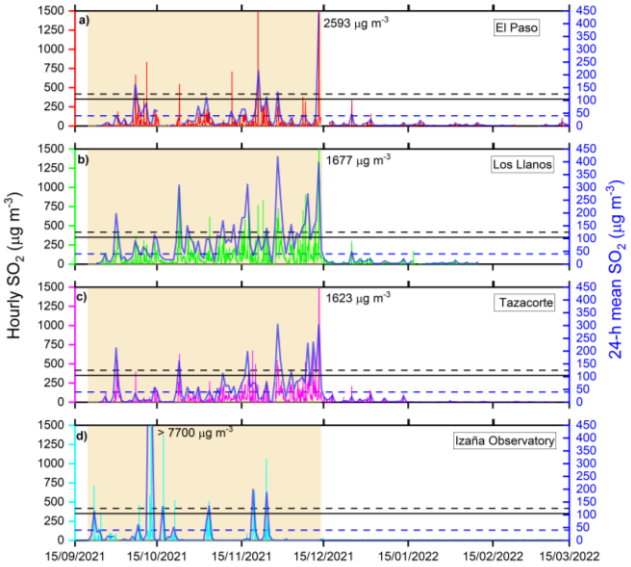

Figure 23.11. Concentrations of SO_2 at a) El Paso, b) Los Llanos, c) Tazacorte and d) Izaña Observatory (15/9/2021–15/3/2022). The left axis indicates hourly mean concentrations and the right axis daily (24-h) mean concentrations (in blue). Reprinted from Milford et al. (2023).

Volcanic aerosols and desert dust both impacted the lower troposphere in a similar height range (~ 0–6 km) during the eruption, providing a unique opportunity to study the combined effect of both natural phenomena.

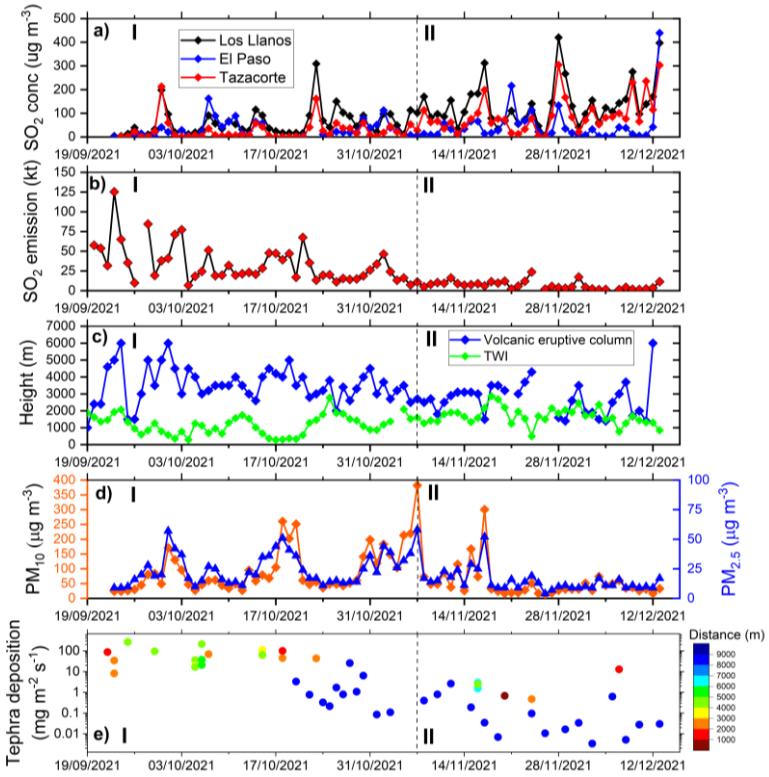

Figure 23.12. Temporal evolution during La Palma volcanic eruption of a) Daily (24-h mean) SO_2 concentrations in La Palma, b) Daily SO_2 volcanic emissions (kt) estimate provided by TROPOMI (credit: ESA, MOUNTS), c) Volcanic eruptive column top height and Trade Wind Inversion (TWI) base height (m a.s.l.). d) Daily (24-h mean) PM_{10} and $PM_{2.5}$ concentrations in Los Llanos and e) Tephra deposition (mg m^{-2} s^{-1}) (note logarithmic scale on the Y axis). The vertical dashed line marks the date 7/11/2021 and separates the volcanic eruption into two phases (I and II). Reprinted from Milford et al. (2023).

The La Palma 2021 volcanic eruption emitted a large amount of SO_2 (~1.84 Tg) into the troposphere over nearly 3 months. To put these SO_2 emissions into context, the total anthropogenic SO_2 emitted from the 27 European Union countries for the whole of 2019 was ~1.66 Tg (EEA, 2021).

The impact of the 2021 volcanic eruption on SO_2 and PM concentrations was strongly influenced by the substantial magnitude of volcanic emissions, the injection height, the strong vertical stratification of the atmosphere in this region and its seasonal dynamics. As a consequence of these modulating factors, SO_2 concentrations at ground-level in La Palma increased during the eruption, showing an opposite temporal trend to SO_2 volcanic emissions (Fig. 23.12).

23.5 Back and forward trajectories

To aid analysis of the La Palma 2021 volcanic plume transport, in the evaluation conducted once the eruption had terminated, FLEXTRA software was utilized to compute both back and forward-trajectories using ERA5 reanalysis data from ECMWF. The software was configured with input data every 6 hours, covering a large area and resolution in both horizontal and vertical dimensions. The strong vertical stratification of the subtropical eastern North Atlantic, which hinders the vertical growth of volcanic plumes and results in a change of wind direction with height, makes FLEXTRA particularly useful in this region. FLEXTRA forward trajectories from the eruptive centre (e.g. Fig. 23.13d-f) and back trajectories were useful in indicating the transport of the volcanic plume and in identifying periods when Izaña Observatory was affected by volcanic emissions (see Section 13 for more details on the back and forward-trajectory calculations).

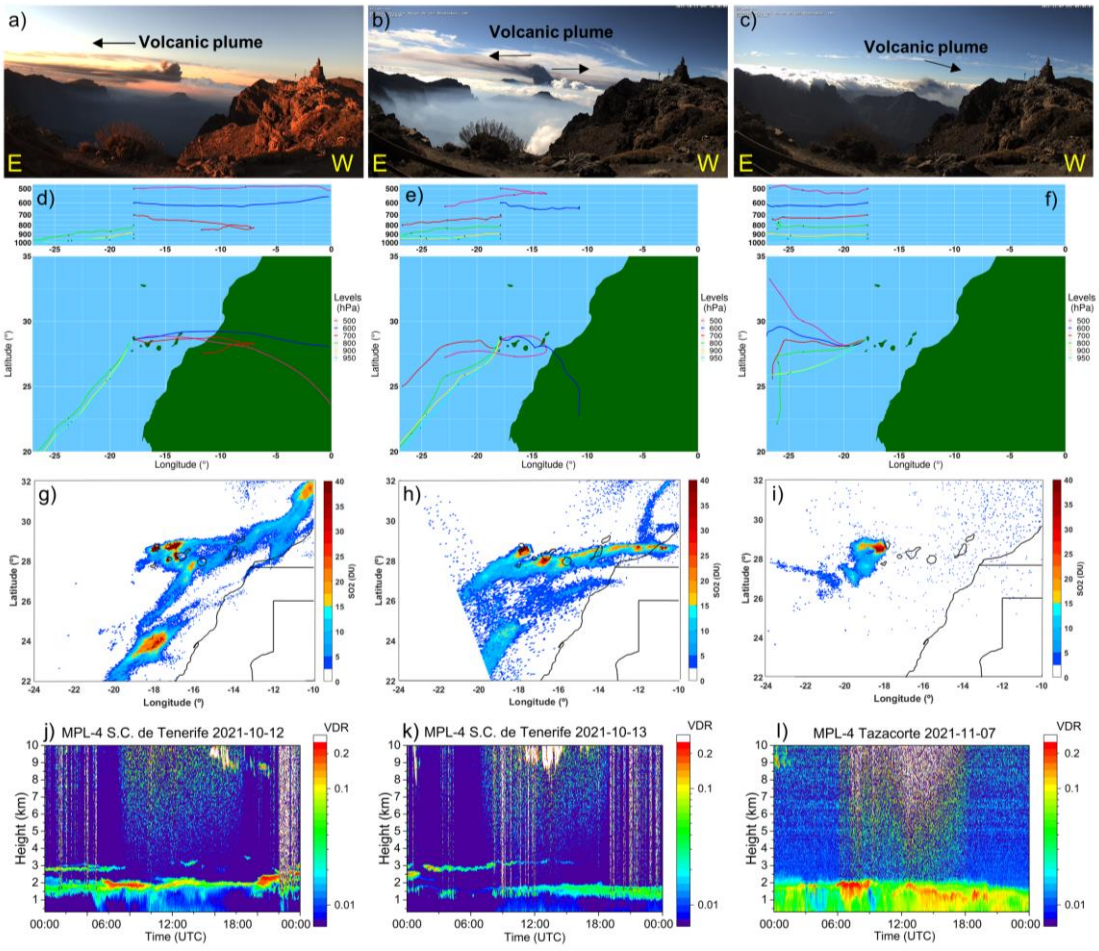

Figure 23.13. Images taken from webcam at Roque de los Muchachos facing south for a) 12/10/2021 07:15 UTC, b) 13/10/2021 10:30 UTC and c) 7/11/2021 09:45 UTC. Credit: Proyecto EELabs, IAC (Instituto Astrofísico de Canarias). Note that the East direction is shown on the left of the image and West on the right. d) to f) Forward trajectories (72 h), starting point at the eruptive centre, from FLEXTRA using ERA5 reanalysis at six pressure levels (950, 900, 800, 700, 600 and 500 hPa). g) to i) Satellite column integrated SO_2 from TROPOMI. Credit: Copernicus Sentinel-5P TROPOMI. Micro-pulse lidar volume depolarisation ratio profiles extracted for Santa Cruz, j) (12/10/ 2021) and k) (13/10/2021) and Tazacorte l) (7/11/2021). Reprinted from Milford et al. (2023).

23.6 Meteors observed during the volcanic eruption

A description of the La Palma 2021 volcanic eruption and its meteors is presented in García et al. (2022a). Some of the images presented in this publication are shown here (Figs. 23.14-23.17).

Figure 23.14. Image of pyroclastic emissions, ash, gases (mainly water vapour) and elemental sulphur deposits on the volcanic cone. Image taken from Tacande (El Paso, 13/11/2021, LuzLux/AEMET).

Figure 23.15. Image of an ash whirlwind over the volcanic lava flow. Image taken from La Montaña de La Laguna (15/11/21, LuzLux/AEMET).

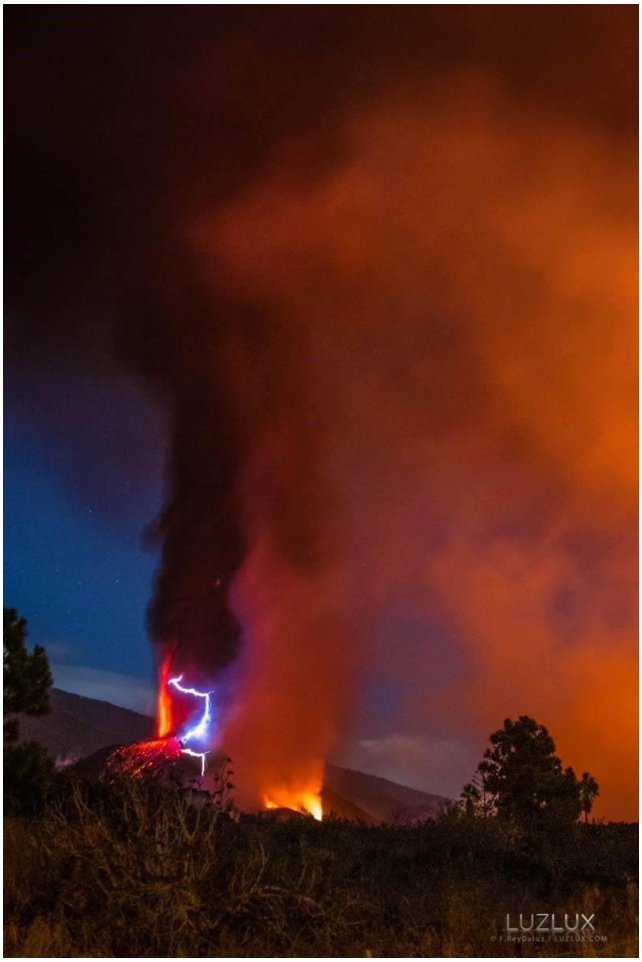

Figure 23.16. Image of volcanic lightning in the volcanic plume. Image taken from Tacande (El Paso, 15/11/21, LuzLux/AEMET).

Figure 23.17. Image of volcanic lightning in the volcanic plume. Image taken from Tacande (El Paso, 15/11/21, LuzLux/AEMET).

23.7 Izaña Observatory

The proximity to La Palma (~140 km) of the Izaña Observatory and its location in the free troposphere at 2373 m a.s.l. (Fig. 23.18), resulted in it being affected at times by the almost unperturbed volcanic plume which allowed various aspects of the volcanic eruption to be studied in greater depth.

23.7.1 In situ SO_2 and Action guide for high levels of volcanic pollution

In addition to the direct impact of the volcanic eruption on air quality in La Palma, several episodes of high levels of SO_2 concentrations were recorded at Izaña Observatory (see Fig. 23.11d). Due to the transport of the volcanic plume injected into the lower-middle layers of the troposphere during the eruption (e.g. Fig. 23.19), SO_2 concentrations measured at IZO were sometimes higher than the values measured at the air quality stations located in La Palma, and on occasions exceeded pollution thresholds established by the European air quality directives and the WHO Air Quality Guidelines.

Figure 23.18. View of the La Palma volcanic plume from the IZO tower on 3 November 2021. In the foreground, the air intake for SO_2 measurement. (Photo: C. Bayo).

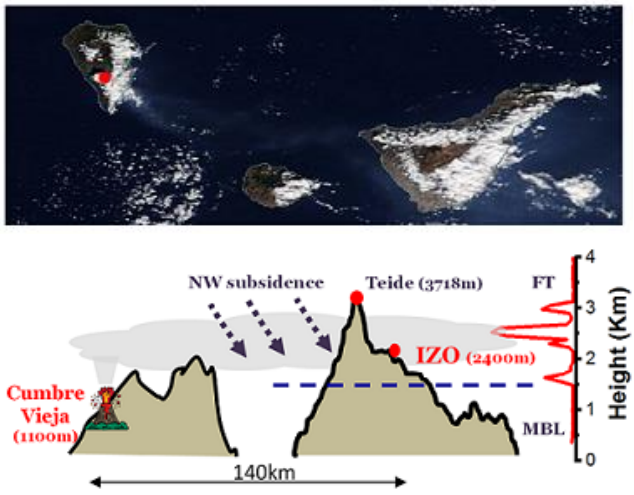

Figure 23.19. Upper panel shows the image captured by the MODIS sensor aboard NASA Terra satellite (red dot indicates the eruptive centre) (https://worldview.earthdata.nasa.gov/) for 19/11/2021, demonstrating the impact of the plume on Tenerife. Lower panel shows the height profile of La Palma and Tenerife islands, plus the aerosol vertical profile (from SCO Lidar) on the right-hand side, also for 19/11/2021.

As a consequence of the first episode of very high levels of volcanic SO_2 recorded at IZO, IARC established an internal operating procedure aimed at minimizing the health risks associated with the presence of volcanic pollution. An alert system with a web interface was developed, which facilitated real-time monitoring of SO_2 concentrations (Fig. 23.20). The alert system was based on information collected in international guidelines, published by Health Departments and by International Volcanic Risk Networks of regions where exposure to the volcanic pollution is much more common, such as Hawaii or Iceland, and on the thresholds established by the European Commission (EC, 2008) and WHO (WHO, 2021). From this emergency IZO procedure, an "Action guide for high levels of volcanic pollution. Izaña Atmospheric Observatory" has been published by AEMET (Prats et al., 2022).

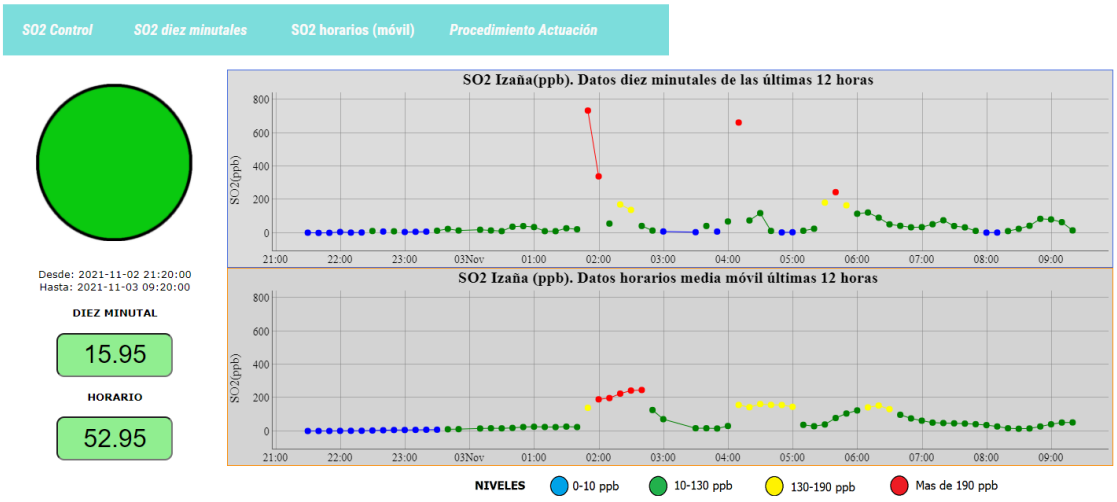

Figure 23.20. Alert system for high levels of volcanic pollution at IZO, applied between 02/11/2021 (21h) and 03/11/2021 (09h). Upper panel shows SO_2 ten-minute mean concentrations. Lower panel shows SO_2 hourly running mean. The colour of the circle indicates the IZO alert level, in accordance with the SO_2 concentration, with specific actions to follow depending on the alert level.

23.7.2 In situ SO_2, CO_2 and CO

As detailed in the previous sections, the transport of the volcanic plume injected into the lower-middle layers of the troposphere during the eruption caused clouds of ash and volcanic gases to disperse over the Canary archipelago and the Atlantic Ocean, as shown in Fig. 23.19. This resulted in the Izaña Observatory recording events of the direct impact of the volcanic dispersion cloud causing the concentrations of gases such as SO_2, CO_2 and CO to exceed, by several orders of magnitude, the values of these gases under usual background conditions (Fig. 23.21). The aerosol vertical profile (from SCO Lidar) for 19/11/2023 is presented in Fig. 23.19 and this demonstrates that the volcanic plume peak was detected at approximately the same altitude as Izaña Observatory (2.4 km a.s.l).

During these events, SO_2 in situ concentrations, one of the main tracers of volcanic emissions (Oppenheimer et al., 2009), frequently exceeded 100 ppb (Fig. 23.21a), with background concentrations below 1 ppb. Simultaneously, these episodes were accompanied by significant increases in other secondary gases emitted, such as CO_2 and CO (Fig. 23.21b-c).

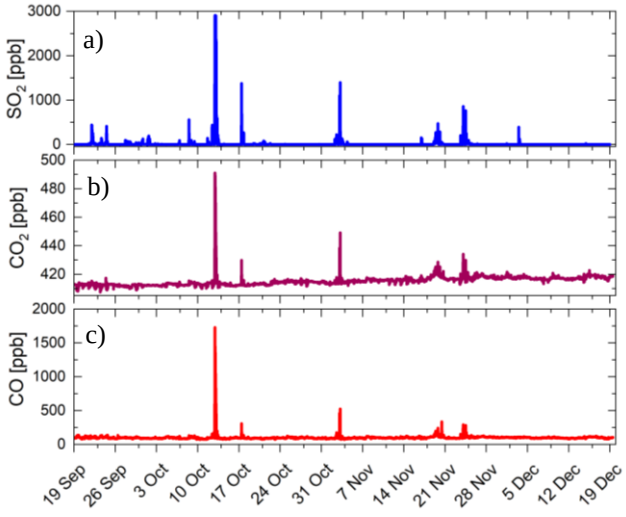

Figure 23.21. Time series of a) SO_2, b) CO_2 and c) CO surface concentrations at Izaña Observatory, 19/9/2021-19/12/2021.

The most intense event was recorded on 12 October 2021, with a duration of 8 hours, during which the measurement range of the SO_2 analyser (3000 ppb) was exceeded. In the same episode, CO_2 reached a concentration of 490 ppm (an increase of 80 ppm with respect to the seasonal value) and CO increased to 1,600 ppb (an increase of 1,500 ppb with respect to the seasonal value). After the episodes, concentrations of these gases returned to their background conditions (SO_2) or their seasonal levels (CO_2 and CO).

23.7.3 Total column SO_2

Total column SO_2 values are available from three independent instruments in Izaña Observatory (Brewer, Pandora, and FTIR). These three techniques showed a good agreement, they were detecting the impact of the volcanic plume during the three months of the 2021 eruption period and observed the maximum total column SO_2 on 24 September 2021 (Fig. 23.22).

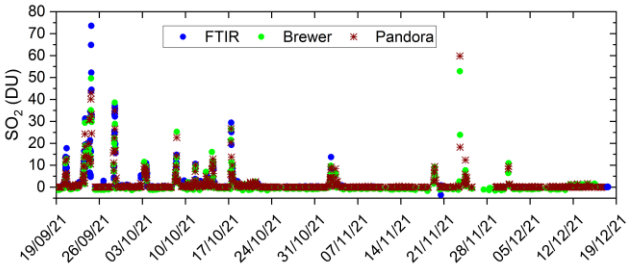

Figure 23.22. Total column SO_2 from Brewer, Pandora, and FTIR instruments in IZO (19/9/2021- 19/12/2021).

Note that the spectrometers measure solar absorption spectra, thus recording the absorption footprint of gases present throughout the atmospheric column, unlike the in-situ analysers (Section 23.7.2), which record concentrations at surface level. An example day (9 October 2021) is shown in Fig. 23.23, in which it is observed that the volcanic plume does not directly affect Tenerife on this day, due to prevailing northerly winds. However, the remote sensing instruments (Brewer, Pandora, and FTIR) only require that the plume to be in the direct path between the Sun and the instrument, as depicted in the lower panel of Fig. 23.23. For more details of the measurement techniques see García et al. (2022c), Hedelt et al. (2022) and Zerefos et al. (2017).

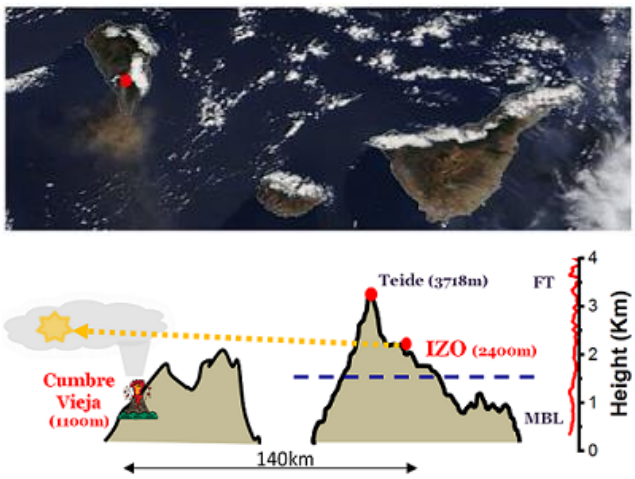

Figure 23.23. Upper panel shows the image captured by the MODIS sensor aboard NASA Terra satellite (red dot indicates the eruptive centre) (https://worldview.earthdata.nasa.gov/) for 9/10/2021. Lower panel shows the height profile of La Palma and Tenerife islands, plus the aerosol vertical profile (from SCO Lidar) on the right-hand side, also for 9/10/2021.

23.7.4 Spectral Aerosol Radiative Forcing and Efficiency of the La Palma Volcanic Plume over the Izaña Observatory

One of the scientific aspects that IARC-AMET investigated in greater depth at the research level was the climate effects of the volcanic aerosols. García et al. (2023b) conducted a study of the spectral direct radiative forcing (ΔF) and efficiency (ΔF^{eff}) estimated from solar radiation measurements performed with an EKO MS-711 grating spectroradiometer at IZO during three events characterised by the presence of different types of aerosols: fresh volcanic aerosols, Saharan mineral dust, and a mixture of volcanic and Saharan dust aerosols.

Three case studies were identified using ground-based (lidar) data, satellite-based (TROPOMI) data, reanalysis data (Modern-Era Retrospective Analysis for Research and Applications, version 2, MERRA-2), and backward trajectories (FLEXTRA), and subsequently characterised in terms of optical and micro-physical properties using ground-based sun-photometry measurements. Despite the ΔF of the volcanic aerosols being greater than that of the dust events (associated with the larger aerosol load present), the ΔF^{eff} was found to be lower (Figure 23.24).

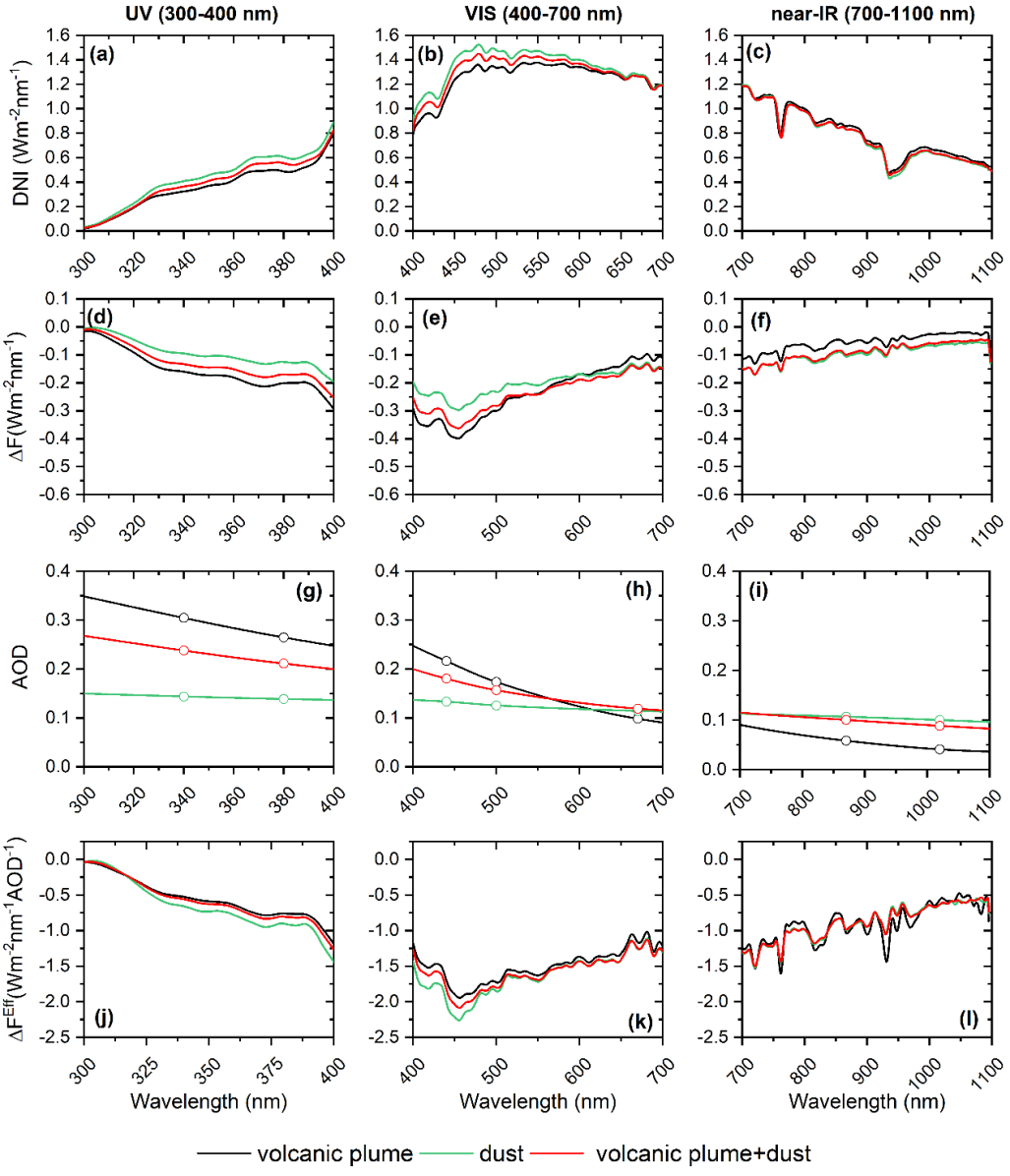

Figure 23.24. Spectral direct normal irradiance (DNI, W m^{-2} nm^{-1}) (a–c), aerosol direct radiative forcing (ΔF, Wm^{-2} nm^{-1}) (d–f), and aerosol direct radiative forcing efficiency (ΔFeff, W m^{-2} $nm^{-1}AOD^{-1}$) (j–l), considering the AOD at each measured wavelength of the EKO (g–i), for the UV (300–400 nm), VIS (400–700 nm), and near-IR (700–1100 nm) spectral ranges at an SZA of 30° and for the three case studies at the IZO: volcanic plume (black), dust (green), and volcanic plume + dust (red). The circles in (g–i) represent the AOD performed by CIMEL-AERONET. Reprinted from García et al. (2023b).

23.7.5 In situ and Column Aerosols

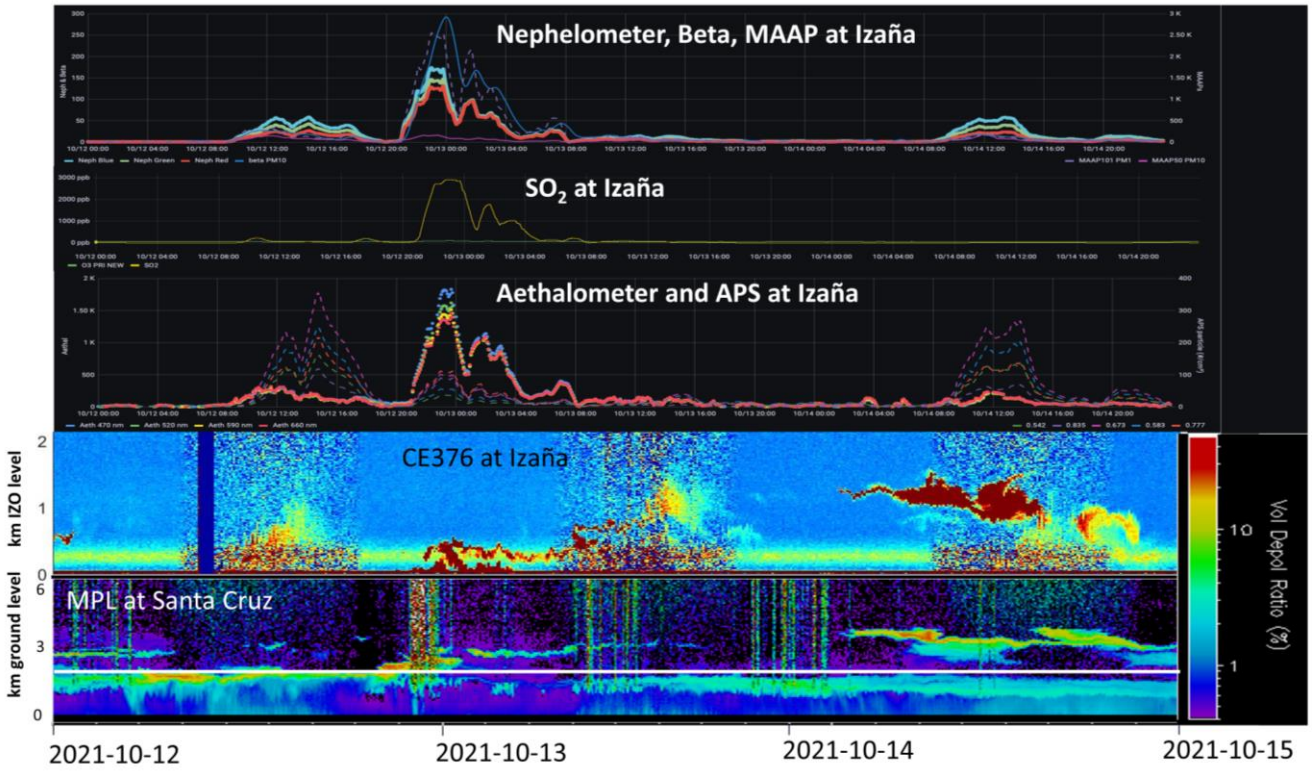

Figure 23.25. Characterization of a volcanic event (12-15 October 2021) at Tenerife from a multi-instrumental perspective. Nephelometer, PM_{10} (Beta), MAAP, Aethalometer, APS and lidar (CE376) measurements were conducted at Izaña Observatory, while MPL lidar measurements were conducted at Santa Cruz Observatory (the white horizontal line indicates the altitude of Izaña Observatory). SO_2 measurements at IZO, conducted with a UV fluorescence analyser (Thermo 43C-TL), were also included in this analysis.

Another aspect of the volcanic eruption being investigated is the study of the aerosol properties of the volcanic plume arriving to Tenerife from a multi-instrumental perspective. Aerosol properties observed with remote and in-situ techniques during a 3-day event are shown in Figure 23.25 along with in situ SO_2 mixing ratio data. This plot shows data from the Aerosol In Situ programme at Izaña Observatory from the following instruments: nephelometer (scattering coefficient in 1/Mm); Beta (PM_{10} in µg m^{-3}); MAAP (black carbon content in ng m^{-3}); Aethalometer (black carbon content in ng m^{-3}) and APS (coarse particle concentration per cm3). SO_2 in situ concentration measured with a UV fluorescence analyser (Thermo 43C-TL) are also shown to aid interpretation. Lidar profiles from Izaña Observatory (CE376) and from Santa Cruz Observatory (MPL-4B) are also shown in the bottom panel of Fig. 23.25 (showing volume depolarization ratio in %).

We can observe at the end of 12 October 2021 the presence of a strong peak in SO_2 mixing ratio (around 3000 ppb) with the subsequent increase in the scattering and absorption of aerosols at Izaña Observatory. Looking at the lidar profiles, we can point to the presence of the volcanic layer reaching Tenerife, probably as a mixture of sulphates and ash, by looking at the depolarization values (< 20%). Another layer was also observed on 14 October 2021, located at about 3.5 km altitude, with no increase of in situ SO_2 at IZO.

This elevated layer was however detected in the atmospheric column by means of remote sensing instruments such as the lidar (CE376), Brewer or Pandora (see Fig. 23.22).

23.8 Low-cost observations

In addition to the measurements described above, a fast deployment of low-cost, multi-sensor system of observations was trialed during the 2021 La Palma volcanic eruption (Pacheco et al., 2022). The experiment consisted of a proximal network of different stations measuring CO_2, SO_2, PM_{10}, $PM_{2.5}$, temperature and humidity; a set of trials to intercept the eruptive plume with weather balloons to measure in-situ the same parameters; a distal aethalometer to detect particles from the distal plume; and a set of buoys to monitor hydroacoustic and environmental parameters in the proximity of the lava deltas. The automatic data processing and different communications were also tested. The results of volcanic plume characterization and real-time data production demonstrated the relevance of this alternative monitoring concept.

23.9 Communication with Media

During the 2021 La Palma volcanic eruption, IARC-AEMET personnel gave various interviews to the media (television, radio and newspaper). Some of these interviews or articles can be found here on the IARC web page.

This section has described some of the activities carried out by IARC-AEMET during the 2021 La Palma volcanic eruption in the emergency response and afterwards in the analysis of data which is still ongoing.

Currently, we have participated as authors or co-authors in the following publications: ACTRIS (2021), Álvarez-Losada et al. (2022), Barreto et al. (2022a, b), Bedoya-Velásquez et al. (2022), Córdoba-Jabonero et al. (2023), García et al. (2022a, b, c), García et al. (2023a, b), Hedelt et al. (2022), Milford et al. (2023), Pacheco et al. (2022), Prats et al. (2022a, b), Salgueiro et al. (2023), Sicard et al. (2022) and Taquet et al. (2022).

23.10 References

ACTRIS, ACTRIS-Spain coordinating unprecedented actions for the Cumbre Vieja volcanic emergency, November 2021. Available at: https://www.actris.eu/news-events/news/actris-spain-coordinating-unprecedented-actions-cumbre-vieja-volcanic-emergency

Álvarez-Losada, O., A. Barreto, O.E. García, R. Román, M. Sicard, V. Rizi, R. Roininen, P.M Romero-Campos, Y. González, S. Rodríguez, R.D. García, C. Torres, M. Iarlori, E. Cuevas, D. Suárez, R. Ramos, C. Córdoba-Jabonero, J. de la Rosa, A. Rodríguez-Gómez, C. Muñoz-Porcar, A. Comerón, A. Bedoya-Velásquez, J.C. Antuña-Sanchez, V. Neustroev, E. Pietropaolo, Y. Lopez-Darias, M.A. López-Cayuela, C. Carvajal-Pérez, J.J. Bustos, O. Álvarez, C. Toledano, C. Aramo, J. Vilches, R. González, F.A. Almansa, R. Ceolato, N. Taquet, Thomas Boulesteix, M. Martínez, N. Prats, A. Redondas, C. Bayo, V. Carreño, C. López, S.L. León, P.P. Rivas, A. Alcántara, F. Parra, C. López, P. Martín, Erupción volcánica de La Palma: caracterización de los aerosoles y gases volcánicos emitidos desde una perspectiva sinérgica, 10ª Asamblea Hispano Portuguesa de GEodesia y Geofísica, Toledo, 28 November-1 December, 2022.

Barreto, O.E. García, R. Román, M. Sicard, V. Rizi, R. Roininen, P.M Romero-Campos, Y. González, S. Rodríguez, R.D. García, C. Torres, M. Iarlori, E. Cuevas, C. Córdoba-Jabonero, J. de la Rosa, A. Rodríguez-Gómez, C. Muñoz-Porcar, A. Comerón, A. Bedoya-Velásquez, J.C. Antuña-Sanchez, V. Neustroev, E. Pietropaolo, Y. Lopez-Darias, M.A. López-Cayuela, C. Carvajal-Pérez, J.J. Bustos, O. Álvarez, C. Toledano, C. Aramo, J. Vilches, R. González, F.A. Almansa, R. Ceolato, N. Taquet, N. Prats, A. Redondas, C. Bayo, R. Ramos, V. Carreño, S.L. León, P.P. Rivas, A. Alcántara, C. López, P. Martín, La Palma Volcano Eruption: Characterisation of Volcanic Aerosols and Gas Emissions from a Synergetic Perspective, International Radiation Symposium (IRS), Thessaloniki (Greece), 4-8 July, 2022a.

Barreto, A., M. Sicard, O.E. García, R. Román, V. Rizi, R. Roininen, P.M Romero-Campos, Y. González, S. Rodríguez, R.D. García, C. Torres, M. Iarlori, E. Cuevas, D. Suárez, R. Ramos, C. Córdoba-Jabonero, J. de la Rosa, A. Rodríguez-Gómez, C. Muñoz-Porcar, A. Comerón, A. Bedoya-Velásquez, J.C. Antuña-Sanchez, V. Neustroev, E. Pietropaolo, Y. Lopez-Darias, M.A. López-Cayuela, C. Carvajal-Pérez, J.J. Bustos, O. Álvarez, C. Toledano, C. Aramo, J. Vilches, R. González, F.A. Almansa, R. Ceolato, N. Taquet, Thomas Boulesteix, M. Martínez, N. Prats, A. Redondas, C. Bayo, V. Carreño, C. López, S.L. León, P.P. Rivas, A. Alcántara, F. Parra, P. Martín, La Palma Volcano Eruption: Characterisation of Volcanic Aerosols and Gas Emissions from a Synergetic Perspective, Congreso Nacional de Medio Ambiente (CONAMA), 21-24 November, Madrid, 2022b.

Bedoya-Velásquez, A.E.; Hoyos-Restrepo, M.; Barreto, A.; García, R.D.; Romero-Campos, P.M.; García, O.; Ramos, R.; Roininen, R.; Toledano, C.; Sicard, M.; Ceolato, R. Estimation of the Mass Concentration of Volcanic Ash Using Ceilometers: Study of Fresh and Transported Plumes from La Palma Volcano. Remote Sens. 14, 5680. https://doi.org/10.3390/rs14225680, 2022

Josse B., Simon P. and V.-H. Peuch, Rn-222 global simulations with the multiscale CTM MOCAGE, Tellus, 56B, 339-356, 2004.

Córdoba-Jabonero, C., M. Sicard, Á. Barreto, C. Toledano, M. Á. López-Cayuela, C. Gil-Díaz, O. García, C. V. Carvajal-Pérez, A. Comerón, R. Ramos, C. Muñoz-Porcar, A. Rodríguez-Gómez, Fresh volcanic aerosols injected in the atmosphere during the volcano eruptive activity at the Cumbre Vieja area (La Palma, Canary Islands): Temporal evolution and vertical impact, Atmospheric Environment, Volume 300, 2023, 119667, ISSN 1352-2310, https://doi.org/10.1016/j.atmosenv.2023.119667.

EEA, 2021. European Union emission inventory report 1990-2019. EEA Report No 05/2021 https://doi.org/10.2800/701303.

García, O.E., Cuevas, E., Rivas, P.P., Torres, C., León-Luis, S.F. and Taquet N. Synergy between surface and column measurements at Izaña Global Atmospheric Watch station: application to the volcanic eruption on La Palma. Information Note ICOS-Spain Nº2. 2021. Available at https://icos-spain.aemet.es/

García, O., Rey, F., Bullón, F., Suárez, D., Cuevas, E., & Ramos, R. (2022a). La erupción volcánica de La Palma y sus meteoros. Revista Tiempo Y Clima, 5(76). https://pub.ame-web.org/index.php/TyC/article/view/2517.

García, O., Suárez, D., Cuevas, E., Ramos, R., Barreto, África, Hernández, M., Quintero, V., Toledano, C., Sicard, M., Córdoba-Jabonero, C., Riz, V., Roininen, R., López, C., Vilches, J., Weiss, M., Carreño, V., Taquet, N., Boulesteix, T., Fraile, E., Torres, C., Prats, N., Alcántara, A., León, S. ., Rivas, P., Álvarez, Óscar, Parra, F., de Luis, J., González, C., Armas, C., Romero, P., de Bustos, J., Redondas, A., Marrero, C., Milford, C., Román, R., González, R., López-Cayuela, M., Carvajal-Pérez, C., Chinea, N., García, R. ., Almansa, F., González, Y., Bullón, F., Poggio, M., Rivera, C., Bayo, C., & Rey, F. (2022b). La erupción volcánica de La Palma y el papel de la Agencia Estatal de Meteorología. Revista Tiempo Y Clima, 5(76). https://pub.ame-web.org/index.php/TyC/article/view/2516

García, O. W. Stremme, N. Taquet, F. Hase, I. Ortega, J. Hannigan, D. Smale, C. Vigouroux, M. Grutter, T. Blumenstock, M. Schneider, A. Redondas Sulphur dioxide from ground-based Fourier transform infrared spectroscopy: application to volcanic emissions, IRWG-NDACC Meeting 2022, 28 June-1 July, 2022c.

García, O., García, R. D., Cuevas-Agulló, E., Barreto, Á., Cachorro, V. E., Marrero, C., Almansa, F., Ramos, R., Álvarez, Ó., and Pó, M.: Spectral Aerosol Radiative Forcing and Efficiency of the La Palma Volcanic Plume over the Izaña Observatory, EGU General Assembly 2023, Vienna, Austria, 24–28 Apr 2023, EGU23-13198, https://doi.org/10.5194/egusphere-egu23-13198, 2023a.

García, R.D.; García, O.E.; Cuevas-Agulló, E.; Barreto, Á.; Cachorro, V.E.; Marrero, C.; Almansa, F.; Ramos, R.; Pó, M. Spectral Aerosol Radiative Forcing and Efficiency of the La Palma Volcanic Plume over the Izaña Observatory. Remote Sens. 2023b, 15, 173. https://doi.org/10.3390/rs15010173

González, P.J., 2022. Volcano-tectonic control of cumbre vieja. Science 375, 1348–1349. https://doi.org/10.1126/science.abn5148.

Hedelt, P., Loyola, D., Redondas, A.., Barreto, A., Garcia, O., Doppler, L. and Reichardt, J. Analysis of the 2021 Cumbre Vieja eruption and the long-range transport of SO_2 to Europe using TROPOMI and ground-based measurements, Sentinel-5P Mission: 5 Years Anniversary Conference, Taormina (Italy), 10 – 14 October 2022.

Milford, C.; Torres, C, Vilches, J.; Gossman, A.K; Weis, F.; Suárez-Molina, D.; García, O.E.; Prats, N.; Barreto, A.; García, R.D.; Bustos, J.J.; Marrero, C. L.; Ramos, R.; Chinea, N.; Boulesteix, T.; Taquet, N.; Rodríguez, S.; López-Darias, J.; Sicard, M.; Córdoba-Jabonero, C.; Cuevas, E. Impact of the 2021 La Palma volcanic eruption on air quality: Insights from a multidisciplinary approach, Science of The Total Environment, Volume 869, 2023, 161652, ISSN 0048-9697, https://doi.org/10.1016/j.scitotenv.2023.161652.

Oppenheimer, C., P. Kyle, F. Eisele, J. Crawford, G. Huey, D. Tanner, S. Kim, L. Mauldin, D. Blake, A. Beyersdorf, M. Buhr, and D. Davis: Atmospheric chemistry of an Antartic volcanic plume, J. Geophys. Res.-Atmos., 115 D04303, doi:10.1029/2009JD011910, 2009.

Pacheco, J., Moutinho, A., Henriques, D., Martins, M., Hernández, P., Oliveira, S., Matos, T., Silva, D., Viveiros, F., Barrancos, J., Henriques, D., Pèrez, N., Padrón, E., Melián, G., Barreto, A., Gonzalez, Y., Rodríguez, S., Cuevas, E., Ramos, R., Fialho, P., Goulart, C., Gonçalves, L., Faria, C., and Rocha, J.: Low-cost, fast deployment multi-sensor observations of the 2021 Cumbre Vieja eruption , EGU General Assembly 2022, Vienna, Austria, 23–27 May 2022, EGU22-8830, https://doi.org/10.5194/egusphere-egu22-8830, 2022.

PEVOLCA, 2021. Scientific Committee Report 25/12/2021: Actualización de la actividad volcánica en Cumbre Vieja (La Palma). . https://info.igme.es/eventos/Erupcionvolcanica-la-palma/pevolca.

Prats, N., Torres, C., Bayo, C., Ramos, R., Cuevas, E. Guía de actuación ante niveles altos de contaminación volcánica. Observatorio Atmosférico de Izaña. AEMET – Publicaciones en línea. Ministerio para la Transición Ecológica y el Reto Demográfico, Agencia Estatal de Meteorología, Madrid, 2022a. NIPO: 666-22-012-X. https://doi.org/10.31978/666-22-012-X.

Prats, N., Torres, C., Bayo, C., Ramos, R., Cuevas, E. (2022b). Guía de actuación ante niveles altos de contaminación volcánica (Guideline for high levels of volcanic pollution). Poster presentado en 10ª Asamblea Hispano Portuguesa de Geodesia y Geofísica, Toledo (España), 28 Nov – 1 Dec 2022.

Salgueiro,V., J.L. Guerrero-Rascado, M.J. Costa, R. Román, A. Cazorla, A. Serrano, F. Molero, M. Sicard, C. Córdoba-Jabonero, D. Bortoli, A. Comerón, F.T. Couto, M.Á. López-Cayuela, D. Pérez-Ramírez, M. Potes, J.A. Muñiz-Rosado, M.A. Obregón, R. Barragán, D.C.F.S. Oliveira, J. Abril-Gago, R. González, C. Gíl-Díaz, I. Foyo-Moreno, C. Muñoz-Porcar, M.J. Granados-Muñoz, A. Rodríguez-Gómez, M. Herreras-Giralda, J.A. Bravo-Aranda, C.V. Carvajal-Pérez, A. Barreto, L. Alados-Arboledas, Characterization of Tajogaite volcanic plumes detected over the Iberian Peninsula from a set of satellite and ground-based remote sensing instrumentation, Remote Sensing of Environment, Volume 295, 2023, 113684, ISSN 0034-4257, https://doi.org/10.1016/j.rse.2023.113684.

Sicard, M.; Córdoba-Jabonero, C.; Barreto, A.; Welton, E.J.; Gil-Díaz, C.; Carvajal-Pérez, C.V.; Comerón, A.; García, O.; García, R.; López-Cayuela, M.-Á.; Muñoz-Porcar, C.; Prats, N.; Ramos, R.; Rodríguez-Gómez, A.; Toledano, C.; Torres, C. Volcanic Eruption of Cumbre Vieja, La Palma, Spain: A First Insight to the Particulate Matter Injected in the Troposphere. Remote Sens. 2022, 14, 2470.

Suárez Molina, D., and García Rodríguez, O., Erupción del volcán de Cumbre Vieja: Aspectos Meteorológicos y Contaminantes, Aula Francisco Morán, Asociación Meteorológica Española (AME), 28 April 2022.

Taquet, N., O. García, R. Campion, T. Boulesteix, W. Stremme,C. Rivera, M. Grutter, A. Barreto, O. Álvarez, S. León-Luis, R. Ramos, V. Carreño, F. Almansa, F. Hase, T. Blumenstock, COCCON activities during the La Palma volcano eruption: gases and aerosols observations, COCCON Meeting (on-line), 23 August 2022.

Zerefos, C. S., Eleftheratos, K., Kapsomenakis, J., Solomos, S., Inness, A., Balis, D., Redondas, A., Eskes, H., Allaart, M., Amiridis, V., Dahlback, A., De Bock, V., Diémoz, H., Engelmann, R., Eriksen, P., Fioletov, V., Gröbner, J., Heikkilä, A., Petropavlovskikh, I., Jarosławski, J., Josefsson, W., Karppinen, T., Köhler, U., Meleti, C., Repapis, C., Rimmer, J., Savinykh, V., Shirotov, V., Siani, A. M., Smedley, A. R. D., Stanek, M., and Stübi, R.: Detecting volcanic sulfur dioxide plumes in the Northern Hemisphere using the Brewer spectrophotometers, other networks, and satellite observations, Atmos. Chem. Phys., 17, 551-574, doi:10.5194/acp-17-551-2017, 2017.

24 Ocean Colour System Vicarious Calibration (OC-SVC)

The European Commission, via its Copernicus programme, invests in operational Earth Observation from space. As part of this programme, Ocean Colour (OC) instruments onboard the Sentinel-3 missions, as well as Sentinel-2, have become an essential source of data at global and regional scales for continuous monitoring, forecasting and alerting on ocean biogeochemistry and the state of marine ecosystems.

Through the Copernicus Marine Environment Monitoring Service (CMEMS), these data are supporting the implementation of European marine and environmental policies, contribute to climate studies, and empower economic activities. These activities include fisheries, aquaculture, shipping, water supply, tourism, offshore operations, and mitigation of health and economic risks associated with poor water quality.

Achieving the Copernicus objectives requires climate-quality ocean colour data with emphasis on accuracy and stability, both for long-term and cross-mission time series. The main challenge resides in the necessary stringent calibration and characterisation of the sensors, because the marine signal is only a small fraction of the radiometry acquired by the satellite at the top of atmosphere.

Limiting the uncertainty of water-leaving radiance to below 5%, as required by the Sentinel-3 Mission Requirement Document and Global Climate Observing System, cannot be achieved today with pre-launch and onboard instrument calibrations alone. Ocean Colour instruments require a complementary System Vicarious Calibration (SVC), i.e. an indirect calibration of the sensor and the processing algorithm through highly accurate and long-term sea-truth measurements (see Fig. 24.1).

EUMETSAT has been planning the development of the OC-SVC infrastructure in coordination with the EC Copernicus Programme, ESA and the EC's Joint Research Centre. The roadmap for the development of the OC-SVC infrastructure is composed of six phases. The first three phases have now been completed. More information about the Copernicus OC-SVC study can be found here.

Phase 3 concerned the infrastructure placement and in 2021, EUMETSAT initiated a study to investigate five candidate locations across European sea waters to select the optimal placement for the potential Copernicus OC-SVC infrastructure. One of the marine sites under consideration in this study is off the island of El Hierro, the furthest south-west island of the Canary Islands (Figs. 24.2 and 24.3).

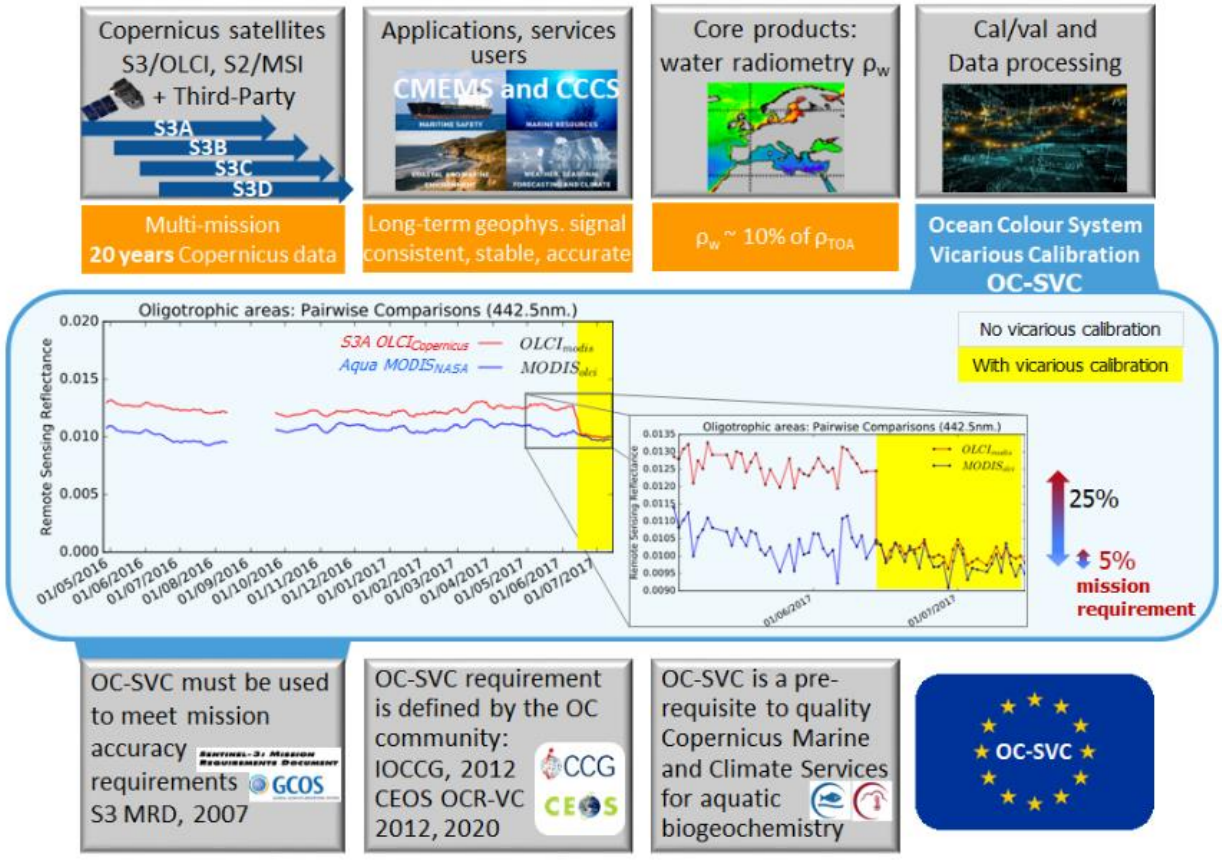

Figure 24.1. Requirements for Copernicus Ocean Colour System Vicarious Calibration Infrastructure. Credit https://www.eumetsat.int/OC-SVC.

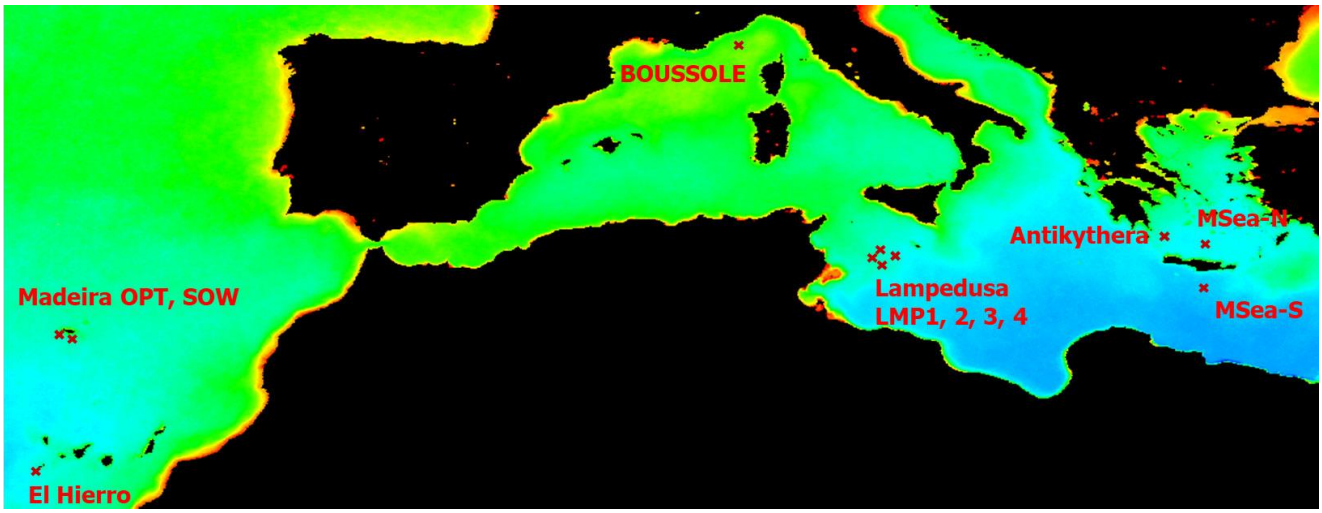

Figure 24.2. Copernicus OC-SVC infrastructure candidate locations. Credit https://www.eumetsat.int/OC-SVC-locations.

A climatological characterisation of the El Hierro candidate site, presenting key atmospheric, oceanographic and environmental features was conducted in conjunction with the Spanish Institute of Oceanography (IEO) (see Cuevas et al., 2021; Fraile-Nuez et al., 2021a, 2021b, 2021c). More information about the Copernicus OC-SVC El Hierro candidate location can be found here.

The study collected and processed suitable climatological and observational data to document various aspects, including the oceanic and atmospheric characterization of the site. The atmospheric characterization included multiple parameters such as cloud cover distribution statistics and wind velocity and direction statistics (Fig. 13.24), as well as information on aerosol parameters and absorbing gases.

In addition to other sources, this information is also derived from a historical dataset consisting of MM5 outputs with a 2 x 2 km horizontal resolution, corresponding to four daily runs that were initialized with ECMWF data. Temporal series were extracted from these data at all points of the domain to enable calculations.

As an example of part of the atmospheric characterization of the site, Fig. 24.4 shows the percentage of hours with wind speed < 6 m s^{-1}, utilising data from the high-resolution model (2 km). This demonstrates the weakening of wind speed, particularly on the leeward sides of the Canary Islands, against the prevailing north-easterly trade-winds. The weakening of wind speed on the island leeward side is observed in each season but is at a maximum in summer.

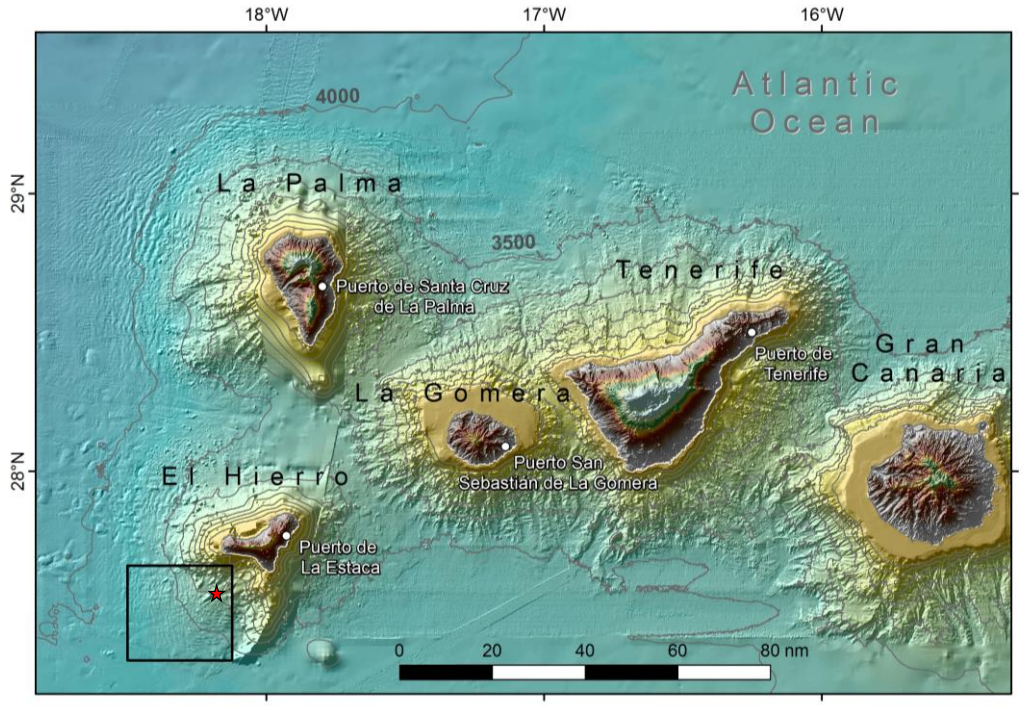

Figure 24.3. Location of the El Hierro OC-SVC candidate site. Reprinted from Fraile-Nuez, et al. (2021b).

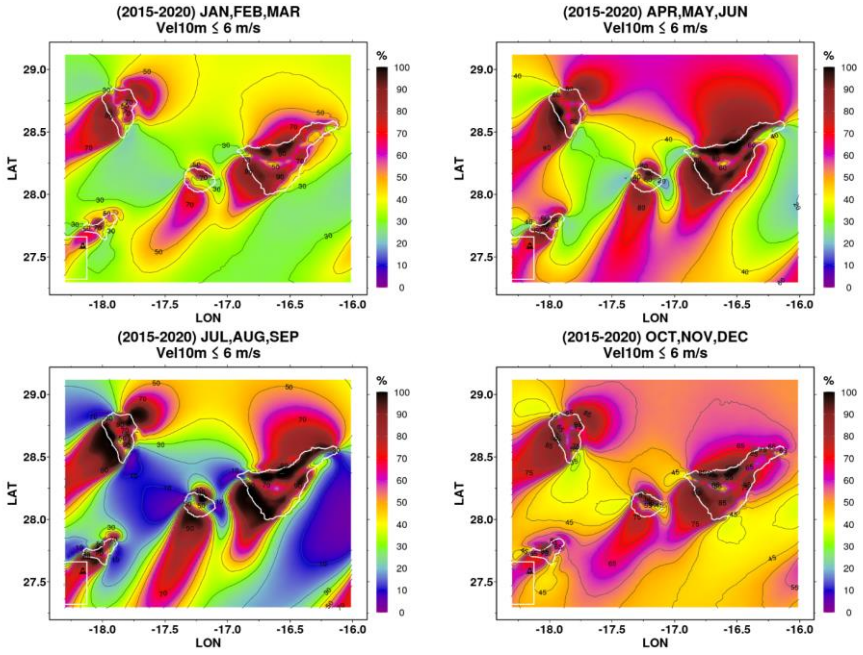

Figure 24.4. Percentage of hours with wind speed < 6 m s^{-1} for each season, data from MM5 (2015-2020). The proposed El Hierro OC-SVC domain is shown in the bottom left corner of the plots. Reprinted from Fraile-Nuez, et al. (2021b).

An international Expert Review Board conducted a review of the Candidate Locations for Copernicus OC-SVC Infrastructure (see EUMETSAT, 2022) and recommended to move to the next phase of the OC-SVC infrastructure roadmap (Fig. 24.5, Phase 4 Engineering Design) with two candidate OC-SVC locations: El Hierro (Spain) and MSEA-S (Crete, Greece).

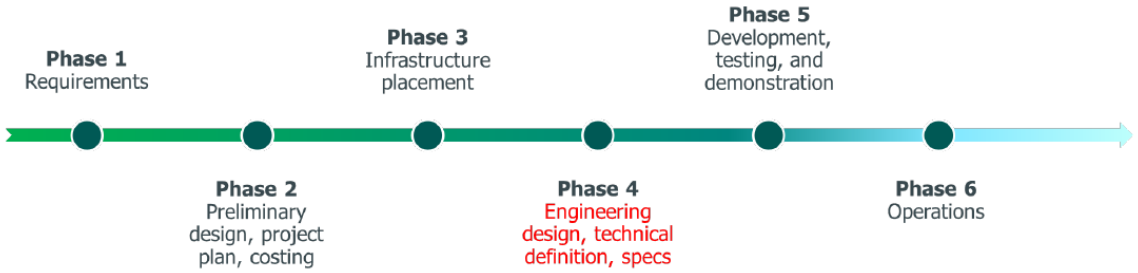

Figure 24.5. Copernicus OC-SVC infrastructure roadmap. Reprinted from EUMETSAT (2022).

24.1 References

Cuevas, E., Milford, C., Fraile-Nuez, E., Arrieta, J.M. and Vélez-Belchí, P. Climatological Characterisation of Ocean Sites for Ocean Colour System Vicarious Calibration: El Hierro (Canary Islands, Spain) Task 2 Report, Annex 4: Statistics and trends in hurricanes for the Canary Islands (EUMETSAT study report, EUMETSAT, Darmstadt, Germany), 2021. https://www.eumetsat.int/media/49928

Fraile-Nuez, E., Cuevas, E., Milford, C., Mosquera, A., Arrieta. J. M., Marrero, C., Vélez-Belchí, P. et al. Climatological Characterisation of Ocean Sites for Ocean Colour System Vicarious Calibration: El Hierro (Canary Islands, Spain), Task 1 Report: Climatological and observational data sets (EUMETSAT study report, EUMETSAT, Darmstadt, Germany), 2021a. https://www.eumetsat.int/media/49924

Fraile-Nuez, E., Cuevas, E., Milford, C., Mosquera, A., Arrieta. J. M., Marrero, C., Vélez-Belchí, P., Bustos, J.J., García, R. D., Barreto, A., García, O., Redondas, A., Romero-Campos, P. M., Berjón, A., Presas-Navarro, C., Palomino, D. and González-Vega, A. Climatological Characterisation of Ocean Sites for Ocean Colour System Vicarious Calibration: El Hierro (Canary Islands, Spain) Task 2 Report: Site Characterisation (EUMETSAT study report, EUMETSAT, Darmstadt, Germany), 2021b. https://www.eumetsat.int/media/49925

Fraile-Nuez, E., Milford, C., Arrieta, J.M., Vélez-Belchí, P., and Cuevas, E. Climatological Characterisation of Ocean Sites for Ocean Colour System Vicarious Calibration: El Hierro (Canary Islands, Spain) Task 2 Report, Annex 3: Physical safety of the El Hierro site (EUMETSAT study report, EUMETSAT, Darmstadt, Germany), 2021c. https://www.eumetsat.int/media/49927

EUMETSAT, Conclusions of the Review of Candidate Locations for Copernicus Ocean Colour System Vicarious Calibration Infrastructure (EUMETSAT study report, EUMETSAT, Darmstadt, Germany), EUM/RSP/REP/22/1303790, v5D, 27 July 2022. https://www.eumetsat.int/media/49961

25 Capacity Building Activities

During 2021-2022 IARC participated in various capacity building activities, some of which are described here. For further details of these activities, see individual sections or the IARC webpage.

25.1 InDust training school for operators of sun-photometers in North Africa

A training course funded by the Cost Action InDust and coordinated by IARC-AEMET and University of Valladolid was held in Izaña on 21-24 September 2021. Despite the COVID restrictions, 11 participants from Spain, Morocco and Tunisia joined the training course.

Figure 25.1. Participants from Morocco and Tunisia in the InDust training school held at Izaña Observatory, 21-24 September 2021.

The training focused on developing the skills of personnel from various remote stations in North Africa in operation of Cimel CE318 sun photometers that participate in AERONET. Various training activities related to the installation, uninstallation, monitoring and maintenance of the CE318 were carried out, as well as practical experiences to solve common problems related to the operation of this type of instrumentation. The purpose is to guarantee the quality of the data supplied by these stations, which play a key role in modelling of aerosol.

25.2 SDS-WAS West Africa Senegal Workshop: on-line, 3-4 February 2021

The MAC-CLIMA project aims to generate a meteorological and ocean observation system and use these observations to promote resilience and adaptation to climate change. The objectives of MAC-CLIMA are to promote the progressive creation of an institutional, scientific and social network among the countries of the cooperation area to work, in a coordinated manner, for the adaptation to and mitigation of climate change.

The cooperation area is made up of the outermost regions of Madeira, Azores and the Canary Islands and the three geographically close countries that have accepted to participate in the programme: Cape Verde, Senegal and Mauritania.

Figure 25.2. Some of the participants of the SDS-WAS West Africa Senegal Workshop, held on-line, 3-4 February 2021.

AEMET organised the SDS-WAS West Africa Workshop: Products and Forecast, and Instrumentation Guide Senegal Edition, which was held on-line, on 3-4 February 2021, in the framework of the MAC-CLIMA/INTERREG project. The objectives of the workshop were to train the personnel of the Senegal Meteorological Service in the use of the forecast products of the WMO-SDS-WAS NAMEE Regional Center, as well as in the management of the installed equipment and in the treatment of the data.

25.3 Monitoring and modeling of the chemical composition of the atmosphere: on-line, 27 September – 15 October 2021

Dr Natalia Prats (IARC-AEMET) participated in a training course, entitled: “Monitoring and modeling of the chemical composition of the atmosphere” held on-line, on 27 September - 15 October 2021. The training course was organized and coordinated by Isabel Martínez Marco (Head of Applications Area, Dept. Development and Applications, AEMET) in the framework of the WMO Regional Meteorological Training Centre (RMTC) and the Spanish Agency for International Development Cooperation (AECID).

The Knowledge Transfer, Exchange and Management Plan for the Development of Spanish Cooperation in Latin America and the Caribbean —INTERCOONECTA— which has been launched by the AECID, is an institutional strategic commitment to support cooperation in strengthening institutional capacities through the transfer and exchange of knowledge. In this way, INTERCOONECTA's general objective is to contribute to the generation of capacities in Institutions and social actors involved in human development in the region, and with the capacity to develop and implement public policies aimed at achieving greater social cohesion.

The online training course "Monitoring and modeling of the chemical composition of the atmosphere (theoretical phase)" is included in the INTERCOONECTA 2019 plan, and in turn in the International Training Strategic Plan (2021-22) of the WMO RMTC in AEMET/Spain.

The main objective is to strengthen the technical training of the professionals of the Ibero-American Meteorological and Hydrological Services that allow them to offer a better service to society through knowledge of the main chemical components and aerosols that affect health, their observation through appropriate and special networks of observation, the prediction of their concentration levels through the use of modeling of the chemical composition of the atmosphere and the preparation of warnings to the population when harmful thresholds for health are exceeded.

More than 20 students from Latin America and the Caribbean (México, Colombia, Argentina, República Dominicana, El Salvador, Costa Rica, Uruguay, Chile, Panamá, Paraguay, Honduras, Perú, Venezuela, etc.) attended this workshop. The practical phase took place in Guatemala in March 2023.

26 Scientific Communication

The main tool of scientific communication of the IARC is, undoubtedly, its webpage (http://izana.aemet.es). Scientific information and articles are regularly posted there. Also, there is a Wikipedia page. In this section, we give details of some of the science communication activities during the 2021-2022 period.

26.1 International Day of Women and Girls in Science: 17 February 2021

At a time when most of the challenges we face (health crisis, energy crisis, environmental crisis, food crisis) depend on Science and Technology, we cannot afford to do without the talent of half the population. For this reason, the Izaña Atmospheric Research Center joined several activities on 17th and 18th February 2021 to celebrate the "International Day of Women and Girls in Science". Dr Omaira García from IARC gave several talks at CEIPS Montessori, IES El Paso and IES José María Pérez Pulido, Santa Cruz de Tenerife (Tenerife), explaining the role of women in science and the scientific activities carried out by IARC, bringing our work closer to the young.

Figure 26.1. Dr Omaira García at the El Paso secondary school (La Palma), 17 Feb 2021, after giving a talk about "Women and Science: What do we do at the Izaña Atmospheric Research Center?".

26.2 Arctic Science Summit Week: March 2021

Dr África Barreto presented in the Arctic Science Summit Week (ASSW) held online in March 2021 a talk titled "Preliminary results on the third lunar/stellar AOD intercomparison campaign at Lindenberg's MOL-RAO Observatory".

26.3 VI Research Conference of the Doctoral Program in Industrial, Computer and Environmental Engineering, University of La Laguna: April 2021

Dr África Barreto presented in the VI Research Conference of the Doctoral Program in Industrial, Computer and Environmental Engineering held online in April 2021 an invited talk titled "Papel de la fotometría lunar y estelar en los estudios atmosféricos y climáticos".

26.4 2nd SOlar Radiation Based Established Techniques for aTmospheric Observations: September 2021

Dr África Barreto presented a talk on Lunar Photometry in the 2nd SOlar Radiation Based Established Techniques for aTmospheric Observations (SORBETTO) Summer School held online in September 2021.

26.5 IPC-XIII/FRC-V Symposium: September 2021

Dr África Barreto presented in the IPC-XIII/FRC-V Symposium held at PMOD (Davos) in September 2021 an invited talk titled "Lunar Photometry".

26.6 ACTRIS Week: October 2021

Dr África Barreto presented in the ACTRIS Week meeting held online between 28-29 October 2021 an invited talk titled "Characterization of volcanic aerosols from a synergetic perspective during Cumbre Vieja (La Palma) eruption".

26.7 e-Profile meeting: November 2021

Dr África Barreto presented in the e-Profile joint ET/TT meeting held online between 8-10 November 2021 an invited talk titled "Cumbre Vieja eruption on La Palma".

26.8 IX Remedia Workshop: Ecological production, sustainability and circular economy in the face of climate change: April 2022

Dr Omaira García presented an invited talk titled "Monitoring of atmospheric concentrations of greenhouse gases from various observation platforms", at the IX Remedia Workshop: Ecological production, sustainability and circular economy in the face of climate change, Córdoba (España), 21-22 April 2022.

26.9 Scientific Conferences on Light Pollution (Meteorology and Astronomy): May 2022

Dr África Barreto presented in the Scientific Conferences on Light Pollution (Meteorology and Astronomy) organized by Kuffner Observatory (Austria) held online in May 2022 an invited talk titled "Daily monitoring of atmospheric aerosols with the CE318-T photometer".

26.10 Spanish Meteorological Association (AME): 28 April 2022

David Suárez Molina (AEMET) and Dr Omaira García (IARC-AEMET) gave a presentation online to the Asociación Meteorológica Española (AME) (Spanish Meteorological Association) on 28 April 2022 (Fig. 26.2) entitled "Erupción del volcán de Cumbre Vieja: Aspectos Meteorológicos y Contaminantes". This presentation addressed the role of AEMET during the La Palma 2021 volcanic eruption. These activities included weather monitoring and prediction, monitoring and prediction of volcanic plume transport, assessment of the impact of volcanic emissions on air quality on the island of La Palma and in the Canary Islands region, as well as observation of key atmospheric compounds.

Figure 26.2. David Suárez Molina and Dr Omaira García gave a presentation online to the Asociación Meteorológica Española (AME) (Spanish Meteorological Association) on 28 April 2022, explaining the role of AEMET during the La Palma 2021 volcanic eruption.

26.11 La Palma: 18 September 2022

David Suárez Molina on behalf of AEMET and Dr Omaira García on behalf of IARC-AEMET, attended an event in La Palma on 18 September 2022, thanking the scientific community who participated in the emergency response during the La Palma 2021 volcanic eruption (Fig.26.3).

Figure 26.3. Dr Omaira García and David Suárez at the event to give thanks to the scientific community who participated in the emergency response during the La Palma 2021 volcanic eruption, 18 September 2022.

26.12 Climate Change and the current reality in the Canary Islands: 14 December 2022

David Suárez Molina and Dr Omaira García participated in the televised conference: "Climate Change in the world and the current reality in the Canary Islands", organized by the Diario de Avisos Foundation, in Santa Cruz de Tenerife, 14 December 2022 (Fig. 26.4).

Figure 26.4. David Suárez Molina and Dr Omaira García at the televised conference: "Climate Change in the world and the current reality in the Canary Islands", organized by the Diario de Avisos Foundation, Santa Cruz de Tenerife, 14 December 2022.

26.13 TeideLab images: 2021-2022

TeideLab is an initiative created between the Teide Cable Car Company and various other institutions, including IARC to produce high quality content that advances and disseminates knowledge about the natural, scientific, cultural and recreational values of Teide National Park. It seeks to facilitate collaboration between different institutions, both those with a direct presence in Teide National Park, as well as those that are particularly relevant to the interests of the Park.

Figure 26.5. Photographic images taken during the "Teide Clouds Laboratory" project from Izaña Observatory by Daniel López.

The "Teide Clouds Laboratory" project, which started in December 2015, is one of four projects within TeideLab. The project is the result of a collaboration between the IARC, the Teide Cable Car Company, and the renowned Astrophotographer Daniel López, with the main aim of registering meteorological phenomena in Teide National Park using high quality photographic images and high temporal resolution "time-lapse" videos. Cameras have been placed within the main Izaña Observatory technical tower and in a "Cloud Tower" outside the observatory to allow diurnal and nocturnal photographic images to be captured remotely (e.g. Fig. 26.5). A video presentation of the "Teide Clouds Laboratory" project can be found here. Daily sunrise and sunset images of Teide National Park collected in the TeideLab project are shared with the public through the AEMET Twitter account (e.g. Fig. 26.6).

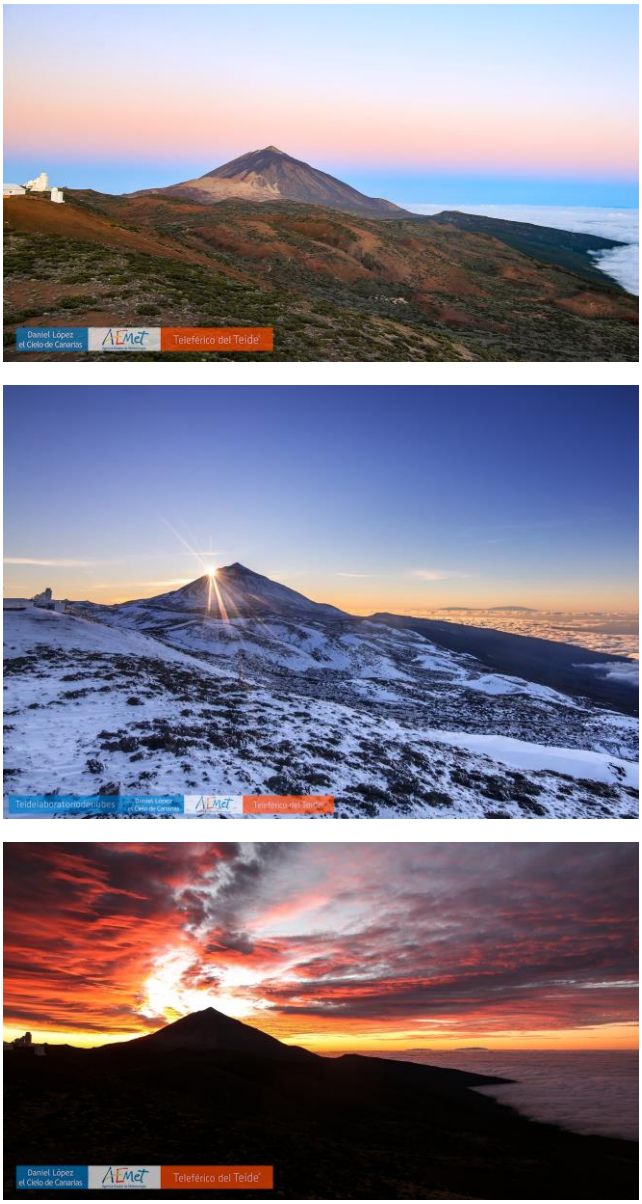

Figure 26.6 Sunrise and sunset images from Izaña Observatory "Teide Clouds Laboratory" project by Daniel López.

27 Publications

27.1 List of peer-reviewed papers

2022

Alberti, C., Hase, F., Frey, M., Dubravica, D., Blumenstock, T., Dehn, A., Castracane, P., Surawicz, G., Harig, R., Baier, B. C., Bès, C., Bi, J., Boesch, H., Butz, A., Cai, Z., Chen, J., Crowell, S. M., Deutscher, N. M., Ene, D., Franklin, J. E., García, O., Griffith, D., Grouiez, B., Grutter, M., Hamdouni, A., Houweling, S., Humpage, N., Jacobs, N., Jeong, S., Joly, L., Jones, N. B., Jouglet, D., Kivi, R., Kleinschek, R., Lopez, M., Medeiros, D. J., Morino, I., Mostafavipak, N., Müller, A., Ohyama, H., Palmer, P. I., Pathakoti, M., Pollard, D. F., Raffalski, U., Ramonet, M., Ramsay, R., Sha, M. K., Shiomi, K., Simpson, W., Stremme, W., Sun, Y., Tanimoto, H., Té, Y., Tsidu, G. M., Velazco, V. A., Vogel, F., Watanabe, M., Wei, C., Wunch, D., Yamasoe, M., Zhang, L., and Orphal, J.: Improved calibration procedures for the EM27/SUN spectrometers of the COllaborative Carbon Column Observing Network (COCCON), Atmos. Meas. Tech., 15, 2433–2463, https://doi.org/10.5194/amt-15-2433-2022, 2022.

Barreto, Á., Cuevas, E., García, R. D., Carrillo, J., Prospero, J. M., Ilić, L., Basart, S., Berjón, A. J., Marrero, C. L., Hernández, Y., Bustos, J. J., Ničković, S., and Yela, M.: Long-term characterisation of the vertical structure of the Saharan Air Layer over the Canary Islands using lidar and radiosonde profiles: implications for radiative and cloud processes over the subtropical Atlantic Ocean, Atmos. Chem. Phys., 22, 739–763, https://doi.org/10.5194/acp-22-739-2022, 2022a.

Barreto, Á., García, R. D., Guirado-Fuentes, C., Cuevas, E., Almansa, A. F., Milford, C., Toledano, C., Expósito, F. J., Díaz, J. P., and León-Luis, S. F.: Aerosol characterisation in the subtropical eastern North Atlantic region using long-term AERONET measurements, Atmos. Chem. Phys., 22, 11105–11124, https://doi.org/10.5194/acp-22-11105-2022, 2022b.

Bedoya-Velásquez, A.E.; Hoyos-Restrepo, M.; Barreto, A.; García, R.D.; Romero-Campos, P.M.; García, O.; Ramos, R.; Roininen, R.; Toledano, C.; Sicard, M.; Ceolato, R. Estimation of the Mass Concentration of Volcanic Ash Using Ceilometers: Study of Fresh and Transported Plumes from La Palma Volcano. Remote Sens. 14, 5680. https://doi.org/10.3390/rs14225680, 2022

Byrne, B., Baker, D. F., Basu, S., Bertolacci, M., Bowman, K. W., Carroll, D., Chatterjee, A., Chevallier, F., Ciais, P., Cressie, N., Crisp, D., Crowell, S., Deng, F., Deng, Z., Deutscher, N. M., Dubey, M., Feng, S., García, O., Griffith, D. W. T., Herkommer, B., Hu, L., Jacobson, A. R., Janardanan, R., Jeong, S., Johnson, M. S., Jones, D. B. A., Kivi, R., Liu, J., Liu, Z., Maksyutov, S., Miller, J. B., Miller, S. M., Morino, I., Notholt, J., Oda, T., O'Dell, C. W., Oh, Y.-S., Ohyama, H., Patra, P. K., Peiro, H., Petri, C., Philip, S., Pollard, D. F., Poulter, B., Remaud, M., Schuh, A., Sha, M. K., Shiomi, K., Strong, K., Sweeney, C., Té, Y., Tian, H., Velazco, V. A., Vrekoussis, M., Warneke, T., Worden, J. R., Wunch, D., Yao, Y., Yun, J., Zammit-Mangion, A., and Zeng, N.: National CO_2 budgets (2015–2020) inferred from atmospheric CO_2 observations in support of the Global Stocktake, Earth Syst. Sci. Data Discuss. [preprint], https://doi.org/10.5194/essd-2022-213, in review, 2022.

Chang, K.-L., Cooper, O. R., Gaudel, A., Allaart, M., Ancellet, G., Clark, H., Godin-Beekmann, S., Leblanc, T., Van Malderen, R., Nédélec, P., Petropavlovskikh, I., Steinbrecht, W., Stübi, R., Tarasick, D.W., Torres, C., (2022). Impact of the COVID-19 economic downturn on tropospheric ozone trends: An uncertainty weighted data synthesis for quantifying regional anomalies above western North America and Europe. AGU Advances, 3, e2021AV000542, https://doi.org/10.1029/2021AV000542, 2022.

Di Tomaso, E., Escribano, J., Basart, S., Ginoux, P., Macchia, F., Barnaba, F., Benincasa, F., Bretonnière, P.-A., Buñuel, A., Castrillo, M., Cuevas, E., Formenti, P., Gonçalves, M., Jorba, O., Klose, M., Mona, L., Montané Pinto, G., Mytilinaios, M., Obiso, V., Olid, M., Schutgens, N., Votsis, A., Werner, E., and Pérez García-Pando, C.: The MONARCH high-resolution reanalysis of desert dust aerosol over Northern Africa, the Middle East and Europe (2007–2016), Earth Syst. Sci. Data, 14, 2785–2816, https://doi.org/10.5194/essd-14-2785-2022, 2022.

Hannigan, J.W., I. Ortega, S. B. Shams, T. Blumenstock, J. E. Campbell, S. Conway, V. Flood, O. García, D. Griffith, M. Grutter, F. Hase, P. Jeseck, N. Jones, E. Mahieu, M. Makarova, M. De Mazière, I. Morino, I. Murata, T. Nagahama, H. Nakijima, J. Notholt, M. Palm, Anatoliy Poberovskii, M. Rettinger, J. Robinson, A. N. Röhling, M. Schneider, C. Servais, D. Smale, W. Stremme, K. Strong, R. Sussmann, Y. Te, C. Vigouroux, T. Wizenberg, Global atmospheric OCS trend analysis from 22 NDACC stations. Journal of Geophysical Research: Atmospheres, 127, e2021JD035764. https://doi.org/10.1029/2021JD035764, 2022.

García, O. E., Sanromá, E., Hase, F., Schneider, M., León-Luis, S. F., Blumenstock, T., Sepúlveda, E., Torres, C., Prats, N., Redondas, A., and Carreño, V.: Impact of instrumental line shape characterization on ozone monitoring by FTIR spectrometry, Atmos. Meas. Tech., 15, 4547–4567, https://doi.org/10.5194/amt-15-4547-2022, 2022.

García, O. E., Sanromá, E., Schneider, M., Hase, F., León-Luis, S. F., Blumenstock, T., Sepúlveda, E., Redondas, A., Carreño, V., Torres, C., and Prats, N.: Improved ozone monitoring by ground-based FTIR spectrometry, Atmos. Meas. Tech., 15, 2557–2577, https://doi.org/10.5194/amt-15-2557-2022, 2022.

Schneider, M., Ertl, B., Diekmann, C. J., Khosrawi, F., Weber, A., Hase, F., Höpfner, M., García, O. E., Sepúlveda, E., and Kinnison, D.: Design and description of the MUSICA IASI full retrieval product, Earth Syst. Sci. Data, 14, 709–742, https://doi.org/10.5194/essd-14-709-2022, 2022.

Schneider, M., Ertl, B., Tu, Q., Diekmann, C. J., Khosrawi, F., Röhling, A. N., Hase, F., Dubravica, D., García, O. E., Sepúlveda, E., Borsdorff, T., Landgraf, J., Lorente, A., Butz, A., Chen, H., Kivi, R., Laemmel, T., Ramonet, M., Crevoisier, C., Pernin, J., Steinbacher, M., Meinhardt, F., Strong, K., Wunch, D., Warneke, T., Roehl, C., Wennberg, P. O., Morino, I., Iraci, L. T., Shiomi, K., Deutscher, N. M., Griffith, D. W. T., Velazco, V. A., and Pollard, D. F.: Synergetic use of IASI profile and TROPOMI total-column level 2 methane retrieval products, Atmos. Meas. Tech., 15, 4339–4371, https://doi.org/10.5194/amt-15-4339-2022, https://amt.copernicus.org/articles/15/4339/2022/, 2022.

Sicard, M.; Córdoba-Jabonero, C.; Barreto, A.; Welton, E.J.; Gil-Díaz, C.; Carvajal-Pérez, C.V.; Comerón, A.; García, O.; García, R.; López-Cayuela, M.-Á.; Muñoz-Porcar, C.; Prats, N.; Ramos, R.; Rodríguez-Gómez, A.; Toledano, C.; Torres, C. Volcanic Eruption of Cumbre Vieja, La Palma, Spain: A First Insight to the Particulate Matter Injected in the Troposphere. Remote Sens. 2022, 14, 2470.

Taylor, T. E., O'Dell, C. W., Crisp, D., Kuze, A., Lindqvist, H., Wennberg, P. O., Chatterjee, A., Gunson, M., Eldering, A., Fisher, B., Kiel, M., Nelson, R. R., Merrelli, A., Osterman, G., Chevallier, F., Palmer, P. I., Feng, L., Deutscher, N. M., Dubey, M. K., Feist, D. G., García, O. E., Griffith, D. W. T., Hase, F., Iraci, L. T., Kivi, R., Liu, C., De Mazière, M., Morino, I., Notholt, J., Oh, Y.-S., Ohyama, H., Pollard, D. F., Rettinger, M., Schneider, M., Roehl, C. M., Sha, M. K., Shiomi, K., Strong, K., Sussmann, R., Té, Y., Velazco, V. A., Vrekoussis, M., Warneke, T., and Wunch, D.: An 11-year record of XCO2 estimates derived from GOSAT measurements using the NASA ACOS version 9 retrieval algorithm, Earth Syst. Sci. Data, 14, 325–360, https://doi.org/10.5194/essd-14-325-2022, 2022.

Tu, Q., Hase, F., Schneider, M., García, O., Blumenstock, T., Borsdorff, T., Frey, M., Khosrawi, F., Lorente, A., Alberti, C., Bustos, J. J., Butz, A., Carreño, V., Cuevas, E., Curcoll, R., Diekmann, C. J., Dubravica, D., Ertl, B., Estruch, C., León-Luis, S. F., Marrero, C., Morgui, J.-A., Ramos, R., Scharun, C., Schneider, C., Sepúlveda, E., Toledano, C., and Torres, C.: Quantification of CH4 emissions from waste disposal sites near the city of Madrid using ground- and space-based observations of COCCON, TROPOMI and IASI, Atmos. Chem. Phys., 22, 295–317, https://doi.org/10.5194/acp-22-295-2022, 2022.

Tu, Q., Hase, F., Chen, Z., Schneider, M., García, O., Khosrawi, F., Blumenstock, T., Liu, F., Qin, K., Lin, S., Jiang, H., and Fang, D.: Estimation of NO_2 emission strengths over Riyadh and Madrid from space from a combination of wind-assigned anomalies and machine learning technique, Atmos. Meas. Tech. Discuss. [preprint], https://doi.org/10.5194/amt-2022-176, in review, 2022.

Vandenbussche, S.; Langerock, B.; Vigouroux, C.; Buschmann, M.; Deutscher, N.M.; Feist, D.G.; García, O.; Hannigan, J.W.; Hase, F.; Kivi, R.; Kumps, N.; Makarova, M.; Millet, D.B.; Morino, I.; Nagahama, T.; Notholt, J.; Ohyama, H.; Ortega, I.; Petri, C.; Rettinger, M.; Schneider, M.; Servais, C.P.; Sha, M.K.; Shiomi, K.; Smale, D.; Strong, K.; Sussmann, R.; Té, Y.; Velazco, V.A.; Vrekoussis, M.; Warneke, T.; Wells, K.C.; Wunch, D.; Zhou, M.; De Mazière, M. Nitrous Oxide Profiling from Infrared Radiances (NOPIR): Algorithm Description, Application to 10 Years of IASI Observations and Quality Assessment. Remote Sens. 2022, 14, 1810. https://doi.org/10.3390/rs14081810, https://www.mdpi.com/2072-4292/14/8/1810

2021

Blumenstock, T., Hase, F., Keens, A., Czurlok, D., Colebatch, O., Garcia, O., Griffith, D. W. T., Grutter, M., Hannigan, J. W., Heikkinen, P., Jeseck, P., Jones, N., Kivi, R., Lutsch, E., Makarova, M., Imhasin, H. K., Mellqvist, J., Morino, I., Nagahama, T., Notholt, J., Ortega, I., Palm, M., Raffalski, U., Rettinger, M., Robinson, J., Schneider, M., Servais, C., Smale, D., Stremme, W., Strong, K., Sussmann, R., Té, Y., and Velazco, V. A.: Characterization and potential for reducing optical resonances in Fourier transform infrared spectrometers of the Network for the Detection of Atmospheric Composition Change (NDACC), Atmos. Meas. Tech., 14, 1239–1252, https://doi.org/10.5194/amt-14-1239-2021, 2021.

Diekmann, C. J., Schneider, M., Ertl, B., Hase, F., García, O., Khosrawi, F., Sepúlveda, E., Knippertz, P., and Braesicke, P.: The global and multi-annual MUSICA IASI {H_2O, δD} pair dataset, Earth Syst. Sci. Data, 13, 5273–5292, https://doi.org/10.5194/essd-13-5273-2021, 2021.

Dogniaux, M., Crevoisier, C., Armante, R., Capelle, V., Delahaye, T., Cassé, V., De Mazière, M., Deutscher, N. M., Feist, D. G., Garcia, O. E., Griffith, D. W. T., Hase, F., Iraci, L. T., Kivi, R., Morino, I., Notholt, J., Pollard, D. F., Roehl, C. M., Shiomi, K., Strong, K., Té, Y., Velazco, V. A., and Warneke, T.: The Adaptable 4A Inversion (5AI): description and first XCO2 retrievals from Orbiting Carbon Observatory-2 (OCO-2) observations, Atmos. Meas. Tech., 14, 4689–4706, https://doi.org/10.5194/amt-14-4689-2021, 2021.

Edgardo Sepúlveda, E., Cordero, R.R., Damiani, A., Feron, S., Pizarro, J., Zamorano, F., Kivi, R., Sánchez, R. Yela, M., Jumelet, J., Godoy, A., Carrasco, J., Crespo, J.S., Seckmeyer, G., Jorquera, J.A., Carrera, J.M., Valdevenito, B., Cabrera, S., Redondas, R., & Rowe, P-M.: Evaluation of Antarctic Ozone Profiles derived from OMPS LP by using Balloon borne Ozonesondes, Nature Scientific Reports; 11:4288, https://doi.org/10.1038/s41598-021-81954-6, 2021.

Evangeliou, N., Platt, S.M., Eckhardt, S., Lund Myhre, C., Laj, P., Alados-Arboledas, L., Backman, J., Brem, B.T., Fiebig, M., Flentje, H., Marinoni, A., Pandolfi, M., Yus-Dìez, J., Prats, N., Putaud, J.P, Sellegri, K., Sorribas, M., Eleftheriadis, K., Vratolis, S., Wiedensohler, A. and Stohl, A. Changes in black carbon emissions over Europe due to COVID-19 lockdowns, Atmos. Chem. Phys., 21, 2675–2692, https://doi.org/10.5194/acp-21-2675-2021, 2021

García, R.D.; Cuevas, E.; Cachorro, V.E.; García, O.E.; Barreto, Á.; Almansa, A.F.; Romero-Campos, P.M.; Ramos, R.; Pó, M.; Hoogendijk, K.; Gross, J: Water Vapor Retrievals from Spectral Direct Irradiance Measured with an EKO MS-711 Spectroradiometer-Intercomparison with Other Techniques, . Remote Sens. 2021, 13, 350. https://doi.org/10.3390/rs13030350.

García, O. E., Schneider, M., Sepúlveda, E., Hase, F., Blumenstock, T., Cuevas, E., Ramos, R., Gross, J., Barthlott, S., Röhling, A. N., Sanromá, E., González, Y., Gómez-Peláez, Á. J., Navarro-Comas, M., Puentedura, O., Yela, M., Redondas, A., Carreño, V., León-Luis, S. F., Reyes, E., García, R. D., Rivas, P. P., Romero-Campos, P. M., Torres, C., Prats, N., Hernández, M., and López, C.: Twenty years of ground-based NDACC FTIR spectrometry at Izaña Observatory – overview and long-term comparison to other techniques, Atmos. Chem. Phys., 21, 15519–15554, https://doi.org/10.5194/acp-21-15519-2021, 2021.

Gonzalez,Y.; Commane,R.; Manninen,E.; Daube,B.C; Schiferl,L.D.; McManus,J.B.; McKain,K.; .Hintsa,E.J; Elkins, J.W.; Montzka, S. A.; Sweeney, C.; Moore,F.; Jimenez,J.-L.; Campuzano Jost, P.; . Ryerson, T. B;. Bourgeois, I; Peischl, J.; C. R.,Thompson; Ray,E.; Wennberg, P. O.; Crounse, J.; Kim, M.; Allen, H. M.; Newman, P. A.; Stephens, B. B.; Apel, E. C.; Hornbrook, R. S.; . Nault, B. A; Morgan, E.; Wofsy, S. C.: Impact of stratospheric air and surface emissions on tropospheric nitrous oxide during ATom. Atmos. Chem. Phys.21, pp. 11113 – 11132. 22/07/2021, https://doi.org/10.5194/acp-21-11113-2021

Gui, K., Che, H., Wang, Y., Xia, X., Holben, B.N., Goloub, P., Cuevas-Agulló, E., Yao, W., Zheng, Y., Zhao, H., Li, L., Zhang, X.: A global-scale analysis of the MISR Level-3 aerosol optical depth (AOD) product: Comparison with multi-platform AOD data sources, Atmospheric Pollution Research, 12, 12, 101238, ISSN 1309-1042, https://doi.org/10.1016/j.apr.2021.101238, 2021.

Hintsa, E. J., Moore, F. L., Hurst, D. F., Dutton, G. S., Hall, B. D., Nance, J. D., Miller, B. R., Montzka, S. A., Wolton, L. P., McClure-Begley, A., Elkins, J. W., Hall, E. G., Jordan, A. F., Rollins, A. W., Thornberry, T. D., Watts, L. A., Thompson, C. R., Peischl, J., Bourgeois, I., Ryerson, T. B., Daube, B. C., Gonzalez Ramos, Y., Commane, R., Santoni, G. W., Pittman, J. V., Wofsy, S. C., Kort, E., Diskin, G. S., and Bui, T. P.: UAS

Chromatograph for Atmospheric Trace Species (UCATS) – a versatile instrument for trace gas measurements on airborne platforms, Atmos. Meas. Tech., 14, 6795–6819, https://doi.org/10.5194/amt-14-6795-2021, 2021.

Marais, E. A., Roberts, J. F., Ryan, R. G., Eskes, H., Boersma, K. F., Choi, S., Joiner, J., Abuhassan, N., Redondas, A., Grutter, M., Cede, A., Gomez, L., and Navarro-Comas, M.: New observations of NO_2 in the upper troposphere from TROPOMI, Atmos. Meas. Tech., 14, 2389–2408, https://doi.org/10.5194/amt-14-2389-2021, 2021

Marquis, J. W., Oyola, M. I., Campbell, J. R., Ruston, B. C., Córdoba-Jabonero, C., Cuevas, E., Lewis, J. R., Toth, T. D., & Zhang, J.: Conceptualizing the Impact of Dust-Contaminated Infrared Radiances on Data Assimilation for Numerical Weather Prediction, Journal of Atmospheric and Oceanic Technology, 38(2), 209-221, https://doi.org/10.1175/JTECH-D-19-0125.1, 2021.

Marseille, C.; Aubé, M.; Barreto, A.; Simoneau, A. Remote Sensing of Aerosols at Night with the CoSQM Sky Brightness Data. Remote Sens. 2021, 13, 4623. https://doi.org/10.3390/rs13224623.

Rodríguez, S., Prospero, J.M., López-Darias, J., García-Alvarez, M.I., Zuidema, P., Nava, S., Lucarelli, F., Gaston, C.J., Galindo,L., Sosa, E., : Tracking the changes of iron solubility and air pollutants traces as African dust transits the Atlantic in the Saharan dust outbreaks, Atmospheric Environment, Vol. 246, 118092, ISSN 1352-2310, https://doi.org/10.1016/j.atmosenv.2020.118092, 2021.

Sha, M. K., Langerock, B., Blavier, J.-F. L., Blumenstock, T., Borsdorff, T., Buschmann, M., Dehn, A., De Mazière, M., Deutscher, N. M., Feist, D. G., García, O. E., Griffith, D. W. T., Grutter, M., Hannigan, J. W., Hase, F., Heikkinen, P., Hermans, C., Iraci, L. T., Jeseck, P., Jones, N., Kivi, R., Kumps, N., Landgraf, J., Lorente, A., Mahieu, E., Makarova, M. V., Mellqvist, J., Metzger, J.-M., Morino, I., Nagahama, T., Notholt, J., Ohyama, H., Ortega, I., Palm, M., Petri, C., Pollard, D. F., Rettinger, M., Robinson, J., Roche, S., Roehl, C. M., Röhling, A. N., Rousogenous, C., Schneider, M., Shiomi, K., Smale, D., Stremme, W., Strong, K., Sussmann, R., Té, Y., Uchino, O., Velazco, V. A., Vigouroux, C., Vrekoussis, M., Wang, P., Warneke, T., Wizenberg, T., Wunch, D., Yamanouchi, S., Yang, Y., and Zhou, M.: Validation of methane and carbon monoxide from Sentinel-5 Precursor using TCCON and NDACC-IRWG stations, Atmos. Meas. Tech., 14, 6249–6304, https://doi.org/10.5194/amt-14-6249-2021, 2021.

Steinbrecht, W., Kubistin, D., Plass-Dülmer, C., Davies, J., Tarasick, D.W., Gathen, P.V., Deckelmann, H., Jepsen, N., Kivi, R., Lyall, N., Palm, M., Notholt, J., Kois, B., Oelsner, P., Allaart, M., Piters, A., Gill, M., Van Malderen, R., Delcloo, A.W., Sussmann, R., Mahieu, E., Servais, C., Romanens, G., Stübi, R., Ancellet, G., Godin-Beekmann, S., Yamanouchi, S., Strong, K., Johnson, B., Cullis, P., Petropavlovskikh, I., Hannigan, J., Hernandez, J.L., Rodriguez, A.D., Nakano, T., Chouza, F., Leblanc, T., Torres, C., Garcia, O., Röhling, A., Schneider, M., Blumenstock, T., Tully, M., Paton-Walsh, C., Jones, N., Querel, R., Strahan, S., Stauffer, R.M., Thompson, A.M., Inness, A., Engelen, R., Chang, K.L., Cooper, O.R., COVID-19 Crisis Reduces Free Tropospheric Ozone across the Northern Hemisphere, Geophysical Research Letters, 48, e2020GL091987, https://doi.org/10.1029/2020GL091987, 2021.

27.2 List of peer-reviewed papers that use IARC data

The following references are studies that use IARC data but do not include IARC-AEMET in the co-authorship.

2022

Karbasi, S., Malakooti, H., Rahnama, M., Azadi, M., 2022. Study of mid-latitude retrieval XCO_2 greenhouse gas: Validation of satellite-based shortwave infrared spectroscopy with ground-based TCCON observations. Sci. Total Environ. 836, 155513. https://doi.org/10.1016/j.scitotenv.2022.155513

Keppens, A.; Compernolle, S.; Hubert, D.; Verhoelst, T.; Granville, J.; Lambert, J.-C. Removing Prior Information from Remotely Sensed Atmospheric Profiles by Wiener Deconvolution Based on the Complete Data Fusion Framework. Remote Sens. 2022, 14, 2197. https://doi.org/10.3390/rs14092197

Kumar, R., He, C., Bhardwaj, P., Lacey, F., Buchholz, R.R., Brasseur, G.P., Joubert, W., Labuschagne, C., Kozlova, E., Mkololo, T., 2022. Assessment of regional carbon monoxide simulations over Africa and insights into source attribution and regional transport. Atmos. Environ. 277, 119075. https://doi.org/10.1016/j.atmosenv.2022.119075

Levin, I., Hammer, S., Kromer, B., Preunkert, S., Weller, R., & Worthy, D. (2022). Radiocarbon in Global Tropospheric Carbon Dioxide. Radiocarbon, 64(4), 781-791. doi:10.1017/RDC.2021.102

Lopez, F.P.A.; Zhou, G.; Jing, G.; Zhang, K.; Tan, Y. XCO2 and XCH4 Reconstruction Using GOSAT Satellite Data Based on EOF-Algorithm. Remote Sens. 2022, 14, 2622. https://doi.org/10.3390/rs14112622

Noël, S., Reuter, M., Buchwitz, M., Borchardt, J., Hilker, M., Schneising, O., Bovensmann, H., Burrows, J. P., Di Noia, A., Parker, R. J., Suto, H., Yoshida, Y., Buschmann, M., Deutscher, N. M., Feist, D. G., Griffith, D. W. T., Hase, F., Kivi, R., Liu, C., Morino, I., Notholt, J., Oh, Y.-S., Ohyama, H., Petri, C., Pollard, D. F., Rettinger, M., Roehl, C., Rousogenous, C., Sha, M. K., Shiomi, K., Strong, K., Sussmann, R., Té, Y., Velazco, V. A., Vrekoussis, M., and Warneke, T.: Retrieval of greenhouse gases from GOSAT and GOSAT-2 using the FOCAL algorithm, Atmos. Meas. Tech., 15, 3401–3437, https://doi.org/10.5194/amt-15-3401-2022, 2022.

Peiro, H., Crowell, S., and Moore III, B.: Optimizing 4 years of CO2 biospheric fluxes from OCO-2 and in situ data in TM5: fire emissions from GFED and inferred from MOPITT CO data, Atmos. Chem. Phys., 22, 15817–15849, https://doi.org/10.5194/acp-22-15817-2022, 2022

Wang, Hengmao & Jiang, Fei & Liu, Yi & Yang, Dongxu & Wu, Mousong & He, Wei & Wang, Jun & Wang, Jing & Ju, Weimin & Chen, Jing. (2022). Global Terrestrial Ecosystem Carbon Flux Inferred from TanSat XCO_2 Retrievals. Journal of Remote Sensing. 2022. 10.34133/2022/9816536.

2021

Dahinden, F., Aemisegger, F., Wernli, H., Schneider, M., Diekmann, C. J., Ertl, B., Knippertz, P., Werner, M., and Pfahl, S.: Disentangling different moisture transport pathways over the eastern subtropical North Atlantic using multi-platform isotope observations and high-resolution numerical modelling, Atmos. Chem. Phys., 21, 16319–16347, https://doi.org/10.5194/acp-21-16319-2021, 2021.

Franco, B., Blumenstock, T., Cho, C., Clarisse, L., Clerbaux, C., Coheur, P.-F., De Mazière, M., De Smedt, I., Dorn, H.-P., Emmerichs, T., Fuchs, H., Gkatzelis, G., Griffith, D. W. T., Gromov, S., Hannigan, J. W., Hase, F., Hohaus, T., Jones, N., Kerkweg, A., Kiendler-Scharr, A., Lutsch, E., Mahieu, E., Novelli, A., Ortega, I., Paton-Walsh, C., Pommier, M., Pozzer, A., Reimer, D., Rosanka, S., Sander, R., Schneider, M., Strong, K., Tillmann, R., Van Roozendael, M., Vereecken, L., Vigouroux, C., Wahner, A., Taraborrelli, D.: Ubiquitous atmospheric production of organic acids mediated by cloud droplets. Nature 593, 233–237. https://doi.org/10.1038/s41586-021-03462-x, 2021.

Klose, M., Jorba, O., Gonçalves Ageitos, M., Escribano, J., Dawson, M. L., Obiso, V., Di Tomaso, E., Basart, S., Montané Pinto, G., Macchia, F., Ginoux, P., Guerschman, J., Prigent, C., Huang, Y., Kok, J. F., Miller, R. L., and Pérez García-Pando, C.: Mineral dust cycle in the Multiscale Online Nonhydrostatic AtmospheRe CHemistry model (MONARCH) Version 2.0, Geosci. Model Dev., 14, 6403–6444, https://doi.org/10.5194/gmd-14-6403-2021, 2021.

Massie, S. T., Cronk, H., Merrelli, A., O'Dell, C., Schmidt, K. S., Chen, H., and Baker, D.: Analysis of 3D cloud effects in OCO-2 XCO2 retrievals, Atmos. Meas. Tech., 14, 1475–1499, https://doi.org/10.5194/amt-14-1475-2021, 2021.

Noël, S., Reuter, M., Buchwitz, M., Borchardt, J., Hilker, M., Bovensmann, H., Burrows, J. P., Di Noia, A., Suto, H., Yoshida, Y., Buschmann, M., Deutscher, N. M., Feist, D. G., Griffith, D. W. T., Hase, F., Kivi, R., Morino, I., Notholt, J., Ohyama, H., Petri, C., Podolske, J. R., Pollard, D. F., Sha, M. K., Shiomi, K., Sussmann, R., Té, Y., Velazco, V. A., and Warneke, T.: XCO2 retrieval for GOSAT and GOSAT-2 based on the FOCAL algorithm, Atmos. Meas. Tech., 14, 3837–3869, https://doi.org/10.5194/amt-14-3837-2021, 2021.

Salmon, A., Quiñones, G., Soto, G., Polo, J., Gueymard, C., Ibarra, M., Cardemil, J., Escobar, R., Marzo, A., 2021. Advances in aerosol optical depth evaluation from broadband direct normal irradiance measurements. Sol. Energy 221, 206–217. https://doi.org/10.1016/j.solener.2021.04.039

Zhang, Y., Jacob, D. J., Lu, X., Maasakkers, J. D., Scarpelli, T. R., Sheng, J.-X., Shen, L., Qu, Z., Sulprizio, M. P., Chang, J., Bloom, A. A., Ma, S., Worden, J., Parker, R. J., and Boesch, H.: Attribution of the accelerating increase in atmospheric methane during 2010–2018 by inverse analysis of GOSAT observations, Atmos. Chem. Phys., 21, 3643–3666, https://doi.org/10.5194/acp-21-3643-2021, 2021.

Zhang Siqi, Bai Yan, He Xianqiang, Huang Haiqing, Zhu Qiangkun, Gong Fang. 2021. Comparisons of OCO-2 satellite derived XCO2 with in situ and modeled data over global ocean. Acta Oceanologica Sinica, 40(4): 1–8, doi: 10.1007/s13131-021-1844-9

27.3 Conference Presentations/Posters

2022

Adriaensen, S., Taylor, S., Toledano, C., Woolliams, E., Barreto, A., Berjón, A., De Vis, P., Bouvet, M.: Lunar Irradiance Model of ESA (LIME) and its application for PROBA-V radiometric calibration, Living Planet Symposium – ESA, Bonn (Germany), 23-27 May, 2022.

Álvarez, O., A. Barreto, O. García, F. Hase, T. Blumenstock, E. Sepúlveda, S. F. León-Luis, V. Carreño, A. Alcántara, F. Almansa, Aerosol properties by ground-based COCCON FTIR spectrometry, International Radiation Symposium (IRS), Thessaloniki (Greece), 4-8 July, 2022.

Álvarez, O., O. García, A. Barreto, F. Hase, T. Blumenstock, E. Sepúlveda, S. León-Luis, V. Carreño, A. Alcántara, R.D. García, F. Almansa, M. Schneider, Spectral Aerosol Optical Depth Retrievals by ground-based COCCON FTIR spectrometry, TCCON/COCCON/NDACC Meeting 2022 (online), 22-24 June, 2022.

Álvarez-Losada, O., A. Barreto, O.E. García, R. Román, M. Sicard, V. Rizi, R. Roininen, P.M Romero-Campos, Y. González, S. Rodríguez, R.D. García, C. Torres, M. Iarlori, E. Cuevas, D. Suárez, R. Ramos, C. Córdoba-Jabonero, J. de la Rosa, A. Rodríguez-Gómez, C. Muñoz-Porcar, A. Comerón, A. Bedoya-Velásquez, J.C. Antuña-Sanchez, V. Neustroev, E. Pietropaolo, Y. Lopez-Darias, M.A. López-Cayuela, C. Carvajal-Pérez, J.J. Bustos, O. Álvarez, C. Toledano, C. Aramo, J. Vilches, R. González, F.A. Almansa, R. Ceolato, N. Taquet, Thomas Boulesteix, M. Martínez, N. Prats, A. Redondas, C. Bayo, V. Carreño, C. López, S.L. León, P.P. Rivas, A. Alcántara, F. Parra, C. López, P. Martín, Erupción volcánica de La Palma: caracterización de los aerosoles y gases volcánicos emitidos desde una perspectiva sinérgica, 10ª Asamblea Hispano Portuguesa de GEodesia y Geofísica, Toledo, 28 November-1 December, 2022.

Barreto, O.E. García, R. Román, M. Sicard, V. Rizi, R. Roininen, P.M Romero-Campos, Y. González, S. Rodríguez, R.D. García, C. Torres, M. Iarlori, E. Cuevas, C. Córdoba-Jabonero, J. de la Rosa, A. Rodríguez-Gómez, C. Muñoz-Porcar, A. Comerón, A. Bedoya-Velásquez, J.C. Antuña-Sanchez, V. Neustroev, E. Pietropaolo, Y. Lopez-Darias, M.A. López-Cayuela, C. Carvajal-Pérez, J.J. Bustos, O. Álvarez, C. Toledano, C. Aramo, J. Vilches, R. González, F.A. Almansa, R. Ceolato, N. Taquet, N. Prats, A. Redondas, C. Bayo, R. Ramos, V. Carreño, S.L. León, P.P. Rivas, A. Alcántara, C. López, P. Martín, La Palma Volcano Eruption: Characterisation of Volcanic Aerosols and Gas Emissions from a Synergetic Perspective, International Radiation Symposium (IRS), Thessaloniki (Greece), 4-8 July, 2022.

Barreto, A., M. Sicard, O.E. García, R. Román, V. Rizi, R. Roininen, P.M Romero-Campos, Y. González, S. Rodríguez, R.D. García, C. Torres, M. Iarlori, E. Cuevas, D. Suárez, R. Ramos, C. Córdoba-Jabonero, J. de la Rosa, A. Rodríguez-Gómez, C. Muñoz-Porcar, A. Comerón, A. Bedoya-Velásquez, J.C. Antuña-Sanchez, V. Neustroev, E. Pietropaolo, Y. Lopez-Darias, M.A. López-Cayuela, C. Carvajal-Pérez, J.J. Bustos, O. Álvarez, C. Toledano, C. Aramo, J. Vilches, R. González, F.A. Almansa, R. Ceolato, N. Taquet, Thomas Boulesteix, M. Martínez, N. Prats, A. Redondas, C. Bayo, V. Carreño, C. López, S.L. León, P.P. Rivas, A. Alcántara, F. Parra, P. Martín, La Palma Volcano Eruption: Characterisation of Volcanic Aerosols and Gas Emissions from a Synergetic Perspective, Congreso Nacional de Medio Ambiente (CONAMA), 21-24 November, Madrid, 2022.

Berjon, A., Redondas, A., Rimmer, J.S., López-Solano, J., Parra-Rojas, F., Carreno, V.: Eubrewnet. Sharing data with other databases (WOUDC, NDACC, EVDC). Talk presented at Nordic Ozone and UV group annual meeting 2022 (Kjeller, Norway), April 26, 2022.

Bjorklund, R. C. Vigouroux, O. García, Dan Smale, J. Hannigan, N. Jones and I. Ortega, IRWG Ozone update: summary, IRWG-NDACC Meeting 2022, 28 June-1 July, 2022.

Bouvet, M., Turpie, K., Barreto, A., Bialek, A., Brown, S., De Vis, P., Fahy, J., Gaton, J., Gonzalez, R., Maxwell, S.E., Toledano, C., Rice, J.P., Adriaensen, S., Stone, T.C., Woodward, J.T., Woolliams, E. Validating a lunar model used to verify in-flight radiometric performance of Earth observation satellites: a metrological approach, Metrology for Climate Action, September 2022.

García, R.D., A. Barreto, E. Cuevas, O.E. García, R. Ramos, F. Almansa, M. Pó, and K. Hoogendijk, Spectral aerosol radiative forcing of the Saharan dust events in June 2021 over Tenerife Island, International Radiation Symposium (IRS), Thessaloniki (Greece), 4-8 July, 2022.

García, R.D., E. Cuevas, R. Ramos, A. Redondas and V.E. Cachorro. "Status of the Izaña BSRN station in 2022", 17th BSRN Scientific Review and Workshop (hybrid, Ispra, VA, Italy) 27-30 June, 2022.

García Rodríguez Omaira Elena; Cuevas Agulló, Emilio; Rivas Soriano, Pedro Pablo; León Luis, Sergio Fabián. Inter-comparison of CO_2, CO and CH_4 mixing ratios obtained by in-situ and remote measurements techniques in the Izaña Atmospheric Observatory. ICOS Science Conference 2022. 12-14 September, 2022.

García, O., Monitorización de las concentraciones de gases de efecto invernadero desde diversas plataformas de observación, IX Remedia Workshop, Córdoba (Spain), 21-22 April, 2022.

García, O. W. Stremme, N. Taquet, F. Hase, I. Ortega, J. Hannigan, D. Smale, C. Vigouroux, M. Grutter, T. Blumenstock, M. Schneider, A. Redondas Sulphur dioxide from ground-based Fourier transform infrared spectroscopy: application to volcanic emissions, IRWG-NDACC Meeting 2022, 28 June-1 July, 2022.

González Ramos, Y., Popovici, I., Barreto, A., Sanchez-Barrero, M.F., Pronieswki, L., Victori, S., Almansa, A.F., Ramos, R., Cuevas, E. Characterization of Recent Aerosol Events Occurring in the Subtropical North Atlantic Region Using a CIMEL CE376 GPN Micro-LiDAR, International Laser Radar Conference 2022, July 2022.

González Ramos, Y., Sanchez-Barrero, M.F., Barreto, A., Victori, S., Popovici, I., Pronieswki, L., Almansa, A.F., Cuevas, E.. Optical Properties of Aerosols travelling over the Subtropical North Atlantic determined with a CIMEL CE376 LiDAR: from Saharan dust to Volcanic aerosols, American Geophysical Union (AGU), December, 2022.

López-Solano, J., Redondas, A., Gröbner, J., Maret, B., Lakkala, K., León-Luis, S.F., Carreño, V., Berjón, A., Parra-Rojas, F.C.: New UV products in EUBREWNET. Talk presented at Nordic Ozone and UV group annual meeting 2022 (online), April 27, 2022.

Hedelt, P., D. Loyola, A. Redondas, A. Barreto, O. Garcia, L. Doppler, J. Reichardt, Analysis of the 2021 Cumbre Vieja eruption and the long-range transport of SO2 to Europe using TROPOMI and ground-based measurements, Sentinel-5P Mission: 5 years anniversary, Taormina (Italy), 10 – 14 October, 2022.

Pacheco, J., Moutinho, A., Henriques, D., Martins, M., Hernández, P., Oliveira, S., Matos, T., Silva, D., Viveiros, F., Barrancos, J., Henriques, D., Pèrez, N., Padrón, E., Melián, G., Barreto, A., Gonzalez, Y., Rodríguez, S., Cuevas, E., Ramos, R., Fialho, P., Goulart, C., Gonçalves, L., Faria, C., and Rocha, J.: Low-cost, fast deployment multi-sensor observations of the 2021 Cumbre Vieja eruption , EGU General Assembly 2022, Vienna, Austria, 23–27 May 2022, EGU22-8830, https://doi.org/10.5194/egusphere-egu22-8830, 2022.

Parra-Rojas, F.C., Redondas, A., Berjón, A., López-Solano, J.: Total ozone uncertainty model implemented on EuBrewNet. Talk presented at Nordic Ozone and UV group annual meeting 2022 (online), 26 April, 2022.

Parra-Rojas, F.C., Redondas, A., Berjón, A., López-Solano, J.: Total ozone uncertainty model implemented on EuBrewNet. Talk presented at Internal Radiation Symposium (Thessaloniki), 4 July, 2022.

Prats, N., Torres, C., Bayo, C., Ramos, R., Cuevas, E. (2022). Guía de actuación ante niveles altos de contaminación volcánica (Guideline for high levels of volcanic pollution). Poster presentado en 10ª Asamblea Hispano Portuguesa de Geodesia y Geofísica, Toledo (España), 28 Nov–1 Dec, 2022.

Qiansi T., F. Hase, M. Schneider, O. García, T. Blumenstock, T. Borsdorff, M. Frey, F. Khosrawi, A. Lorente, C. Alberti, J.J. Bustos, A. Butz, V. Carreño, E. Cuevas, R. Curcoll, C. J. Diekmann, D. Dubravica, B. Ertl, C. Estruch, S. F. León-Luis, C. Marrero, J.-A. Morgui, R. Ramos, C. Scharun, C. Schneider, E. Sepúlveda, C. Toledano, C. Torres Quantification of CH4 emissions from waste disposal sites using ground- and space-based observations of COCCON, TROPOMI and IASI, TCCON/COCCON/NDACC Meeting 2022 (online), 22-24 June, 2022.

Redondas, A., López-Solano, J., Gröbner, J., Maret, B., Lakkala, K., León-Luis, S.F., Carreño, V., Berjón, A., Parra-Rojas, F.C.: UV in EUBREWNET. Poster presented at International Radiation Symposium (Thessaloniki), 4 July, 2022.

Schneider, M., B. Ertl, Q. Tu, C. J. Diekmann, F. Khosrawi, A. N. Röhling, F. Hase, D. Dubravica, O. E. García, E. Sepúlveda, T. Borsdorff, J. Landgraf, A. Lorente, A. Butz, H. Chen, R. Kivi, T. Laemmel, M. Ramonet, C. Crevoisier, J. Pernin, M. Steinbacher, F. Meinhardt, K. Strong, D. Wunch, T. Warneke, C. Roehl, P. O. Wennberg, I. Morino, L. T. Iraci, K. Shiomi, N. M. Deutscher, D. W. T. Griffith, V. A. Velazco, D. F. Pollard, Synergetic use of IASI profile and TROPOMI total column level 2 methane retrieval products, 2022 Living Planet Symposium, Bonn (Germany), 23-27 May, 2022.

Taquet, N., O. García, R. Campion, T. Boulesteix, W. Stremme,C. Rivera, M. Grutter, A. Barreto, O. Álvarez, S. León-Luis, R. Ramos, V. Carreño, F. Almansa, F. Hase, T. Blumenstock, COCCON activities during the La Palma volcano eruption: gases and aerosols observations, COCCON Meeting (on-line), 23 August, 2022.

2021

Barreto, A., García, O.E., Schneider, M., García, R.D., Hase, F., Sepúlveda, E., Almansa, A.F., Cuevas, E., Blumenstock, T. Spectral Aerosol Optical Depth and Angstrom Exponent From Ground-Based Fourier Transform Infrared Spectrometry. Innovation in Atmospheric Sciences Virtual Workshop (online) 18 May, 2021.

Barreto, Á., García, O.E., Schneider, M., García, R.D., Hase, F., Sepúlveda, E., Almansa, A.F., Cuevas, E., and Blumenstock, T., Aerosol properties by ground-based TCCON FTIR spectrometry, TCCON/COCCON/NDACC Meeting 2021 (online), 8-10 June, 2021.

Berjon, A., Redondas, A., López-Solano, J., Carreno, V., Parra-Rojas, F., León-Luis, S.F.: Reprocessing of the RBCC-E triad ozone series. Talk presented at 18th WMO-GAW Brewer Workshop (online), June 14, 2021.

Berjon, A., Redondas, A., López-Solano, J., Carreno, V., Parra-Rojas, F., León-Luis, S.F.: Reprocessing of the RBCC-E Izaña Observatory triad ozone series. Talk presented at Quadrennial Ozone Symposium (online), 9 October, 2021. Available from: http://qos2021.yonsei.ac.kr/

Berjon, A., Redondas, A., Rimmer, J.S., López-Solano, J., Parra-Rojas, F., Carreno, V., León-Luis, S.F.: EUBREWNET Updates. Talk presented at Nordic Ozone and UV group annual meeting 2021 (online), 20 April, 2021.

Blanco, J.J, García-Tejedor, J.I., García-Población, O., Ayuso, S., López-Comazzi, A., Vrublesvskyy, I., Gomis, A., Moure, D., Cuevas, E., Barreto, A., Ramos, R. ICaRO: a new cosmic ray detector at Izaña Atmospheric Observatory, 37th International Cosmic Ray Conference (ICRC 2021), July 2021.

Doppler, L., Barreto, A., Toledano, C., Mazzola, M., Kouremeti, N., Uchiyama, A., Novikov, V., Navas-Guzmán, F., Roman, R., Ritter, C., González, R., Vitale, V., Stone, R., Ivanescu, L., Yamazahki, Schulz, K-H. Preliminary results on the third lunar/stellar AOD intercomparison campaign at Lindenberg's MOL-RAO Observatory, Arctic Science Summit Week 2021 (online), 20-26 March 2021.

García, O.E., E. Sanromá, M. Schneider, F. Hase, S.F. León-Luis, T. Blumenstock, E. Sepúlveda, A. Redondas, V. Carreño, C. Torres, and N. Prats, Ozone monitoring by NDACC FTIR spectrometry: improved retrieval strategy and impact of instrumental line shape characterisation, Quadrennial Ozone Symposium, virtual, 3-9 October, 2021

García, O., Sanromá, E., Schneider, M., Hase, F., León-Luis, S.F., Blumenstock, T., Sepúlveda, E., Redondas, A., Carreño, V., Torres, C., and Prats, N., Ozone monitoring by NDACC FTIR spectrometry: improved retrieval strategy and impact of instrumental line shape characterization, TCCON/COCCON/NDACC Meeting 2021 (online), 8-10 June, 2021.

García, O.E., Eliezer Sepúlveda, Sergio F. León-Luis, Josep-Antón Morgui, Matthias Frey, Carsten Schneider, Ramón Ramos, Carlos Torres, Roger Curcoll, Carme Estruch, África Barreto, Carlos Toledano, Frank Hase, André Butz, Emilio Cuevas, Thomas Blumenstock, Juan J. Bustos, and Carlos Marrero, Monitoring of Greenhouse Gas and Aerosol Emissions in Madrid megacity (MEGEI-MAD), GAW Symposium 2021 (online), 28 June-2 July, 2021.

López-Solano, J., Redondas, A., León-Luis, S.F., Berjón, A., Carreño, V., Parra-Rojas, F.C.: Aerosol Optical Depth in EUBREWNET. Talk presented at Brewer Ozone Spectrophotometer Open Workshop (online), June 14, 2021.

López-Solano, J., Redondas, A., León-Luis, S.F., Berjón, A., Carreño, V., Parra-Rojas, F.C.: Aerosol Optical Depth in EUBREWNET. Talk presented at Nordic Ozone and UV group (NOG) annual meeting 2021 (online), April 21, 2021.

López-Solano, J., Redondas, A., Rimmer, J., Berjón, A., Parra-Rojas, F.C., Carreño, V., León-Luis, S.F.: EUBREWNET: An Overview of Recent Advances. Talk presented at Quadrennial Ozone Symposium (online), October 9, 2021.

Mazzola, M., Toledano, C., Ivanescu, L., Stone, R., Ritter, C., Vitale, V., Doppler, L., Stone, T., Hansen, G. H., Kouremeti, N., Sasamoto, K., McComiskey, A., Barreto, A., Roman, R., Gonzales, R., Cachorro, V., Barnes, J. E., Uchiyama, A., Yamanouchi, T. Aerosol observations in the Arctic from ground-based and satellite systems during T-MOSAIC, Arctic Science Summit Week 2021 (online), 20-26 March 2021.

Navas-Guzmán, F., Martucci, G., Collaud Coen, M., Hervo, M., Barreto, A., López-Solano3, J., Ruiz-Arias, J.A., Lyamani, H., Hüglin, C., Pérez-Ramírez, D., Titos, G., Alonso, M., Alados-Arboledas, L., Brem, B.T., Gysel, M., Haefele, A. Statistical analysis of aerosol hygroscopic properties over Payerne (Switzerland), European Aerosol Conference EAC 2021, September 2021.

Parra-Rojas, F.C., Redondas, A., Berjón, A., López-Solano, J.: Total ozone uncertainty model on Brewer Algorithm. Talk presented at Quadrennial Ozone Symposium (online), October 3, 2021

Parra-Rojas, F.C., Redondas, A., Berjón, A., López-Solano, J.: Total ozone uncertainty model on Brewer Algorithm. Talk presented at WMO-GAW Brewer Workshop (online), June 14, 2021.

Parra-Rojas, F.C., Redondas, A., Berjón, A., López-Solano, J.: A new data set for the Brewer spectrophotometer uncertainty budget in the total ozone column measurements. Talk presented at EGU General Assembly 2021 (online), April 30, 2021. Available from: https://doi.org/10.5194/egusphere-egu21-15316

Parra-Rojas, F.C., Redondas, A., Berjón, A., López-Solano, J.: Total ozone uncertainty model on Brewer Algorithm and its implementation in EuBrewNet. Talk presented at Metrology for Meteorology and Climate Webminar (online), April 26, 2021.

Parra-Rojas, F.C., Redondas, A., Berjón, A., López-Solano, J.: Total ozone uncertainty model on Brewer Algorithm. Talk presented at Nordic Ozone and UV group annual meeting (online), April 20, 2021.

Redondas, A., Parra-Rojas, F.C., Berjón, A., López-Solano, J., Bais, A., Gröbner, J., De Bock, V., Karppinen, T., Vilaplana, J.M.: Eubrewnet Brewer updated algorithm, total ozone in seven European stations: Sodankyla, Davos, Uccle, Thessaloniki, Madrid, El Arenosillo and Izaña. Talk presented at Quadrennial Ozone Symposium (online), October 9, 2021.

Redondas, A., Parra-Rojas, F.C., Berjón, A., López-Solano, J., Bais, A., Gröbner, J., De Bock, V., Karppinen, T., Vilaplana, J.M.: Eubrewnet Brewer updated algorithm, total ozone in seven European stations: Sodankyla, Davos, Uccle, Thessaloniki, Madrid, El Arenosillo and Izaña. Talk presented at Nordic Ozone and UV group annual meeting (online), April 20, 2021.

Schneider, M., Benjamin Ertl, Christopher Diekmann, Farahnaz Khosrawi, Amelie N. Röhling, Frank Hase, Omaira E. García, Eliezer Sepúlveda, Alba Lorente, Jochen Landgraf, Huilin Chen, Rigel Kivi, Thomas Laemmel, Michel Ramonet, Cyril Crevoisier, Martin Steinbacher, Frank Meinhardt, Voltaire A. Velazco, Nicholas M. Deutscher, David Griffith, Dave Pollard, Hartmut Bösch, Tim Trent, Harald Sodemann, Synergetic use of IASI and TROPOMI for generating a tropospheric methane profile product, European General Assembly (online), 19-30 April, 2021.

Schneider M., Ertl B., Diekmann C., Khosrawi F., Röhling A., Hase F., Dubravica D., García O., Sepulveda E., Borsdorff T., Landgraf J., Lorente A., Chen H., Kivi R., Laemmel T., Ramonet M., Crevoisier C., Pernin J., Steinbacher M., Meinhardt F., Deutscher N., Griffth D., Velazco V., Pollard D., Bösch H., Trent T., Sodemann H., Thurnherr I., Synergetic use of IASI and TROPOMI for generating a tropospheric methane profile product, EUMETSAT Meteorological Satellite Conference 2021, online, 20-24 September, 2021

Schneider, M., B. Ertl, C. Diekmann, F. Khosrawi, F. Hase, O. García, Overview on the MUSICA IASI retrieval products, IASI 2021 Conference, Evian (France), 6-10 December, 2021.

Sha, M.K., B. Langerock, D. Dubravica, F. Hase, C. Alberti, T. Borsdorff, A. Lorente, M. Kiel, M. De Mazière, S. Ars, C. A. B. Aquino, B. C. Baier, D. Balis, C. Bes, E. Blandin, T. Blumenstock, H. Boesch, A. Butz, J. Chen, C. Crevoisier, A. Dandocsi, A. Dehn, F. Dietrich, J. Fanklin, M. Frey, S. Jeong, I. Morino, T. Newberger, O. E. Garcia, E. Gottlieb, M. Grutter, P. Heikkinen, N. Humpage, N. Jacobs, R. Kivi, M. Lopez, E. Marais, M. Mermigkas, A. Nemuc, N. Pak, M. Pathakoti, M. Ramonet, S. Roche, A. N. Röhling, H. Ohyama, G. B. Osterman, H. Park, D. Pollard, V. K. Sagar, M.V.R. S. Sai, K. A. da Silva, D. Schuettemeyer, W. Simpson, W. Stremme, N. Taquet, Y. Té, Q. Tu, F. Vogel, D. Wunch, Validation of TROPOMI products using COCCON network data, TCCON/COCCON/NDACC Meeting 2021 (online), 8-10 June, 2021.

Sha, M.S., B. Langerock, M. Kiel, D. Dubravica, F. Hase, T. Borsdorff, A. Lorente, M. De Mazière, C. Alberti, S. Ars, C. A. Bauer Aquino, B. C. Baier, D. Balis, C. Bes, E. Blandin, T. Blumenstock, H. Boesch, A. Butz, J. Chen, A. Dandocsi, A. Dehn, F. Dietrich, J. Franklin, M. Frey, S. Jeong, I. Morino, T. Newberger, O. E García, E. Gottlieb, M. Grutter, P. Heikkinen, N. Humpage, N. Jacobs, R. Kivi, M. Lopez, E. Marais, M. Mermigkas, A. Nemuc, N. Pak, M. Pathakoti, M. Ramonet, S. Roche, A.N. Röhling, H. Ohyama, G.B. Osterman, H. Park, D. Pollard, V. K. Sagar, M.V.R. Sesha Sai, K. A. da Silva, D. Schuettemeyer, W. Simpson, W. Stremme, N. Taquet, Y. Té, Q. Tu, F. Vogel, D. Wunch, Using the COllaborative Carbon Column Observing Network for validating space borne GHG sensors, 17th Internationl Workshop on Greenhouse Gas Measurements from Space (virtual meeting), 14-17 June, 2021.

Steinbrecht, W., D. Kubistin, C. Plass-Dülmer, J. Davies, D.W. Tarasick, P. v. d. Gathen, H. Deckelmann, N. Jepsen, R. Kivi, N. Lyall, M. Palm, J. Notholt, B. Kois, P. Oelsner, M. Allaart10, A. Piters, M. Gill, R. Van Malderen, A.W. Delcloo, R. Sussmann, E. Mahieu, C. Servais, G. Romanens, R. Stübi, G. Ancellet, S. Godin-Beekmann, S. Yamanouchi, K. Strong, B. Johnson, P. Cullis, I. Petropavlovskikh, J.W. Hannigan, J.-L. Hernandez, A. Diaz Rodriguez, T. Nakano, F. Chouza, T. Leblanc, C. Torres, O. Garcia, A.N. Röhling, M. Schneider, T. Blumenstock, M. Tully, C. Paton-Walsh, N. Jones, R. Querel, S. Strahan, R.M. Stauffer, A.M. Thompson, A. Inness, R. Engelen , K.-L. Chang, O.R. Cooper, G.P. Brasseur, I. Bouarar, and B. Gaubert, Free tropospheric ozone reductions due to reduced emissions in the COVID-19 pandemic, Quadrennial Ozone Symposium, virtual, 3-9 October, 2021.

Steinbrecht, W., R. Van Malderen, D. Poyraz, D. Hubert, J. Davies, D.W. Tarasick, P. v. d. Gathen, H. Deckelmann, N. Jepsen, R. Kivi, N. Lyall, B. Kois, P. Oelsner, M. Allaart, A. Piters, M. Gill, G. Romanens, R. Stübi ,G. Ancellet, S. Godin-Beekmann , B. Johnson, P. Cullis, I. Petropavlovskikh, J.-L. Hernandez, A. Diaz Rodriguez, T. Nakano, C. Torres, M. Tully, R. Querel, D.E. Kollonige, R.M. Stauffer, A.M. Thompson, K.-L. Chang, O.R. Cooper, H.G.J. Smit, Ozone Trends in the Lower Stratosphere from Ozone Sondes, Quadrennial Ozone Symposium, virtual, 3-9 October, 2021.

Taylor, S., Toledano, C., Berjón, A. J., Barreto, A., Adriansen, S., Woolliams, E., Bouvet, M. LIME: Lunar Irradiance Model of the European Space Agency, EGU General Assembly (online) 19–30 April 2021.

Vigouroux, C., Blumenstock, T., De Mazière, M., Errera, Q., García, O. E., Grutter, M., Hannigan, J., Hase, F., Jones, N., Mahieu, E., Virolainen, Y., Ortega, I., Palm, M., Rettinger, M., Roehling, A., Smale, D., Stremme, W., Strong, K., Sussmann, R., K., Thölix, L., Wizenberg, T., Trends and variability of ozone total, stratospheric, and tropospheric columns from long-term FTIR measurements of the NDACC network, Quadrennial Ozone Symposium, virtual, 3-9 October, 2021

Vigouroux, C., O. García, J. Hannigan, I. Ortega, Y. Virolainen, D. Smale, M. Grutter, and I. Murata, TOAR-II (Tropospheric Ozone Assessment Report): FTIR contribution, TCCON/COCCON/NDACC Meeting 2021 (online), 8-10 June, 2021.

27.4 Non-peer reviewed papers and reports

2022

Arola, A., S. Basart, A. Benedictow, Y. Bennouna, A.-M. Blechschmidt, E. Cuevas, Q. Errera, H.J. Eskes, J. Kapsomenakis, B. Langerock, A. Mortier, M. Pitkänen, M. Ramonet, A. Richter, M. Schulz, N. Sudarchikova, V. Thouret, T. Warneke, C. Zerefos, Validation report of the CAMS near-real-time global atmospheric composition service: Period September – November 2021, Copernicus Atmosphere Monitoring Service (CAMS) report, CAMS2_82_2022SC1_D82.1.1.1-SON2021.pdf, April 2022, doi:10.24380/e3r1-ga84, 2022a

Arola, A., S. Basart, A. Benedictow, Y. Bennouna, A.-M. Blechschmidt, I. Bouarar, E. Cuevas, Q. Errera, H.J. Eskes, J. Griesfeller, J. Kapsomenakis, B. Langerock, A. Mortier, I. Pison, M. Pitkänen, M. Ramonet, A. Richter, M. Schulz, J. Tarniewicz, V. Thouret, A. Tsikerdekis, T. Warneke, C. Zerefos, Validation report of the CAMS near-real-time global atmospheric composition service: December 2021 – February 2022, Copernicus Atmosphere Monitoring Service (CAMS) report, CAMS2_82_2022SC1_D82.1.1.2-DJF2022.pdf, June 2022, doi: 10.24380/9z4h-5ni, 2022b.

Cuevas, E., Milford, C., Barreto, A., Bustos, J. J., García, O. E., García, R. D., Marrero, C., Prats, N., Ramos, R., Redondas, A., Reyes, E., Rivas-Soriano, P. P., Romero-Campos, P. M., Torres, C. J., Schneider, M., Yela, M., Belmonte, J., Almansa, F., López-Solano, C., Basart, S., Werner, E., Rodríguez, S., Afonso, S., Alcántara, A., Alvarez, O., Bayo, C., Berjón, A., Carreño, V., Castro, N. J., Chinea, N., Cruz, A. M., Damas, M., Gómez-Trueba, V., González, Y., Guirado-Fuentes, C., Hernández, C., León-Luís, S. F., López-Fernández, R., López-Solano, J., Parra, F., Pérez de la Puerta, J., Rodríguez-Valido, M., Sálamo, C., Santana, D., Santo-Tomás, F., Sepúlveda, E. and Serrano, A.: Izaña Atmospheric Research Center Activity Report 2019-2020. (Eds. Cuevas, E., Milford, C. and Tarasova, O.), State Meteorological Agency (AEMET), Madrid, Spain and World Meteorological Organization, Geneva, Switzerland, NIPO: 666-22-014-0, WMO/GAW Report No. 276, https://doi.org/10.31978/666-22-014-0, 2022.

Di Tomaso, E. et al. (2022). MONARCH Regional Reanalysis of Desert Dust Aerosols: An Initial Assessment. In: Mensink, C., Jorba, O. (eds) Air Pollution Modeling and its Application XXVIII. ITM 2021. Springer Proceedings in Complexity.

Springer, Cham. https://doi.org/10.1007/978-3-031-12786-1_33, 2022a.

García, O., Rey, F., Bullón, F., Suárez, D., Cuevas, E., & Ramos, R. (2022a). La erupción volcánica de La Palma y sus meteoros. Revista Tiempo Y Clima, 5(76). Recuperado a partir de https://pub.ame-web.org/index.php/TyC/article/view/2517.

García, O., Suárez, D., Cuevas, E., Ramos, R., Barreto, África, Hernández, M., Quintero, V., Toledano, C., Sicard, M., Córdoba-Jabonero, C., Riz, V., Roininen, R., López, C., Vilches, J., Weiss, M., Carreño, V., Taquet, N., Boulesteix, T., Fraile, E., Torres, C., Prats, N., Alcántara, A., León, S. ., Rivas, P., Álvarez, Óscar, Parra, F., de Luis, J., González, C., Armas, C., Romero, P., de Bustos, J., Redondas, A., Marrero, C., Milford, C., Román, R., González, R., López-Cayuela, M., Carvajal-Pérez, C., Chinea, N., García, R. ., Almansa, F., González, Y., Bullón, F., Poggio, M., Rivera, C., Bayo, C., & Rey, F. (2022b). La erupción volcánica de La Palma y el papel de la Agencia Estatal de Meteorología. Revista Tiempo Y Clima, 5(76). Recuperado a partir de https://pub.ame-web.org/index.php/TyC/article/view/2516

Langerock, B., B., A. Arola, S. Basart, A. Benedictow, Y. Bennouna, A.-M. Blechschmidt, I. Bouarar, E. Cuevas, Q. Errera, H.J. Eskes, J. Griesfeller, J. Kapsomenakis, A. Mortier, I. Pison, M. Pitkänen, M. Ramonet, A. Richter, M. Schulz, J. Tarniewicz, V. Thouret, A. Tsikerdekis, T. Warneke, C. Zerefos, Validation report of the CAMS near-real-time global atmospheric composition service: March – May 2022, Copernicus Atmosphere Monitoring Service (CAMS) report, CAMS2_82_2022SC1_D82.1.1.3-MAM2022.pdf, August 2022, doi:10.24380/akid-u2rr, 2022, 2022.

Prats, N., Torres, C., Bayo, C., Ramos, R., Cuevas, E. (2022). Guía de actuación ante niveles altos de contaminación volcánica. Observatorio Atmosférico de Izaña. AEMET – Publicaciones en línea. Ministerio para la Transición Ecológica y el Reto Demográfico, Agencia Estatal de Meteorología, Madrid, 2022.

WMO, WMO Airborne Dust Bulletin: Sand and Dust Storm Warning Advisory and Assessment System, No. 6 - September 2022, 2022.

2021

Basart, S., García-Pando, C.P., Werner, E., Nickovic, S. and Cuevas-Agullo, E.: Understanding the user's needs in risky sand and dust storm environments in Northern Africa, the Middle East and Europe. In NSF Convergence Workshop on Bringing Land, Ocean, Atmosphere and Ionosphere Data to the Community for Hazards Alerts. AGU, 2021a.

Basart, S., Werner, E., Cuevas, E., García-Pando, C.P. (2022). The WMO Barcelona Dust Regional Center: Linking Research with the Development of Dust User-Oriented Services. In: Mensink, C., Jorba, O. (eds) Air Pollution Modeling and its Application XXVIII. ITM 2021. Springer Proceedings in Complexity. Springer, Cham. https://doi.org/10.1007/978-3-031-12786-1_31, 2021b

Cuevas, E., Auscultando la atmósfera de la Tierra desde el entorno del Parque Nacional del Teide. Durban, N & Martín-Esquivel, JL (Eds.). Ciencia en el Parque Nacional del Teide 2009-2019. Cabildo Insular de Tenerife y Ediciones Turquesa. Santa Cruz de Tenerife. Capítulo VI, ISBN 978-84-16785-84-1, 2021.

Cuevas, E., Milford, C., Barreto, A., Bustos, J. J., García, R. D., Marrero, C. L., Prats, N., Bayo, C., Ramos, R., Terradellas, E., Suárez, D., Rodríguez, S., de la Rosa, J., Vilches, J., Basart, S., Werner, E., López-Villarrubia, E., Rodríguez-Mireles, S., Pita Toledo, M. L., González, O., Belmonte, J., Puigdemunt, R., Lorenzo, J.A., Oromí, P., and del Campo-Hernández, R.: Desert Dust Outbreak in the Canary Islands (February 2020): Assessment and Impacts. (Eds. Cuevas, E., Milford, C. and Basart, S.), State Meteorological Agency (AEMET), Madrid, Spain and World Meteorological Organization, Geneva, Switzerland, WMO Global Atmosphere Watch (GAW) Report No. 259, WWRP 2021-1, 2021a.

Cuevas, E., Milford, C., Fraile-Nuez, E., Arrieta, J.M. and Vélez-Belchí, P. Climatological Characterisation of Ocean Sites for Ocean Colour System Vicarious Calibration: El Hierro (Canary Islands, Spain) Task 2 Report, Annex 4: Statistics and trends in hurricanes for the Canary Islands (EUMETSAT study report, EUMETSAT, Darmstadt, Germany), 2021b. https://www.eumetsat.int/media/49928

Errera, Q., M. Ramonet, N. Sudarchikova, M. Schulz. H. J. Eskes, S. Basart, A. Benedictow, Y. Bennouna, A.-M. Blechschmidt, S. Chabrillat, Christophe, Y., E. Cuevas, A. El-Yazidi, H. Flentje, P. Fritzsche, K.M. Hansen, U. Im, J. Kapsomenakis, B. Langerock, A. Richter, V. Thouret, A. Wagner, T. Warneke, C. Zerefos, Validation report of the CAMS near-real-time global atmospheric composition service: Period March – May 2021, Copernicus Atmosphere Monitoring Service (CAMS) report, CAMS84_2018SC3_D1.1.1_MAM2021.pdf, September 2021, doi:10.24380/qq5mdg18.

Fraile-Nuez, E., Cuevas, E., Milford, C., Mosquera, A., Arrieta. J. M., Marrero, C., Vélez-Belchí, P., Bustos, J.J., Barreto, A., García, R. D., Redondas, A., García, O., Romero-Campos, P. M., Presas-Navarro, C., Palomino, D. and González-Vega, A. Climatological Characterisation of Ocean Sites for Ocean Colour System Vicarious Calibration: El Hierro (Canary Islands, Spain), Task 1 Report: Climatological and observational data sets (EUMETSAT study report, EUMETSAT, Darmstadt, Germany), 2021a. https://www.eumetsat.int/media/49924

Fraile-Nuez, E., Cuevas, E., Milford, C., Mosquera, A., Arrieta. J. M., Marrero, C., Vélez-Belchí, P., Bustos, J.J., García, R. D., Barreto, A., García, O., Redondas, A., Romero-Campos, P. M., Berjón, A., Presas-Navarro, C., Palomino, D. and González-Vega, A. Climatological Characterisation of Ocean Sites for Ocean Colour System Vicarious Calibration: El Hierro (Canary Islands, Spain) Task 2 Report: Site Characterisation (EUMETSAT study report, EUMETSAT, Darmstadt, Germany), 2021b. https://www.eumetsat.int/media/49925

Fraile-Nuez, E., Milford, C., Arrieta, J.M., Vélez-Belchí, P., and Cuevas, E. Climatological Characterisation of Ocean Sites for Ocean Colour System Vicarious Calibration: El Hierro (Canary Islands, Spain) Task 2 Report, Annex 3: Physical safety of the El Hierro site (EUMETSAT study report, EUMETSAT, Darmstadt, Germany), 2021c. https://www.eumetsat.int/media/49927

García, Rosa D. y Cuevas, E., Radiación Solar en el Parque Nacional del Teide. Durban, N & Martín-Esquivel, JL (Eds.). Ciencia en el Parque Nacional del Teide 2009-2019. Cabildo Insular de Tenerife y Ediciones Turquesa. Santa Cruz de Tenerife. Capítulo VIII, ISBN 978-84-16785-84-1, 2021.

Ramonet, M., N. Sudarchikova, M. Schulz. Q. Errera, H. J. Eskes, S. Basart, A. Benedictow, Y. Bennouna, A.-M. Blechschmidt, S. Chabrillat, Christophe, Y., E. Cuevas, A. El-Yazidi, H. Flentje, P. Fritzsche, K.M. Hansen, U. Im, J. Kapsomenakis, B. Langerock, A. Richter, V. Thouret, A. Wagner, T. Warneke, C. Zerefos, Validation report of the CAMS near-real-time global atmospheric composition service: Period June – August 2021, Copernicus Atmosphere Monitoring Service (CAMS) report, CAMS84_2018SC3_D1.1.1_JJA2021.pdf, November 2021, doi:10.24380/6x8f-9630, 2021.

Schulz, M., Q. Errera, M. Ramonet, Sudarchikova, N., H. J. Eskes, S. Basart, A. Benedictow, Y. Bennouna, A.-M. Blechschmidt, S. Chabrillat, Christophe, Y., E. Cuevas, A. El-Yazidi, H. Flentje, P. Fritzsche, K.M. Hansen, U. Im, J. Kapsomenakis, B. Langerock, A. Richter, V. Thouret, A. Wagner, T. Warneke, C. Zerefos, Validation report of the CAMS near-real-time global atmospheric composition service: Period December 2020 – February 2021, Copernicus Atmosphere Monitoring Service (CAMS) report, CAMS84_2018SC3_D1.1.1_DJF2021.pdf, June 2021, doi:10.24380/f540-kb09, 2021.

Sudarchikova, N., M. Schulz, Q. Errera, M. Ramonet, H. J. Eskes, S. Basart, A. Benedictow, Y. Bennouna, A.-M. Blechschmidt, S. Chabrillat, Christophe, Y., E. Cuevas, A. El-Yazidi, H. Flentje, P. Fritzsche, K.M. Hansen, U. Im, J. Kapsomenakis, B. Langerock, A. Richter, V. Thouret, A. Wagner, T. Warneke, C. Zerefos, Validation report of the CAMS near-real-time global atmospheric composition service: Period September - November 2020, Copernicus Atmosphere Monitoring Service (CAMS) report, CAMS84_2018SC3_D1.1.1_SON2020.pdf, March 2021, doi: 10.24380/ rysv-7371, 2021.

Vélez-Belchí, P., Fraile-Nuez, E., Arrieta, J.M., Milford, C. and Cuevas, E. Climatological Characterisation of Ocean Sites for Ocean Colour System Vicarious Calibration: El Hierro (Canary Islands, Spain) Task 2 Report, Annex 2: Proposal for high-volume data communication links (EUMETSAT study report, EUMETSAT, Darmstadt, Germany), 2021. https://www.eumetsat.int/media/49926

WMO, WMO Airborne Dust Bulletin: Sand and Dust Storm Warning Advisory and Assessment System, No. 5 - July 2021, 2021.

28 List of scientific projects

Table 28.1. List of scientific projects at IARC during 2021-2022.

Project Title	Duration	Funding Agency	Project Website	Principal Investigator/ Contact
International network for harmonization of atmospheric aerosol retrievals from ground-based photometers (HARMONIA)	2022-2026	Cost Action CA21119		PI: Stelios Kazadzis (PMOD) PI (IARC-AEMET): Dr África Barreto
Knowledge and climate services from an African observation and Data research Infrastructure (KADI)	2022-2025	HORIZON-INFRA-2021-DEV-01		PI: ICOS ERIC PI (IARC-AEMET): Dr África Barreto – Dr Omaira García
Towards the Next Generation of Sensors for Surveying the Atmospheric Carbon Cycle (CarbonSurvey)	2022-2024	Spanish Ministry of Science and Innovation		PI (UC3M): Dr Marta Ruiz Llata PI (IARC-AEMET): Dr Omaira García
Solutions for Sustainable Access to Atmospheric Research Facilities (ATMO-ACCESS)	2021-2025	H2020-INFRAIA-2018-2020 (H2020)	https://izana.aemet.es/atmo-access-isaf/#home	PI (CNRS): Prof Paolo Laj PI (IARC-AEMET): Dr Natalia Prats
SYNERgies for assessing short- and long-term variations of Aerosols properties in the subtropical North Atlantic (SYNERA)	2021-2023	Spanish Ministry of Science and Innovation		PI (IARC-AEMET): Dr África Barreto
Metrology for aerosol optical properties (MAPP)	2020-2023	EURAMET: European Association of National Metrology Institutes	https://www.pmodwrc.ch/en/MAPP/	PI (SFI Davos): Dr Julian Gröbner PI (IARC-AEMET): Dr África Barreto
Aerosol, Clouds and Trace gases Research InfraStructure (ACTRIS)	2020-2023	H2020-INFRADEV, Grant agreement ID: 871115	https://www.actris.eu/	PI (FMI): Dr Eija Juurola PI (IARC-AEMET): Dr África Barreto
Mac-Clima	2019-2023	MAC2/3.5b/254, Inter-Reg	https://mac-clima.energiagrancanaria.com	Consortium
Climate Risk and Early Warning System (CREWS)	2021-2022	WMO		PI: WMO PI (AEMET): Ernest Werner
Brewer Error Budget in Eubrewnet (BREWEB)	2020-2022	European Space Agency (ESA) 4000117151/16/I-LG KNMI-2020/658	http://www.tropomi.eu/data-products/mission-performance-centre	PI (ESA): Dr Angelika Dehn PI (IARC-AEMET): Alberto Redondas

S5P NItrogen Dioxide and FORmaldehyde Validation using NDACC and complementary FTIR and UV-Vis DOAS ground-based remote sensing data (NIDFORVal)	2016-2023	European Space Agency (ESA) ID28607		PI (BIRA-IASB): Dr Corinne Vigouroux Dr Giai Pinardi PI (IARC-AEMET): Dr Omaira García
Validation of S5P Methane and Carbon Monoxide with TCCON Data (TCCON4S5P)	2016-2023	European Space Agency (ESA)		PI (BIRA-IASB): Dr Filip Desmet PI (IARC-AEMET): Dr Omaira García
Medida de Gases de Efecto Invernadero en Ambientes Urbanos (MEGEI)	2018-ongoing	Meteorological State Agency (AEMET)	https://izana.aemet.es/projects/#megei	PI (IARC-AEMET): Dr Omaira García
SDS-Africa	2007-ongoing	Spanish Agency for International Development Cooperation	__	PI (IARC-AEMET): Dr Emilio Cuevas
GAW-Sahara	2007-ongoing	Spanish Agency for International Development Cooperation	__	PI (IARC-AEMET): Alberto Redondas

For a definition of the acronyms used in the above table, see Section 31.

29 List of major national and international networks, programmes and initiatives

The Izaña Atmospheric Research Center participates in the following national and international networks, programmes and initiatives:

ACTRIS	Aerosols, Clouds, and Trace gases Research InfraStructure
AERONET	AErosol RObotic NETwork
ALC	Automatic Ceilometer and Lidars Network
BSRN	Baseline Surface Radiation Network
CarbonTracker	CO_2 measurement and modeling system developed by NOAA to keep track of sources and sinks of carbon dioxide around the world
CarbonTracker Europe	
CARS	ACTRIS Centre for Aerosol Remote Sensing
CCRES	ACTRIS Centre for Cloud Remote Sensing
COCCON	Collaborative Carbon Column Observing Network
EAN	European Aeroallergen Network
EARLINET	European Aerosol Research Lidar Network
E-GVAP	EUMETNET GNSS Water Vapour Programme
E-PROFILE	EUMETNET Profiling Programme
EPN	EUREF Permanent Network
EUBREWNET	European Brewer Network
EUMETNET	European Meteorological Network
GAW	WMO Global Atmosphere Watch Programme
GCOS	Global Climate Observing System
GEOMON	Global Earth Observation and Monitoring of the Atmosphere
GLOBALVIEW-CO2	
GLOBALVIEW-CH4	
GLOBALVIEW-CO	
GLOBALVIEW-CO2C13	
GURME	WMO GAW Urban Research Meteorology and Environment project
ICOS	Integrated Carbon Observation System
LOTUS	Long-term Ozone Trends and Uncertainties in the Stratosphere
MPLNet	Micro-Pulse Lidar NETwork
NDACC	Network for the Detection of Atmospheric Composition Change
NOAA/ESRL/GMD CCGG Cooperative Air Sampling Network	
Pandonia Global Network	
PHOTONS	PHOtométrie pour le Traitement Opérationnel de Normalisation Satellitaire

RBCC-E	Regional Brewer Calibration Center for Europe
REA	Red Española de Aerobiología
REDMAAS	Red Española de DMAs Ambientales
SDS-WAS	WMO Sand and Dust Storm Warning, Advisory and Assessment System
SPALINET	Spanish and Portuguese Aerosol Lidar Network
SPARC	Stratosphere-troposphere Processes And their Role in Climate
TCCON	Total Carbon Column Observing Network
TOAR	Tropospheric Ozone Assessment Report
WCCAP	World Calibration Centre for Aerosol Physics
WDCGG	World Data Centre for Greenhouse Gases
WDCRG	World Data Center for Reactive Gases
WOUDC	World Ozone and Ultraviolet Data Center
WRC-WORCC	World Radiation Centre-World Optical Depth Research and Calibration Center
WRC-WCC-UV	World Radiation Centre-World Calibration Center-Ultraviolet Section
WRDC	World Radiation Data Centre

30 Staff

Research Staff			
Name	**Position**	**Email**	**Personal Web Page**
Dr Emilio Cuevas-Agulló[a]	Izaña Atmospheric Research Center: Former Director	ecuevasaATaemet.es	ResearchGate Google Scholar
Carlos J. Torres García	Izaña Atmospheric Research Center: Director[b] Reactive gases and Ozonesondes Programme: Head	ctorresgATaemet.es	ResearchGate
Óscar Alvarez Losada	Column Aerosols Programme	proyecto_kadiATaemet.es	ResearchGate
Dr África Barreto	Column Aerosols Programme: Head	abarretovATaemet.es	ResearchGate
Juan J. de Bustos-Seguela	Meteorology Programme McIdas and Eumetcast Manager	jbustossATaemet.es	ResearchGate
Dr Omaira E. García-Rodríguez	FTIR Programme: Head	ogarciarATaemet.es	ResearchGate Google Scholar
Ignacio Mármol Fernández[c]	In situ Aerosols Programme	proyecto_atmo_accessATaemet.es	
Carlos L. Marrero de la Santa Cruz	Meteorology Programme: Head	cmarrerodATaemet.es	
Dr Francisco Parra Rojas[d]	Ozone and UV Programme	proyecto_breweb_ciaiATaemet.es	
Dr Natalia Prats Porta	ATMO-ACCESS Project Manager	npratspATaemet.es	ResearchGate
Alberto Redondas-Marrero	Ozone and UV Programme: Head	aredondasmATaemet.es	ResearchGate Google Scholar
Pedro Pablo Rivas Soriano	Greenhouse Gases and Carbon Cycle Programme: Head	privassATaemet.es	
Pedro M. Romero-Campos	Radiation and Water Vapour Programme: Head	promerocATaemet.es	

[a]Retired in August 2023, [b]From 1 Sept 2023, [c]Joined IARC in 2022, [d]Left IARC in 2021-2022

Research Staff from other Institutions				
Name	**Affiliation**	**Programme**	**Email**	**Personal Web Page**
Dr Antonio F. Almansa-Rodríguez	CIMEL	UV-Vis Photodiode Array Spectrometer development	f-almansaATcimel.fr	
Dr Alberto Berjón	TRAGSATEC	Ozone and UV Programme	aberjonATtragsa.es	ResearchGate
Nayra Chinea	SIELTEC/ TRAGSATEC	Reactive Gases and Ozonesondes Programme	nayra.chineaATsieltec.es	
Dr Rosa D. García-Cabrera	TRAGSATEC /UVA	Radiation Programme	rgarci47ATtragsa.es	ResearchGate
Dr Yenny González	CIMEL	Column Aerosols Programme	y-gonzalezATcimel.fr	ResearchGate
Dr Sergio León-Luís	TRAGSATEC	ICOS	sleon2ATtragsa.es	ResearchGate
Dr Javier López-Solano	TRAGSATEC	Ozone and UV Programme	jlopez15ATtragsa.es	ResearchGate
Dr Celia Milford		In situ Aerosols Programme	cmilford2ATgmail.com	ResearchGate
Daniel Santana	LuftBlick	Ozone and UV Programme	daniel.santanaATluftblick.at	
Dr Eliezer Sepúlveda[a]	TRAGSATEC	FTIR Programme	esepulveATtragsa.es	
Dr Noemie L. Taquet[a]	TRAGSATEC	FTIR Programme	ntaquetATtragsa.es	

[a]Joined IARC in 2023

Technical Staff		
Name	**Position**	**Email**
Antonio Alcántara-Ruíz	Meteorological Observer/GAW technician	aalcantararATaemet.es
Concepción Bayo-Pérez	Meteorological Observer/GAW technician	cbayopATaemet.es
Virgilio Carreño-Corbella	Meteorological Observer/GAW technician	vcarrenocATaemet.es
Néstor J. Castro-Quintero[a]	IT specialist	ncastroqATaemet.es
Antonio M. Cruz-Martín	IT specialist	acruzmATaemet.es
Cándida Hernández-Hernández	Meteorological Observer/GAW technician	chernandezhATaemet.es
Rocío López-Fernández	IT specialist	rlopezfATaemet.es
Ramón Ramos-López	Scientific instrumentation and infrastructures: Head	rramoslATaemet.es
Enrique Reyes-Sánchez	Scientific instrumentation and infrastructures	ereyessATaemet.es
Antonio Serrano-De la Torre	Scientific instrumentation and infrastructures	aserranotATaemet.es
Pablo González-Sicilia[b]	Postgraduate training scholarship: AEMET	becas2022_proy03@aemet.es
Jorge Guerola-Campos[b]	Postgraduate training scholarship: AEMET	becas2022_proy05@aemet.es
Jose Iván Martín-Herrera[b]	Postgraduate training scholarship: AEMET	becas2022_proy01@aemet.es
Celia Rey-Díaz[b]	Postgraduate training scholarship: AEMET	becas2022_proy07@aemet.es

[a]Left IARC in 2023, [b]Joined IARC in 2023

Administration Staff			
Name	**Position**	**Email**	**Personal Web Page**
Dr Emilio Cuevas-Agulló[a]	Izaña Atmospheric Research Center: Former Director	ecuevasaATaemet.es	ResearchGate Google Scholar
Carlos J. Torres García[b]	Izaña Atmospheric Research Center: Director	ctorresgATaemet.es	ResearchGate
Marcos Damas-García	Driver	mdamasgATaemet.es	
Antonio Naranjo-Zamudio[c]	Administration trainee	practicaprofesional13ATaemet.es	
Dr Natalia Prats Porta	Project Manager	npratspATaemet.es	ResearchGate
J. Félix Santo Tomás-Castro	Accounting officer	jsantotomascATaemet.es	

[a]Retired in August 2023, [b]From 1 Sept 2023, [c]Joined IARC in 2023

31 List of Acronyms

ACE-FTS - Atmospheric Chemistry Experiment - Fourier Transform Spectrometry

ACMAD - African Centre of Meteorological Application for Development

ACSO - Absorption Cross Sections of Ozone

ACTRIS - Aerosol, Clouds and Trace Gases Research Infrastructure

ADF - aerosol radiative forcing

AE - Angstrom Exponent

AECID - Agencia Española de Cooperación Internacional para el Desarrollo (Spanish Agency for International Development Cooperation)

AEMET - Agencia Estatal de Meteorología (State Meteorological Agency)

AEROCOM - Aerosol Comparisons between Observations and Models

AERONET - AErosol RObotic NETwork

AF - Radiative Forcing

ALC - Automatic Ceilometer and Lidars Network

AMISOC - Atmospheric MInorSpecies relevant to the OzoneChemistry at both sides of the Subtropical jet

ANACIM - Agence Nationale de l'Aviation Civile et de la Météorologie

ANAtOLIA - Atmospheric moNitoring to Assess the availability of Optical LInks through the Atmosphere

ANN - Artificial Neuronal Networks

AOD - Aerosol Optical Depth

APS - Aerosol Polarimetry Sensor

ARTI - African Residence Time Index

ATC - Atmospheric Thematic Center (ICOS)

ATMOZ - Traceability for atmospheric total column ozone

AQG - Air Quality Guideline

BC - Black Carbon

BDCN - Banco Nacional de Datos Climatológicos (National Climatological Data Base)

BDFC - Barcelona Dust Forecast Centre

BIRA-IASB - Royal Belgian Institute for Space Aeronomy

BSC-CNS - Barcelona Supercomputing Centre – National Supercomputing Centre

BSRN - Baseline Surface Radiation Network

BTO - Botanic Observatory

CALIMA - Cloud, Aerosols and Ice Measurements in the Saharan Air Layer

CAMS - Copernicus Atmosphere Monitoring Service

CARS - Centre for Aerosol Remote Sensing

CARSNET - China Aerosol Remote Sensing NETwork

CBL - Convective Boundary Layer

CCD - Charge-coupled device

CCGG - Carbon Cycle Greenhouse Gases group

CCI - Climate Change Initiative

CCLs - Central Calibration Laboratories

CCN - Cloud Condensation Nuclei

CEAM - Centro de Estudios Ambientales del Mediterráneo (Mediterranean Center for Environmental Studies)

CEILAP - Laser and Applications Research Center

CEIP - Colegio de Educación Infantil y Primaria (School of Infant and Primary Education)

CEOS - Committee on Earth Observation Satellites

CIMH - Caribbean Institute for Meteorology and Hydrology

CIMO - Commission for Instruments and Methods of Observations

CINDI - Cabauw Intercomparison campaign Nitrogen Dioxide measuring Instrument

CMA - China Meteorological Administration

CNR - National Research Council of Italy

CNRS - Centre National de la Recherche Scientifique (French National Centre for Scientific Research)

COALITION - Characterization Of AerosoLs In The subtropIcal nOrth atlaNtic

COCCON - Collaborative Carbon Column Observing Network

COP – Conference of the Parties

CoSQM - Color Sky Quality Meter

COST - European Cooperation in Science and Technology

CPCs - Condensation Particle Counter

CPT - Cold Point Tropopause

CRDS - Cavity Ring-Down Spectroscopy

CREWS - Climate Risk and Early Warning System

CRR - Convective Rainfall Rate

CSIC - Consejo Superior de Investigaciones Científicas (Spanish National Research Council)

CWT - Concentration Weighted Trajectory

DBM - Daumont, Brion & Malicet

DMN - Direction de la Météorologie Nationale

DNI - Direct Normal Irradiance

DOAS - Differential Optical Absorption Spectroscopy

DOD - Dust Optical Depth

DQO - Data Quality Objective

DREAM - Dust REgional Atmospheric Model

DS - Direct Sun

DSCR - Digital Sky Colour Radiometer

DTCAN - Delegación Territorial de AEMET en Canarias (Territorial Delegation of AEMET in the Canary Islands)

DU - Dobson Unit

DVB - Digital Video Broadcast

DWD - Deutscher Wetterdienst (German National Meteorological Service)

EAN - European Aeroallergen Network

ECC - Electrochemical concentration cell

ECD - Electron Capture Detector

ECMWF - European Centre for Medium-Range Weather Forecasts

ECMWF-IFS - European Centre for Medium-Range Weather Forecasts - Integrated Forecasting System

ECN - Energy research Centre of the Netherlands

ECV - Essential Climate Variable

EGVAP - EUMETNET GPS Water Vapour Programme

EMA - Egyptian Meteorological Authority

EMPA - Eidgenössische Materialprüfungs- und Forschungsanstalt (Swiss Federal Laboratories for Materials Science and Technology)

EMPIR - European Metrology Programme for Innovation and Research

EMRP - European Metrology Research Programme

Eolo-PAT EOLO-Predicción Aerobiológica para Tenerife

EPA - Environmental Protection Agency

EPS - Ensemble Prediction System

ERA4CS - European Research Area for Climate Services

ERA-Interim – ECMWF global atmospheric reanalysis from 1979

ERDF - European Regional Development Fund

ERIC - European Research Infrastructure Consortium

ESA - European Space Agency

ESA-CALVAL – European Space Agency Calibration and Validation project

ESFRI - European Strategy Forum on Research Infrastructures

ESRL - Earth System Research Laboratory

ESTOC - Estación de Series Temporales en el Océano de las Islas Canarias

ET-ACMQ - Expert Team -Atmospheric Composition Measurement Quality

ETC - Extraterrestrial constant

EUBREWNET - European Brewer Network

EU COST - European Cooperation in Science and Technology

EUDAT - European Data Infrastructure

EUMETNET - European Meteorological Network

EUMETSAT - European Organisation for the Exploitation of Meteorological Satellites

EURAMET - European Association of National Metrology Institutes

EVDC - ESA Validation Data Center

EVOLUTION - EValuation of aerOsol LUnar measuremets at the saTellIte cOmmunication chaNnels

FCS - Fraction Clear Sky

FID - Flame Ionization Detector

FLC - Ferroelectric Liquid Crystal

FLEXTRA - FLEXible TRAjectories

FMI - Finnish Meteorological Institute

FNL - Final Analysis Data

FOV - Field Of View

FRC-V Fifth Filter Radiometer Comparison

FRM - Fiducial Reference Measurements

FRM4DOAS - FRM for DOAS

FT - Free Troposphere

FTIR - Fourier transform infrared spectroscopy

FTS - Fourier Transform Spectrometry

FW2 - Fitting Window 2

FW5 - Fitting Window 5

FWHM - Full Width at Half Maximum

GAW - Global Atmosphere Watch

GAW-PFR - Global Atmosphere Watch - Precision Filter Radiometer

GAWSIS - GAW Station Information System

GCOS - Global Climate Observing System

GC-RGD - Gas Chromatography Reduction Gas Analyser

GDAS - Global Data Assimilation System

GEO – Geostationary Orbit

GEOS-5 -Goddard Earth Observing System model

GFS - Global Forecast System

GHG - Greenhouse Gas

GLOBE - Global Learning and Observations to Benefit the Environment

GLONASS - Global Navigation Satellite System

GMD - Global Monitoring Division

GMES - Global Monitoring for Environment and Security

GNSS - Global Navigation Satellite System

GOA - Atmospheric Optics Group

GOA-UVA - University of Valladolid Atmospheric Optics Group

GOME - Global Ozone Monitoring Experiment

GPS - Global Positioning System

GRASP - Generalized Retrieval of Aerosol and Surface Properties

GRUAN - Global Climate Observing System Reference Upper-Air Network

GSR - Global Solar Radiation

HEGIFTOM - Harmonization and Evaluation of Ground-based Instruments for Free Tropospheric Ozone Measurements

H2020 - Horizon 2020

HIRLAM - High Resolution Limited Area Model

HYSPLIT - Hybrid Single Particle Lagrangian Integrated Trajectory Model

IAC - Instituto de Astrofísica de Canarias (Institute of Astrophysics of the Canary Islands)

IAEA - International Atomic Energy Agency

IAGOS - In-Service Aircraft for a Global Observing System

IARC - Izaña Atmospheric Research Center

IASI -Infrared Atmospheric Sounding Interferometer

ICOS - Integrated Carbon Observation System

ICP-AES - Inductively Coupled Plasma Atomic Emission Spectroscopy

ICP-MS - Inductively Coupled Plasma Mass Spectroscopy

IDAEA - Instituto de Diagnóstico Ambiental y Estudios del Agua (Institute of Environmental Assessment and Water Research)

IEO - Instituto Español de Oceanografía (Spanish Institute of Oceanography)

IES - Instituto de Educación Secundaria (Institute of Secondary Education)

IGAC - International Global Atmospheric Chemistry Project

IGACO - Integrated Global Atmospheric Observations

IGN - Instituto Geográfico Nacional de España (Spanish National Geographic Institute)

IG3IS - Integrated Global Greenhouse Gas Information System

ILAS - Improved Limb Atmospheric Spectrometer

IMAA - Institute of Methodologies for Environmental Analysis

IMK-ASF - Institut für Meteorologie und Kimaforschung - Atmosphärische Spurengase und Fernerkundung (Institute of Meteorology and Climate Research - Atmospheric Trace Gases and Remote Sensing)

IN - Ice Nuclei

INAR - Institute for Atmospheric and Earth System Research

INM - Institut National de la Météorologie

INSTAAR - Institute of Arctic and Alpine Research

INTA - Instituto Nacional de Técnica Aeroespacial (Spanish National Institute for Aerospace Technology)

INTERCOONECTA - Knowledge Transfer, Exchange and Management Plan for the Development of Spanish Cooperation in Latin America and the Caribbean

IO3C - International Ozone Commission

IPCC - Intergovernmental Panel on Climate Change

IPMA - Instituto Português do Mar e da Atmosfera (Portuguese Institute for Sea and Atmosphere)

IR – Infrared

ISAF - Izaña Subtropical Access Facility

IUP - Institut für Umweltphysik (Institute of Environmental Physics)

IZO - Izaña Observatory

JRC - Joint Research Centre

KADI - Knowledge and climate services from an African observation and Data research Infrastructure

KIT - Karlsruhe Institute of Technology

LAP - Laboratori d'Anàlisis Palinològiques (Laboratory of Palynological Analysis)

LEO - Low Earth Orbit

LIDAR - Laser Imaging Detection and Ranging

LIME - Lunar Irradiance Model ESA

LOA - Laboratoire d'Optique Atmosphérique (Atmospheric Optics Laboratory)

LR - Lidar Ratio

LUT – Look Up Table

MAAP - Multi Angle Absorption Photometer

MAPP - Metrology for Aerosol oPtical Properties

MARS - Meteorological Archival and Retrieval System

MAXDOAS - Multi Axis Differential Optical Absorption Spectroscopy

MBL - Marine Boundary Layer

McIDAS - Man Computer Interactive Data Access System

MEDA - Mars Environmental Dynamics Analyzer

MetUN - Met Office Unified Model

MEE - Mass Extinction Efficiency

MERRA-2 Modern-Era Retrospective Analysis for Research and Applications, version 2

MFRSR - Multi Filter Rotating Shadow-Band Radiometer

MGA - Modified Geometrical Approach

MICINN - Ministerio de Ciencia, Innovación y Universidades (Spanish Ministry of Science, Innovation and Universities)

MIPAS - Michelson Interferometer for Passive Atmospheric Sounding

MIR - Middle Infrared

MISR - Multi-angle Imaging SpectroRadiometer

MITECO - Ministerio para la Transición Ecológica y el Reto Demográfico (Spanish Ministry for the Ecological Transition and the Demographic Challenge)

MLO - Mauna Loa Observatory

MM5 - Mesoscale Model

MOCAGE - Modèle de Chimie Atmosphérique de Grande Echelle

MODIS - Moderate Resolution Imaging Spectroradiometer

MOL-RAO - Meteorologisches Observatorium Lindenberg - Richard Aßmann-Observatorium

MOSAIC - Multidisciplinary drifting Observatory for the Study of Arctic Climate

MPA - Moon phase angle

MPL - Micro Pulse Lidar

MSG - Meteosat Second Generation

MUSICA - MUlti-platform remote Sensing of Isotopologues for investigating the Cycle of Atmospheric water

NAFDI - North African Dipole Intensity

NA-ME-E - The Regional Centre for Northern Africa, Middle East and Europe

NAO - North Atlantic Oscillation

NAS - Network-Attached Storage

NASA - National Aeronautics and Space Administration

NASA MPLNET - The NASA Micro Pulse Lidar Network

NCEP - National Centers for Environmental Prediction

NDACC - Network for the Detection of Atmospheric Composition Change

NDIR - Non Dispersive Infrared

NEMS - NOAA Environmental Modeling System

NGAC - NEMS GFS Aerosol Component

NIDFORVal - NItrogen Dioxide and FORmaldehyde Validation

NIES - National Institute for Environmental Studies

NILU - Norwegian Institute for Air Research

NIPR - National Institute of Polar Research of Japan

NIR - Near Infrared

NIST - National Institute for Standards and Technology

NMHSS - National Meteorological and Hydrological Services

NMMB - Nonhydrostatic Multiscale Model on the B-grid

NMME - North American Multi-Model Ensemble

NOA - National Observatory of Athens

NOAA - National Oceanic and Atmospheric Administration

NORS - Demonstration Network Of ground-based Remote Sensing Observations in support of the Copernicus Atmospheric Service

NPF - New Particle Formation

NRT - Near Real Time

OC-SVC - Ocean Colour System Vicarious Calibration

ODSs - Ozone Depleting Substances

OMI - Ozone Monitoring Instrument

ONM - Office National de la Météorologie

OLI - Operational Land Imager

OSC - ozone slant column

O3S-DQA Ozonesonde Data Quality Assessment

OT - Ozone Tropopause

PAR - Photosynthetically Active Radiation

PBS - Polarizer Beam Splitter

PEVOLCA- Plan Especial de Protección Civil y Atención de Emergencias por Riesgo Volcánico en la Comunidad Autónoma de Canarias

PFR - Precision Filter Radiometer

PI - Principal Investigator

PIXE - Particle-Induced X ray Emission

PLOCAN - Oceanic Platform of the Canary Islands

PM - Particle Matter

PM-LCS - Particle Matter – Low Cost Sensors

PMOD - Physikalisch-Meteorologisches Observatorium Davos

PSR - Precision Solar Spectroradiometer

PTB - Physikalisch-Technische Bundesanstalt (National Metrology Institute of Germany)

PV - Potential Vorticity

PWV - Precipitable Water Vapour

QA - Quality Assurance

QASUME - Quality Assurance of Spectral Ultraviolet Measurements

QA4EO - Quality Assured Data for Earth Observation communities

QC - Quality Control

QUIMA - Institute of Oceanography and Climate Change

RA - Row Anomaly

R&D - Research and Development

R+D+I – Research, Development & Innovation

RBCC-E - Regional Brewer Calibration Center for Europe

RCF - RIMO Correction Factor

REA - Red Española de Aerobiología (Spanish Aerobiology Network)

REDMAAS - Red Española de DMAs Ambientales (Spanish Network of Environmental DMAs)

RGB - composite - Red Green Blue composite

RH - Relative Humidity

RIMO - ROLO Implementation for Moon-photometry Observation

RMSE - Root Mean Square Error

RMTC - WMO Regional Meteorological Training Centre

ROLO - RObotic Lunar Observatory model

RSMC-ASDF - Regional Specialized Meteorological Centre with activity specialization on Atmospheric Sand and Dust Forecast

RTM - Radiative Transfer Model

SAF - Satellite Application Facilities

SAG - Scientific Advisory Group

SAL - Saharan Air Layer

SALAM - Air Layer Air Mass characterization

SAO - Smithsonian Astrophysical Observatory

SBSTA - Subsidiary Body on Scientific and Technical Advice

SCIAMACHY - Scanning Imaging Absorption Spectrometer for Atmospheric Chartography

SCILLA - Summer Campaign for Intercomparison of Lunar measurements of Lindenberg's Aerosol

SC-MINT - Standing Committee on Measurement, Instrumentation and Traceability

SCO - Santa Cruz Observatory

SD - Sunshine Duration

SDM - Standard Delivery Mode

SDR - Shortwave downward radiation

SDS - Sand and Dust Storm

SDS-WAS - Sand and Dust Storm Warning Advisory and Assessment System

SEAIC - Sociedad Española de Aerobiología e Inmunología Clínica (Spanish Society of Aerobiology and Clinical Immunology)

SeaWIFS - Sea-Viewing Wide Field-of-View Sensor

SEM - Standard Error of the Mean

SHL - Saharan Heat Low

SI - International System of Units

SIOS - Svalbard Integrated Arctic Earth Observing System

SMN - Argentinian Meteorological Service

SMPS - Scanning Mobility Particle Sizer

SOC - Stratospheric Ozone Column

SOL - Significant Obstructive Lesions

SONA - Sistema de Observación de Nubes Automático (Automatic cloud observation system)

SOP - Standard Operating Procedure

SPARC - Stratosphere-troposphere Processes And their Role in Climate

SPC - Science Pump Corporation

SSDM - Server Meteorological Data System

STJ - Subtropical Jet Stream

STS - Sky Temperature Sensor

STT - Stratosphere-to-troposphere

SWIR - short-wave infrared

SWVID - Stable Water Vapor Isotope Database

SYNERA - SYNERgies for assessing short- and long-term variations of Aerosols properties in the subtropical North Atlantic

SYNOP - Surface Synoptic Observation

SZA - Solar Zenith Angle

TNA - Trans National Access

TOB - Tropospheric Ozone Burden

TOC - Total Ozone Column

TPO - Teide Peak Observatory

TSP - Total Suspended Particles

TT - Thermal Tropopause

UAB - Universidad Autónoma de Barcelona (Autonomous University of Barcelona)

UFPs - Ultrafine Particles

ULL - University of La Laguna

ULPGC - University of Las Palmas de Gran Canaria

UNAM - National Autonomous University of Mexico

UNEP - United Nations Environment Programme

UNFCCC - United Nations Framework Convention on Climate Change

UPC - Universitat Politècnica de Catalunya

UPS - Uninterruptible Power Supply

UT – Upper Troposphere

UTC - Coordinated Universal Time

UTLS - Upper Troposphere Lower Stratosphere

UV - Ultraviolet

UVA - University of Valladolid

VAAC - Volcanic Ash Advisory Centre

VIS - Visible

VMR - Volume Mixing Ratio

VOS - Volunteer Observing Ship

WCC - World Calibration Center

WCCAP - World Calibration Centre for Aerosols Physics

WCRP - World Climate Research Programme

WDCA - World Data Centre for Aerosols

WDCGG - World Data Centre for Greenhouse Gases

WDCRG - World Data Center for Reactive Gases

WIGOS – WMO Integrated Global Observing System

WMO - World Meteorological Organization

WORCC - World Optical Depth Research and Calibration Center

WOUDC - World Ozone and Ultraviolet Data Center

WRC - World Radiation Center

WS-CRDS - Wavelength-Scanned Cavity Ring-Down Spectroscopy

WWRP - World Weather Research Programme

XS - Cross Section

ZHD - Zenith Hydrostatic Delay

ZSR - Zenith Sky Radiance

ZTD - Zenith Total Delay

32 Acknowledgements

A dedicated, enthusiastic and motivated team formed by scientific, technical and administrative staff is the key factor to run a centre like IARC. This report summarizes the activities carried out by IARC in 2021-2022 and is an expression of recognition of work done by each and every one of the people working in IARC and in all the institutions which collaborate with IARC.

The WMO Global Atmosphere Watch Programme has been an excellent framework within which to develop our activities, where we have always found great assistance and support. IARC has been contributing to the GAW Programme since it was established in 1989 and we thank the WMO and its associated bodies for their work in coordinating and developing the GAW Programme and for its continuing support to all the IARC activities.

We would like to express our sincere gratitude for the extraordinary effort carried out by IARC and AEMET personnel and all collaborating organisations, to assist in the emergency deployment as part of the response to the volcanic eruption that occurred in La Palma from 19 September-13 December 2021. The dedication of time and resources was a key example of the collaborative expertise of the scientific community providing a service to society.

In addition, although this period is not included in the 2021-2022 activity report, we would like to thank all the emergency personnel who showed an exceptional dedication to controlling and extinguishing the forest fire which occurred in Tenerife in August 2023. Their work made it possible to keep critical infrastructure such as the Izaña Observatory safe.

We are grateful for the strong support to IARC from the former Director of Planning, Strategy and Business Development (DPEDC-AEMET), Ana M. Casals Carro, who has always shown a high level of interest and enthusiasm for all the IARC activities. We also thank Ms Ana Melgar (DPEDC-secretary) for assisting us in many ways.

We thank Miguel Ángel García-Couto, Head of AEMET Documentation Service, for his support in the final publication of this report and other technical publications. We also thank the AEMET central library team, headed by Elena Morato who have always provided invaluable help.

We express our sincere gratitude to all those institutions, included in this report, which work closely with IARC and collaborate on both national and international projects. These collaborations are crucial to the activities at all the IARC facilities and provide an enriching and synergistic research environment.

Back cover photograph: Teide, taken from Izaña Observatory (Photo: Daniel López TeideLab project)

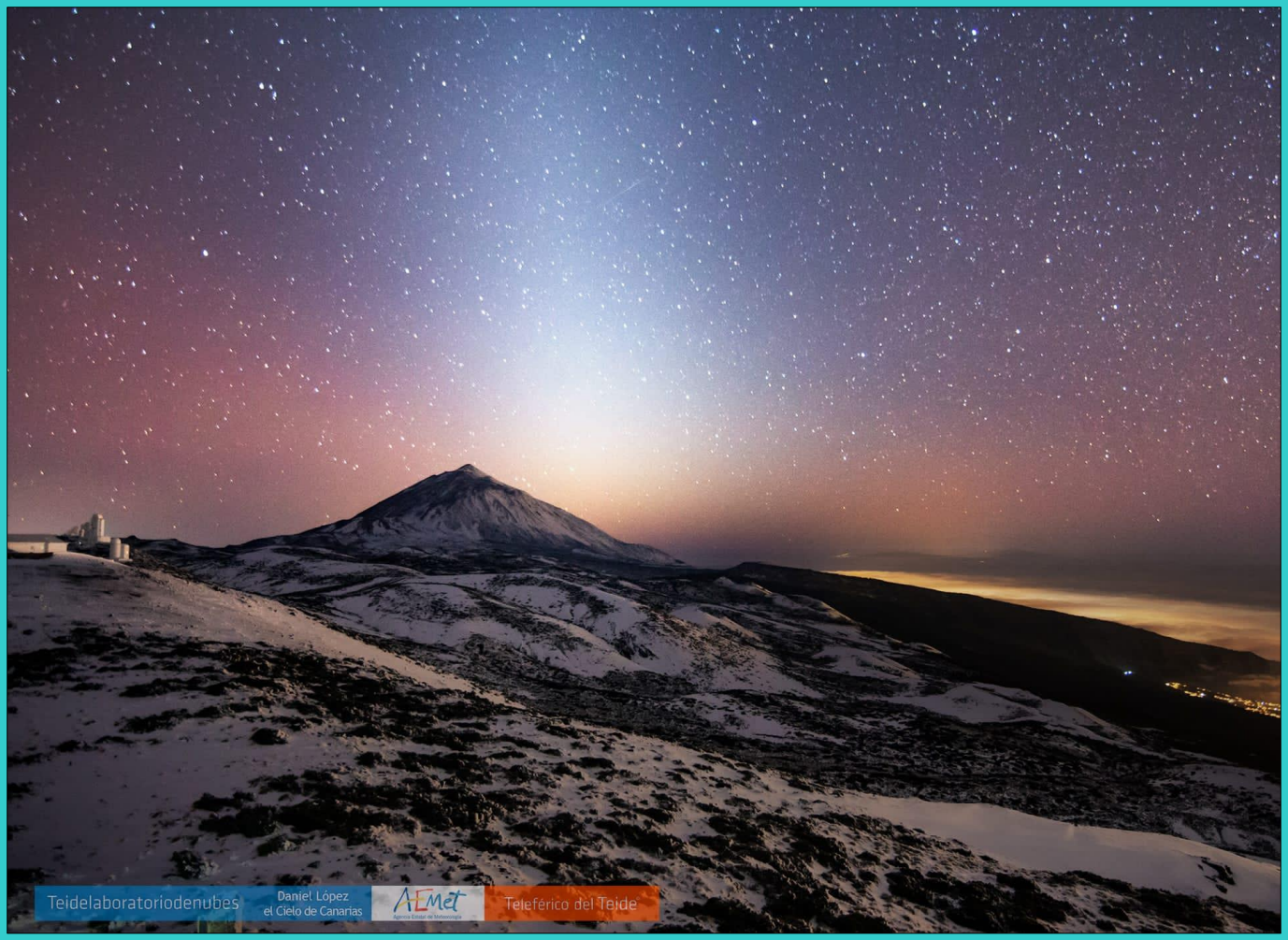

For more information, please contact:
Izaña Atmospheric Research Center
Calle La Marina, 20, Planta 6
Santa Cruz de Tenerife
Tenerife, 38001, Spain
http://izana.aemet.es